LEABHARLANN CHOLÁISTE NA TRÍONÓIDE, BAILE ÁTHA CLIATH | TRINITY COLLEGE LIBRARY DUBLIN
Ollscoil Átha Cliath | The University of Dublin

Terms and Conditions of Use of Digitised Theses from Trinity College Library Dublin

Copyright statement

All material supplied by Trinity College Library is protected by copyright (under the Copyright and Related Rights Act, 2000 as amended) and other relevant Intellectual Property Rights. By accessing and using a Digitised Thesis from Trinity College Library you acknowledge that all Intellectual Property Rights in any Works supplied are the sole and exclusive property of the copyright and/or other IPR holder. Specific copyright holders may not be explicitly identified. Use of materials from other sources within a thesis should not be construed as a claim over them.

A non-exclusive, non-transferable licence is hereby granted to those using or reproducing, in whole or in part, the material for valid purposes, providing the copyright owners are acknowledged using the normal conventions. Where specific permission to use material is required, this is identified and such permission must be sought from the copyright holder or agency cited.

Liability statement

By using a Digitised Thesis, I accept that Trinity College Dublin bears no legal responsibility for the accuracy, legality or comprehensiveness of materials contained within the thesis, and that Trinity College Dublin accepts no liability for indirect, consequential, or incidental, damages or losses arising from use of the thesis for whatever reason. Information located in a thesis may be subject to specific use constraints, details of which may not be explicitly described. It is the responsibility of potential and actual users to be aware of such constraints and to abide by them. By making use of material from a digitised thesis, you accept these copyright and disclaimer provisions. Where it is brought to the attention of Trinity College Library that there may be a breach of copyright or other restraint, it is the policy to withdraw or take down access to a thesis while the issue is being resolved.

Access Agreement

By using a Digitised Thesis from Trinity College Library you are bound by the following Terms & Conditions. Please read them carefully.

I have read and I understand the following statement: All material supplied via a Digitised Thesis from Trinity College Library is protected by copyright and other intellectual property rights, and duplication or sale of all or part of any of a thesis is not permitted, except that material may be duplicated by you for your research use or for educational purposes in electronic or print form providing the copyright owners are acknowledged using the normal conventions. You must obtain permission for any other use. Electronic or print copies may not be offered, whether for sale or otherwise to anyone. This copy has been supplied on the understanding that it is copyright material and that no quotation from the thesis may be published without proper acknowledgement.

A STUDY OF THE EFFECTS OF THIN DYKE INTRUSIONS ON MUDROCK

by

Jacqueline Connolly

A thesis presented in accordance with the requirements for the degree of
Doctor of Philosophy

Department of Geology, Trinity College Dublin

September 2002

TRINITY COLLEGE
2 3 APR 2003
LIBRARY DUBLIN
THESIS
7323

DECLARATION

I hereby declare that the work in this thesis is entirely my own, unless otherwise stated, and has not previously been submitted to the University of Dublin or any other university. Reproduction in whole or part of this work is authorised, provided that the source is acknowledged, at the discretion of the depository library of the University of Dublin.

I give permission for the Library to lend or copy this thesis upon request.

Jacqueline Connolly

Jacqueline Connolly

SUMMARY

The aim of this work is to examine the thermal response of mudrock to the short lived heating event induced by dyke intrusion. The work examines five Carboniferous mudrock horizons, intruded by Tertiary olivine tholeiitic dykes. Two of the mudrock sample horizons (named CK and CQ) were collected from the Carrickleck Quarry in the Kingscourt Outlier and are cut by a 1.5m wide dyke. The other three mudrock horizons (named BC, cMd and NSD) were collected from the north Antrim coast, near Ballycastle, and are cut by a 4m wide dyke. The mudrock horizons were sampled at up to 30 positions over 7-80m from the dyke, with sampling density increasing within *c.* 1m from the dyke margin. Samples were processed and analysed for vitrinite reflectance, spore colour, spore fluorescence, palynofacies, clay mineralogy, illite crystallite size, and bulk chemistry. In addition a numerical model was used to estimate the temperatures reached in the two dyke aureoles. The stratigraphic age of the Ballycastle rocks was determined using palynology.

Vitrinite reflectance results show background values of *c.* 1% R_r. However as the dyke is approached the values increase exponentially to *c.* 3.6% R_r at Carrickleck and 5.5% R_r at Ballycastle before dropping to *c.* 3% R_r at Carrickleck and 3.8% R_r at Ballycastle within *c.*20cm from the contact. However, background VR values from coal lenses in the cMd horizon and at the Gobb Colliery section, *c.* 2km away were as low as 0.5% R_r.

Spore colour index (TAI) increases steadily as the dyke is approached, from a background level of around 2 rising to 5 at the contact.

Spore fluorescence was observed to decrease in intensity and was eventually quenched within *c.* 1.5m from the contact at recorded vitrinite reflectance values of *c.* 1.5% R_r (Carrickleck) and 1.5% R_r (Ballycastle).

Palynofacies analysis shows a gradually darkening organic assemblage. There is a significant increase in amorphous organic matter (AOM), from *c.* 30% (Carrickleck), 20% (Ballycastle) in background samples up to *c.* 95% (Carrickleck), 90% (Ballycastle) within *c.*1m (Carrickleck) and 1.5m (Ballycastle) of the dyke contact. There is a concomitant decrease in non-woody plant tissue, palynomorphs and brown wood.

Clay mineral assemblages are all dominated by kaolinite and illite/smectite. The kaolinite XRD reflection diminishes in size within *c.* 0.7m of the dyke contact at VR values of *c*1.5%R_r. The illite/smectite XRD reflection shows diminished intensity, sharpens and narrows within 1-1.5m from the dyke contact.

Illite crystallite best mean sizes, calculated using MUDMASTER are small, < 4nm, in all horizons.

Stratigraphic palynology suggests that the NSD mudrock horizon in the NC miospore zone of the Pendleian (Upper Mississippian). 23 spore genera were identified in background samples. Only two genera were consistently identifiable right into the contact, *Lycospora* sp. and *Densosporites* sp..

Numerical modelling (Delaney 1988) suggests maximum temperatures in the host rock at the dyke contact to be 535°C (Carrickleck) and 550°C (Ballycastle). The model also calculates *c.* 0.42 years for the contact temperature to drop to below 200°C and *c.* 42 years for the dyke centre and contact to return to the ambient temperature of the host rock at Carrickleck. Applied to Ballycastle the model calculates *c.* 4 years for the contact temperature to drop to less than 200°C and *c.* 200years for the dyke centre and contacts to return to the ambient temperature of the host rock.

The thicker North Star Dyke has effected higher vitrinite reflectance values, a result of the longer cooling time and sustained heat flow. The 'apparent' trend reversal of the vitrinite reflectance values within *c.* 0.2m from the contact has been assumed to be due to a situation whereby pore space over pressure has retarded the reaction.

Spore fluorescence survives to higher vitrinite reflectance values at Ballycastle than Carrickleck. Spore fluorescence is quenched at a vitrinite reflectance of *c.* 1.3%R_r in a simple burial setting.

The inability to identify spore genera in the same numbers into the margin is a testament to the destructive influence of the dyke on the organic material and to the robust genera, *Lycospora* sp and *Densosporites* sp., which can be identified all the way into the dyke contact.

Concomitant darkening of material and shift in the percent content of the palynofacies groups, towards an AOM dominated palynofacies has been interpreted as a reflection of the destruction of the organic material due to heating. This is something that might lead to the misrepresentation of the palynofacies, i.e. it might be mis-identified as an over-mature AOM rich, (and possibly therefore source rock) lithology.

Literature and experimental evidence shows that kaolinite can be 'destroyed' at *c.*550°C. The marked reduction of the kaolinite peak might be assumed to represent a thermal contour. Illite crystallinity is represented as measure of the symmetry and breadth of the 001 peak. The increased symmetry and narrowing of this peak in the clay traces represents increased maturity, however the decreased intensity of the peak shows that the material is also diminishing in concentration within the sample.

Comparison of modelled thermal profiles to VR results implies that VR within *c.*1m of the contacts grossly underestimate $T_{max.}$ The temperature profiles are similar but disparity in this region suggests that the vitrinite reflectance was suppressed possibly by vaporised fluids at the contact.

ACKNOWLEDGEMENTS

I would like to express my gratitude to Enterprise Ireland for funding this project for three years, and to the Trinity Trust Travel Fund, which has aided and abetted my attending a plethora of varied and fascinating conferences in many far-flung and exotic locations.

To my supervisor, Professor Geoffrey Clayton, for his support and guidance, I would like to express my most sincere thanks.

Thankyou to all of the Geology Department teaching staff 'old guard' and new, for all of their enthusiasm and encouragement.

I would like to thank all of the departmental non-academic staff. Special thanks should be extended to Frank who has provided so much help, support and entertainment from the Palynology Lab. for all five of my years here, 'Hendron'; to Declan who has always been able to help with the many computer problems that follow in my wake, and to Joann for always being there and helping whenever I asked.

To all of my 'palynology group' predecessors, I owe a great debt of gratitude as the seeds of this project are to be found in their theses.

I would like to acknowledge and thank all of the geology postgrad's with whom I have had both the honour and pleasure of working with during my time at Trinity.

Finally, I would like to thank my family for their constant support, for which I will always be grateful.

DEDICATION

This work is dedicated to

John Tate Abernethy

CONTENTS

TITLE

DECLARATION

SUMMARY

ACKNOWLEDGEMENTS

DEDICATION

TABLE OF CONTENTS

LIST OF FIGURES

LIST OF TABLES

1 AIMS AND OBJECTIVES 1

1.1 AIMS 1

1.2 PREVIOUS WORK 1

1.3 THESIS FRAMEWORK 2

2 GEOLOGY AND SAMPLING STRATEGY 3

2.1 REGIONAL GEOLOGY 3
2.1.1 IRELAND IN THE MISSISSIPPIAN (LOWER CARBONIFEROUS) (Metcalfe 1997, Menning *et al.* 2000) 3
2.1.2 IRELAND AND THE TERTIARY VOLCANICS AND IRELAND 4

2.2 GEOLOGICAL BACKGROUND AND SETTING 6
2.2.1 BALLYCASTLE 6
2.2.1.1 GENERAL GEOLOGY 6
2.2.1.2 DYKE AND SETTING 7
2.2.2 CARRICKLECK AND THE KINGSCOURT OUTLIER 8
2.2.2.1 GENERAL GEOLOGY 8
2.2.2.2 DYKE AND SETTING 11

2.3 SAMPLING STRATEGY 12
2.3.1 SAMPLING AT BALLYCASTLE 15
2.3.2 SAMPLING AT KINGSCOURT 16

3 PETROGRAPHY AND GEOCHEMISTRY OF THE DYKES AND GEOCHEMISTRY OF THE HOST ROCKS 17

3.1 PETROGRAPHY OF THE INTRUSIONS 17
3.1.1 THE NORTH STAR DYKE 17
3.1.2 THE CARRICKLECK DYKE 17
3.1.2.1 CALCITE VEINING IN THE CARRICKLECK DYKE 18

3.2 MAJOR AND TRACE ELEMENT ANALYSIS OF DYKE AND COUNTRY ROCK **19**
3.2.1 BALLYCASTLE 19
3.2.1.1 NORTH STAR DYKE SAMPLES 19
3.2.1.2 NSD SAMPLE HORIZON 20
3.2.2 CARRICKLECK 20

4 VITRINITE AND VITRINITE REFLECTANCE **23**

4.1 THE CONCEPTS OF COALIFICATION, RANK AND MATURATION **23**

4.2 VITRINITE **25**
4.2.1 PHYSICAL AND CHEMICAL EVOLUTION OF VITRINITE 26
4.2.2 VITRINITE REFLECTANCE 26
4.2.2.1 VITRINITE OPTICAL ANISOTROPY 29
4.2.2.2 OPTICAL PROPERTIES OF VR IN DISPERSED ORGANIC MATTER 32

4.3 TIME AND TEMPERATURE; THEIR EFFECT ON VR AND INFLUENCE ON THERMAL MODELLING **32**
4.3.1 TEMPERATURE AND TIME 33
4.3.1.1 TIME AND TEMPERATURE INCLUSIVE MODELS 33
4.3.1.2 TEMPERATURE DEPENDENT MODELS 37

4.4 SAMPLE PREPARATION FOR VITRINITE REFLECTANCE **38**
4.4.1 ORGANIC MATTER extraction 38
4.4.2 PREPARATION FOR VITRINITE REFLECTANCE 39
4.4.2.1 SLIDE MOUNTING FOR VR 39
4.4.2.2 BLOCK MOUNTING FOR VR 40
4.4.3 SAMPLE PREPARATION FOR COAL SAMPLES 40
4.4.3.1 UNORIENTED COALS 40
4.4.3.2 ORIENTED COALS 40

4.5 VITRINITE REFLECTANCE ANALYSIS **41**
4.5.1 THE REFLECTANCE MICROSCOPE AND IMAGE ANALYSIS SETUP 41
4.5.2 MEASURING VITRINITE REFLECTANCE 41
4.5.3 PARTICLE COUNT 42
4.5.4 VITRINITE IDENTIFICATION 42
4.5.5 POSSIBLE PROBLEMS AND ERRORS WITH VR 43
4.5.6 PRESENTATION OF RESULTS 44

4.6 RESULTS **44**
4.6.1 RESULTS FOR THE CARRICKLECK DYKE AUREOLE 44
4.6.1.1 BACKGROUND AND SETTING THE SCENE 44
4.6.1.2 CK HORIZON TRAVERSE RESULTS 44
4.6.2 THE NORTH STAR DYKE AUREOLE 46
4.6.2.1 BACKGROUND - THE GOBB SECTION RESULTS 46
4.6.2.2 THE BC HORIZON TRAVERSE 46
4.6.2.3 THE CMD HORIZON TRAVERSE 48
4.6.2.4 THE NSD HORIZON TRAVERSE 48
4.6.2.5 COAL LENSES IN THE CMD HORIZON 48

4.7 VR CONVERSION TO PALAEOTEMPERATURE (°C) USING THEORETICAL EQUATIONS/PUBLISHED CALIBRATIONS 50

4.8 DISCUSSION 55
4.8.1 THE GOBB SECTION BALLYCASTLE 55
4.8.2 VR AUREOLE PROFILES 55
4.8.2.1 OBSERVATION 55
4.8.2.2 DISCUSSION 56
4.8.3 MINERALISATION OF THE COAL LENSES IN THE CMD HORIZON 59
4.8.4 TEMPERATURE CONVERSION OF VR IN THE DYKE AUREOLES 60

4.9 CONCLUSIONS 61

5 CLAYS AND CLAY ANALYSIS 62

5.1 CLAYS AND CLAY MINERALS IDENTIFIED IN XRD 62
5.1.1 CLAY MINERALS 62
5.1.1.1 KAOLINITE 65
5.1.1.1.1 PHYSICAL AND CHEMICAL CHARACTERISTICS 65
5.1.1.1.2 IDENTIFICATION 66
5.1.1.1.3 OCCURRENCE 66
5.1.1.2 PYROPHYLLITE 66
5.1.1.2.1 PHYSICAL AND CHEMICAL PROPERTIES 67
5.1.1.2.2 IDENTIFICATION 67
5.1.1.2.3 OCCURRENCE 67
5.1.1.3 CHLORITE 67
5.1.1.3.1 PHYSICAL AND CHEMICAL CHARACTERISTICS 68
5.1.1.3.2 IDENTIFICATION 68
5.1.1.3.3 OCCURRENCE 68
5.1.1.4 ILLITE 69
5.1.1.4.1 PHYSICAL AND CHEMICAL CHARACTERISTICS 69
5.1.1.4.2 IDENTIFICATION 69
5.1.1.4.3 OCCURRENCE 70
5.1.1.5 SMECTITE 70
5.1.1.5.1 PHYSICAL AND CHEMICAL CHARACTERISTICS 70
5.1.1.5.2 IDENTIFICATION 70
5.1.1.5.3 OCCURRENCE 70
5.1.1.6 ILLITE/SMECTITE 71
5.1.1.6.1 IDENTIFICATION 72
5.1.2 NON CLAY MINERALS IDENTIFIED IN XRD 73
5.1.2.1. GYPSUM $CaSO_4.2H_2O$ 73
5.1.2.2 HALITE NaCl 73
5.1.2.3 CALCITE $CaCO_3$ 73
5.1.2.4 Fe Mg CARBONATES 73
5.1.2.5 APATITE $Ca_5(F,Cl)(PO_4)_3$ 74
5.1.2.6 PYRITE FeS_2 74
5.1.2.7 QUARTZ SiO_2 74
5.1.2.8 FELDSPARS 74
ALKALI FELDSPARS 74
PLAGIOCLASE FELDSPARS 75

5.2 CLAY MINERALOGY AS AN INDICATOR OF METAMORPHIC CONDITIONS **75**
5.2.1 CLAYS AND CLAY MINERALOGY IN AN IGNEOUS AUREOLE 77

5.3 X-RAY DIFFRACTION **78**
5.3.1 THE X-RAY DIFFRACTOMETER AND OPERATOR CONDITIONS 79
5.3.2 SAMPLE PREPARATION FOR CLAY ANALYSES 79
5.3.2.1 AIR DRIED SAMPLES 80
5.3.2.2 ETHYLENE GLYCOL SOLVATION 80
5.3.2.3 DIMETHYL SULPHOXIDE (DMSO) SOLVATION 80
5.3.2.4 HEATING A SAMPLE 81
5.3.2.5 PRESENTATION OF RESULTS 81
5.3.3 SAMPLE PREPARATION FOR MUDMASTER ANALYSIS 81
5.3.3.1 PRESENTATION OF RESULTS 82

5.4 CLAY MINERALOGY RESULTS **82**
5.4.1 CARRICKLECK 82
5.4.1.1 ILLITE 83
5.4.1.2 KAOLINITE AND CHLORITE 83
5.4.2.3 QUARTZ 83
5.4.1.3 CARRICKLECK CLAYS SUMMARY 85
5.4.2 BALLYCASTLE 86
5.4.2.1 SMECTITE 86
5.4.2.2 ILLITE 87
5.4.2.3 KAOLINITE AND CHLORITE 87
5.4.2.4 CARBONATES 88
5.4.2.5 QUARTZ 88
5.4.2.6 FELDSPAR 88
5.4.2.7 BALLYCASTLE CLAYS SUMMARY 90

5.5 THE 'ILLITE CRYSTALLITE' DEBATE **90**

5.6 MUDMASTER: A PROGRAM FOR CALCULATING CRYSTALLITE SIZE DISTRIBUTIONS AND STRAIN FROM THE SHAPES OF X-RAY DIFFRACTION PEAKS (Eberl *et al.* 1996) **93**

5.7 MUDMASTER BEST MEAN SIZE RESULTS **93**
5.7.1 CARRICKLECK 94
5.7.1.1 CK HORIZON 94
5.7.1.2 CQ HORIZON 94
5.7.2 BALLYCASTLE 94
5.7.2.1 BC HORIZON 94
5.7.2.2 cMd HORIZON 97
5.7.2.3 NSD HORIZON 97

5.8 DISCUSSION **97**
5.8.1 MINERALOGY OF THE <2μm FRACTION OF DYKE AUREOLE SAMPLES 97
5.8.2 BMS VALUES AND VR 99
5.8.2.1 CARRICKLECK 99
5.8.2.2 BALLYCASTLE 99

BC 99
cMd 99
NSD 100
5.8.3 BMS AND APPARENT INTENSITY PROFILES 100
5.8.3.1 CARRICKLECK 100
5.8.3.2 BALLYCASTLE 100
BC 100
cMd 100
NSD 103
5.8.4 GENERAL 103

5.9 CONCLUSIONS 104

6 SYSTEMATIC PALYNOLOGY 105

6.1. NOMENCLATURE AND CLASSIFICATION, SPORE MORPHOLOGY AND DESCRIPTIVE TERMINOLOGY 105

6.2 SAMPLE PREPARATION AND PALYNOLOGICAL ANALYSES 105
6.2.1 ORGANIC MATTER EXTRACTION 105
6.2.2 PREPARATION FOR PALYNOLOGICAL ANALYSES 105
6.2.3 TRANSMITTED LIGHT MICROSCOPE 106
6.2.4 STRATIGRAPHIC PALYNOLOGY AND COUNT 106
6.2.5 PRESENTATION OF RESULTS 106

6.3 SYSTEMATIC PALYNOLOGY RESULTS 106

6.4 DISCUSSION 157
6.4.2 PALYNOSTRATIGRAPHY 157
__6.4.2 SPORE RANGE FLUCTUATION AND DESTRUCTION 157

6.5 CONCLUSIONS 158

7 THERMAL ALTERATION OF SPORES AND OTHER ORGANIC MATTER 161

7.1 INTRODUCTION 161

7.2 THERMAL ALTERATION AND MATURATION OF SPORES 161

7.3 SPORE COLOUR SCALES 162
7.3.1 USING SPORE COLOUR SCALES 165
7.3.2 AOM COLOUR ALTERATION 165
7.4 FLUORESCENCE 166
7.4.1 WHY USE FLUORESCENCE? 167
7.4.2 WHY DO SPORES AND AOM FLUORESCE? 167
7.4.3 USING SPORE AND AOM FLUORESCENCE 168
7.4.4 THE FADING EFFECT 168

7.5 SAMPLE PREPARATION 170
7.5.1 ORGANIC MATTER EXTRACTION 170

7.5.2 PREPARATION FOR PALYNOLOGICAL ANALYSES 170
7.5.3 SPORE COLOUR USING THE TRANSMITTED LIGHT MICROSCOPE 170
7.5.3.1 PRESENTATION OF RESULTS 170
7.5.4 SPORE FLUORESCENCE 170
7.5.4.1 PRESENTATION OF RESULTS 170

7.6 RESULTS 171
7.6.1 CARRICKLECK: TAI 171
7.6.1.1 CK SAMPLE HORIZON 171
7.6.1.2 CQ SAMPLE HORIZON 171
7.6.2 CARRICKLECK: FLUORESCENCE 171
7.6.2.1 CK SAMPLE HORIZON 171
7.6.2.2 CQ SAMPLE HORIZON 173
7.6.3 BALLYCASTLE: TAI 175
7.6.3.1 cMd SAMPLE HORIZON 175
7.6.3.2 BALLYCASTLE, NSD SAMPLE HORIZON 175
7.6.4 BALLYCASTLE: FLUORESCENCE 175
7.6.4.1 cMd SAMPLE HORIZON 175
7.6.4.2 NSD SAMPLE HORIZON 175

7.7 DISCUSSION 177
7.7.1 TAI 177
7.7.2 FLUORESCENCE 178

7.8 CONCLUSIONS 179

8 PALYNOFACIES 180

8.1 DEFINITIONS AND INTRODUCTION 180
8.1.1 DEFINITIONS 180
8.1.2 INTRODUCTION 180

8.2 THE SUBDIVISION OF ORGANIC MATTER 181

8.3 OBSERVED ORGANIC MATERIAL 184

8.4 CLASSIFICATION SCHEMES USED IN THIS WORK 194

8.5 PARTICLE COUNT 197

8.6 PALYNOFACIES RESULTS 197
8.6.1 CARRICKLECK BACKGROUND 197
8.6.2 BALLYCASTLE 201

8.7 THERMAL ALTERATION AND PALYNOFACIES 203
8.7.1 PARTICLE SIZE VARIATION 203
8.7.2 TRANSLUCENT WOODY MATERIAL 204
8.7.3 NON-WOODY PLANT DEBRIS 204
8.7.4 OPAQUE ORGANIC MATTER 205
8.7.5 PALYNOMORPHS 205

8.7.6 AOM 206
8.7.7 THE TERNARY PLOT OF TYSON (1995) AND PALYNOFACIES CHARACTERISATION 207

8.8 SUMMARY 219

8.9 DISCUSSION 219

8.10 CONCLUSIONS 220

9 THERMAL MODELLING 222

9.1 INTRODUCTION 222
9.1.1 THERMAL CONDUCTIVITY AND DIFFUSIVITY -TEMPERATURE DEPENDENT THERMAL PROPERTIES 222
9.1.1.1 FACTORS INFLUENCING CONDUCTIVITY (K) AND DIFFUSIVITY (k) 225
9.1.2 LATENT HEAT OF MAGMATIC CRYSTALLISATION 225
9.1.2.1 FACTORS INFLUENCING THE LATENT HEAT OF MAGMATIC CRYSTALLISATION 226

9.2 PROGRAMS FOR THE CONDUCTIVE COOLING OF DYKES WITH TEMPERATURE-DEPENDENT THERMAL PROPERTIES AND HEAT OF CRYSTALLISATION (after P.T. Delaney 1988) 226
9.2.1 INTRODUCTION 226
9.2.2 FOUR PROGRAMS; FIVE SOLUTIONS 227
9.2.3 THE WORKING MODEL 228

9.3 ASSUMPTIONS OF THE MODELS FOR THE NORTH STAR AND CARRICKLECK DYKES 231

9.4 INPUT DATA 231
9.4.1 INDIVIDUAL DATA INPUT AND EXPLANATION 231
9.4.1.1 AMBIENT TEMPERATURE OF HOST ROCK 231
BALLYCASTLE 232
9.4.1.2 TEMPERATURE OF INTRUDING MAGMA 232
CARRICKLECK 232
9.4.1.3 SOLIDUS TEMPERATURE 233
9.4.1.4 DYKE WIDTH 233
9.4.1.5 THERMAL PROPERTIES OF ROCKS 235

9.5 RESULTS 236
9.5.1 MODELLING THE CARRICKLECK DYKE 236
9.5.2 MODELLING THE NORTH STAR DYKE 238

9.6 DISCUSSION 242

9.7 CONCLUSIONS 245

10 CONCLUSIONS 246

BIBLIOGRAPHY 248

APPENDICES

APPENDIX I DATA TABLES

APPENDIX II VITRINITE REFLECTANCE HISTOGRAMS

APPENDIX III PLATES

APPENDIX IV PALYNO-DICTIONARY

LIST OF FIGURES

Figure 2.1 Palaeogeographic maps of Ireland in Viséan and Namurian times (after Ziegler 1990)..... 5

Figure 2.2 Palaeogeographic maps of Ireland (a) in the Tertiary (after Anderton et al. 1993), (b) Tertiary dyke swarms and volcanics in northeast Ireland (adapted after Emeleus and Preston 1969)..... 5

Figure 2.3 Generalised geology of the Ballycastle area (after Wilson and Robbie1966, Wilson 1972, Goodhue 1996 and Evans pers. comm. 2002)..... 9

Figure 2.4 The North Star Dyke (photograph courtesy of Dr. R. Goodhue) and a generalised log of the foreshore. Marked on the foreshore, the approximate positions of the 3 main sample horizons..... 10

Figure 2.5 Generalised geology of the Kingscourt Outlier (after Strogen et al. 1995, Fernandez 2000)13

Figure 2.6 The Carrickleck Dyke exposed in the face of the Carrickleck Quarry, intruding the Carrickleck Shales. Sample horizons CK and CQ are marked and a generalised log (after Fernandez 2000) and vitrinite profile (Fernandez 2000) are presented. The vitrinite profile illustrates a gradually increasing VR with depth, i.e. that the lithologies are free from the influence of the Barley Sill intruded geographically and stratigraphically higher (photograph courtesy of Dr. P. Fernandez)..... 14

Figure 3.1 Whole rock element oxide and trace element discrimination diagrams..... 21

Figure 3.2(a) Whole rock element oxide variation in the NSD horizon and in the North Star Dyke samples IG1 and IG3. NOTE: Y-axis is on a logarithimic scale..... 22

Figure 3.2(b) Whole rock element oxide variation in the CK horizon and data from the Carrickleck Dyke. NOTE: Y-axis is on a logarithmic scale..... 22

Figure 4.1 Chemical evolution of coalification with respect to volatile matter (dry ash free), atomic ratio H/C, carbon dry ash free content and hydrogen. This is presented relative to coal rank, hydrocarbon fluids and vitrinite reflectance (compiled from Teichmüller 1987, Taylor et al. 1998).... 24

Figure 4.2 Increasing aromatisation, resulting in condensation and ordering of aromatic units parallel to bedding plane during coalification of vitrinite. After Teichmüller and Teichmüller 1984 in Taylor et al. 1998, Teichmüller 1987, Stach et al. 1982..... 27

Figure 4.3 Basin maturity chart showing correlation of metamorphic zone, depth, temperature, vitrinite reflectance, hydrocarbon zones and coal rank (after Merriman 1999)..... 28

Figure 4.4 The course of isorank lines. (a) pre-orogenic lines tend to run parallel to bedding, (b) syn-orogenic coalification they tend to lie obliquely and (c) post-orogenic they are lying horizontally, if the lithological column was buried and the original reflectance values were overprinted (after Stach et al. 1982). 29

Figure 4.5 The vitrinite indicatrix, represented by an ellipsoid with three rectangular axes, the length of these axes being proportional to the refractive index of any beam vibrating parallel to it (i.e. travelling perpendicular to it). Here they are labelled a, b and c; where a represents the minimum refractive index and the fast ray (R_{min}), c represents the maximum refractive index and the slow ray (R_{max}) and b represents the intermediate ray perpendicular to the a-c plane 30

Figure 4.6 Relationship between increasing R_{min} and R_{max} and R_{max} and R_r 31

Figure 4.7 Modification of Karweil's (1955) plot of burial time and temperatures versus volatile matter in coal. Volatile matter is shown on the upper part of top the horizontal line, vitrinite reflectance on the lower part of the top horizontal line. Numbers on curves are burial times in millions of years. Burial temperature scale, in degrees C, is on left side of figure. Volatile matter values converted to vitrinite reflectance values based on Stach et al. (1982). Karweil's original curves are from 10 - 300 million year burial times and as they are a simple repeating logarithmic function, the curves were extrapolated to lower vitrinite reflectance values for shorter burial times after a R_o value of 0.28% at 20°C for an assumed burial time of 100,000yrs. The vitrinite reflectance value of 5.0%R_r and volatile matter values of 3 and 4 % are from Bostick (1979), (after Price 1983). 35

Figure 4.8 The relationship between LOM and effective heating time of Hood et al 1974 (in Hood et al. 1975) 35

Figure 4.9 Vitrinite reflectance profile through the CK horizon in the Carrickleck Dyke aureole and relative coal rank. 45

Figure 4.10 Locality map for the disused Gobb Colliery and coal samples Cl9 to Cl16 (section adapted from Sheet 5 of the Ordnance Survey of Northern Ireland) and simplified log of the Gobb Colliery section (after Evans 1998, pers. comm..) Vitrinite reflectance profile for the Gobb section in the Ballycastle area 47

Figure 4.11 VR profiles and relative coal rank through the NSD, cMd and BC horizons in the North Star Dyke aureole 49

Figure 4.12 Compilation of temperature profiles from the CK horizon in the Carrickleck aureole; BC, cMd and NSD horizons in the North Star Dyke aureole using the temperature conversion of Barker and Pawlewicz (1986) 52

Figure 4.13 Compilation of temperature profiles from the CK horizon in the Carrickleck aureole; BC, cMd and NSD horizons in the North Star Dyke aureole using the temperature conversion of Barker (1988) 53

Figure 4.14 Compilation of temperature profiles from the CK horizon in the Carrickleck aureole; BC, cMd and NSD horizons in the North Star Dyke aureole using the temperature conversion of Barker and Goldstein (1990) 54

Figure 5.1 An assemblage of 2 tetrahedral sheets sandwiching an octahedral sheet, representing the 2:1 clay mineral. 62

Figure 5.4 Contrasting views of illite 'crystallite' material. (a) 3-D schematic of illite and chlorite crystallites containing various types of lattice imperfection 'observed' in lattice-fringe images (after Warr and Nieto 1998); (b) the 2-D representation of the I/S crystallite shown as either a MacEwan crystallite or as a stack of fundamental particles (modified from Altaner and Bethke 1988, Altaner et al. 1988, Moore and Reynolds 1997) 92

Figure 5.5 Best Mean size for the CK and CQ horizons in the aureole of the Carrickleck dyke. Note that the profiles might be described as having a similar pattern over the length of the aureole that they both cover. 95

Figure 5.7 Comparison of the MUDMASTER Best Mean crystallite Size (BMS) results for illite in the CK and CQ horizons with the illite and kaolinite intensity profiles 101

Figure 6.1 Revised scheme for the classification of sporites after Smith and Butterworth (1967) modified after Dettmann (1963) 107

Figure 6.2 NSD horizon palynological age/biozone. 158

Figure 6.3 Spore genus assemblage variation in the NSD horizon. 159

Figure 6.4 Assemblage variation and the effect on palynostratigraphic recognition 160

Figure 7.1 Scales and correlation charts/reviews of various authors; correlated using vitrinite reflectance. 163

Figure 7.2 Spores/pollen exine coloration with geothermal maturation (coalification). TAI=Thermal Alteration Index, a scale based on vitrinite reflectance measured by reflected light under oil. Fluorescence refers to the tendency of exines to fluoresce (visible light when exposed ultraviolet light).

Exine is the coal maceral consisting of exines; vitrinite is a maceral of woody or similar plant origin. Compiled from Traverse (1988) and Pearsons colour chart issued by Phillips (1984). 164

Figure 7.3 Fluorescence energy exchange..... 166

Figure 7.4 The fading effect observed by van Gijzel after 30 minutes exposure to fluorescent light: (a) the fluorescence of the mineral bituminous groundmass' of oil-source rocks. Fading is positive (maximum wavelength shortens/intensity increases) in immature sediments, but negative (longer wavelength/decrease in intensity) within the 'Oil window' until fluorescence is lost at ca. 1.2%.(b) the fading effect observed for spore fluorescence. Fading is positive (shorter maximum wavelength/increase in intensity) at all stages of thermal maturation until fluorescence is lost (c. 1.2% R_r). (From McPhilemy 1989; after van Gijzel 1982) 169

Figure 7.5 Spore TAI and fluorescence in the CK horizon of the Carrickleck Dyke aureole; plus the 'predicted' fluorescence quenching point, based on vitrinite reflectance..... 172

Figure 7.6 (i) The fading effect after 30 minutes exposure to fluorescent light:(a) on spore fluorescence in the CK sample horizon and on AOM in the CQ sample horizon. Fading is negative (decrease in intensity, but no visible change in wavelength). Observed from samples recording 1.03 -1.10%Rr to 1.46%Rr until fluorescence is lost 1.40/1.49% Rr. (b) on AOM fluorescence in the cMd sample horizon. Fading is positive and observed in samples up to cMd6 (VR=0.94%Rr) 173

Figure 7.6 (ii) investigating the fading effect in: (a) CK29, (Lycospora sp.), (b) CQ3.0 (AOM particle), (c) cMd8, (Densospora sp.) (d) NSD 24 (unidentified spore) Images acquired after 1 minute, 10 minutes, 20 minutes and 30 minutes. (a) and (b) both exhibit negative fading, which has taken full effect within the first 5 minutes of exposure. (c) and (d) show positive fading (mild), which is strongest after 30 minutes..... 174

Figure 7.7 Spore TAI and fluorescence extinction and predicted fluorescence extinction (based on vitrinite reflectance) recorded in the NSD and cMd horizons of the North Star Dyke aureole..... 176

Figure 8.1 Examples of the different morphologies exhibited by woody tissue, after Tyson (1995)... 185

Figure 8.2 Schematic representation of leaf, cuticle (Teichmüller 1982) and cuticle cellular patterns (after Tyson 1995)..... 187

Figure 8.3 Morphological classification of microforaminiferal linings (after Stancliffe 1985) 189

Figure 8.4 Examples of the basic spore morphologies (outline seen in polar view) and the various germinal opening marks 190

Figure 8.5 The reaction of hylogen, melanogen, phyrogen and amorphogen to heating. Adapted from Bujak et al. 1977 after Bayliss 1974, 1975 195

Figure 8.6 Ternary AOM-Phytoclast-palynomorph plot (after Tyson 1993, 1995) 195

Figure 8.7 Background palynofacies in the (a) CQ and (b) CK horizons in the Carrickleck quarry.... 199

Figure 8.8 Background palynofacies characterisation (Tyson 1995) for the (a) CK and (b) CQ horizons from the Carrickleck Quarry, and the (c) NSD and (d) cMd horizons from Ballycastle 200

Figure 8.9 Background palynofacies at Ballycastle (a) cMd horizon and (b) the NSD horizon 202

Figure 8.10 Organic matter particle size variation in the Carrickleck Dyke and North Star Dyke aureoles 208

Figure 8.11(i) Translucent woody material content and size variation in the Carrickleck Dyke aureole 209

Figure 8.11(ii) Translucent woody material content and size variation in the North Star Dyke aureole 210

Figure 8.12 Non-woody plant content and size variation in the Carrickleck and North Star Dyke aureoles 211

Figure 8.13 AOM content and size variation in the Carrickleck Dyke and North Star Dyke aureoles 212

Figure 8.14(i) Palynomorph and OOM content and size variation in the Carrickleck Dyke aureole... 213

Figure 8.14(ii) palynomorph and OOM content and size variation in the North Star Dyke aureole.... 214

Figure 8.15 (i) Palynofacies variation in the Carrickleck Dyke aureole (a) CQ horizon (b) the CK horizon 215

Figure 8.15 (ii) Palynofacies variation in the North Star Dyke aureole (a) cMd horizon (b) NSD horizon 216

Figure 8.16 (i) Samples through the Carrickleck Dyke aureole plotted on the ternary plot of Tyson (1995). (a) the CK horizon; (b) the CQ horizon 217

Figure 8.16 (ii) samples through the North Star Dyke aureole plotted on the Ternary plot of Tyson (1995). (a) the NSD horizon (b) the cMd horizon 218

Figure 9.1 Variation of thermal diffusivity and conductivity with temperature for different lithologies (after Delaney 1987, 1988, data from Touloukian et al. 1981) 224

Figure 9.2 (a) Ternary phase diagram for the Albite-Anorthite-Diopside system at 1bar (Bowen 1915). A ternary system contains three binary systems: (b) Albite-Anorthite phase diagram, (c) Anorthite-Diopside phase diagram, and (d) Diopside-Albite phase diagram. 234

Figure 9.3 Modelled T_{max} and VR estimated temperature from the CK horizon in the Carrickleck dyke aureole. VR estimated temperatures beyond the aureole are expected to exceed those of the model as it has been assumed that maximum burial occurred in the Late Carboniferous. 236

Figure 9.4 Modelled Temperature (T) profiles at selected time intervals the Carrickleck dyke aureole with VR estimated temperatures from the CK horizon. 237

Figure 9.5 The thermal evolution through time of the dyke centre (-0.75m), the contact (0m) and some points in the Carrickleck Dyke aureole 237

Figure 9.6(i) Modelled Temperature (T) profiles for the North Star Dyke aureole with VR estimated temperatures from the BC, cMd and NSD horizons. Assumed ambient temperature of host rocks (a) 24°C, (b) 37°C, and (c) 56°C. Profiles representing temperatures through the aureole at points in time (where the time is represented in days) 239

Figure 9.6(ii) Modelled Temperature (T) profiles for the North Star Dyke aureole with VR estimated temperatures from the BC, cMd and NSD horizons. Assumed ambient temperature of host rocks (d) 86, (e) 102°C, and (f) 148°C. Profiles representing temperatures through the aureole at points in time (where the time is represented in days) 240

Figure 9.7 Modelled T_{max} profiles in the North Star Dyke aureole based on the various estimated ambient temperatures of host rock at time of intrusion. VR estimated temperatures from the NSD, BC, cMd horizons 241

Figure 9.8 Four models of Barker (1998) describing four styles of heat transfer after the intrusion of a dyke. SIMPLE CONDUCTIVE – after intrusion pore water does not vaporise and is assumed to have negligible effect as a heat sink. COMPLEX CONDUCTIVE – after intrusion, pore water is assumed to absorb heat and vaporise. INCIPIENT CONVECTION – rapid cooling of the dyke after intrusion causes a rise of heated fluids near the dyke without the development of a recharge system.

CONVECTION CELL – after intrusion a convection cell featuring the buoyant rise of heated fluids next to the dyke and recharge to the cooled fluids away from the dyke..... 244

LIST OF TABLES

Table 4.1 The relative terms of coalification, maturity and metamorphism with approximate range in vitrinite reflectance 25

Table 4.2 Subdivision of the maceral group vitrinite after the ICCP system 1998. 26

Table 4.3 Reflectance standards used in this study 41

Table 4.3 Calculated background and maximum temperatures calculated for each horizon after Barker and Pawlewicz (1986), Barker (1988) and Barker and Goldstein (1991), where θ is the temperature and the subscript $_{BG}$ refers to Background, $_{max}$ to maximum, $_{c}$ to contact; T_{peak} refers to the maximum temperature calculated from the vitrinite reflectance values using the methods of the authors named above 51

Table 5.1 The classification of clay phyllosilicates (from Moore and Reynolds 1997, based on Hower and Mowatt 1966, Bailey 1980, Brindley 1981 and Środoń 1984). z=charge per formula unit. 64

Table 5.2 the maximum and minimum recorded values, and respective sample numbers for the best mean crystallite size, calculated by the MUDMASTER software for each of the samples horizons. 94

Table 8.1 Comparison of selected palynofacies schemes 183

Table 8.2 Description and classification of organic materials observed in palynological preparations of this work. 193

Table 8.3 Comparative uses of the four main categories used by Burgess (1974) and Bujak et al. (1977) 194

Table 8.4 Organised comparison between categories of count scheme in this work and the scheme of Bujak et al. (1977) and Tyson (1995) 196

Table 9.2 'Basic' sample input data for analytical and/or numerical model solutions 229

Table 9.3 The effect of varying test parameters. wnen = whole time numerical solutions; θ_{ci}=initial contact temperature; θ_c = contact temperature; basic solution is the solution for the parameters cited in Table 9.2 230

1 AIMS AND OBJECTIVES

1.1 AIMS

The estimation of the thermal maturity of source rock using organic indicators is widely practised. Considerable uncertainty exists concerning the relative importance of temperature and time in the complex reactions involved in the 'maturation' of organic matter in sedimentary rocks and on the associated changes in clay mineralogy. The principal objectives of this project are to (1) investigate the changes exhibited by the various maturity indicators that can be used to determine peak palaeotemperatures attained by sedimentary rocks in a dyke aureole, (2) to use computer modelling to determine theoretical time-temperature distributions through the dyke aureoles and (3) to compare the results of the maturity indicators with those of the theoretical model.

1.2 PREVIOUS WORK

Previous work carried out in dyke aureole settings has recorded the rapid response of vitrinite reflectance, (VR), (Bishop and Abbott 1995, Goodhue 1996, McCormack 1998), spore colour and spore fluorescence (Goodhue 1996). In some cases clay crystallinity and mineralogy (Esposito and Whitney 1995, McCormack 1998) and Total Organic Content, (TOC), (Bishop and Abbott 1995, Goodhue and Clayton 1998) were also examined. These studies have taken in a variety of stratigraphic horizons *e.g.* Carboniferous, Jurassic and Tertiary country rock intruded by igneous Tertiary dykes or sills. McCormack (1998) concluded from his study that the response rate of VR is in the order of tens of years and is not a cumulative response, i.e. once established the reflectance can only be modified by exposure to a higher temperature. Bishop and Abbott (1995) and Goodhue (1996) observed a general reduction in TOC with proximity to the dyke, and also recorded a maximum TOC at approximately 50% dyke thickness in the country rock. The work of Esposito and Whitney (1995) looked at the effects of thin igneous intrusions on the diagenetic reactions in Tertiary rocks. It recorded a decrease in illite/smectite expandability with proximity to the intrusion, a decrease in kaolinite as chlorite increased and the increased replacement of carbonates. The study also recorded that VR (from coals) although locally affected does not react to the intrusions on a regional scale, even where that study was concerned with large bodied sills (thicknesses of 4 - 26m).

Computer modelling of the temperature distributions through dyke aureoles, undertaken by Bishop and Abbott (1995), Goodhue (1996) and McCormack (1998) have all predicted

curves that are similar to that recorded by VR, but that predict higher temperatures than those calculated from the VR.

1.3 THESIS FRAMEWORK

In chapter two both background geology and detailed geology for each of the sample localities are discussed along with sampling strategy.

Chapter three considers the lithology and geochemistry of both dykes and the geochemistry of the host rocks.

Chapter four deals with vitrinite and vitrinite reflectance, theory and results. Here the concepts of 'maturation' and 'coalification' are considered and the concept of time and temperature and their effect on vitrinite reflectance and influence on thermal modelling are discussed. Sample results from the aureoles of each horizon are presented and these results are discussed.

Chapter five examines clays and other minerals identified in the samples using X-ray diffraction methods. The concept of clay mineralogy as an indicator of metamorphic conditions is discussed. Sample results are presented and discussed. 'MUDMASTER a program for calculating crystallite size distributions and strain from the shapes of X-ray diffraction peaks'(Eberl *et al.* 1996), was used in an attempt to study illite crystallite best mean size distribution through the aureoles. Sample results and discussion are presented at the end of the chapter.

Chapter six presents systematic palynological results for one of the mudrock horizons from Ballycastle. Systematic palynology was used to accurately date the horizon. The destruction of the spore range through this horizon in the dyke aureole was also recorded and discussed.

Chapter seven records the reaction of spore colour and fluorescence at both localities. The results are presented and discussed and also related to vitrinite reflectance results.

Chapter eight deals with the changes in palynofacies assemblages for each of the sampled horizons. Changes observed in each horizon as the dyke is approached are discussed in detail and compared. Results and discussion are presented.

Chapter nine presents a thermal model based on the work of Delaney (1987, 1988). The theoretical heat flow and maximum temperature curve through the dyke aureole was calculated for each setting. These results are compared to those attained through the study of the vitrinite reflectance in the horizon samples.

Chapter ten contains final conclusions and discussion of this work.

2 GEOLOGY AND SAMPLING STRATEGY

2.1 REGIONAL GEOLOGY

2.1.1 IRELAND IN THE MISSISSIPPIAN (LOWER CARBONIFEROUS) (Metcalfe 1997, Menning *et al.* 2000)

The Carboniferous can be split into two divisions the Mississippian (Lower Carboniferous) and Pennsylvanian (Upper Carboniferous) (Metcalfe 1997, Menning *et al.* 2000). It is the Mississippian division that is addressed in this section. Carbonate rocks dominate much of the Irish Mississippian. Towards the top of the Irish Mississippian increasing amounts of terrigenous mudstone and sandstone are observed.

A northwards transgression marked the beginning of the Carboniferous, covering the south and the Irish midlands and encroaching on the northern area of Ireland. At this time Ireland was in tropical latitudes, and as the sea transgressed, shallow water carbonate shelf deposition became common over much of the midlands area, with the development of localised deeper water sedimentation in the disconnected basins such as the Shannon Basin and the Dublin Basin. In the south, the South Munster Basin also developed deeper water sedimentation. Meanwhile, in the north sedimentation was that of carbonates and mixed terrigenous sediments. The Shannon and Dublin basins of the early Carboniferous contain lithofacies similar to that seen in the midlands but in greater thicknesses. By the Viséan the transgression had extended the area of marine deposition, and deeper water basins developed, with bounding shallow shelves, thus creating a greater contrast in accumulating sediments (see figure 2.1). The northwest region was experiencing fluviatile deposition in the Viséan, while in the northeast, north of the Lower Palaeozoic Longford - Down inlier, Viséan deposition is thought to have been dominated by fault controlled differential subsidence, reflected in major changes in facies and thicknesses. The northern extent of the margin is thought to have been close to marine deposition from the Viséan onwards. By the end of the Viséan, marine sedimentation was dominant across the entire region. The end of the early Carboniferous, the beginning of the Namurian, sees a switch to dominantly terrigenous rocks, with some few limestones and coals. This is a diachronous transition, which came with the development of large broad river systems, probably as a consequence of uplift.

There is evidence of early Carboniferous volcanics. Tournaisian tuffs of unknown source and Viséan volcanics related to volcanic centres seen in Munster are found in Cork and the Limerick volcanic region. There are also tuff layers and agglomerates seen in the Dublin Basin and Northern Ireland. (The information for this section was acquired from

Sevastopulo 1981, Sevastopulo and Wyse-Jackson 2001, and to a lesser extent Anderton *et al.* 1993. For Carboniferous palaeogeographic maps, after Ziegler 1990, see figure 2.1).

2.1.2 IRELAND AND THE TERTIARY VOLCANICS AND IRELAND

Much of northwestern Europe experienced tectonic activity during the Tertiary, namely by the opening of the Atlantic Ocean in the north and Alpine tectonics to the south. The siting and timing of the extensive volcanism, which characterises the British Tertiary Volcanic Province, are linked to the opening of the North Atlantic Ocean. Northeast Ireland was on the southern most extent of the British Tertiary Volcanic Province (Wilson and Robbie 1966). The end Cretaceous saw a period of widespread uplift and denudation (Wilson and Manning 1978), but while the southeast of Britain became inundated by the return of shallow marine conditions (Richey 1961), the northwest experienced the onset of extensive volcanic activity. In northeast Ireland basalt lavas poured out over the land surface in a series of eruptions, with inter basaltic horizons recognised in north Antrim (Wilson 1972). Following the basaltic lavas came acid magmas, some explosively breaking the surface, while others remained confined by sediments (Richey 1961). Late in the volcanic history, the intrusion of vast masses of basic rock, as sills and laccoliths occurred. "Tensional cracks in the crust gave lines of weakness along which vertical sheets of basalt welled up to form dykes, often in swarms aligned northwest, which converged on the major foci of the plutonic centres, such as the Mournes and Slieve Gullion" (Wilson 1972). Consequently, there are many dykes in the northern half of Ireland, although unlike the Tertiary Igneous of Scotland, they are not closely associated with a volcanic centre (Preston 1981, Mussett *et al.* 1988). They are commonly relatively narrow (0 - 15m) and have been interpreted as flash injections *i.e.* swift, single intrusive events, intruded at the end of the igneous process. However there are some older feeders, which are usually wider (up to km scale). Over 300 dykes are known in the Belfast area alone, indicating a crustal stretch of up to 4%.

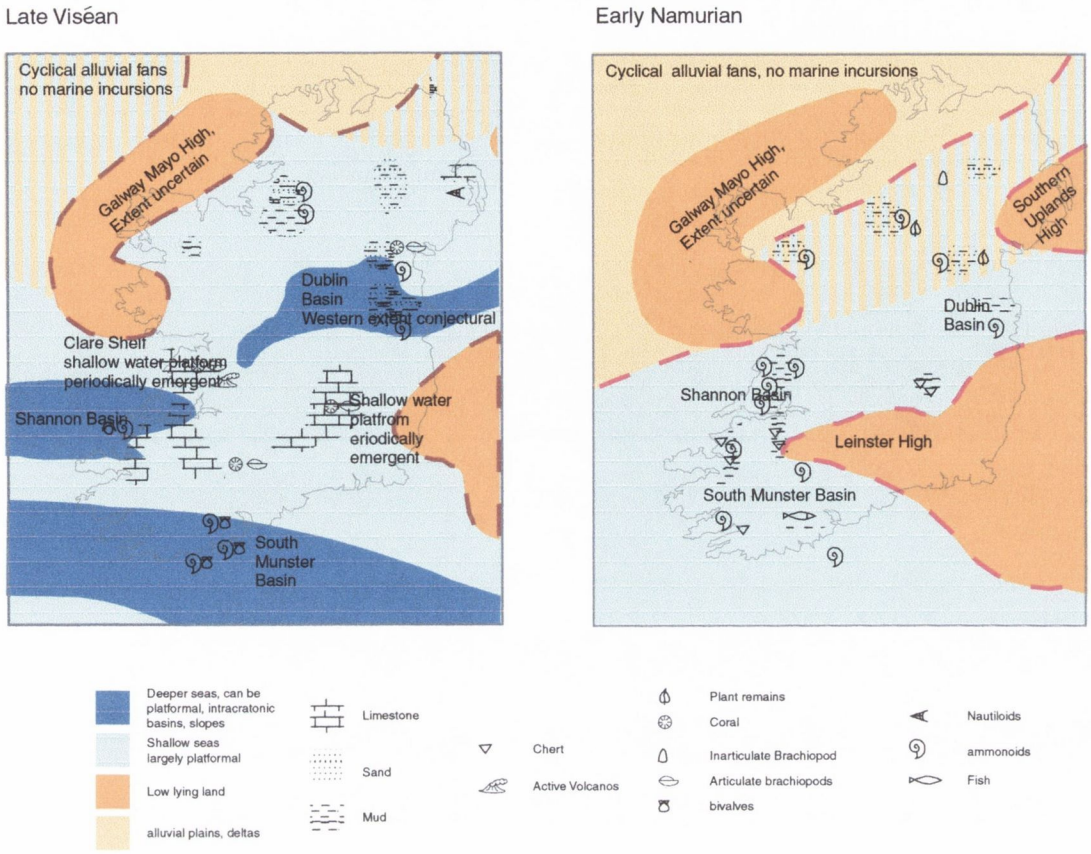

Figure 2.1 Ireland in Vis an and Namurian times (after Ziegler, 1990)

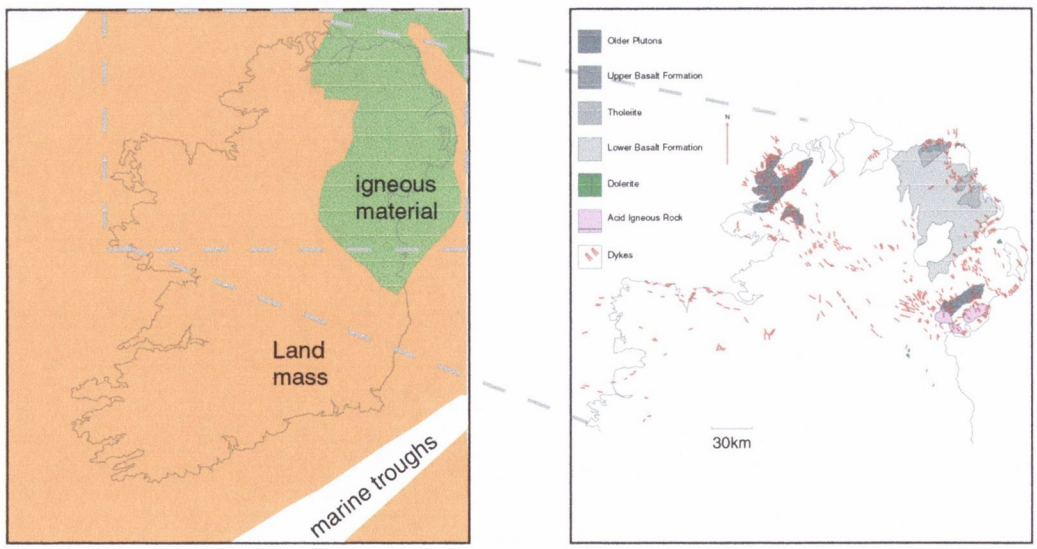

Figure 2.2 (a) Ireland in the Tertiary (after Anderton et al. 1993), (b) Tertiary dyke swarms and volcanics in North East Ireland (adapted after Emeleus and Preston 1969)

2.2 GEOLOGICAL BACKGROUND AND SETTING

2.2.1 BALLYCASTLE

2.2.1.1 GENERAL GEOLOGY

Ballycastle is situated on the northern coast of County Antrim. In general the area is one of moderate relief with a long and steep coastline. The area that this study focuses on is one dominated by Carboniferous sedimentary lithologies and Tertiary igneous rocks (see figure 2.3). The Carboniferous rocks form a conformable sequence of 600 - 700m (Wilson and Robbie 1966, Wilson 1972), of mixed marine and non-marine strata. The lower 550m of the section is Viséan and the upper 100 - 150 m, lower Namurian (Whitaker and Butterworth 1978). The lower part of the succession is represented by basaltic lavas, which overlie conglomerates, arenaceous sandstones and nodular limestones, all of which rest unconformably on Dalradian metasediments (Wilson and Robbie 1966). The lavas are followed by a series of interbedded tuffs and mudstones, followed by arenites and argillites, which contain several coal seams and a number of marine and non-marine fossiliferous horizons. The beginning of the Upper Carboniferous is marked by the Main Coal, and the succession displays marine and continental lithologies.

The Ballycastle Carboniferous succession has been compared to the Scottish Carboniferous outlier in Kintyre by Robbie and Wilson (1966), Wilson (1972), and Whitaker and Butterworth (1978). Although precise correlation is difficult, it is proposed that the successions are sufficiently similar to correlate (Wilson and Robbie 1966). Whitaker and Butterworth (1978) have used palynological evidence to suggest that the miospore assemblage up to the Main Coal is comparable to that of the P1 and P2 zones described from elsewhere in the British Isles. They have also compared the assemblage to those recorded by Sullivan and Marshall (1966) from the Upper Sedimentary Group of Ayrshire and from the 'Yoredale Series' of the Roman Wall district of Northumberland of Marshall and Williams (1970).

The Tow Valley Fault is the largest fault in the Ballycastle area, trending NNE - SSW and down-throwing Cretaceous chalk and Tertiary basalt against Carboniferous and Dalradian 'basement'. The E-W trending Great Gaw Fault downthrows Carboniferous rocks to the north in an oblique slip, normal fault movement, and terminates against the Tow valley Fault. There are also a number of smaller NNW-SSE trending faults.

The Tertiary basalts are bounded by the northern margin of the Tow Valley Fault west of Ballycastle, however there is also much evidence of Tertiary igneous activity to the east

of the town of Ballycastle in the form of sills and dykes. The most imposing intrusion is the Fair Head sill that caps a headland (Fair Head) to the east of Ballycastle. It has a maximum thickness of 82m and thins to the southeast and west. The olivine dolerite sill has intruded Carboniferous sediments. The Gobb sill, capping workings of the (disused) Gobb Colliery, is another large coarse olivine dolerite sill, east of Ballycastle. It shows similar although not so well developed columnar jointing to the Fair Head Sill.

2.2.1.2 DYKE AND SETTING

The North Star Dyke outcrops on the foreshore below the road east of the North Star Colliery. It is a 4m wide, Tertiary, olivine dolerite dyke, which has been associated with the north Antrim and Down dyke swarm (NNW trend) (see figure 2.3). The intrusion dips steeply to the west at *c.* 85., trending *c.* 346.. The dyke is a, *c.* 4m wide, composite of three intrusions, the first, intruded by the second, which was in turn, intruded by the third (3.1m, 0.6m and 0.3m, oldest to youngest, outer to inner). The first and widest of the intrusions has chilled margins of up to 16cm, seen as a finer grained doleritic selvage. The secondary and tertiary intrusions, are much narrower, and show very fine chilled margins, with strong jointing perpendicular and parallel to the contacts. Petrological evidence shows some slight compositional variation between the outermost chilled margin and the inner sections of the dyke.

The sediments on the foreshore are late Viséan to early Namurian in age and dip at the shallow angle of *c.* 08. to the SSW. The rock exposed on the foreshore represents a deepening sequence of marine and brackish facies. The section represents a 'coarsening up' sequence. The top of the sequence is represented by silty beds, finely laminated towards the top, interbedded with coal-lense bearing mudstones; these are preceded by a mudstone unit with lenses of shelly material and very fine sands; below this are more mudstone horizons, massive, each capped by a concentration of shelly debris. Towards the bottom is a thin limestone horizon rich in shelly fossiliferous material, such as ostracod and gastropod debris. The bottom of the sequence is a mudstone horizon with concretions (see figure 2.4). Palynological analyses suggests that these rocks were formed near the end Mississippian, straddling the Viséan-Namurian boundary, in the NC palynomorph zone. One valve of a *Posidoniella* sp. was recovered from just below one of the sampled mudstone horizons. The presence of this flaky, fragile, fossil implies very quiet depositional conditions. The absence of laminations and other sedimentological

structures in these mudrocks with the concentration of shelly indeterminate material towards the top of beds might indicate substantial bioturbation.

The Gobb Sill caps a cliff ESE of the North Star Dyke. The Tertiary sill has a maximum thickness of *c.* 20m and is intruded into shales below the Hawkes Nest Coal. It is the closest, exposed igneous body to the North Star Dyke and the possibility of its overprinting or interfering with the thermal affect of the North Star Dyke has been investigated and discounted in this work (see chapter 4).

2.2.2 CARRICKLECK AND THE KINGSCOURT OUTLIER

2.2.2.1 GENERAL GEOLOGY

Kingscourt is located in east central Ireland within the Longford - Down Massif (see figure 2.5). The area is a flat lying region of low hills where relief rarely exceeds 150m. The Kingscourt Outlier is a Carboniferous - Permo-Triassic outlier, surrounded by Lower Palaeozoic rocks and faulted to the west and north with an unconformable boundary east and south. The outlier extends 30km north to south and 25km east to west. Jackson (1955, 1965) described an almost complete, if condensed, succession of Namurian rocks overlain by a thin sequence of Langsettian, (Westphalian A), sediments. Upper Permian and Lower Triassic rocks rest unconformably on Carboniferous sediments close to the Kingscourt Fault. Although positioned within the Longford - Down Massif, the Kingscourt Outlier is considered to be an integral part of the Dublin Basin succession (Strogen *et al.* 1995, Fernandez 2000).

The most complete Irish Carboniferous succession is observed in the Kingscourt Outlier. During its deposition, the Kingscourt Outlier was on the northern margin of the Dublin Basin (Fernandez 2000). Upper Viséan, shelf limestones (Pickard and Jones 1992), were progressively overlapped in a northwards direction, by Pendleian, black shales and sandstones and the Arnsbergian, Carrickleck sandstones (Jackson1965). This is thought to be the result of the southwards progradation of deltaic systems. The Carrickleck sandstone is followed by the Carrickleck shale (sampled horizons are from this formation), which is succeeded by sandstone dominated 'grits', with shale intervals (Chokierian-Kinderscoutian). The development of repeated cyclothemic sequences is observed, typically with marine bands at the base and coarse grained capping sandstones. There are also examples of fireclays at the top of some of the earlier sequences. The last of the cyclothems, with the Cabra Shale at its base and topped by the Cabra Sandstone, is overlain by the *Gastrioceras cumbriense* marine band, followed by siltstones

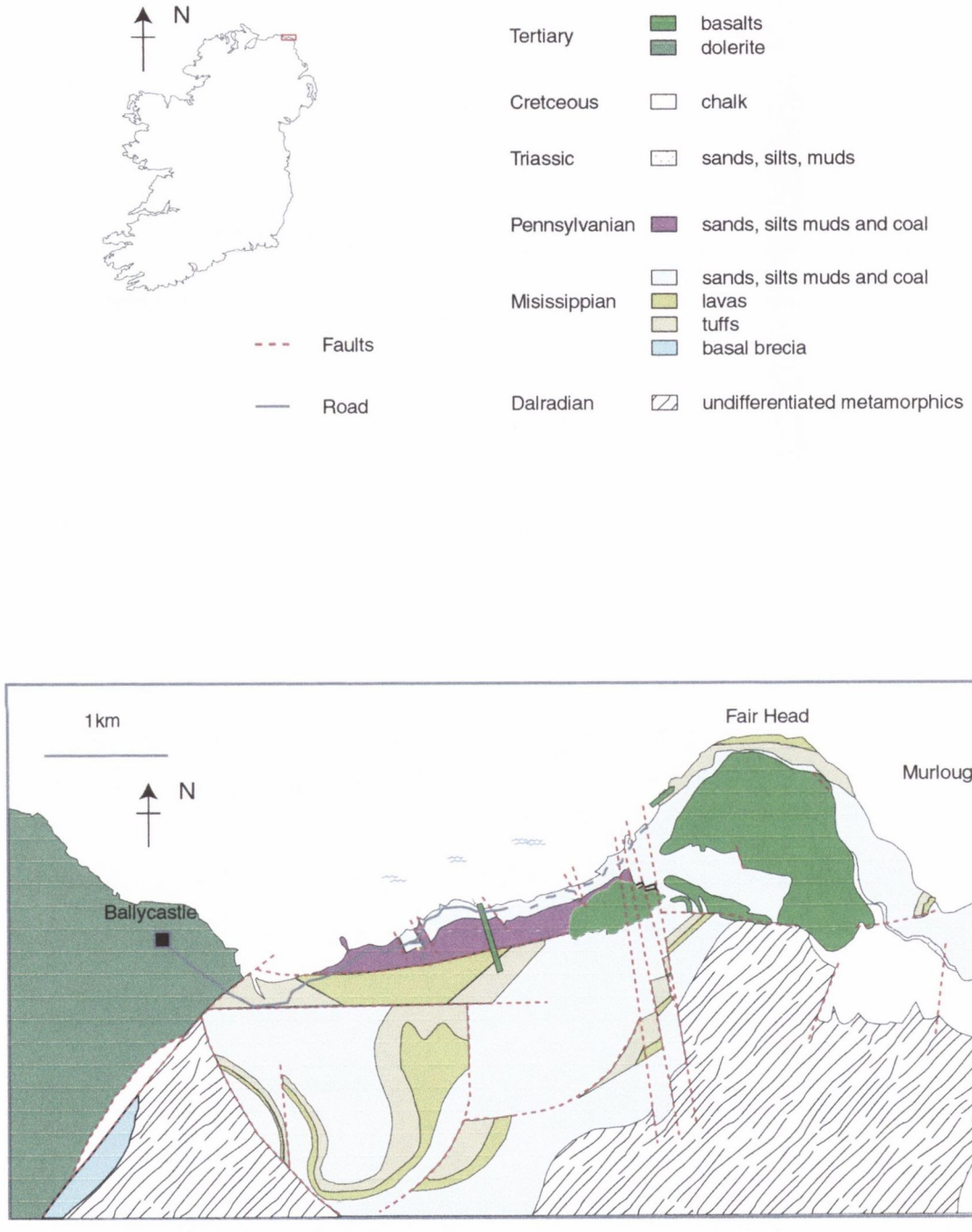

Figure 2.3 Generalised geology of the Ballycastle area (after Wilson and Robbie1966, Wilson 1972, Goodhue 1996 and Evans pers. comm. 2002)

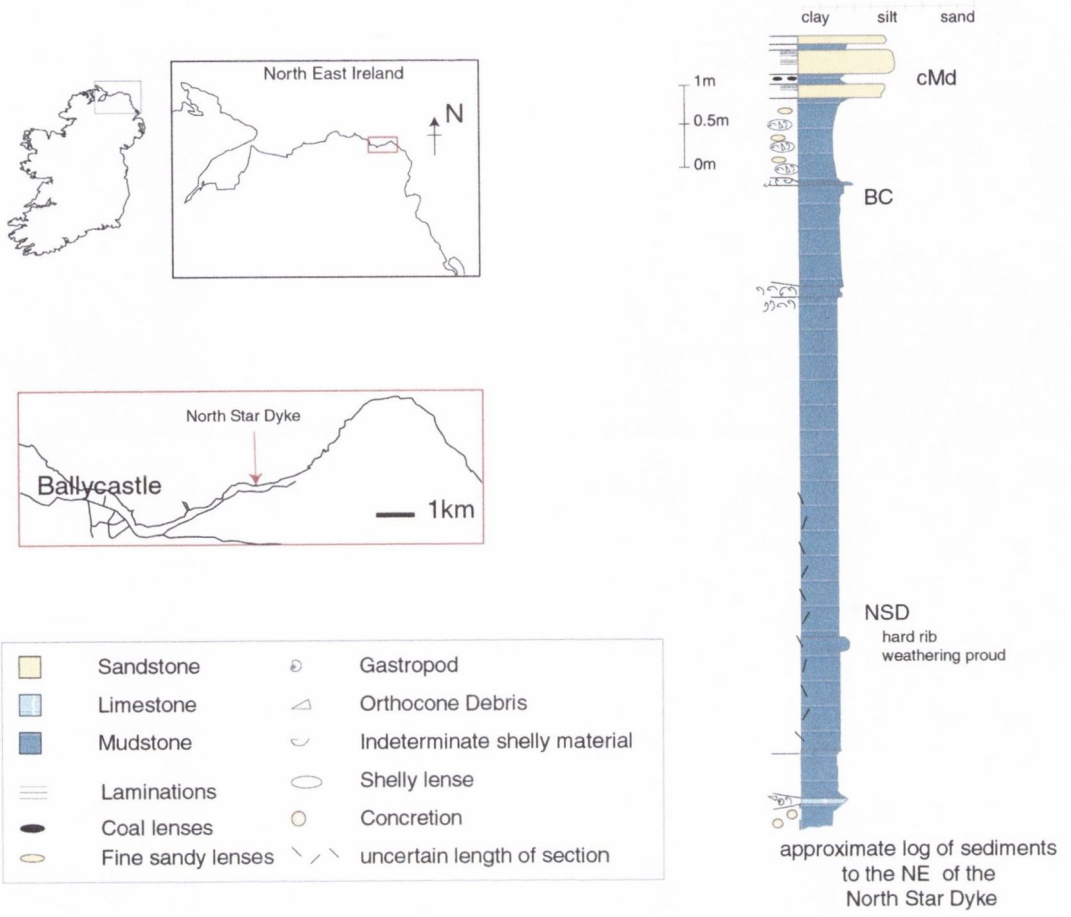

Figure 2.4 The North Star Dyke (photograph courtesy of Dr. R. Goodhue) and a generalised log of the foreshore. Marked on the foreshore, the approximate positions of the 3 main sample horizons.

and fine grained sandstones passing upwards into the Westphalian (Jackson 1965, Fernandez 2000). Red conglomerates and sandstones of the Late Permian lie unconformably atop the Langsettian (Visscher 1971) sedimentary lithologies, which consist of dark shales, thin laminated sandstones and siltstones and some thin coals (Fernandez 2000).

The Permo-Carboniferous lithologies of the Kingscourt Outlier are cut by the Donegal - Kingscourt dyke swarm, which includes dykes trending northwest to southeast and is linked to a major phase of extensional tectonics *c.*60Ma (Macintyre *et al.* 1975). New K-Ar ages for dolerite intrusions in County Fermanagh, considered to be a part of this swarm, have yielded an older age of *c.*69Ma (Johnston and Rundle 1993). This would imply that at least some of the dyke swarm is related to a Late Cretaceous volcanic centre. Mussett *et al.* (1988) have shown that the main period of onshore volcanic and igneous activity in northeast Ireland was during the Palaeogene and it is therefore assumed here that the Carrickleck Dyke is Palaeogene in age.

2.2.2.2 DYKE AND SETTING

The Carrickleck Quarry is situated on the east-southeast side of the Kingscourt Outlier (see figure 2.5). The Carrickleck Dyke outcrops in the disused quarry [approximate Grid Reference 282 500, 290 000]. The quarry floor is the top of the Carrickleck Sandstone, while the quarry face is composed of the Carrickleck Shale Formation, a succession of early Namurian (Arnsbergian), shallowing silty, muddy sediments deposited in a deltaic environment of fluctuating marine and brackish waters. The outcropping mudrock units show two characteristic groupings. Unit A appears massive and has a blocky fracture, while Unit B is darker, more fissile, with a stronger tendency towards a laminate structure. Units A and B are repeated twice in the quarry face (see figure 2.6). The lower Unit A (A1), has pyrite nodules, not observed in the upper Unit A (A2), although much of unit A2 is inaccessible. There are also some macrofossils observed in A1, namely gastropods and bivalves. Unit B is characterised by siderite concretions near the base, and a calcareous component. Macrofossils present include brachiopods, goniatites and *Posidonia* sp. (Fernandez 2000). The quarry face unfortunately acts as a conduit for runoff waters for some of the upland to the northwest, so that Unit B particularly can be quite 'grubby'. The rocks have a relatively low dip of 10. to the north.

These units describe a transgressive trend, where units A1 and A2, lacking typical marine fossils, represent brackish depositional conditions and units B1 and B2 indicate marine

conditions (Fernandez 2000). These units can also be characterised by their clay mineralogy where the brackish units A1 and A2 typically have expandable illite, kaolinite, chlorite and quartz in the <2. m fraction, the marine units are dominated by very minor amounts of quartz and trace quantities of illite.

These lithologies are intruded by the Carrickleck Dyke, a 1.5m wide Tertiary, single intrusion, olivine basalt dyke. The dyke is associated with the Donegal - Kingscourt dyke swarm (NW trend) (see figure 2.2). It is intruded along a high angle fault plane, dipping at 79. to the northeast, trending 278., displacing the Carboniferous rocks either side by several centimetres (downthrown to the northeast). Whether the dyke intruded an existing fault plane or whether the intrusion offered a line of weakness which accommodated subsequent movement is not clear. There is a fine grained dolerite contact of up to 1cm. Post intrusion hydrothermal fluids have exploited the contact plane, evidence of such can be seen in the presence of calcite veining in the dyke margin, although there is no observed veining in the host rock.

The Barley Sill, a Tertiary basaltic intrusion, can be seen in outcrop to the NNW of the Carrickleck Quarry. It is intruded into Arnsbergian and Sabdenian sediments (Jackson 1965), and despite its proximity, it does not appear to have overprinted or interfered with the thermal affect of the Carrickleck Dyke (Fernandez 2000).

2.3 SAMPLING STRATEGY

A dyke may cross-cut a number of lithologies. If the intrusion represents a single event, it may be considered to act as a single, localised heat pulse. A dyke is by definition a sheet like body of igneous rock, which is discordant to the bedding of the host rock. Where this discordance is near perpendicular then the geometrical relations can be described as relatively simple, both stratigraphically and thermally (i.e. the heat transmitted can be considered in 2 dimensions). Courtesy of the Tertiary igneous activity in the region that is now Britain and Ireland, there is an abundance of Tertiary dykes intruding Carboniferous rock in Ireland.

Carrickleck and Ballycastle were chosen for the relative simplicity, similarity and accessibility of the sites. At each site, Upper Mississippian/Lower Pennsylvanian, low angle sediments are intruded, at near right angles, by thin (<5m), Tertiary doleritic dykes. In each case, the dykes have had a localised effect and although there are other large

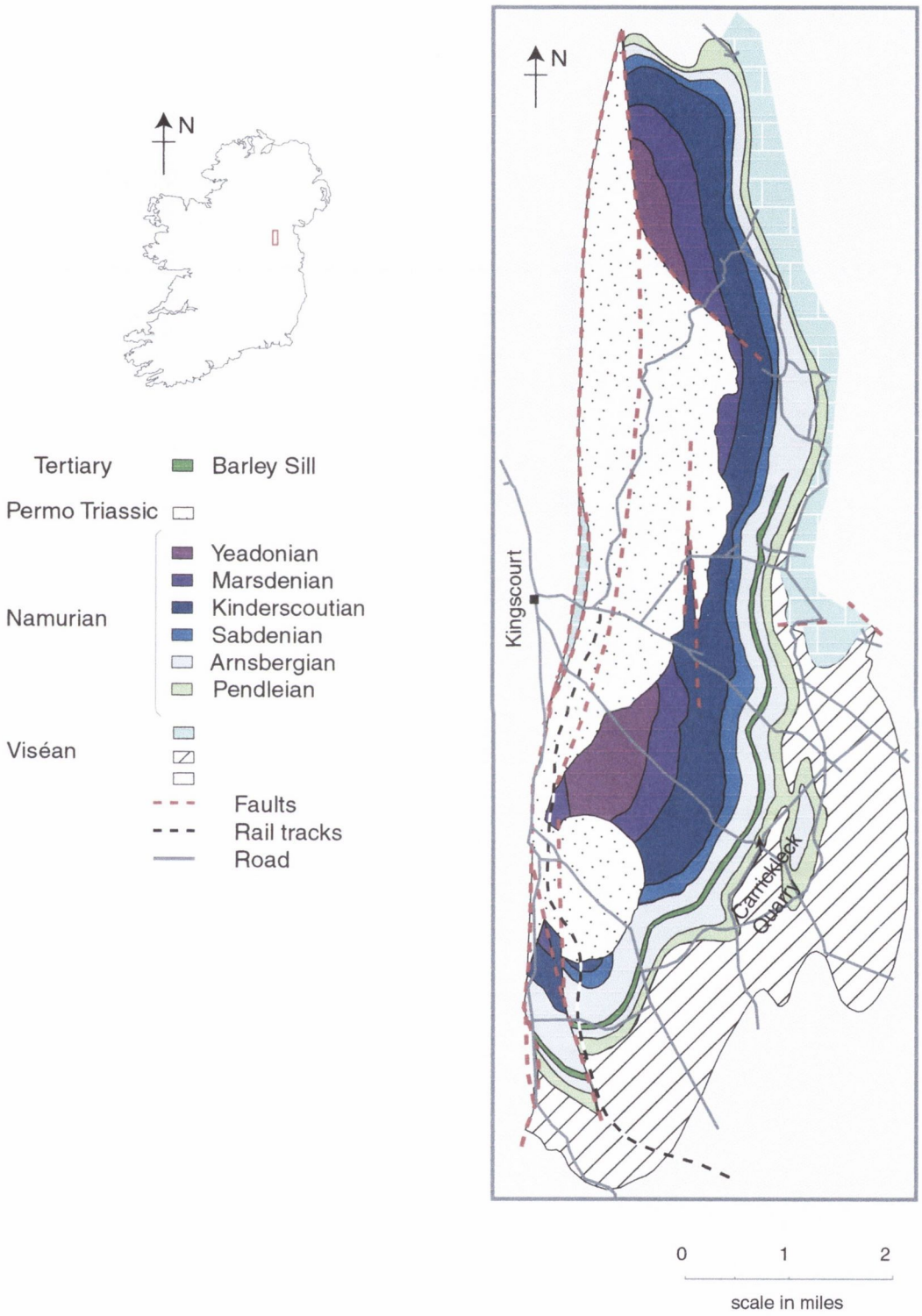

Figure 2.5 Generalised geology of the Kingscourt Outlier (after Strogen et al. 1995, Fernandez 2000)

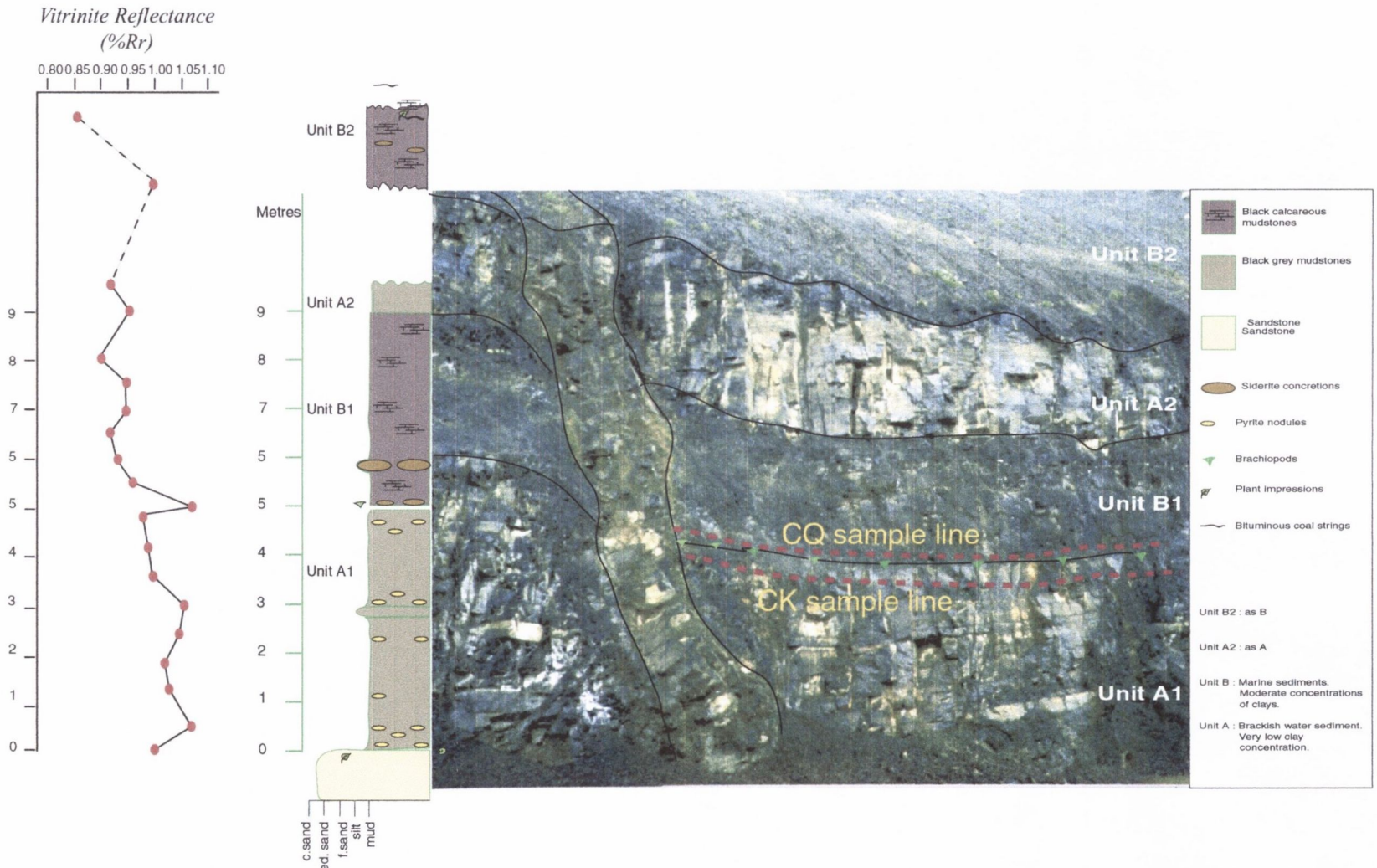

Figure 2.6 The Carrickleck Dyke exposed in the face of the Carrickleck Quarry, intruding the Carrickleck Shales. Sample horizons CK and CQ are marked and a generalised log (after Fernandez 2000) and vitrinite profile (Fernandez 2000) are presented. The Vitrinite profile demonstrates that the lithologies in the quarry face are free from the influence of the Barley sill (photograph courtesy of Dr. P. Fernandez).

igneous bodies nearby, these do not appear to have overprinted or interfered with the intrusive heat associated with the dykes. There is also little field evidence of extensive fluid movements in or near either of the dyke aureoles.

Five sedimentary lithological horizons were sampled from the dyke aureoles; 3 from the North Star Dyke aureole at Ballycastle and two from the Carrickleck Dyke aureole near Kingscourt. Samples were collected such that there was a greater sampling density closer to the dyke, and a sample from each horizon which was far enough away from the dyke so that it would represent material unaffected by the intrusion. Each of the five sampled horizons were dark mudrock because this lithology is believed to provide the greatest chances of finding appropriate organic materials as well as clay minerals. Material was also collected from the dykes.

2.3.1 SAMPLING AT BALLYCASTLE

Three horizons have been collected by various workers over the course of several years. The BC horizon is a mudstone lithology that was sampled by Goodhue, Clayton and Doff (Goodhue 1996). 11 samples were collected between 0.73 and 11.42m from the contact *. The sample closest to the dyke was used in its entirety by 1997. The coastal section where the North Star Dyke outcrops is often obscured by seaweed and marine debris, making it impossible to ensure that the same horizon would be sampled when the site was re-visited. The NSD horizon was sampled by McCormack, Clayton, Goodhue and Doff (McCormack 1998). 24 samples were collected from this horizon, between 0.04 and 10.11m from the contact*. The cMd horizon is a mudstone horizon with coal lenses which was sampled by Connolly, Clayton, Goodhue Gould and Wagner. 8 mudrock samples were collected, 3 oriented coal samples and 1 unoriented coal sample were collected between 0.45 and 2.42m from the contact* . Stratigraphically the cMd horizon is slightly younger than the BC horizon which is in turn younger than the NSD horizon.

Three samples were collected (by Goodhue in 1999) from the North Star Dyke; one from the western outer margin of the first intrusion, one from the centre of the first intrusion (0.90m from the dyke margin) and a third from the centre of the third intrusion (2m from the dyke margin).

8 coal samples were collected from the Gobb Section ESE of Ballycastle, within 1km of the North Star Dyke (see figure 2.4), in order to establish background vitrinite reflectance

* Perpendicular distance from the dyke

values, and to investigate whether the overlying Gobb Sill has had any significant thermal effect on the sedimentary lithologies in its immediate vicinity.

2.3.2 SAMPLING AT KINGSCOURT

Two horizons have been collected from the Carrickleck quarry. The CQ horizon was sampled, by Fernandez in 1996, from near the base of unit B1. Nine samples were collected between 0.09 and 2.7m from the contact* . The CK horizon was sampled (by Connolly, Clayton, Fernandez, McCormack and McCaughan 1997) from unit A1. 30 samples were collected between 0.07 and 72m from the contact. See figure 2.6.

Two samples were collected from the Carrickleck Dyke; one from the dyke margin and one at 0.6m from the dyke margin.

3 PETROGRAPHY AND GEOCHEMISTRY OF THE DYKES AND GEOCHEMISTRY OF THE HOST ROCKS

3.1 PETROGRAPHY OF THE INTRUSIONS

3.1.1 THE NORTH STAR DYKE

The North Star Dyke is an aphanitic – microcrystalline, olivine-phyric basalt. Thin section petrography shows that all three intrusions appear to be petrographically similar (see Appendix III plates 1-3). They are holocrystalline, inequigranular, and fine to medium grained. A subophitic texture with lath shaped plagioclase chadocrysts and pyroxene oikocrysts is common. Olivine is present only in the form of phenocrysts and is commonly altered or partly altered to a brown amorphous material, possibly saponite, (apparently preferentially with respect to the other minerals present). Feldspars can show a seriate texture from *c.* 0.05 – 0.50mm (acicular and lath shaped). Opaque minerals are present in quantities of no more than 5%.

The chilled outer margin of the first intrusion of the North Star Dyke, is also inequigranular and holocrystalline but with a more dominant and finer grained groundmass of acicular feldspar. There is a high degree of alteration of this material represented by a brown and pale green amorphous material, (possibly saponite?) in the groundmass. Olivine phenocrysts are highly altered and (more commonly than the central sections of the dyke) entirely altered to the brown material also observed in the other samples and groundmass. The larger feldspar laths can show preferential alignment, paralleling the dyke wall. The most notable (and possibly significant) variation from the central dyke sections, after the grain size, is the absence of pyroxene in the chilled margin. There are some veinlets, approximately 0.1mm wide, filled with a material that is opaque in plane polarised and cross polarised light.

3.1.2 THE CARRICKLECK DYKE

(See Appendix III plates 4-6)

The Carrickleck Dyke is an aphanitic – microcrystalline, olivine-phyric basalt. Thin section petrography shows that the basalt is holocrystalline, inequigranular, porphyritic with a fine grained groundmass and olivine phenocrysts up to *c.* 4mm.

The groundmass consists dominantly of fine grained lath shaped and acicular feldspars with variably sized augites and olivines. Subophitic texture is not uncommon, with feldspar chadocrysts. Opaque minerals make up approximately 5-10% of this rock matrix. Olivine phenocrysts are usually euhedral, and fractured (sometimes with a curved

fracture) and often highly altered. Some of the alteration material seems to have a greenish brown colour, which may indicate chloritization, or saponite.

3.1.2.1 CALCITE VEINING IN THE CARRICKLECK DYKE

(See Appendix III plates 7-9)

Calcite veining is observed in the CK dyke samples. The veins are a function of brittle deformation, implying that dilation occurred after the dyke had solidified and probably after it had substantially cooled. There are some en echelon type veins. Unfortunately, when collecting the dyke samples the material was not marked for oriented petrological work.

The vein fill consists of calcite and ferroan calcite. Cross cutting features expressed by the veins imply that there were at least two phases of dilation and calcite fill.

PHASE 1 is assumed to represent dilation, with the accompanying space accommodating ferroan calcite fill. The ferroan calcite has a characteristic blue-blue green cathode luminescence (CL). These veins are clearly a function of brittle fracture, and show an anastamosing vein network. This ferroan calcite exhibits fibrous growth, which is often taken to reflect precipitation in over-pressured systems (Parnell *et al.* 2000). The fibres are generally perpendicular to the vein wall. However, there are some cases where the growth shows a tendency towards bowing or 's'-shaped growth (sinistral sense), indicating growth under a pressure regime.

PHASE 2 involves further dilation, with the accommodation space being filled by a calcite, which has a characteristic orange colour under CL. The veining for this phase has exploited some of the same planes of weakness as phase one, and so the calcite is often clearly associated with the ferroan calcite and can be seen to be replacing, the phase one vein fill in places. Phase 2, shows 'varved' calcite vein fill in some of the material, fibrous growth, a blocky euhedral crystalline fill in the thicker veins (4mm across) and a network of very fine veins which heavily alter the olivine crystals that they come in contact with. The varved calcite shows sequential iron rich/poor layers. Fibrous calcite veins have concentrated iron content at the vein/dyke interface. The very fine anastamosing network of veins tends to be iron rich carbonate. This iron concentration is thought to be associated with the strong alteration of dyke, and is particularly prevalent in olivine alteration. The euhedral calcite crystals have pockets with strong negative shape, which parallel crystal faces, as do trails of these pockets (see Appendix III, plate 9). However, in spite of these characteristics typical of fluid inclusions (Rankin 1989),

further investigation showed that there was no liquid in these spaces. It is possible that what might have been there has escaped through decrepitation or that these spaces are actually filled by a crystalline solid. There was a limited amount of sample collected and for further investigation larger sample should be available, limitations of time in this project have meant that this work must be left here.

The veining observed in the Carrickleck dyke occurred as a function of brittle fracture. It is postulated here that the dyke was at least cool, if not cold at the time of fracturing. The consequent calcitic fills are thought to be a result of fluids that have exploited, and possibly facilitated movement along the fault plane, which the dyke has intruded. It is possible that the veining is an expression of displacement along the fault, although further field evidence should be collected before this could be substantiated or negated.

3.2 MAJOR AND TRACE ELEMENT ANALYSIS OF DYKE AND COUNTRY ROCK

(see Appendix I, Table 2 for list of all raw data and normalised results for whole rock major element oxides and trace element analysis)

3.2.1 BALLYCASTLE

Whole rock major element oxide analysis and trace element analysis was carried out on two of the North Star Dyke samples, one from the chilled outer margin and one from the main intrusion. Whole rock element oxide analysis was carried out on 5 samples from the NSD sample horizon (NSD 1, 3, 5, 15 and 24).

3.2.1.1 NORTH STAR DYKE SAMPLES

While there is little variation between the element oxide results (see figure 3.1) for the 2 igneous samples, the margin sample is enriched in Ba and Cr relative to the dyke 'body' sample. There is also a variation in the amount of H_20 for the two samples, although the CO_2 content is quite similar for both. These quantities are often taken as reflecting alteration of the igneous material.

It may be possible that the Ba source in these samples was an artefact of the dyke being submerged so often in the North Atlantic (pers. comm. Dr. D. Doff 1998)

CIPW normalised element oxide data identifies the dyke samples (IG2 and IG3) as metaluminous, silica saturated, tholeiitic basalt (see figure 3.1 and Appendix III). Trace

element discrimination diagram for Ti, Zr and Y relates the basalt to divergent plate boundary tectonics.

3.2.1.2 NSD SAMPLE HORIZON

The greatest variation seen in the element oxides (see figure 3.2(a)) in the sedimentary NSD lithology is a reduction in CaO content from 16.32% to 0.51% (background to the margin sediments); MgO is also depleted in the margin samples relative to background samples. SiO_2 is enriched in samples beside the dyke relative to the background sediments as is Al_2O, Na_2O, FeO, MnO, TiO_2 and Cr_2O_3. Insufficient numbers of samples in this horizon were analysed to be able to say anything very useful about these data as an independent trend relative to the dyke.

3.2.2 CARRICKLECK

Whole rock element oxide analysis carried out on 5 samples from the CK sample horizon (CK 1, 2, 6, 18 and 30, see figure 3.2(b)). The dyke samples were highly altered and so it was deemed unreasonable to use XRF analyses.

Samples near the dyke show enrichment in SiO_2, CaO, Na_2O and K_2O relative to the background material, and depletion in Al_2O_3. However an insufficient number of samples were run for XRF analysis for these data to be used to describe a trend in the sedimentary lithologies relative to the dyke.

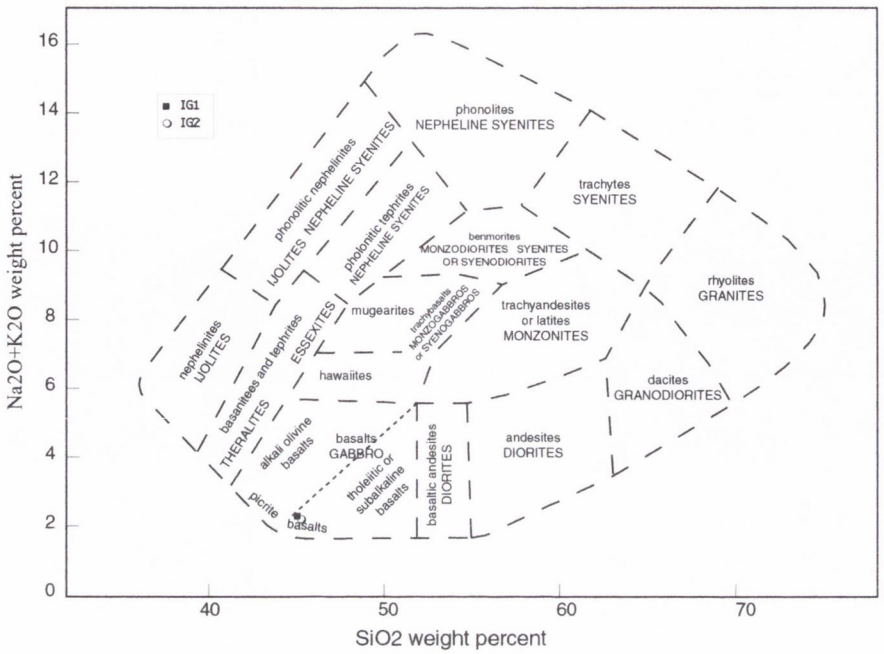

A basic nomenclature of the more common igneous rocks based on their silica and alkali contents (after Cox et al. 1979). This places the North Star Dyke samples in the tholeiitic or subalkaline basalt section.

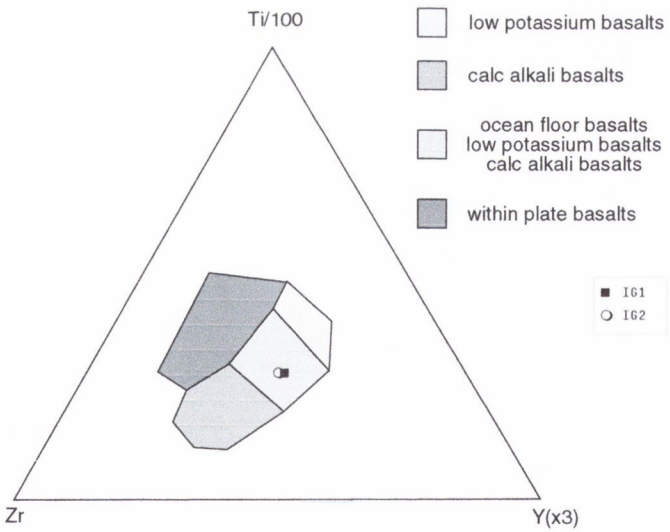

Trace element discrimination diagram using Ti, Zr and Y, (Pearce and Cann 1973) which implies that the basalts are related to divergent margin tectonic setting

Figure 3.1 Whole rock element oxide and trace element discrimination diagrams

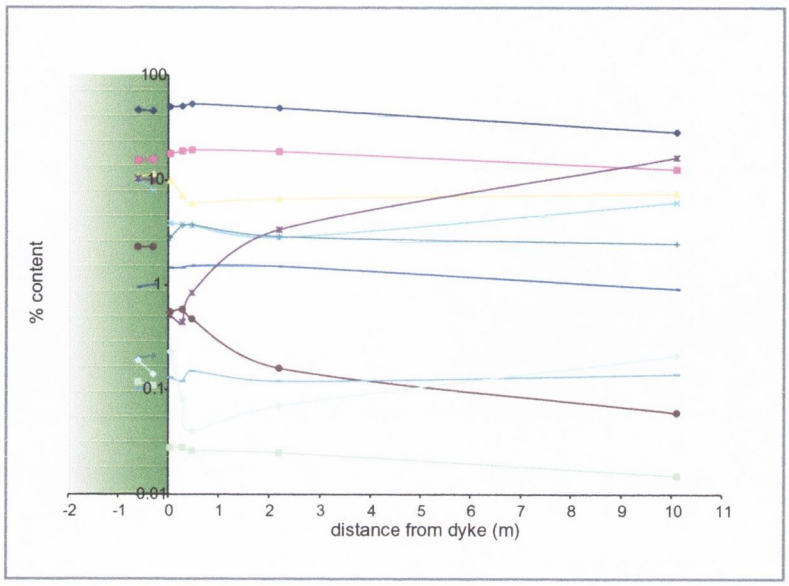

Figure 3.2(a) whole rock element oxide variation in the NSD horizon and in the North Star Dyke samples IG1 and IG3. NOTE: Y-axis is on a logaritimic scale.

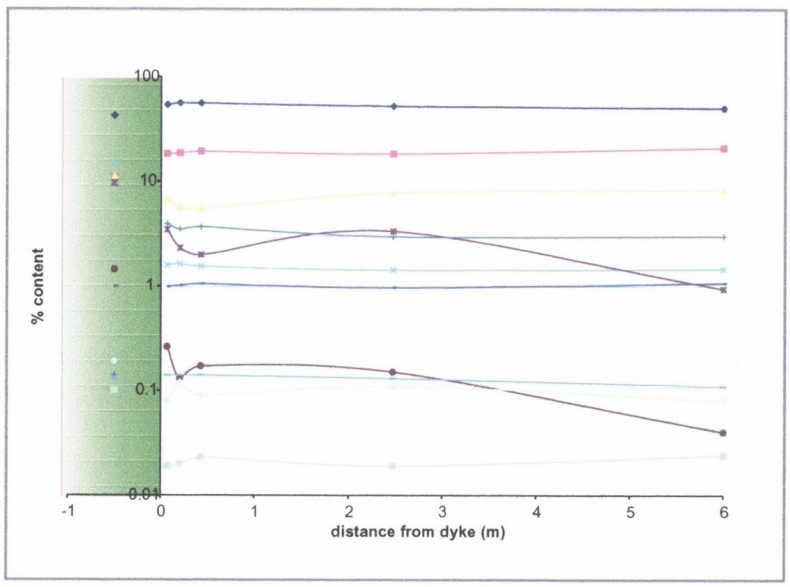

Figure 3.2(b) whole rock element oxide variation in the CK horizon and data from the Carrickleck dyke. NOTE: Y-axis is on a logaritimic scale.

4 VITRINITE AND VITRINITE REFLECTANCE

4.1 THE CONCEPTS OF COALIFICATION, RANK AND MATURATION

Organic matter reacts sensitively to rise of rock temperature and to a lesser extent pressure. This is particularly useful in the estimation of rock diagenesis and low-grade metamorphism (where coalification takes place) because coalification is irreversible (Stach *et al.* 1982, Barker 1983, Price 1983, Teichmüller 1987, Taylor *et al.* 1998 among others), and reacts in some situations more sensitively to rise in temperature and pressure than mineral transformations (Teichmüller 1987). The terms coalification, rank and maturation are terms commonly used in literature to describe these changes.

Coalification refers to the transformation of plant material into coal. This takes place in two stages – (a) biochemical degradation, this is the chemical decomposition of botanical matter aided by organisms; followed by (b) physico-chemical degradation caused by conditions of burial, when water is squeezed out and pore size reduced. As burial progresses oxygen and hydrogen are released during thermal cracking, with water and carbon dioxide (CO_2). This is thought to occur at temperatures between 30-100. C (Teichmüller 1987), followed by the further release of hydrogen in methane (CH_4) at temperatures up to 200. C (Teichmüller1987).

Coal rank refers to the degree of coalification, from the peat stage through lignite, sub-bituminous coal, bituminous coal, anthracite and meta-anthracite to the stage of semi graphite. Rank increase is characterised by a rise in C content and vitrinite reflectance, a decrease in volatile matter and moisture content and an initial rise in H content followed by a decrease to less than 2%.

Metamorphism undergone by organic material in sedimentary rocks other than coal also involves the expulsion of volatiles and liquids. The term 'thermal maturity' or 'maturity' is used as a measure of the degree to which this metamorphism has progressed (see figure 4.1 and table 4.1).

Carbonisation, according to Gray and Boucot (1975), occurs through a rapid charring, thermal degradation or decomposition (pyrolysis) of organic material. It may occur under a variety of pressure conditions. It is a purely thermal decomposition of the original organic material that occurs during a short time interval as a result of a rapid rise in temperature to a relatively high level. Like coalification, carbonisation of

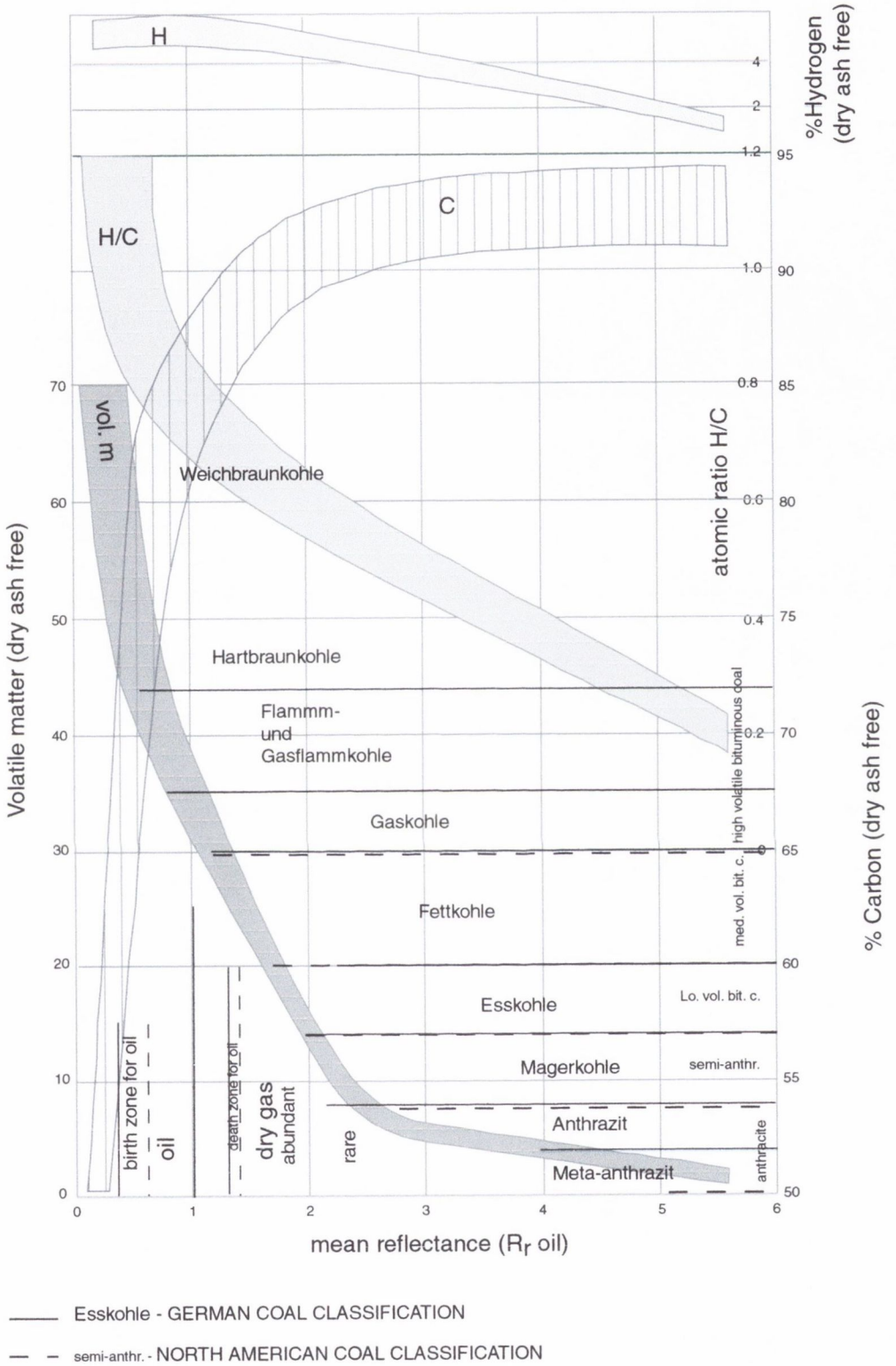

Figure 4.1 Chemical evolution of coalification with respect to volatile matter (dry ash free), atomic ratio H/C, carbon dry ash free content and hydrogen. This is presented relative to coal rank, hydrocarbon fluids and vitrinite reflectance (compiled from Teichmüller 1987, Taylor et al. 1998)

METAMORPHISM	MATURITY	COAL RANK	VITRINITE REFLECTANCE (mean random reflectance, $\%R_r$)
Diagenesis	Immature	sub-bituminous	< 0.5-0.6%
Catagenesis	Mature	sub-bituminous to semi-anthracite	0.5-0.6% to 2.0 – 2.3%
Metagenesis	Overmature	semi anthracite to pre-graphite??	> 2.0 – 2.3%

Table 4.1 The relative terms of coalification, maturity and metamorphism with approximate range in vitrinite reflectance

organic material involves aromatisation and may end in the formation of coke or graphite if the temperature gets high enough. The temperature difference that separates the thermochemical effects of coalification and carbonisation is less critical than the rate of temperature increase. For example, natural cokes have been formed by the thermal energy generated in close proximity to either an intrusive or extrusive igneous body (Gray and Boucout 1975).

4.2 VITRINITE

Vitrinite is one of the main maceral groups of coal (see table 4.2). Stopes first used the term 'maceral' in 1934, derived from the term 'maceration' (a method of breaking up rock by steeping it in water) (Stopes 1935). The main maceral groups are vitrinite, inertinite and liptinite. They are distinguished by their colour, reflectance, chemical composition and physical properties. Although each coal maceral follows a different coalification path, they each become more visually alike as the process progresses.

"The term vitrinite designates a group of macerals whose colour is grey and whose reflectance is generally between that of the associated darker liptinites and lighter inertinites over the rank range in which three respective maceral groups can be recognised" (ICCP system 1998). See table 4.2. This is a woody maceral occurring in most post-Silurian grey/black shales and is a dominant constituent of coals.

Huminite is a term used for the potentially more morphologically distinct precursors of vitrinite that occur only in immature rocks (i.e. where reflectance is less than or equal to

0.5% R_r). Palynologists and geochemists are frequently guilty of using vitrinite as a general term without regard to the rank of the host rock.

GROUP	VITRINITE	
SUBGROUP Telovitrinite	Detrovitrinite	Gelovitrinite
MACERAL Telinite	Vitrodetrinite	Corpogelinite
Collotelinite	Collodetrinite	Gelinite

Table 4.2 Subdivision of the maceral group vitrinite after the ICCP system 1998.

4.2.1 PHYSICAL AND CHEMICAL EVOLUTION OF VITRINITE

Vitrinite is essentially a coalification product of humic substances, which originate from the lignin and cellulose of plant cell walls (Taylor *et al.* 1998). With compaction and burial vitrinite loses porosity and moisture content. It is characterised by high oxygen content relative to the other macerals. With progressive coalification carbon content increases as oxygen content decreases. Hydrogen content peaks at a mean random reflectance value equivalent to *c.* 1.0-1.1% (ICCP system 1998). At a very basic molecular level vitrinite consists of clusters of aromatic rings (7-7.5Å across) connected by aliphatic groups. As coalification progresses the aliphatic chains are removed and the aromatic rings coalesce (up to >15 angstroms). With this increasing condensation and aromatisation, ordering is also imposed on the molecular units, principally in response to thermal stress (Murchison *et al.* 1985), and where overburden pressure is the principal pressure they tend to align parallel to bedding (see figure 4.2).

4.2.2 VITRINITE REFLECTANCE

Vitrinite reflectance is the ratio of the light reflected from a polished vitrinite surface to that of the source (incident light) expressed in %. Reflectance depends on the refractive index and the absorption index of vitrinite and on the refractive index of the medium through which it is travelling, usually immersion oil or air, according to the Beer equation:

The Beer Equation

(4.1) $$R=([(n-n_0)^2 + n^2K^2]/[(n+n_0)+n^2K^2)100$$

where R = vitrinite reflectance

n = vitrinite refractive index

n_0 = refractive index of oil/air

K = vitrinite absorption index

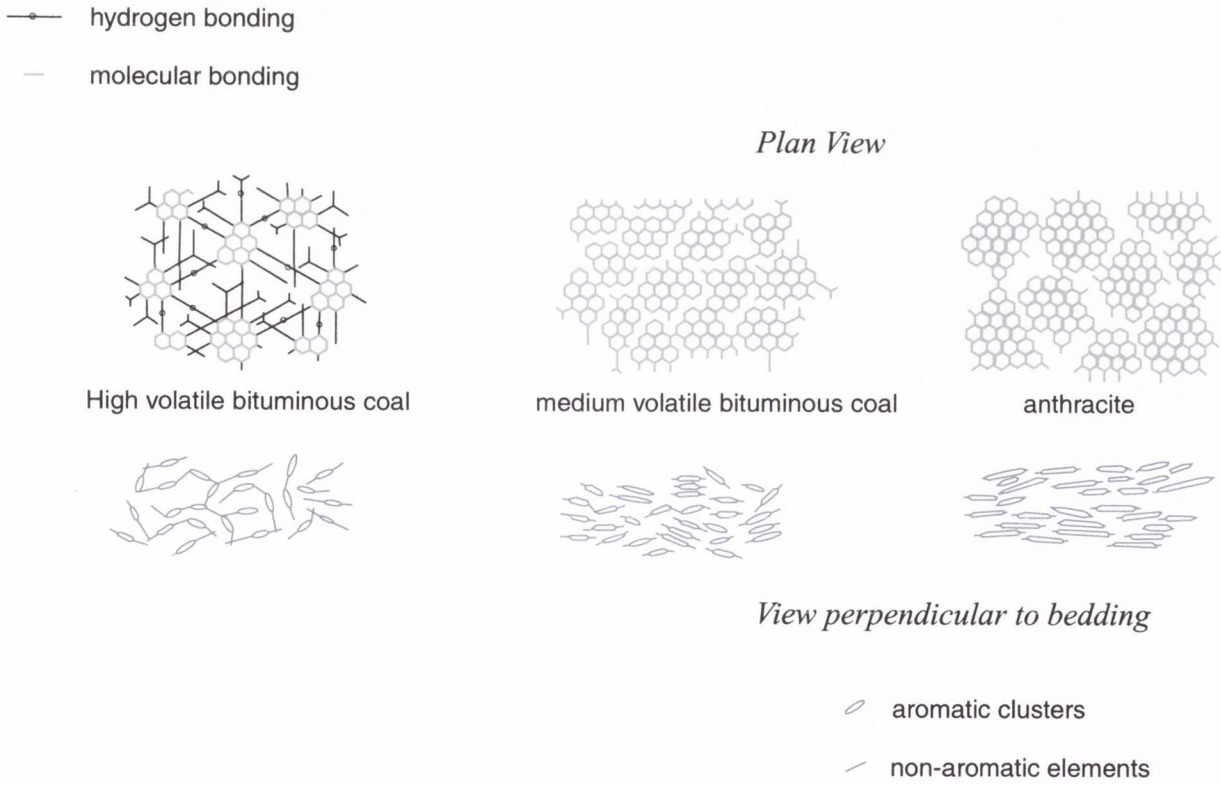

Figure 4.2 Increasing aromatisation, resulting in condensation and ordering of aromatic units parallel to bedding plane during coalification of vitrinite. After Teichmüller and Teichmüller 1984 in Taylor et al. 1998, Teichmüller 1987, Stach et al. 1982.

Vitrinite reflectance generally increases with burial (see figure 4.3). This can be expressed as a function of temperature (Stach *et al.* 1982, Price 1983, Levine and Davis 1984, Murchison *et al.* 1985) from 0.2 % R_r at *c.* 20. C to 8.0 % R_r at *c.* 400. C (where R_r is mean random reflectance). The thermal response of vitrinite is a non - retrograde reaction (Stach *et al.* 1982, Price 1983, Teichmüller 1987). Burial also involves increasing pressure with depth. The reflectance of vitrinite is related to its molecular structure. Increasing reflectance can be correlated with the increasing condensation, aromatisation and ordering undergone by the vitrinite molecular units

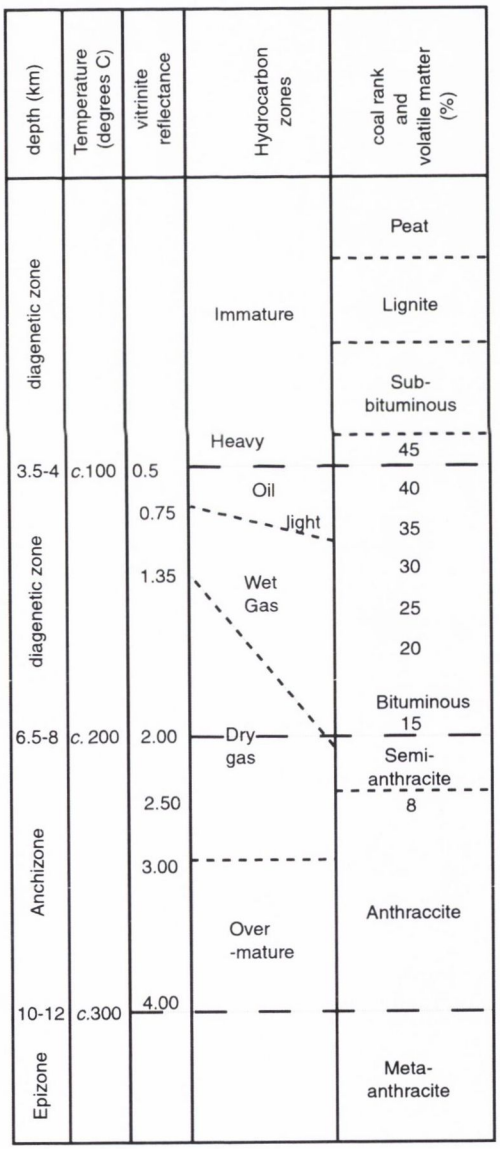

Figure 4.3 Basin maturity chart showing correlation of metamorphic zone, depth, temperature, vitrinite reflectance, hydrocarbon zones and coal rank (after Merriman 1999)

principally in response to thermal stress (Murchison *et al.* 1985). Overburden pressure also encourages these units to align, and where overburden is the dominant acting pressure then the units will tend to align parallel to bedding. Where the effective tectonic stress is other than the gravitational load of the overburden, the vitrinite molecular units tend to align along the line of maximum stress (see figure 4.4).

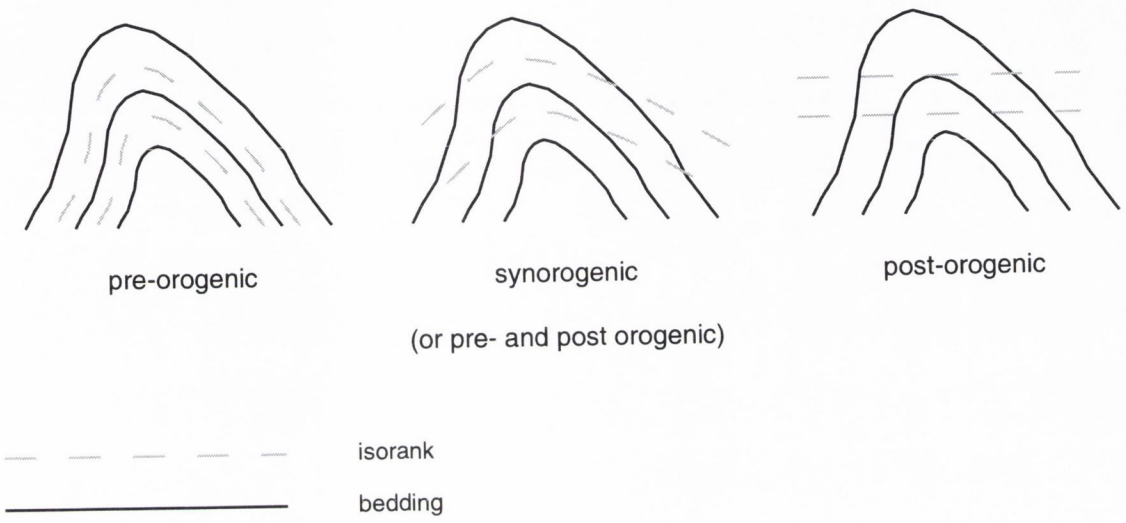

Figure 4.4 The course of isorank lines. (a) pre-orogenic lines tend to run parallel to bedding, (b) syn-orogenic coalification they tend to lie obliquely and (c) post-orogenic they are lying horizontally, if the lithological column was buried and the original reflectance values were overprinted (after Stach et al. 1982).

Work has been carried out by Dalla Torre *et al.* (1997) over a pressure range of 0.5 to 20 Kbar, temperatures of 200 to 350. C and run durations of 2, 4 and 7 days. Results showed that applied pressure can lower vitrinite reflectance and that this 'suppression' is enhanced when the starting material is wet. Other workers have shown that overpressure and high hydrostatic pressure can retard chemical coalification by hindering the removal of coalification gases (McTavish 1978, Teichmüller 1987, Price and Wenger 1992, Carr 2000, Zou and Peng 2001).

4.2.2.1 VITRINITE OPTICAL ANISOTROPY

An anisotropic substance has different physical properties when measured in different directions. In low rank coals (less than 0.7%R_r), vitrinite is basically optically isotropic

(Ting 1981), that is optical properties are the same when measured in all directions. As coal rank increases, bireflectance develops. Bireflectance or optical anisotropy is the difference or ratio between the maximum and minimum reflectance (R_{max} and R_{min}). The progressive ordering of the molecular layers, with rank increase, leads to a more organised reflective surface (see figure 4.2). It follows that as coalification progresses the difference between R_{max} and R_{min} increases so that bireflectance (R_{max} - R_{min}) or optical anisotropy increases. Under idealised burial conditions, vitrinite develops an anisotropic nature similar to that of a uniaxially negative material, so the crystallographic/optic axis (minimum reflectance) would develop perpendicular to the sedimentary bedding plane (see figure 4.5). Bireflectance is most pronounced in the anthracite rank. The development and increase of anisotropy with coal rank is a general rule except in some cases, for example, where coalification is caused by contact metamorphism (ICCP system 1998).

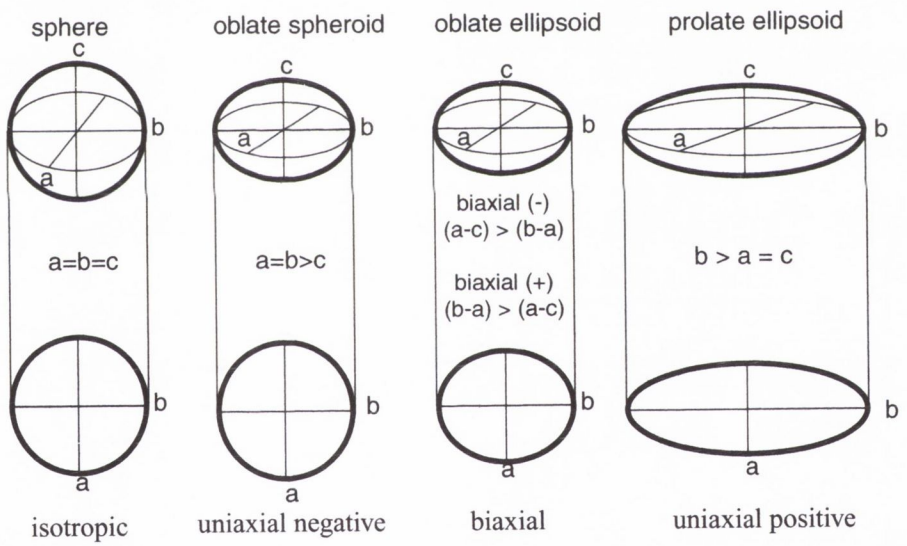

Figure 4.5 The vitrinite indicatrix, represented by an ellipsoid with three rectangular axes, the length of these axes being proportional to the refractive index of any beam vibrating parallel to it (i.e. travelling perpendicular to it). Here they are labelled a, b and c; where a represents the minimum refractive index and the fast ray (R_{min}), c represents the maximum refractive index and the slow ray (R_{max}) and b represents the intermediate ray perpendicular to the a-c plane.

Different thermal regimes and tectonic forces can affect vitrinite anisotropy. While temperature tends to promote the chemical evolution of vitrinite, pressure tends to promote the physical evolution of vitrinite. In an ideal burial situation the two progress in tandem.

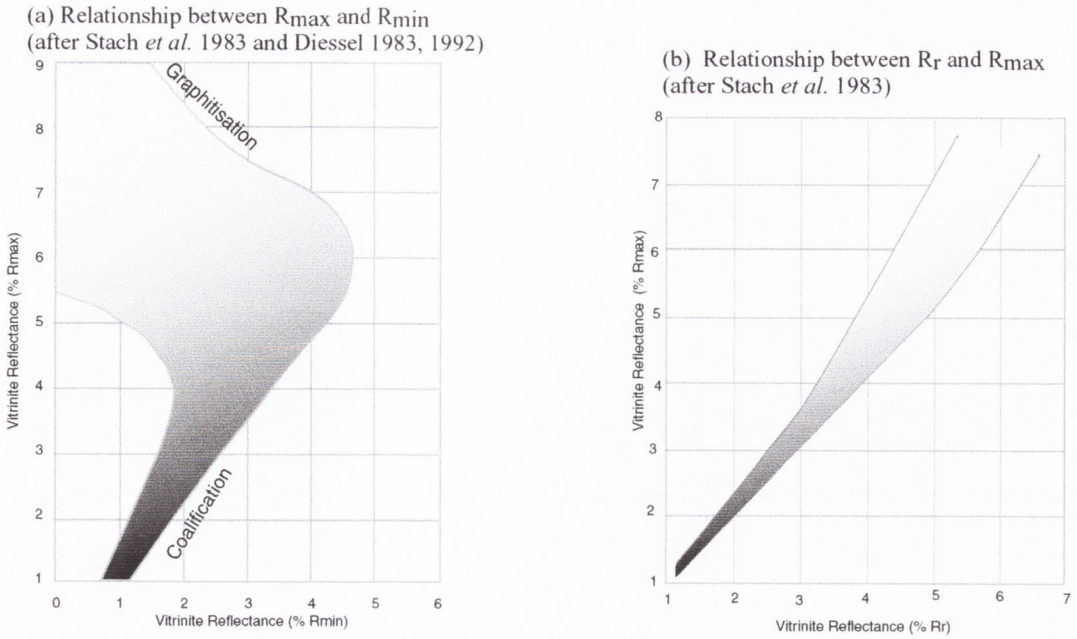

Figure 4.6 Relationship between increasing R_{min} and R_{max} and R_{max} and R_r

Tectonic pressure apparently promotes the parallel ordering of the molecular units normal to the direction of the maximum tectonic stress. This can lead to abnormal increases of maximum reflectance and bireflectance (Stach *et al.* 1982, Taylor *et al.* 1998). Tectonic shearing can also cause a sharp increase in bireflectance (Bustin *et al.* 1995a & b, Ross and Bustin 1997). The relationship between thrust planes and localised increase in vitrinite reflectance has been reported (Teichmüller and Teichmüller 1967, Bustin 1983) and was attributed to short lived, heating due to either frictional and/or geothermal heating during strike slip faulting (Teichmüller 1987, Taylor *et al.*1998). The high temperatures and pressures induced in these situations have also been quoted as a mechanism for natural graphite formation (Bonijoly *et al.* 1982, Bustin *et al.* 1995a & b). Tectonic pressure may also 'disturb' the ordering of the aromatic lamellae and give rise to biaxial anisotropy (Levine and Davis 1984, Teichmüller 1987). Levine and Davis (1984) have suggested that the aromatic lamellae of vitrinite tend to polymerise in the direction of the minimum compressive stress and stack in the direction of maximum compression, thus indicating the tectonic regime that was last imposed. The presence or absence of uniaxial or biaxial vitrinite has been used in conjunction with other methods to indicate the relative timing between thermal and kinematic events (Levine and Davis 1984, Grieve 1991, Houseknecht and Weesner 1997).

4.2.2.2 OPTICAL PROPERTIES OF VR IN DISPERSED ORGANIC MATTER

The small size of vitrinite particles in organic matter residues, extracted from sediments for strew slides and vitrinite stubs, makes the measurement of R_{max} and R_{min} difficult, particularly when the stage must be rotated, if the microscope cannot be accurately centred then the small fragment will move away from the measuring aperture on rotation. This has led to the use of a fixed stage position with the polariser out of the optical train (random) or in the optical path (average)(Murchison *et al.* 1995). It is also a problem that measurements taken, for R_{max} and R_{min}, may be apparent but not true due to lack of control on particle orientation. This problem is also caused by the inhomogeneity of clastic rocks. The differing hardness of vitrinite and the mineral particles in many lithologies means that during compaction the relatively harder minerals are pressed into the softer vitrinite. This can disturb the normally parallel molecular micelles and biaxial anisotropy may develop due to the transverse stress. The use of 'mean random reflectance' (R_r of Taylor *et al.* 1998) is thus the more reasonable approach in these cases, where R_r is "the mean reflectance of all reflectance values of a polished surface" (Teichmüller 1987, Taylor *et al.* 1998) and is measured using a fixed stage, with the polarizer out of the optical path. This is a useful method for measuring vitrinite reflectance when the vitrinite particles are small and studied in the form of dispersed organic matter. Ting (1977) has proposed the statistical relationship for R_{max} and R_r of:

(4.2) $$\text{Mean } R_{max} = 1.06 \, (\text{Mean } R_r)$$

Work carried out on coal from the Upper Silesian Coal Basin, Poland, has yielded the following relationship (Komarek and Morga 2001), between R_{max} and R_r:

(4.3) $$R_{max} = 1.090(R_r) - 0.052$$

4.3 TIME AND TEMPERATURE; THEIR EFFECT ON VR AND INFLUENCE ON THERMAL MODELLING

Rock temperature increases with depth of subsidence or burial, resulting in coalification in tectonically undisturbed sequences. This relationship is known as Hilt's Law. The rate of rank increase with depth depends on a number of interdependent factors such as the geothermal gradient, rate of subsidence, heating rate, heat conductivity of the underlying and accompanying rocks, the rank parameter being examined and the rank range, which

the coal has reached. Vitrinite is one of the more successful and popular rank (maturation) indices. Although this is the case, a complete understanding of the influence of time spent at a specific temperature on rank in the geological column is not yet agreed upon.

4.3.1 TEMPERATURE AND TIME

While temperature is indisputably a dominant influence on the increasing rank of vitrinite, the role played by time has long been debated. In pursuit of a resolution to this debate two approaches for modelling the thermal evolution of vitrinite have been proposed. One is a time dependent model, where the amount of time spent at a particular temperature is presumed to be of import in vitrinite maturation. Work attempting to model vitrinite rank increase using time and temperature are largely based around the chemical kinetics of the first order reaction rates predicted by the Arrhenius equation.

The second model assumes a time independent approach, where time is not considered to be a controlling factor, and the vitrinite is assumed to represent the maximum temperature to which it was exposed.

4.3.1.1 TIME AND TEMPERATURE INCLUSIVE MODELS

The Arrhenius equation:

(4.4) $$K = A\exp^{-E/RT}$$

where K = rate constant
A = frequency factor
E = activation energy
T = temperature in . K
R = the gas constant

The Arrhenius equation theoretically expresses the exponential temperature dependence on the rate of a chemical reaction (Connan 1974). A first order reaction should by definition describe a straight line when the reaction extent is plotted on a logarithmic scale against reaction time on an arithmetic scale (Price 1983).

One of the earliest attempts to incorporate time and temperature in predictive calculations was the work of Karweil (1955). He proposed that coals heated over a short period of time could attain the same rank as coals heated over a longer period at lower temperatures. Unfortunately, most of the samples considered by Karweil in this study were from areas in Germany, riddled with igneous intrusions. Karweil's work assumed a

constant thermal gradient, but didn't consider the possibility of higher palaeogeothermal gradients caused by intrusive and hydrothermal events. This was however a fundamental piece of work, which considered the concept of geological time and organic metamorphism. The samples were used to calculate the necessary activation energies of coal to reach their present rank. Assuming these reactions follow first order Arrhenius reaction kinetics Karweil produced a nomogram for predicting coal rank from burial history (see figure 4.7).

Lopatin (1971) developed the use of the Arrhenius equation to predict the rank of organic matter if exposed to specific temperatures for specific time periods. This was based on an observation that Karweil's (1955) nomograph predicted lower coal rank, particularly at greater depth, than were found in the Munsterland No. 1 borehole. The model is known as the Temperature Time Index (TTI)(Figure 4.7). It is known that reaction rate varies with temperature (Robert 1988, Allen and Allen 1991, Huang 1996). The TTI proposes that reaction rates double with every 10. C rise in temperature and represents the sum of the temperature adjusted durations of burial, based on this reaction rate. Lopatin (1971) assumed a mean set of kinetic parameters, which progressed as first order reactions, with activation energies equivalent to 8.4 – 30 kcal mol^{-1}. Price (1983) measured activation energies of 40 – 80 kcal mol^{-1}, in laboratory experiments and other authors have also noted that they are quite low for the entire rank range (Hood *et al.* 1975, Wood 1988). Wood (1988) observed that, "the use of a mean set kinetic parameters for one reaction rather than several sets of kinetic for parallel reactions (that more closely model the decomposition of kerogen) tends to underestimate the significance of early and late reactions in the calculated maturity index". The TTI (Lopatin 1971, later modified by Waples 1980) was widely used in industry for some time.

Figure 4.8 shows the relationship proposed by Hood *et al.* (1975), between VR, T_{max} and effective heating time, the latter defined as the "time span during which the coal was within 15. C of its maximum burial temperature" (Taylor *et al.* 1998). This was based on a scale for the 'Level of Metamorphism of organic matter' or the LOM. The LOM, consists of a scale from 0-20, equivalent to the coal ranks of lignite to the upper extent of the anthracite rank, and relates temperature to time for organic maturation, LOM, based on the chemical kinetics proposed by Karweil (1955), calculates the reaction rate approximately doubling every 10. C (similar to the TTI).

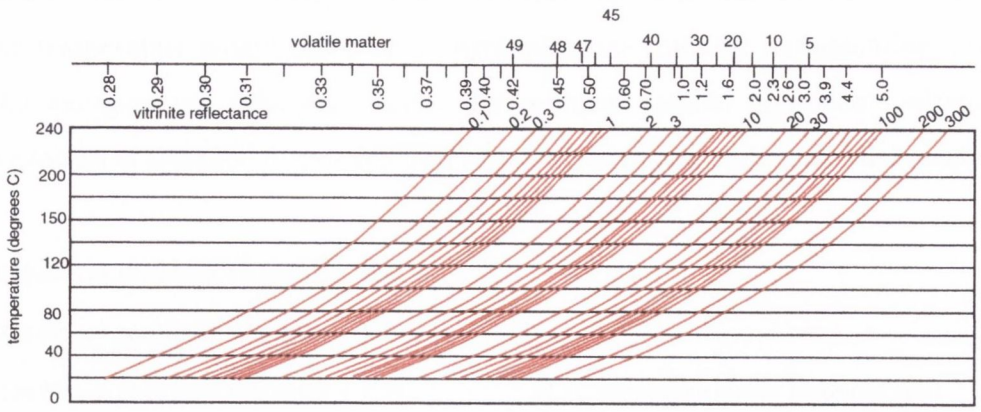

Figure 4.7 Modification of Karweil's (1955) plot of burial time and temperatures versus volatile matter in coal. Volatile matter is shown on the upper part of top the horizontal line, vitrinite reflectance on the lower part of the top horizontal line. Numbers on curves are burial times in millions of years. Burial temperature scale, in degrees C, is on left side of figure. Volatile matter values converted to vitrinite reflectance values based on Stach et al. (1982). Karweil's original curves are from 10 - 300 million year burial times and as they are a simple repeating logarithmic function, the curves were extrapolated to lower vitrinite reflectance values for shorter burial times after a R_o value of 0.28% at 20°C for an assumed burial time of 100,000yrs. The vitrinite reflectance value of 5.0%R_r and volatile matter values of 3 and 4 % are from Bostick (1979), (after Price 1983).

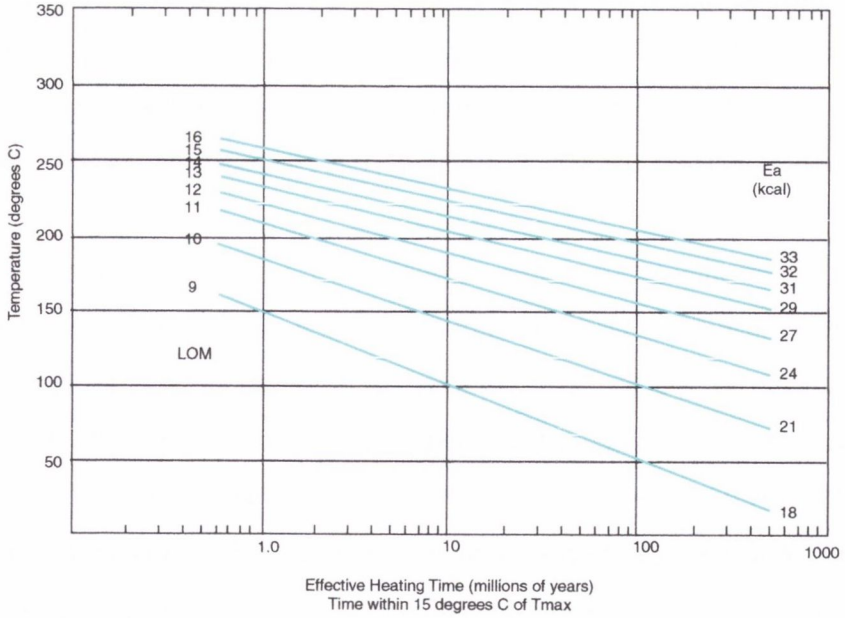

Figure 4.8 The relationship between LOM and effective heating time of Hood et al 1974 (in Hood et al. 1975)

Burnham and Sweeney (1989) suggested the chemical kinetic model 'EASY%R_o'. This is another time-temperature model based on an Arrhenius rate equation but assuming a range of activation energies and taking a "first order reaction parallel approach", where the maturation process is assumed to proceed as a series of four independent parallel reactions:

Vitrinite $\rightarrow$ residual vitrinite + H_2O

Vitrinite $\rightarrow$ residual vitrinite + CO_2

Vitrinite $\rightarrow$ residual vitrinite + CH_n (CH_n represents higher hydrocarbons)

Vitrinite $\rightarrow$ residual vitrinite + CH_4

This is an important assumption. Vitrinite has a wide range of reactivity, as some reactions may have gone to completion others may not yet have started (Sweeney and Burnham 1990). The EASY%R_o model is not unlike the approach of Mackenzie and Quigley (1988). The assumption of first order reactions however is a fundamental flaw in these models (Barker 1983, Price 1983, Landais *et al.* 1993). Although first order reactions can be generated in the laboratory using dry material (Price 1983), this is not generally the situation found in nature, where the system tends to be partially open or closed, pressurised and water wet. The introduction of parallel reactions does to some degree compensate for this, but doesn't fully realise the system parameters. A number of authors have quoted reaction times for stabilisation of the maturation process for vitrinite during burial diagenesis: 1,000 – 10,000 yrs (Barker 1983, Price 1983), 1 to 10 million yrs (Kisch 1987, Barker 1988).

There is disagreement among workers in this field about how important time is as a factor in maturation with respect to lower and higher temperature regimes. Some authors have concluded that time, as a factor in the lower temperature regimes, is more important than at the higher end of the temperature scale, others believe the opposite. Gretener and Curtis (1982) wrote, "The effect of temperature is exponential to that of time linear. At very low temperatures (<50. C) the conversion rate (kerogen to hydrocarbon) is so slow that time has no influence. At high temperatures (>130. C) the reaction proceeds at such a high rate that time also plays no important role. The effect of time is noticeable in the range of 70 - 100. C, where intermediate conversion rates prevail." Due to the effect of duration of heating and varying palaeogeothermal histories it is impossible to relate a particular degree

particular degree of coalification to a precise temperature. Typical coalification temperatures are 100-170°C for bituminous coals and 170-250°C for anthracites.

4.3.1.2 TEMPERATURE DEPENDENT MODELS

A number of authors believe that vitrinite reflectance is set by the peak temperature (Gretener and Curtis 1982, Barker 1983, Price 1983, Barker and Pawlewicz 1986, Pollastro and Barker 1986). Barker (1983) states that after a heating duration of 10^4 yrs (virtually inconsequential on the geological timescale), time has little or no further influence on the reaction. A study carried out by Koch and Schellschmidt (2001) found no influence of time on the thermal maturation of organic material observed in Germany.

Price (1983) reviewed and rebuked much of the work (pre- 1983), which attempted to incorporate time as a controlling factor in organic maturation or rank increase. He did not accept that the first order reaction kinetics, pivotal in most of these models could be substantiated in nature. He believed that although time may *appear* in some circumstances to have a correlation with the thermal evolution of vitrinite in reality it is "actually a consequence of the fact that the older the sediment is, the greater the chance it has had of being affected by a major geologic event with an accompanying high heat-flow." Price (1983) went on to propose that vitrinite be used as an absolute palaeogeothermometer.

Barker and Pawlewicz (1986) compiled maximum temperatures from over 35 systems using samples rich in humic matter. The data spanned a range of maximum burial temperatures (T_{max}) of 25-325°C and R_r values ranging from 0.2 – 4.0 $\%R_r$. Their burial reconstruction indicated that the effective heating duration for these systems ranged between 10,000 and 10 million years. Using this information and plotting $\%R_r$ against T_{max} a least squares fit linear regression equation was calculated

(4.5) $$Ln(R_r) = 0.0078\ T_{max} - 1.2$$

Concluding that vitrinite reflectance is highly dependent on maximum temperature.

Barker and Halley (1986), studied palaeotemperatures indicated by fluid inclusions, $\%R_r$ and oxygen isotope data from the Dellaware Basin, Texas. Using this data and the major axis regression method of Till (1974), Barker (1988) proposed the equation

(4.6) $$T(.C) = [Ln(R_r)*104]+148$$

This equation was modified from Barker and Pawlewicz (1986) as "we now think that it is better to use a regression method that allows error to be present in both the independent and dependent variable" (Barker 1988). This equation predicted peak temperatures from $\%R_r$ that were more "compatible with other geothermometers and burial history reconstruction" (Barker 1988). Johnsson *et al.* (1993) found equation 4.6 to correlate more closely with the results predicted by the kinetic models of Burnham and Sweeney (1989) and Sweeney and Burnham (1990) than equation 4.5 or 4.7.

Barker and Goldstein (1990) proposed the equation:

(4.7) $$T_h = [(\ln R_m) + 1.26]/0.00811$$

This work was based on the assumption that "aqueous fluid inclusions in calcite re-equilibrate during over heating, and therefore some homogenisation temperatures (T_h) record a temperature close to the maximum reached by the rock" (Barker and Goldstein 1990). Using data for T_h and the maximum temperatures (T_{peak}) that were assumed to be at maximum burial, the authors illustrated close agreement between T_h and T_{peak}. Then comparing $T_{h\ mode\ (or\ mean)}$ to R_r and again using least squares fit produce equation 4.7. This equation is very similar to that of Barker and Pawlewicz (1986), which supported the suggestion that VR is more closely controlled by maximum temperature than time duration.

Tobin and Claxton (2000) selected samples from "burial (non-hydrothermal)" systems in 19 basins from 16 countries with ages that range from the Precambrian to the Miocene. Using an empirical approach they calibrated re-equilibrated calcite fluid inclusion data and vitrinite reflectance data. The vitrinite reflectance data ranged from 0.5 – 1.4%R_r. VR was plotted against the homogenisation temperature (T_h). The resulting relationship is:

(4.8) $$\%R_r = 2.1113\ (\log T_h) - 3.2640$$

4.4 SAMPLE PREPARATION FOR VITRINITE REFLECTANCE

4.4.1 ORGANIC MATTER EXTRACTION

All samples were initially washed under water and left for at least 24 hours to dry. The sample material was then broken into small chips and 10g was weighed and placed into polythene, lidded bottles. The material was tested for carbonates which, where present,

were removed using 10% HCl. After all carbonates were removed, the HCl was neutralised and decanted. HF was then added, enough to completely cover the sample, to remove any silicates. The sample bottles were placed in a water bath, maintained at a constant temperature of 60. C, where they were left for at least 48 hours under HF and stirred twice daily. When the silicates were completely broken down the HF solution was very carefully decanted, and topped up with water, at least 6 times. The final number of decants was dependant on whether the decanted water reacted to lime or not *i.e.* when it was neutralised. At this stage approximately one third of the organic residue was placed in a glass phial and stored under water. The rest of the organic residue was then sieved through a 20μm mesh and the >20. m fraction was stored in a glass phial under water and used for vitrinite reflectance, palynological content and characteristics (*i.e.* palynofacies, stratigraphic palynology, spore colour and spore fluorescence work).

4.4.2 PREPARATION FOR VITRINITE REFLECTANCE

Two methods have been employed in mounting organic residue for the analysis of vitrinite reflectance (VR).

4.4.2.1 SLIDE MOUNTING FOR VR

This first method involves spraying one side of a glass cover slip (no.1 thickness, 22 x 22 mm surface area) with a teflon based releasing agent. Once dried a dilute solution of organic residue was pippetted onto the tefloned side of the cover slip. When dry the cover slip was mounted onto a glass slide (1.2/1.4mm thickness, 76 x 26mm surface area) using MetSet mounting medium. After the resin had hardened the cover slip was removed and the mount was hand polished on silicon carbide (SiC) grinding paper for wet grinding, grit 1200, using a figure of eight motion usually for no more than eight turns to remove all of the teflon. The resin slide is then polished using a series of polishing alumina suspensions, 1.0 – 0.05μm. The first polish uses 1.0μm alumina. The sample was hand held for 2 - 3 minutes at 250 RPM on the lap, while a constant figure of eight motion was described. The final polish uses 0.05 alumina, the sample is exposed to 3minutes at 250 RPM and 1 minute at 125 RPM. After each sample the polish lap is cleaned either under running water using a plastic bristled brush or in the ultrasonic bath. This is done to remove any pyrite that might have been dislodged during lapping. This method of mounting vitrinite on a glass slide was practiced after the method described by McCormack (1998), adapted from Hillier and Marshall (1988).

In 1999 the acquisition of MetSet resin was no longer possible and so vitrinite samples were necessarily mounted in blocks.

4.4.2.2 BLOCK MOUNTING FOR VR

This involves the use of greater quantities of residue and resin (EpoThin resin). Sieved organic residue is pippetted onto a petri dish and allowed to dry. It is then powdered/separated, using a razor blade, and a small amount of resin added to the residue. The now organic residue rich resin is then pippetted into a small plug, allowed to settle for a few minutes and then topped up with resin. Once cured the resin plug is removed and polished as with the slide except it receives 3 - 4 minutes at 250 RPM using 1.0 alumina and 4 - 6 minutes using the 0.05 alumina.

Use of glass-mounted vitrinite makes it possible to switch between reflected and transmitted light. This is particularly advantageous when identifying vitrinite particles. This method also uses less organic residue, and is quicker to polish. Alternatively, the vitrinite stub is more robust, is quicker and easier to prepare and can carry a substantial amount of organic residue in one stub, if required.

4.4.3 SAMPLE PREPARATION FOR COAL SAMPLES

4.4.3.1 UNORIENTED COALS

Unoriented coal samples were collected with the intention of measuring mean random reflectance (%R_r). 5g of sample was selected and crushed to a powder. The powder was then mounted in a resin plug (in the same way as the organic residue in 2.1.2 as for block mounting) and polished for reflectance studies.

4.4.3.2 ORIENTED COALS

Where the sample was oriented it was mounted whole, and oriented, in the same resin as in 2.1, and then cut (1) *c.* perpendicular to the bedding plane/*c.* parallel to strike and (2) *c.* perpendicular to the bedding plane/*c.* perpendicular to strike. These surfaces and the topmost surface of the lens, were then polished as for VR block mounting except that it was sometimes necessary to use SiC grinding paper, 320 grit, first to remove the layer of resin covering the top of the coal.

4.5 VITRINITE REFLECTANCE ANALYSIS

4.5.1 THE REFLECTANCE MICROSCOPE AND IMAGE ANALYSIS SETUP

The apparatus consists of the Leitz Ortholux II MPV compound binocular microscope with a stabilised light source (12volt, 100 watt halogen lamp), rotating stage; light controlling apertures, Berek prism type vertical illuminator and a removable polariser. The objective lens has magnification of 50, and is strain free. One eyepiece has cross wires; both has a magnification of 10. The light source is turned on 30 minutes before use each time, to allow it to stabilise. Attached to the microscope is a black and white camera, which is in turn connected to a Leica PC and the downloaded image is analysed using the Leica image analysis software.

4.5.2 MEASURING VITRINITE REFLECTANCE

Vitrinite reflectance is the ratio of the light reflected from a polished vitrinite surface to that of the source (incident light) expressed in %. Reflectance depends on the refractive index and the absorption index of vitrinite and on the refractive index of the medium through which it is travelling, usually immersion oil or air. Vitrinite reflectance is measured using a reflected light source and a receiver, which has been calibrated using 2 or more standards. The standards used throughout this study are listed in table 4.1.

Standard type	*%R_r in oil*	*%R_r in air*
Spinel (McCrone No.307)	0.42	7.17
Glass (Leitz no.998)	1.23	9.60
Cubic zirconia (McCrone No.319)	3.28	13.90
Silicon Carbide (McCrone No.339)	7.54	20.70

Table 4.3 Reflectance standards used in this study

R_r is measured using a fixed stage position, with the polarizer out of the optical path. 100 readings are taken for each sample where possible. Where less than one hundred readings were taken it has been noted in the appendix with the appropriate sample.

R_{min} and R_{max} are measured by rotating the sample through 360.° at 22.5.° intervals, and with the polariser in taking 50 readings per interval. This is done for each of the three surfaces mentioned in section 2.1.2.1, for each of the samples.

Reflectance measurements are taken under oil with a refractive index of 1.5193 at a constant room temperature of 19-20. C.

4.5.3 PARTICLE COUNT

Stach *et al.* (1982) suggests that, based on statistical methods, the optimum number of measurements required for an accurate estimate (within +/- 2%) for the mean random reflectance of vitrinite (%R_r) is 100 for coals and 50 for dispersed organic matter (DOM). However, Barker and Pawlewicz (1993) suggest that by Stach's arguing for 100 measurements for coals then at least 100 readings for DOM should also be taken. This was reasoned by the fact that as "the degree of precision of the mean is directly proportional to the standard deviation of the population" and accounting for the fact that the standard deviation of DOM %R_r is generally greater than for that of coals, then there should also be at least 100 readings for DOM. However the findings of Barker and Pawlewicz (1993) suggested that even were there only a maximum of 20 - 30 particles the precision is in "good agreement with the general precision of one decimal place recommended for" %R_r measurements on DOM.

In this study when measuring DOM, 100 readings were taken, as there is a general abundance of vitrinite in the samples. For samples where it was not possible to find 100 readings due to a scarcity of vitrinite the number of particles counted was noted and has been recorded (see appendix II).

When measuring maximum reflectance (%R_{max}) and minimum reflectance (%R_{min}) of the oriented coals a maximum of 50 readings were taken for each angle. This is justified using the arguments of Barker and Pawlewicz (1993).

4.5.4 VITRINITE IDENTIFICATION

For this work when identifying vitrinite the sample is scanned to get the 'eye in' for finding the particles wit the following features:

The operator wants to see

- . A blocky maceral with a solid linear outline, rounded edges suggests reworking and arcuate edges suggests that it may be a member of the fusinite group.

- A particle that fits the above description, which has a mid to light grey reflectance colour.
- A structureless particle, with low relief.
- Optical anisotropy, particularly in high-ranking samples.
- Where possible relict cell-structure can make identification much easier and the mistaken identification of bitumen for vitrinite can be ruled out.
- If there is something that can definitely identified as something other than vitrinite e.g. semifusinite then this particles its reflectivity was measured and this was sometimes used as a rough guide as to what to expect for vitrinite.
- Ideally a vitrinite particle that has a scratch free, relatively homogenous surface that is large enough to allow reflectance measurement
- There is often associated pyrite

4.5.5 POSSIBLE PROBLEMS AND ERRORS WITH VR

1. One of the biggest problems related to VR is the misidentification of vitrinite.
2. VR for a coal generally results in histograms with narrow normal distribution, and a single peak. VR from other sedimentary rocks tend to result in more complex distribution. This seems to imply that the selection of indigenous vitrinite can be difficult.
3. Correctly identifying primary vitrinite is difficult in rocks containing both primary (autochthonous) and secondary (reworked, allochtonous) vitrinite.
4. Identifying whether or not VR is 'real', suppressed or retarded. The presence of the exinite-liptinite group macerals may have a suppression effect as a result of the impregnation of bitumen produced by this group.
5. Poorly polished sample with scratches and relief can result in a reduction of the measured VR.
6. The presence of moisture in samples reduces the measured VR (Carr 2000). This is only a problem in immature to early mature coals (0.7%R_o), where the vitrinite is still porous enough to retain moisture and can be overcome by storing the polished block in a dessicator overnight before measuring.
7. Vitrinite is not a single constituent with a restricted range of optical properties. Vitrinite reflectance can vary depending in the original plant material and the diagenetic conditions that it was subjected (Buiskool Toxopeus 1983).

4.5.6 PRESENTATION OF RESULTS

Raw data are presented in Appendices I (tables) and II (histograms). Plates of whole rock coal samples are available in Appendix III, plates 10-12.

4.6 RESULTS

Samples of both the Carrickleck Dyke and the North Star Dyke were systematically collected from mudstone horizons in the dyke aureoles, with greater sampling density in the area directly adjacent to the dyke. Samples were also collected between 10 and 80m from the dykes so that vitrinite reflectance beyond the influence of the dykes could be established as a background maximum. All distances quoted are perpendicular distance from the dyke contact.

4.6.1 RESULTS FOR THE CARRICKLECK DYKE AUREOLE

4.6.1.1 BACKGROUND AND SETTING THE SCENE

The Carrickleck dyke is intruded along a fault plane showing displacement across the fault. The timing of this movement is unclear. There is evidence of post intrusion fluid flow, with calcite veining cross cutting the dyke margin. There is no observed veining in the host rock. It seems that the fluid exploited the interface between the dyke and the fault plane as a conduit for flow. It is assumed that the temperature of these fluids cannot have been as high as that of the intruding magma.

4.6.1.2 CK HORIZON TRAVERSE RESULTS

Samples from the CK horizon of the Carrickleck Dyke aureole yielded sufficient vitrinite for 100 measurements per sample. Vitrinite reflectance data show normal distribution, which implies a single vitrinite population. There is no evidence from the vitrinite reflectance work that the vitrinite was reworked. This implies that the reflectance data obtained from samples beyond the influence of the Carrickleck Dyke aureole represent the maximum temperature experienced by the host rock, assuming that there were no other unknown localised heat sources in the vicinity. This maximum temperature is assumed to have been generated through burial.

Values of 1.08-1.10%R_r were recorded from samples collected *c.* 60 - 70m from the dyke (see figure 4.9). Vitrinite reflectance values first rise above 1.10%R_r at *c.* 4.5m from the dyke and remain between 1.10 and 1.20%R_r up to 1.6m from the dyke. From here there is

an accelerated rise in VR with proximity to the dyke. Maximum $\%R_r$ is recorded not in the sample collected closest to the dyke but at 0.20m from the dyke which records a VR of $3.65\%R_r$. The sample closest to the dyke records a VR of $3.09\%R_r$. The VR profile in the CK horizon reflects increasing coalification or rank with proximity to the dyke. The background is in the high volatile bituminous stage, 4.5 – 0.8m records a gradual increase through the medium volatile bituminous stage, at 0.6m the aureole is set at the low volatile bituminous stage, the cluster of samples between *c.* 0.4m and the dyke margin all rank as anthracites ($3.09\text{-}3.65\%R_r$).

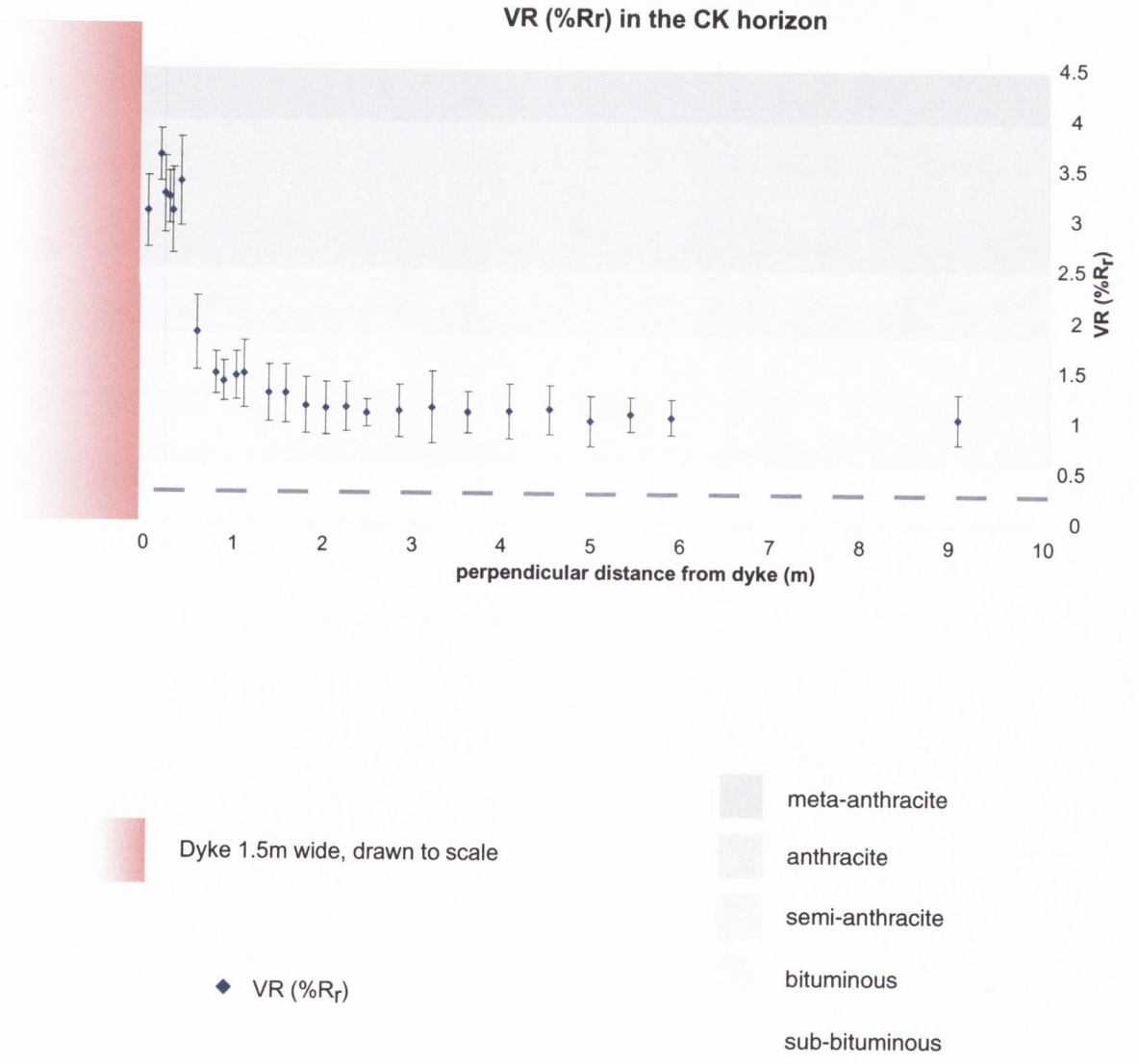

Figure 4.9 Vitrinite reflectance profile through the CK horizon in the Carrickleck Dyke aureole and relative coal rank.

4.6.2 THE NORTH STAR DYKE AUREOLE

4.6.2.1 BACKGROUND - THE GOBB SECTION RESULTS

Vitrinite reflectance data collected from Carboniferous coal samples (Clayton *et al.* 1989) and organic rich shales (pers. comm. Evans 1998) from the Ballycastle area have yielded vitrinite reflectance results of *c.* 0.5 and 0.6 $\%R_r$ (sub-bituminous). Coal samples collected from the Gobb section (CL9-16, refer to section 2.3.1) ESE of Ballycastle (within 1km of the North Star Dyke) record a modal VR between *c.* 0.5 and 0.6$\%R_r$ (see figure 4.10). However sample Cl9 records a VR of 1.14$\%R_r$. Sample Cl16, was collected from a coal horizon immediately below a massive sandstone. This sample also shows an elevated reflectance value, at 0.78$\%R_r$, relative to the rest of the profile. There is not a large enough data set to hang any theory on this one spurious point, however there are a number of possible situations that may be responsible.

Sampling of the horizons adjacent to the North Star Dyke occurred over a number of years (see chapter 3). Three horizons have been used for the vitrinite study in this work. They have been called the BC, cMd and NSD horizons.

'Background' BC and NSD horizon samples at a distance of *c.* 11m and 10m respectively from the dyke record a VR of 1.10 and 1.25$\%R_r$. However in the cMd horizon, at 3.5m from the dyke, a reflectance value of 0.55$\%R_r$ is recorded.

4.6.2.2 THE BC HORIZON TRAVERSE

The BC horizon yields vitrinite with reflectance values that range from 1.09 – 1.98$\%R_r$ over a distance of 11.4 – 1.6m from the dyke contact (see figure 4.11, Appendix I, table 3). There was originally one more sample collected from nearer the dyke. However by the time this work began there was no sample left. This sample horizon concurs with the reflectance values yielded by the NSD samples. 'Background' values of *c.* 1.09 – 1.11$\%R_r$ are recorded between 11.5 and 8m from the dyke. Between 6.3 and 3.2m from the dyke, reflectance values range from 1.16 – 1.2$\%R_r$. From 2.5 to 1.6m, the reflectance profile gradually steepens from 1.34 – 1.98$\%R_r$ respectively. So from 11m to 1.5m from the dyke the horizon records VR values that progressively increase through bituminous rank, and semi-anthracite at 1.6m from the dyke margin.

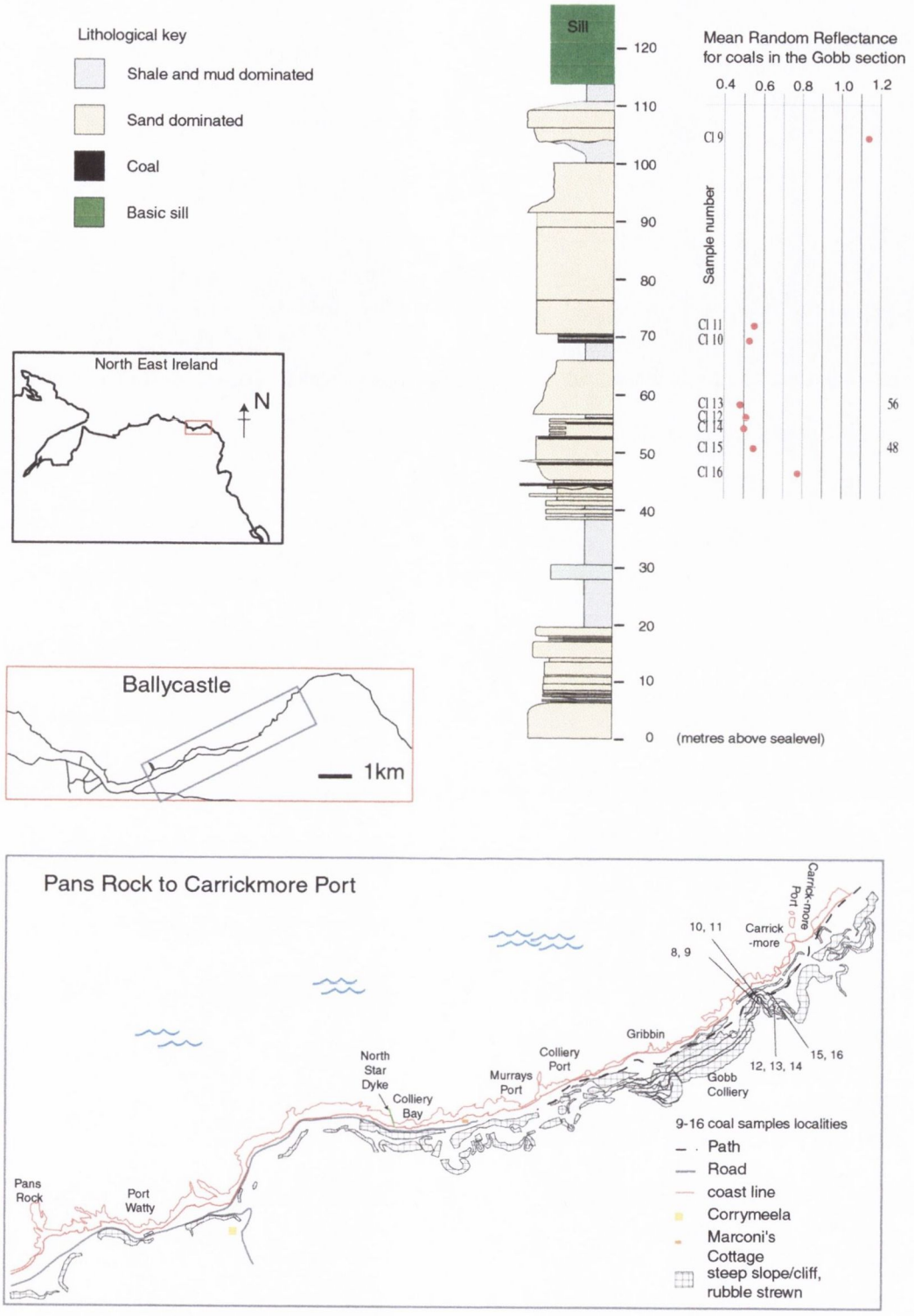

Figure 4.10 Locality map for the disused Gobb Colliery and coal samples Cl9 to Cl16 (section adapted from Sheet 5 of the Ordnance Survey of Northern Ireland) and simplified log of the Gobb Colliery section (after Evans 1998, pers. comm..) Vitrinite reflectance profile for the Gobb section in the Ballycastle area

4.6.2.3 THE cMd HORIZON TRAVERSE

'Background' reflectance values for the cMd horizon are taken as the reflectance value yielded by the sample collected furthest from the dyke *i.e.* 0.55%R_r at 3.55m from the dyke (see figure 4.11 and appendix I, table 4). Reflectance values rise gradually through the interval 3.55 - 1.6m from 0.55 to 0.94%R_r. The profile climbs steeply between 1.6m and 0.6m where the maximum reflectance is recorded at 5.45%R_r. Again, this is not the sample collected closest to the dyke; at 0.4m from the dyke a reflectance of 5.2%R_r is recorded. These values profile a progressive rise from sub-bituminous to meta-anthracite. Sub-bituminous rank (0.55%R_r) at 3.6m, by 2.6m it is in the bituminous rank, at 1.0m the horizon is in the semi-anthracite range, by 0.8m anthracite rank is reached, beyond 0.6m meta anthracite rank is recorded.

4.6.2.4 THE NSD HORIZON TRAVERSE

The NSD horizon has a range of VR values from 1.03 – 5.55%R_r; this ranges in coal rank from bituminous coal to meta anthracite (see figure 4.11 and appendix I, table 4). The background values are not very tightly constrained, but for distances of 2-10m from the dyke VR ranges from 1.03 – 1.25%R_r. Between 2 and 0.6m there is a progressive increase in VR from 1.30 – 3.40%R_r. The profile becomes very steep to accommodate the increasing reflectance values over such a short distance between *c.*1m - 0.3m (maximum VR). 0.5 – 0.3m yields the highest VR values ranging between 4.68 and 5.55%R_r (meta-anthracite rank), values do not progressively increase in a regular manner. The samples closest to the dyke show relatively lower values at 3.87 and 3.84%R_r (anthracite rank).

4.6.2.5 COAL LENSES IN THE cMd HORIZON

The cMd horizon contains coal lenses, which yield reflectance values of *c.* 0.5%R_r. %R_{max} and %R_{min} reflectance work was carried out on oriented coal lens samples (Co1, Co2 and Co4) collected from the cMd horizon at 4.5 and 2.5m. These samples do not show any optical, anisotropic evidence of deformation other than compaction. See Appendices I and II for reflectance results for samples Co1, 2 and 4.

There is carbonate mineralisation of fracture networks in samples Co2 and Co4, which show multiple fracture systems. Sample Co1 is also mineralised although the mineral fill and fracture system is slightly different.

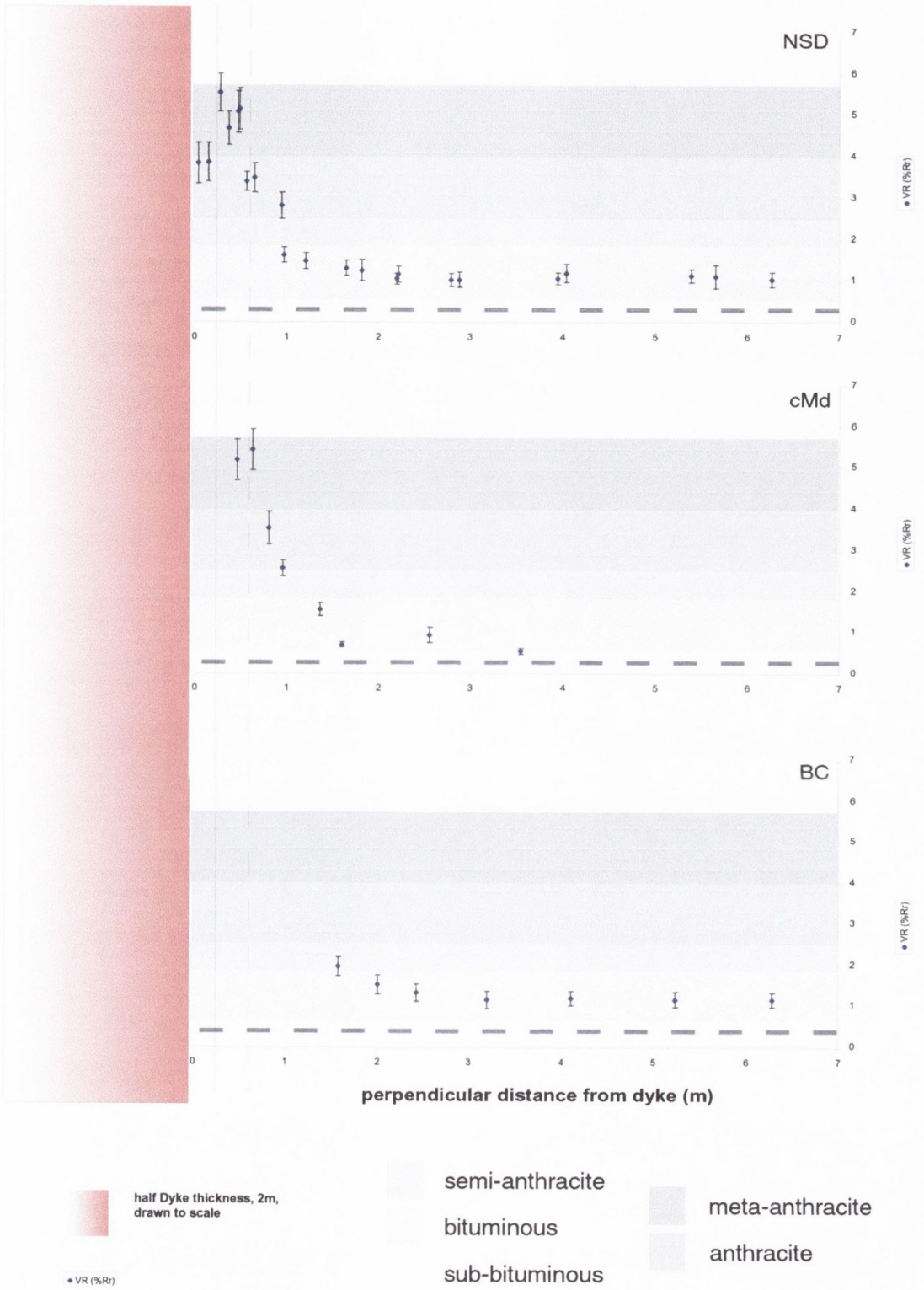

Figure 4.11 VR profiles and relative coal rank through the NSD, cMd and BC horizons in the North Star Dyke aureole

4.7 VR CONVERSION TO PALAEOTEMPERATURE (°C) USING THEORETICAL EQUATIONS/PUBLISHED CALIBRATIONS

The burial histories of the areas investigated have not been accurately ascertained. There are large sections of Irish post-Carboniferous history that can only be postulated. In spite of the fact that burial modelling might be a useful method to establish a feasible background temperature, it was considered not to be within the scope of this work to investigate these problems. It was therefore deemed unreasonable to attempt to model the burial history using the time temperature models previously described, based on the large number of uncertainties (refer to chapter 2).

Vitrinite reflectance data were converted to maximum temperatures (°C) (termed T_{peak} after Barker and Goldstein 1990) (see table 4.3, and Appendix IV) using methods published by Barker and Pawlewicz (1986), Barker (1988), and Barker and Goldstein (1990).

The temperature conversion of Barker and Pawlewicz (1986) (see figure 4.12) the greatest range of temperatures for the reflectance data, yielding the lowest background temperature and the highest temperatures in the area proximal to the contact (T_{max}). Relative to Barker and Goldstein (1990) (see figure 4.13), Barker and Pawlewicz (1986) methods calculate lower temperatures for vitrinite reflectance less than *c.* 2.3%R_r, and higher temperatures for vitrinite reflectance greater than 2.52%R_r. The temperature conversion of Barker (1988) (see figure 4.14) relative to Barker and Goldstein (1990) yields lower temperatures. The difference between the estimated temperatures increases as the reflectance values increase. Relative to Barker and Pawlewicz (1986), Barker (1988) calculates higher temperatures at reflectance values less than 0.76%R_r, and lower temperatures at reflectance values greater than 0.77%R_r.

		Barker & Goldstein 1990	Barker 1988	Barker & Pawlewicz 1986
BC	$T_{peak \cdot BG}$	158	166	173
	$T_{peak \cdot max}$	219	241	243
cMd	$T_{peak \cdot BG}$	86	77	91
	$T_{peak \cdot max}$	324	371	364
	$T_{peak \cdot c}$	319	365	358
NSD	$T_{peak \cdot BG}$	158	166	173
	$T_{max \cdot max}$	326	374	366
	$T_{max \cdot c}$	288	326	322
CK	$T_{peak \cdot BG}$	154	166	173
	$T_{peak \cdot max}$	283	320	316
	$T_{peak \cdot c}$	265	298	296

Table 4.3 Calculated background and maximum temperatures calculated for each horizon after Barker and Pawlewicz (1986), Barker (1988) and Barker and Goldstein (1991), where . is the temperature and the subscript $_{BG}$ refers to Background, $_{max}$ to maximum, $_{c}$ to contact; T_{peak} refers to the maximum temperature calculated from the vitrinite reflectance values using the methods of the authors named above

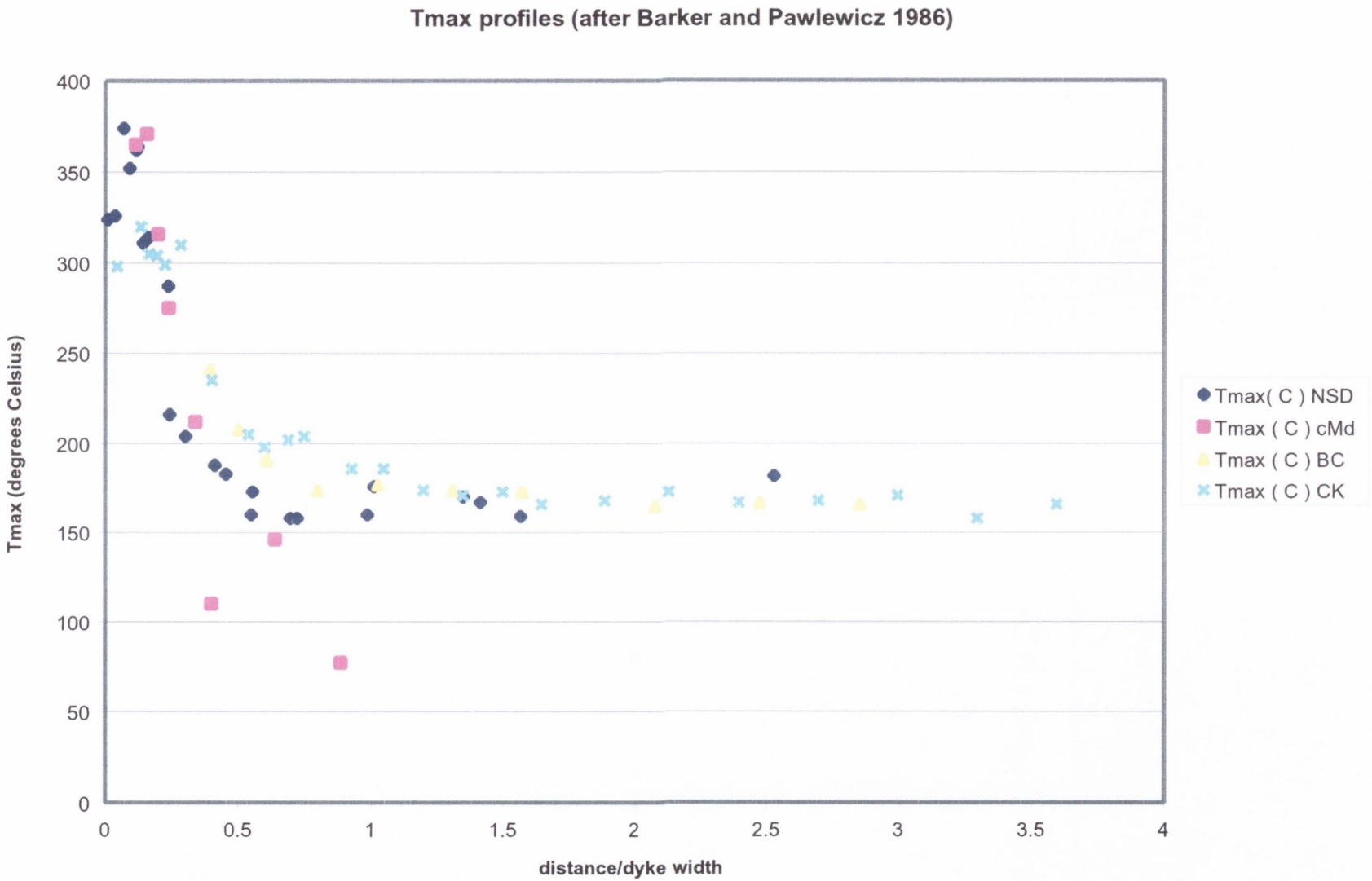

Figure 4.12 Maximum temperatures Tmax calculated from VR using the temperature conversion equation of Barker and Pawlewicz 1986

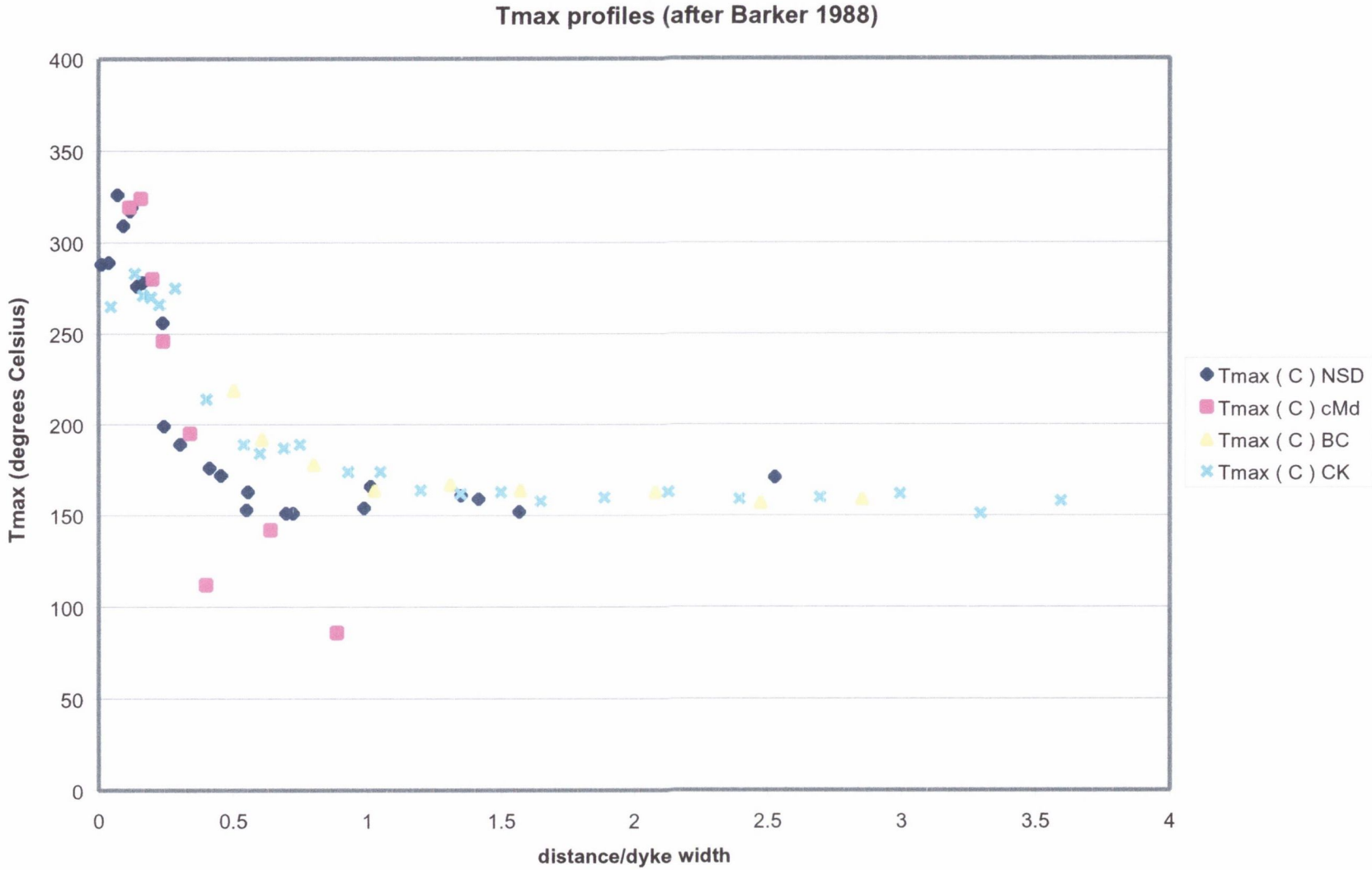

Figure 4.13 Maximum temperatures (Tmax) calculated from VR using the temperature conversion equation of Barker 1988

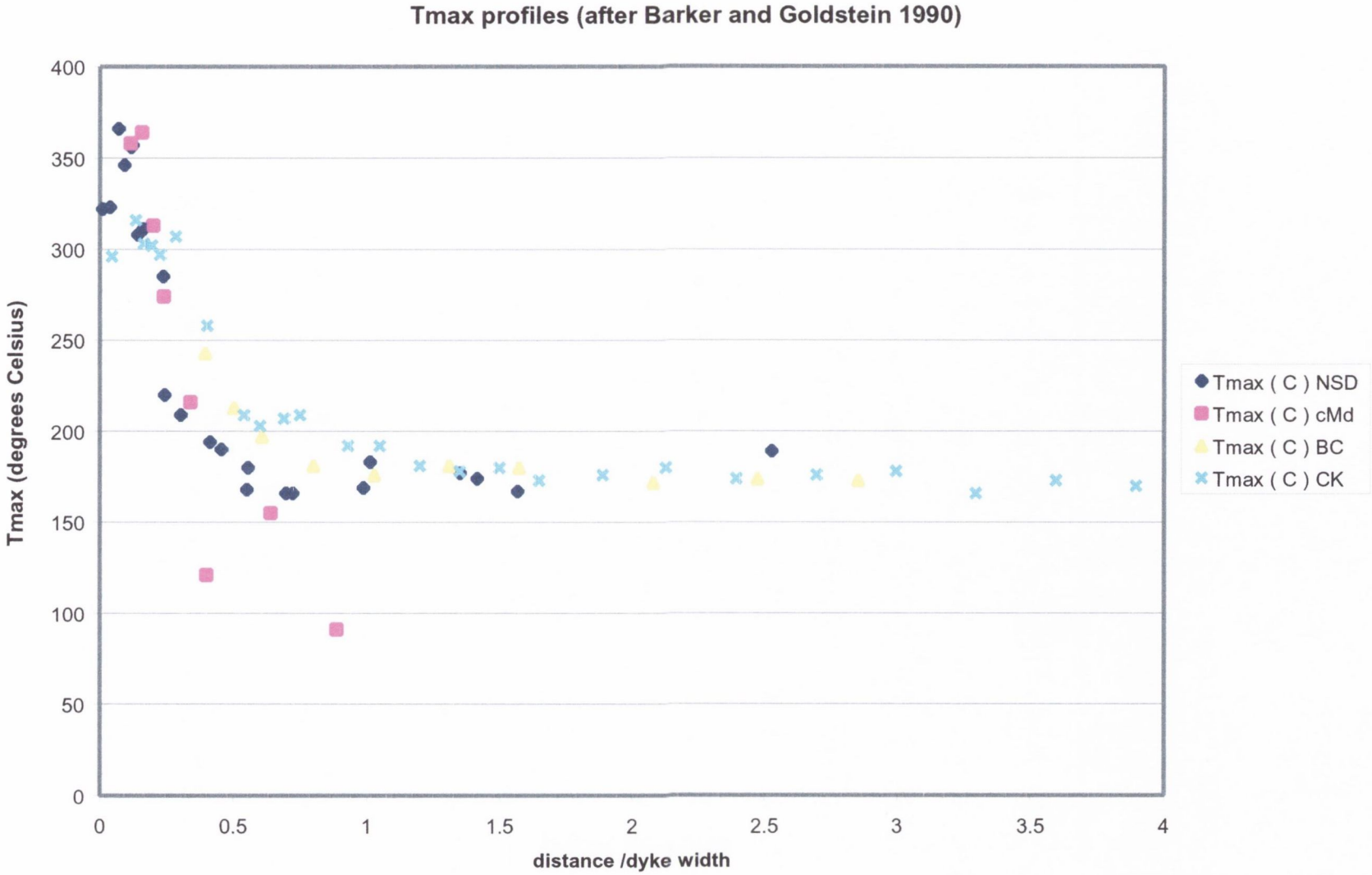

Figure 4.14 Maximum temperatures (Tmax) calculated from VR using the temperature conversion equation of Barker and Goldstein 1990

4.8 DISCUSSION

4.8.1 THE GOBB SECTION BALLYCASTLE

The coal horizon of Cl9 is approximately 14m below the Gobb sill, whose vertical extent is unknown. It is assumed that the relatively elevated reflectance value is due to proximity to the overlying sill.

1. The log of the Gobb section records a continuous sequence, however the slopes of the disused Gobb colliery are grassed over and have a covering of patchy rubble and scree. The profile shows reflectance values increasing between Cl13 and Cl16, and a particularly steep increase between Cl15 and Cl16. If this were due to burial, the rank increase would be expected to be more regular and a geothermal gradient of $1.2\%R_r\ km^{-1}$ could be invoked. However, compared to the material above, it would not be unreasonable to suggest that the profile might suggest that there could be another igneous intrusion in the rocks not very much further down the column. There is no field evidence for this nor has any such igneous body been reported in any of the literature reviewed on the area.
2. It is also be possible that the VR of Cl16 may be due to different depositional conditions and or different vitrinite sub-maceral content (Veld *et al.* 1996, Carr 2000). Veld *et al.* (1996) related VR and hydrogen indices differences in coals that couldn't be differentiated by their telocollinite:desmocollinite ratio to their depositional environment, quoting fluviatile influenced environment to have had significantly lower VR, than those formed under deltaic conditions. The lithologies in the area represent fluctuating influence between marine and brackish waters (pers. comm. Evans 1998) so this hypothesis may not be disregarded.
3. It is also possible that the higher VR readings are a result of localised heating by fluid movement (although there is no field or laboratory evidence for this).
4. Finally the option for operator error is not to be ignored. It is worthy of note however that the majority of the samples from this section are in accord with the values quoted by Evans (1998) and Clayton *et al.* (1989).

4.8.2 VR AUREOLE PROFILES

4.8.2.1 OBSERVATION

1. There is enough vitrinite in each of the horizons, CK (Carrickleck), NSD, BC and cMd (Ballycastle) to ensure statistically sound results
2. The CQ horizon, from Carrickleck, is barren of vitrinite

3. All VR profiles show an increase in VR with proximity to the dyke
4. VR from the aureole of the thicker, multiple intrusion, North Star Dyke records higher VR_{max} values than VR from the aureole of the thinner, single intrusion, Carrickleck Dyke.
5. Maximum values recorded from both dyke aureoles are not recorded from samples collected closest to the dyke/host rock contact
6. CK, NSD and cMd horizon VR profiles all exhibit trend reversal for samples closest to the dyke
7. Irregular VR profile in the CK traverse between 0.2 and 0.4m
8. Variation in background VR at Ballycastle-(i)similar values for the BC and NSD horizons variance to the VR cMd horizons and (ii) reflectance values measured from coal samples are generally lower than those measured from vitrinite extracted from mudrock horizons
9. In the North Star Dyke aureole, VR_{max} is recorded at 0.3m from the dyke contact in the NSD horizon, at 0.6m from the dyke/sediment contact in the cMd horizon. These distances are equivalent to approximately 7% and 16% of the dyke thickness ([(measured distance from the dyke)/(dyke thickness)]x100).
10. VR_{max} is recorded at 0.2m from the dyke/sediment contact, which is a distance equivalent to approximately 14% of the dyke thickness.
11. VR_{max} is recorded at greater distances from the dyke/sediment contact in the North Star Dyke aureole than in the Carrickleck aureole.

4.8.2.2 DISCUSSION

All vitrinite reflectance profiles from lithologies intruded by both dykes show a general trend of increased VR with proximity to the dyke. This implies that vitrinite reacted to the swift heat pulse emitted by dyke intrusion at both locations and that vitrinite reacts, in geological time, swiftly and is sensitive to temperature increase.

It is not surprising to note that VR_{max} recorded from the host rocks intruded by the North Star Dyke (5.55%R_r and 5.45%R_r) are higher than VR_{max} recorded from the host rocks intruded by the thinner Carrickleck Dyke (3.65%R_r). The North Star Dyke is *c.*4m thick and Carrickleck Dyke is less than half this thickness at *c.*1.5m. Thus the North Star Dyke had a greater volume of hot magma and therefore a greater body of heat. The North Star Dyke is also a composite body of 3 intrusions, meaning that magma flow would have been prolonged relative to the single intrusion that is the Carrickleck Dyke. Sustained flow and

the thicker body of the North Star Dyke implies that it must have sustaining the elevated temperatures for a longer period of time than might have been sustained by the Carrickleck Dyke.
Assuming that both situations were sufficiently similar at time of intrusion this implies that vitrinite reflectance is sensitive to temperature and although vitrinite can react very quickly to temperature increase, time is still a very important factor, i.e. it can only register the equivalent reflectance value for the temperature to which it is exposed if it is given sufficient time to react.

At the North Star Dyke VR_{max} is recorded at 0.3m from the dyke in the NSD traverse, at 0.6m from the dyke in the cMd traverse. These different distances of recorded VR_{max} may be a reflection of different lithological characteristics, such as conductivity, permeability, contained connate waters. It is considered by this author more likely to be related to differences in the original starting material/vitrinite measured from each horizon (i.e. the vitrinite measured in each of the horizons may be of different origins).

NSD and BC have similar background reflectance values (*c.*1.1%R_r); cMd records background VR values at *c.* 50% lower (*c.* 0.5%R_r).
NSD and cMd show what appears to be a sharper increase, closer to the dyke than the BC curve, which has a shallower slope and more consistent VR along its length. There is an incipient problem with the BC horizon and interpretation of the vitrinite results. There was insufficient sampling in the area closest to the dyke, to allow detailed examination of how the vitrinite from this horizon reacted in the area closest to the dyke.
NSD and cMd both record maximum reflectance values of approximately 5.5%R_r. However, cMd records maximum reflectances at a distance, twice that seen in the NSD horizon, 0.6m and 0.3m respectively. cMd is not as densely sampled as the NSD horizon in the region directly adjacent to the dyke. If there were more samples collected at lesser distances from the dyke in the cMd horizon, then maximum reflectance values might have been observed closer to the dyke. Alternatively, it may be an expression of a differing conductivity, organic composition or something that has not yet been considered in this work. (Future work).

VR_{max} is recorded at 0.20m from the Carrickleck Dyke. This VR_{max} is recorded closer to the Carrickleck dyke than the VR_{max} values recorded in the North Star Dyke aureole. This

is probably another consequence of the heat generated by the thicker, multi-intrusion North Star Dyke relative to the Carrickleck Dyke.

The CK, NSD and cMd horizons all exhibit a trend reversal in VR values for samples closest to the dyke. This reversal at the contact with an intrusion is not uncommon (Raymond and Murchison 1988, Khorasani *et al.* 1990, Bishop and Abbott 1995, Barker *et* al. 1998), but nor has it not been universally recorded. The mechanism responsible for this trend reversal is not understood. Various authors have made observations on this phenomena. (a) Khorasani *et al.* (1990) have shown increased molecular disorder in vitrinite close to intrusions. From their work, they conclude that these reversals tend to be observed in thermal aureoles that are relatively wide for the intrusion thickness, and assert that "such aureoles develop when the intrusion is emplaced after considerable lithification of the sediments and the background temperature has substantially raised the rank level of the sedimentary organic matter or coals prior to intrusion" (Khorasani *et al.* 1990). (b) Other authors have suggested that the difficulty in attaining large, uniformly polished vitrinite for measurement is partly to blame, because of increasingly finer sized granular anisotropy, due to progressively smaller and more variable reflectance domains (Bishop and Abbott 1995, Barker 1998).

While this author would definitely not dispute the above reckonings of other authors she would also like to offer the following as possible reasons for this trend:

(1) Perhaps there was some volume of connate water present in the rocks at time of intrusion. These waters would have been drawn to and concentrated at the contact and vaporised. If this was the case then the contact will experience the greatest pressure, exerted by the expelled fluids (overpressure), which will be sustained until all of the fluid has been expelled and has dissipated out into the rock. The fluid would create a situation whereby the contact would experience (a) an increased conductivity, and (b) overpressure. The enhanced conduction should have acted to accelerate heat flow away from the dyke, and the overpressure would have had a retarding effect on rank increase in the area immediately adjacent to the dyke. The idea that there may have been fluids expelled from the dyke should not be immediately discarded as there is evidence in the changing clay mineralogy through the dyke and aureole (further discussed and explored in chapter 5), and the veining of the coals may also suggest this situation.

(2) Alternatively, duration and rate of heating during intrusion may have played a major role in the trend reversal. Vitrinite maturation involves complex parallel reactions that do

not occur simultaneously and involve the expulsion of fluids. Is it possible that the very swift initial pulse of heat that is experienced on contact with the intruding magma, causes the rate of some but not all of these reactions to accelerate or decelerate, thereby changing progression along the reaction path. Or the rapid heat fluctuations at intrusion may have started some reactions, and brought them part way but not to completion, leaving them incomplete and without enough material left to re-initiate and progress to completion.
(3) a combination of both (1) and (2).

The CK VR profile not only records the maximum VR at 0.2m from the dyke, but the area between 0.4 and the dyke margin shows an elevated and slightly irregular pattern. Fluid flow along the contact area, or heat of friction if there was movement along the fault, post intrusion, in the Carrickleck situation may have contributed to the erratic vitrinite reflectance values recorded adjacent to the dyke. However this is probably not the sole reason.

4.8.3 MINERALISATION OF THE COAL LENSES IN THE CMD HORIZON

The vein/fracture system of the coal samples Co4 and Co2 (see Appendix IV, plates 4.2-4.3) are quite complicated and appear to have been introduced to the coal lenses in a number of different phases, and have been divided into 3 phases:

Phase 1 = sub-horizontal complex fracture networks. The fracture networks enclose slivers of coal that are generally lens shaped, particularly towards the outer edges of the body of the coal lense. Thinner veinlets are concentrated at the outer edges of the coal lenses and slightly thicker veinlets are observed further into the body of the lens. The fracture network is mineralised by ankerite, and to a lesser degree, calcite, (*pers. comm.* Sevastopulo 2002), causing vertical dilation. This fracture system is considered to be a result of compression due to lithostratigraphic load. The compression of the coal lense is expressed in this phase as shearing at the contacts, with the more competent centre remaining intact, resulting in net elongation. The mineralisation is thought to be a function of diagenesis.

Phase 2 = parallel, vertical – oblique, normal fractures, which crosscut and displace the horizontal veins and fracture system of phase 1. The fracture system of phase 2 is exploited by mineralisation. This phase is one of net elongation and is considered to be a result of continued compression/compaction with burial. It is suggested that as dehydration progressed with burial, and with mineralisation of the phase 1 fractures, the coal body becomes more competent. The overburden pressure, increasing with burial, eventually

causes the coal lense to fracture in this very brittle fashion of high angle normal faults resulting in net horizontal elongation. The fracture system dilated with the mineralisation, which may have been syn- or post faulting and is believed to be a function of later (than phase 1) diagenesis. The timing is unclear. The mineral fill for these faults does not react to HCl, nor does it stain red in the presence of Alizarin red solution, implying that it is not calcite, nor does the mineralisation pick up the potassium ferri-cyanide stain. The presence of dolomite in the XRD traces and the hardness of the veinlets seem to imply that the veinlets are a 'pure' dolomite.

Phase 3 = Pyrite, over prints phase 1 and 2 veinlets, and forms an outer lining for the base of the coal lense. Sometimes the pyrite is observed to surround muddy sediment found within, but near the edge of, the coal lense. Disseminated pyrite is also observed throughout the coal lens. It is interesting to note that there is consistent pyrite mineralisation, concentrated in a thin layer at the bottom of all the coal lenses. This might be interpreted as an indication of a coal/sediment interface reaction due to microbial action at the time of deposition.

Iron rich mineralisation of Co1 (red material, see appendix IV plate 4.1) is concentrated to the lower half of the coal material.

4.8.4 TEMPERATURE CONVERSION OF VR IN THE DYKE AUREOLES

The temperature profiles serve to demonstrate the substantial temperature increase in a dyke aureole, as recorded by vitrinite. They also demonstrate contrasting R_{max} and R_c, recorded by vitrinite in similar lithologies, from the same aureoles. For example in the North Star Dyke aureole none of the sampled horizons cMd, NSD and BC, calculate the same T_{peak} at the same distance along the length of the sample lines. It might also be noted that T_{peak}, calculated from VR, underestimates the predicted contact temperatures, based on heat flow models. This is a well-substantiated observation (Erren and Bredewout 1991, Bishop and Abbott 1995, Goodhue 1996, Barker 1998, McCormack 1998). For further discussion on this topic refer to chapter 9.

Temperature conversion of VR, using any of the published equations discussed in section 4.7, calculate maximum temperatures which are no more than 0.25 the value of the generally accepted temperature (1100 – 1200°C) of an intruding magma. This seems to imply that either (a) the conversion equations are invalid, (b) these conversion equations are invalid in the situation under investigation, (c) the vitrinite from the aureole samples closest to the dykes did not have sufficient time exposed to the elevated temperatures of

the intruding dykes to fully equilibrate and reflect these temperatures – after all the time factor seems to be relevant as the samples collected from the North Star Dyke contain the highest VR_{max} and therefore T_{peak}, or (d) there was another factor, which retarded the evolution of the vitrinite during the intrusion events.

4.9 CONCLUSIONS

Vitrinite reflectance is sensitive to, and reacts quickly to increased temperatures. However, vitrinite takes longer to equilibrate at higher temperatures.

VR_{max} is recorded further from the North Star Dyke than from the Carrickleck Dyke. The thicker, multiple intrusion, North Star Dyke can maintain elevated temperatures for longer, and so the vitrinite gets more time to adjust to the elevated temperatures.

The reverse trend of VR values observed in the areas directly adjacent to the dykes may be due to a number of causes. It is thought however that they are due primarily to VR retardation, caused by overpressure created by vaporised fluids (probably connate waters) at the time of intrusion.

Vitrinite from directly adjacent to a dyke, does not register the true temperature to which it was exposed. Although longer periods of exposure to elevated temperatures results in higher reflectance values, in neither dyke aureole are there reflectance values which might be assumed to represent *c.* 1150°C (approximate temperature of intruding magma).

Temperature conversion equations reviewed and used in this work are either invalid in a dyke intrusion situation or are inadequate to relate the reflectance values of vitrinite in a dyke aureole, particularly vitrinite from less than 0.5m distance from the dyke.

Discrepancies in VR values between the NSD and cMd horizons is thought to be due to differences in the original vitrinite. Further work would need to be considered to confirm this.

Coal beyond the influence of the dyke yields background VR of 0.5%R_r, but vitrinite recovered from clastic sediments yield VR of 1.1-1.2%R_r. This might be interpreted in a number of ways:

1. Vitrinite recovered from the clastic lithologies might have been reworked.
2. Operator error with respect to correct identification of vitrinite
3. The obviously different depositional environments may have led to the concentrations of different starting vitrinites and thus varying maturation paths, leading to contrasting VR values

Mineralisation of the cMd coal lenses was probably a result of diagenesis.

5 CLAYS AND CLAY ANALYSIS

Clay is a general term that refers to a naturally occurring material composed primarily of fine-grained minerals, <2μm, which is generally plastic at appropriate water contents and will harden when dried or fired. Clay usually contains phyllosilicates but it may also contain associated phases that do or do not impart plasticity, and organic matter. The term is usually used in reference to rock.

A **clay mineral** refers to a specific phyllosilicate mineral. Most clay minerals conveniently occur in the clay-sized fraction *i.e.* <2μm.

5.1 CLAYS AND CLAY MINERALS IDENTIFIED IN XRD

5.1.1 CLAY MINERALS

Clay minerals are hydrous aluminium silicates and are classified as phyllosilicates or layer silicates. Phyllosilicates have a highly layered atomic structure, which leads to a tendency towards a perfect (001) cleavage and a platy, friable morphology. These layers can consist of two basic constructs; edge linked octahedra or corner linked tetrahedra. These are the basic building blocks for the phyllosilicates and dictate, to a degree, the properties, physical and chemical, that the clay mineral will possess. The clay mineral structure can be described in terms of the ratio of these sheets e.g. a 2:1 phyllosilicate is a construct of 2 tetrahedral sheets to 1 octahedral sheet.

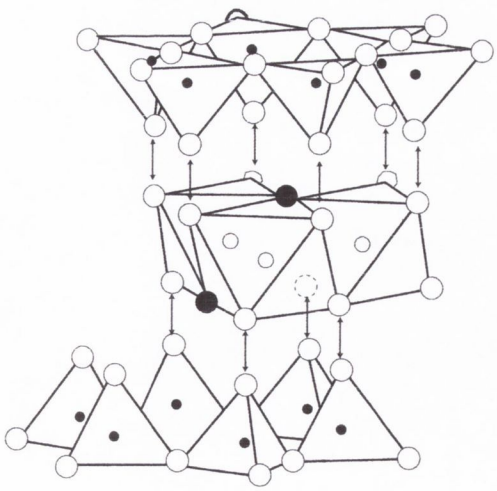

Figure 5.1 An assemblage of 2 tetrahedral sheets sandwiching an octahedral sheet, representing the 2:1 clay mineral. The large black balls represent hydroxyls; small black balls represent tetrahedrally coordinated cations. Small colourless balls are the octahedrally coordinated cations and colourless big balls are oxygens (after Moore and Reynolds 1997)

The **tetrahedral** sheet consists of corner-linked tetrahedra. Each tetrahedron consists of a central four-coordinated atom (e.g. Si, Al, or Fe) surrounded and linked by covalent bonds

to four oxygen atoms that in turn are linked with other nearby atoms. The dominant (central atom) cation (T) to fill this central position is Si^{4+}, Al^{3+} is not uncommon and Fe^{3+} is not so common. The general T/O (where O represents oxygen) ratio for the tetrahedron is T_2O_5.

The **octahedral** sheet consists of edge-linked octahedra. Each octahedron consists of a central six-coordinated metallic atom (e.g. Al, Mg or Fe) surrounded and linked by covalent bonds to six oxygen (O) or hydroxyl (OH) groups that in turn are linked with other nearby metallic atoms, in this way serving as inter-unit linkages to hold the sheet together. The dominant cations of the octahedral sheet is Al^{3+}, Mg^{2+}, Fe^{2+} and Fe^{3+}, however all of the other transition elements except Sc can assume the octahedral cation position.

In layer silicates, octahedral sheets are either gibbsite like, $Al(OH)_3$, or brucite-like, $Mg(OH)_2$. In the latter the cation – anion ratio is 2:1. In a brucite sheet with divalent cations all three of the sites around each hydroxyl must be filled to have electrical neutrality. Layer silicates with this arrangement are described as **trioctahedral**.

Layer silicates with gibbsite like octahedral sheets have a cation – anion ratio of 1:3. To have electrical neutrality only two Al^{3+} cations are needed instead of three Mg^{2+} cations. Thus only two of every three octahedral sites must be filled. These are termed **dioctahedral** layer silicates.

Clay minerals have charges on their surfaces, which determine ion-exchange capacities. There are 2 types of charge; surface layer charge, known as **layer** or **permanent charge** and charge on the broken edges of the mineral structure, known as **variable charge**, i.e. where the structure pattern ends with broken bonds. The **total charge** of a particle is the sum of the permanent charge and the variable charge.

Where a clay mineral has a permanent charge the variable charge is usually less than 1% of the total charge. The variable charge is a function of the pH of the liquid in which the clay mineral is or has been immersed, whereas the permanent charge is independent of the pH.

Some minerals swell with water, others do not. The influence of the layer charge of a mineral extends only a few water layers away from the surface (Moore and Reynolds 1997). Water forms a coordination sphere or shell around most cations, which is more tightly held around some of these cations than others. Water in the interlayer space is

Layer Type	Group	Subgroup	Species
1:1	Serpentine – kaolin (z~0)	Serpentines (Tr) Kaolins	Chrysotile, antigorite, Lizardite, berthierine, odinite Kaolinite, dickite, Nacrite, halloysite
2.1	Talc – Pyrophyllite (z~0)	Talc (Tr) Pyrophyllite (Di)	
2.1	Smectite (z~0.2 - 0.6)	Tr smectite Di smectites	Saponite, hectorite Montmorillonite, beidellite, nontronite
2.1	Vermiculite (z~0.6 – 0.9)	Tr vermiculites Di vermiculites	
2:1	Illite (0.6>z<0.9)	Tr illite Di illite	Illite, glauconite
2.1	Mica (z~2.0)	Tr micas Di micas	Biotite, phlogopite, lepidolite Muscovite, paragonite
2.1	Brittle mica (z~2.0)	Brittle micas	Margarite
2.1	Chlorite (z variable)	Tr, Tr chlorites Di, Di chlorites Di, Tr chlorites Tr, Di chlorites	Common name based on Fe^{2+}, Mg^{2+}, Mn^{2+}, Ni^{2+} Donbassite Sudoite, cookeiite No known examples!!
2:1	Sepiolite-Palygorskite	Inverted ribbons	(with z variable)

Table 5.1 The classification of clay phyllosilicates (from Moore and Reynolds 1997, based on Hower and Mowatt 1966, Bailey 1980, Brindley 1981 and Środoń 1984). z=charge per formula unit.

dynamic i.e. it is rotating and stretching and does not freeze even at temperatures of –30°C. Water in this position is in a state somewhere between bulk liquid and ice.

Swelling clay minerals seem to take in water as single, double or triple layers of water. Swelling or expansion is exclusively along the [001] or Z crystallographic direction.

Water in the interlayer space of expandable clay minerals is controlled by three factors 1. the polar nature of the water molecule; 2. the size and charge of the cations in the interlayer space; 3. the value and localisation of the charges on the adjacent silicate layers.

Expanded clay minerals carry water into the depositional sites. During diagenesis it is released, carrying cations and anions in solution.

5.1.1.1 KAOLINITE

'Kaolin' the word was derived from the Chinese *kualing*, the name of a Chinese mountain, meaning high ridge (Bailey 1988), which was an early source of clays. It has been used to define a group of 1:1 layer silicates, of which kaolinite is a member and the most common.

5.1.1.1.1 PHYSICAL AND CHEMICAL CHARACTERISTICS

Kaolinite has a generalised chemical formula of

$$Al_4Si_4O_{10}(OH)_8. \qquad \text{(Moore and Reynolds 1997)}$$

It is a 1:1, dioctahedral phyllosilicate and has no layer charge or a very small layer charge, which is because all the tetrahedral cation sites are usually occupied by Si^{4+} and the octahedral sites by all Al^{3+} or all Mg^{2+}. If there is substitution in one sheet of a 1:1 layer silicate, there is almost always a compensating substitution in the other sheet so that neutrality is maintained (Moore and Reynolds 1997). However if analysed in detail there may be from 0.1-10% vermiculitic, micaceous, smectitic or some layer combination present in kaolinites (Talibudeen and Goulding 1983, Moore and Reynolds 1997). In nature small amounts of cation substitution can take place. Al can substitute for Si in the tetrahedral sheet; Fe, Ti and Mn can replace Al in the octahedral sheet. The interlayer cation is usually K, but substitution for Ca and Na is not unusual (Newman and Brown 1987). In nature there is always a variable charge due to the broken bonds at the edges of the mineral.

Kaolinite can take the form of vermicular stacks (books) of plates or a platy fine material. Kaolinite has a triclinic structure, unlike its 2-layer polytypes dickite and nacrite, which are monoclinic. Dickite occurs as a hydrothermal mineral and occasionally as an authigenic sedimentary mineral. Nacrite is rare in nature and occurs only in hydrothermal environments (Bailey 1988). Kaolinite does not absorb water and therefore does not expand when it comes into contact with water. It does however swell when solvated in certain organic substances e.g. dimethylsulphoxide.

5.1.1.1.2 IDENTIFICATION

Kaolinite is identified by its first two basal reflections at [001], 12.4°2θ, 7.2Å and [002], 24.8°2θ, 3.6Å. The [002] reflection for kaolinite occurs below 25°2θ, 3.56Å. This is a distinguishing feature as the kaolinite [001], 12.4°2θ, 7.2Å and [002], 24.8°2θ, 3.6Å peaks can overlap with chlorite [002] 12.5°2θ, 14.24Å and [004] 25°2θ, 3.56Å peaks respectively.

It can also be difficult to distinguish kaolinite from some of the other group members. The kaolinite polytypes 'dickite' and 'nacrite' are not as common as kaolinite; where they do occur they are usually associated with hydrothermal alteration. They are impossible to distinguish from kaolinite on the basis of their basal XRD reflections (Moore and Reynolds 1997).

Kaolinite becomes amorphous/the structure is destroyed when heated to 550°C, and when solvated with the organic solution dimethylsulphoxide (DMSO) the first order reflection swells to 11.2Å (Moore and Reynolds 1997).

5.1.1.1.3 OCCURRENCE

Kaolinite is a widespread clay mineral in clastic sedimentary rocks. It can occur as a detrital constituent in nearshore deposits or as an authigenic phase in, for example, sandstones. It is commonly found as a diagenetic mineral filling pore spaces. It is also a major component of the mantle regolith particularly in weathering profiles and hydrothermally altered felsic rocks. It can be formed by the weathering or alteration of aluminosilicate minerals, such as plagioclase and muscovite. In order to form kaolinite, ions like Na, K, Ca, Mg and Fe must first be leached away by the weathering or alteration process. This leaching is favoured by acidic conditions (low pH).

The breakdown products of kaolinite can react with (where) available Fe and Mg to form illite and chlorite. However, when a system is Al rich and Fe poor, the tendency is to form pyrophyllite (Merriman 2002b)

5.1.1.2 PYROPHYLLITE

The name is derived from the Greek *pyr* 'fire' and *phyllon* 'leaf' in reference to its tendency to peel when heated.

5.1.1.2.1 PHYSICAL AND CHEMICAL PROPERTIES

Pyrophyllite has a generalised chemical formula of:

$Al_2Si_4O_{10}(OH)_2$ (Moore and Reynolds 1997)

This is a basic, 2:1, dioctahedral, aluminium phyllosilicate, without layer charge. Pyrophyllite should not have any substitution or interlayer material in the ideal case, however in nature there may be some small amount of substitution in the Al and Si octahedral and tetrahedral sites. Al can substitute for Si in the tetrahedral sheet, this is compensated by the change of O^{2-} to OH^-. However in nature this is never a complete transformation and the extra charge allows for the attraction of some few cations in the interlayer, namely K, Na and Ca. Ti, Fe, Mg and Mn can substitute for Al in the octahedral layer.

This is a soft mineral with good cleavage due to very weak interlayer bonding and varying degrees of stacking order.

5.1.1.2.2 IDENTIFICATION

Pyrophyllite is identified by the presence of the basal reflection series: [001] 9.6°2θ, 9.2Å, [002] 19.2°2θ, 4.6Å and [003] 28.8°2θ, 3.06Å. These reflections may not always be observed as they can be overlapping with the illite, quartz and chlorite reflection series.

5.1.1.2.3 OCCURRENCE

Pyrophyllite forms principally in metamorphic rocks. In pyrophyllite-bearing mudrocks pyrophyllite often "first appears in the lower anchizone or in the late diagenetic zone as a regular (R1) interstratified pyrophyllite smectite" (Merriman 2002). Pyrophyllite can be the end member product of the reaction series Kaolin→ dickite-nacrite ($+SiO_2$)→ pyrophyllite, and has been reported in minor amounts in clay assemblages in the British Isles (Merriman 2002a).

5.1.1.3 CHLORITE

The name 'chlorite' derives from the Greek, *chloros*, meaning green, a colour characteristic of many chlorites.

5.1.1.3.1 PHYSICAL AND CHEMICAL CHARACTERISTICS

Chlorite consists, generally, of a negatively charged 2:1 layer, and a negatively charged interlayer octahedral sheet (Moore and Reynolds 1997). Usually trioctahedral, chlorites can also be mixed dioctahedral/trioctahedral, these are called sudoites (Moore and Reynolds 1997), and are quite rare. A generalised chemical formula for chlorite is

$$(Mg, Fe, Al)_{12}(Si_5Al_3)O_{20}(OH)_{16}$$ (adapted from Deer *et al.* 1982)

Chlorites are hydrous silicates usually incorporating the medium sized cations Mg, Al and Fe. The chemistry of chlorite is highly variable and dependent on the whole rock chemistry, pressure and temperature conditions. Chlorite can enjoy cation substitution of small amounts of Al for Si. The solid solution series of Mg-Fe-Al means cation variation in the octahedral sheet. Fe^{2+} and Fe^{3+} are also quite variable, and Ti and Mn can also substitute in very small amounts in the cation sites in the octahedral sheet.

5.1.1.3.2 IDENTIFICATION

High-Fe chlorite commonly has weak odd-order reflections, so weak that they may not appear on the XRD trace. In mutual mixtures the kaolinite ([001] and [002] at 12.4°2θ, 7.16Å and 24.8°2θ, 3.57Å) and chlorite ([002] and [004], at 12.5°2θ, 7.08Å and 25.0°2θ, 3.56Å) basal reflection series superimpose one on the other. The positive identification of chlorite is provided by the presence of the peaks at [001] 6.2°2θ, 14.24Å and [003], 18.8°2θ, 4.73Å. Where the chlorite [001] and [003] reflections are absent DMSO solvation should shift any kaolinite peaks, or heating the sample to 550°C for 1hour should make any kaolinite amorphous to XRD and shift the chlorite [001] 6.2°2θ, 14.24Å peak to 6.3-6.4°2θ, 14.02-13.8Å, and the chlorite 002, 003, and 004 peaks are weakened.

5.1.1.3.3 OCCURRENCE

Chlorite is a common accessory mineral in low to medium grade metamorphic rocks. In fact the regional metamorphic greenschist facies is named for the green of the chlorite that it contains. It occasionally forms in igneous, usually secondarily by deuteric or hydrothermal alteration of low ferromagnesian minerals (Bailey, 1988). In sedimentary rocks chlorite can occur both as detrital and authigenic crystals. Authigenic crystals can be derived from aggradation of less organised sheet silicates. Detrital crystals can be products

of the degradation of pre-existing ferromagnesian minerals and crystallisation from dilute solutions of its components, and by pro-grade alteration of smectite. Chlorites are also found in shales at the highest grades of diagenesis; in soils; as a product of neoformation on the surface of sand grains in porous sandstones, where they may be the alteration product of kaolins; as a replacement of carbonate grains; as matrix in carbonate rocks and in geothermal and low temperature hydrothermal systems.

5.1.1.4 ILLITE

The term 'illite', was first introduced by Grim *et al* (1937) in honour of the state of Illinois, coined for the mica like clay minerals commonly found in argillaceous rocks.

5.1.1.4.1 PHYSICAL AND CHEMICAL CHARACTERISTICS

A generalised chemical structure for illite is:

$$K_2Al_4(Si_6Al_2)O_{20}(OH)_4 \qquad \text{(Moore and Reynolds 1997)}$$

The interlayer cation is usually K, although some substitution of Ca and Na for K is commonly found in natural systems. Illite is a 2:1, dioctahedral phyllosilicate. In their definition of illite, some workers will allow small amounts of interlayer minerals in illite (up to 10%), others will not. It is quite rare in nature to find a pure illite without any interlayer minerals. A common definition for illite (Bailey 1984, Moore and Reynolds 1997) allows up to 5% interstratified layers. These are most commonly smectite but can be vermiculite or chlorite.

Illite is characterised by a rational series of basal reflections with d-spacing of 10Å. Środoń *et al.* (1992) describe all illite layers having a charge of 0.89. Cation substitution in the illite structure can occur in the tetrahedral sheet as Al for Si; in the octahedral sheet, Fe, Ti and Mn can replace Al.

5.1.1.4.2 IDENTIFICATION

Illite is characterised by a rational series of basal reflections with d(001) of 10Å. This is routinely identified as illite mixed with smectite. The basal reflection patterns produce peaks at *c.* 8.9*, 17.8, 26.7*, and 35.9°2θ (* implies that the peak is one of the more intense peaks).

5.1.1.4.3 OCCURRENCE

Illitic material is the most abundant clay mineral in mud-rocks. It can occur in one of the following manners, detrital material, recycled, the product of weathered silicates (primarily feldspars e.g. the weathering of an acidic igneous rock can lead to the formation of illite) or as the diagenetic product of other clay minerals. Illite can form on the exterior layer of grains in porous sandstones, taking the form of thin wiry hairs, described as 'hairy illite'. Illitic material can also form in hydrothermal and metamorphic environments. Most marine illite is detrital; in fact very little illite is thought to form in the sea (Środoń and Eberl 1984).

5.1.1.5 SMECTITE

5.1.1.5.1 PHYSICAL AND CHEMICAL CHARACTERISTICS

Smectite is the name for a group of 2:1 layer type, 'swelling' clay minerals. They have cation substitution in both the tetrahedral and octahedral positions. General formulas for dioctahedral and trioctahedral smectites are:

Dioctahedral $(M^{+}_{x+y}nH_2O)\ (R^{3+}_{2-y}R^{2+}_{y})(Si_{4-x}Al_x)_{10}(OH)_2$

Trioctahedral $(M^{+}_{x+y}nH_2O)\ (R^{3+}_{3-y}Li^{2+}_{y})(Si_{4-x}Al_x)_{10}(OH)_2$

$(M^{+}_{x-y}nH_2O)\ (R^{2+}_{3-y}R^{2+}_{y})(Si_{4-x}Al_x)_{10}(OH)_2$ (Bailey 1984)

5.1.1.5.2 IDENTIFICATION

Smectite readily accepts water and many other liquids into the interlayers. The degree of hydration of the cations can be variable from layer to layer, resulting in non-conformable basal reflections and making identification very difficult. One solution to this problem is to solvate the material in ethylene glycol, which expands the basal spacings to constant values near 5.2°2θ, 17Å.

5.1.1.5.3 OCCURRENCE

Smectites occur in sedimentary and retrograde metamorphic rocks, in deposits of hydrothermal origin, in some pyroclastic rocks (e.g. bentonites) and soils. An important source of smectite is the alteration of volcanic glass with a relatively high Si content or by the alteration of other clay minerals e.g. illite, chlorite or kaolinite. Most important in smectite formation is the presence of sufficient Mg, such that poor drainage and weathering of a basic rock can lead to the formation of smectite whereas good drainage

and weathering of a basic rock can lead to the formation of kaolinite. In fact prolonged leaching of smectite can lead to the formation of kaolinite. Smectite also appears to precipitate directly in pore spaces of sandstone forming a wispy growth on the outer rim of the sand grains and apparently forms in weathering environments characterised by slow movement of water, whether in swampy lowlands or in arid or semi-arid regions (Berner 1971). Smectites also occur as hydrothermal alteration products as metalliferous veins or deposits and near hot springs and geysers, sometimes as the outer part of a zoned deposit along with chlorite. The zoning of the alteration products is attributed to migrating gaseous fluids, the composition of which changes with the reaction with wall rock. Some positive factors in the formation of smectite are poor drainage, alkali conditions, Ca availability and a paucity of K.

5.1.1.6 ILLITE/SMECTITE

Illite/smectite (I/S) is an interstratified clay mineral that exhibits properties of both illite and smectite (Altaner and Bethke 1988). Illite is generally agreed to be more stable than smectite at higher temperatures. It has long been recognised that smectite rich I/S minerals in sedimentary and contact metamorphic environments change with time to more illite rich minerals upon burial and heating. The reaction, termed smectite illitization by some, can drive petroleum migration (Burst 1969, Bruce 1984) and cause geopressures (Powers 1967, Bethke 1986). Just how the transition from smectite to illite/smectite to illite takes place is not yet understood. Hower *et al.* (1976) argued that the transition takes place according to the following reaction

K-feldspar + smectite → illite + chlorite + quartz

although there are many alternative routes (Merriman 2002). Three of the most important variables in the illite to smectite transition are temperature, time and the availability of K. Temperature or heat energy, to stimulate the reaction, can come from a number of sources: 1. burial and geothermal gradient; 2. hydrothermal fluids and 3. intrusion of an igneous body. There are those who have described a reaction in which all smectite reacts to form illite at the same time. Proponents of this idea have called this punctuated diagenesis (Morton, 1985, Ohr *et al.* 1991, Freed and Peacor 1992). The illitization reaction is in part time dependent. It has been noted that %smectite in I/S values are not significantly affected by a sill like intrusion unless they are very near the contact (Esposito and Pollastro 1995, Smart and Clayton 1985). It has been postulated that the transformation of illite/smectite of low expandability occurs too slowly to reflect the effect of minor intrusions except where

near the contact (Smart and Clayton 1985), for example the circulating alkaline hydrothermal water associated with the Cuilin Centre of Skye, was probably rich in K and Na derived from leaching of K-feldspars and plagioclase in granites (Taylor and Forester 1971). Thus pore water may have aided the destruction of smectite (Andrews 1987). Acid solutions generated in or near an overlying coal have opened illite layers thereby forming I/S; expandability increases towards the coal where leaching was most intense. A small reversal of this trend noted beside the coal was postulated to represent a local increase in K^+ derived from vegetal matter. The chemical composition of pore waters in contact with clay is also important in the illitization of smectite, specifically the activity of K^+ and Na^+ ions (Long and Neglia 1968, Shaw 1980 in Andrews 1987).

Expandability is a measure of the percentage of swelling interlayers in I/S. The expandable nature of the I/S clay, and the generally observed decrease in expandability, increased ordering and decrease in imperfections of the material with burial led to the attempt to quantify the expandability and order of this mixed layer clay. A term used to describe 'order-disorder' is the **Reichweite** ("the reach back"), R. This is a means of expressing "the probability, given layer A, of finding layer B next to it" (Moore and Reynolds 1997). The nomenclature expresses how far the influence of the first layer extends or reaches. For example for the R3 sequence, ISII, the first I (illite) has influence that reaches three positions to the last I, such that each smectite would be surrounded by at least 3 illite layers. Order for both components occurs when the composition is exactly 50% smectite and 50% illite for R1.

The **intensity ratio** (Ir) of Środoń and Eberl (1984), is the ratio of the I/S (001):(003) reflections of an air-dried oriented solution divided by the ratio of the (001):(003) I/S reflections of the ethylene glycol solvated oriented solution. A ratio of 1 indicates no swelling layers; while Ir >1 indicates the presence of expandable layers.

(5.1) $$Ir = (I[001]/I[003])_{\text{air dried}}/(I[001]/I[003])_{\text{glycolated}}$$

5.1.1.6.1 IDENTIFICATION

Where an I/S phase is present at *c.* 8.8°2θ, 10Å XRD peaks are broadened and made asymmetrical by the presence of mixed layering and order-disorder of the I/S phase. Greater smectitic content and disorder tends to shift the 8.8°2θ, 10Å peak to lower angles. Over the course of the illitization reaction (*i.e.* as ordering increases and illite content increases) the reflection drifts towards 10Å, and the peak should narrow.

5.1.2 NON CLAY MINERALS IDENTIFIED IN XRD

5.1.2.1. GYPSUM $CaSO_4.2H_2O$

Gypsum is probably the most common sulphate in sediments. The word derives from the Greek *gypsos* 'plaster' and 'cement'. Gypsum is identified by the reflection series [020] 11.58°2θ, 7.56Å, [121], 20.84°2θ, 4.27Å, [141], 29.18°2θ 3.059Å. Gypsum is commonly found in clays and limestones, sometimes associated with sulphur.

5.1.2.2 HALITE NaCl

Halite, the word was derived from the Greek *hals* meaning 'salt', describing the mineral, which is a common salt. It was used in the preparation of samples for PVP-10 intercalation and thus has been artificially introduced into samples. It is identified by the reflection at 31.7 °2θ (2.82Å).

5.1.2.3 CALCITE $CaCO_3$.

The name as derived from the Greek *chalx* meaning 'lime', and is identified by the [104] reflection at 29.42 – 29.6°2θ (3.03Å).

5.1.2.4 Fe Mg CARBONATES

The following of the Fe Mg carbonates are mentioned as they have been identified in hand specimen in the coal lenses of the cMd horizon and both have very similar reflections that are difficult to tell apart.

DOLOMITE $CaMg(CO_3)_2$,

Dolomite was named after Deodat de Dolomieu (1750-1801), a French mineralogist, and is identified by the [104] reflection at 30.92°2θ (2.89Å).

ANKERITE $Ca(MgFe)(CO_3)_2$

Ankerite was named after the Professor M.J. Anker, Styrian mineralogist, and is identified by the [104] reflection at 30.82°2θ (2.91Å)

Carbonates found in clays are usually those having rhomdohedral, calcite-type structures (Brown 1984). The3 carbonates above are all trigonal carbonates, and form an limited solid solution series usually involving the replacement of Ca by Mg, Fe and/or Mn. Calcite and dolomite can occur as primary sediments.

5.1.2.5 APATITE $Ca_5(F,Cl)(PO_4)_3$

Apatite the name derives from the Greek *apate* 'deceit', in allusion to its commonly being confused with other minerals. It is found in all kinds of rocks e.g. in igneous rocks, (especially pegmatites) and metamorphosed limestones, and is a common detrital mineral.

5.1.2.6 PYRITE FeS_2

Pyrite is the most widespread sulphide mineral and is often found as an accessory mineral in igneous rocks; in hydrothermal ore veins; contact metamorphic deposits; anaerobic sediments. Oxidation of pyrite in shales often leads to the formation of iron sulphates in association with clays. The name comes from the Greek *pyr* meaning 'fire', possibly in reference to the sulphurous smell that it gives off when struck. Pyrite is identified by its reflection at 33.02°2θ (2.7Å)

5.1.2.7 QUARTZ SiO_2

Quartz derives from the German word *Quarz.* It was first introduced in a German medieval miners language, although the original meaning is now lost.

Common quartz (also known as alpha quartz) is one of the polymorphs of silica and is stable up to 573°C. This alpha quartz is identified by the [100], and [101] reflections at 20.8°2θ (4.27Å) and 26.6-9°2θ, (3.34Å). Quartz is an important rock-forming mineral, and found in acid igneous rocks, in many metamorphic rocks, as hydrothermal vein fill and in many sedimentary rocks as a detrital constituent or as cement.

5.1.2.8 FELDSPARS

Feldspars are the most important single group of rock forming silicate minerals. They are tectosilicates (3-dimensional framework structures). Feldspars are either monoclinic or triclinic, and four chemically distinct groups exist – potassium/alkali feldspars, sodium feldspars, calcium feldspars, and barium feldspars. At high temperatures there is a continuous series of solid solution between potash feldspars and soda feldspar, but at low temperatures only a limited solid solution is possible.

ALKALI FELDSPARS

MICROCLINE $KAlSi_3O_8$

Microcline (of Greek derivation *micros* 'small' and *klinen* 'to incline' in reference to the twinning effect) is a triclinic member of the alkali feldspar group, the general name for

triclinic potassium feldspar. It is the 'potash feldspar' that usually forms intergrowths with quartz (graphic granite) and with albite (perthite) in granite pegmatite. It is also a relatively common detrital mineral in many sedimentary rocks. Microcline is identified by the presence of a reflection at 27.5°2θ, (3.24Å)

PLAGIOCLASE FELDSPARS

Plagioclase describes a solid solution series of sodium to calcium triclinic feldspars. The sodium plagioclases are found mainly in alkali rich rocks (granites and syenites) while the calcium rich end members are characteristic of basic rocks (basalts).

Albite ($Na(AlSi_3O_8)$), from the Latin *albus* meaning 'white', in allusion to its colour, is the Na rich end member of the plagioclase Na – Ca series. It is identified by the presence of the reflection at 27.95°2θ, (3.19Å)).

Anorthite, from the Greek negative prefix *an-* with *orthos* 'upright' in allusion to the oblique crystal form, is the Ca rich end member of the plagioclase series is identified by the presence of two peaks at 27.8°2θ (3.21Å) and 28°2θ, (3.18Å) of equal magnitude.

5.2 CLAY MINERALOGY AS AN INDICATOR OF METAMORPHIC CONDITIONS

The presence of kaolinite and smectite is dependent on both the metamorphic grade and compositional factors (Kisch 1987). As kaolinite shows only minor compositional variations and is replaced by a discontinuous reaction, its compositional dependence is easier to ascertain. Kaolinite in shales tends to be replaced in the 1.2 – 1.9%R_r range, but can persist to at least 2.2%R_r. For example studies of deeply buried Carboniferous sequences in the Arkoma basin indicate that kaolinite is present to thermal maturities of R_r=1.9 – 2.1% (Spötl *et al.*) equivalent to the lower anchizone. However in sandstones at temperatures of 120°C and greater kaolinite to dickite transformations have been reported (Frey and Robinson 1999). However, it has been shown that the disappearance of kaolinite differs substantially depending on the associated lithology, and kaolinite has been observed in kaolinite-coal tonsteins and underclays of anthracite rank (Kisch 1969). Although the replacement of kaolinite is strongly dependent on the concentration of cations such as K, Mg and Fe, it does not appear to be affected by the cation activities imposed by the solution (Velde and Nicot 1985). Kaolinite goes to its polytypes, nacrite and dickite, with increasing metamorphic grade. Kaolinite transforms to the more stable dickite at about

3km depth below the seafloor, at about 120°C, in sandstone reservoirs on the continental shelf of Norway (Moore and Reynolds 1997). Thus, the disappearance of kaolinite in well-defined assemblages appears to be a good indicator of metamorphic grade, however nacrite and dickite are indistinguishable from kaolinite using XRD (Moore and Reynolds 1997) and are simply identified as kaolinite.

Authigenic chlorites are found in shales at the highest grades of diagenesis and in geothermal and low temperature hydrothermal systems. Chlorite is one part of the mineral assemblage which represents the greenschist facies. Hayes (1970) and Kisch (1983) (from Frey 1987) suggested that chlorite polytypism was a potentially useful geothermometer. However the polytypes are difficult to distinguish using XRD and detrital chlorites may hamper analysis and interpretation.

The presence of abundant, discrete, smectite in mudstones normally indicates immature lithologies, of early diagenetic zone, with depths of burial less than 4km and palaeotemperatures that have not exceeded *c.*100°C (pers. comm. Kemp and Rochelle 1998).

The most prominent changes in the clay mineralogy of sedimentary rocks upon burial diagenesis are the progressive disappearance of kaolinite and smectite and the emergence of illite and chlorite as the major phyllosilicates at the onset of anchizone metamorphism (Kisch 1987). The discontinuous nature of the smectite to illite reaction through mixed layers upon burial has been documented in a large number of papers. Two major 'clay dehydration stages' can be distinguished (Perry and Hower 1972), the first corresponding to the disappearance of discrete smectite, and the second corresponding to the reduction of the percentage expandable layers from about 35 to 20%. At the latter stage regular stacking order tends to appear. Kisch (1983) attempted to correlate the depth and temperature intervals of this reduction in expandable layers with the geothermal gradients, both based on measurable borehole temperatures. However since then, the palaeothermal gradients in several Mesozoic and Palaoegene basins have been recognised as having been much higher at the time of diagenetic alteration, than they are at present. The correlation with borehole temperatures thus must be abandoned except for geothermal areas and for young sedimentary basins in which the present temperatures can be taken to be reasonably maximal (Merriman and Kemp 1996).

Kisch (1987) is quoted as having published "The most consistent divergence from the predominant relationship between illitization and chloritization of smectite and coal rank is

found in areas that underwent strong, particularly short-lived heating during or after burial". For instance, in the Carboniferous of the Alston Block of the northern Pennines of England, Smart and Clayton (1985) found high VR of mainly 2.5 – 4%R_{max} for a distance of about 1.5 times the thickness of the Whin Sill, whereas with the exception of a very strong drop where sample sites are very close to the contact, the sill had little effect on the smectite layers in I/S. "Under the effect of a steep palaeogeothermal gradient the illitization of smectite, and the degree of clay-mineral alteration in general, lags behind the progress of coalification, resulting in the association of a low degree of clay mineral metamorphism with higher than usual coal ranks" (Kisch 1987).

There is a wealth of data from a number of sources that suggest that phyllosilicates in diagenetic and very low-grade metamorphic conditions do not reflect thermodynamic equilibria (Guggenheim *et al.* 2002).

The mineralogy of very low-grade metaclastites is dominated by the non-diagnostic assemblage illite + chlorite + quartz +/- feldspars +/- carbonates. Nevertheless, the occasional presence, or the first appearance, of pyrophyllite, rectorite, mixed layer paragonite/muscovite, paragonite, lawsonite, stilpnomelane and Mg-Fe-carpholite may be helpful for mineral zoning purposes. Whenever possible the mineralogical investigation of very low-grade metaclastites should be combined with coal rank and fluid inclusion studies.

5.2.1 CLAYS AND CLAY MINERALOGY IN AN IGNEOUS AUREOLE

The lithology, chemical composition and texture of the rocks into which igneous sills were intruded can influence solution chemistry, water availability and starting mineralogy. Reaction rates in clays heated close to igneous intrusions are many orders of magnitude faster than those which occur during basin evolution, and they promote direct transformation of smectite to muscovite without intermediate products (Merriman 2002). Late intrusions into previously buried and tectonised mudrocks can simplify a clay assemblage (Merriman 2002).

Kaolinite commonly decreases in abundance immediately near an intrusion (Goodhue 1996, Esposito and Whitney 1995, McCormack 1998, *pers. comm.* Kemp and Rochelle 1998). Emplacement may have led to the dissolution of kaolinite. Chlorite, on the other hand, has been reported to increase in abundance in the vicinity of the intrusions and decrease at increasing distances, replacing mafic grains such as biotite (Esposito and

Whitney 1995). The relationship between the intrusions and chlorite and kaolinite content is not however always consistent (Esposito and Whitney 1995, McCormack 1998).

Lynch and Reynolds (1985) observed a smectite to illite transition series with an increase in I/S content with proximity to a dyke intruded into smectite bearing shales along a line perpendicular to the intrusion, whereas in burial the total amount of illite smectite seems to decrease with depth. Smart and Clayton (1985) noted that %S in I/S values are not directly related to an intrusion (the Whin Sill) except where close to the contact. They explained this by saying that the transformation of illite/smectite of low expandability occurs too slowly to reflect thermal effects of minor intrusions except where close to the contact.

The formation of authigenic carbonate minerals, such as calcite, dolomite and siderite, in rocks near intrusions have been reported by Esposito and Whitney (1995). They have taken this to imply that Ca, Mg and Fe were mobile at least over short distances. Whether the ions came from fluids released by cooling intrusions or from dissolution of framework grains is unclear, but they believed their presence may have locally inhibited the illitization reaction.

5.3 X-RAY DIFFRACTION

X-rays are a form of electromagnetic radiation of very short wavelength (10 - 10^{-2} nm). They are produced when high-speed electrons, accelerated by high voltage in an evacuated tube, strike a metal object.

In 1895, W.C. Roentgen (1845 - 1923) discovered that when electrons were accelerated by a high voltage in a vacuum tube and allowed to strike a glass or metal surface inside the tube, fluorescent minerals some distance away would glow and film would become exposed. Roentgen attributed these effects to a new type of radiation and called the radiation X-rays after the algebraic symbol *x*, the unknown quantity.

Max von Laue (1879 - 1960) around 1912 showed that if the atoms in a crystal were arranged in a regular array that the crystal served as a grating for very short wavelengths, the scattered X-rays presenting the peaks and troughs of a diffraction pattern. Thus he showed in a single blow that X-rays have a wave nature and that crystals have a regular structure.

This work has been developed into the X-ray diffraction (XRD) analysis of crystals that is commonly used today to identify and investigate crystals.

The theory and technique of X-ray diffraction was developed around 1912 - 13 by W.H. Bragg (1862 - 1942) and his son W.L. Bragg (1890 - 1971). The Bragg equation - derived

by and named after W.L. Bragg - describes the relationship between the angle of the incident X-ray beam and the crystal lattice.

$$n\lambda = 2d\sin\theta$$

n=an integer - nth reflecting plane

λ= the X ray wavelength (nm)

d=the lattice plane spacing in the crystal lattice (nm)

θ=the angle between the incident beam and the reflecting plane of atoms

2.1 the Bragg equation

Thus if the wavelength of the X-ray is known and the angle at which constructive interference occurs is known (or measured) the distance 'd' can be obtained and this is the basis for X-ray crystallography.

XRD techniques provide rapid and inexpensive analyses of clays.

5.3.1 THE X-RAY DIFFRACTOMETER AND OPERATOR CONDITIONS

The X-ray diffractometer used was a Phillips PW1540 diffractometer. A Cu Kα anode was used with standard conditions of 40Kv and 20mA. A Ni-filter was used as a secondary monochromator. The diffractometer was set to 1° divergence slits, a 0.2mm receiving slit and a time constant of 1 second. Peak profiles were recorded as .csv (comma separated values, compatible with exel) and .cpi (comma point indexed compatible with Traces v4) files and examined in the Traces v4 software for PC.

The oriented <2μm fraction sample was run for general clay mineralogy were run at $2°2\theta min^{-1}$ from 2 to 35° 2θ. Oriented <2μm fraction PVP-10 treated samples were run at $1°2\theta min^{-1}$ from 2-20°2θ.

5.3.2 SAMPLE PREPARATION FOR CLAY ANALYSES

All samples are washed under tap water and left for at least 24 hours to dry. The sample is then crushed using a mortar and pestle and sieved through a 0.5mm mesh and then further crushed in an agate mortar and pestle. 5gms of powder was collected for each sample where possible.

5.3.2.1 AIR DRIED SAMPLES

5gm of the prepared powder is placed in a 100ml, graduated cylinder with 5ml of dispersing solution (Calgon or 10% Na Hexametaphosphate) and then topped up to the 100ml mark with deionised water. The cylinder is then capped, shaken vigorously and left to settle for 3 hours. After 3 hours a sample of the <2μm fraction from 3.9cm depth is removed from the cylinder (after Stokes Law using the Atteburges cylinder method) and pippetted onto a glass slide (after the method of Gibbs 1965). The solution is allowed to dry and then run immediately.

After the first run of a sample from the air-dried preparation it was evident that further work was necessary to elucidate the true mineralogy of the samples. For this a number of further techniques were used.

5.3.2.2 ETHYLENE GLYCOL SOLVATION

This is a method used here to: (1) identify or negate the presence of smectite (2) to separate the smectite 001 peak or the mixed layer illite/ expandable mineral from the illite 001 peak. An air-dried preparation is run in the X-ray diffractometer and then solvated in ethylene glycol at 60°C for at least 6 hours. When cooled and removed from the ethylene glycol saturated atmosphere the slide is run immediately. The following indicators of expandability are apparent after glycolation:

(1) the 001 'illite' reflection becomes more asymmetric and features a low angle tail or shoulder. A tail or shoulder also appears on the side of the 003 'illite' reflection

(2) the 001 'illite' reflection is displaced to a higher angle, and the 003 'illite' reflection is displaced to a lower angle

(3) the intensity of the 001 reflection decreases relative to the 003 reflection

5.3.2.3 DIMETHYL SULPHOXIDE (DMSO) SOLVATION

Solvating in DMSO is a method used to positively identify kaolinite. This is made possible by swelling the kaolinite structure. It is useful, especially where an iron rich chlorite and a kaolinite fraction are both present in the same sample. The method employed is as follows: an air-dried sample is prepared and run. The slide is then placed into a DMSO rich atmosphere and left at 60°C for at least 12 hours so that the sample is completely solvated. When cooled and removed from the DMSO saturated atmosphere the sample is run immediately.

5.3.2.4 HEATING A SAMPLE

Some clay structures are destroyed after having been exposed to certain temperatures. The sample is prepared and run as for air dried and then heated in an oven to the required temperature and then run for X-ray diffraction immediately. As long as the necessary temperature is below that of 550°C the sample preparation is as for the air-dried sample. Where the sample is to be heated to 550°C or above the sample is pippetted onto a piece of tile.

5.3.2.5 PRESENTATION OF RESULTS

Presentation, interpretation and discussion of results are presented in chapter 5. Tabulated data for mineralogical identification using XRD are presented in Appendix V.

5.3.3 SAMPLE PREPARATION FOR MUDMASTER ANALYSIS

All samples are washed under tap water and left for at least 24 hours to dry. The sample is then crushed using a mortar and pestle and sieved through a 0.5mm mesh and then further crushed in an agate mortar and pestle. 8g of powder is collected for each sample. The powder is split in 2: 5gms for the standard air-dried preparation and 3gms for crystallite thickness measurements using the MUDMASTER software of Eberl *et al.* (1996).

3gm of the prepared powder is placed in a 50ml glass beaker and covered with 25ml of a 1mol solution NaCl. This is left to stand for at least 12 hours or until the sample is Na saturated. The excess liquid/NaCl solution is removed by decanting 7 times or until the excess water doesn't turn silver nitrate cloudy. The repeated decanting is facilitated by the use of a centrifuge to keep the lighter, <2μm fraction, out of suspension. The Na saturated sample is now placed in a 50ml graduated cylinder and topped to 50ml by deionised water. The cylinder is capped and shaken vigorously and allowed to settle for 3 hours. As before the <2μm fraction is removed from a depth of 3.9cm and is pippetted onto clock glass and allowed to dry. 2.5mg of this sample is then thoroughly mixed with an aqueous solution of PVP-10 (2.0ml deionised water, 1mol solution PVP - 10 and 2.5mg <2μm fraction, Na saturated sample), (PVP - 10 is polyvinylpyrrolidone, molecular weight = 10,000). The sample and PVP-10 solution was mixed in the TCD Geochemistry laboratory by putting the mixture in a 10ml lidded glass bottle and placing it in a paint shaking machine which shakes the sample very vigorously for 10 minutes. The sample goes lumpy if there is too much PVP-10, not enough and the sample doesn't swell completely. The aliquot is then

pippetted onto a silicon metal wafer and allowed to dry. The reaction could be enhanced by heating at 60°C for at least 1 hour. The silicon wafer is cut perpendicular to the (100) plane and glued to a glass slide. This is necessary as the silicon wafer cut in this direction produces a much lower background 'noise' in XRD than the standard amorphous glass slides, which produce quite a lot of 'noise'. Some of the silicon wafers do however produce peaks at 28°2θ and 14.36°2θ and 69°2θ due to the direction in which they were cut. All of the silicon wafer slides were kindly donated to the department by Dr. Denis Eberl.

Once dried the sample is run on the XRD machine, in steps of 0.02°2θ. The illite 001 peak is analysed using the Excel 5 program MUDMASTER of Eberl *et al.* (1996).

5.3.3.1 PRESENTATION OF RESULTS

Tabulated data is presented in Appendix I; XRD raw data and compilation traces are presented in Appendix V; graphs, discussion and interpretation of the data are presented in chapter 5.

5.4 CLAY MINERALOGY RESULTS

5.4.1 CARRICKLECK

Two mudstone horizons were sampled in the Carrickleck Quarry. The XRD traces for each of the horizons reveal a very similar clay mineralogy of kaolinite dominated assemblage with illite, illite-smectite, and chlorite; minor amounts of quartz; trace amounts of feldspar, pyrophyllite, dolomite and calcite only in some of the samples (refer to Appendix V, figures 1 and 2). Gypsum dominates samples CK 7 and CQ0.8, 0.5m and 0.8m from the dyke respectively (see appendix I for sample lists and minerals present).

There is a general reduced mineral reflection intensity in the CK XRD traces for samples nearest to the dyke contact relative to that observed for samples at greater distance from the dyke. There is a tentative identification of pyrophyllite in sample CK8. Quartz is most dominant in sample CK7, which is also a gypsum dominated sample. Quartz reflectance shows a decrease in intensity towards the dyke from that point (refer to Appendix V, figure 1).

The CQ horizon shows a similar intensity reduction towards the dyke margin. General intensity values for CQ illite and kaolinite are lower than in the CK horizon. The CQ

horizon has a consistent carbonate content and a more dominant quartz component than the CK horizon (refer to Appendix V, figures 1 and 2).

5.4.1.1 ILLITE

For both horizons the illite 001 reflection was broad, asymmetric with the development of a broadened low angle shoulder and was invariably measured at less than 10Å. The 002 reflection was also broad but symmetrical. The illite 003 reflection was asymmetric with a high angle shoulder and broad. The presence of common quartz in the sample meant that the quartz 101 and illite 003 reflections were interfering. Solvating samples in ethylene glycol did not produce a 17Å peak, but the broad, illite 001 reflection, collapsed to a narrower, sharper peak with a more complicated left shoulder reflection. The 003 reflection also sharpened and the high angle shoulder collapsed, becoming more symmetrical. This has been interpreted to imply the presence of poorly ordered, mixed layer expandable illite, with a low percentage of expandable layers. Illite 001 shows a general intensity decrease with proximity to the dyke. However the decrease is not constant, but shows a tendency to increase and decrease with an almost regular frequency through the horizon (refer to Appendix V, figure 2 and figure 5.2).

5.4.1.2 KAOLINITE AND CHLORITE

The significant peaks for kaolinite and chlorite overlap in both CK and CQ horizons. The uneven peaks of the chlorite diffraction patterns were observed in some of the traces but were rarely intense enough to consistently appear above 'background' or other interfering reflections on the trace. The presence of chlorite was confirmed by heating the same sample to 550°C, and solvation in DMSO.

The kaolinite 001 peak /chlorite 002 peak, is observed to decrease in intensity with proximity to the dyke. However this is not a gradual intensity decrease. In fact the intensity profile describes gradually decreasing 'packages', defined on either side by a major drop in value (see figure 5.2).

5.4.2.3 QUARTZ

Quartz is a dominant component in the CQ XRD traces, however with proximity to the dyke the quartz [101] reflection becomes less prominent, although it does not entirely disappear. The CK horizon has a minor amount of quartz although the reflection is never

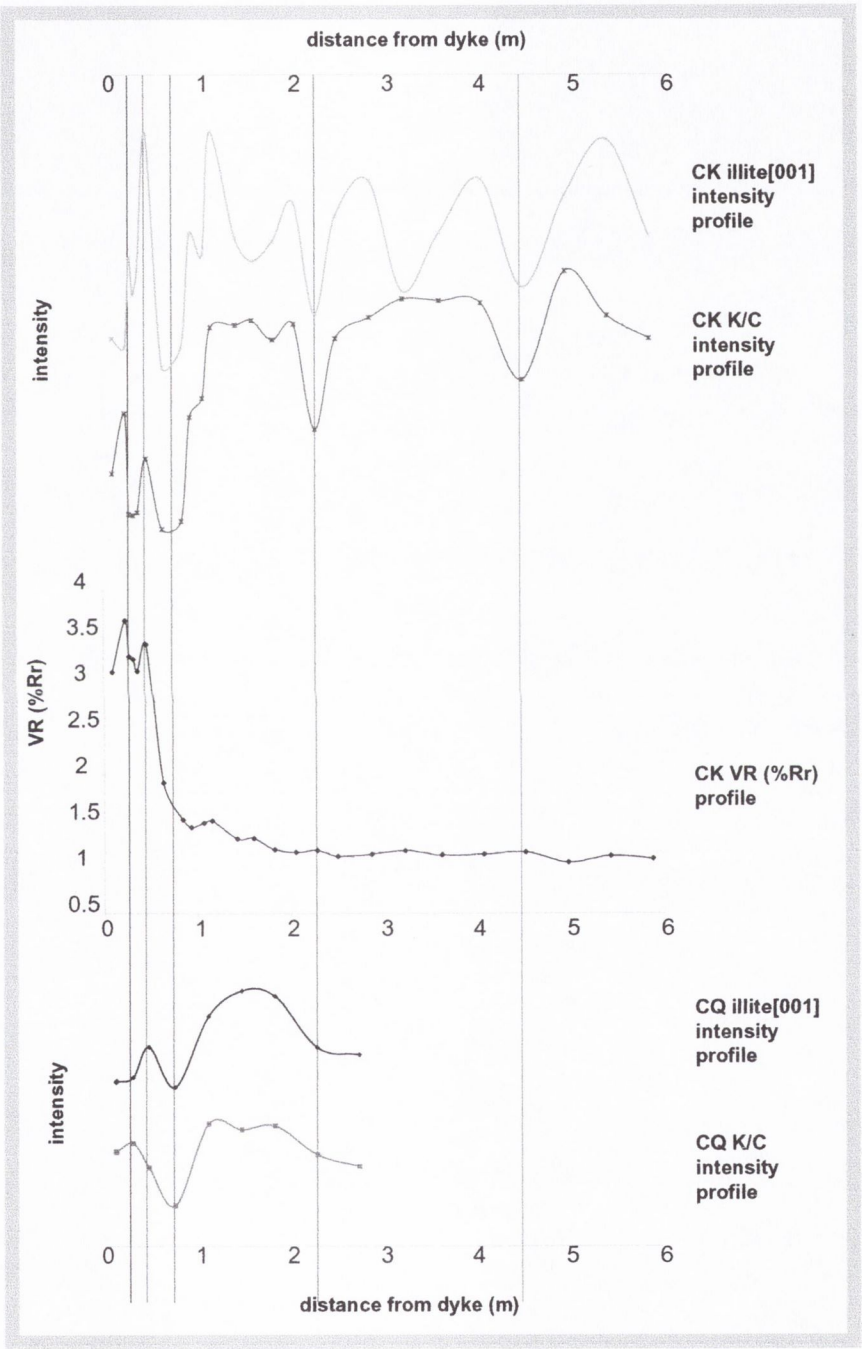

Figure 5.2 Illite, K/C (kaolinite/chlorite) apparent intensity profiles for CK and CQ horizons and the CK VR profile. Correlating the coincident kinks/slope changes in each of the profiles, which can be correlated between the mineralogy and the VR of a single horizon and also between both the CK and CQ horizons.

quite as dominant in the traces as it is in the CQ horizon. It does however become more dominant in the traces as the dyke is approached.

5.4.1.3 CARRICKLECK CLAYS SUMMARY

There is an apparent decrease in the smectitic content (the illite reflections sharpen although the intensity values decrease) in both the CK and CQ horizons adjacent to the dyke.

Kaolinite decreases most dramatically at 0.8m from the dyke. Although there is a continued fluctuation within this 1m region the reflection intensity never regains the stronger peaks seen at distances beyond 1m from the dyke.

Each of the defining drops in intensity seen in the kaolinite profiles coincide with a drop in the apparent illite peak intensity. The lowest values coincide with the lowest value for illite intensity, (see figure 5.2) and show rapid intensity fluctuation in values within the area of the highest recorded VR values (see figure 5.2).

Pyrophyllite is identified in CK8, *c.* 0.6m from the dyke. This is the same position of the lowest illite and kaolinite intensity values. Quartz reflections decrease in intensity with proximity to the dyke, although they become more dominant on the XRD traces

The lowest apparent illite intensity coincides with the sharpest slope increase on the VR profile. The maximum illite intensity coincides with the main break in slope for the VR profile, although beyond this there is an intensity decrease towards the dyke while VR values fluctuate apparently randomly. The kaolinite apparent intensity drops dramatically where there is a strong break in slope of the VR with a large drop in value at the same point in the aureole, and the kaolinite intensity profile increases and decreases at the same points in the aureole as the VR, all the way into the dyke.

If relative intensities of the traces are taken to be a rough representation of the relative 'amounts' of clay in the sample then these results would appear to imply that kaolinite and illite are decreasing in amount as the dyke is approached. The varying intensity profiles show a regular pattern that may be indicative of convective influence.

5.4.2 BALLYCASTLE

There were three mudstone horizons sampled from the North Star Dyke aureole. Each of the horizons shows similar basic clay mineralogy (see Appendix V figures 3-5).

The BC horizon traces are dominated by chlorite, and kaolinite; there are minor amounts of illite with a mixed layer component, calcite and dolomite; traces of quartz, feldspar and apatite were also observed. The XRD traces of cMd samples are characterised by the presence of a dominating smectite peak and minor to trace amounts of a calcium plagioclase and apatite adjacent to the dyke; chlorite and kaolinite dominate the profiles at greater distance, where smectite no longer produces coherent reflections and calcium plagioclase is not observed. There are also minor amounts of illite, with trace amounts of quartz, potassium feldspars, pyrite and dolomite. The NSD horizon can be similarly characterised although apatite is identified as a trace component up to 2.8m from the dyke.

5.4.2.1 SMECTITE

XRD analysis shows smectite as the dominant clay mineral in samples closest to the dyke from the NSD and cMd horizons. Smectite was also identified in XRD profiles of the North Star Dyke itself (see Appendix V, figure 6).

In the NSD horizon the 'discrete' smectite phase can be traced up to 1m from the dyke margin. The 12.5Å (air dried) peak showed a dramatic drop in intensity between 1-1.21m, beyond this point the smectite peak drifts to higher angles and does not produce a discrete reflection on glycolation. What was observed on glycolation was a sloping shoulder on the lower angles of the illite 001 reflection. Where the discrete smectite phase disappears from the traces the kaolinite 001 and 002 /chlorite 002 and 004 peaks increase in intensity. It might be possible to interpret this as kaolinite being preferentially destroyed or leached with the neoformation of smectite.

The cMd horizon XRD traces are dominated by the 001 smectite reflection up to *c.* 1m from the dyke. At *c.* 1.4m from the dyke there was a dramatic drop in intensity, the peak lost sharpness and drifted to higher angles and glycolated traces no longer contained a discrete peak. By 1.6m there were only trace amounts of smectite visible in the XRD reflections.

The BC sample horizon does not have samples closer than *c.* 1.5m from the dyke. According to the NSD and cMd horizons, this is beyond the range of this smectite phase. The BC samples were not dominated by smectite. There is an increase in the smectitic component from 11-2.5m from the dyke, which is followed by a drop in the smectitic

component, at 2m and 1.5m. Solvating these samples in ethylene glycol does not produce a discrete smectite peak.

5.4.2.2 ILLITE

Illite is not a major component in any of the BC, cMd or NSD horizons. The BC profile shows a maximum illite intensity at *c.* 2.4m and maximum drop in intensity at *c.* 2m. The cMd traces show minimum recorded illite intensity at *c.*1.5m.

The NSD apparent illite intensity profile is much more irregular and any pattern difficult to discern. Illite intensities from glycolated traces are predictably lower, particularly within 2m of the dyke. Solvating the NSD samples in ethylene glycol effectively halved the illite peak intensity values and smoothed the profile (see figure 5.3). There is a final rise in illite apparent intensity within 0.5m of the dyke margin, even after glycolation.

Solvating the samples in ethylene glycol rarely produced a sharp 10Å peak in any of the North Star Dyke horizons, but did result in a broad shoulder to the left of the illite 001 reflection. This might imply that there is not a lot of smectite in the I/S and/or that it is very poorly ordered.

5.4.2.3 KAOLINITE AND CHLORITE

As in the Carrickleck samples the kaolinite and chlorite peaks from the BC, cMd and NSD traces overlap and interfere. The main peaks are 12.4 and 24.9/25 °2θ, the odd order chlorite reflections were rarely observed. The dominance of the 12.4 over 24.9/25 °2θ reflections suggests the presence of an iron rich chlorite fraction.

All 3 horizons recorded an increasing kaolinite intensity with proximity to the dyke, maximum intensity occurring beyond 2m from the dyke contact. Each of the profiles showed a decreased intensity at *c.* 2m from the dyke, although the BC profile has a more extreme decrease than either the cMd or NSD.

The intensity reduction of the 12.4 and 24.9/25 °2θ reflections not only coincides with the first appearance of a discrete smectite reflection but also with the greatest drop in the apparent illite intensity and the sharpest increase in the VR profile. The area beside the dyke where the higher VR values are recorded reflects the greatest drop in kaolinite, reflections followed by a slight rise in peak intensity.

5.4.2.4 CARBONATES

Calcite and (Fe, Mg) carbonates were present in all of the North Star Dyke sample horizons in minor to trace amounts. These minerals were present most consistently in the BC sample horizon. Calcite peak intensity is seen to gradually increase as the (Fe, Mg) carbonates intensity decreases (see figure 5.3), as the dyke is approached. Generally what is observed in the profile is where the calcite peak shows an increased reflection intensity the (Mg, Fe) carbonate peak records a lowered intensity and vice versa. Calcite is the dominant intensity of the two in the sample, collected closest to the dyke (*c.* 1.6m from the dyke margin).

5.4.2.5 QUARTZ

Quartz is present in trace amounts in the <2μm fraction XRD traces for each the three horizons, but significantly lessens and disappears from the traces with proximity to the dyke. For the cMd horizon quartz is last identified at 0.6m, for the NSD horizon quartz is last identified at 0.4m from the dyke and for the BC horizon quartz is present in very trace amounts only and is not observed at 1.5m from the dyke.

5.4.2.6 FELDSPAR

Calcium plagioclase, is identified in the North Star Dyke <2μm XRD trace. It is also identified in the NSD and cMd samples adjacent to the dyke margin. Calcic plagioclase forms at relatively high temperatures for example anorthite forms at *c.*> 1300°C at 1kbar in the pure diopside:anorthite phase system (see figure 9.4). In the impure natural state this crystallisation temperature can be lowered, particularly in the presence of water.

In the NSD horizon, calcium plagioclase is a major constituent of the <2μm fraction adjacent to the dyke margin. The reflection intensity of the calcium plagioclase weakens in samples further from the dyke, and was last observed at *c.* 0.6m, from the dyke margin. Microcline was identified in the NSD horizon at 0.95m from the dyke and background samples. A problem with identifying the feldspars in the XRD traces is the presence of the quartz and expandable illite reflections. This is also the <2μm fraction that is being observed and the main representative feldspar fraction is the >2μm fraction. Solvating in ethylene glycol revealed a sodic feldspar (?Albite) peak in the glycolated NSD11 sample at 1.21m from the dyke, and microcline in NSD14 1.82m from dyke.

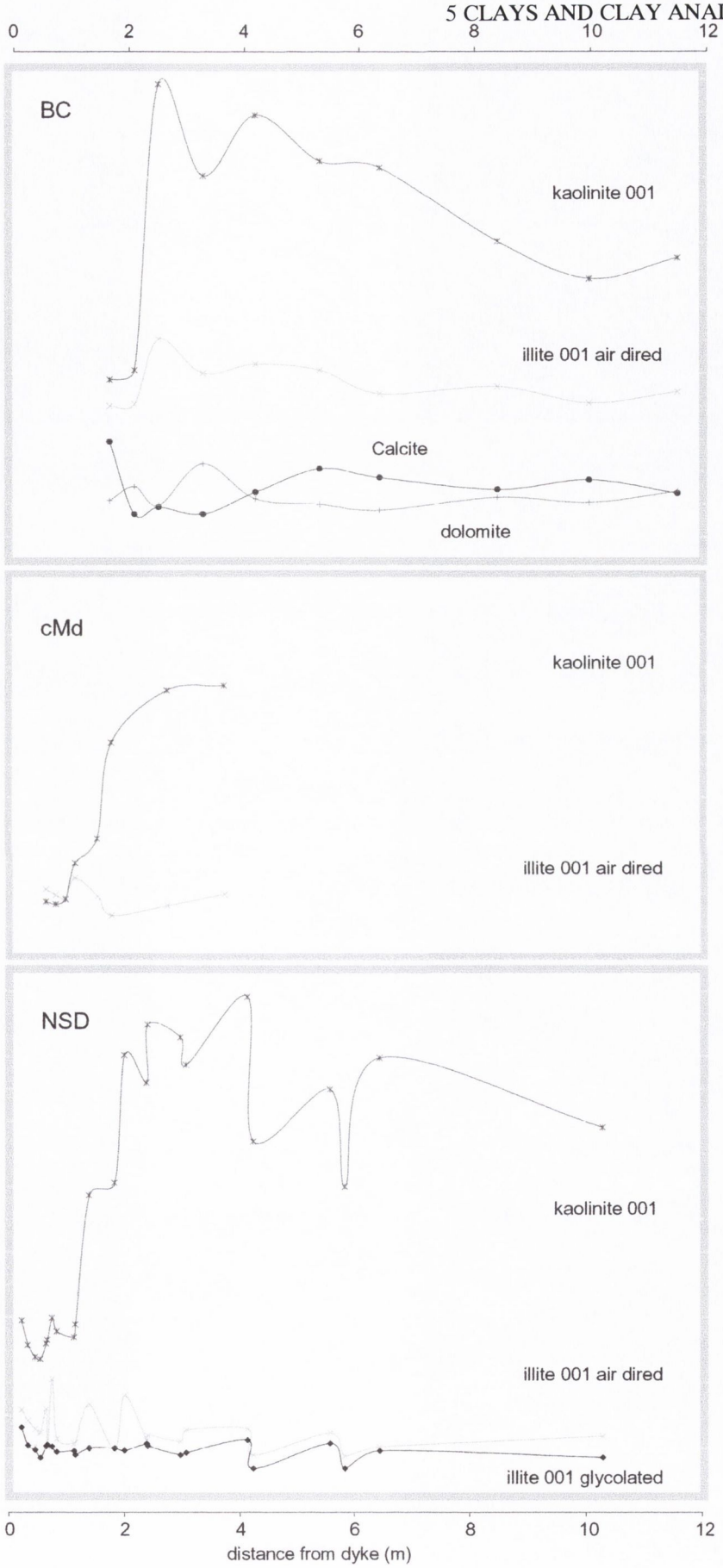

Figure 5.3 Kaolinite /chlorite, illite and carbonate peak intensity variation in the BC, cMd and NSD horizons.

Calcium plagioclase was recorded in the cMd horizon up to 0.8 - 0.9m from the dyke. Microcline was identified at 1.6m and was observed as a trace component in background samples.

Microcline is identified in some of the BC samples, up to 2m from the dyke. It is only present in trace amounts.

5.4.2.7 BALLYCASTLE CLAYS SUMMARY

Calcium plagioclase is present in samples adjacent to the dyke in cMd and NSD horizons (≤0.97 and ≤0.47 respectively).

In samples adjacent to the dyke a discrete smectite peak is observed (≤ 0.96m in the cMd horizon and ≤0.97m in the NSD horizon).

The appearance of a discrete smectite peak is coincident with the drop in kaolinite intensities in the cMd and NSD horizons (refer to Appendix V, figures 3-5).

Maximum and minimum illite intensities are coincident with the kaolinite maximum intensity and kaolinite intensity drop respectively in the BC horizon. The same cannot be said for the cMd and NSD horizons (refer to Appendix V, figures 3-5 and figure 5.3). In the cMd horizon, at *c.*2m from the dyke illite intensity values increase, towards the dyke, reaching a maximum value at *c.* 1.5m from the dyke. Illite intensity values are then seen to decrease with proximity to the dyke. Kaolinite intensity values are observed to decrease with proximity to the dyke from *c.*2m from the dyke (refer to figure 5.3).

The reduced intensities of the kaolinite/chlorite reflections, in the various horizons, with proximity to the dyke may be due to heat or leaching with the concomitant formation of smectite.

There is a constant carbonate presence in the BC traces, although the dominant carbonate type varies through the aureole (refer to Appendix V figure 3 and figure 5.3).

Quartz reflections decrease in intensity in regions proximal to the dyke ((refer to Appendix V, figures 3-5).

5.5 THE 'ILLITE CRYSTALLITE' DEBATE

There are 2 equally valid ways to describe illitic crystals composed of illite and smectite, the MacEwan crystallite (MacEwan 1956, 1958, 1980) and fundamental particles (Nadeau *et al.* 1984).

MacEwan crystallites are described as stacks of crystals (non hydrous illite and hydrous expandable smectite), which diffract coherently. The Markov theory was developed to explain the XRD patterns of I/S minerals (Altaner and Bethke 1988b). This theory proposes that I/S consists of crystallites about 10nm thick or greater that are composed of stacked illite (dehydrated K rich interlayers with Al rich tetrahedral sheets) and smectite interlayers (hydrated interlayers with exchangeable cation sites and Si-rich tetrahedral sheets). In the Markovian theory each stacking sequence is known as a MacEwan crystallite (Hendricks and Teller 1942 and MacEwan 1956, 1958). The Markovian theory holds that I/S consists of crystallites that can accumulate during XRD experiments to give the appearance of MacEwan crystallites (Altaner and Bethke 1988b), (see figure 5.4 (b) for schematic representation of the MacEwan crystallite and the fundamental particle models).

The theory of fundamental particles is based on observations made using TEM. Nadeau *et al.* (1984, 1985) found I/S particles to consist of fundamental particles, each of which was small but an integral number of nm thick, using TEM Pt shadowing. They proposed that the interfaces between the crystallites could hydrate so that random accumulation can occur during preparation and behave like MacEwan crystallites. The fundamental particles act as illite and the hydrous interface form smectite layers.

An unresolved question is whether either the fundamental particle theory or the MacEwan crystallite or both adequately describe the crystallite sizes of I/S minerals in nature. McHardy *et al.* (1982) estimated crystallite thicknesses of filamentous I/S from sandstone pores using SEM. They concluded that these clays were more like the fundamental particle than the MacEwan crystallite. However, lattice fringe images of the crystallites of I/S from bentonites show crystallites that are closer in thickness to the MacEwan crystallites than to the fundamental particle (Peacor 1998).

It has been suggested that the formation of fundamental particles might be due to osmotic cleaving of the MacEwan crystallite along the smectitic interlayer due to Na saturation and Li saturation (Altaner and Bethke 1988, Altaner *et al.* 1988) while others have suggested that cleaving along the same layer due to grinding during sample preparation is the cause (Ahn and Peacor 1986)

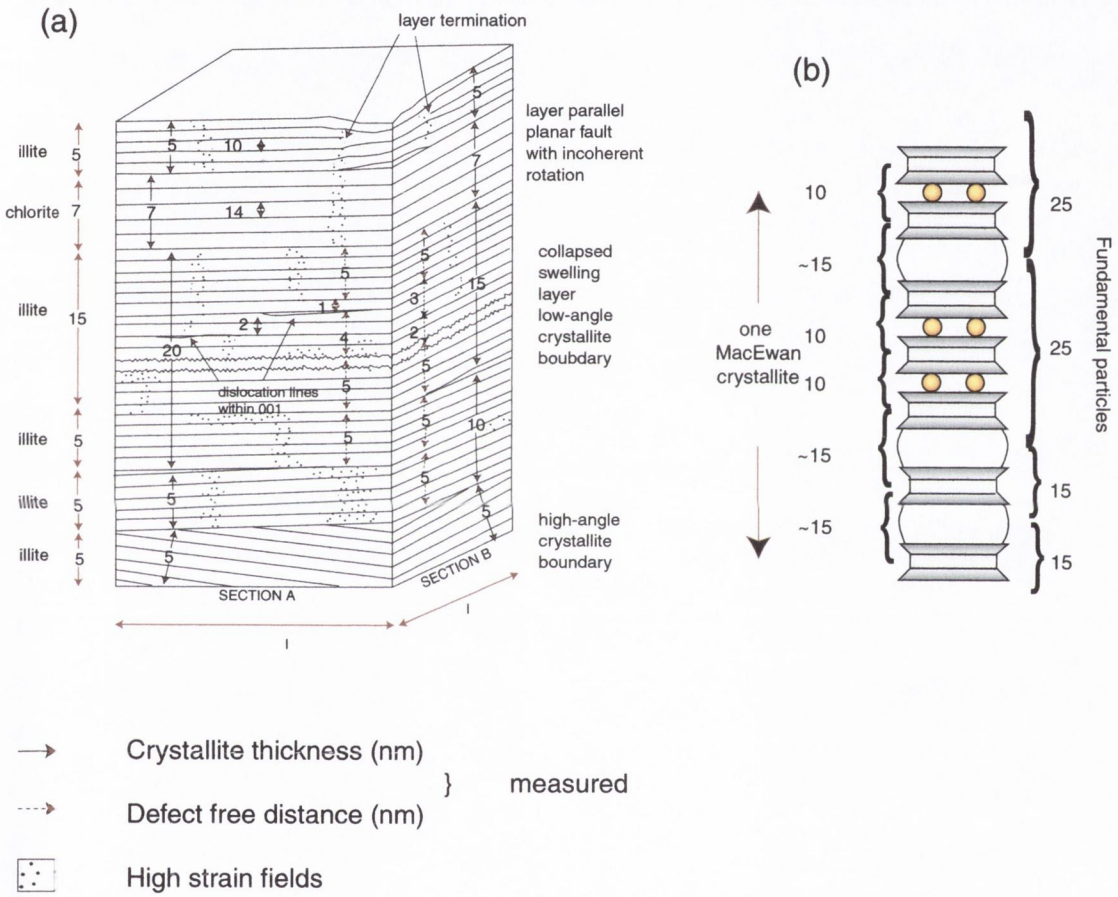

Figure 5.4 Contrasting views of illite 'crystallite' material. (a) 3-D schematic of illite and chlorite crystallites containing various types of lattice imperfection 'observed' in lattice-fringe images (after Warr and Nieto 1998); (b) the 2-D representation of the I/S crystallite shown as either a MacEwan crystallite or as a stack of fundamental particles (modified from Altaner and Bethke 1988, Altaner et al. 1988, Moore and Reynolds 1997)

5.6 MUDMASTER: A PROGRAM FOR CALCULATING CRYSTALLITE SIZE DISTRIBUTIONS AND STRAIN FROM THE SHAPES OF X-RAY DIFFRACTION PEAKS (EBERL *et al.* 1996)

"The Bertaut Warren Averbach technique (BWA) is based on the fourier analysis and can be used to analyse XRD reflections, and permits determination of the area weighted mean size of the coherent scattering domain (CSDs). The distribution of these sizes and fluctuations in the d-spacings (micro strains) of the CSDs measures Fundamental Crystallite size" (Drits *et al.* 1998). (CSD is a term used to describe a stack of parallel layers (Drits *et al.*1998)).

MUDMASTER uses a modified version of the BWA to measure crystallite size distributions and strain in minerals, particularly in clay minerals (Środoń *et al.* 1992). This method uses XRD, but XRD peaks are broadened and made asymmetrical by mixed layering, high background values and the presence of multiple minerals, which might produce similar reflections. This might imply that the BWA cannot be applied. However this has been dealt with by Na saturation and dehydration, followed by pvp-10 saturation, which eliminates the effect of interlayer swelling, and by placing the solution on a silicon wafer cut along the 010 axis, which reduces background interference on the trace (Eberl 1998).

The MUDMASTER program (Eberl *et al.* 1993, 1996) has been somewhat controversial since its introduction. MUDMASTER tends to calculate smaller crystallite sizes than TEM methods (Warr and Nieto 1998). This discrepancy has not, however, been satisfactorily explained by users of either method. Part of the inconsistency might be due to the different techniques being used, the sample preparation and the 'visualisation' of the material being measured. Figure 5.4 illustrates the schematics of the crystallites idealised by each group of workers.

5.7 MUDMASTER BEST MEAN SIZE RESULTS

The results from the MUDMASTER software revealed relatively small 'crystallite' sizes in each setting for all horizons. Calculated values range from a maximum of 4.0nm to 2.9nm minimum values (see table 5.2).

Sample Horizon	Max. Best Mean (nm)	Min Best Mean (nm)
CK	4.0	3.1
CQ	3.8	3.1
NSD	3.6	2.9
BC	3.2	3.0
CMd	3.6	2.9

Table 5.2 the maximum and minimum recorded values, and respective sample numbers for the best mean crystallite size, calculated by the MUDMASTER software for each of the samples horizons.

5.7.1 CARRICKLECK

5.7.1.1 CK HORIZON

MUDMASTER calculated illite best mean crystallite sizes are all quite small, ≤ 4.0nm. Maximum crystallite size was recorded within 0.3m of the dyke at 4nm. One of the lowest crystallite sizes was recorded directly adjacent to the dyke. There appear to be at least 3 sequences of increasing and decreasing crystallite sizes described by the profile, which flatten and extend with distance from the dyke (see figure 5.5).

5.7.1.2 CQ HORIZON

Results from the CQ horizon show a variation between 3.8 and 3.1nm in best mean size. The profile describes a varying pattern of increasing and decreasing crystallite size, like the CK horizon the profile seems to show a repeating arch profile, with the smallest calculated values recorded from samples closest to the dyke (see figure 5.5).

5.7.2 BALLYCASTLE

5.7.2.1 BC HORIZON

The BC horizon has best mean calculated crystallite sizes of 3.1 – 3.2 nm. These are very small crystallite sizes, but the results are consistent throughout the samples. The profile describes a virtually straight line(see figure 5.6).

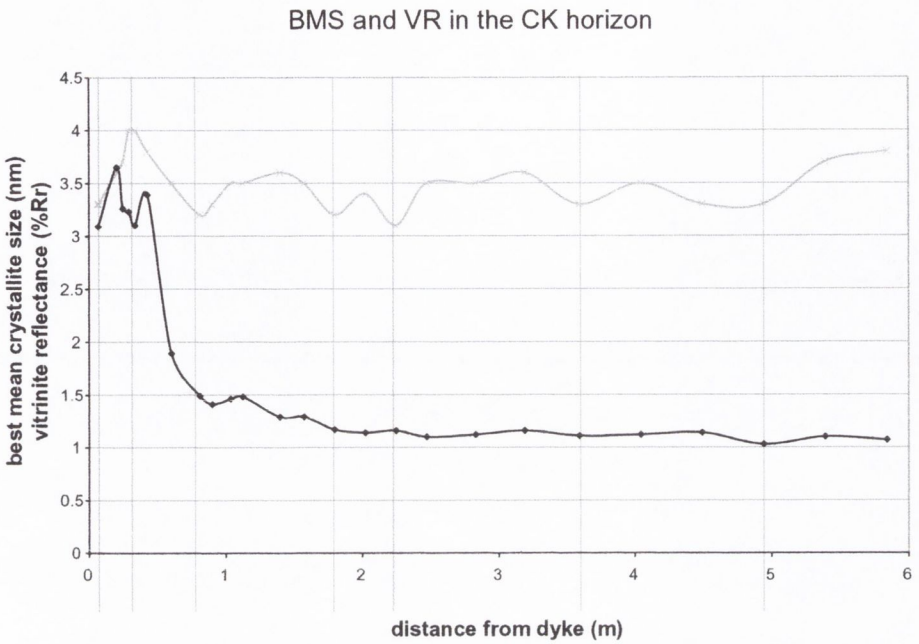

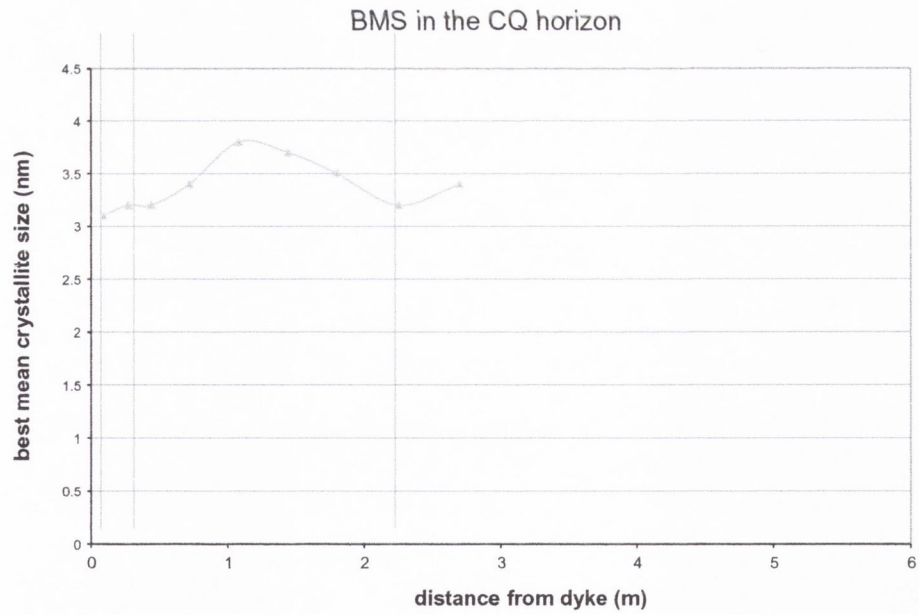

Figure 5.5 Best Mean size for the CK and CQ horizons in the aureole of the Carrickleck dyke. Note that the profiles might be described as having a similar pattern over the length of the aureole that they both cover.

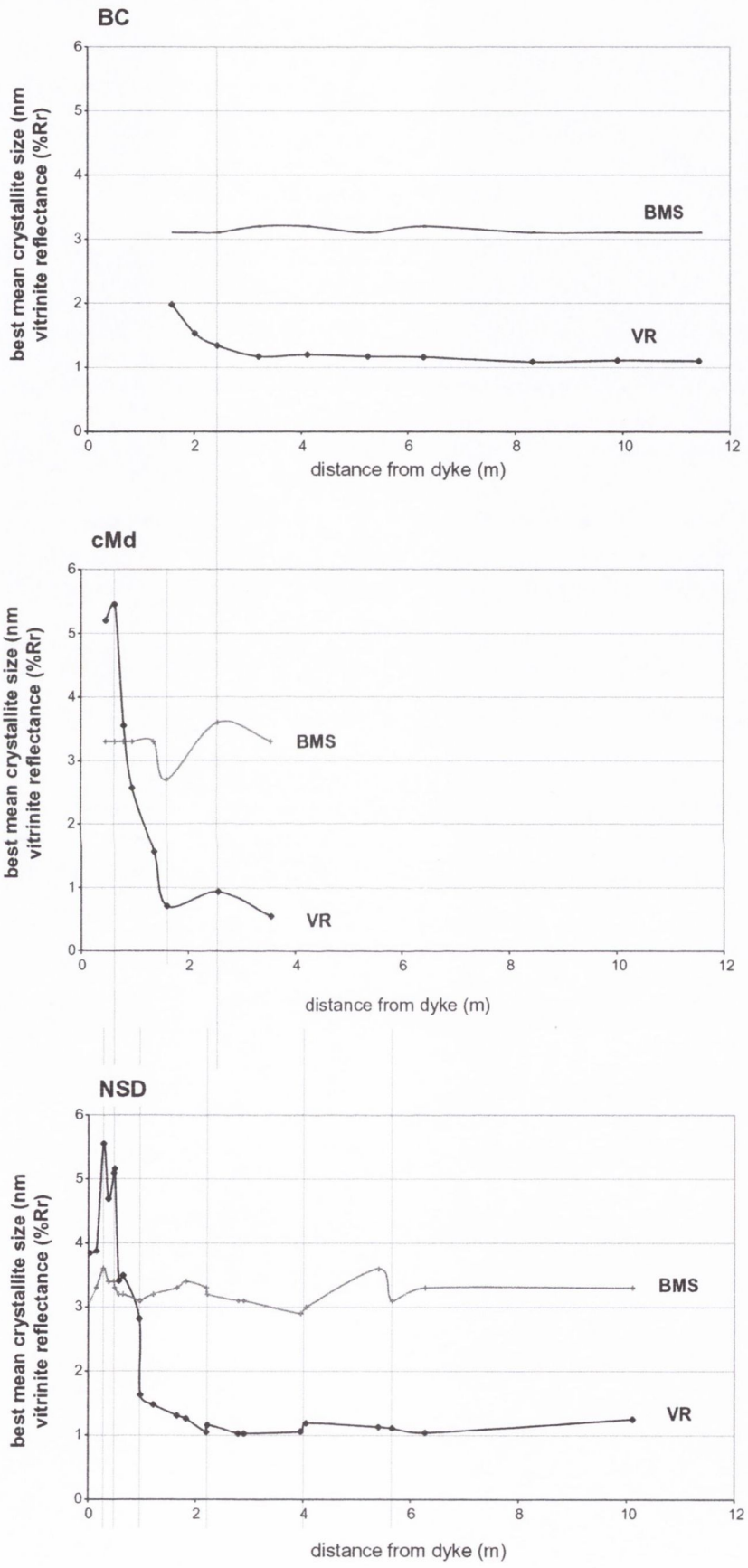

Figure 5.6 Calculated best mean crystallite size (BMS) for the BC, cMd and NSD horizons in the North Star Dyke aureole.

5.7.2.2 cMd HORIZON

The cMd horizon results have a maximum and minimum best mean size of 3.6 and 2.9nm respectively. These values are recorded between *c.* 2.5 and 2.0m from the dyke. The profile shows maximum variation beyond 1.5m from the dyke. The four samples closest to the dyke yield values of 3.3nm (see figure 5.6).

5.7.2.3 NSD HORIZON

The NSD horizon results show a maximum and minimum best mean size of 3.6 and 2.9 nm. These values are calculated from samples between 5.5 and 4 m from the dyke contact respectively. The data profile describes what might be postulated to approximate a straight line if more samples were collected. The data can be described as detailing a series of increasing and decreasing crystallinity sizes. However the pattern is not particularly coherent (see figure 5.6).

5.8 DISCUSSION

5.8.1 MINERALOGY OF THE <2μm FRACTION OF DYKE AUREOLE SAMPLES

The mineralogy observed for the sample horizons from the Carrickleck and Ballycastle are not unusual for mudstones (for examples of similar mineral suites for mudstones and shales refer to Moore and Reynolds 1999, Frey 1987, Esposito and Whitney 1995, among others).

Kaolinite/chlorite and expandable illite are the dominant clay minerals in each of the horizons. Smectite is also presen in the cMd and NSD horizons

If relative intensities of the traces are taken to be a rough representation of the relative 'amounts' of clay in the sample then these results would appear to imply that kaolinite and illite are decreasing in amount as the dyke is approached. The varying intensity profiles show a regular pattern that may be indicative of convective influence.

Non-clay minerals are more prevalent in the XRD traces closer to the dyke but this is a function of the decreased 'amounts' of the clay minerals in these samples. All non clay minerals are present in trace-minor amounts. Quartz is present in each of the horizons throughout. At Ballycastle some of the samples (NSD1, 5, cMd1, 3) contain apatite; NSD1-6 and cMd1-4 contain plagioclase. Apatite is not identified beyond 0.5m in the NSD horizon and 0.8m in the cMd horizon, and plagioclase is not identified beyond 0.5m and

1m in the NSD and cMd horizons. Intensity of the plagioclase peak increases with proximity to the dyke in both horizons. Both of these minerals are also present in the dyke itself (see Appendix V, figure 6).

Kaolinite is one of the dominant clays for both localities. The peak intensity drops quite dramatically as the dykes are approached with the major intensity drop occurring at 0.8m (CK) 2m (BC), 1.4m (cMd) and 1.0m (NSD) from the dyke at equivalent VR of 1.5%R_r, 1.5% R_r, 1.6% R_r and 1.5%R_r, respectively. As with the fluorescence exercise (chapter 7), although the positions (m) in the dyke aureole do not concur, the kaolinite intensity drop occurs at positions with approximately the same VR values. These reflectance values can be converted to a maximum temperature of *c.*210°C after Barker and Goldstein (1990) (refer to section 4.3.1.2). This evidence combined with the known fact that the kaolinite structure can be destroyed at temperatures ≥ 550°C in the laboratory (unpublished personal experimental work, Moore and Reynolds 1989 and Brindley and Brown 1984), would suggest that this is what has occurred in the aureole samples. The kaolinite has been partially destroyed.

In the horizon samples from Ballycastle kaolinite concentration drops dramatically in the same region as smectite appears.

The sharpening of the 10Å illite peak, observed in the XRD traces as the dyke is approached, is often associated with clays of increasing 'maturity'. The concomitant decrease in peak intensity with proximity to the dyke might suggest that the illite content is also decreasing.

In the CK horizon the lowest apparent illite intensity coincides with the sharpest slope increase on the VR profile (refer to figure 5.2). The maximum illite intensity coincides with the main break in slope for the VR profile, although beyond this there is an intensity decrease towards the dyke while VR values fluctuate apparently randomly. The kaolinite apparent intensity drops dramatically where there is a strong break in slope of the VR with a large drop in value at the same point in the aureole, and the kaolinite intensity profile increases and decreases at the same points in the aureole as the VR, all the way into the dyke.

At Ballycastle smectite has a discrete peak in both the cMd and NSD horizons within 1.36m and 1.21m respectively, which increases in intensity with proximity to the dyke. This is contrary to expected character of smectite. However the smectite peak is also observed in the XRD traces for the North Star Dyke itself, indicating fluid dyke/host rock interaction.

The reduced quartz intensities in the <2μm fraction in the region closest to the dyke might imply that this silica was soaked up in the formation of the plagioclase. It is possible that hydrothermal fluids may have leached or carried excess Ca from the fluid dyke, and deposited it within a 40-60cm distance of the margin (*pers. comm.* Dr. V. Troll 2002). The appearance and increase of smectite, plagioclase and apatite concentration towards the dyke margin within this same region and the presence of these same minerals within the dyke might be taken to reinforce the idea of some kind of fluid exchange between sediment and dyke.

5.8.2 BMS VALUES AND VR

5.8.2.1 CARRICKLECK

Comparing the VR and BMS in the CK horizon (see figure 5.5) shows a general change towards the dyke and the most extreme variation in the region within 1m of the dyke contact. What can also be seen is that there is some general correlation between the undulating profiles. The maximum positive break in slope of the VR profile is matched by the BMS profile i.e. where the maximum increasing VR values are recorded in the CK horizon the BMS values are also increasing implying that there are bigger crystallites associated with the higher reflectances of this part of the aureole. And as the VR profile inverts against the dyke contact, so too does the BMS profile. The wavy profile of the VR might be compared to a modelled heat flow profile of Barker 1988, modelled to represent fluid flow in an aureole.

5.8.2.2 BALLYCASTLE

BC

The VR profile of the BC horizon is the most regular of this setting and the BMS profile for this horizon is virtually flat. The regularity of the profiles compared to the irregular nature of the cMd and the NSD profiles is the most striking thing about these results and may represent differences in bulk chemistry or physical characteristics (e.g. porosity, permeability or inherent pore fluids) in this lithology at the time of intrusion relative to the cMd and NSD horizons (see figure 5.6).

cMd

The cMd horizon VR and BMS profiles show accord approaching the dyke up to c.1.5m from the dyke. This coincides with the marked change in slope observed for the illite and

K/C apparent intensity profiles, it is also where the VR profile shows a positive break in slope. The 'kink' in the BMS profile is followed by a flat trace at 3.2nm, between c. 1.5m and the dyke margin, in spite of the increasing reflectance values recorded by the vitrinite. This might be interpreted to represent an area close to the dyke where the clay chemistry is no longer reacting in tandem with the vitrinite.

NSD

The NSD BMS and VR profiles appear to be messy and irregular, variously kinked and irregularly fluctuating values. However when these profiles are compared some of the kinks can be correlated across the profiles and the major break in slope described by the VR at *c.* 1.5m from the dyke, is followed by the BMS profile, although lagging by *c.*0.5m. The maximum, recorded BMS (3.6nm) in this region is matched by the maximum, recorded VR (5.55 $\%R_r$).

5.8.3 BMS AND APPARENT INTENSITY PROFILES

5.8.3.1 CARRICKLECK

Superimposing the BMS profile on the illite[001] and kaolinite apparent intensity profiles, it becomes apparent that they are describing similar patterns. For the CK horizon the pattern similarity seems to be particularly strong when comparing any of the profiles with the kaolinite profile.

5.8.3.2 BALLYCASTLE

BC

Comparing the flat BMS profile of the BC horizon, to the varying intensity profile, it would appear that the illite BMS is not related to the varying illite reflection intensities.

cMd

The BMS profile for the cMd horizon shows some similarity to the apparent intensity profiles for illite and kaolinite. At *c.*1.5m from the dyke there is a distinct 'kink' in the BMS profile, which matches a negative break in slope for the kaolinite intensity profile and a positive break in slope for the illite intensity profile at *c.* 1.5m from the dyke. BMS calculated sizes remain at 3.2 nm within the area of 1.5m from the dyke, while the intensity illite and kaolinite intensities continue to vary.

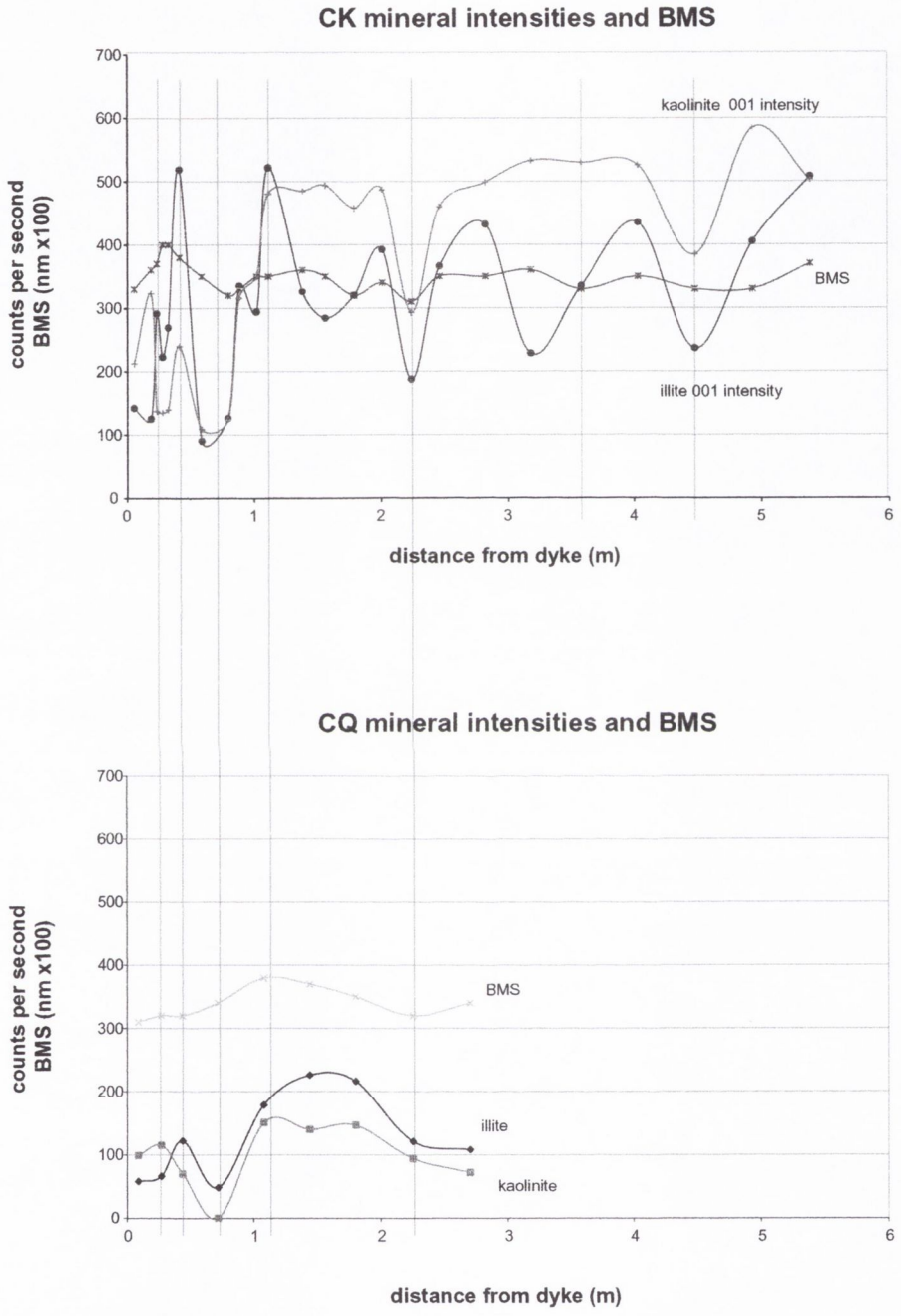

Figure 5.7 Comparison of the MUDMASTER Best Mean crystallite Size (BMS) results for illite in the CK and CQ horizons with the illite and kaolinite intensity profiles

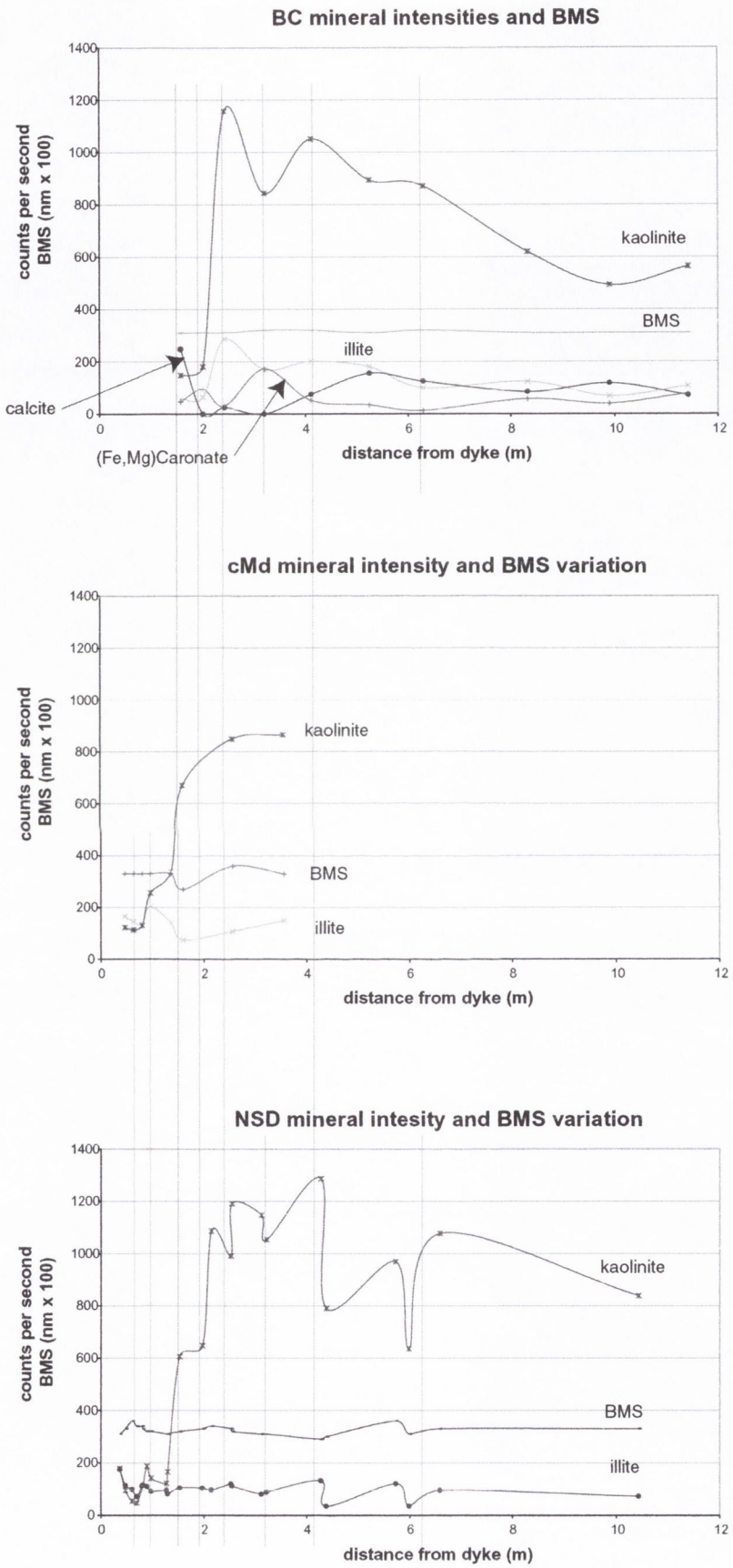

Figure 5.8 comparison of the MUDMASTER Best Mean crystallite Size (BMS) results for illite and the illite and kaolinite intensity profiles in the BC, cMd and NSD and the calcite and (Fe, Mg) carbonate intensity profiles in the BC horizons.

NSD

The NSD BMS profile is particularly random in appearance as are the illite and kaolinite/chlorite intensity profiles. They are full of irregular 'kinks', and increase and decrease in BMS values. However superimposing these profiles one upon the other reveals that these 'kinks' can be correlated between the profiles (see figure 5.8) if somewhat loosely. An aside – one of the most pronounced slope breaks in the mineralogical data occurs in the region of *c.* 1.5m from the dyke, as is seen for the cMd horizon. Three sharp 'kinks' observed in the BMS profile are reflected in the illite apparent intensity profile, at *c.*5.5m from the dyke, 4m from the dyke and 2.2m from the dyke. They can be seen in the kaolinite intensity profile as marked drops in value at these same positions along the aureole. The area within 1.5m of the dyke is the most apparently chaotic. However, where the illite apparent intensity profile shows the minimum values in this region the BMS profile records some of the highest values for this horizon.

5.8.4 GENERAL

The fact that there are correlations to be drawn, and that much can be seen to be changing relative to the dyke would imply that some of the variations in the clays through the aureole are related to the intrusion. There is a general drop in expandable illite intensity in a region approximately 40%(NSD)-50%(CK) dyke thickness from the dyke margin. At the same point there is also a considerable drop in kaolinite intensity. Within this region for each mineral the intensity and BMS values vary. The presence of smectite in the North Star Dyke and the aureole rocks closest to the dyke margin indicates that fluid assisted host-rock/dyke interaction occurred. In the Carrickleck situation there is an apparent decrease in the smectitic content (the illite reflections sharpen although the intensity values decrease). The wave like patterns described by the intensity profiles is reminiscent of the modelled heat transfer in a dyke aureole with a convective component (Barker 1988). It is interesting to note that for samples within one meter of each of the dykes a scatter of data is observed that is apparent in XRD mineralogical intensities, BMS data and VR, and far from being as random as it might appear, correlative profiles can be produced for each of these data sets from any one horizon. This is true for both the Carrickleck Dyke (CK horizon) and the North Star Dyke (NSD horizon) settings. It would appear from the data described by clays and clay analysis that fluids were probably present in both dyke aureoles at the time of intrusion. It is unlikely that a convective influence became established as a dominant factor in the heat distribution of the cooling dykes.

5.9 CONCLUSIONS

There were fluids available to transport elements parallel to bedding, and the transport and precipitation of these elements were influenced to some extent by the dykes. It would appear that most of the changes observed occur within

The heat of dyke intrusion had a destructive effect on some of the clay minerals in the aureole mudrock horizons. Kaolinite is particularly sensitive to this, suffering a massive intensity drop in both aureoles at VR values of *c.* 1.5-1.6%R_r, equivalent to a maximum temperature of *c.*210°C (after Barker and Goldstein 1990). This temperature is well less than half the temperature necessary to destroy the kaolinite structure using heat in the laboratory.

The illite peak decreases in intensity and 'sharpens' with proximity to the dykes, reflecting the expected increase in 'illite crystallinity'.

There is a strong likelihood that there were fluids present at the time of intrusion, and that there has been host rock/dyke fluid interaction. This is particularly true for the North Star Dyke.

Illite crystallite BMS are very small for each horizon, but they do present size fluctuations coincident with varying mineral intensities, and maximum sizes are observed in samples closest to the dyke.

Correlation between the VR and BMS profiles is indicative of the crystallite size being related, although not strongly, to the thermal influence of the dyke

The wave like patterns described by the intensity profiles is reminiscent of the modelled heat transfer in a dyke aureole with a convective component (Barker 1988, see chapter 9).

The influence of the post intrusion calcite fluid did not have a far reaching effect on the observed mineralogy of the aureole mudrocks at Carrickleck.

6 SYSTEMATIC PALYNOLOGY

PALYNOLOGY: Hyde and Williams (1944) derived the term from the Greek verb *palunein* (meaning to sprinkle, to dust), to encompass the study of fossil spores and pollen. Today the working term includes the study of all organic walled microfossils found in sedimentary rocks (Traverse 1988, Tyson 1995).

This section deals with a palynological study of sporess carried out in the Ballycastle, NSD sample horizon. This was done for the following reasons:

1. to determine the age of the horizon.
2. to assess the resistance of different spore genuses in the NSD dyke aureole to the destructive effect of the short-lived, elevated temperatures, due to dyke intrusion, and therefore:
3. to observe the variation in spore assemblage in the aureole samples due to the thermal influence of the dyke.

The study involved a count of 250 indeterminate and identified spores, and 250 identified spores per sample examined. 21 samples were examined. The samples were prepared and mounted as per. chapter 2.

6.1. NOMENCLATURE AND CLASSIFICATION, SPORE MORPHOLOGY AND DESCRIPTIVE TERMINOLOGY

The suprageneric classification used in this work is that proposed by Dettmann (1963) and modified by Smith and Butterworth (1967). Descriptive terminology used is essentially that of Grebe (1971).

6.2 SAMPLE PREPARATION AND PALYNOLOGICAL ANALYSES

6.2.1 ORGANIC MATTER EXTRACTION

(see section 4.4.1)

6.2.2 PREPARATION FOR PALYNOLOGICAL ANALYSES

A small amount of organic residue using Cellusize as a dispersing agent was mounted on a glass cover slip (no.1, 22 x 40mm surface area) and allowed to dry overnight. The dry cover slips and residue are then mounted onto labelled glass slides (0.8/1.0mm thickness,

76 x 26mm surface area) using the mounting medium elvacite. The slides were left for 24-48 hours to dry to allow the elvacite to dry.

6.2.3 TRANSMITTED LIGHT MICROSCOPE

The microscope used in this study is a Nikon transmitted light, binocular microscope, with an OSRAM XENOPHOT 12V 50W, halogen, light source.

6.2.4 STRATIGRAPHIC PALYNOLOGY AND COUNT

Miospores were studied in transmitted white light. Descriptive terminology of Grebe (1971), and the classification of Smith and Butterworth (1968) were used. Analyses of the spore numbers present were based on counts of 350 per slide. The number was assumed after a number of cumulative counts were taken.

6.2.5 PRESENTATION OF RESULTS

All data are tabulated and presented in Appendix I. Graphic representations of the results are presented in chapter 6. Plates of identified sporomorphs are found in Appendix III, plates 13-15. A systematic description for each of the sporomorph species, and or genus is presented in chapter 6.3.

6.3 SYSTEMATIC PALYNOLOGY RESULTS

A total of 25 spore genus and 42 species are identified in the NSD horizon. Photomicrographs of most of the spores described are illustrated in Appendix III, plates 13-15. All sizes are given in microns and all images are at x500 magnification. Following is a list of all the miospore species identified followed by systematic diagnoses and description:

Diagnostic feature	CATEGORY													Rank
	SPORITES													Anteturma
Aperture	TRILETES						TRILETES			HILATES			ALE-TES	Turma
Stratification	ACAVATI-TRILETES		LAMINATI-TRILETES		PSEUDO-SACCITRILETES	PERINO-TRILETES	ACAVATO-MONOLETES		CAVATO-MONOLETES	ACAVATI-HILATES	CAVATI-HILATES			Suprasubturma
Equatorial featues	AZONOTRILETES	ZONOTRILETES	AZONOLAMINATITRILETES	ZONOLAMINATITRILETES			AZONOMONOLETES	ZONOMONOLETES			AZONOCAVATIHILATES	ZONOCAVATIHILATES		Subturma
Sculpture / equatorial thickening and/or extension	LAEVIGATI APICULATI MURORNATI	AURICULATI TRICRASSA CINGULATI	TUBERCULORNATI	CRASSITI CINGULICAVATI PATINATI	MONOPSEUDOSACCITI POLYPSEUDOSACCITI		LAEVIGATOMONOLETI SCULPTATOMONOLETI				EPITYOMATI OPERCULATI			Infraturma

Figure 6.1 Revised scheme for the classification of sporites after Smith and Butterworth (1967) modified after Dettmann (1963)

TABLE OF CONTENTS FOR SPORE SYSTEMATICS

Calamospora parva 110
Calamospora sp. 111
Leiotriletes priddyi 111
Leiotriletes sphaerotriangularis 112
Leiotriletes tumidus 113
Punctatisporites nitidus 113
Punctatisporites minutus 114
Punctatisporites planus 114
Punctatisporites viriosus 115
Retusotriletes incohatus 116
Videospora glabrimarginata 117
Anaplanisportes globulus 118
Lophptriletes sp. 119
Pustulatisporites papillosus 119
Raistrickia nigra Love 120
Tricidarisporites fasciculatus 121
Verrucosipsorites nodusus 122
Dictoytriletes c.f. pactilis 123
Microreticulatisporites concavus 124
Secarisporites remotus 125
Triquitrites marginatus 126
Tripartites vetustus 127
Knoxisporites stephanopherous 128
Knoxisporites triradiatus 128
Murospora intorta 129
Reticulatisporites polygonalis 131
Reticulatisporites reticulatus 132
Rotaspora knoxi 133
Stenozonotriletes bracteolus 134
Stenozonotriletes coronatus 134
Diatomozonotriletes sp. 135

Crassispora maculosa 136
Cingulizonates bialatus 137
Cirratriradiites elegans 138
Cirratriradiites cf. praetergranulates 139
Cristatisporites sp. 140
Densosporites anulatus 141
Densosporites intermedius 141
Densosporites regalis 142
Densosporites spinifer 143
Densosporites sp. 143
Densosporites triangularis 143
Lycospora noctuina 145
Lycospora pusilla 145
Potoniespores cf. delicatus 146
Discernisporites sp. 148
Discernisporites micromanifestus 148
Endosporites c.f. micromanifestus 149
Grandispora spinosa 150
Rugospora corporata 151
Scholzospora campyloptera 152
Schulzospora elongata 152
Schulzospora ocellata 153
Perotriletes perinatus 154
Laevigatosporites minor 155
Laevigatosporites vulgaris 156

Anteturma SPORITES H. Potonié 1893

Turma TRILETES (Reinsch) Dettman 1963

Suprasubturma ACAVATITRILETES Dettman1963

Subturma AZONOTRILETES (Luber) Dettman 1963

Infraturma LAEVIGATI (Bennie and Kidston) R. Potonié 1956

Genus: CALAMOSPORA, Schopf, Wilson and Bentall 1944

Type species: C. *hartungiana* Schopf in Schopf, Wilson and Bentall 1944, p51, fig. 1

Diagnosis: (Potonié and Kremp1955, p. 46; translation in Smith and Butterworth 1967, p. 130) "Trilete miospores, that is isospores, microspores and megaspores , the latter possibly up to 350µm (cf. Hartung 1933, p.106). Laesurae generally shorter, or only slightly longer, than one-half the radius of the equatorially flattened spore; occasionally indistinct. Suture sometimes open

Remarks: The genus encompasses thin, smooth, usually folded, simple acamerate miospores of variable size. This study follows Smith and Butterworth 1967, p.130-138, in using the following size categories to differentiate between species (where no significant haptotypic features are):

1. <55µm *C. parva*
2. 55-75µm *C.pallida*
3. >75-100µm *C.microrugosa*

Affinity: Eleutherophyllaceae, Sphenophyllaceae, Calamitaceae, Equisetaceae, and Noeggrathiineae in Potonié (1962), Protopityales (Walton 1957).

Occurrence: NSD 14, 18, 20, 23

Calamospora parva Guennel 1958

Holotype: Guennel 1958, fig. 16, p. 71. Sample 66 slide 4104; equatorial diameter 38µm.

Type Locality: Outcrop Coal, upper Block b zone, Daviess Co., Indiana; USA. Pottsville Series.

Diagnosis: (from the description in Guennel 1958, p.70) "Amb circular to elliptical. Laesurae 1/3 of radius. Exine thicker and darker in contact areas. Folding common."

Remarks: Conforms with the original description. All specimens observed are folded. Not often identified as the folding of most of the *Calamospora* spp. is so complete that an accurate measurement of the equatorial diameter is not possible.

Size: 32(37)45µm (Guennel 1958);

Size present study: 41.25μm (based on 4 specimens)

Range: LL-CM, Tournaisian of Ireland. Higgs *et al.* 1988

Westphalian, Smith and Butterworth 1967.

Calamospora sp.

Description: circular, smooth outline. Laevigate. Trilete, straight, variable length. Contact mark often open; straight, simple. Exine thin; yellow.

Remarks: all spores broken or heavily folded making the differentiation of species difficult.

Size present study: 55-95μm (based on 24 samples)

Present in samples: N24, N22, N23, N22, N20, N19, N18, N17, N16, N15, N14, N11

Genus: LEIOTRILETES (Naumova) Potonié and Kremp 1954

1932 *Sporonites sphaerotriangulus* Loose in Potonié, Ibrahim and Loose, p. 451, pl18, fig 45

1933 *Laevigati-sporites sphaerotriangulus* (Loose); Ibrahim, p. 20

1944 *Punctati-sporites sphaerotriangulatus* (Loose); Schopf, Wilson and Bentall 1944, p. 31.

1950 *plani-sporites sphaerotriangulatus* (Loose); Knox, p. 316, pl. 17, fig. 214

1954 *Leiotriletes sphaerotriangulus* (Loose); Potonié and Kremp, p. 120.

Type species: L.*sphaerotriangulus* (Loose) Potonié and Kremp 1954

Holotype: Potonié and Kremp 1955 pl. 11, fig 107 after Loose. Preparation IV21, f2 (m/ol).

Diagnosis: (Potonié and Kremp 1954 p.20; translation in Smith and Butterworth 1967 p. 121). "Trilete isospores or microspores with smooth margin and triangular amb having distinctly concave, or slightly to rather convex sides. Providing the triangular shape is still obvious or the three proximal pyramidal faces are rather steep, the spores belong to *Leiotriletes*. The angles of the amb are roughly rounded or blunt. Occasionally infrapunctate to infrareticulate. Trilete rays are generally greater than one half of radius."

Size: 30-66 μm (Potonié and Kremp 1955)

Range/occurrence: Langsettian to Bolsovian (Smith and Butterworth 1967)

Affinity: Filicales, Remy and Remy (1957). Further evidence of filicinean affinity is given in Potonié (1962).

Leiotriletes priddyi (Berry) Potonié and Kremp 1955

1937 *Zonales-sporites priddyi* Berry

1944 *Granulati-sporites(?) priddyi* (Berry); Schopf Wilson and Bentall 1944 p.33

1950 *Plani-sporites priddyi* (Berry); Knox, pg 316, pl 17, fig. 20

1955 *Leiotriletes priddyi* (Berry); Potonié and Kremp, p.38

Holotype: Berry1937, p.159; text-fig. 2. Preparation L1, 91 49.4

Diagnosis: (from Berry 1937, p156; in Smith and Butterworth 1967). Amb triangular, often slightly convex between angles. Laesurae two thirds of radius. Exine laevigate, clear (?without infrasculpture), and very thin.

Size: not more than 35µm (Berry 1937);

Size present study: 25(28)33µm (based on 4 specimens)

Range: Namurian to Duckmantian (Smith and Butterworth 1967)

Sample present: N23, N22, N20, N17

Leiotriletes sphaerotriangularis (Loose) Potonié and Kremp 1954

1932 *Sporonites sphaerotriangularis* Loose in Potonié Ibrahim and Loose, P. 451, pl. 18, fig. 45

1933 *Laevigati-sporites sphaerotriangularis* (Loose); Ibrahim, p. 20

1944 *Punctati-sporites sphaerotriangularis* (Loose); Schopf, Wilson and Bentall, p. 31

1950 *Plani-sporites sphaerotriangularis* (Loose); Knox, p. 316, pl. 17, fig. 214

1954 *Leiotriletes sphaerotriangularis* (Loose); Potonié and Kremp, p. 120

Holotype: Potonoié and Kremp 1955, pl. 11, fig. 107 after Loose. Preparation IV21, f_2 (m/ol).

Type locality: Bismarck Seam Ruhr Coalfield, Germany; Upper Westphalian B

Diagnosis: (Potonié and Kremp 1955, p. 41; translation in Smith and Butterworth 1967, p. 123) "amb triangular, sides in part slightly convex. Laesurae extend nearly to the equator. Exine weakly infrapunctate."

Size: 40-60µm (Potonié and Kremp 1955); 38(46)55µm (Smith and Butterworth 1967);

Size present study: 45(46.5)50µm (based on 5 specimens)

Remarks: Rounded triangular, slightly concave to convex, to circular; smooth outline; trilete, laesurae straight, simple, extend 1/3 to 2/3 of spore radius; exine laevigate, thin, yellow to orange.

Occurrence/ range: Langsettian to Bolsovian (Smith and Butterworth 1967)

Present in samples: N18, N15

Leiotriletes tumidus Butterworth and Williams (1958)

Holotype: Smith and Butterworth (1967) Pl.1, fig. 11, slide T32/1, in collection of Coal survey Laboratory, Sheffield.

Type Locality: Kilsyth coking seam at 1,097 ft, in Cawder Cuilt borehole, Central Coalfield, Scotland Namurian A.

Diagnosis: (from Butterworth and Williams 1958 p. 359, in Smith and Butterworth 1967). Size 34 – 52 μm, elongated triangular in outline; spore coat smooth. Proximal hemisphere tumid; trilete rays long, typical with ray folds.

Remarks: Triangular, rounded, straight or convex; margin smooth; spore coat thin, colour pale yellow to yellow, laevigate. Trilete, laesurae, 2/3 radius or greater, frequently reaching almost to the equator; margins simple or very slightly raised, can be slightly darker where thickened

Size: 34(42)52μm (Butterworth and Williams 1958);

Size present study: 35(39.6)43.5μm based on 8 samples

Range: Viséan and Namurian (Smith and Butterworth 1967)

Genus: PUNCTATISPORITES (Ibrahim 1933) Potonié and Kremp 1954

Type species: *P. punctatus* Ibrahim 1933.

Diagnosis: (original description Ibrahim 1933, emended diagnosis Potonié and Kremp 1954, p.120, translation Smith and Butterworth 1967 p.125). "Trilete isospores or microspores having a circular, or near-circular, equatorial outline with a mere suggestion of triangular shape. Margin smooth, as exine devoid of ornamentation. Structure not recognizable or only discernible owing to the presence of punctuation, infrareticulation, or infragranulation (which must not be confused with a granulation causing roughness of the margin). On occasions, punctuation is no more than locally visible, as for instance, along the trilete rays. Rays generally longer than one-half the radius at the equator."

Affinity: Psilophytopsida, Flicales (Primofilices and Leptosporangiatae) and other Pteropsida in Potonié 1962.

Punctatisporites nitidus Hoffmeister, Staplin and Malloy 1955

Holotype: Hoffmeister, Staplin and Malloy 1955, pl. 36, fig. 4. Preparation 9, ser. 18, 659. Equatorial diameter 34μm.

Type locality: Shale at 2,072ft. Carter No. 3 borehole (TCO-82), Webster County, Kentucky, USA; Hardinsburg Formation, Chester Series.

Diagnosis: (Smith and Butterworth 1967, p. 127) "Amb circular. Laesurae simple, about two-thirds of radius. Arcuate compression folds common. Exine laevigate to faintly granulose, about 2μm thick."

Size: 31-43μm (Hoffmeister, Staplin and Malloy 1955); 30-38μm (Hacquebard 1957); 30(43)57μm (Smith and Butterworth 1967)

Size present study: equatorial diameter 35-37μm (based on 3 specimens)

Range/occurrence: Namurian (Smith and Butterworth 1967)

Present in samples: N18, N15, N14

Punctatisporites minutus Kosanke 1950

Holotype: Kosanke 1950, pl 16, fig. 3, maceration 584, slide 7, 29μm

Type Locality:?Woodbury Coal, Jasper County, Illinois, U.S.A.; McLeansboro Group.

Diagnosis: (from description in Kosanke 1950, p.15, in Smith and Butterworth 1967, p. 126). "Originally spherical in shape with the spore coat variously folded. Laesurae distinct, two thirds of radius, lips slightly developed. Exine 1-5μm thick and minutely punctate."

Size: 27-33μm (Kosanke 1950); 22(27)32μm (based on 18 specimens; Smith and Butterworth 1967);

Size present study: 22μm (based on 2 specimens)

Remarks: circular; smooth outline; laesurae usually straight; contact areas sometimes slightly darkened. Folding slight or absent. The size difference and apparent thickness is used to identify this spore.

Range/occurrence: LL-CM biozones (Higgs *et al.* 1988); CM-TS biozones (McPhilemy 1989); Recorded from coal and other rocks of Viséan age from Scotland by Love 1960; Namurian (Smith and Butterworth 1967).

Punctatisporites planus Hacquebard 1957

Holotype: Hacquebarrd 1957, pl. 1, fig. 12. M101, slide 4, at 31.2 by 96.3 dialux.

Type Locality: Occurrence Horton group, Nova Scotia, West Gore and Blue Beach samples.

Diagnosis: (Sullivan 1965)

Original description: (Hacquebard 1957) "spores radial, trilete simple; circular to subcircular in proximal view; trilete simple, two thirds to three fourths spore radius; surface smooth to very slightly infragranulose; spore coat 2 μm thick; occasionally one major compression fold"

Remarks: Conforms to original description (Hacquebard 1957 p. 308), sometimes folded making measurement difficult; not unusual to find specimens degraded to a certain degree.

Size: diameter 50-64μm (based on twelve specimens Hacquebard 1957).

Size present study: 49-50.5μm based on 5 specimens

Range: Kinderhookian, Mississippian (Clayton *et al.* 1998); Mississippian (Hacquebard 1957); Upper Mississippian (Sullivan 1965).

Present in samples: N23, N22, N18, N14

Punctatisporites viriosus Hacquebard 1957

1994 *P. varius* Lu: 188, pl. 1, figs 33, 34

Holotype: M101, slide 1 at 48.4 by 112.9 dialux, Hacquebard (1957), pl.1, fig. 13

Diagnosis: (original description of Hacquebard (1957), p.308-9) "Spores radial, trilete; outline circular to subcircular, generally proximo-distally oriented; trilete distinct, lips low and bordered by single row of minute pits that may be noted after careful focusing, sutures occasionally broad, one-half to two thirds spore radius; surface essentially smooth to slightly rough, some specimens show slightly darker colour in contact areas; spore coat 2.5-3μm thick; small arcuate compression folds occasionally present; diameter 68-83μm (on twelve specimens)."

Description: subcircular to subtriangular; smooth outline; trilete, laesurae straight to slighty sinuous (but sinuous appearance may be due to compaction), may have thickened lips which will be darker, extend ½ to 2/3 of spore radius, laesurae usually closed but may be split; spore coat thick, amber brown to brown; in the larger specimens it is not unusual to observe obliquely compressed spores where to legs of the trilete mark outline part of the spore margin. Some of the spores in this study exceed the quoted size range of Hacquebard (1957) but otherwise fit the description.

Size: equatorial diameter 63-100μm; exine thickness 2-4μm

Size in present study: 72-98μm (based on 5 specimens)

Remarks: Agrees with description of Hacquebard (1957) although the size range allotted in this study exceeds that quoted by Hacquebard (1957).

Range/occurrence: Horton Group, Nova Scotia, West Gore and Blue Beach samples Mississippian

Present in samples: N20, N23, N22, N16

Infraturma RETUSOTRILETI Streel 1964

Genus: RETUSOTRILETES Naumova emend Streel 1964

Type species: *R. simplex* Naumova 1953

Retusotriletes incohatus Sullivan 1964

Holotype: Sullivan 1964, p. 1251-1252, pl. 1 figs. 5-7; Higgs, Clayton and Keegan 1988, p 52, pl2. fig.20

Diagnosis: (Sullivan 1964 p.1251-2, in Higgs *et al.* 1988, p. 52) "Radial, trilete, acamerate miospores. Amb circular, subcircular or rounded triangular. Trilete mark distinct to indistinct, sutures distinct or indistinct, straight, extending between two third and four fifths of spore radius, frequently accompanied by either low narrow lips or low elevated folds, which decrease in height towards ends of sutures. Ends of sutures fuse laterally with well defined curvaturae which define contact areas with thinner exine. Exine laevigate, thicker outside curvaturae and thinner with tendency to being infrapunctate in contact areas. Exine 2-4μm thick."

Size: 32(54)75μm;

Size in present study: 51x45, 46x60μm

Remarks: Agrees with original diagnosis. Subcircular, smooth outline; thick exine, amber in colour.

Range/occurrence: Upr. Devonian, Strunian, LL biozone England; Tournaisian, CM biozone, England, Owens (pers. comm.); VI-PC biozones (Higgs 1996)

Present in samples: N24, N18

Genus: VIDEOSPORA Higgs and Russell 1981

1971 *Punctatisporites glabrimarginatus* Owens

Type Species: *V. glabrimarginatus* (Owens)

Diagnosis: (Higgs and Russell 1981) "Trilete acamerate miospores. Mb subcircular to rounded triangular. Distal surface laevigate. Proximal surface ornamented with conate, granulate, spinose, baculate or verrucate elements which may be discrete and or fused, and of regular or irregular distribution. Suturae extending ½ to 3/4 almost the total spore diametes, simple or with labra. Exine thin, commonly folded and mmaybe thickened at the proximal pole."

Videospora glabrimarginata (Owens) Higgs and Russell 1981

Holotype: Owens

Description: (Higgs and Russell 1981) "Amb subcircular. Suturae straight, simple, length half to three quarters of the spore radius. Exine 1,5μm in thickness thickened immediately adjacent to the suturae particularly at the proximal pole, thus forming a darkned triangular area. Distal surface laevigate. Proximal surface ornamented with grana. Ornament is concentrated at the proximal pole, along the suturae (thus amplifying the exinal darkening in this region), and in triangular areas at the sutural terminations. The equatorial and outer interradial areas of the proximal surface laevigate or sparsely ornamented. Compression folds common."

Size: 65(77)98μm (Higgs and Russell 1981);

Size in present study: 47.5μm (based on 1 specimen)

Range/occurrence: *V. glabrimarginatus* initially described from the Frasnian Griper Bay Formation of Melville Island, Arctic Canada. There have since been two records in Ireland, from the Sherkin Formation (Givetian-Frasnian) of West Cork by Clayton and Graham (1974) and from the early Tournaisian 'Old Red Sandstone' facies at Hook Head, Co. Wexford by Higgs 1975.

Present in samples: N14

Infraturma APICULATI (Bennie and Kidston) Potonié 1954

Genus: ACANTHOTRILETES (Naumova) Potonié and Kremp1954

Type species: *A.ciliatus* (Knox) Potonié and Kremp 1954.

Diagnosis: (Potonié and Kremp 1954 p. 133; translation in Smith and Butterworth 1967, p. 177). "Trilete isospores or microspores. Exine ornamented with spinae between which there is little or no spoace. Scarcely any blunting of the gradually tapered spinae, the length of which is more than twice their diameter."

Range: Viséan to Namurian A (Arnsbergian); A.triquetrus Upper Duckmantian and Bolsovian (Smith and Butterworth 1967).

Affinity: Unknown

Remaks: Amb subtriangular; convex to straight sided with rounded angles. Outline modified by spinae closely spaced. Spinae 3-5μm in length; no more than 1.5μm at base, gradually tapering towards distal terminus. All specimens are broken or damaged; contact mark not visible. Exine moderately thin; all specimens yellow.

Size: 25-45μm (based on 5 specimens)

Present in samples: N24, N23, N19, N18, N15

Genus: ANAPLANISPORITES Jansonius 1962

Type species: *A. telephorus* Klaus 1960

Diagnosis (Jansonius 1962, in Smith and Butterworth 1967, p.165) "Trilete miospores; equatorial outline sircular to subcircular; exine relatively thin, distally with numerous warts, granules or low coni, usually not more than 2μm; ornaments regularly disposed, uniform in size and shape, showing on equatorial outline but only barely extending into proximal face; dehiscence area without ornamentation, essentially laevigate; sutures more or less distinct, mostly over half radius in length; dehiscene area relatively large."

Anaplanisporites globulus (Butterworth and Williams) emend.1948 Knox, p.158, fig 19

1958 *Apiculatisporis globules* Butterworth and Williams p.363, pl. 1 figs 26, 27

Holotype: Plate 7, fig 6 (Smith and Butterworth 1967). Preparation T38/1 in collection of Coal Survey Laboratory Sheffield.

Diagnosis: (emended from Butterworth and Williams 1958, p. 363, in Smith and Butterworth, 1967, p. 168, pl.7 fig. 6, 7). "Amb broadly rounded or triangular. Laesurae simple, straight, one half to two thirds of radius. Ornament restricted to distal surface, variable, consisting of small coni or verrucae, widely and irregularly spaced; approximately 15 to 30 project round the equator. Proximal face laevigate."

Size: 32(36)46μm

Size in present study: 43x48μm (based on one specimen)

Range: Namurian A (Arnsbergian) (Smith and Butterworth 1967)

Affinity: unknown

Present in samples: N15

Genus: LOPHOTRILETES (Naumova) Potonié and Kremp 1954

Type species: *L. gibbosus* (Ibrahim) Potonié and Kremp

Diagnosis: (Potonié and Kremp 1954, p. 129; translation in Smith and Butterworth 1967, p. 155) "Trilete isospores or microspores, of similar structure to *Apiculatisporitis,* but with the equatorial outline distinctly triangular rather than circular; sides generally convex, sometimes concave. Forms with very convex sides approaching a circle in equatorial outline are included in *Apiculatisporis.*"

Affinity: The spores of the fern *Sphyropteris* cf. *boenschi* Stur figured by Remy and Remy (1957, pl. 2, fig. 7) appear to be of *Lophotriletes* type.

Lophptriletes sp.

Description: triangular, straight, rounded; trilete, laesurae straight, extend to edge of central body. Specimen is degraded and not adequately preserved to allow speciation.

Size in present study: 48.6x45μm

Present in samples: N15

Genus: PUSTULATISPORITES Potonié and Kremp 1954

Type species: *P. pustulatus* Potonié and Kremp 1954

Diagnosis: (Potonié and Kremp 1954, p. 134; translation in Smith and Butterworth 1967, p. 168) "Trilete isospores or microspores. Exoexine with individual widely spaced grana, warts or short blunt coni. The intervals between the sculptural elements are generally so wide that more than sufficient space is left for additional ornamentation elements are generally so wide that more than sufficient space is left for additional ornamentation elements of the same size. The bases of these elements are in contact only here and there and therefore never assume a polygonal shape."

Affinity: unknown

Pustulatisporites papillosus (Knox) Potonié and Kremp 1955

1948 Type 16K Knox, text-fig. 13

1950 *Triquitrites papillosus* Knox, p. 327, pl. 17, fig. 234

1955 *Pustulatisporites papillosus* (Knox); Potonié and Kremp, p. 82

Lectotype: Pl. 7, fig. 9, Smith and Butterworth 1967. Knox did not designate a holotype. A specimen marked by Knox on her preparatrion 360A has been chosen as the lectotype (T84/1 in collection of Coal Survey Laboratory, Sheffield) by Smith and Butterworth (1967). Dunfermline Splint Seam, Lumphinnans No. 1 borehole, West Fife Coalfield, Scotland; Namurian A (Arnsbergian)

Diagnosis: (Butterworth and Williams 1958, p. 365, in Smith and Butterworth 1967, p.168) "Amb triangular, sides slightly concave, straight or slightly convex, angles rounded or truncate, outline modified to varying degree by ornament. Laesurae simple, straight, extending almost to margin. Ornament distal, of widely spaced verrucae, or short bacula, up to 5μm in diameter and 8μm in height, slightly tapering with blunt or well-rounded

apices; ornamentation variable on any one specimen; proximal surface laevigate. Exine moderately thick.

Size: Lectotype 45μm, 37(50)65 Butterworth and Williams 1958; 40μm (based on 1 specimen)

Occurrence: Namurian A (Arnsbergian) (Smith and Butterworth 1967)

Present in samples: N18

Genus: RAISTRICKIA Schopf, Wilson and Bentall 1944

Type species: R.*grovensis* Schopf in Schopf, Wilson and Bentall 1944

Diagnosis: (Potonié and Kremp 1955, p. 85; translation in Smith and Buterworth 1967) Trilete isospores and microspores. Exine largely covered with bacula, i.e. roughly cylindrical ornamentation. In some cases fairly distinct cone shaped elements appear interspersed with bacula. The individual bacula are thinner, or barely thicker, at the base than over their entire length; alternatively, they showmarked broadening at the root only. At their top ends the bacula are generally unpointed, only slightly pointed, or rounded; they are in fact often abruptly truncated. This truncation is apparently partly a secondary phenomenon, as seems to be borne out by the irregular fracture, sometimes by the raggedness at the ends, and frequently by a distinct variation in bacula length. The bacula vary appreciably in thickness, by as much as a factor of two. Frequently the bacula tend to split at their ends into two or more papillae.

Affinity: Filices, Radforth 1938, 1939; Mamay 1950.

Raistrickia nigra Love 1960

Diagnosis: Radial, trilete, acamerate miospores. Amb circular to broadly rounded triangular. Trilete mark distinct, laesurae simple, straight, extending up to two thirds of the spore radius. Exine relatively thick, ornamented with relatively sparsely distributed baculae. Elements are more or less regular in form, more or less equal in width and height (5-6μm), with normally rounded but occasionally blunt to roundly tapered terminations. Ornament restricted to the distal surface and more equatorial portions of the proximal surface.

Size: 60-75μm; 45(58)61μm (based on 13 specimens)

Remarks: The distinctive form of the squat, rounded broad based baculae distinguishes this species from all other species assigned to the genus Raistrickia.

Range: "NM-NC (Asbian (Viséan) – Pendleian (Namurian)) miospore zones Kora, 1993. Abu Rodeiyim well, Sinai, Egypt; Abu Thora Fmn., Late Viséan" (pers. comm. Owens 2000)

Genus: TRICIDARISPORITES Sullivan and Marshall 1964

Type species: *T. balteolus* Sullivan and Marshall, sp. *nov.*

Diagnosis: (from Sullivan and Marshall 1964, p. 268) "Radial trilete miospores; amb triangular with concave to convex sides and rounded apices; trilete rays distinct or obscured by ornamentation; proximal surface laevigate; distal and equatorial surfaces ornamented with grana, cones, pila or spines; equatorial ornamentation elements largest along the interradial margins (up to about two and a half times the size of the distal ornamentation), reduced or absent at the apices; ornamentation elements along the interradial margins of the equator discrete or laterally coalescent."

Tricidarisporites fasciculatus (Love 1960) Sullivan and Marshall 1964 comb. nov.

1960 *Tricidarisporites (al. Procoronaspora) fasiculatus* (Love1960) Sullivan and Marshall 1966 new comb.

Holotype: *Procoronospora fasiculatus* Love 1960, p. 112-113, pl. 1, fig. 2; text-fig. 2.

Diagnosis: (Love 1960, p. 112; in Smith and Butterworth 1967, p. 164) "Triangular with almost straight interradial sides, apices narrowly rounded; trilete rays almost to the apices, lips thickened; ornament of granules only on distal surface and on the interradial equatorial margins where about 15 granules appear on each one; equatorial apices and proximal surface laevigate."

Description: Rounded, straight to convex, triangular; exine quite thick, yellow; proximal surface laevigate; distal surface densely ornamented with grana and pila; grana *c.* 0.5µm in diameter; equatorial elements pilose; pila 1.5-2µm long at the center of the interradial margin tapering towards the apices; pila about 0.5 µm wide at the base and 0.8µm wide at the top.

Size: 41-47µm (Sullivan and Marshall 1966 based on 4 specimens);

Size in present study: 38µm (based on 1 specimen)

Range/occurrence: Scottish Viséan (Sullivan and Marshall 1966); Lower Oil-Shale Group of Scotland (Love 1960)

Present in samples: N23

Genus: VERRUCOSISPORITES Ibrahim (1933), Smith and Butterworth emend. (1967)

Type species: *V. verrucosus* (Ibrahim) Ibrahim 1933

Diagnosis: (Smith and Butterworth 1967, p. 147) "Trilete isosipores and microspores. Amb circular, subtriangular or roundly triangular. Margin generally crenulate but may be undulate to irregularly lobate. Laeurae grenerally simple, if ridgedd, lips not exceeding height of ornament, length variable from one-half to length of spore radius. Exine predominantly verrucate but sculptural elements may include some small proportion of rugulae, coni or bacula. Sculpture generally comprehensive but size of eleents may be reduced in contacta reas. In plan view shape circular, polygonal, phaseolate or irregular; in profile may be dome-shaped or sides may taper to varying dgrees and the apices may be flat, obliquely truncate or well rounded, height equal to or less than breadth. Sculptural elements generally closely spaced but distance variable, generally not greater than maximum diameter of verrucae. Number of elements projecting from margin usually greater than 10 but rarely exceeding 100. Exine thickness (including sculpture) rarely exceeds 10μm."

Affinity: Filicales, Remy and Remy (1957).

Verrucosipsorites nodusus Sullivan and Marshall 1966

Holotype: pl. 1, fig 20, pg 369 (Sullivan and Marshall 1966) from shale below the Blackbyre Limestone.

Diagnosis: Trilete radial spores; amb subcircular to oval; rays straight, extending up to ¾ of spore radius; exine ornamented with verrucae up to 4-5μm wide an 2μm high; can have broadened terminations, broadly rounded to blunted crests.

Size: equatorial diameter 34(38)48μm; verrucae up to 4-5μm wide, up to 2μm high (Sullivan and Marshall 1966)

Size in present study: 42.5(52.7)64μm (7 specimens) N

Present in samples: N24, N22, N19, N16, N15

Infraturma MURORNATI Potonié and Kremp 1954

Genus: CONVOLUTISPORA Hoffmeister, Staplin and Malloy 1955

Type species: *C. florida* Hoffmeister, Staplin and Malloy

Diagnosis: (Smith and Butterworth 1967, p. 183) "Spores radial, trilete; circular to subcircular, probable original spherical shape indicated by lack of orientation; preference;

ornamentation closely packed overlapping anastomosing vermiculate or obervermiculate ridge like proceeded, often causing a convoluted or coarsely reticulate-punctate appearance; trilete rays short, usually simple, but may have distinct lips, often obscured by the overlapping ridges; spore coat thick, lacking conspicuous folding, translucent; diameter 40-150μm."

Affinity: The dispersed spores of *Senftenbergia pennaeformis* Brongiart, figured by Radforth (1938, pl. 1, figs 2,6, and 7) would appear to belong to Convolutispora rather than to *Camptotriletes* Naumova as suggested by Potonié (1962, p. 106)

Remarks: circular to triangular; uneven outline, smooth anastamosing convolute ornament if various width and density; exine of moderate thickness, colour varies from yellow to amber brown; contact mark when visible trilete, straight, extends to equator, can be open, can show thickening

Present in samples: N24, N23, N22, N20, N19, N18, N17, N16

Genus: DICTYOTRILETES (Naumova) emend Smith and Butterworth 1967

Type species: *D. bireticulatus* (Ibrahim) Potonié and Kremp 1954

Diagnosis: (emended from Potonié and Kremp 1954 p144 by Smith and Butterworth 1967, p 144). "Radial, trilete miospores. Exine with, reticulate sculpture. Arrangement of muri may give a well defined or poorly defined reticulum. The muri may project at the amb, or may be low and scarcely recognizable. Lumina regular, or highly variable in shape, generally greater than 6μm in diameter. Reticulum may be confined to distal surface."

Affinity: Reticulate spores have been recovered from *Sclerocelyphus oviformis* Mamay (1954) but the systematic position of this fructification is uncertain.

Dictoytriletes c.f. pactilis Sullivan and Marshall 1966

Holotype: Specimen illustrated in pl.2 fig 3 from the shale below the Backbyre limestone. Size 6μm

Diagnosis: (from Sullivan and Marshall 1966 pg 271). "Amb circular to oval, sometimes approaching a polygonal outline. Trilete rays not observed. Muri about 1μm thick (exact thickness difficult to measure) and up to 14μm high, frequently preserved parallel with the equator About 10 muri cross the equator. Lumina irregularly polygonal, 10-18μm in diameter. Parallel sided compression folds often surround the equator."

Size: 52(58)63μm

Remarks: circular; contact mark not visible; muri less than 1μm thick; all specimens broken; lumina polygonal; specimens are both in a poor state of preservation. Although they are most likely to be *D. pactilis* it is not that they exhibit features that do not agree with the original diagnosis but that there is not enough left of the spore to definitely name it as such.

Range: Viséan, Scotland (Sullivan and Marshall 1966); Lower Oil Shale group, Scotland (Love 1960)

Sample present: N16

Genus: MICRORETICULATISPORITES (Knox) Potonié and Kremp 1954 *non sensu* Bharadwaj

Type species: *M. lacunosus* (Ibrahim) Knox 1950

Diagnosis: (Potonié and Kremp 1954, p. 143; translation in Smith and Butterworth 1967, p. 190) "Trilete isospores and microspores. Amb triangular to circular. Exine extrareticulate with small lumina not much greater than 6μm in diameter, mostly smaller. Muri sometimes imperfect and branched, with lumina having a corresponding shape. Occasionally muri vary in height and are sometimes inclined to the perpendicular. Margin finely notched to undulating."

Affinity: Filicales. Spores of *Scolecopteris iowensis* Mamay 1950 (p. 249, pl. 5, fig. 25) may belong to *Microreticulatisporites* according to Potonié (1962, p. 99)

Remarks: A number of spores fit this genus but do not retain sufficient detail for all of them to be designated to an appropriate species. The microreticulate ornament is the main feature used for identification however they fit the genus diagnosis.

Present in samples: N18, N15

Microreticulatisporites concavus Butterworth and Williams 1958

Holotype: Plate 11, fig. 1, after Butterworth and Williams 1958, pl. 1, fig. 56. Preparation T45/1 in collection of Coal Survey Laboratory, Sheffield. 44μm

Type locality: Seam at 1,872 ft. 7in., Righead borehole, West Fife Coalfield, Scotland; Arnsbergian.

Diagnosis: (from Butterworth and Williams 1958, p. 367, in Smith and Butterworth 1967, p. 190) "Amb triangular, angles broadly rounded, interradial margins concave. Laesurae two-thirds radius. Ornamentation finely microreticulate, distinct and regular."

Size: 30(40)52μm (Butterworth and Williams 1958)

Size in present study: 30x35µm (based on one sample)

Remarks: Agrees with original description. Rounded triangular concave-straight; irregular outline; trilete; laesurae straight, simple, extend to equator; microreticulate ornament;

Range/occurrence: Namurian (Smith and Butterworth 1967)

Present in samples: N22

Genus: SECARISPORITES Neves 1961

Type species: *S. lobatus* (Neves 1961)

Diagnosis: (Neves 1961,) "Trilete, iso- or microspores, equatorial outline subcircular, ovate to subtriangular. The exoexine is expanded into a series of lobate outgrowths which are of such dimensions as to give rise to an outer zone or pseudo-flange in the compressed spores. The outer zone is not continuous and deep indentations frequently occur between the bulbous lobes. The distal polar region of the spores is covered by an ornament of loosely spaced ridges and warts."

Secarisporites remotus Neves 1961

Holotype: 56µm, Neves 1961, pl. 32, fig 9, p. 262

Type locality: Non-marine shales with *Carbonicola exporrecta*, Hipper Sick, Derbyshire (Loc. 12), Yeadonian stage.

Diagnosis: (Neves 1961, p. 262) "Equatorial diamaeter triangular, sides straight to slightly concave. Apices rounded; kyrtome built up from a series of small, bluntly conical elements, which also occur scattered in the interradial regions."

Size: 45-60µm (Neves 1961)

Size in present study: 30(41)54µm (based on 4 specimens)

Range/occurrence: Upper Namurian B-Namurian C (Neves 1961).

Present in samples: N22, N18, N14

Subturma ZONOTRILETES Waltz 1935

Infraturma AURICULATI (Schopf) Dettmann 1963

Genus: TRIQUITRITESPORITES (Wilson and Coe) Potonié and Kremp 1954

Type species: *T. arculatus* Wilson and Coe 1940

Diagnosis: (Potonié and Kremp 1954, p. 153; translation in Smith and Butterworth 1967, p. 201) "Trilete isospores, or microspores; amb approximately triangular. Exine at angles

only slightly thickened and therefore appears to be darker (valvae) or shows fairly small projections, which are either pointed or rounded, the rounded projections being described as auriculae. These auriculae tend to become inflated and more or less to protrude cushion-wise beyond the contour of the spore in contrast to the auriculae of *Tripartites*. Occasionally the three valvae, or auriculae, may be found joined by a narrow flange at the equator."

Affinity: Potonié (1962) provides no definite evidence for the palaeobotanical affinities of this type of spore. A possible filicean relationship has been suggested by Schopf, Wilson and Bentall (1944, p. 46)

Triquitrites marginatus Hoffmeister, Staplin and Malloy 1955

Holotype: pl. 39, fig. 12, p. 397, (Hoffmesiter, Staplin and Malloy, 1955) TCO-82, 2072 ft., slide 1, ser. 15,789, Hardinsburg formation

Type locality: TCO-82, 2072 ft, Hardinsburg Formation, Illinois, U.S.A.

Diagnosis: (from original description in Hoffmeister, Staplin and Malloy, 1955, p. 397) "Spores radial, trilete; axial view sublenticular; proximal view subtriangular, radial margins convex, interradial margins concve; equatorial flange distinct, widest at radial margins, narrow or absent at the interradial margins; central body levigate, flange faintly fluted, thicker than central body; trilete rays distinct, simple, almost equal to central body radius; spore coat relatives thick, lacking conspicuous folding, translucent"

Size: 42-61μm (Hoffmeister, Staplin and Malloy 1955);

Size in present study: 35(37)45μm (based on 8 specimens)

Remarks: Conforms to original description.

Range/occurrence: Hardinsburg Formation, Upper Mississippian (Hoffmeister, Staplin and Malloy 1955)

Genus: TRIPARTITES (Schemel 1950) Potonié and Kremp 1954

Type species: *T. vetustus* Schemel 1950

Diagnosis: (from Potonié and Kremp 1954, p. 154; translation in Smith and Butterworth 1967, p. 207) "trilete isospores, or microspores, approximately triangular at equator. Exine at the angles broadens to form auriculae (radial crassitudes) generally much larger and more lobate (or spatulate) than in *Triquitrites* – hence virtually tri-lobal at equator, not unlike treoil. Auriculae are often found to be radially plicated (unlike *Triquitrites*) due to their more membranous character, when they may sometimes also be rather short and

broad. The auriculae may be joined at the equator by a flange." size range 30-70μm (Hoffmeister, Staplin and Malloy 1955).

Tripartites vetustus Schemel 1950

Holotype: Schemel 1950, pl. 40, fig. 11. Preparation in collection of Missouri Geological Survey.

Type locality: 24 in. coal about 550ft. above top of Madison Formation, Draggett County, U.S.A.; Mississippian.

Diagnosis: (from description in Schemel 1950, p. 242; in Smith and Butterworth 1967, p. 209) "Amb subtriangular, angles broadly rounded or blunt, interradial margins modately to strongly concave. Laesurae 1-2μm shorter than radius in length. Equatorial flange widest at corners and very narrow, or absent, in the interradial regions; plicated in the widest portions. Flange laevigate; remainder of exine laevigate to minutely punctate."

Size: 30-40μm (Schemel 1950); 30-37μm (Hoffmeister, Staplin and Malloy 1955); 30(42)50μm (Smith and Butterworth 1967);

Size in present study: 35-36μm (based on 4 specimens).

Range/occurrence: Upper Viséan and Namurian (Smith and Butterworth 1967); Upper Mississippian (Hoffmeister Staplin and Malloy 1955)

Present in samples: N17, N15

Infraturma CINGULATI (Potonié and Klaus) Dettmann 1963

Genus: KNOXISPORITES Potonié and Kremp 1954, Neves and Playford 1961

Type species: *K. hageni* Potonié and Kremp 1954

Diagnosis: (Neves and Playford 1961, report to commission International de Microflore du Paléozoïque; in Smith and Butterworth 1967, p. 218). "Trilete isospores or microspores with an equatorial flange (cingulum) which is of more or less uniform thickness throughout its width, possibly tapering slightly in the immediate vicinity of the equator. The distal hemisphere of the spores is characterised by variably disposed radial and/or concentric bands of thickening. The equatorial outline of the cingulum is circular to rounded-triangular, more or less conformable with that of the spore body, departing from it locally where the fusion of radial elements and the flange produces a swollen node of thickening. Small, thickened lobes may project from the cingulum on to the proximal surface of the spore body.

Affinity: unknown.

Knoxisporites stephanopherous Love 1960

Diagnosis: (Love 1960, pp 118-119, pl. 2 fig 1) "Radial, trilete, cingulated miospores. Amb circular, subcircular to rounded triangular. Trilete mark distinct, sutues straight, extending to margin spore body, simple or accompanied by low narrow thickened labra which typically become expanded equatorially to form triangular thickened areas which fuses onto the proximal surface of the cingulum. Exine laevigate. Intexine forming spore body rarely discernible. Exoexine developed into second ring of thickening mid-way between the equator and the distal pole with irregular radially oriented thickened ribs in theinter radial positions sometimes connecting it to the cingulum. An area of distal polar thickening is also developed on the exoexine, 5-10μm in diameter."

Size: Equatorial diameter 40-90μm

Range/occurrence: Lower Oil Shale Group Scotland (Love 1960); Coal Measures of South Wales (Sullivan 1962); Innimore Bay Scotland (Love and Neves, 1963); Viséan-Namurian (pers. comm. B.Owens)

Present in samples: N15 e.f. S35.2

Knoxisporites triradiatus Hoffmeister, Staplin and Malloy 1955

Holotype: TCO-82, 2087ft, slide 6, ser. 18,939 (pl 37, fig 12)

Locality: Hardinsburg Formation, TCO-82; occasional occurrence

Diagnosis and description: (original description in Hoffmeister, Staplin and Malloy 1955) "Spores radial, trilete; outline circular, sometimes circular, sometimes folded into a roughly rectangular shape; arcuate compression folds indicate a probable subspherical form; orientation usually proximal-distal; proximal surface smooth; equatorial thickening or girdle broad, with three acute inward projections at the radial positions which extend to or slightly beyond the ends of the trilete rays; distal surface smooth, three bands of thickening radiate from the pole to join the equatorial girdle, and are rotated 60 degrees from the trilete mark of the proximal surface; trilete rays distinct, lips moderate, length two thirds spore radius; spore coat sub transparent, colour amber brown; diameter 50-88μm."

Remarks: agrees with original description. Triangular, convex, rounded; smooth outline Trilete, laesurae extend to edge of centre area.

Size: Holotype-80x86μm, girdle 10μm, distal bands 12μm; present study:

Size in present study: Equatorial diameter 75x81μm; Body 56x56μm; distal bands up to 10μm

Range/occurrence:

Present in samples: N18

Genus: MUROSPORA Somers 1952

1952 *Murospora* Somers, p.20

1954 *Simozonotriletes* (Naumova 1939) ex Potonié and Kremp, p. 159; pl. 12, fig. 53

1958 *Simozonotriletes* Potonié and Kremp; Sullivan, p. 126-127

1958 *Westphalensisporites* Alpern, p. 78

Type species: *M. kosankei* Somers 1952.

Type Locality: Lower Jubilee Seam, Sidney Coalfield; Nova Scotia, Pennsylnanian

Diagnosis: (Carson 1995, after Somers 1952, p20) "Trilete, radial spores. Rays extend along the whole radii of spore body. Prominent lips, not elevated, arcuate ridges are not developed. Triangular in transverse section; sides moderately and regularly concave; corners rounded, wedge shaped or blunt. Spore wall is extremely thick (4-9μm). Ornamentation of spore wall ranges from laevigate to slightly granulose at the corners. Rarely folded."

Size: equatorial diameter 45x40μm; spore body 35x35

Size in present study: 35-47.5μm N

Affinity: unknown

Remarks: one specimen was found that fitted the diagnosis for this genus but could not be speciated. Following is a description:

subcircular to subtriangular (convex, rounded) radial spore; outline modified by murornate sculpture; cingulate (4-7.5μm); Trilete, indistinct or distinct; moderately thick exine; crange to amber brown

Sample present: N24, N22

Murospora intorta (Waltz) Playford 1962

1938 *Zonotriletes intortus* Waltz *in* Luber and Waltz, p. 22 (no description; pl. 2, fig. 24

1954 *Simozonotriletes intortus* (Waltz) Potonié and Kremp 1954, p. 159

1956 *Simozonotriletes intortus* (Waltz) Ischenko, p 88-89; pl. 17, fig. 204

Lectotype: Luber and Waltz 1938, p. 22, pl. 2, fig. 24 (designated by Horst)

Type locality: Moscow Brown Coal; Tournaisian or Viséan. Neotype, Horst (1955, pl. 22, fig. 52) Upper Silesia; Westphalian A. Holotype, designated by Hacquebard and Barss (1957, pl. 5, fig, 1), Canada; Lower Carboniferous.

Diagnosis: (Sullivan 1958, p. 127; in Smith and Butterworth 1967, p. 237) "Trilete rays extend almost to margin of the central area; lips thin, intertectum narrow, remainder as for genus"

Description: triangular, rounded, straight to concave sides; outline smooth; body subtrialngular with concave sides and rounded apices, smooth conformable with spore outline, spore body laevigate; trilete; laesurae distinct, simple, straight, length at least two-thirds spore body radius; cingulum well defined, laevigate; uniform or may be perceptibly thicker and/or broader about apices.

Size: 33(44)57µm (Playford 1962);

Size in present study: equatorial diameter 52.5-60µm, cingulum7.5-15µm (based on 2 specimens)

Range/occurrence: Lower Carboniferous (numerous workers) to Middle Westphalian B (Nottinghamshire) (Playford 1962)

Middle Westphalian A-Westphalian B (Sullivan 1958 under synonym *S. intortus*)

Comment: Same species named in Smith and Butterworth (1967) as *Simozonotriletes intortus* (waltz) Potonié and Kremp.

Samples present: N17, N16

Genus: RETICULATISPORITES (Ibrahim) Neves 1964

Type species: *R.reticulatus* Ibrahim 1932

Diagnosis: (Neves 1964, p. 106; in Smith and Butterworth 1967, p. 220). "Trilete isospores or microspores with a differentiall thickened cingulum. Equatorial outline rounded triangular to somewhat polygonal; irregular embayments in the outline may occur particularly in poorly preserved, larger specimens. Outline of spore cavity triangular to sub-circular.

Cingulum has a peripheral zone of thickening and a further band of thickening adjacent to and slightly over lapping the spore cavity outline. Between the thickened bands the cingulum has a concentric zone in which the exine is relatively thinner. Thickened nodes commonly develop in the peripheral band of thickening, particularly in the inter-radial positions.

The distal surface of the spores is distinguished by a network of muri [*R. reticulatus* and *R.(knoxisporites) margarethae* (Hughes and Playford) comb. Nov.] or by linear bars of exinal thickening [i.e. *Reticulatisporites polygonalis* (Ibrahim) Loose, 1934]. Bifurcation of the muri and linear thickenings is common and various patterns are to be found on the distal surface."

Affinity: Unknown

Remarks: A number of spores recognizable as being reticulate fitted the genus description but did not retain enough detail to allow them to be designated a species.

Present in samples: N23, N22, N20, N18, N16, N14

Reticulatisporites polygonalis (Ibrahim) Smith and Butterworth 1967 emend.

1932 *Sporonites polygonalis* Ibrahim in Potonié, Ibrahim and Loose, p. 447, pl. 14, fig. 8

1933 *Laevigato-sporites polygonalis* Ibrahim, p. 19, pl. 1, fig. 8

1934 *Reticulati-sporites polygonalis* Ibrahim; Loose, p. 155, pl. 7, fig. 16

1955 *Knoxisporites polygonalis* (Ibrahim) Potonié and Kremp, p.117, pl. 16, fig. 318, text-fig. 33

1964 *Reticulatisporites polygonalis* (Ibrahim); Neves, p. 1066

Holotype: Potonié and Kremp 1955, pl. 16, fig 318 after Ibrahim. Preparation A40, b5 (or)

Type locality: Ägir Seam Ruhr Coalfield, Germany; top of Westphalian B.

Diagnosis: (emended from Potonié and Kremp 1955, p.117; in Smith and Butterworth 1967 p. 221) "More or less polygonal in polar compression, but shape very variable due to oblique compression and folding; outline smooth and undulate, due to radial thickenings. Laesurae simple or if ridged, elevation slight; one-half to two thirds of radius. Three zones of cingulum clearly defined, the inner broader than the outer zone. The degree of separation of these thickened zones varies. Exine ornament on distal surface prominent, but reduced proximally; pattern varies in detail but distally consists essentially of a single triangle, or a more or less polygonal structure formed by the bands which connect to the cingulum at interradial positions by three prominent muri. Proximally three bands arising in radial positions pass polewards from the cingulum to meet the laesurae; bands of thickening may also pass towards the proximal pole for shortest distances from other positions on the cingulum. Exine laevigate or scabrate (?infrasculpture); moderately thick.

Size: 79(91)110µm (Smith and Butterworth 1967); 40(51)60µm (based on three specimens)

Remarks: spores are smaller than those recorded by Smith and Butterworth (1967) but they otherwise conform to the diagnosis of Potonié and Kremp (1955).

Range/occurrence: Langsettian, Duckmantian and Bolsovian (lowest part) (Smith and Butterworth 1967).

Present in samples: N24, N22

Reticulatisporites reticulatus (Ibrahim) Ibrahim 1933

1932 *Sporonites reticulatus* Ibrahim in Potonié, Ibrahim and Loose, p. 447, pl. 14, fig. 3

1933 *Reticulati-sporites reticulatus* Ibrahim, p. 33, pl. 1, fig. 3

1938 *Azonotriletes reticulatus* (Ibrahim); Luber in Luber and Waltz, pl. 7, fig. 99

Holotype: p. 222, pl. 14, fig. 16, Smith and Butterworth 1967, after Ibrahim. Preparation B5, b2 (or)

Type locality: Ägir seam, Ruhr Coalfield, Germany; top of Westphalian

Diagnosis: (expanded from Potonié and Kremp 1955, p.112; in Smith and Butterworth 1967, p. 222). "Amb subcircular, sub-angular, or more or less polygonal. Outline smooth, somewhat modified by radial ornament. Laesurae simple, straight, one half to 2/3 of radius. In polar impression cingulum clearly differentiated into 3 zones. Exine ornament comprises bands of thickening, which extend a short distance from equator to proximal pole and form a reticulate pattern distally. Muri broader than high; number of distal muri reaching equator 6 to 15, rarely more. Exine of proximal face and distal lumina laevigate, moderately thick."

Size: 75-90µm; 49(54)60µm (based on 6 specimens)

Range/occurrence: Langsettian to Westphalian D (Smith and Butterworth 1967); base of the Namurian C to top Westphalian (Clayton *et al.* 1977)

Present in samples: N24, N22, N18, N16, N14

Genus: ROTASPORA (Schemel 1950) emend. Smith and Butterworth 1967

Type species: *R. fracta* Schemel 1950

Diagnosis: (in Smith and Butterworth 1967, p. 226, emended from description in Schemel 1950, p.241). "Spores radial, trilete, zonate. Amb circular to subcircular; body triangular to subtriangular. Laesurae simple, generally almost equal to body radius in length. Zona may be reduced in width radially. In the uncompressed state of the zona, if broad, may be directed downwards from the equator in a distal direction thereby forming a 'collar'. Compression results in a broa zona in the radial positions lying distally over the angles of the spore body while projecting horizontally in the inerradial regions. Ornament, laevigate to verrucate, may be different on the body and the zona. Exine relatively thick."

Size range: 28-46μm

Affinity: unknown

Rotaspora knoxi Butterworth and Williams 1958

1948 Knox, p. 157, text-fig. 5

1958 *Rotaspora knoxi* Butterworth and Williams 1958, p. 37, pl.3, figs 21-23

Holotype: (Smith and Butterworth 1967) pl. 15, fig.15, Preparation T56/1 in collection of Coal Survey Laboratory, Sheffield.

Type Locality: Lower Garscadden Irontone Seam at 1,010ft 2in., Cawder Cuilt borehole, Central Coalfield, Scotland; Namurian A.

Diagnosis: (from Butterworth and Williams 1958, p. 378 in Smith and Butterworth 1967, p. 228). "Amb triangular, angles broadly rounded, sides convex; body triangular, less rounded. Laesurae simple, straight, extendiong two-thirds to three-quarters body radius. Zona broadest in interradial areas, narrow at angles; cingulum with narrow peripheral rim. Exine smooth, body vitreous in appearance."

Description: Width of zona in the interradial area up to 5μm. Thickened peripheral rim of zona, up to 3μm wide, often linked to the body by thin, closely spaced radial thickenings. Exine relatively thick.

Size: 36(32)44μm (Butterworth and Williams 1958)

Size in present samples: 35μm (based on 2 samples).

Remarks: triangular, rounded, convex; smooth outline; contact area slightly darker, Trilete, laesurae, straight, simple, extend half to two-thirds spore diameter; laevigate; thickened peripheral rim of zona

Occurrence/Range: Viséan and Arnsbergian (Smith and Butterworth 1967); 1st occ mid Asbian (mid NM graptolite zone; base ME biozone) continues beyond Viséan (pers. comm. Dr. B. Owens)

Genus: STENOZONOTRILETES (Naumova 1937) emend. Hacquebard 1957

Type Species: *S. conformis* Naumova 1953

Diagnosis/description: (from Hacquebard 1957, p. 313) "Spores radial, trilete; triangular, subcircular or circular in proximal view; trilete not always distinct, rays long, at least three fourths radius of central area; rim narrow, rounded (not cuneiform), surrounding central area like a tire around a wheel; ornamentation of central area infragranulose, punctate or smooth, rim essentially smooth to slightly rough; diameter 37 to 119 μm."

Stenozonotriletes bracteolus (Butterworth and Williams) Smith and Butterworth *comb. nov.* 1967

1958 *Lycospora bracteola* Butterworth and Williams, p 375, pl. 3 figs. 26, 27

Holotype: pl. 14, fig. 1 (Smith and Butterworth 1967). Preparation T57/1 in collection of Coal Survey Laboratory, Sheffield.

Type locality: Lower Hirst Seam at 1,854 ft. 2 in., Kincardine borehole, West Fife Coalfield, Scotland.

Diagnosis: (Butterworth and Williams 1958; in Smith and Butterworth 1967, pg. 217) "Amb circular to rounded triangulae, outline smooth to denticulate. Laesurae straight, extending to inner margin of cingulum. Exine covered by small grana. Cingulum approximately one-quarter of total spore radius."

Size: (Butterworth and Williams 1958) 36(43)54μm;

Size in present study: 54μm (based on 1 specimen)

Range/Occurrence: Namurian (Smith and Butterworth 1967), Viséan, coal and shale in the Lower Oil Shale Group of Scotland (Love 1960)

Present in samples: N16

Stenozonotriletes coronatus Sullivan and Marshall 1966

Holotype: Specimen illustrated in Sullivan and Marshall (1966), p.278-279, pl. 3, fig. 2, from the shale below the Blackbyre Limestone. Size 43μm.

Diagnosis: (Sullivan and Marshall 1966, p. 278) "distal surface ornamented with small cones or spines up to 1.5μm high and wide; narrow equatorial cingulum frequently corroded; tecta up to three quarters of radius of spore cavity."

Description: circular to rounded triangular; trilete; laesurae distinct, straight to slightly sinuous, simple, extending from two thirds to three-quarters of spore radius; cingulum 1.5-3μm wide; exine ornamented with small cones, tubercles or spines. Elements 0.5-1.5μm high and wide; not densely distributed; ornamentation usually extends on to the cingulum. Margin of cingulum frequently corroded.

Size: 37(46)55μm (Sullivan and Marshall 1966);

Size in present study: 37.5(42)46 μm (based on 8 specimens)

Range: Appears at the beginning of the TC zone and disappears by the end of the NC zone (Clayton *et al.* 1984)

Present in samples: N24, N23, N19, N18, N16, N15

Infraturma TRICRASSITI Dettmann 1963

Genus: DIATOMOZONOTRILETES (Naumova) Playford 1963

Type species: *D. saetosus* (Hacquebard and Barss) Hughes and Playford 1961

Diagnosis: (Playford 1963, p. 646 in Smith and Butterworth 1967 p. 213). " Microspores radial, trilete; spore body triangular or subtriangular in equatorial outline. Laesurae usually well defined and long; simple or accompanied by lips. Spore body almost entirely encompassed by prominent zona (corona) consisting of numerous strongly developed, mainly discrete saetae (fimbriae) emanating radially from equatorial margin of spore body. Saetae are particularly well developed in central interradial equatorial regions, characteristically exhibiting a gradual diminution in size towards the triangular apices of the spore, where they may be either absent or considerably reduced. Saetae pointed or blunt; sometimes fused, at least in part, but always remain recognizable, individually within the corona as distinct structural entites. Spore body often sculptured, particularly on distal surface"

Affinity: unknown

Diatomozonotriletes sp.

Description: trilete, radial spore. Triangular, straight, rounded; irregular outline. Saetae emanating from equatorial margin at least 14 on inter radial area, none visible on apices of equatorial margin, saetae vary in length-longer in centre of interradial area and shorter towards the apices. Contact mark visible; straight apparently simple closed trilete mark; spore body has pyrite round the inner margin. Exine moderate thickness.

Size: equatorial diameter 24µm; saetae 1.5-4µm

Remarks: Only one specimen found in this horizon. Although the specimen is smaller than most species in this genus it is possible that this is an immature member of the species. The postion of the saetae and the shape of the spore would imply that it is otherwise in the correct genus.

Present in sample: N22

Suprasubturma LAMINATRILETES Smith and Butterworth 1967

Subturma ZONOLAMINATRILETES Smith and Butterworth 1967

Infraturma CRASSITI Bharadwaj and Venkatachala emend. Smith and Butterworth 1967

Genus: CRASSISPORA (Bhardwaj 1957) emend. Sullivan 1964

Type species: C. *kosankei* (syn C.*ovalis*) (Potonié and Kremp) Bharadwaj 1957

Diagnosis: (generic description in Sullivan 1964, p. 375). "Radial trilete miospores. Amb circular to oval, or roundly triangular. Exoexine finely to coarsely infrapunctate; crassitudinous thickening at the equator. Distal surface ornamented with cones and, occasionally, spines; proximal surface without ornamentation. Intexine thin and translucent, outline rarely seen; margin conformable to equator of the spore. Apical papillae visible in intertectal areas. These are particularly well seen in over-macerated specimens. Trilete rays usually indistinct, sometimes accompanied by folds."

Remarks: The above generic description given by Sullivan (1964) is considered by the authors to constitute an emendation of Bharadwaj's diagnosis (1957b, p.125) in which it is stated that the ornament covers the entire exine. Sullivan also mentions other features not referred to in the original description.

Affinity: Rettschlag and Remy (1954, pl. 4, fig. 1) isolated spores from *Sigillariostrobus ciliatus* which resemble *Crassispora.*

Crassispora maculosa (Potonié and Kremp) Bharadwaj 1957 emend.

1948 23K Knox, p. 158, fig. 26

1950 *Verrucoso-sporites* maculosus (Knox);

1955 *Apiculaisporites maculosus* (Knox); Potonié and Kremp, p. 78

1954 *Crassispora maculosa* (Knox); Sullivan, p. 376

Lectotype: Plate 18, fig. 8. Knox did not select a holotype in 1950. A specimen identified by Knox on a slide in the authors possession is therefore designated as lectotype. Knox preparation 360A (T83/1 in collection of Collection of Coal Survey Laboratory Sheffield).

Type Locality: Dunfermlinne Splint Seam, Lumphinnans No. 1 Colliery, West Fife Coalfield, Scotland; Namurian A.

Diagnosis: (Smith and Butterworth 1967, p.234) "Amb circular. Laesurae ridged; ridges narrow and flexuose, one-half to three quarters of spore radius. Equatorial crassitude narrow and weakly developed. Exine with fine and dense granulate infrasculpture and distally covered at fairly regular intervals with grana and coni not exceeding 2μm in height. Proximal surface laevigate."

Remarks: Conforms to diagnosis. Subcircular; outline modified by coni or grana, which can vary in size and distribution density. Contact mark trilete, extends one third to three quarters of spore radius, laesurae straight, simple; oblique compression common for most specimens; single fold due to compression.

Size: 76-121µm (Knox) 67-100µm (based on 14 specimens from NSD horizon)

Range: Viséan to Namurian (Smith and Butterworth1967 pg236); extinction base Arnesbergian, TK zone (Owens 1996)

Present in samples: N24, N23, N22, N20, N19, N18, N16, N15

Infraturma CINGULICAVATI Smith and Butterworth 1967

Genus: CINGULIZONATES (Dybová and Jachowicz) Butterworth, Jansonious, Smith and Staplin 1964

Type species: C.*bialatus* (Waltz) *comb. nov.*

Diagnosis: (Butterworth, Jansonious, Smith and Staplin in Staplin and Jansonious 1964, p. 105). 'Spore trilete; outline convexly triangular to subcircular; two layered; central body (intexine) thin, psilate; outer layer complex, central proximal area thin, minutely sculptured to psilate, sutural ridges or grooves distinct but fine, reaching to the cuesta; cuesta distinctly raised, sometimes internally vacuolated; outer portion of zona much lower than the cuesta, sometimes sculptured; in section, outer portion of zona tapered and relatively thin; distal surface of outer layer generally differentiated into two zones, the central distal area (usually granulose or verrucose) and the zona.'

Affinity: Lycopsida (Chaloner 1958)

Remarks: A number of cingulate but highly degraded spores have been seen in these samples. The trilete mark is rarely visible. There may be some visible projections. Amb is usually triangular to subtriangular; rounded and convex. The body shape usually conforms to the shape of the amb. The flange thins towards the edge and has a grainy appearance.

Cingulizonates bialatus (Waltz) Smith and Butterworth 1967

1938 *Zonotriletes bialatus* in Waltz in Luber and Waltz, p.22, pl. 4, fig. 51

1941 *Zonotriletes bialatus* var. *undulates* Waltz in Luber and Waltz p. 28, pl.5, figs. 71a, b.

1941 *Zonotriletes bialatus* var. *costatus* Waltz in Luber and Waltz, p. 29, pl. 5, fig. 72.

1956 *Densosporites bialatus* (Waltz); Potonie and Kremp, p.114

1956 *Hymenozonotriletes bialatus* var. *undulates* (Waltz); Ischenko, p.63, 64; pl. 12, figs.135-137

1957 *Cingulizonates tuberosus* Dybová and Jachowicz, p. 171, pl. 53, figs. 1-4

1958 *Densosporites striatus* (knox); Butterworth and Williams, p. 380, pl. 3, fig. 36

Holotype: Not designated

Type locality: Bed 6, Verkhni-Goubakhin Colliery, Kalinin Shaft, kizel region, U.S.S.R.; Lower Carboniferous.

Diagnosis: (Waltz, in Luber and Waltz 1941, in Smith and Butterworth 1967, p.260). "Body rounded-triangular or ovate. Rays seldom seen but somewhat shorter than radius of spore body. Flange thin, broad, with undulating surface and irregular margin; inner edge thickened, smooth or striated, sometimes with large tubercules projecting into the inner outer flange."

Remarks: Agrees with original description. Trilete mark rarely seen. Flange thin, broad. Inner edge thickened, smooth or striated. Sometimes larger ornament projecting in to the upper flange

Size: 70-80μm (Luber and Waltz 1938); 25-60μm (Luber and Waltz 1941); 46(60)77 (Playford 1963); 27(37)45μm (Smith and Butterworth 1967)

Size in present study: 28(37)50μm (based on 25 specimens)

Range: Viséan and Namurian (Smith and Butterworth 1967)

Present in samples: N24, N23, N22, N20, N19, N18, N17, N16

Genus: CIRRATRIRADITES Wilson and Coe 1940

(Taken from Playford 1962)

Type Species: *C. saturni* (Ibrahim) Schopf, Wilson and Bentall 1944

Remarks: Subtriangular to rounded; trilete, laesurae straight, thickened and raised, thicker and higher over center area thinning out as ectending towards equator; thin flange, apparently striated, extends from edge of center area apparently cupping the center area; distal area spinose

Present in samples: N22, N20, N16

Affinity: Microspores showing close resemblance to *Cirratriradites anulatus* Kosanke and Brokaw (in Kosanke 1950) have been recovered from the herbaceous, heterosporous lycopod *Selaginellites suissei* Zeiller (Chaloner 1954) and also from the detached heterosporous strolibus *S.crassicinctus* Hoskins and Abbott (1956).

Cirratriradiites elegans (Waltz) Schopf, Wilson and Bentall 1944

1938 *Zonotriletes elegans* Waltz in Luber and Waltzs, p 15; pl 3, fig 32

1956 *Cirratriradites elegans* (Waltz) Potonié and Kremp, p. 126

1958 *Hymenozonotriletes elegans* (Waltz) Ischenko, p67; pl. 7, fig. 88

Diagnosis: (Taken from Playford 1962 description) 'Spores radial trilete; amb convexly subtriangular, conformable with spore body outline. Laesurae distinct, straight; extending to zona, frequently reaching equator; accompanied by conspicuous, smooth, elevated, thickened lips, having maximum development on spore body, extending 4-6µm on either side of laesurae. Spore body, more or less smooth, often folded, shows equatorial decrease in thickness; radially pitted or channeled in corroded specimens.

Size: Equatorial diameter 70-128µm; body diameter 44-63µm (Playford 1962);

Size in present study: Equatorial diameter 55-75µm; body diameter 25-40µm (based on 2 specimens)

Remarks: Conforms to Playfords (1962) description. Triangular convex, angular; outline modified by projections that line and project from the zona. Contact mark trilete; Laesurae straight thickened extending almost to the equatorial margin.

Range: Viséan to Namurian (Luber and Waltz 1938; Ischenko 1958); Lower Carboniferous (Playford 1962)

Present in samples: N24, N18

Cirratriradiites cf. praetergranulates Hoffmeister Staplin and Malloy 1957

Holotype: TCO-82, 2071 ft., slide 10, ser, 18,821, Hardinsburg formation; dimensions 44x48µm, flange 5.6µm. Pl 57, fig 4.

Diagnosis: (taken from Hoffmeister Staplin and Malloy description 1957) "Spores radial trilete; shape lenticular, proximal outline subtriangular; equator marked by a moderately wide flange; central body outline indistinct; surface of both central body and flange equally granulose; trilete rays distinct, lips moderately developed extending to outer flange margin as thickenings; spore coat thin, translucent to transparent."

Size: 43-48µm, flange 3.7-6.0 µm (Hoffmeister Staplin and Malloy 1957); 55x55µm, cirgulum 5-10µm (based on 1 specimen).

Remarks: Spore sub triangular; convex; outline smooth; trilete, laesurae straight, simple extend to equator, appear to be slightly raised, more extreme over center area and lower as exends to equator; granulose ornament, not dense.

Range/occurrence: Upper Mississippian (Chester series; Hardinsburg fm; Illinois) (Hoffmeister, Staplin and Malloy 1957).

Sample present: N18

Genus: CRISTATISPORITES (Potonié and Kremp) Butterworth, Jansonious, Smith and Staplin 1964

Type species: *C. indignabundus* (Loose) Potonié and Kremp 1954

Diagnosis: (Butterworth, Jansonious, Smith and Staplin 1964, p.108; found in Smith and Butterworth pg 253). 'Spores Trilete; outline subtriangular to subcircular; two layered; intexine often indistinct, when preserved almost fills the exoexinal cavity, sculpture absent-minor; ring of setae, apiculae, granules or small pits; sutural ridges or grooves often indistinct, terminated by the setose ring; zona beyond the setae psilate or with scattered granules or small apiculae; spore margin irregular with small scattered processes, or strongly incised if the distal sculpture carries to equatorial margin; distal sculpture prominent, often mammoid or with warts that in part bear setose tips; inner surface of exoexine may be minutely foveolate and vacuolated.'

Affinity: Lycopsida, Chaloner 1962.

Cristatisporites sp.

Description: Sub circular to subtriangular, convex rounded amb. Outline modified by multiple dense processes of variable size and multiple termination (base width 0.5-5µm, process length 0.5-7µm). Body sub circular to sub triangular. Contact mark not visible. Heavy ornamentation means the spore has an amber colour in transmitted light.

Remarks: Specimen similar to that described above is illustrated in Tschudy and Scott, Aspects of Palynology, p.227. There is no description or diagnosis nor is the specimen named to species level.

Size: equatorial diameter max. 63µm (Tschudy and Scott);

Size in present study: equatorial diameter 55x60-65µm; body 25(30)x29(30)µm.

Sample present: N23 M49.4; N16 S29.2

Genus: DENSOSPORITES (Berry) Butterworth, Jansonius, Smith and Staplin (1964)

Type species: *D. covensis* Berry 1937

Diagnosis: (Butterworth, Jansonius, Smith and Staplin 1964, p.101). "Spores trilete; outline convexly triangular to subcircular; two layered; intexine (central body) thin, psilate or faintly roughened, laesurae indistinct, apical papillae sometimes present; proximal surface of outer layer evenly arched or with zona slightly raised above the central proximal area; sutural ridges weak to strong; sometimes connected at their extremities to the zonal

region; proximal sculpture generally absent or minor except for scalloping of the zona in some species, faint roughening or granulosity of the central distal area usually differentiated from distal sonal surface, usually granulose; zona psilate, granulose, spinose, apiclose, verrucose etc.; internal vacuoles (rods) rare or absent." Note that 'zona' applies to the structural feature referred to by the authors of Smith and Butterworth (1967) as a cingulum.

Affinity: Lycopsida (Bharadwaj 1958)

Densosporites anulatus (Loose) *comb. nov.*

1932 *Sporonoites anulatus* Loose in Potonié, Ibrahim and Loose, p.451, pl. 18, fig 44.

1934 *Zonales-sporites* (*Annulati-sporites*) *anulatus* Loose, p.151

1944 *Densosporites annulatus* (Loose); Schopf, Wilson and Bentall, p.40

1956 *Denso-sporites reynoldsburgensis* Kosanke, p. 33, pl. 6, figs. 9-11

1950 *Anulatisporites anulatus* (Loose); Potonié and Kremp, p.112, pl.. 17, figs. 365-372

Holotype: Potonié and Kremp 1956, pl. 17, fig. 365 after Loose, preparation III31, b5 (m/or). Bismarck seam, Ruhr Coalfield, Germany; Upper Westphalian B.

Diagnosis: (Potonié and Kremp 1956, p. 112; translation, in Smith and Butterworth 1967, p. 239) "Cingulum relatively uniform and smooth, having scaly structure. Amb smooth. Central area relatively much lighter than cingulum. Infragranulation obscure. Tetrad mark scarcely discernible."

Size: Eq. diam. 32(48)56: Cing. width 4(7)11; 33(40) 43 : 6(8)12; 26(34)42 : 4(7)9; 28(37)42 : 5(8)11 Smith and Butterworth 1967; 37.5, 35-60 Holotype, Potonié and Kremp 1956.

Remarks: Agrees with original decription. Amb subtriangular. Outline smooth. No contact mark observed on any of the specimens. Central body can be absent but where present is thin and laevigate. Cingulum narrow, tapering only slightly towards the equator, laevigate, 40-45% of spore diameter.

Range/occurrence: Viséan to Lower Westphalian C (Smith and Butterworth 1967)

Present in samples: N24, N22, N19; N18

Densosporites intermedius Butterworth and Williams (1958)

1958 *Densosporites intermedius* Butterworth and Williams, p. 379, pl. 3, figs, 38, 39

1955 *Densosporites tenuis* Hoffmeister, Staplin and Malloy, p. 387, pl. 36, figs. 18, 19 and 23

Holotype: plate 19, fig. 19 (in Smith and Butterworth 1967, p. 240), preparation T61/1 in collection of Coal Survey Laboratory, Sheffield. Spore diameter 35-36μm; 37(43)51; Cingulum width 8(11)15

Type Locality: Seam at 2,082 ft. 2 in., Righead borehole, West Fife Coalfield, Scotland; Namurian A.

Diagnosis: (Butterworth and Williams 1958, p. 379; in Smith and Butterworth 1967, p.240-1). "Outline round to rounded triangular. Central area thin, unornamented, or slightly granular. Tetrad mark not always seen; rays narrow, extending to the edge of the central area. Cingulum broad, roughly one-half spore radius; differentiated into a darker, thicker, inner zone and a lighter equatorial zone. Margin smooth or slightly notched."

Size: 37((43)51μm (Smith and Butterworth, 1967)

Size in present study: 36(40)51μm (based on 18 specimens)

Remarks: Laesurae faint, rarely visible, length slightly greater than radius of central area. Intexine often absent, where present, thin, laevigate, frequently folded. Proximal central area of exoexine can be slightly granulate. Cingulum about 50% of total diameter.

Range: Viséan to Westphalian A (Smith and Butterworth 1967).

Densosporites regalis (Bharadwaj and Venkatachala) Smith and Butterworth 1967

1961 *Cristatisporites regalis* Bharadwaj and Venkatachala, p 33, pl. 6, figs. 101-104

1963 *Densosporites spitsbergensis* Playford, p. 627, pl. 89, figs. 1-5

Holotype: Bharadwaj and Venkatachala 1961, pl.6, fig. 101. Preparation at Birbal Sahni Institute of palaeobotany, Lucknow, India. 95μm; 62-100μm, cingulum 18-26 between the angles, up to 35 at the angles.

Diagnosis: (Bharadwaj and Venkatachala 1961, p. 33, in Smith and Butterworth 1967 p.242) "Radial, subtriangular angles blunt and conical, central body hyaline girdled by a dark brown cingulum, 18-26μm wide between the angles, proximal exine granulose and distal spinose. Extrema lineamenta granulose, Y mark prominent and extending into the cingulum."

Size: 62-100μm (Bharadwaj and Venkatachala 1961); 40(55)80μm (Smith and Butterworth 1967);

Size in present study: 50x45μm (based on one sample)

Remarks: Laesurae not visible; ornament variable; distal spinae more prominent towars the inner margin of the cingulum than at the equator. Cingulum about 50% of total diameter.

Range: Viséan (Smith and Butterworth 1967).

Densosporites spinifer Hoffmeister Staplin and Malloy 1955

Holotype: TCO-82, 2075ft., sl. 3, ser. 19,055 (pl.36, fig. 17); 42X46 μm, equatorial region approximately 10μm.

Type locality:, shale at 2075 ft., Carter No. 3 borehole (TCO-82), Webster County, Kentucky U.S.A.; Hardinsburg formation, Chester series.

Diagnosis: (Smith and Butterworth 1967, p 243) "Spores radial, trilete; outline convexly subtriangular; equatorial region of nearly equal thickness throughout its width, only slightly thinner at outer margin, almost opaque; ornamentation central body coarsely granulose, spines of equatorial region scattered to crowded, 2-6 μm long, sometimes divided, extremely variable in shape and disposition; outer margin spinose; trilete sutures, when preserved, extend slightly into the thickened equatorial region; diameter 32-48μm. Almost opaque equatorial region characterises this species."

Remarks: Agrees with original description. Subtriangular, convex sides; coarsely granulate body, equatorial region dense scattered spinae. Cingulum about 44% of the total diameter

Range: Viséan Namurian (Smith and Butterworth 1967, p.244)

Size: Holotype 46x52μm, 32-48μm equatorial diameter; equatorial diameter 31(36)46 μm : cingulum width 5(8)11; equatorial diameter 33(40)53μm : cingulum width 6(9)15μm (Smith and Butterworth 1967 p. 244);

Size in present study: 30-49μm (based on 6 specimens)

Present in samples: N24, N23, N14

Densosporites sp.

Description: subcircular; smooth outline; contact mark trilete, laesurae simple, straight, extends to edge of central area; central area subtriangular to circular; ornamented; zona laevigate, thick, tapers towards equator, up to 50% of spore diameter; exine moderately thick, dark yellow.

Size in present study: equatorial diameter 45x50μm; centre area 25x30μm based on one specimen

Present in samples: N16

Densosporites triangularis Kosanke 1950

1950 *Denso-sporites triangularis* Kosanke, p.34, pl. 7, fig. 1

1958 *Densosporites spongesus* Butterworth and Williams, p. 380, pl. 3, figs. 40, 41

Holotype: Kosanke 1950, pl. 7, fig. 1. Preparation 144, slide 3. 'Sub-Babylon' Coal, Fulton County, Illinois, U.S.A.; Tradewater Group.

Diagnosis: (from description in Koanke 1950, p. 34, in Smith and Butterworth 1967, p. 244). 'Outline subtriangular. Tetrad mark indistinct. Proximal and distal central areas granulose to vermiculate. Equatorial portion, measuring about 55% of spore diameter, tapers slightly and is variously spinose or punctate.

Size: Holotype: equatorial diameter 58.8x58.8µm, 52-65 : cingulum width 12-19; equatorial diameter 40(51)50 µm : cingulum width 8(12)17µm (Smith and Butterworth 1967)

Size in present study: equatorial diameter 41(47)54µm : cingulum width 9(11.5)16µm

Remarks: Conforms to original description. Subtriangular to triangular, convex, rounded; one end usually longer than the other two; tetrad mark not always visible, where visible extends on to the cingulum; cingulum spinose in area closest to the central body area

Present in samples: N24, N23, N22, N20, N19, N18, N17

Genus: LYCOSPORA (Schopf, Wilson and Bentall 1944) Potonié and Kremp 1954; Somers 1972 emend.

Type species: *L. micropapillata* (Wilson and Coe) Schopf, Wilson and Bentall 1944, considered as a junior synonym of *L. Pusilla* (Ibrahim) emend.

Diagnosis: (translated from Somers 1972) Iso- or microspores, trilete, cinguli or cingulizonate. Maximum diameter around 15 to 50µm. Convex triangular to subcircular equatorial contour seen in polar view; in equatorial view the proximal profile is convex angular, the distal profile convex rounded. Margins generally smooth to finely rugose, but perhaps neatly/cleanly(?) cut. Sutures clear, straight, continuing at least as far as the side of the internal cingulum and sometimes as far as the equator, without narrowing to a point; rarely simple, generally labra +/-thickening, straight to sinuous. The exine is divided in two layers; intexine weakly separated from the exoexine, smooth, very thin, occasionally visible; exoexine complex, thin on the central part, thickened towards the equator. Equatorial formations are composed of an internal partial thickening (Cingulum:C) and an external partial thinning (Zona:Z); the zona perhaps rudimentary, rarely absent; the size of Z+C varies from 1/10 to a little more than 1/3 of the radius (R) of the entire spore, the size of C is less than 1/5R; the relative size of C to Z varies. In Transverse thin section, cuniform equatorial thickening; internal part (cingulum) relatively thickened and part of the external equator (zona) often strongly effilee. Ornamentation of the central part, which

comprises of the labra and the cingulum, can be punctate, microgranulose, granulose, verrucose to rugulose; the zona is smooth or microgranulose to verrucose with sometime a fibrous radial structure or perforations; the ornamentation perhaps reduced on the proximal face. Secondary folds are frequently at the limits of the central part/cingulum.

Affinity: Lycopsida. Arborescent Lepidodendra (Chaloner 1953b, Felix 1954, Abbott 1963; Lepidocarpon (Andrews and Pannell 1942)

Lycospora noctuina (Butterworth and Williams 1958), reviewed by Y.Somers 1972

Holotype: Pl.1., fig. 3; pl. 11, fig. I (in Somers 1972). Preparation T.54/I, National Coal Board, Coal survey Laboratory, Sheffield, England.

Type locality:9" coal at 256'II", sondage Darnley no. 3, Central Coalfield, Ecoss; Upper Limestone Group, Namurian A.

Diagnosis: (Smith and Butterworth 1967, expanded from diagnosis in Butterworth and Williams 1958, p.376). 'Amb rounded triangular; outline smooth or minutely indented, sometimes undulate. Laesurae ridges, straight or flexuose, up to 2μm in width and height, extending to inner, thickened zone of cingulum and sometimes beyond. Cingulum (including flange) relatively broad 4-8μm in width. Exine of central area and inner zone of cingulum finely granulate. A small number of large grana, or verrucae, or rugulae 1-3μm broad and variable in length, occur distally in the central area within the cingulum; flangeof cingulum laevigate, finely granulate, or with small circular, or radially elongate, dissections. Exine of central area thin.

Size: Holotype 36: 30-45 (Butterworth and Williams 1958), 31(35)38, 27(36)47 Smith and Butterworth (1967), 25(28)32.5μm (based on 10 specimens)

Remarks: Agrees with original diagnosis. Triangular, convex, rounded; oultine smooth; trilete, laesurae smooth, straight, ridges, extend to edge of center area, cingulum thicker at inner edge thinning towards the equator; central area thin with rugulose ornament

Range: Namurian A, Viséan, Westphalian A (Smith and Butterworth 1967)

Lycospora pusilla (Ibrahim) (Schopf, Wilson and Bentall) Somers 1972

1932 *Sporonites pusillus* Ibrahim in Potonié, Ibrahim and Loose, p. 448, pl. 15, fig. 20

1933 *Zonales-sporites pusillus* Ibrahim, p.32, pl.2, fig. 20

1934 *Granulati-sporites pusillus* (Ibrahim) Loose, p. 146, pl.7, fig.3

1938 *Zonotriletes pusillus* (Ibrahim) Waltz in Luber and Waltz, p.13, pl.3, fig 33

1944 *Lycospora pusillus* (Ibrahim) Schopf, Wilson and Bentall, p.54

Holotype: Pl. 1, fig.13; pl 11, fig. 6-8 (Somers 1972). Preparation B27, al(0); Staatl. Geologische Kommission Berlin. 38μm. Diameter 25-40μm; C+Z/R:1/10 (after Potonié and Kremp 1956)

Type locality: Couche Agir, Ruhr basin, Germany; Horster Schichten supérieures, Westphalian B (Upper)

Diagnosis: (translated from Somers 1972) Equatorial contour rounded triangular to almost circular; margin smooth to finely denticulate. Sutures clear, simple where with labra, straight to slightly 'flexueuses', which continues at least as far as the central area, it often continues into the cingulum or as far as the equator. The size of these equatorial features is variable, greatest at 1μm, at 1/10 to a little less than 1/3 of the radius of the spore; the zona perhaps rudimentary, or the smaller size equal or greater than the cingulum. Exine of the central area and of the cingulum is regularly punctate, microgranulose to granulose; zona smooth, punctate or very finely microgranulose, present sometimes a slight radial fibrous structure or small circular perforations along the radial. Exine of the central area is thin, often ornamented with small secondary folds parallel to the equator.

Size: 28(35)41μm (based on 25 specimens)

Range: 1st occurrence base TS zone, Mid Arundian continues beyond the top Viséan (Clayton *et al.* 1977)

Present in samples: All samples

Genus: POTONIESPORES Artüz 1957

Type species: *P. bizonales* Artüz 1957

Description: (Playford 1962), Concise differentiation of the equatorial girdle into an inner thickened portion and an outer membrabnous zone.

Potoniespores cf. delicatus Playford 1962

Holotype: Preparation P180B/4, 24.7 95.1. L1202

Type locality: Birger Johnsonfjellet (sample G1102), Spitsbergen;

Diagnosis: (Playford 1962, pg. 643-644, pl. 91, figs. 12-13) "Radial, trilete, zonate miospore. Amb subtriangular, conformable with the spore body outline. Trilete mark distinct, sutures straight, more or less simple, extend to or almost to the equatorial margin of spore body. Intexine of spore body thin, laevigate or infrapunctate, amb subtriangular with rounded apices and markedly concave to slightly convex sides. Exoexine extended in

the equatorial plane to form differentially thickened zona consisting of a prominent thickened inner zone and a thinner outer zone commonly possessing radially oriented placations. Approximately half to two thirds of the width of the zona occupied by inner thicker zone, margin between two parts clearly defined. Exoexine laevigate."

Size: Overall equatorial diameter 50(58)69μm, equatorial diameter of spore body 23(27)33μm (Playford 1962).

Size in present study: 35μm (1 sample)

Range/Occurrence: Lower Carboniferous (Playford 1962), TC-NM zone (Clayton *et al.* 1977)

Present in samples: N16

Infraturma PATINATI Butterworth and Williams 1967

Genus: THOLISPORITES Butterworth and Williams 1958

Type species: *Tholisporites scoticus* Butterworth and Williams 1958, p. 382, pl. 3, fig. 48

Diagnosis: (Butterworth and Williams 1958, p.318-382, in Carson 1995, p. cxv) "Trilete iso- or microspores possessing a central body enclosed on the distal side by a thick distal patina. (A patina is here defined as an exinal thickening which extends over the entire area of one hemisphere so long as one or other pole remains free). The patina in this genus extends for a short distance beyond the equator proximally, enclosing the body both distally and equatorially so that the bodyis exposed only over a relatively small area surrounding the proximal pole. Body circular. Equatorial outline of spore circular. In lateral view the distal outline is semicircular, the proximal convex or pyramidal."

Remarks: There is one spore recognized to fit in this genus (N15 S35.2). It has not been designated a species.

Size: 46μm (based on one specimen)

Present in samples: N15

Subturma PSEUDOSACCITRILETES Richardson 1965

Infraturma MONOPSEUDOSACCITI Smith and Butterworth 1967

Genus: DISCERNISPORITES Neves emend. Neves and Owens 1966

Type Species: *Discernisporites irregularis* Neves 1958 (in Neves and Owens 1966)

Diagnosis (emended in Neves and Owens 1966 p 357) Trilete radial, camerate miospores in which the equatorial extension of the exoexine contains a single, continuous chamber peripheral to the intexine. Equatorial outline of spores convexly triangular, outline of intexine often subcircular; proximo-distal orientation common, indicating an original discoidal shape. Exine layers laevigate or with fine infrapunctate or infragranulate structure. Ornamentation or modification of the contact faces may be present; limbus absent. Trilete rays usually accompanied by long folds of the exoexine, lips thin often featuring intense flexures near proximal pole."

Discernisporites sp.

Description: Triangular, convex, rounded; outline smooth; camerate; trilete; raised folds following trilete mark extend to equator. Body triangular, straight, rounded; exoexine very fine, brown; intexine brown, appears to be thicker than the exoexine, laevigate?; exoexine laevigate to very finely infraounctate.

Size: equatorial diameter 35x40µm; body 30x25µm (based on one specimen)

Present in samples: N23

Discernisporites micromanifestus (Hacquebard) Sabry and Neves

Description: (Pers comm. B. Owens) "Radial, trilete, camerate miospore. Amb and outline of the inner body convexly subtriangular. Trilete mark distinct, laesurae straight, commonly obscured by elevated flexuous exoexinal folds which extend tapering in height almost to the equatorial margin of the spore. Exine composed of two layers, Intexine thin laevigate, forming inner body. Exoexine relatively thin closely appressed to the intexine on the proximal surface but separated in the equatorial plane and over the entire distal surface but infragranulose to laevigate. Equatorial ‚margin non-limbate."

Size: equatorial diameter55-100µm; Body diameter 35-70µm.

Remarks: Agrees with the description of B. Owens; triangular, convex, rounded; outline modified by micrograna on the equator; contact mark trilete, laesurae, straight, thickened, raised, extend to edge of central area, slightly darkened.

Range: Coquel and Moreau Benoit 1986. Ghadames Basin, Libya; Tournaisian-Viséan, Palynozones 12-14; Moureau-Benoit, 1989; Ghadames Basin, Libya; Pragian-strunian, Palynozones 2-11; Coquel and Latreche, 1989. Illizi Basin, Algeria; Illerene Fm., Strunian-Lower Tournaisian, Palynozones 1-2; Upper Binem-Dalma Fms., Late Femennian/Strunian – Late Tournaisian, Palynozones 11-13.

Present in Samples: N23; N16

Genus: ENDOSPORITES Wilson and Coe 1940

Type species: *E. ornatus* Wilson and Coe 1940

Diagnosis: (Extension of Wilson and Coe 1940, in Smith and Butterworth 1967 pg 270) "Trilete pseudosaccate microspores in which the intexine and exoexine are separated distally. In polar compression the intexine (central body) is surrounded by the pseudosaaccus, both of them being round, or rounded-triangular. Laesurae do not extend beyond the equator of the body. The pseudosaccus usually possesses a limbus."

Affinity: "Chaloner (1953a, 1958b) has reported the occurrence of microspores very similar to *Endosporites globiformis* (Ibrahim) Schopf, Wilson and Bentall 1944 in the lycopod cone *Polysporia mirabilis* Newberry 1873 (syn. Lepidostrobus zea Chaloner 1953a). Earlier, schopf, Wilson and Bentall (1944 p. 45) stated that Endosporites is related to some of the Pennsylvanian Cordaitaleans because of the presence of E. pelucidus-type spores within the strobilus Cordaianthus shulerei Darrah 1940. This attribution of Endosporites has been discounted by Wilson (1960 p31) because he has shown that *E. Pelucidus* is more correctly assigned to the genus Florinites (see Wilson 1958)" (Smith an dButterworth 1967).

Endosporites c.f. micromanifestus Hacquebard 1957

1956 *Hymenozonotriletes* aff. Variabilis Naumova; Ischenko, p. 62; pl. 11, figs. 129, 130

1957 *Endosporites micromanifestus* Hacquebard, p. 317; pl. 3, fig. 16

1960 *Auroraspora micromanifestus* (Hacquebard) Richardson, p.51

Diagnosis: (Taken from Playford 1962 description pg 648) "Spores radial trilete; amb convexly subtriangular. Laesurae distinct, accompanied by elevated, rather irregular, flange like lips that frequently extend to the equator. Central body thin, often folded, infragranulate.

Size: Equatorial diameter 42(67)95µm; body diameter 28(44)65µm."

Range: Viséan–Namurian, Northern Ireland (Whitaker and Butterworth 1978); Scottish Viséan (Sullivan and Marshall 1966, Love 1960), Lower Carboniferous Spitsbergen (Hughes and Palyford 1961) Tournaisian-Viséan-Namurian, Western extension of the Donetz Basin (Ischenko 1956); Lowermost Mississippian, Nova Scotia (Hacquebard 1957);

Present in: N15

Genus: GRANDISPORA Hoffmeister, Staplin and Malloy 1955

Type species: G. *spinosa* Hoffmeister *et al.* 1955

Diagnosis: Hoffmesiter *et al.* 1955 describe this genus as follows: " Spores radial, trilete; central body enclosed by a bladder, both subcircular; central body laevigate(?); possibly punctate to granulose, possibly laevigate, with prominent scattered spines; trilete rays weak, simple, apparently extend to edge of central body; central body wall only slightly thicker than the bladder wall, translucent."

Remarks: Hacquebard (1955) states that the spinose bladder distinguishes this genus from Endosporites; only one species, the genotyoe, was assigned to this genus. This species occurs in the Upper Missiissippian of the United States; it measures 100-143 μm in diameter. The Horton samples contain two types that may be included in Grandispora, giving the genus a size-range of 62-143 μm.

Grandispora spinosa Hoffmeister, Staplin and Malloy 1955

Holotype: TCO-82, 2077ft, slide 6, ser. 19,311 (pl.39, fig. 10) diameter 118μm, central body 84x95μm

Type Locality: TCO-82, Hardinsburg formation, Chester Series, Upper Mississippian, Illinois;

Description: Spores radial, trilete; proximal view of both central body and bladder circular to subcircular; both bladder and central body punctate to slightly granulose; bladder of equal width around the central body, spinose, processes 2-8 μm long and 8-25μ apart; trilete indistinct, simple, perhaps extends to edge of central body; dimensions 100-143 μm, central body 84-100μm.

Remarks: Circular, camerate, spinose spores. Trilete mark not visible in specimens, spores broken, inner body circular; processes on bladder; processes vary in size from 1.5μm – 6μm;

Size: equatorial diameter 65(100)135μm, body diameter 57(84)100μm (based on 5 specimens)

Range: Chester Series, Upper Mississippian (Hoffmeister Staplin and Malloy 1957)

VF – bottom of SO miospore zones.

Present in samples: N23, N20, N18, N16, N15

Genus: RUGOSPORA Neves and Owens 1966

Type species: *R. corporata* Neves and Owens 1966 (S.G. No. 6.8.19)

Diagnosis: (from Neves and Owens 1966, pg.350-351, pl. II, figs. 4-5. "Trilete, camerate miospores; two exine layers attached only in the region of the trilete mark. Equatorial outline subcircular to oval. Intexine thin, laevigate, often indistinct due to spore wall pigmentation and ornament, when it appears as a darker subcircular region in the polar position. Exoexine bears a characteristic microverrucose ornament and a persistent series of folds or placations, which give the spores an irregular, corrugated appearance. Folds are not orientated in a regular manner. Trilete often indistinct due to nature of exoexine; rays simple, extending almost to the margin of intexine sac, lips thin."

Rugospora corporata Neves and Owens 1966

Holotype: S.G. No. 6.8.19

Type locality: Marine shales with Gastrioceras cancellatum, Crowborough Wood (GR SJ 902556), Staffordshire

Diagnosis: (Neves and Owens 1966) "spores radial, trilete, camerate. Equatorial outline subcircular to oval. Trilete rays simple, straight, extend to or almost to the marginof the intexine sac, lips thin. Sac like intexine distinct to obscure; circular to subcircular in outline; thin with series of concentric folds at the margin. Attachment to exoexine in region of trilete rays only. Exoexine decorated with an ornament of small, subcircular to irregularly shaped verrucae up to 4μm in diameter, and which show variable density on both proximal an distal surfaces. These elements are superimposed on a series of narrow, flat topped exinous folds, up to 30μm long and 3-6μm wide, which are irregular in outline and randomly oriented."

Size: Exoexine diameter 105-175μm, intexine sac 66-102μm (Neves and Owens 1966).

Size in present study: Exoexine 140μm (intexine 125μm?) N

Remarks: Agrees with original diagnosis. Large amount of pyrite infilling.

Range/occurrence: Southern Pennines and Stainmore Outlier - Namurian A-Namurian C (Neves and Owens 1966).

Present in samples: N22

Genus: SCHULZOSPORA Kosanke 1950

Type species: S.*rara* Kosanke 1950

Diagnosis: (expanded from Kosanke 1950 p. 53, in Smith and Butterworth 1967 p. 273). 'Radial, trilete spores with a bilateral appearance due to the presence of an elliptical pseudosaccus. Body spherical, equatorial limit marked by a darker annular zonee about 3-5µm wide. Laesurae straight, simple, never exceeding body radius in length. Ornament of body and pseudosaccus uniformly punctate, granulate, or minutely reticulate. Exine thin, not exceeding 2µm. Folding of the pseudosaccus is common.

Affinity: "Remy and Remy (1955b) have isolated a species of *Schulzospora* from the pteridosperm fructifaction *Simplotheca silesiaca* Remy and Remy from the Namurian of Lower Silesia."

Occurrence/range: 1st occ base TC zone (mid Holkerian) continues beyond Viséan

Schulzospora campyloptera (Waltz) Hoffmeister, Staplin and Malloy 1955

1884 No.619, Reinsch, p. 60, pl. 22, fig. 231D

1938 *Zonotriletes campylopterus* Waltz in Lubr and Walttz, p. 16, pl. 3, fig. 39, and pl. A, fig. 15

1955 *Schulzospora campyloptera* (Waltz); Hoffmeister, Staplin and Malloy, p. 396

1958 *Dilobozonotriletes campylopteras* (Waltz); Ischenko, p. 94, pl. 12, figs. 160, 161

Holotype: Not known

Type locality: Seam 46, Skakulin Colliery, Selizharovo, Moscow Basin

Diagnosis: (Luber and Waltz 1938, C.E.D.P. French translation no. 1443, in Smith and Butterworth 1967). 'Outline approximately oval; pseudosaccus thin, of variable width, three or four times wider at equator than at poles, giving the spore an oval rather than a round shape; pseudosaccus margin crenulated. Laesurae indistinct, rays one-third to two-thirds spore radius, not all of equal length. Exine microreticulate, more distinct on the pseudosaccus than on the body.

Size: 90-114µmx65-75µm, body 60-70µm; 76(87)100x44(55)62µm, body 46(48)60µm (Smith and Butterworth 1967);

Size in present study: equatorial diameter 81(87)95 x 52(58.4)64µm; Body 47(52)57µm (based on 6 specimens)

Range: Viséan and Namurian (Smith and Butterworth 1967)

Schulzospora elongata Hoffmeister, Staplin and Malloy 1955

Holotype: Hoffmeister Staplin and Malloy 1955, pl. 39, fig. 2; preparation 1, ser. 15800, 30-6 µm

Type locality: 2072 ft., Carter No. 3 borehole (TCO-82), Webster County, Kentucky, U.S.A.; Hardinsburg Formation, Chester Series.

Diagnosis: (from description in Hoffmeister, Staplin and Malloy 1955, p. 396). "Spores radial trilete; outline elongate-oval; central body enclosed by bladder; bladder faintly folded; ornamentation central body smooth to slightly granulose, bladder granulose to finely reticulate; trilete rays distinct, approximately three-fourths central body radius; central body coat moderately thick, translucent, bladder coat very thin, transparent."

Remarks: the extremely elongate shape characterises this species and the extra length distinguishes it from *S. campyloptera.*

Range: Viséan and Namurian (Smith and Butterworth 1967)

Size: equatorial diameter 52(63)76x24(40)52, body 30(39)48;

Size present study: equatorial diameter 50(66076x30(39)44, body 28(37)46x26(34)40

Schulzospora ocellata (Horst) Potonié and Kremp 1956

1943 *Triletes (Zonales) ocellatus* Horst, (thesis) figs. 40, 41

1955 *Schulzospora ocellata* (Horst) Potonié and Kremp in Horst, p. 195, pl. 21, figs. 4a, b.

1956 *Schulzospora ocellata* (Horst); Potonié and Kremp, p. 166

non 1958 *Schulzospora ocellata* (Horst) Potonié and Kremp; Butterworth and Williams pl. 4, fig, 15

Holotype:Horst 1955, pl. 21, figs. 40a, b. Preparation IV 68, 20.5, 75.8

Type locality: Osmana seam, Michael Colliery, Moravska-Ostrava; Namurian A

Diagnosis: (Horst 1955, p.195; in Smith and Butterworth 1967, p. 275) "Microscopes with fine infragranulation. Amb oval to round. Body thin-walled. Pseudosaccus circular to oval, darkest at the boundary of grey body. The rays sometimes reach to this boundary; generally however they are shorter. Spores with a ruptured tetrad mark, in which the exine is generally torn outwards are rare. The body, the size of which varies from 25-59µm almost always lies obliquely to the length of the spore."

Size: equatorial diameter: 76(92)110x60(69)88µm, body: 56(66)77x52(61)74;

Size present study: equatorial diameter: 106x94 µm, body: 66x64µm (based on 1 specimen).

Remarks: Not common in the NSD horizon.

Present in samples: N22

Genus: PEROTRILETES Couper emend Evans 1970

Type species: *Perotriletes granulatus*

Diagnosis: Camerate-zonate spores with a diaphanous exoexine and ornamented distal surface (Higgs and Clayton 1988)

Perotriletes perinatus Hughes and Playford 1961

Holotype: Hughes and Playford 1961 pg. 33; preparation P003/4, 42.8, 95.1 Dialux 1, pl. 2 figs. 7-10 pg. 33.

Type locality: Sample B685, Lower Carboniferous, Spitsbergen

Diagnosis: (Hughes and Playford 1961, pg. 33) "Spores radial, trilete; amb circular to triangular, usually convexly subtriangular. Perine very thin, hyaline, laevigate to finely granulate, loose fitting, usually wrinkled and folded, standing out 4-10μm beyond equatorial margin of spore body. Laesurae 2/3 to 5/6 radius of spore body, straight and sometimes with weak, narrow labiae. Exine laevigate, thickness 2.5-4μm."

Size: 44(67)90μm; 40-45μm (based on 2 specimens)

Description: agrees with diagnosis of Hughes and Playford. Circular, with very fine perine. Trilete, laesurae straight, simple extend almost to edge of spore inner body; laevigate; fine perine, folded laevigate

Range/occurrence: Lower Carboniferous

Present in samples: N23, N17

Turma MONOLETES Ibrahim 1933

Suprasububturma ACAVATOMONOLETES Dettmann 1963

Subturma AZONOMONOLETES Luber 1935

Infraturma LAEVIGATOMONOLETES Dybová and Jachowicz 1957

Genus: LAEVIGATOSPORITES Ibrahim 1933

Type species: *L. vulgaris* Ibrahim 1933

Diagnosis: (Potonié and Kremp 1954, p. 165; translation in Smith and Butterworth 1967, p. 281). "Monolete spores. Outline smooth. Laevigate to infrapunctate. Amb more or less oval; shape in meridian plane, phaseolate. Distal margin slightly, and not, as in *Latosporites*, markedly convex; polar axis therefore relatively shorter than in *Latosporites*. Exine always sculptureless. Monolete mark straight."

Affinity: "*Sphenopsida* and *filicales*. The larger forms of Laevigatosporites (those exceeding about 35μm in length) have so far only been obtained from the *Sphenopsida*.

Reed (1938) described spores with a length of 50μm from a *Calamitean* type fructification. Andrews and Maamay (1951) recovered spores ranging from 20 to 40μm in length from a species of Bowmanites and Remy (1960 and 1961) isolated spores with size ranges from 35 to 50 μm and 55 to 70 μm from two other species of Bowmanites. The smaller forms of Laevigatosporites have been recovered from the *sphenopsida* by Baxter (1950) and from the *Filicales* by Mamay (1950)" (Smith and Butterworth 1967).

Remarks: *Laevigatosporites minimus*, *L. minor* and *L. vulgaris* have been differentiated by virtue of their size as the diagnostic descriptions are otherwise identical. Thus an attributed size range is used to distinguish between the species:

L. minimus is less than 35μm

L. minor is 35-64μm

L. vulgaris is 65-100μm

Laevigatosporites minimus (Wilson and Coe) Schopf, Wilson and Bentall 1944

1940 *Phaseites minimus* Wilson and Coe, p.183, pl.1, text-fig. 5

1944 *Laevigato-sporites minimus* (Wilson and Coe);Schopf, Wilson and Bentall, p.37

Holotype: Wilson 1958, pl. 1, fig. 5 after Wilson and Coe (1940). Preparation 121P. Size 25μm, length 20-30μm width in equatorial view 16-20μm

Type locality: What Cheer Clay Products Company Mine, What Cheer, Keokuk County, Iowa, U.S.A.; Des Moines Series.

Diagnosis: (in Smith and Butterworth 1967, p.283). "Amb oval, shape in equatorial view phaseolate. Laesura simple, greater than one-half of spore diameter in length. Exine very thin, folding infrequent."

Range: Westphalian D (Smith and Butterworth 1967)

Size: 32-35μm (based on 4 specimens)

Laevigatosporites minor Loose 1934

1932 *Sporonites vulgaris* Ibrahim in Potonié, Ibrahim and Loose, in part

1933 *Laevigato-sporites vulgaris* Ibrahim, in part.

1934 *Laevigatosporites vulgaris minor* Loose, p. 158, pl. 7, fig. 12

1957a *Laevigatosporites minor* (Loose) Potonié and Kremp; Bharadwaj, p.109, pl. 29, figs. 8,9.

Holotype: Loose 1934, pl. 7, fig. 12. Preparation V29 a. Type locality Bismarck seam, Ruhr Coalfield, Germany; Upper Westphalian B.

Diagnosis: (from Ibrahim 1933, p.39; in Smith and Butterworth 1967, p 284). "Amb oval, shape in equatorial view, phaseolate; margin smooth. Laesura about two thirds of spore length. Exine laevigate to faintly punctate (?infrasculpture), about 1µm thick."

Size: 40-70µm (Loose 1943); 45-65µm (Bharadwaj 1957); 37(44)50µm, 44(55)64µm, 34(50)68µm (Smith and Butterworth 1967)

Size in present study: 37-65µm (based on 9 specimens)

Range/occurrence: Namurian-Westphalian D (Smith and Butterworth 1967).

Present in Samples: N24, 23, 22, 20, 19, 18

Laevigatosporites vulgaris Ibrahim 1933

1932 Sporonites vulgaris Ibrahim in Potonié, Ibrahim and Loose, P. 448, pl. 15, fig. 16

1933 Laevigato-sporites vulgaris Ibrahim, p. 39, pl. 2, fig. 16

1940 Phaseolites desmoinesensis Wilson andCoe, p. 182, pl. 1, fig. 4

1944 Laevigatosporites desmoinesensis (Wilson and Coe); Schopf, Wilson and Bentall, p. 37

Holotype: Potonié and Kremp 1956, pl. 19, fig. 429 after Ibrahim. Preparation B31, c6 (or).

Type locality: Ägir seam, Ruhr Coalfield, Germany; top of Westphalian B.

Diagnosis: (from Ibrahim 1933, p. 39, in Smith and Butterworth 1967). "Amb oval, shape in equatorial view, phaseolate; margin smooth. Laesurawe about two-thirds of lengthof spore Exine laevigate to faintly punctate (?infrasculpture) about 1µ thick."

Description: Laesurae simple, rather longer than one half the spore diameter [27(38)55µm in lergth]. Exine laevigate; occasionally slightly scabarate.

Range: Westphalian B (Smith and Butterworth 1967).

Size: 69.5; 56-77µm

Present in samples: N24, 23, 19

6.4 DISCUSSION

6.4.2 PALYNOSTRATIGRAPHY

The spore assemblage suggests that the horizon can be placed in the NC zone (see figure 6.2), straddling the Viséan-Namurian boundary. Some of the key spores present are *Grandispora spinosa, Leiotriletes tumidus, Schulzospora campyloptera, Schulzospora ocellata, Raistrickia nigra, Rotaspora knoxi,* and *Stenozonotriletes coronatus.*

Work carried out by Whitaker and Butterworth (1978) has placed the Viséan Namurian boundary at the Main Coal in the Ballycastle area (refer to figure 4.11). This conclusion was drawn after comparison of assemblages found in the Ballycastle area with assemblages found in Scotland and Northumberland known to be Lower Carboniferous in age. The NSD horizon is located stratigraphically below the Main Coal. There were no macrofossils of stratigraphic significance recovered from the NSD horizon for this work. The assemblage observed in the NSD horizon contains elements of both the VF and NC horizons. This is not unusual at this stratigraphic level, and some of the key spores used in the recognition of the NC biozone, such as *Bellisporites nitidus,* and *Reticulatisporites carnosus*, have not been observed. To fully clarify this disparity a further detailed palynological study would need to be undertaken in the area.

6.4.2 SPORE RANGE FLUCTUATION AND DESTRUCTION

The identified assemblage in the NSD horizon is dominated by the spore genus *Lycospora*, and the species *L. pusilla*. Indeterminate spores dominate the assemblage, with *c.*40% in the background samples which increases to 70-80% of the spore count in the samples adjacent to the dyke.

25 spore genera that appear in the spore count. Not all 25 spore genus are recorded in any one of the sample slides (see figure 6.3), there is an average of 11 genus identified in each of the background samples. The number of identifiable spore genera drops markedly at sample N11 (1.21m from dyke, 1.48% VR). There is an average of 3 identifiable genera in each of the samples N11-N1. The miospore genus' *Lycospora* and *Densosporites* and the miospore species, *L. pusilla,* are identifiable in the samples closest to the dyke margin. The destruction of the spores affects the ability to determine a palynostratigraphic age for a sample collected adjacent to the dyke margin.

A comment on the progressive destruction of the various species: this might also reflect the more resistant nature of the genera *Lycospora* and *Densospora*. However when considering this it must also be taken into account that these two genera also dominate the assemblage.

6.5 CONCLUSIONS

The NSD horizon should be placed in the NC zone of the Carboniferous, straddling the Viséan-Namurian boundary.

Sporomorphs are destroyed in a dyke aureole, the destructive influence being greater with proximity to the dyke.

Only the more robust spore genera such as *Lycospora* and *Densospora* survive into the dyke contact.

Rock samples gathered in proximity to an intrusion are difficult to date using palynostratigraphy.

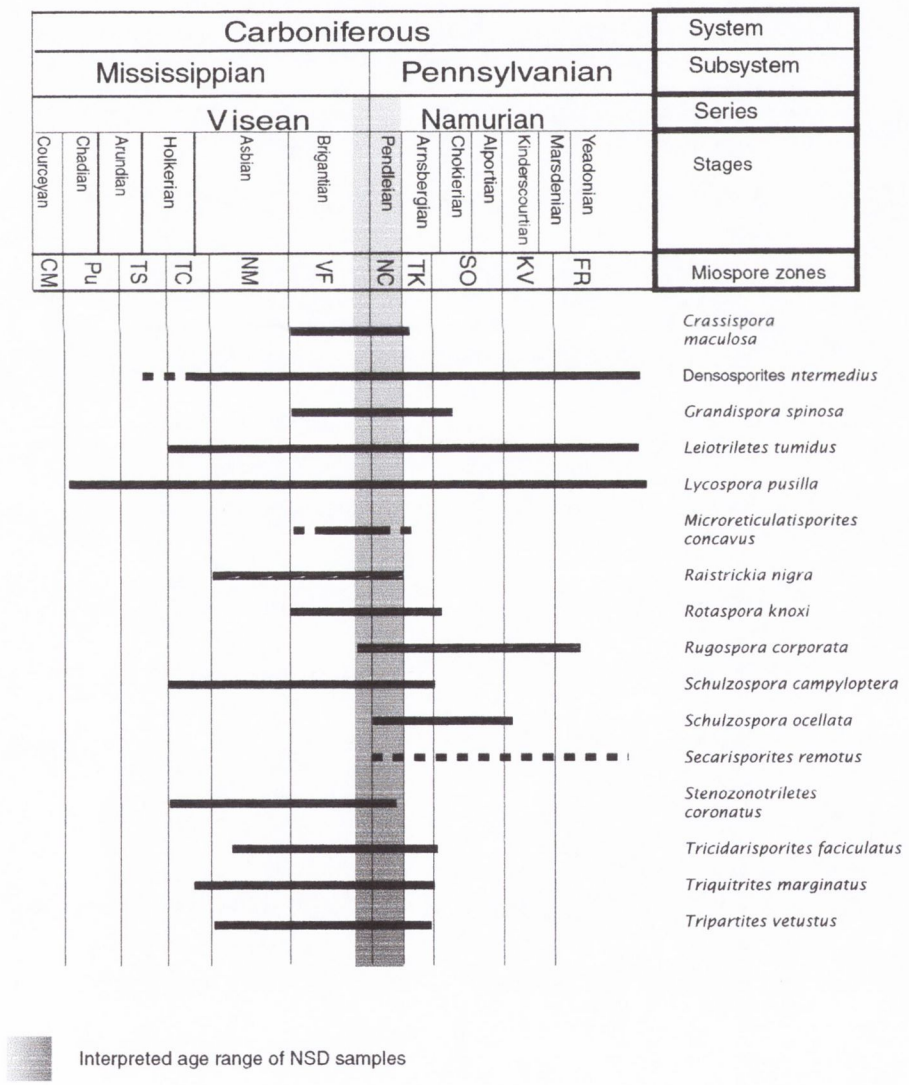

Figure 6.2 NSD horizon palynological age/biozone.

Sample No	Dist. from (	VR (%Rr)
NSD1	0.04	3.78
NSD2	0.15	3.72
NSD3	0.28	4.69
NSD4	0.37	5.61
NSD5	0.47	5.47
NSD6	0.49	5.16
NSD7	0.57	3.41
NSD8	0.65	3.49
NSD9	0.95	2.82
NSD10	0.97	1.63
NSD11	1.21	1.48
NSD14	1.82	1.26
NSD15	2.2	1.05
NSD16	2.22	1.16
NSD17	2.89	1.03
NSD18	2.79	1.03
NSD19	3.95	1.06
NSD20	4.05	1.19
NSD21	5.4	1.13
NSD22	5.66	1.11
NSD23	6.27	1.04
NSD24	10.11	1.25

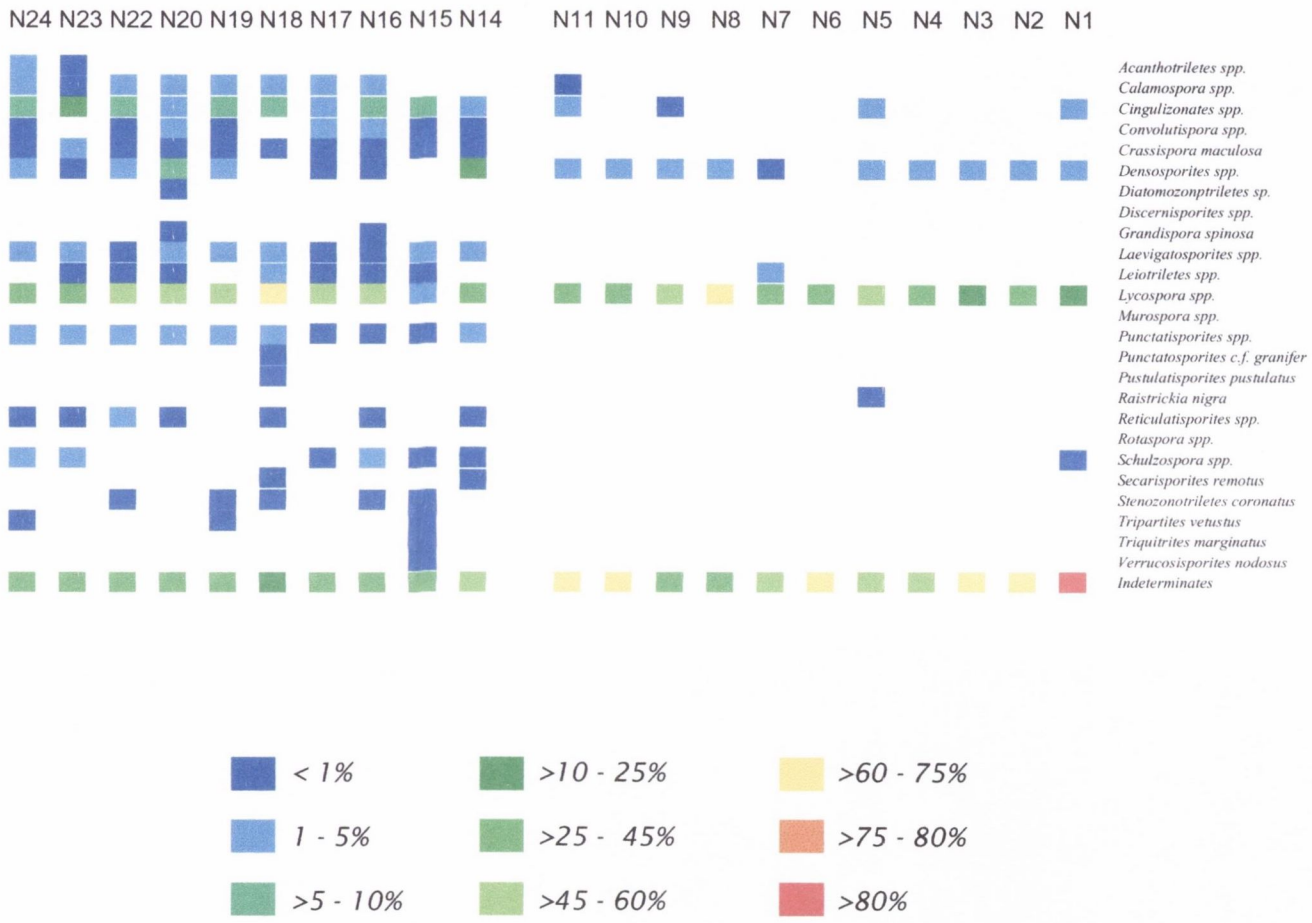

Figure 6.3 Spore genus assemblage variation in the NSD horizon

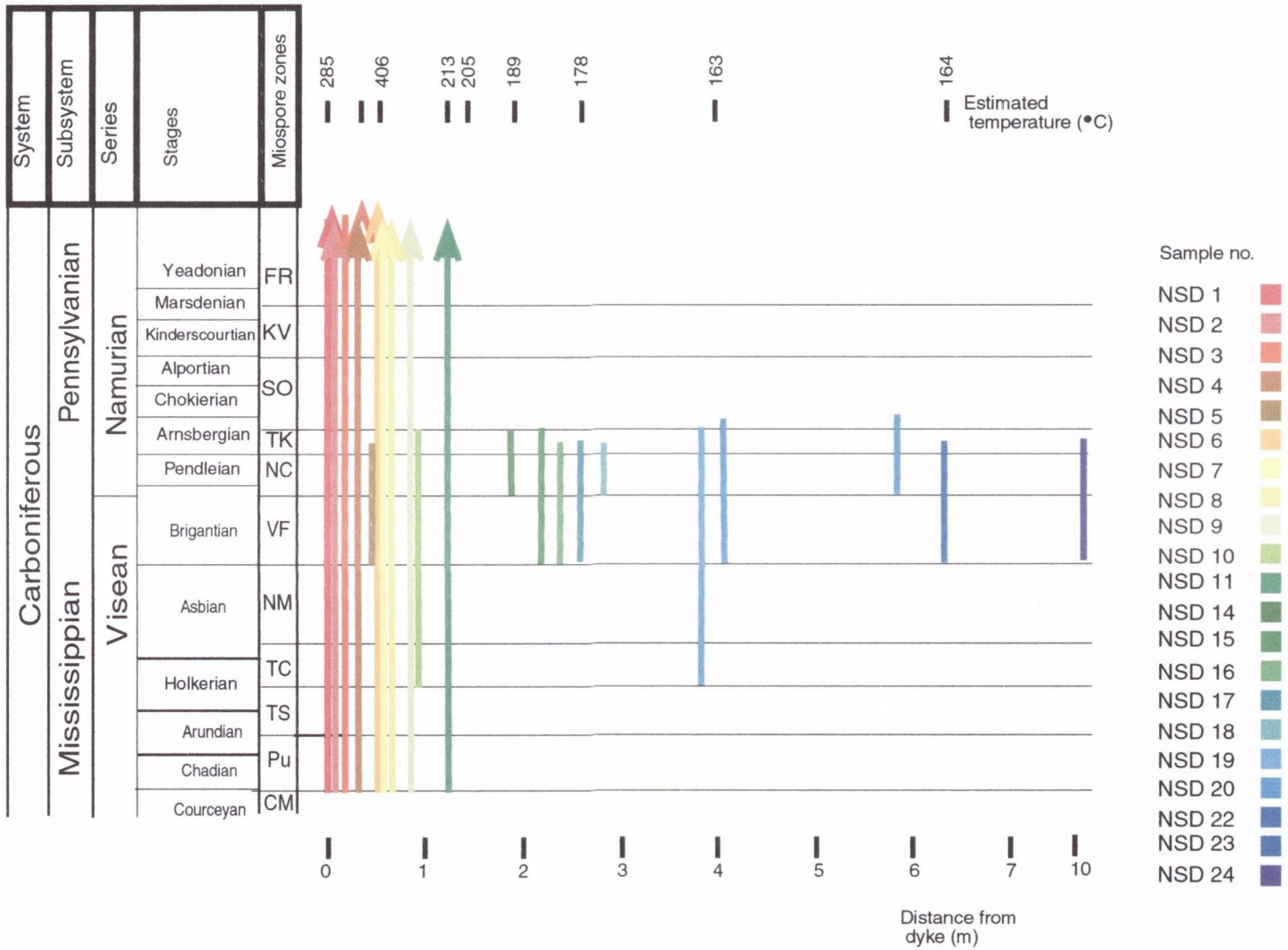

Figure 6.4 Assemblage variation and the effect on palynostratigraphic recognition

7 THERMAL ALTERATION OF SPORES AND OTHER ORGANIC MATTER

7.1 INTRODUCTION

Stadnichenko (1929) published one of the first works to note that spores have a different colour dependant on the degree of coalification of the rocks in which they were found. It is now known that spores, pollen and other organic material such as acritarchs, conodonts and scolecodonts, will alter in colour reflectance and fluorescent properties in response to increasing coalification or under the influence of temperature alone.

7.2 THERMAL ALTERATION AND MATURATION OF SPORES

Sediments recovered from >5,500m do not tend to yield palynofloras. This is due to the spores having been destroyed by the high temperatures and pressures at such depths (Traverse 1988). However the temperature at which organic matter decomposes depends in part on the rank (or degree of coalification) of the starting product (Cook *et al.* 1972).

Sediment burial leads to rising temperature and pressure over a period of time. Burial affects the evolution of organic material. For example in some palynomorphs (e.g. spores, pollen or acritarchs) there is an associated loss of hydrogen (H) and oxygen (O) with a concomitant increase in carbon (C) concentration (Stach *et al.* 1982, Taylor *et al.* 1998). Increasing temperature with burial is also reflected in the physical, visible properties of the palynomorphs as increasing opacity, increasing incident light reflective values and changes in fluorescent properties (decreased fluorescence intensity and colour changes) (Frey *et al.* 1987, Taylor *et al* 1998). These properties of varying translucency of isolated palynomorphs allow the estimation of the rank of sedimentary, organic palynomorph bearing rocks other than coal, *e.g.* assessing the maturity of oil prone lithologies. Spores and pollen actually begin to change colour before co-occurring acritarchs, which, in turn, change before chitinazoa (Gray and Boucout 1975). In fact spores and pollen are said to be among the most sensitive palynomorphs to metamorphism, and this is especially true for very low grade metamorphism (Gray and Boucout 1975) and material below semi anthracite grade.

Experimental work of McIntyre (1972) showed that spore colour could be altered in a very short time (days). Spores exposed to temperatures <200°C showed very little effect, at temperatures >200°C the colour was altered and at temperatures >270°C there was a significant colour alteration. The extent of the darkening appeared to be controlled by the peak temperature. Yule *et al.* (2000) reported that spores, artificially heated, progressed through a similar series of colours to those recovered from spores matured in rock through

burial, even though the chemical evolution differed. Thus the maximum temperature that the rock and sporopollenin were exposed to appeared to be reflected by the colour change the pollen and spores exhibit; however the colour may not necessarily represent the coalification or rank of the sediments.

7.3 SPORE COLOUR SCALES

A number of spore colour scales have been proposed (Staplin 1969 (TAI), Correia 1971, Jones and Edison 1978, Batten 1980 & 1982, Fisher *et al.* 1981, Collins 1990 (SCI Robertson group) and Pearson 1982 & 1984) (see figure 7.1) and adopted with varying degrees of success. No one scale has been universally accepted although the Thermal Alteration Index (TAI) of Staplin 1969 is well used throughout literature. All of these scales are based on observer-determined colours from a 5 to 20 point scale. The colours range from pale yellow or colourless to black with some discrepancy between authors as to exactly what the vitrinite reflectance value and temperature is at which spores are altered to black. The scales of Staplin, Correia, Fisher *et al.* and Collins are based on standard specimens. This makes access to the scales difficult and expensive. The scale of Pearson consists of a range of Munsell colours, ranging from pale yellow to black. It was adopted by the Phillips petroleum company and distributed in 1981, and an updated version was also distributed in 1984. The scale of Pearson is readily accessible and easily utilized but it cannot be entirely accurate with respect to the spore colour. However, it was available in this department and was used in this subjective study.

A CAUTIONARY NOTE: vitrinite and sporopollenin have different compositions and so do not follow the same evolutionary pathways, thus they exhibit different kinetic behaviour through varied burial and thermal histories. "Any vitrinite calibration should be regarded as a general equivalent and invaluable cross check on thermal maturity level but never inter-convertible" (Marshall and Yule 1999).

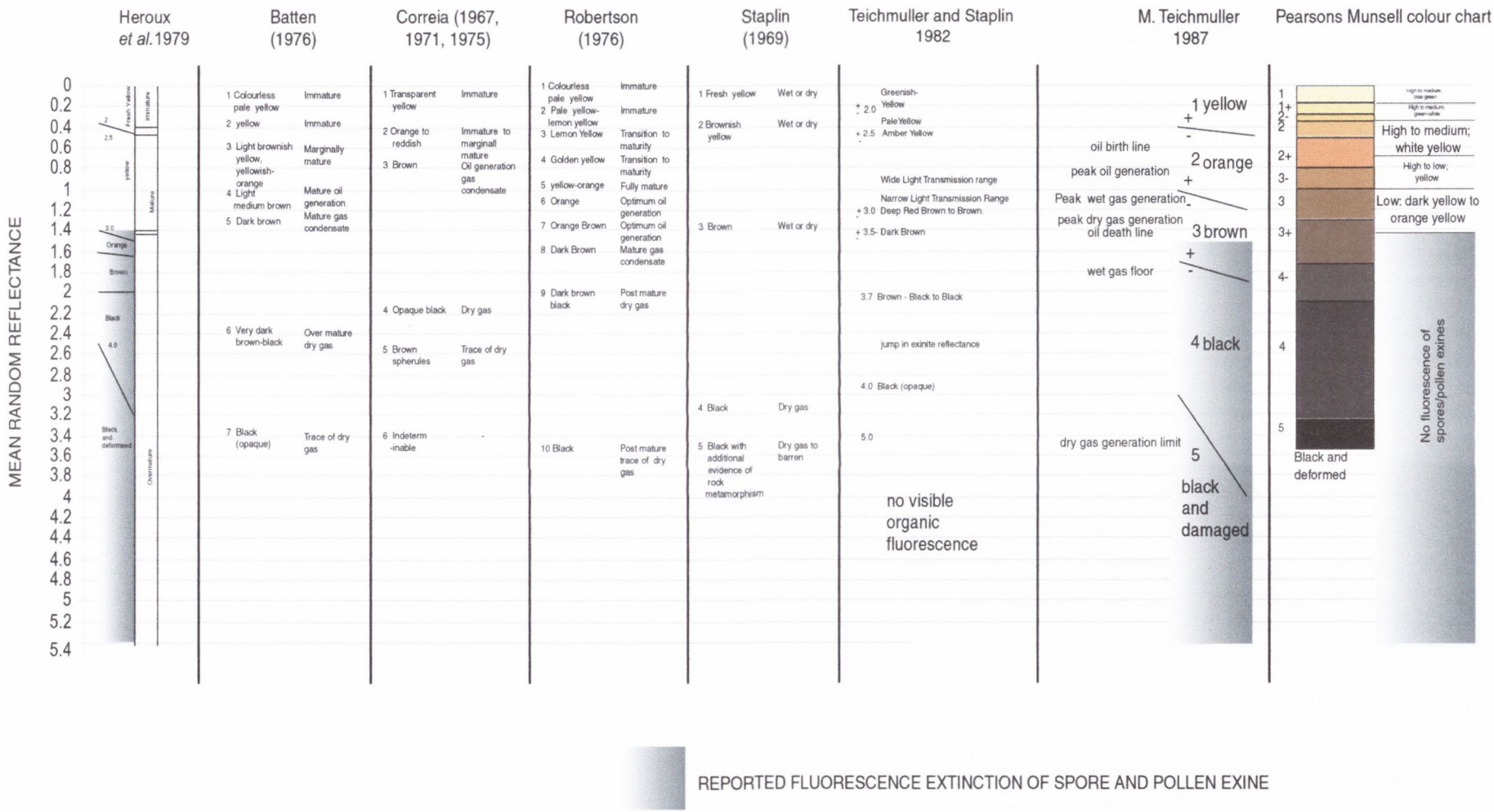

Figure 7.1 Scales and correlation charts/reviews of various authors; correlated using vitrinite reflectance

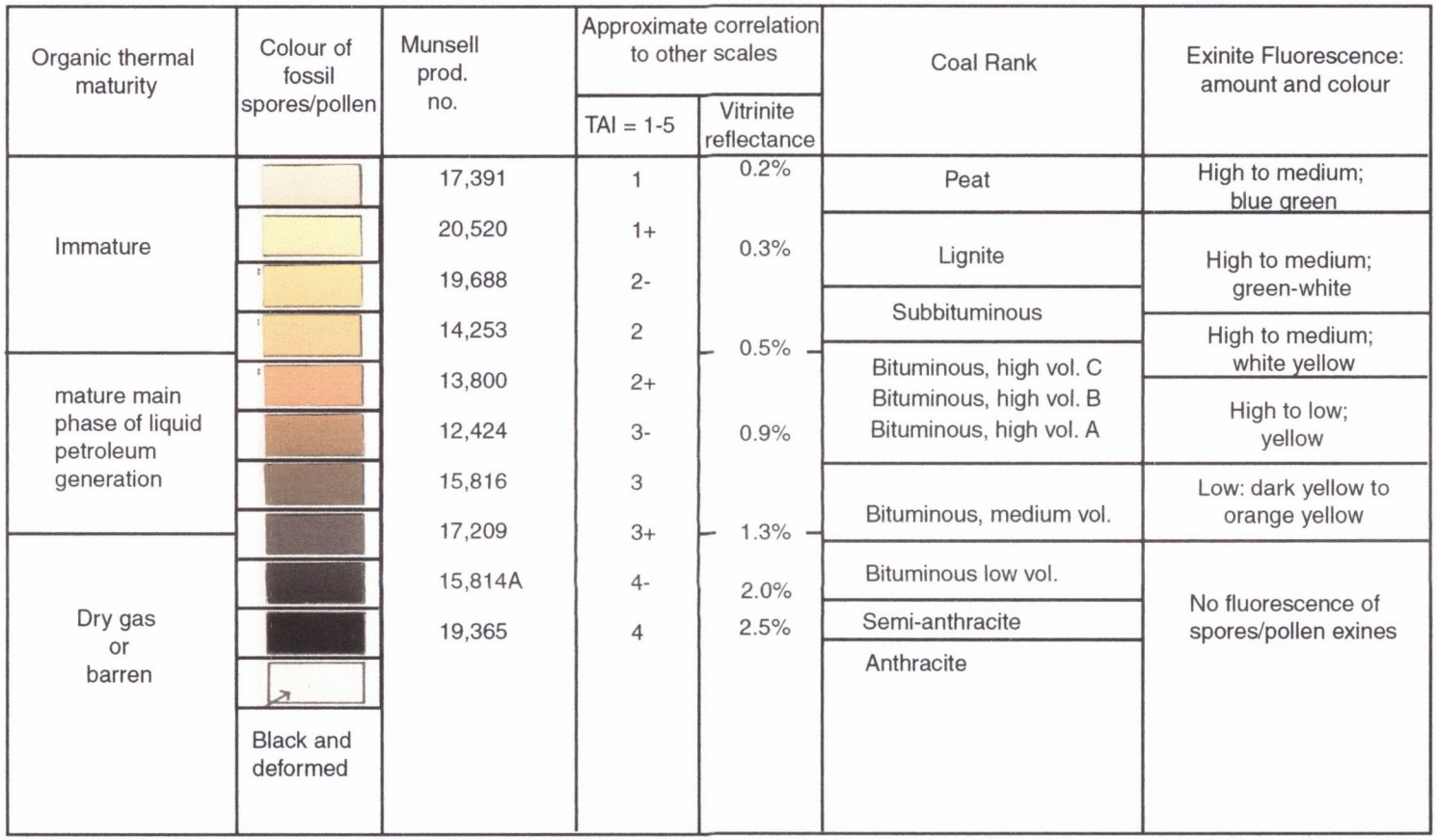

Figure 7.2 Spores/pollen exine coloration with geothermal maturation(coalification). TAI= Thermal Alteration Index, a scale basedon vitrinite reflectance measured by reflected light under oil. Fluorescence refers to the tendency of exines to fluoresce (to visible light when exposed to ultraviolet light). Exinite is the coal maceral consisting of exines; vitrinite is a maceral of woody or similar plant origin.
Compiled from Traverse (1988) and Pearsons colour chart issued by Phillips (1984) .

7.3.1 USING SPORE COLOUR SCALES

When using spore colour analysis it is necessary that the worker is aware of the following:

- Variations in wall thickness will cause a variation in the amount of transmitted light and therefore a variation in spore colour. Thus a thicker walled spore may appear darker in transmitted light. This also makes camarate and heavily ornamented spores an inappropriate choice for spore colour alteration analyses.
- The final colour of a spore, particularly after lower temperature thermal alteration, is dependent on the colour of the starting product. Most spore colour scales assume a starting colour of pale yellow/green. To fit this parameter a thin walled, psilate spore is more appropriate than a thick walled or heavily ornamented spore. It is also useful if the colour of the spore on deposition or at least at reflectances of less than 0.5% was pale yellow/green.
- To ensure that the results/observations are consistent and that there is no bias due to differences in wall thickness, ornamentation, starting colour etc. one spore type, identified to species level where possible, should be used throughout one body of work and for comparative studies.

The spore *Lycospora pusilla* was used in this work where it could be found. Unfortunately it was not possible to identify many of the Lycospores in the Carrickleck samples beyond *Lycospora sp.* This problem was due to the poor state of preservation.

7.3.2 AOM COLOUR ALTERATION

Spores are not always present in the rock being examined. Colour alteration in response to thermal maturation or rank increase is not a phenomenon specific to the sporopollenin alone. In fact all particulate organic matter (except opaque organic matter) can be observed to alter in colour in response to heightened thermal stimuli. The AOM fraction of a palynofacies has long been associated with hydrocarbons, specifically oil generation. The true potential is of course dependent on the original material now constituting the AOM. This amorphous fraction is commonly found in most rocks, in greater or lesser amounts. The colour changes of AOM due to thermal alteration are broadly similar to those seen in spores (Burgess 1974, Peters *et al.* 1977, Marshall 1990, Batten 1996) and have been correlated using different quantitative and qualitative methods (Staplin 1969, Burgess 1974, Peters *et al.* 1977, Robison *et al.* 2000). One of the biggest difficulties associated with AOM colour analysis is in the fact that the material can have a variable thickness even

across a single particle. When choosing the particles that were to be used for analysis the worker should aim to pick particles that have as uniform a thickness as possible and appear to consist of the same material (for more information and further discussion of AOM types see chapter 8).

7.4 FLUORESCENCE

Fluorescence is the adsorption of one type of light, followed by the emission of light of another colour. Usually the wavelength of the outgoing light is longer than that of the incoming light (because the electrons are going from a state of excitation to the ground state (figure 7.3).

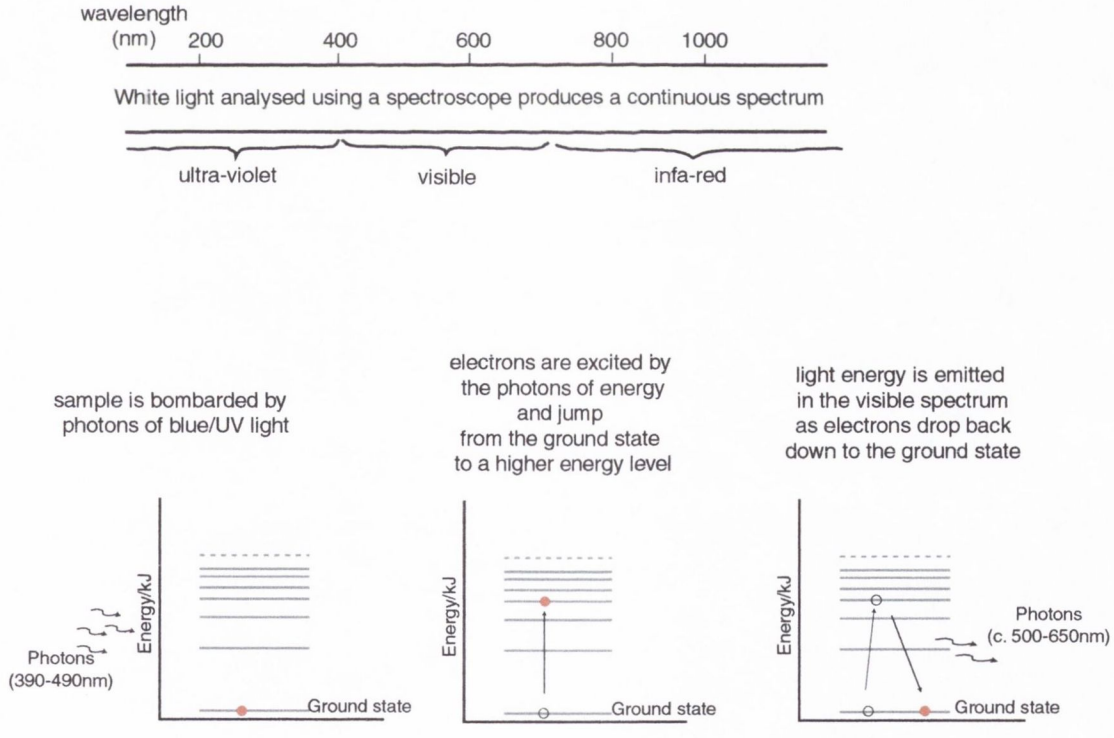

Figure 7.3 Fluorescence energy exchange

7.4.1 WHY USE FLUORESCENCE?

There are some organic molecules and compounds that exhibit fluorescence properties when irradiated with UV or blue light (447nm). This is observed in most liptinitic-exinitic material. Fluorescence observations with organic material can be the primary source of identification, either by obviating fine structure, distinguishing between particles that are stuck together or overlapping, or by differentiating bituminous from solid hydrocarbon particles (Grayson, 1981). The surficial nature of the emitted fluorescence (because the radiation only penetrates to a very shallow depth) gives a better 3-D appreciation of the surface relief and fine morphology of palynomorphs than transmitted light. AOM often masks the presence of palynomorphs. The nature of the fluorescing material can often reveal these hidden contents that are otherwise invisible in transmitted light, (unless the sample has been oxidised to the degree whereby fluorescence is quenched). Fluorescence can also enhance very fine membranous like materials that appear as only fine filmy material in transmitted light and may otherwise be missed (Grayson 1981, Tyson 1995). Fluorescence observations can also be used for assessing the proportion of highly oil-prone constituents and the state of preservation of AOM and palynomorphs (Gregory *et al.* 1991). The quenching of spore fluorescence usually marks the top of the oil window in hydrocarbon producing rocks (1.2 – 1.5% R_r) and occurs in the second coalification jump (1.2 – 1.6%R_r).

7.4.2 WHY DO SPORES AND AOM FLUORESCE?

"Fluorescence is not produced by the general hydrogen rich nature of the oil-prone kerogens but by particular compounds that exhibit specific types of carbon bonds or heteroaromaticity. However fluorescence is enhanced when these fluorophors are dispersed throughout an aliphatic medium (hence the association with oil-prone rocks)" (Tyson 1995).

Thermal influence causes the spectral fluorescence to shift to a longer wavelength (towards the red end of the spectrum) as rank increases (Ottenjahn *et al.*, 1975, 1974, Creaney, 1989). Polymerisation, aromatisation and condensation during maturation result in altered colour of fluorescence; green – yellow – orange – red/brown - no visible fluorescence (Staplin 1982, Creaney 1989, Tyson 1995). There is also a progressive decline in intensity, especially at VR = 0.8 to 0.9 % R_r and fluorescence disappears completely between VR = 1.2 – 1.5 %R_r (Staplin 1969, Ting 1977, Tyson 1995). Obviously this visual scale is a very subjective method but it is useful, cheap and allows quick assessment. It has also been

shown to have reasonable correlation with other thermal indices in burial settings (Ting 1977, Staplin 1982, Teichmüller 1987, Traverse 1988).

7.4.3 USING SPORE AND AOM FLUORESCENCE

Fluorescence assessment is, in part, dependent on the mounting medium. It is important that the medium doesn't have a storing fluorescence, which would mask that of the particles. Elvacite is used in preparations in this work as it gives a dark green background.

Apparent fluorescence increases with the power of the objective lens so relative observations should be based on a standard magnification. In this work x400 magnification was used.

Fluorescence intensity is known to vary with the thickness of the irradiated material. Fluorescence properties are also affected by state of preservation as well as organic matter source, oxidation and microbial degradation.

AOM of algal derivations shows a very intense fluorescence, even more intense than spores of the same rank. It should never be assumed that amorphous material is terrestrially sourced when it is non-fluorescent, especially where it is all non-fluorescent. In many marine sediments non-fluorescent amorphous material usually represents degraded plankton derived AOM.

7.4.4 THE FADING EFFECT

This refers to the phenomenon where fluorescence intensity may increase or decrease over time. It has been variously named 'light etching' (Jacob 1964), 'fading or photochemical effect' (Van Gijzel 1982) and 'alteration' (Ottenjann 1988). In this work the term 'fading' is used.

"Positive alteration is a result of photochemical change of the molecular structure of organic matter in coal and oil shales. It is considered that the irradiation generates additional chemical bonds. The fluorescence increases with multiplied excitable bonds. A general relationship is that the lower the level of maturation the more reactive the organic matter and the stronger the positive alteration. The effect of negative alteration is considered to be a result of evaporation and or partial polymerisation. The extent of negative alteration is thought to finger print the amount of secondary fluid bitumen." (Ottenjann 1988). When the intensity decreases the significant loss of intensity occurs within the first minute (Ottenjann 1988). The 'fading' of spores on exposure to fluorescence is unclear (Stach *et al.* 1986).

Van Gijzel (1981, 1982) suggested the application of the concepts of fluorescence microscopy to kerogen concentrates. This work used a qualitative assessment of the fluorescence properties of palynological preparations, specifically of *Lycospora sp.* and AOM particles, to examine sample maturation.

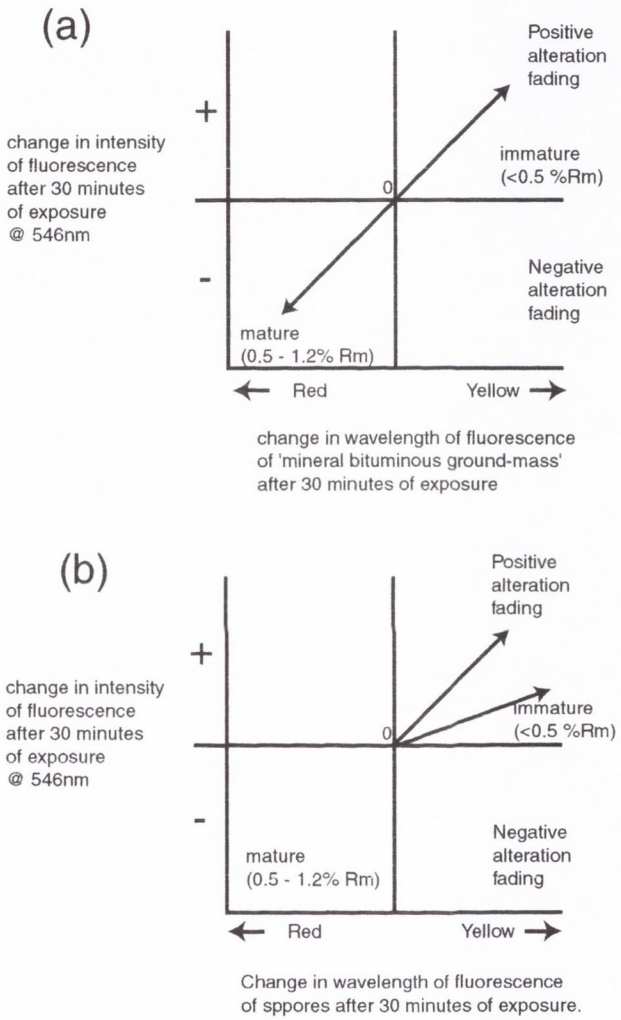

Figure 7.4 The fading effect observed by van Gijzel after 30 minutes exposure to fluorescent light:

(a) the fluorescence of the mineral bituminous groundmass' of oil-source rocks. Fading is positive (maximum wavelength shortens/intensity increases) in immature sediments, but negative (longer wavelength/decrease in intensity) within the 'Oil window' until fluorescence is lost at ca. 1.2%.

(b) the fading effect observed for spore fluorescence. Fading is positive (shorter maximum wavelength/increase in intensity) at all stages of thermal maturation until fluorescence is lost (c. 1.2% R_r). (From McPhilemy 1989; after van Gijzel 1982)

7.5 SAMPLE PREPARATION

7.5.1 ORGANIC MATTER EXTRACTION

See section 4.4.1

7.5.2 PREPARATION FOR PALYNOLOGICAL ANALYSES

See section 6.2.2

7.5.3 SPORE COLOUR USING THE TRANSMITTED LIGHT MICROSCOPE

Spores were studied under transmitted white light. *Lycospora pusilla*, and *Lycospora* sp. where *Lycospora pusilla* could not be recognised, was chosen as the representative spore whose colour was to be recorded form each of the samples. The spore colour was given a representative number based on the Munsell colour chart of Pearson (1984).

The microscope used in this study is a Nikon transmitted light, binocular microscope, with an OSRAM XENOPHOT 12V 50W, halogen, light source.

7.5.3.1 PRESENTATION OF RESULTS

The plates and data are presented in graphical form in chapter 7.

7.5.4 SPORE FLUORESCENCE

Spore fluorescence was studied using a Leitz Wetzlar Dialux-20 binocular microscope. The microscope was attached with an incident fluorescent tube (Ploemopak 2.4) and with a violet and blue +12 filter block with a band of 390 - 490nm. This system was allowed to stabilize for 30 minutes prior to the observation of sample fluorescence.

Lycospora pusilla and *Lycospora* sp. were chosen and subjected to up to 3 minutes of excitation after which their fluorescence colour was recorded. The colour referenced correlates with that seen in figure 7.1.

7.5.4.1 PRESENTATION OF RESULTS

Plates 16-20 are presented in Appendix III.

7.6 RESULTS

7.6.1 CARRICKLECK: TAI

7.6.1.1 CK SAMPLE HORIZON

The material in the CK sample horizon is quite mature, with a background vitrinite reflectance of 1.03 – 1.10%R_r. The spore colour of the background material is 2+ to 3- (CK30 – CK12). CK11 is estimated to exhibit a spore colour of 3, CK 10 looks to be 3/3+, CK9 to 6 are 3+, CK 5 is 4-, CK4 is 4, CK3 is 4-, and CK2 and 1 are 5 (black and deformed). The spores with the highest TAI are found in the samples closest to the dyke. The samples closest to the dyke do not yield vitrinite with the highest reflectance. The highest VR is recorded from CK6 where the recorded TAI is 3+ (see Appendix III plate 16).

7.6.1.2 CQ SAMPLE HORIZON

AOM in the background CQ sample horizon is light brown in colour, from CQ3.0 – 2.0. CQ1.6 is dark brown, CQ1.2 is brown, CQ0.8 is dark brown, CQ0.6 is dark brown/black and CQ 0.3 and CQ0.1 are black (see Appendix III plate 17).

7.6.2 CARRICKLECK: FLUORESCENCE

7.6.2.1 CK SAMPLE HORIZON

The *Lycospora* sp. is not the most intensely fluorescing particle in the CK sample horizon. In fact the *Densosporites* has a fluorescence of greater intensity. *Densospora* sp. is not common enough to use for this work, nor is it a spore of uniform thickness.

Not all of the Lycospores fluoresce in any one sample. This may simply be a function of the thermal maturity of the material or it may represent different sources for spores e.g. some may have been subjected to greater oxidation or biodegradation before final deposition, some of the spores may be reworked. All of the fluorescing material in the CK sample horizon fluoresces orange to red-brown, with a very low intensity. Furthermore the material exhibits a negative fading, effective within less than 3 minutes of exposure to irradiation (see figure 7.6). This fading effect is more pronounced with proximity to the dyke, and lycospores with a very weak fluorescence have been observed to lose all fluorescence within 1 minute of continuous irradiation. In spite of fading, fluorescence is recorded up to CK11 (which is very, very weak and still exhibiting negative fading), with a TAI of 3 and a VR of 1.46%R_r. At CK10 there is no visible organic fluorescence (TAI = 3/3+, VR =1.41%R_r). This is at a slightly higher VR than is reported by some authors (see

figures 7.1 and 7.2). Fluorescence quenching is quoted to occur at the following VR: 1.35%R_r (Staplin 1969), 1.10 – 1.15%R_r (Ting 1977), 1.2 – 1.5%R_r (Tyson 1995), less than 1.5%R_r (Teichmüller 1987).

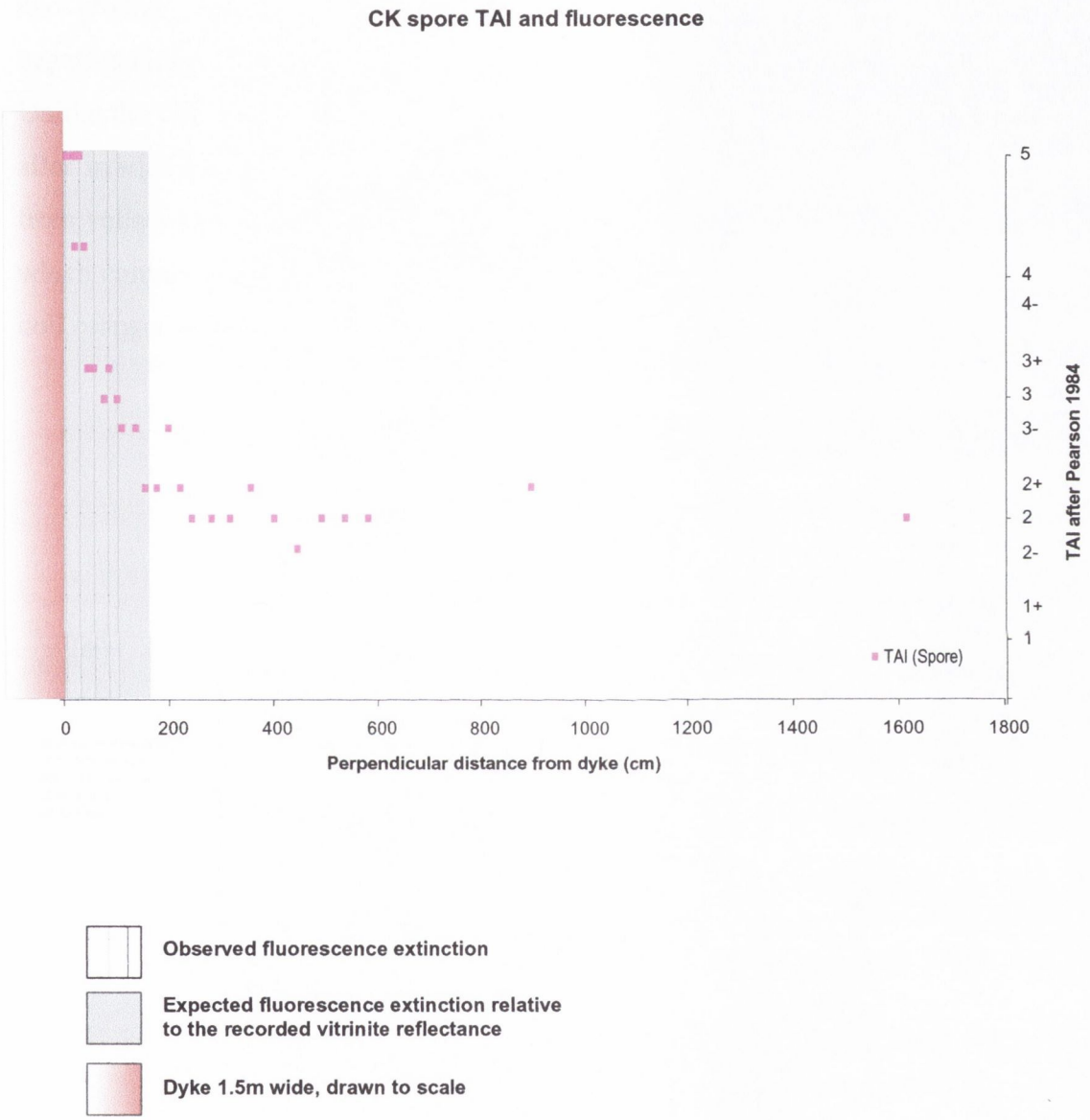

Figure 7.5 Spore TAI and fluorescence in the CK horizon of the Carrickleck Dyke aureole; plus the 'predicted' fluorescence quenching point, based on vitrinite reflectance.

7.6.2.2 CQ SAMPLE HORIZON

There was very little vitrinite in the CQ samples so there are no VR readings for this horizon. Nor are there many spores present in the samples. In fact the material was up to 80% AOM and so AOM colour and fluorescence alteration were assessed in this horizon.

CQ AOM fluoresces, unlike the AOM in the CK horizon. The AOM fluorescence of the background samples in the CQ horizon is yellow, of moderate intensity and exhibits negative fading, effective within less than 5 minutes of irradiation.

Unlike the CK horizon, the fading effect is never seen to lead to extinction of fluorescence after irradiation of a particle. AOM fluorescence shows decreasing intensity and a shift from yellow to red/brown due to the fading effect. CQ1.2 is the sample closest to the dyke, which contains fluorescing AOM (brown in colour, fluorescence intensity very weak and a dull orange/brown). CQ0.8 does not have any fluorescing organic material.

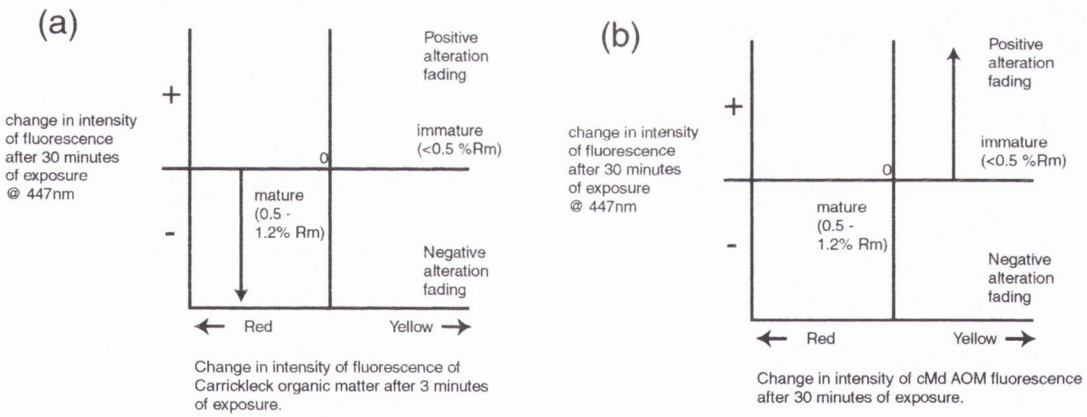

Figure 7.6 (i) The fading effect after 30 minutes exposure to fluorescent light:

(a) on spore fluorescence in the CK sample horizon and on AOM in the CQ sample horizon. Fading is negative (decrease in intensity, but no visible change in wavelength). Observed from samples recording 1.03 -1.10%Rr to 1.46%Rr until fluorescence is lost 1.40/1.49% Rr. (b) on AOM fluorescence in the cMd sample horizon. Fading is positive and observed in samples up to cMd6 (VR=0.94%Rr)

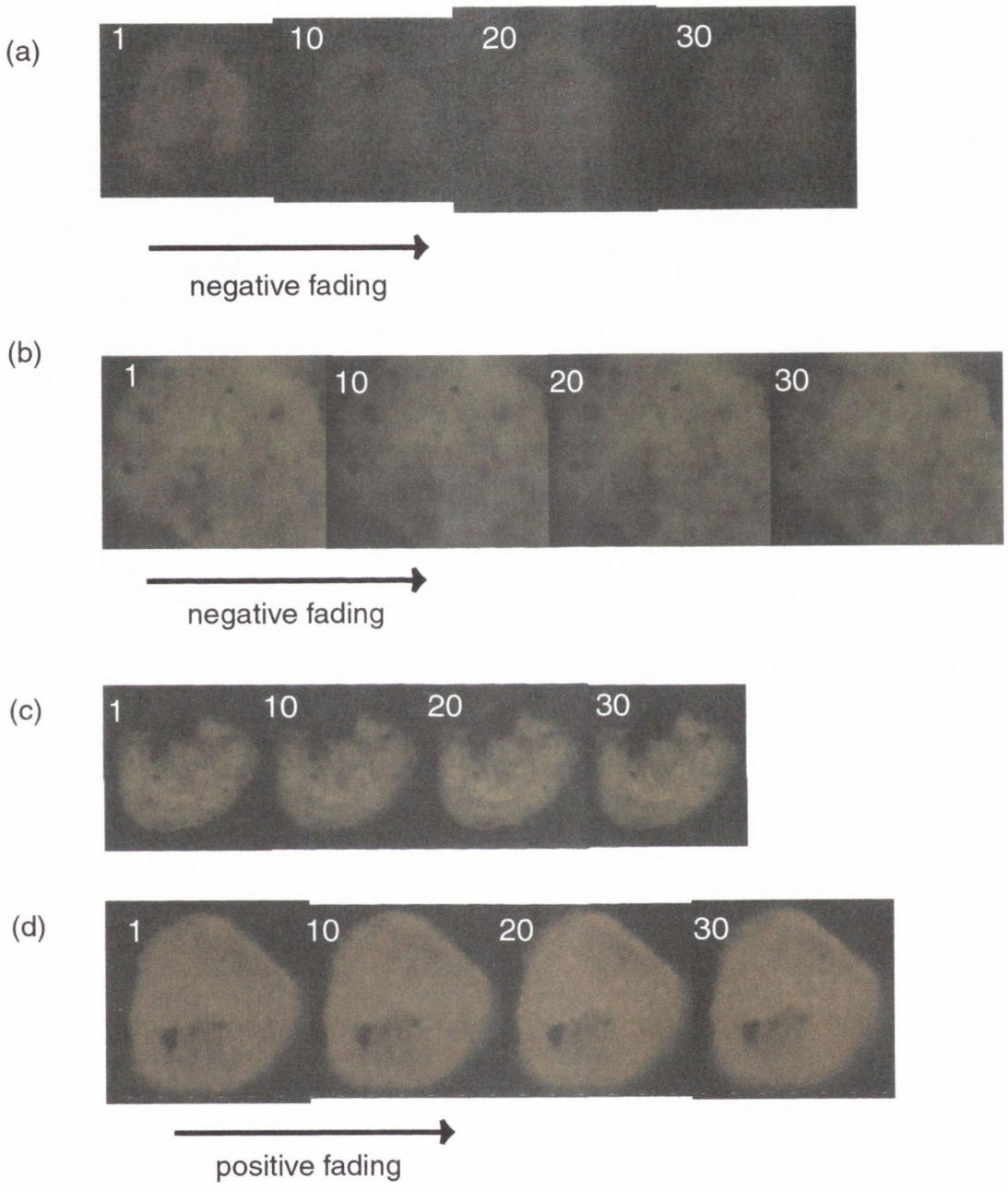

Figure 7.6 (ii) investigating the fading effect in: (a) CK29, (Lycospora sp.), (b) CQ3.0 (AOM particle), (c) cMd8, (Densospora sp.) (d) NSD 24 (unidentified spore) Images acquired after 1 minute, 10 minutes, 20 minutes and 30 minutes. (a) and (b) both exhibit negative fading, which has taken full effect within the first 5 minutes of exposure. (c) and (d) show positive fading (mild), which is strongest after 30 minutes.

7.6.3 BALLYCASTLE: TAI

7.6.3.1 CMD SAMPLE HORIZON

The TAI of the background cMd horizon is 2/2- (VR=0.55 – 0.94%R_r) in samples cMd8 – 6. There is a marked change in TAI to 3+ (dark brown) at cMd5 (VR=1.57%R_r). TAI is 3+ for cMd4 and 3+/4- for cMd3 (VR=2.57 and 3.55%R_r respectively) and 4- for cMd2 and 1 (VR=5.45 and 5.2 %R_r respectively).

7.6.3.2 BALLYCASTLE, NSD SAMPLE HORIZON

The NSD horizon is sampled at 10.11m perpendicular distance from the dyke. The background material contains spores with a TAI of 2-/2 (VR=1.03 – 1.25 R_r). This TAI is maintained in all samples from NSD24 –15 (10.11 – 2.2m perpendicular distance from the dyke contact). NSD14 has a TAI of 3- (1.82m from dyke, VR=1.26R_r). NSD11 – 8 have a TAI of 3/3+ (1.21 – 0.65m from the dyke respectively, VR=1.48 – 3.49%R_r respectively). NSD7, 6 have a TAI of 4-, NSD5 and 4 have a TAI of 4 NSD has a TAI of 4-/4 and NSD2 and 1 have a TAI of 4/5.

7.6.4 BALLYCASTLE: FLUORESCENCE

7.6.4.1 CMD SAMPLE HORIZON

Fluorescence in the cMd horizon has a moderately strong intensity in the background samples of cMd8 and 7, with a bright yellow fluorescence, exhibited after 10 minutes irradiation (positive fading, see figure 7.6(ii)). Sample cMd6 shows a marked drop to weak intensity with an orange-brown fluorescence colour. This is the last sample to exhibit fluorescence. Sample cMd5, with a TAI of 3+, shows a complete absence of fluorescence(see figure 7.7).

7.6.4.2 NSD SAMPLE HORIZON

Fluorescence in the NSD sample horizon is moderately intense in the background but it varies even within single samples. This is not very surprising considering the VR range within these rocks. There is no observed fading effect, positive or negative (see figure 7.6(ii)). The fluorescence colour of the background material is orange to red-brown also in keeping with the VR observed. Spore fluorescence is not uniform within a single sample, i.e. there is some variation in intensity between spores in any single sample but there is no fading effect, positive or negative, observed. The most representative Lycospore for each sample was chosen. NSD14 is the last sample to

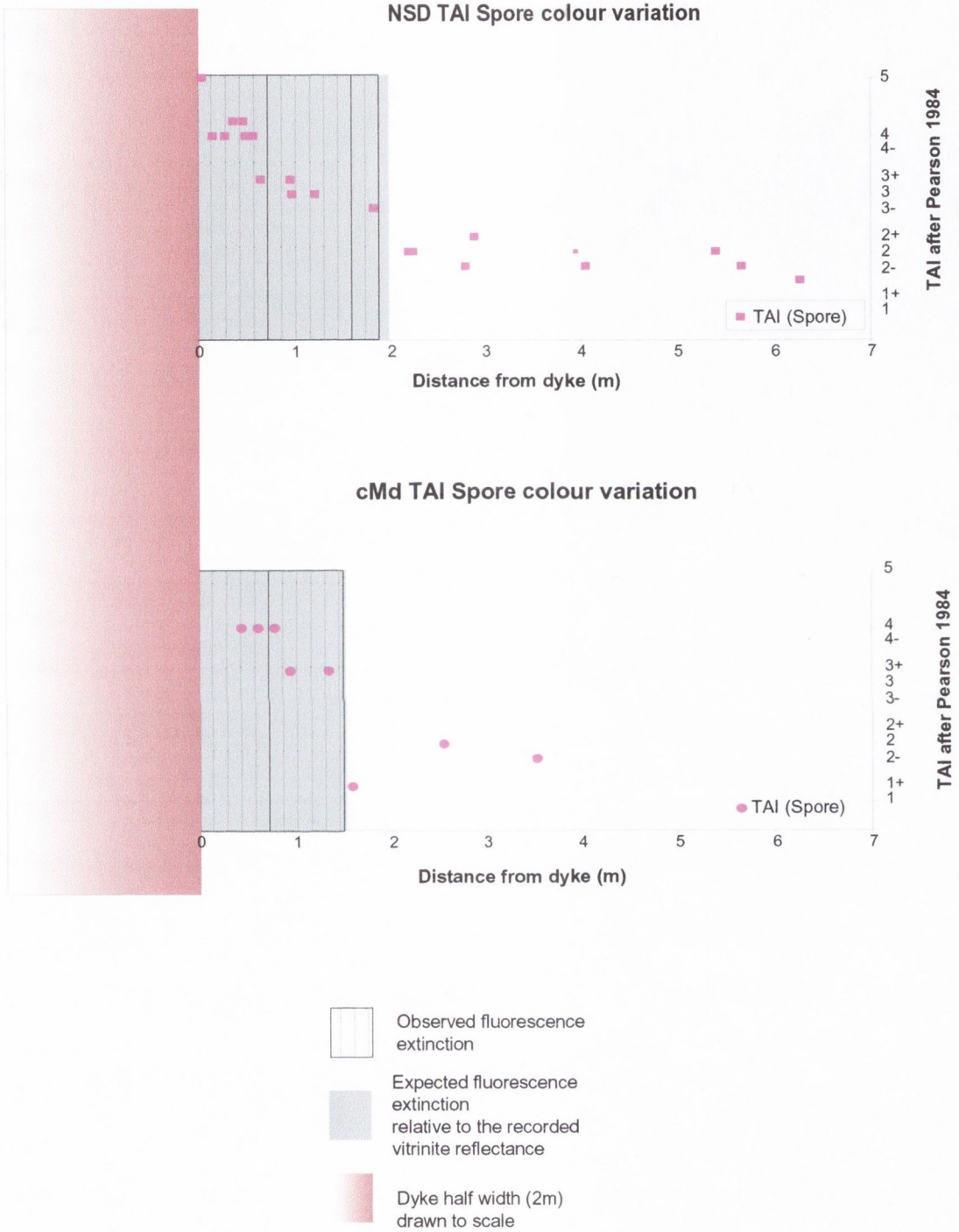

Figure 7.7 Spore TAI and fluorescence extinction and predicted fluorescence extinction (based on vitrinite reflectance) recorded in the NSD and cMd horizons of the North Star Dyke aureole.

exhibit spore fluorescence(see figure 7.7).. The fluorescence is very weak and a dull red-brown colour. There is no fluorescing organic material in NSD11.

7.7 DISCUSSION

7.7.1 TAI

TAI for each horizon gives a reasonable 'maturity' estimate of the background samples, in that the background TAI values agree with the background VR results. The thermal alteration index is showing consistency in each horizon with VR in the background samples.

AOM colour in the CQ horizon also alters, through a similar colour series as the spores of the CK horizon.

AOM colour alteration might also be used with a TAI, however, the material colour changes need to be calibrated.

TAI results show a trend of low TAI to high TAI, as the distance from the dyke decreases, for each of the samples horizons.

Showing that the spore TAI is reacting to the dyke.

TAI results, through the respective aureole horizons, are not 'in step' with the equivalent VR results. For example, spores with the highest TAI are found in the samples closest to the dykes.

This implies that the spore colour changes occur quite rapidly in response to the heat of intrusion.

However, these samples closest to the dyke do not yield vitrinite with the highest reflectance. This can be seen in the CK horizon at Carrickleck, where one of the highest VR readings is recorded from sample CK6 at 0.4m from the dyke (VR= 3.4%R_r) where the recorded TAI is 3+. Sample CK1 (0.07m from the dyke) has a recorded TAI of 5 (black and deformed), and VR of 3.1%R_r.

It would be expected that the spores with the highest TAI would occur in the samples with the highest VR but this is not always the case. In fact in the CK and NSD horizons where both spore TAI and VR were recorded, it was observed that the highest TAI values are always recorded from material that was closest to the dyke, while the maximum VR values are usually recorded from samples that are displaced 0.2-0.5m from the dyke/sediment contact.

This might be seen to imply that there is another factor acting in this scenario, other than heat affecting the thermal evolution of the vitrinite in the area directly adjacent to

the dyke. This also shows that the TAI although not as accurate an indicator for lithological maturity, is more dependant on temperature than vitrinite in this case.

7.7.2 FLUORESCENCE

In each of the sample horizons, some of the material examined from the background samples does fluoresce. However, fluorescence intensity varies between particles within any individual sample, and across an individual particle. Fluorescence is a qualitative science. Comparison is the best way to implement this tool. One would assume that this makes the use of fluorescence in the study of thermal maturity quite blunt for very specific/accurate work.

Particle fluorescence can have a characteristic 'fading' effect, which tends to be something that is characteristic of an entire sample, rather than typical of a single particle within a sample.

Fluorescence intensity decreases with proximity to the dykes, without exception, for each of the sample horizons, in spite of the difficulty with varied particle fluorescence. This is not a new observation and can be related to the heat experienced by the host rocks when the dyke was intruded and as it cooled, that is decreased fluorescence of organic material is a reflection of the temperatures to which it was exposed. Spore fluorescence reacts quickly, in geological time, to elevated temperatures.

Fluorescence quenching occurs at approximately the same position in both the CQ and the CK horizons, between 1.2 and 0.8m, even though AOM was being examined in the case of the CQ horizon and spores were being used in the case of the CK horizon.

Fluorescence quenching occurs at a greater distance from the dyke in the sample horizons collected from the North Star Dyke aureole (1.8-1.7m for NSD and 1.6-1.4m for cMd) than those collected from the Carrickleck Dyke aureole (1.0-1.1m for CK and 1.2-0.8m for CQ). This is assumed to be a reflection of the effect of the multi-intrusion thicker North Star Dyke relative to the single intrusion thinner Carrickleck Dyke.

Fluorescence is quenched in the NSD and cMd horizons at different positions, 1.8-1.7m for NSD (1.5 –1.3%R_r respectively) and 1.6-1.4m for cMd (0.7-1.6%R_r respectively). While the positions in the dyke aureole do not overlap, the VR values

do. This would appear to be a reflection of a difference in the properties of the cMd and NSD horizons.

Fluorescence quenching is generally accepted to occur at c. 1.4%R_r (refer to figure 6.5). Fluorescence quenching occurs in the CK horizon at an equivalent VR of *c.* 1.5%R_r, and in the North Star Dyke aureole horizons - NSD 1.5 –1.3%R_r and cMd 0.7-1.6%R_r. It would appear that fluorescence quenching is occurring in the dyke aureoles at VR values slightly greater than those expected, from burial maturation studies. It would tentatively be suggested that fluorescence is reacting faster than VR, although more work would need to be undertaken to confirm this result.

Fluorescence quenching is not reversed in the area adjacent to the dyke, where there is also a reverse trend in the VR results.

7.8 CONCLUSIONS

The thermal alteration index is showing consistency in each horizon with VR in the background samples.

AOM colour in the CQ horizon alters through a similar colour series as the spores of the CK horizon.

AOM colour alteration might also be used as a TAI, however, the material colour changes need to be calibrated.

Spore and AOM colour changes occur quite rapidly in response to the heat of intrusion.

TAI, although not as accurate or specific an indicator for lithological palaeotemperature, is more dependant on temperature than vitrinite, in this case at least.

Spore fluorescence reacts quickly, in geological time, to elevated temperatures.

Fluorescence quenching in the Carrickleck Dyke and the North Star Dyke aureole sample horizons indicates that the North Star Dyke has a more extensive aureole.

Fluorescence appears to react faster than VR to temperature, and maybe, like TAI, is also more temperature dependant than VR. More work would need to be undertaken to confirm this result. If fluorescence reacts more quickly than VR, then perhaps in the exploration operations, if the rock assessed contains material with a similar VR/spore fluorescence discrepancy it might be assumed that the core is adjacent to an intrusion and that the 'maturity' that is being assumed for this horizon is misleading.

8 PALYNOFACIES

8.1 DEFINITIONS AND INTRODUCTION

8.1.1 DEFINITIONS

Facies describes a spatially segregated and broadly coeval body of sediment deposited within a specific depositional environment or by a specific depositional mechanism (Tyson, 1995).

Palynofacies Powell *et al.* (1990) defines palynofacies as a distinct assemblage of hydrochloric acid (HCl) and hydrofluoric acid (HF) insoluble particulate organic matter (palynoclasts), whose composition reflects a particular sedimentary environment. The term palynofacies has been used in other works to describe a facies based only on the palynomrph distribution (Cramer and Diez 1972, Traverse 1988), however the term is used in the former sense in this work and is treated as an indication of a set of characteristics that can help to characterise the rock, rather than a method for definitive identification.

Palynofacies analysis is defined as the identification of characteristics of rock facies through the palynological study of their contained organic matter (after Combaz 1964, Powell 1990, Tyson 1995, Batten 1999). Thus, analysis requires that all types of HCl and HF resistant organic matter recovered from rock or sediment samples by palynological extraction methods are examined. Only three components survive HF and HCL, they are chitin, sporopollenin and cutin. Palynofacies analysis is a useful if blunt tool.

8.1.2 INTRODUCTION

Palynofacies is a term originally introduced by Combaz (1964) to include the "total complement of acid resistant organic matter recovered from a sediment or sedimentary rock by acid processing techniques using HCl and HF" (Durand 1980, after Combaz 1964). The term and its definition, proposed by Combaz, were not immediately accepted (Sigal, 1965, derided the term calling it "illogical" and "superfluous"). Since then there have been a confusing number of classification schemes through the literature. These schemes are often more readily applicable only to the facies types and settings from which they have been derived (Alpern 1970, Alpern *et al.* 1972, Batten 1973, 1982a & b Hart 1986, Tyson 1995). Palynofacies publications have increased in frequency from the 1980s onwards, since the recognition of the possible aid it can offer in hydrocarbon exploration (Brooks 1981, Batten 1982, Lorente 1990, Traverse 1994 and Smith 1996).

In this work, palynofacies analysis has been implemented for the following uses and reasons:

1. In association with other methods, palynofacies analysis is used to help characterise the horizon that is being examined through a dyke aureole.
2. Because preferential destruction of spores and other particulate organic matter occurs in rocks that have been subjected to heating, palynofacies analysis has been used to record some of the progressive visible changes in the sedimentary particulate organic matter through the dyke aureole.
3. Palynofacies analysis is a quick and inexpensive method that can be applied to any rock bearing particulate organic matter.

It is very important not to over interpret the results of palynofacies analysis, particularly in relation to point 1. There is only a very limited portion of the particulate organic matter, potentially available for deposition in sediments, that will finally become entombed. For example; marine organic matter production is controlled by light, temperature and nutrient content of the seawater. The accumulation of organic matter into the sediments depends on equilibrium processes, which not only preserve and concentrate but also degrade and dilute the organic matter. It is estimated that less than 1% of the produced organic matter is eventually preserved in sediments (Durand 1980, Brooks 1981, Tyson 1995). Thus, palynofacies is a method of analysis best used in conjunction with others. Although it can be used as a single method to imply certain facies affinities, it cannot be used alone to define a sedimentary facies.

Most terrestrial matter accumulates within fluvial – lacustrine systems in estuaries and in the nearby offshore. Once in the sea, it tends to be found in the inner shelf area where it is often rendered finely particulate by reworking and biological degradation (Batten 1996a). The bulk of the organic matter in sediments is preserved in detrital, anoxic environments. High phytoclast abundances have been related to the occurrence of turbidites (Tyson 1995). Winnowing of sediments in high-energy environments may lead to a concentration of phytoclasts in unexpected locations (Batten 1999, 1996a, Goodhue 1996).

8.2 THE SUBDIVISION OF ORGANIC MATTER

Organic matter contained in sediments includes all plant and animal remains, such as spores and pollen, plant fragments, whole/fragments of animal carapaces or carapace

linings, algal remains etc. The production of terrestrial organic matter is most common along continental margins (Brooks 1981).

For the implementation of palynofacies analysis it is important to categorise the fossilised organic matter. However, previous workers in the field have not been prone to agreement on the classification schemes used. Listed below are some of the schemes proposed and used by previous workers. (summarised in table 7.1)

Batten (1996a) proposes four main categories; palynomorphs, structured plant debris, unstructured amorphous material and soluble compounds, extractable by organic solvents. The first three of these categories are extracted from the sediment or rock using (and are resistant to) HCl and HF and are regarded as palynological matter and can be studied petrographically.

Tyson (1995) has a similar classification scheme to that of Batten (1996a). Although they differ somewhat in the placement of the zooclast subgroup, they are essentially the same, differentiating between structured and structureless particulate organic matter and more or less subdividing from there. Batten (1996a) does add a further element of subjectivity by including a separate category for reworked material. Although it might seem to be an obvious addition, it would take a practiced eye to consistently be able to differentiate the correct material for this category particularly if only using transmitted light. Both Batten (1996) and Tyson (1995) present classification schemes that are very comprehensive.

Smith (1996) used a classification adapted after the Amsterdam Palynological Organic Matter Classification, 2nd edition, as defined at Aix-en-Provence, France (September 1992). The scheme, although agreed upon in Amsterdam has not been widely accepted, (perhaps due to the fact that it has never been published and so is not readily accessible) and used only in a modified form such as that of Smith (1996).

Davies *et al.* (1991) developed a scheme for specific work; to describe the transition from largely fluviatile, late Devonian Old Red Sandstone, to the mainly marine, early Dinantian, Lower Limestone, Shale Group in South Wales. The sequences examined delivered a relatively limited range of material. This is a succinct scheme that again is not comprehensive in not including amorphous group of OM, which is prevalent in so many OM rich sediments.

The classification scheme of **Hart (1986)** is broadly divided into Phytoclasts and Protistoclasts, Sclerotoclasts. These are then further subdivided by their state of degradation, morphology and structural framework. This scheme would appear to be even more subjective than many of the others.

Combaz (1964)	Alpern (1970)	Correia (1971)	Bujak *et al* (1977)	Habib (1979)	Masran and Pocock (1981)	Davies *et al* (1991)	Smith (1996)	Tyson (1995)			Batten 1996a		
Debris Vegetaux	Phytoterrestes	Tracheides	Hylogen From woody material	Tracheids,	Terrestrial (structured)	Woody Plant Debris Hylogen	Brown woody material Black brown woody material	Woody Tissue	Macrophyte debris	Phytoclast	Structured Organic Matter	PhytoClasts	wood (Black and brown) charcoal and other black phytoclasts cuticle other non-cuticular tissue Tubes, filaments, hairs
		Ligneuse	Melanogen opaque organic material	Cuticle	Charcoal	Melanogen	Black Woody Material Black particulate organic matter	Charcoal					
	Fungi		Phyrogen non woody plant material including palynomorohs		Terrestrial (structured) Fungi	Non-woody Tissue Tubes	Other plant Tissue	cuticle Other non-woody tissue				Zooclasts	
								Fungal Hypahe	Fungal Debris				
Microfossiles	Spores	Vegetale		Classopollis, bisaccates and small sporomorphs Large Fern Spores	Spores and Pollen	Spores	Non saccate miospores	Spores Pollen	Sporomorph	Palynomorph	Structured	Palynomorphs	Spores and pollen Fungal sclerotia Dinoflagellate cysts Acritarchs Prasinophyte algae Chlorococcolea Green Algae Cyanobacteria Chitinozoans Foraminiferal linings Scolecodonts Miscellaneous
	Organismes autonomes Zooplankton and zoobenthos			Dinoflagellates	Structured Aqueous	Organic walled Micro Plankton		Acritarchs Dinofl-agellates	Organic walled Phytoplankton				
						Scolecodonts		Foramini-feral linings Scolecodonts	Zoomorphs				
								Graptolite fragments Arthropod Fragments		Zooclast			
Matiere Organique Amorphe	Bitumes Bacteries	Colloidale	Amorphogen amorphous: structureless organic matrerial	Globular Debris Comminuted Debris Shredded Debris	Resins Biodegraded Aqueous Biodegraded Terrestrial Amorphous		Orange Brown structureless matter Grey Brown structureless organic matter Fluffy Structureless matter	Resins Gels AOM		Amorphous Organic Matter	Non-Structured	Structureless Organic Matter	gelified matter Resin and Amber Solid Bitumen AOM AOMT AOMA
												Reworked Organic Matter	

Table 8.1 Comparisons of selected palynofacies schemes.

Brooks (1981) has a trifold scheme, which divides between unstructured/amorphous insoluble material, morphologically structured-partly structured material and soluble organic compounds that can be extracted into organic solvents.

Masran and Pocock (1981) used a scheme based on botanical and coal petrological classification of palynodebris. One reasons for not adopting this scheme is the possible confusion that can occur with the crossover between transmitted and reflected light terminologies.

The scheme of **Habib (1979)** is a type specific study, as can be seen by the missing categories. Although the work neatly displays expected trends through sediments of differing terrigenous supply, the overall palynofacies terms have been classified into 5 separate categories.

Bujak *et al.* (1977) used a classification scheme also employed by Manum and Throndsen (1978), some of the terms also being used by Davies *et al.* (1991). This is one of the less complicated schemes used in the literature. Although it does not show specific space for the 'zooclasts' of Batten (1996) and Tyson (1995) it is readily adapted and used.

Some of the first schemes such as that of **Combaz (1964)**, **Alpern (1970)** and **Correia (1971)**, used broad categories. These are relatively easy to use, although some do not give full scope to all of the potentially available material.

8.3 OBSERVED ORGANIC MATERIAL

One of the problems faced in the literature is the various use/misuse of terminology. Any palynological terms used in this work that might be misconstrued have been defined, as applied in this work, in Appendix IV.

Woody tissue

Recognition and identification: woody fragments can be lath shaped, equidimensional, needle like fragments, tubular, pitted or banded and most will tend to have an angular outline(see figure 8.1). Woody tissue is quite a thick resilient material and cellular structure is commonly retained. Literature records a very weak fluorescence for immature woody material (<5.0 $\%R_r$) (Tyson 1995 and references therein). This is not observed in any of the material studied in this work. The material is generally light to dark brown/black to entirely opaque.

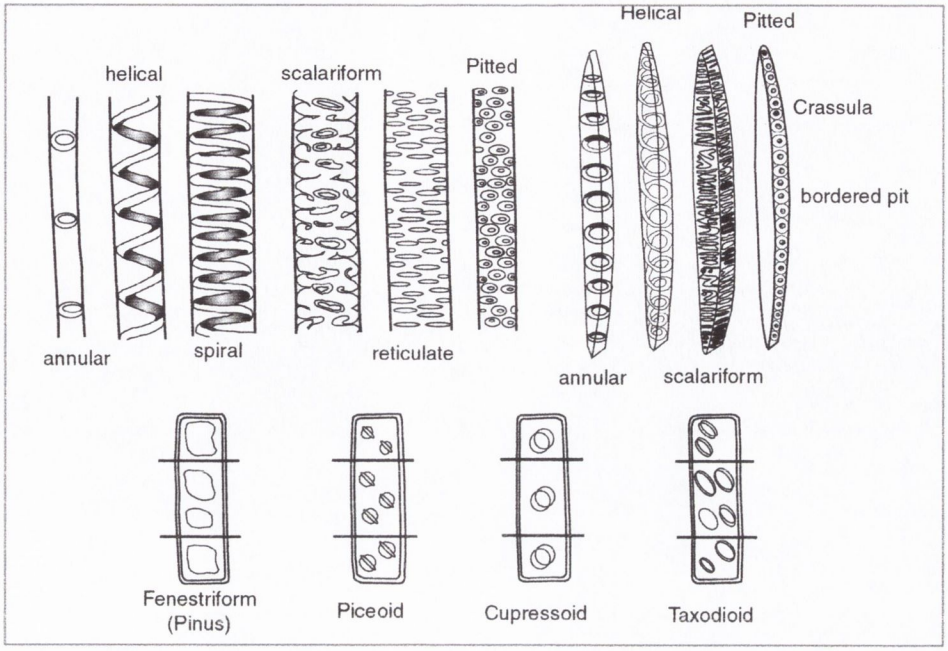

Figure 8.1 Examples of the different morphologies exhibited by woody tissue, after Tyson (1995)

Difficulties in identification: some of the thicker pieces of woody tissue may appear to be opaque. When this material is observed at higher magnification (at least x400 magnification) and/or with the stage flooded with light it may be possible to observe some colour around the edges of the particle or at a thinner piece of the fragment. As the rock reaches higher stages of maturation this problem becomes greater.

Biological affinities and miscellaneous detail: The majority of the dispersed organic matter preserved in sediments can be classified as terrestrially derived wood (Tyson 1995 and Batten 1996). Its relatively good preservation rate is due to the high lignin content of these tissues, lignin being strongly resistant to degradation (spore exine and xylem are two of the most indestructible forms of plant tissue). "Most woody tissue found in palynological preparations is derived from the ligno-cellulosic tissues of terrestrial macrophytes and probably represents the fragments of strongly lignified mechanical support and vascular tissue of the secondary xylem of arborescent angio- and gymnosperms" (Tyson 1995). The wood of angiosperms (deciduous) appears to be more prone to degradation than that of modern gymnosperms (Batten 1996a), with the bulk of the woody tissue recovered from brown coals being of mainly coniferous origin (Teichmüller 1982, Tyson 1995 and Batten 1996a). This may due to a lesser lignin content, greater chemical susceptibility, and swifter fungal invasion in the former (Brooks 1981 and Tyson 1995).

Xylem elements, such as tracheid and vessels are commonly observed in palynological preparations. Tracheids are elongate, spindle shaped, closely packed cells. Fossilised, they are generally fragmentary in preparations (Brooks 1981, Tyson 1995 and Batten 1996). The fragments can be tubular, pitted or banded and most will tend to have an angular outline. These particles are generally brown to dark brown/black to entirely opaque. The colour variation in woody particles is due to the fragments thickness, "oxidation, desiccation and fungal mouldering" of the originally brown material (Tyson 1995). Oxidation is said to be the most important of the three processes. Hart (1986) observed varying states of oxidation in modern sediments dependent on the depositional environment.

Comparisons have been made between the distribution of woody material in ancient (post Silurian) and modern material (McPhilemy 1989, Tyson 1995, Batten 1996 and Batten 1999). Woody particles are relatively common in near shore settings and re-deposited sandy silty deposits and in those relatively oxidising facies in which less resistant materials have been selectively destroyed (Tyson 1995).

Opaque organic matter (OOM)

Recognition and identification: material assigned to this category is entirely opaque and has a definite outline. The fragments can be lath shaped, equidimensional, needle shaped/splinters, rounded or angular. They may or may not show remnant cellular structure. See table 8.2, Appendix III plates 20-26.This material does not fluoresce.

Difficulties in identification: One of the problems with this group is the possible mis-identification of pyrite. Although pyrite is generally recognisable by its framboidal nature this is not always the form it takes. Reflected light is an easy means for the identification of pyrite because, as for charcoal and black wood, pyrite has a very high reflectance, higher than either charcoal or black wood. It is easier to recognise in incident light at high magnification.

Biological affinities: This group contains particles such as charcoal, oxidised land plant tissue (*e.g.* black wood) and recycled coalified material. Some workers have found the distribution of opaque phytoclasts to be similar to that of woody debris in modern sediments (Tyson 1995 and references within). The work of Claret *et al.* (1981) on Cenozoic sediments of the Niger delta, found opaque phytoclasts to be frequent in marine and littoral facies, they have also been noted in barrier beach and offshore sands (Bustin 1988), and fluvial lower (subaerial) delta plain and estuarine or inter distributary and

coastal dominated sediments (Habib and Miller 1989). These facies are also low in palynomorphs, have high plankton content and common reworked palynomorphs and freshwater algae (Tyson 1995).

Cuticle

Recognition and identification: (see figure 8.2) using transmitted light cuticle appears as very fine, pale yellow to colourless material. For the purposes of this work, material is only identified as cuticle where remnant cellular structure is observed. Cuticle is so thin that it is often folded. Cuticle fluoresces up to VR of *c.* 1% (Tyson 1995).

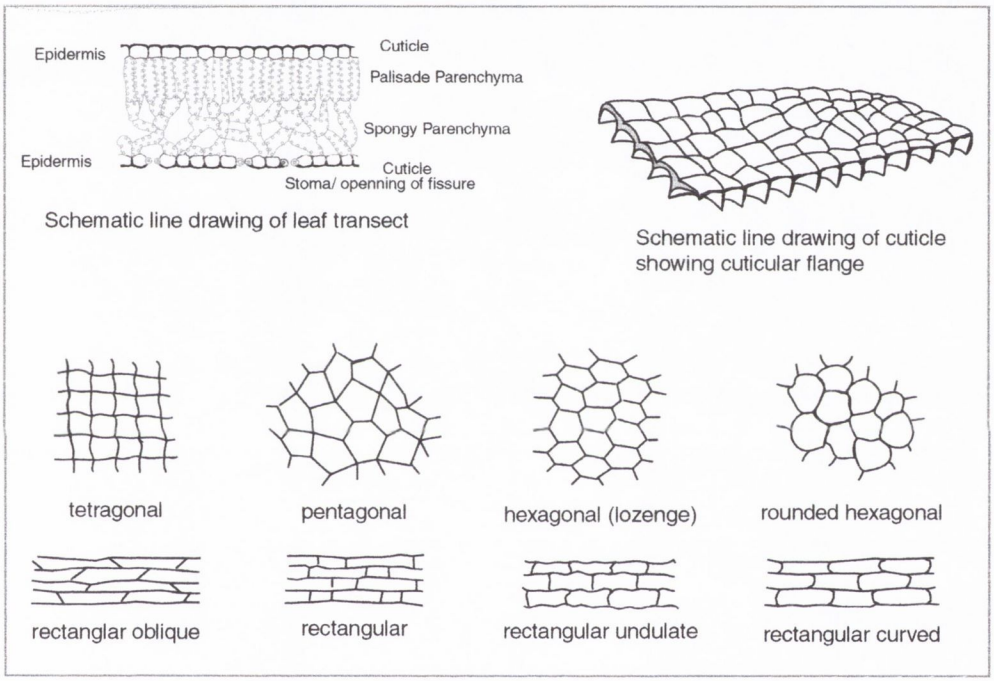

Figure 8.2 Schematic representation of leaf, cuticle (Teichmüller 1982) and cuticle cellular patterns (after Tyson 1995)

Biological affinities: Cuticle is a surface feature of the exposed parts of most vascular plants, the purpose of which is to reduce desiccation (Thomas and Spicer 1987). It is not present in aquatic plants and is thought to have evolved after the plant colonisation of land. Fossil evidence for the early occurrence of cuticle is ambiguous. Durable sheets of cells occur as early as the Precambrian and are common from the late Silurian on. The problem would appear to be in relating the cuticle to land plant. Animals produce cuticle-like coverings, which in the dispersed fossil state may be indistinguishable from those of plant origin (Taylor 1982).

Cuticle tends to be associated hydrodynamically with the sand and silt fraction of sediments and is commonly found in delta top, prodelta and estuarine-mangrove facies or in proximal siliciclastic submarine fan facies. According to Tyson (1995), this fraction of palynofacies is rarely found in distal anoxic facies in great quantities.

Non- woody non-cuticular plant tissue

Recognition and identification: non-woody plant tissue has a very fine cellular structure. It may be fibrous, ribbed or membranous in appearance. Plant tissue is often folded in palynological preparations and can range in colour from almost colourless-pale yellow to amber. Some plant tissue can fluoresce.

Biological affinities: cellulose makes up most of the non-lignified tissues such as colenchyma and thin walled parenchyma (or ground tissue) of the cortex (i.e. the non-epidermal, non-vascular tissue), (Batten 1996), whereas woody material is strongly lignified. As cellulose degrades up to three times faster than lignin (Tyson 1995), such tissues degrade much faster than the vascular, lignified tissue of the woody material. This is reflected in the greater degree of bacterial colonization in streams and the more rapid degradation of the non-woody plant material. In ancient sediments, remains of such non-woody tissues seem to be most common in non-marine and deltaic facies. They are rare in most marine facies unless introduced by re-deposition. Aquatic plants have a much lower chance of surviving to the fossil record than their terrestrial counterparts. This is especially true if they are growing in a well-oxygenated environment (Tyson 1995, Batten 1996). As for cuticle, non-woody plant material is found with the sand and silt fraction in transport.

Acritarchs

Recognition and identification: Acritarchs can be spherical to polygonal bodies that can have an array of external sculptures and processes, or can be entirely smooth. There is much variation in both the external ornamentation and the thickness of the cysts making the colour and resistance of these ambiguous bodies variable. The acritarchs identified in this work are spherical, and without ornamentation. The cysts are flattened with distinctive folding. In transmitted light the cysts vary in colour from pale yellow (leiosphaerids) to amber (tasmanitids). Acritarchs are known to fluoresce.

Biological affinities and miscellaneous detail: Acritarchs are mostly marine green algal cysts (Traverse 1988). As a group, they have a very varied form. Pre 1960 the group was referred to as hystrichosphaerids, and often had dinoflagellates included in the group.

Major revisions by Evitt (1963a & b) brought in the new name of acritarchs and reassigned the dinoflagellates to the appropriate grouping (Tappan 1980, Traverse 1988). Some acritarchs *e.g. Tasmanites* and *Leiosphaeridia* have been placed in the algal division Prasinophyta (Tappan 1980).

Microforaminiferal linings

Recognition and identification: Microforaminiferal lining types tend to be described under the general headings of isolated chamber, uniserial, biserial, coiled and combined (Stancliffe 1989) (see figure 8.3). In this work uniserial, biserial and coiled microforaminiferal linings were observed. The lining appears fragile and shows a series of spherical chambers connected by a centrally developed neck. The linings are usually brown in colour and non-fluorescing.

Biological affinities: Microforaminifera range from the Cambrian to Recent. Microforaminiferal linings are described in the literature from Late Devonian to Recent. Most published material on microforaminiferal linings deals with Jurassic sediments and younger (Clarke and Verdier 1967, Lam and Porter 1977, Davies 1985, Stancliffe 1989). Microforaminiferal linings are defined as "the acid resistant organic remains (chitinous tectin) found in palynological preparations which are thought to be the inner linings of microforaminiferal tests" (Stancliffe 1989). The remains are thought to be

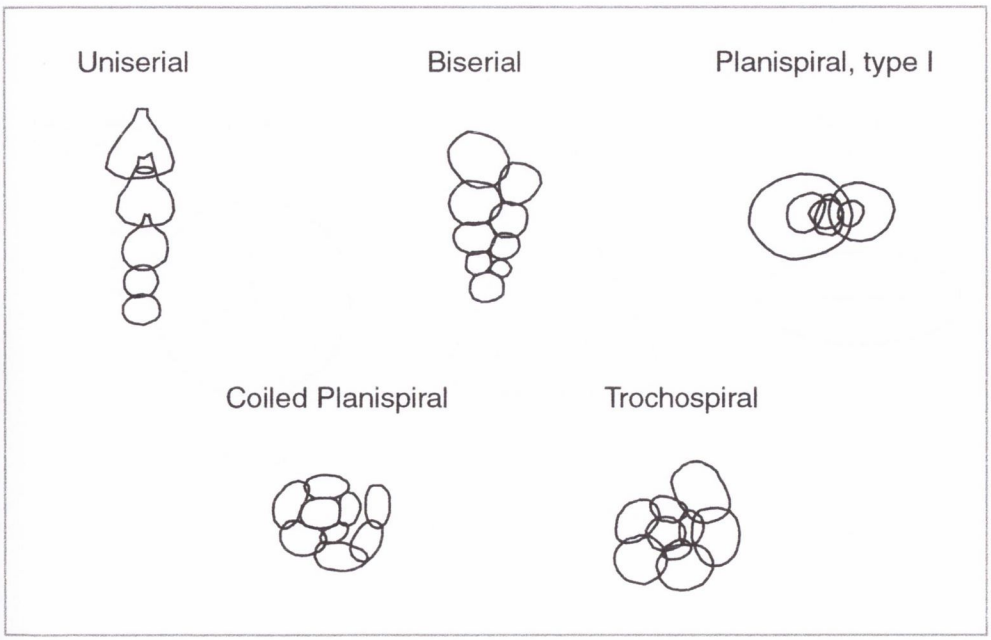

Figure 8.3 Morphological classification of microforaminiferal linings (after Stancliffe 1985)

exclusively marine (Decommer 1982), and mainly from benthic forms (Bradford 1977, De Vernal 1992, Tyson 1995). Any occurrences in terrestrial sediments are likely to be the products of reworking. "He (Bradford 1977) also found higher counts of linings in the Arabian Gulf samples where the sediment is coarse, water depth is shallower with a high salinity and higher summer temperatures" Stancliffe (1989). In modern sediments microforaminiferal lining concentrations are found to be largest related to current upwellings and that occurrences decreased with an increase in water depth. In sedimentary rocks, the linings are commonly associated with melanogen or amorphous organic material (Stancliffe 1989). Microforaminiferal linings vary in size from 50 - 200μm (Tyson 1995)

Sporomorphs

Recognition and identification: Sporomorphs vary in shape (generally spherical, triangular or oval), size (50-200μm miospores, >200μm megaspore) and ornamentation. Spores of vascular plants are often characterised by the well-formed and consistently placed germinal aperture. The form of this aperture in spores is trilete, monolete or where there is no obvious trilete or monolete mark the spore is described as alete (see figure 8.4). Spores generally fluoresce up to 1.2 $\%R_r$. Their colour in transmitted light varies depending on exine thickness and coalification level. Even at the immature stages, there is a range of colour in transmitted light from colourless to pale yellow, yellow, orange or amber.

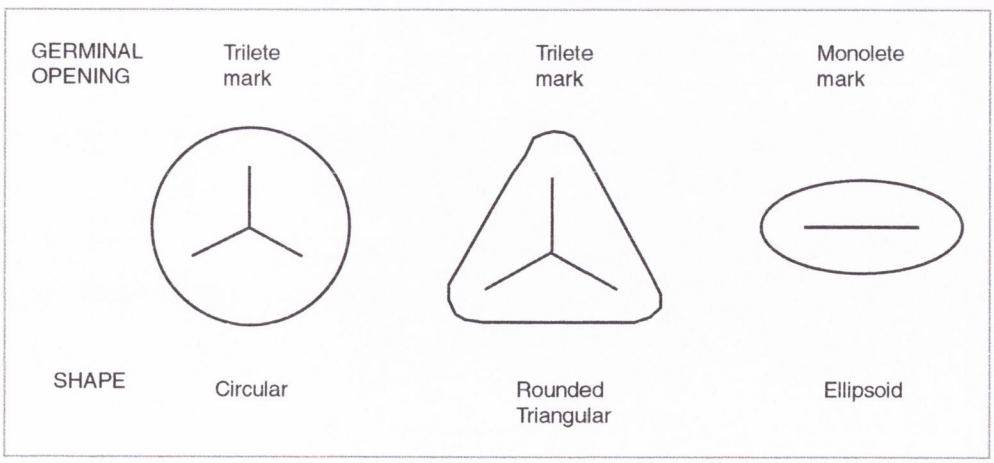

Figure 8.4 Examples of the basic spore morphologies (outline seen in polar view) and the various germinal opening marks

Biological affinities: Miospores are abundant in a wide range of terrestrial and marine facies in part because they are readily transported (Davies *et al.* 1991). The exine of miospores consists of a highly resistant material called sporopollenin. Large and strongly ornamented trilete spores tend to be more abundant in fluvio-lacustrine, delta top and back delta/swamp and near shore/estuarine facies than elsewhere (Tyson 1995, Batten 1996). Where transport has been a minor influence, miospore masses and megaspores may be preserved in abundance locally, especially in abandoned channels and lagoonal silts (Batten 1996). Small thin-walled, unornamented spores and non-saccate pollen grains are more likely to be numerous in muddy non-marine or marine offshore facies (Batten 1996). The settling rates of most sporomorphs is comparable to that of fine silt grade quartz (Tyson 1995), thus most sporomorphs and palynomorphs are concentrated in the clay to silt size fraction. Sediment with >30 – 40% sand fraction tends to have a lesser abundance of palynomorphs (Tyson 1995). In cases where miospore assemblages and other organic matter are both diverse and abundant, it can be assumed that accumulation was not far from the source vegetation (Batten 1999).

In ancient sedimentary rocks, spores can be found in almost all marine rock types, although they tend to be more abundant in the siltstones. (Pollen is not really developed until the late Carboniferous and so is not discussed in this work).

Megaspores have been found to be abundant in fluvial marsh and lagoonal sediments. They are usually most abundant in medium to coarse silts and decrease markedly in clays (Tyson 1995). Megaspores have been found in both continental and open marine settings as well as proximal facies (Davies 1991) where they occurred as infrequent fragments.

Scolecodonts

Recognition and identification: Scolecodonts look like a saw blade, often curved but sometimes straight. Scolecodonts consist of thick and resistant "part calcified and sclerotoproteinaceos ('chitinous')" (Tyson 1995) material.

Biological affinities: Scolecodonts are chitinous jaws of small polychaetous annelid worms (Tyson 1995). They are commonly found as disarticulated parts of the mouth lining of the worms (Traverse 1988). A refractory element, the scolecodont generally occurs in low concentrations in sediments and sedimentary rocks. Scolecodonts are most commonly found in shallow marine facies, although they have been recovered from deeper water lithologies (Davies 1991). The modern polychaete worm is a marine animal particularly tolerant of oxygen deficiency and may occur in abundance in dys- to suboxic environments

(Tyson 1995). However, the absence of scolecodonts cannot be taken as an anoxic indicator due to their infrequency in sediments.

Amorphous Organic Matter

Recognition and identification: AOM is a structureless mass of degraded organic matter of mixed, often unknown affinities. Observed AOM has shown a variety of colour even in one sample preparation. It can be yellow/brown, brown or a grey/black colour. It seems to be generally accepted that terrestrially derived material (terrestrial plant material biodegraded under aerobic aquatic conditions; Masran and Pocock 1981) tends to have a weaker fluorescence than the marine equivalent (assuming it to be degraded algae type) (Masran and Pocock 1981, Tyson 1995, Batten 1996). It was also suggested by the experimental work of Masran and Pocock (1981) that biodegradation of terrestrial plant material under anaerobic conditions is expected to be a yellow orange to orange brown colour, and under aerobic conditions is an orange brown mixed with grey black coloured material. Biodegradation of marine material in a reducing environment produces a neutral grey-black material often rich in organo pyrite. One of the problems with assumptions based on colour and auto fluorescence is the spectral changes exhibited by the material through varying stages of maturity and oxidation.

Biological affinities and miscellaneous detail: Some AOM has been attributed to various zoomorph grazing habits or bacterial and fungal degradation of organic material (Tyson 1995, Batten 1996), however it can also be a mass of coagulated particulate matter (Davies 1991, Tyson 1995, Batten 1996). AOM may be the remains of degraded terrestrially derived material (biodegradation of terrestrial plant material under aerobic aquatic conditions Masran and Pocock 1981) or that of marine derived degraded algae (Masran and Pocock1981, Tyson 1995, Batten 1996).

Where AOM is present in an assemblage, it has a tendency to dominate, especially in a marine lithology (Tyson 1995). Higher percentages of AOM have been found in ancient sand-poor, clay or limestone rich facies. This phenomenon has been ascribed to the hydrodynamic sorting of material in the delta leading to a lower concentration of sporomorphs and phytoclast material. AOM has a tendency to be the dominant constituent in distal, carbonate, dysoxic or eutrophic environments with a low phytoclast input (Tyson 1995). Unidentifiable coagulated particulate matter tends to be the dominant AOM of terrestrial sediments. It may not even be possible to recognise the particulate nature of the

	Biological Origin	Terrestrial Aquatic	Main Compositional Component	Degradation?	Auto-Fluorescence	Colour in TL	Characteristics in TL	Age Range	Facies implications	Tyson (1995) Classification	Bujak *et al* (1977) Classification	example plate at < 1.2 %Rr	
Woody tissue	derived from xylem material of macrophytes	terrestrial originsV	composed of up to 50 - 60% Lignin	Resistant to degradation. Option for reworking and survivng distal tranport	*sensu stricto* yes but very, very weak	Amber-brown-dark brown/b;ack.	Usually angular in O/L, blocky - to lath shaped, tubular, pitted, spindle	Common from the Silurian to present	lagoonal facies, delta top, Sst	Phytoclast	Hylogen		Dark brown balck, Tracheid NSD 23
Opaque Organic matter	unknown, various affinities	not always possible to identify	various	Resistant to degradation	no	Opaque, Black	variable	cannot quantify	various	Phytoclast	Melanogen		Angular, lath shaped opaque material NSD 23
Cuticular Tissue	epidermal tissue of higher land plants, usually the cuticle of a leaf	terrestrial	cutin	easily degraded	yes	pale yellow, colourless	thin sheet like bodies, cna have remnant fossil cell structure	common from late Silurian to recent	More common in terrestrial lithologies or sed.s depo.d not far from source	Phytoclast	Phyrogen		Angular, equidimensional, with rectangular cell structure CK 13
Non-woody, non-cuticular Phytoclasts	tissue of vascular land plants	Terrestrial	cellulose	degrades up to 3 times faster than lignified woody tissue	yes	colourless, pale yellow, amber	ref plates Variable	common form Silurian to present assumung terre origins	as for cuticle	phytoclast	Phyrogen		Ribbed Plant tissue NSD 23
Acritarchs	Presumed reproductive cysts of algal bodies	aquatic, marine brackish or fresh water	sporopollenin	resistant to degradation	yes	colourless/pale yellow/green	spherical, smooth, an array of sculptural features and processes	Proterozoic to recent (Traverse 1988)	marine sediments, brackish water sediments.	Group: Palynomorph, subgroup: Phytoplankton	Phyrogen		Acritarch, Tasmanitid NSD 23
Sporomorphs	pollen and spores the seeds of plants	terrestrial	sporopollenin	resistant to degradation	yes	pale yellow/green - orange/amber	variuos, shapes, ornamentation, size and markings	Upr Ordovician to recent (Thomas and Spicer 1987, Clayton)	almost all facies can contain sporomorphs	Group: Palynomorph, subgroup: sporomorph	Phyrogen		Discernisporites sp. NSD 23
Scolecodonts	chitinous mouthpartsof marine annelid worms (polychaetes)	marine	chitin	resistant to degradation	??????	amber/dark brown	similar to the blade of a saw!	Cambrian to recent (Traversr 1988)	where in situ, suboxic environ but can be reworked or transported	Group: Zoomorph, subgroup: scolecodont	not included in Bujak et al Classn. Phyrogen		both from CK 30
AOM	degraded organic matter	and /or	mixed origins	moderate resistance to degradation	yes, stronger in the marine algalily derived AOM	pale yellow - dark brown	Structureless, fluffy or coagulated OM	unknown	common in sand poor clay or limestone rich environments	Group: AOM subgpuoup: AOMM AOMT	AOM	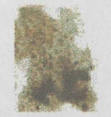	brown AOM with Spore NSD 20
Foraminiferal Test Lining	chitinous tectin linings of foraminifera	marine	chitinous tectin	resistant to degradation	yes	brown	spherical chambers connected by a thin neck	Devonian (?) to recent	most marine lithologies	Group: Palynomorph Subgroup: Zoomorph	not mentioned in the work of Bujak et al, Phyrogen		Uniserial foraminiferal lining CK 22

Table 8.2 Descriptions and classifications of material observed in palynological preparation (images not to scale)

AOM without fluorescence microscopy or SEM work. These techniques may reveal particles such as hidden sporomorphs or fragments of plant material.

8.4 CLASSIFICATION SCHEMES USED IN THIS WORK

The classification categories considered in the palynofacies count are based on size, colour, biological and morphological affinities, preservational state, thermal alteration.

The first scheme used for analysis is that of Bujak *et al.* (1977a & b), who had in turn adapted their scheme after Burgess (1974). Bujak *et al.* found the scheme of Burgess (1974) practical and straightforward. However the botanical connotations of the terms used by Burgess (1974) were dropped and replaced by terms, which are morphologically defined by Bujak *et al.* (1977). This approach is a useful introductory method.

Burgess (1974)	Herbaceous	Woody	Coaly	Amorphous
Bujak, Barss and Williams (1977)	Phyrogen	Hylogen	Melanogen	Amorphogen

Table 8.3 Comparative uses of the four main categories used by Burgess (1974) and Bujak et al. (1977)

Bujak *et al.* (1977) define their categories in the following manner: "Amorphogen comprises unorganised, structureless organic material which may be finely disseminated or coagulated into fluffy masses. Phyrogen comprises all non-opaque, recognizable plant matter that is not of woody origin. Melanogen is all opaque organic material." Some of these same terms are used in the more developed scheme of Davies *et al.* (1991). Bustin (1988) uses the terms 'structured woody organic matter', 'opaque organic matter', 'cuticles, pollen etc.' and 'amorphous organic matter', which represent the divisions of hylogen, melanogen, phyrogen and amorphogen respectively of Bujak *et al.* (1977)(see figure 8.5). The way in which these four types of organic material respond to heating has been graphically illustrated by Bayliss (1975).

The use of the more complicated analysis scheme of Tyson (1995) (see figure 8.6) means that the material can be compared to more recent works. This is also a more detailed work and is more a facies oriented study than a means to assess hydrocarbon generating potential.

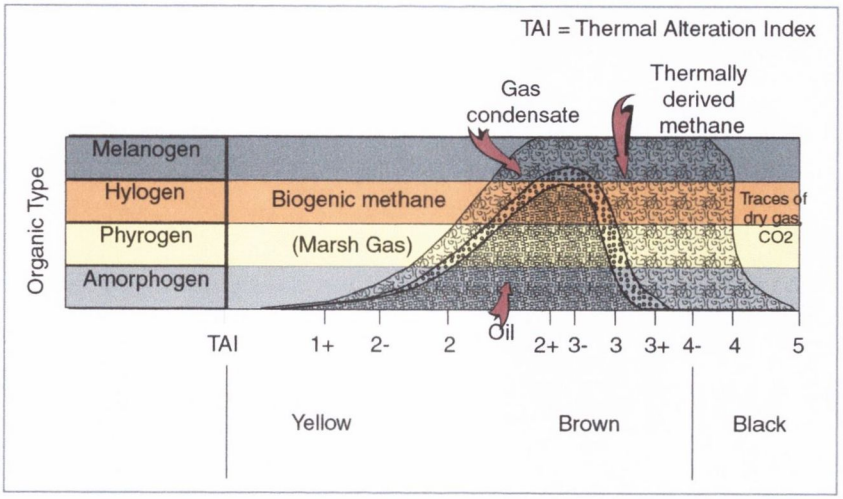

Figure 8.5 The reaction of hylogen, melanogen, phyrogen and amorphogen to heating. Adapted from Bujak et al. *1977 after Bayliss 1974, 1975.*

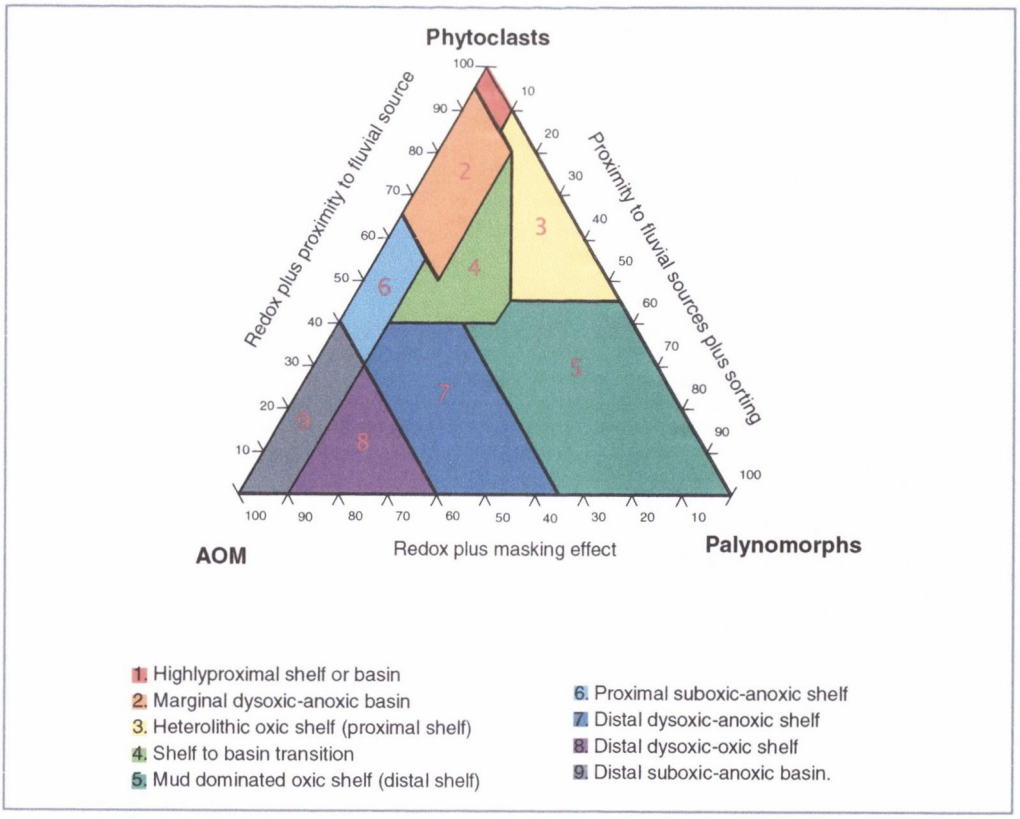

Figure 8.6 Ternary AOM-Phytoclast-palynomorph plot (after Tyson 1993, 1995)

The classification categories considered in the palynofacies count are based on material observed in the preparation, size, colour biological and morphological affinities, and the state of preservation. The categories used can be placed as subdivisions into the schemes of Tyson (1995) and Bujak *et al.* (1977), allowing the data to be presented in a variety of forms.

Bujak et al. 1977	Connolly 2002	Tyson 1995
Hylogen	Translucent Wood	Phytoclasts
Melanogen	Opaque Organic matter	
Phyrogen	Ribbed tissue	
	Membranous tissue	
	Fibrous tissue	
	Plant material of no definitive structure	
	Spores	Palynomorphs
	Other Palynomorphs	
	Scolecodonts	
AOM	AOM	AOM
	CPM	
	Unknown affinities	

Table 8.4 Organised comparison between categories of count scheme in this work and the scheme of Bujak et al. (1977) and Tyson (1995)

8.5 PARTICLE COUNT

A count of 350 particles was undertaken for each sample, this number was assigned based on a number of cumulative counts undertaken on some of the aureole samples. The classification schemes of Bujak *et al.* (1977a & b)and Tyson (1995) were used.

8.6 PALYNOFACIES RESULTS

8.6.1 CARRICKLECK BACKGROUND

CK Observations: the CK traverse shows a high percentage of non-woody plant material and wood. In the un-sieved fraction there is an abundance of very fine 'fluffy' material, which cloaks much of the rest of the sample. The sieved fraction has an abundance of plant tissue and woody debris as well as much framboidal pyrite. The percentages of spores in the 'background samples' vary between 2-15%. They are mainly trilete, with some monolete spores. The spores tend to be poorly preserved making identification difficult. Tasmanitids and Leiosphaerids have been identified although they are rare. Scolecodonts have also been seen but again they are scarce. Although both acritarchs and scolecodonts were observed in the material neither appeared in the count. There is a reasonably high proportion of wood in the samples most of which is dark brown. Unlike the palynomorphs much of the woody material is reasonably well preserved. Variations in the colour were observed, although this could be due to variable thickness, or to the inclusion of reworked material. Non-woody material such as cuticle and other epidermal tissues are abundant but, as for the palynomorphs, they are quite poorly preserved, with most of the material looking quite 'ragged'. There is an average of 10% opaque organic matter in the background samples. This material is usually lath shaped, exhibiting little or no obvious structure. There are some examples of black wood. The degraded state of the material means that there were always a number of particles that could not be easily consigned to any one category. These particles were described and categorised as 'indeterminate'.

CK interpretation: Applying the scheme of Bujak *et al.* (1977a & b) the percentages of hylogen, melanogen, phyrogen and AOM vary even within the background samples (see figure 8.7 (a)). This is due to the AOM content variation. The AOM content is very high in the unsieved fraction. Depending on whether the sieving was lengthy (more than 3minutes) and or vigorous enough to completely remove all AOM the proportion of AOM in the sample residue can vary. However, the average hylogen content is 26%, the average melanogen content is 8%, the average AOM content is 28% and the average phyrogen content is 36%.

Adapting the data to Tyson's ternary plot (1995) the background data of CK is seen to cluster in the marginal dysoxic-anoxic basin facies (see figure 8.8(a)). The state of preservation of much of the plant debris suggests either long distance transport, or, that it has spent some time in an oxygenated environment where it possibly suffered biodegradation. The varying states of preservation of the more susceptible plant material (cutin and cellulose based material), the angularity of the brown wood fragments and the large amounts of the finer AOM lost after sieving, may indicate that the latter explanation of bacterial activity was responsible for the degraded state of the material.

CQ Observations: in marked contrast with the CK line of the quarry face CQ has a very high yellow/brown AOM content even after sieving. Again, there is a fine amorphous fraction lost during sieving. Although phytoclasts and palynomorphs are represented, they are always rare and as before, the relative content apparently decreases towards the dyke. At no time is there a high woody content nor is there a high content of opaque organic matter. There is also quite a lot of framboidal pyrite in the prepared residue. Figures 8.7(b) shows AOM as the major component. There is very little hylogen, phyrogen or melanogen.

CQ Interpretation: Plotting the background data on the ternary diagram of Tyson (1995) places the material in the distal suboxic-anoxic basin (8.8(b)). The high percentages of AOM are associated with bacterial degradation and a quiet, low energy environment permitting preservation of the material. The material is not very strongly fluorescent and is generally brown-yellow in colour although there is also some dark brown-black material. The AOM can also contain small grains of pyrite within the main body of the material. The colour of the amorphous material is in keeping with the observations of Masran and Pocock (1981) for the experimental biodegradation of terrestrial plant material under aerobic conditions.

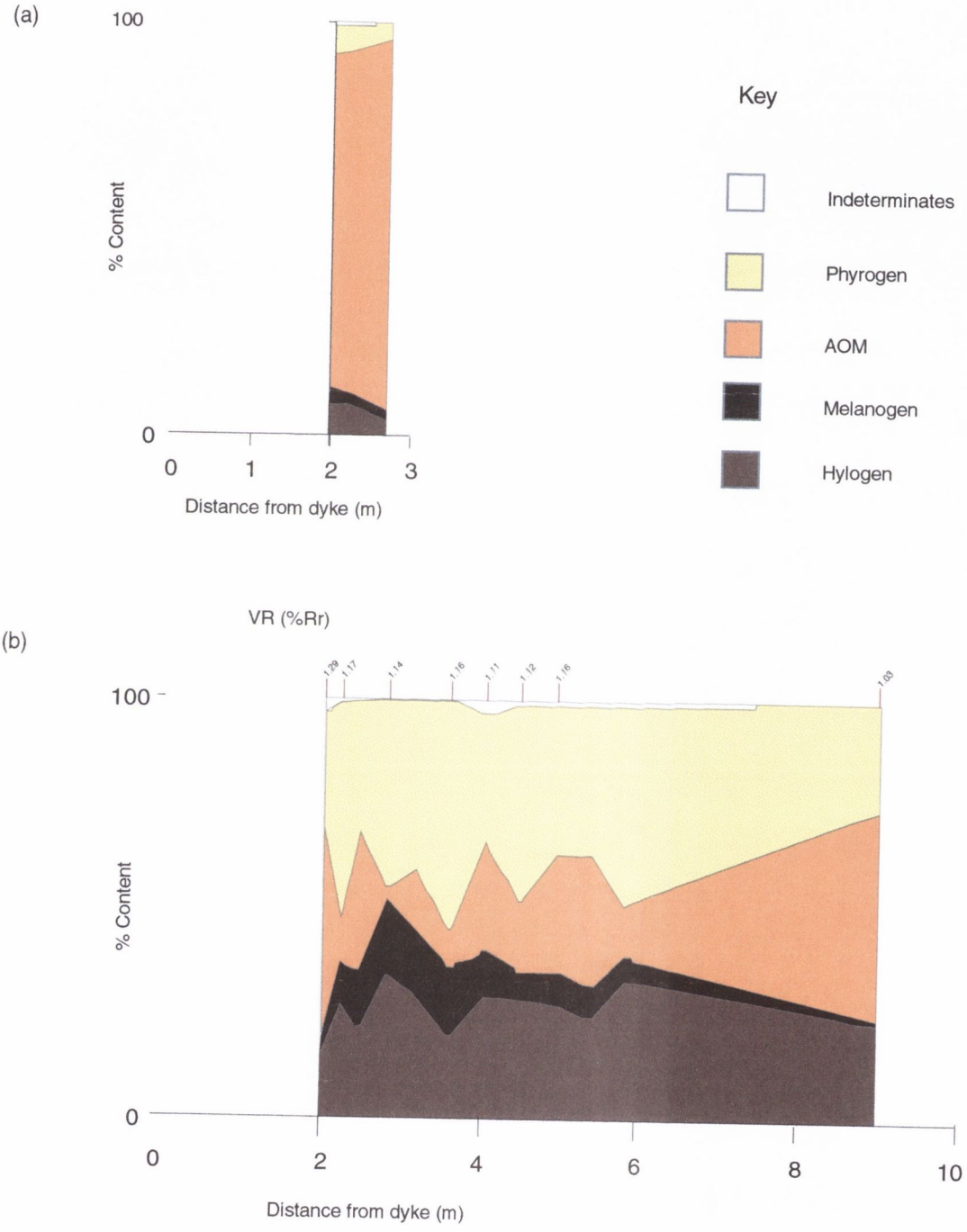

Figure 8.7 Background palynofacies in the (a) CQ and (b) CK horizons in the Carrickleck quarry

(a) CK

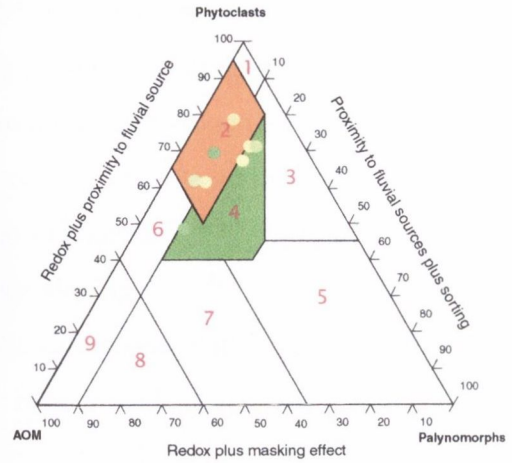

Sample	Perp Dist. from dyke (cm)	Palyn-omorphs	Phyto-clasts	AOM	VR (%Rr)
	359.52	15.83113	71.50396	12.66491	1.11
	404.46	7.94702	64.56954	27.48344	1.12
	449.4	13.89646	68.11989	17.98365	1.14
	494.34	9.657321	62.3053	28.03738	1.03
	539.28	6.695464	62.41901	30.88553	1.1
	584.22	16.15599	72.14485	11.69916	1.07
	898.79	1.944444	50.83333	47.22222	1.07
	1617.83	5.18732	33.42939	61.38329	1.07
	6291.56	8.908046	50	41.09195	1.1
	7190.35	7.650273	69.67213	22.6776	1.08

(c) NSD

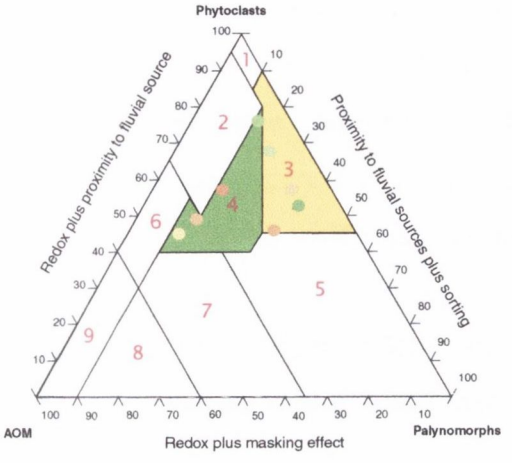

Sample	Perp Dist. from dyke (cm)	Palyn-omorphs	Phyto-clasts	AOM	VR (%Rr)
	2.2	16.42157	56.86275	26.71569	1.05
	2.22	34.48276	46.15385	19.3634	1.03
	2.89	14.75728	48.54369	36.69903	1.06
	2.79	33.66093	56.75676	9.58231	1.03
	3.95	11.11111	45.27778	43.61111	1.06
	4.05	12.36264	61.26374	26.37363	1.19
	5.4	10.16166	68.82217	21.01617	1.13
	5.66	22.86501	66.94215	10.19284	1.11
	6.27	14.4357	74.54068	11.02362	1.04
	10.11	37.67313	51.80055	10.52632	1.25

(b) CQ

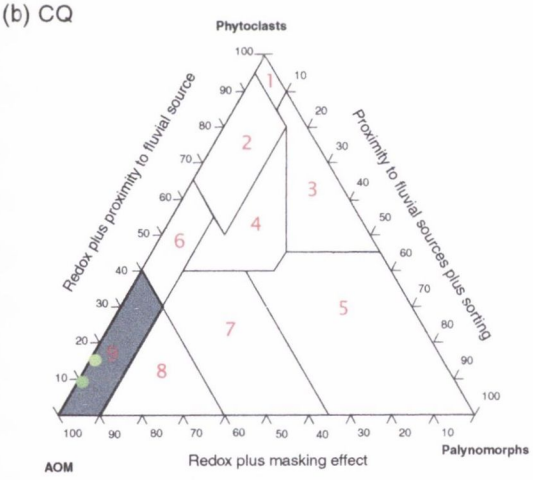

Sample	Perp Dist. from dyke (cm)	Palyn-omorphs	Phyto-clasts	AOM
	80.89	0.57971	15.65217	83.76812
	89.88	0	9.537572	90.46243

(d) cMd

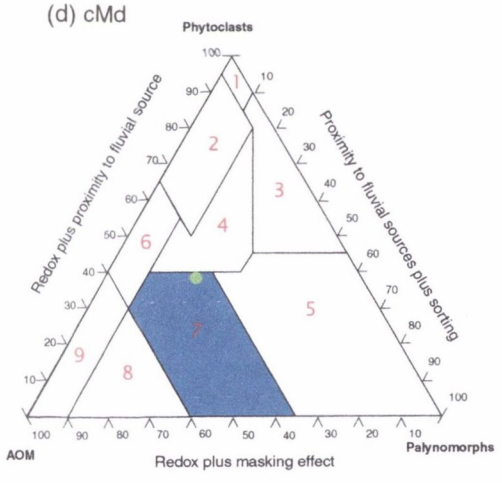

Sample	Perp Dist. from dyke (cm)	Palyn-omorphs	Phyto-clasts	AOM	VR (%Rr)
	60.22	21.53392	38.93805	39.52802	0.55

(e) 2. Marginal dysoxic-anoxic basin
3. Heterolithic oxic shelf (proximal shelf)
4. Shelf to basin transition
7. Distal dysoxic-anoxic shelf
9. Distal suboxic-anoxic basin.

Figure 8.8 Background palynofacies characterisation (Tyson 1995) for the (a) CK and (b) CQ horizons from the Carrickleck Quarry, and the (c) NSD and (d) cMd horizons from Ballycastle

8.6.2 BALLYCASTLE

cMd observations: samples beyond the aureole of the North Star Dyke, contain a large proportion of palynomorphs and plant debris, including woody material. There is a dominance of hylogen and phyrogen in the background samples (see figure 8.9(a)). AOM content is variable and in high proportions (see figure 8.9(a) and figure 8.13g & h). As is seen in Carrickleck there is also a fine amorphous fraction (<20μm), which was discarded when sieving.

cMd interpretation: Using the ternary diagram of Tyson (1995) (figure 8.8(d)) data for the background samples of the cMd line plots in the shelf to basin transition and marginal dysoxic-anoxic basin. The material from this horizon is relatively well preserved. Although there was a fraction of fine amorphous material, it was removed by sieving. The high palynomorph content (maximum of 20%) and a reasonable diversity of spores might imply a shelf depositional environment. Again, the colour of the AOM would indicate aerobic conditions with biological degradation (Masran and Pocock 1981). The background material of the cMd line plots in a shelf to basin transition or marginal dysoxic-anoxic basin on the ternary diagram of Tyson (1995). The former interpretation is preferred. The presence of the fine fraction of amorphous material may imply a significant biodegradational activity, which has not gone to completion, and that has not affected all of the material as much of the organic matter observed under the microscope appears to be in a relatively good state of preservation.

NSD observations: background samples from the NSD horizon have a high phytoclast and palynomorph (37% NSD24 VR=1.07% R_r) content. The palynomorphs tend to be well preserved allowing for identification at least to genus level of a reasonable number at all stages through the aureole. There is a greater miospore range in the Ballycastle group of samples compared to the Carrickleck suites, and all of the material appears to be in a better state of preservation. As with all of the other samples in the unsieved state, there is a high proportion of fine amorphous material 'cloaking' the rest of the organic material. The woody material from this horizon does show some variety in shape, structure and colour. Mostly tracheidal fragments are observed. These are usually angular in outline and blocky to lath shaped. There are some darker fragments that might be more rounded but only slightly. The opaque organic matter is a small constituent in this facies ranging between 0.6% and 8% in the background samples (see

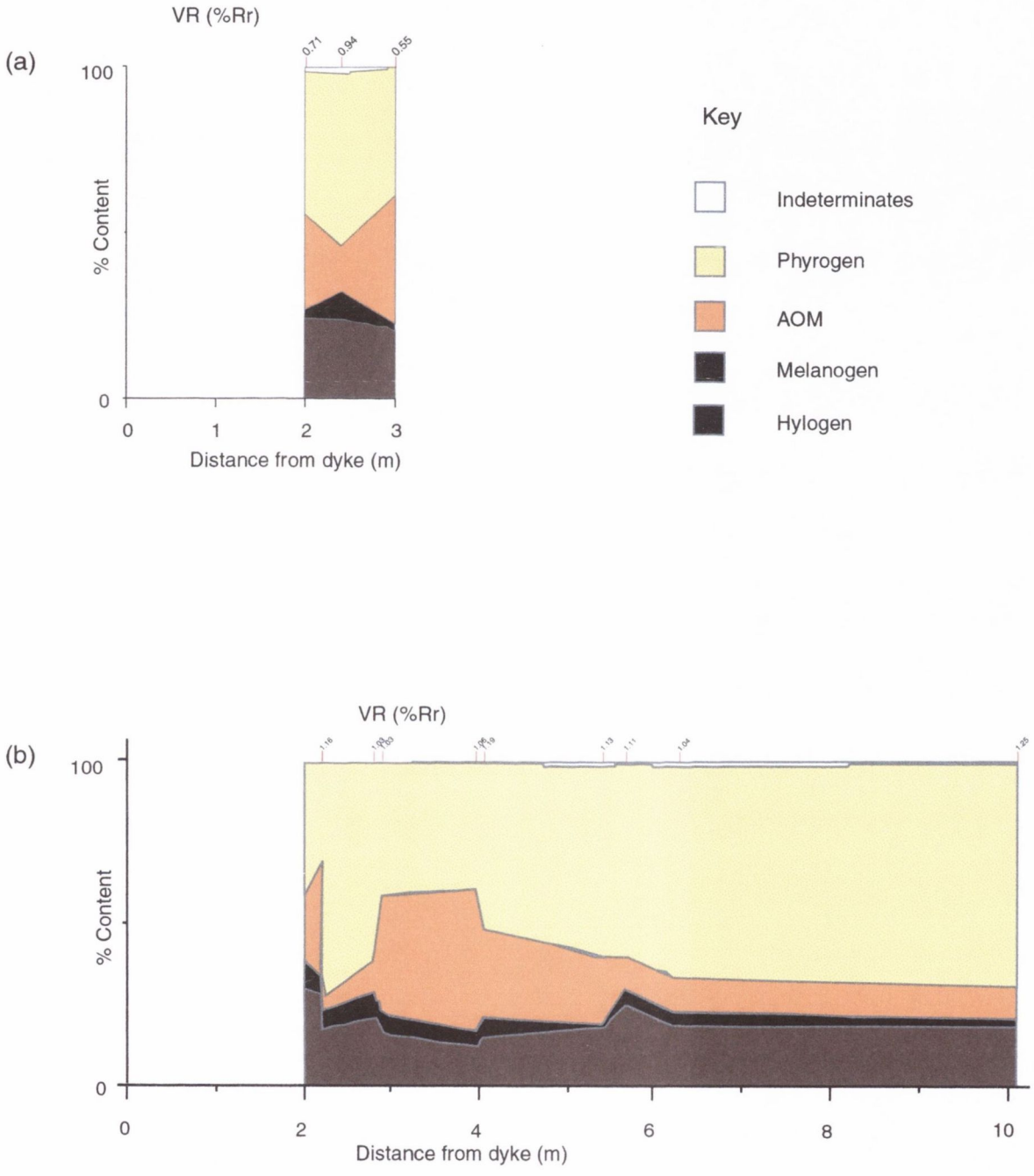

Figure 8.9 Background palynofacies at Ballycastle (a) cMd horizon and (b) the NSD horizon

figures 8.9(b) and 8.14(ii)c & e). The OOM in this horizon does not tend to show structure but does have a solid outline. The fragments are usually lath shaped but can be either angular or rounded. Whether this is related to reworked and autochthonous material or to a varying composition of the opaque material cannot be answered in this study. There is quite alot of framboidal pyrite, some of which is associated with the AOM, however some is also associated with spores and plant material.

NSD interpretations: The range of miospores found in this horizon and their preservational state suggests that the NSD horizon was deposited closer to shore than any of the others described here. The state of preservation and variety of the plant material in this horizon also supports this assertion. However, it could also be argued that there was less microbial activity or that the environment was less oxygenated. The presence of AOM in both the very fine fraction (<20μm) and the >20μm fraction could suggest microbial degradation. The colour of the AOM is the same as that of the other horizons described here; amber-brown with some black amorphous bodies. The amorphous material does not have a strong fluorescence. A strong fluorescence is expected from marine algal material at this VR (1.07%R_r) (Masran and Pocock 1981). It is therefore possible that the AOM is biodegraded terrestrial material.

Tysons classification shows the NSD background material clustering in the heterolithic oxic shelf and shelf to basin transition, which might be read as a distal oxic shelf (see figure 8.8(c)).

8.7 THERMAL ALTERATION AND PALYNOFACIES

8.7.1 PARTICLE SIZE VARIATION

Particle size variation was recorded through both the Carrickleck Dyke aureole and the North Star Dyke aureole (see figures 8.10). Both the CK and the CQ lines show a marked dominance of organic material < 1250μm^2 at distances of greater than and up to *c.*150cm from the dyke margin (VR of 1.29% R_r; *c.* 192°C). Nearer to the dyke margin the material becomes dominated by particles smaller than 1250μm^2.

The North Star Dyke aureole material appears to be quite random in the size distribution although contrary to the findings from the Carrickleck aureole both samples show a dominance of the larger size fraction material in the area adjacent to the dyke. This is attributed to the larger size fraction of AOM that develops in this region. Some of this larger fraction AOM is coagulated particulate material. This dominance of the larger

fraction AOM in the area adjacent to the dyke might also be due to preferential destruction of other particles and these being the particles that are more robust in the aureole environment.

8.7.2 TRANSLUCENT WOODY MATERIAL

Woody material accounts for up to 26% of the contained organic matter in some of the sediments being examined (see figures 8.11). All samples processed for palynofacies show a range in proportions of translucent wood. Equally, all samples show a very general decreasing trend in proportion (to < 1% in some cases), which appears to be accelerated in the region directly adjacent to the dyke margin. The colour of the translucent woody material is variable. For all traverses there is a general darkening of the woody fragments, towards the dyke, until they are almost all so dark that the main determination is a combination of structural recognition in conjunction with examination at high magnification to see any colour or translucence around the edges. Although wood can fluoresce weakly at very low rank (<VR=0.5% R_r (Tyson 1995)), the lowest VR observed is in the cMd line at 0.55% R_r and there is no observed fluorescing wood.

8.7.3 NON-WOODY PLANT DEBRIS

Non-woody plant tissue is present in the NSD line in quantities of up to 50%, in the cMd line up to 33%, the CK line contains up to 43% and the AOM dominated CQ line has a maximum of 11%. For each of the traverses (see figures 8.12) this percentage drops below 10% within 1m from the dyke. There is an interesting phenomenon in the NSD and CK traverses. The samples closest to the dyke tend to have an increased percentage of woody plant material within this 1m zone. The NSD traverse increases up to >10% but the CK line exhibits a leap from <5% to >30% at 7cm from the dyke (VR=3.09, 296°C (Barker and Goldstein 1990)). This may be due to either, loss of the AOM fraction during sieving thus enhancing the apparent dominance of non-woody fraction in the sample, or for some reason there are preferable preservation factors at work in the area directly adjacent to the dyke.

The non-woody plant tissue tends to be yellow-yellow/orange in the background samples. This colour darkens as the dyke is approached, the material becomes brown and eventually black at 0.6m from the dyke in the CK traverse, 0.3m in the CQ traverse, 1.21m in the NSD traverse and 0.96m in the cMd traverse.

Undifferentiated all of non-woody plant tissue fluoresces but this fluorescence is entirely extinguished by a VR = *c.*1.0-1.2%R_r, regardless of the form or the line in which it is seen.

8.7.4 OPAQUE ORGANIC MATTER

Opaque organic matter content remains approximately the same throughout all of the lines. CK does show a decreased % within 10cm of the dyke margin but again the sample closest to the dyke has an anomalously high content <25% at 7cm. This is not seen in any of the other lines. One point maybe worth noting is that the opaque organic matter is the only fraction that tends to be preserved in the >50 size fraction and this is true for all of the lines and this size dominance generally remains unchanged (see figures 8.13).

8.7.5 PALYNOMORPHS

(see figures 8.14) For CK there is a maximum content of 17% at > 3m from the dyke. <3m (VR=1.12% R_r, T=176°C) from the dyke there is >11% content in any of the samples. By 1m (VR- 1.46% R_r, T= 207°C) there is <4% in any of the samples, <0.5m (VR= 3.3% R_r, T=307°C) there is <2% palynomorph content in any of the samples.

CQ contains <1.5% palynomorphs at any time.

The NSD line has the greatest percentage of contained palynomorphs at 37% maximum. This proportion is not constant. The abundance and range of spores decreases with proximity to the dyke. At distances >2.2m (VR=1.2% R_r, 189°C (Barker and Goldstein 1990)) from the dyke the abundance range can vary from 8% (at 5.4m from the dyke) to 37% (at 10.1m from the dyke). At <2.2m all samples contain < 20%, and at distances of <1m (NSD10, 0.97m from dyke, VR=2.5% R_r, 262°C) from the dyke no sample contains more than 5% palynomorphs.

cMd contains a maximum of *c.* 20% palynomorphs. This is seen to decrease with proximity to the dyke. The most rapid decrease in values is seen between *c.* 2.0 and 1.5 m where there is a reduction from *c.* 18% - 4% respectively. In the area of 1m - 0.5 m from the dyke there is a drop from 2.5% - >1% and in the last sample at a distance of <0.5m from the dyke there is only *c.* 2% content.

For colour and fluorescence descriptions please see chapter 6.2, and figures 7.17 – 7.20.

For palynomorph quantity study please see chapter 6.1

8.7.6 AOM

AOM in the CK line is less than 40 % at >3m from the dyke. At <3m, from the dyke the range broadens from 4% to 50% content. <0.6m from the dyke the AOM content increases to 80% - 96% content. The sample directly adjacent to the dyke (7cm) has a much lower value of 33%.

The <1250μm^2 AOM size fraction is dominant throughout the CK line. There is a change in content in the >1250μm^2 fraction however. The larger fraction is constantly <10% up to 1m from the dyke. At *c.*1m from the dyke however the >1250μm^2 fraction increases from 5% to 36% at 0.2m and then decreases to 14% at 0.07m from the dyke. All AOM material is black by 0.6m(VR 1.89 %R_r)(see Appendix III, plates 20-22).

The CQ palynofacies is AOM dominated. Through the aureole the proportion is seen to dip from 90% - 67% between 2.7m and 0.7m respectively, and then increase again to a maximum of 90% (range of 90% - 86%) between 0.4m and the dyke margin. There is a size variation in the AOM particle size in the CQ line where the material is dominantly >1250μm^2, at 1m-3m from the dyke. However, at >1m from the dyke the material is dominantly <1250μm^2. All AOM material is black by 0.3m, (see Appendix III, plate 23).

AOM in the NSD traverse shows an increase in proportion towards the dyke. Between 10m and 5.6m (1.1 -1.2 % R_r) from the dyke the AOM content is well below 20%. Between 5.66m and 2m (VR=1.11 and 1.2% R_r respectively) from the dyke margin the content shows a relatively wide range from 10% - 42%. At 0.8m the content drops to 13% followed by an immediate increase up to a maximum of 88% content at 0.6/0.5 m (*c.* 4% R_r, VR maximum) from the dyke. From this point the trend shows a down turn and drops to 76% at 0.04m (3.78% R_r, 320°C).

AOM particle size does not appear show any major trends in the NSD line, there being an irregular mix in dominating fractions through the aureole. However it is interesting to note that the >1250μm^2 size fraction dominates in the area less than or equal to 0.5m from the dyke margin. All AOM material is black by 0.97m(VR 1.62% R_r) (see Appendix III, plate 25 & 26), and figure 8.13 AOM variation in the NSD traverse in the North Star Dyke aureole).

cMd AOM content drops from 40% at 2.4 m from the dyke to 14% at just less than 2m. Between 2m and *c.* 1m there is an increase to 83% content and a levelling of at 89-91%

content between 0.8m and 0.45m from the dyke margin. All AOM material is black by 1.36m from the dyke margin (VR 1.57%R_r) (see Appendix III, plate 24, and figure 8.13 AOM variation in the cMd traverse in the North Star Dyke aureole).

8.7.7 THE TERNARY PLOT OF TYSON (1995) AND PALYNOFACIES CHARACTERISATION

On Tyson's ternary plot CK material plots in 6 different facies. Background samples plot in either the 'shelf to basin transition', the 'highly proximal shelf or basin'; 'marginal dysoxic-anoxic basin' or 'proximal suboxic-anoxic shelf' one stray sample plots in a 'distal dysoxic-anoxic shelf' area. Samples CK11, 8 -2 all plotted in an area representative of a distal suboxic-anoxic basin, and the anomalous CK 1 plots on the edge of the area representing a proximal suboxic-anoxic shelf. The sample with the highest %AOM is also the sample in this line to have experienced the maximum VR i.e. CK2, 0.20m from the dyke, 3.65% R_r, 316°C.

CQ samples all plot in the area 9, representing a distal suboxic-anoxic basin (see figure 8.16 (i)b).

10 NSD traverse samples closest to the dyke, 0.04m - 0.97m, max VR= 4.69% R_r (at NSD 4, 0.37m), min=2.51% R_r (NSD 10, 0.04m), plot in area 9, a 'distal suboxic-anoxic basin' without exception. Samples NSD - 6, 7, 8 and 9 cluster together, furthest down the area, i.e. with the highest relative AOM quantities, these are also the samples with the highest recorded VR. NSD11 falls into area 6, which represents a proximal suboxic-anoxic shelf. The rest of the samples fall into the following categories, (4) shelf to basin transition, (3) heterolithic oxic shelf (proximal shelf).

cMd samples plot from (7) distal dysoxic-anoxic shelf (cMd 8), to (4) a shelf to basin transition (cMd 7), to (2) marginal dysoxic-anoxic basin (cMd 6) and finally to (9) a distal suboxic-anoxic basin. Again the samples that have recorded the highest VR are clustered at the bottom left of the diagram (cMd 1,2,3 have VR of 5.2% R_r, 358°C, 5.45% R_r, 364°C and 3.55% R_r, 316°C respectively).

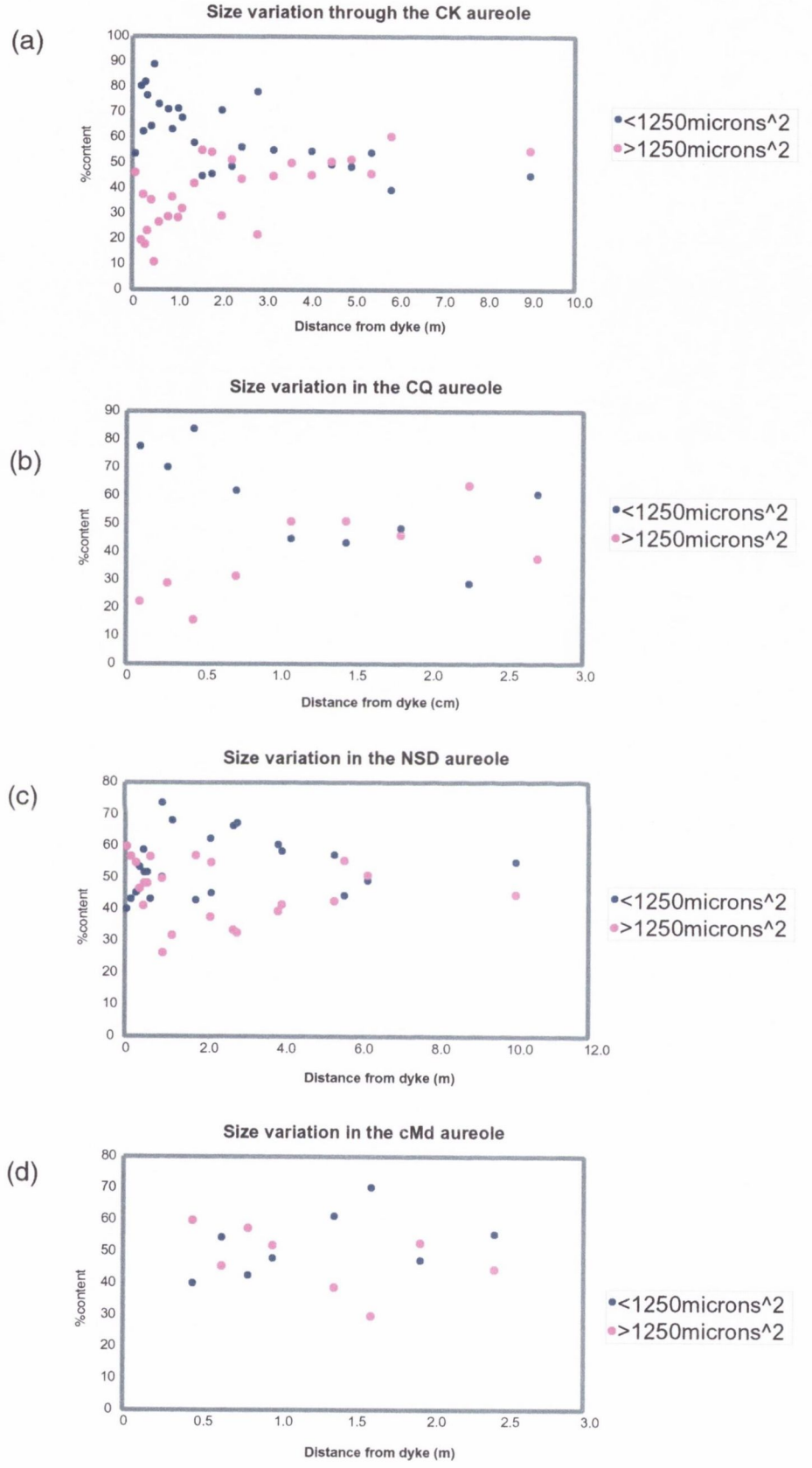

Figure 8.10 Organic matter particle size variation in the Carrickleck Dyke and North Star Dyke aureoles

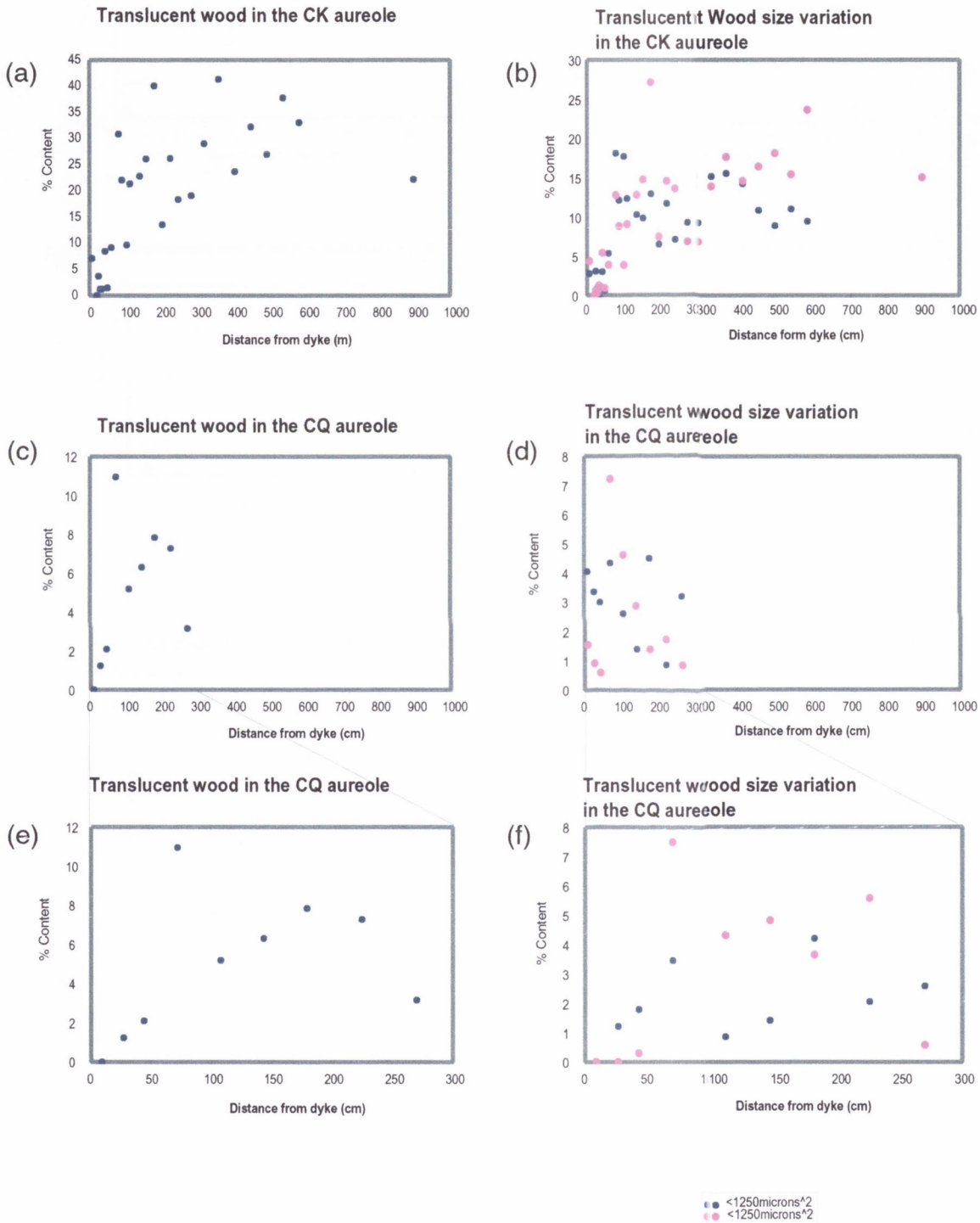

Figure 8.11(i) Translucent woody material content and size variation in the Carrrickleck Dyke aureole

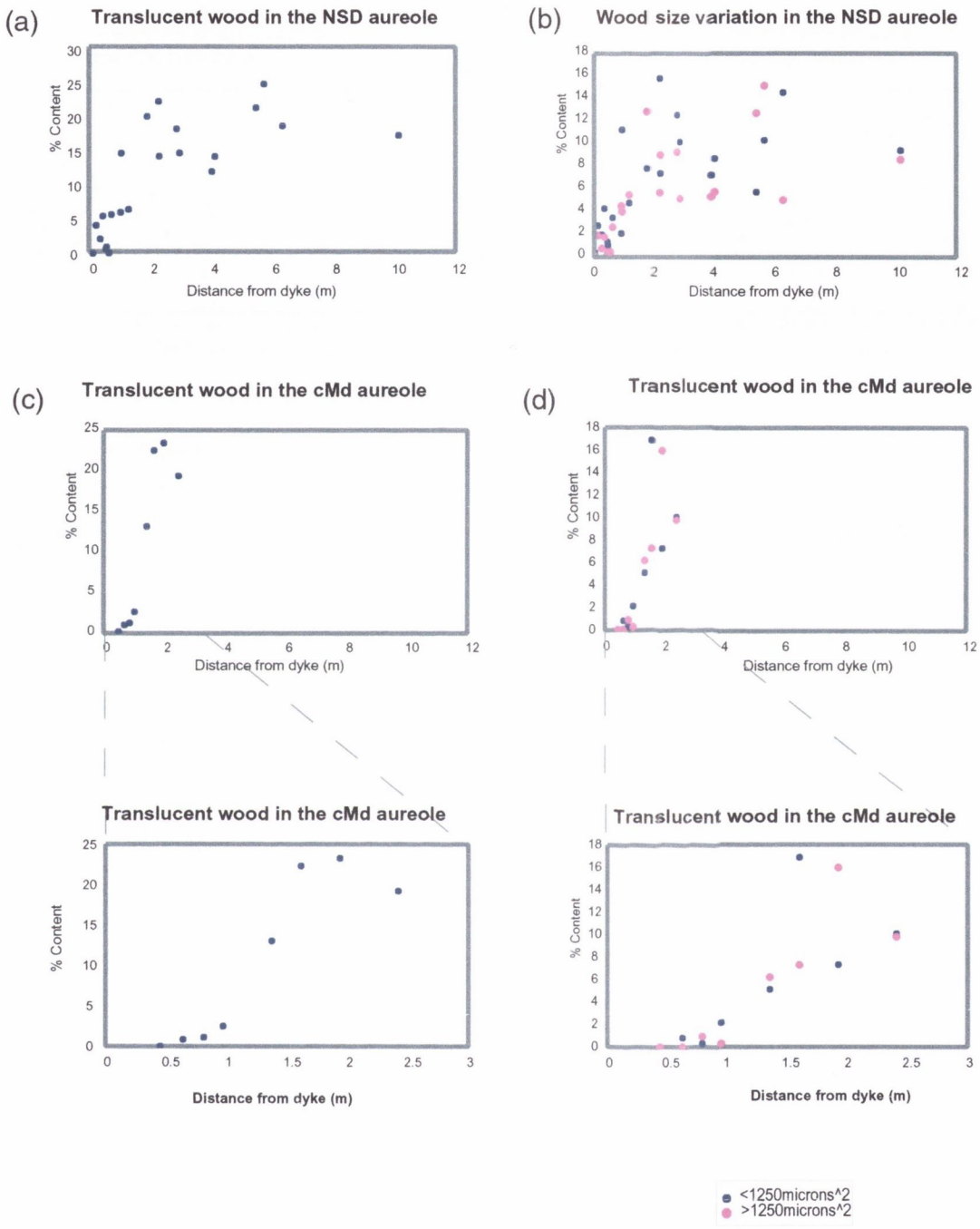

Figure 8.11(ii) Translucent woody material content and size variation in the North Star Dyke aureole

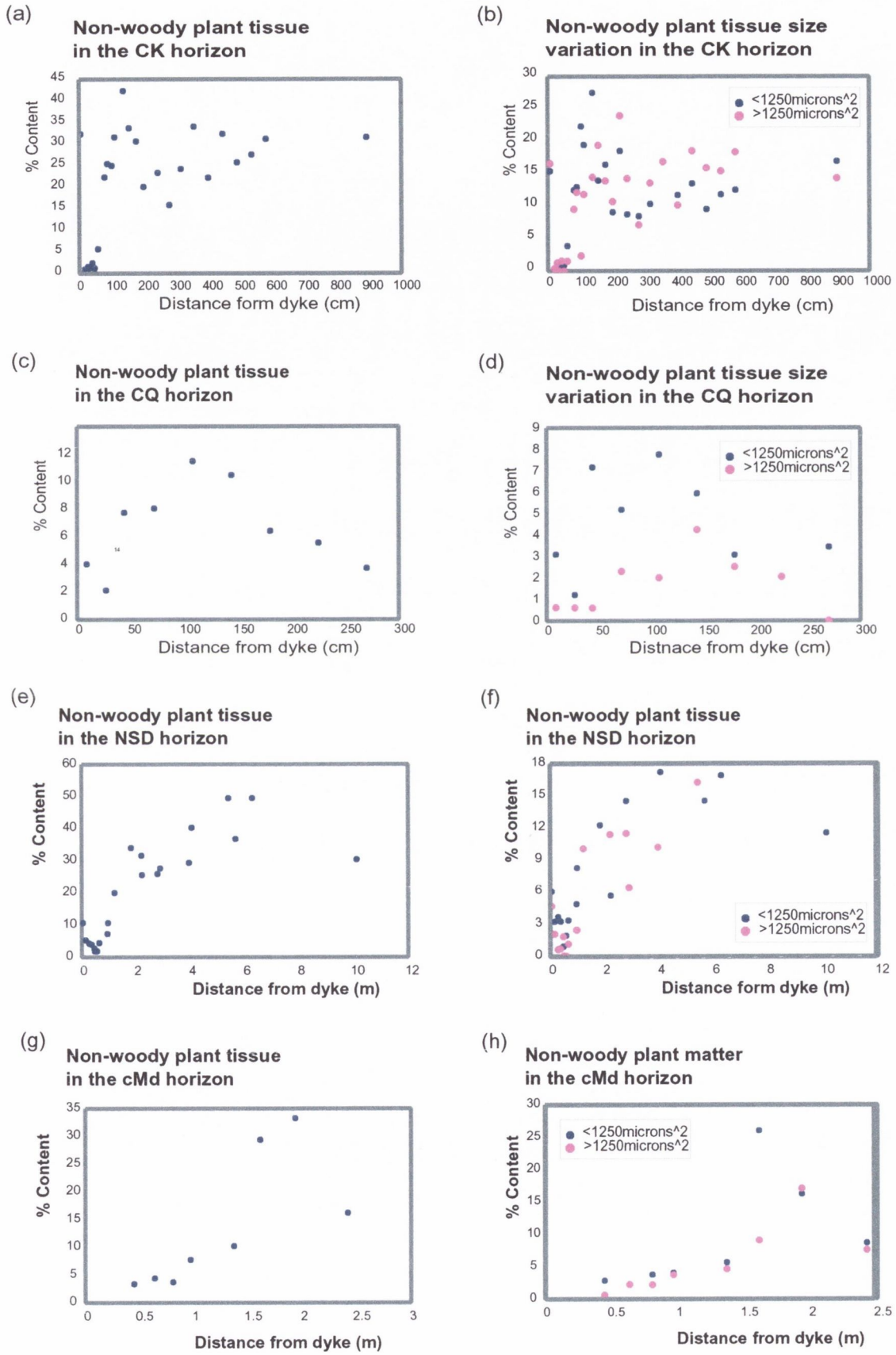

Figure 8.12 Non-woody plant content and size variation in the Carrickleck and North Star Dyke aureoles

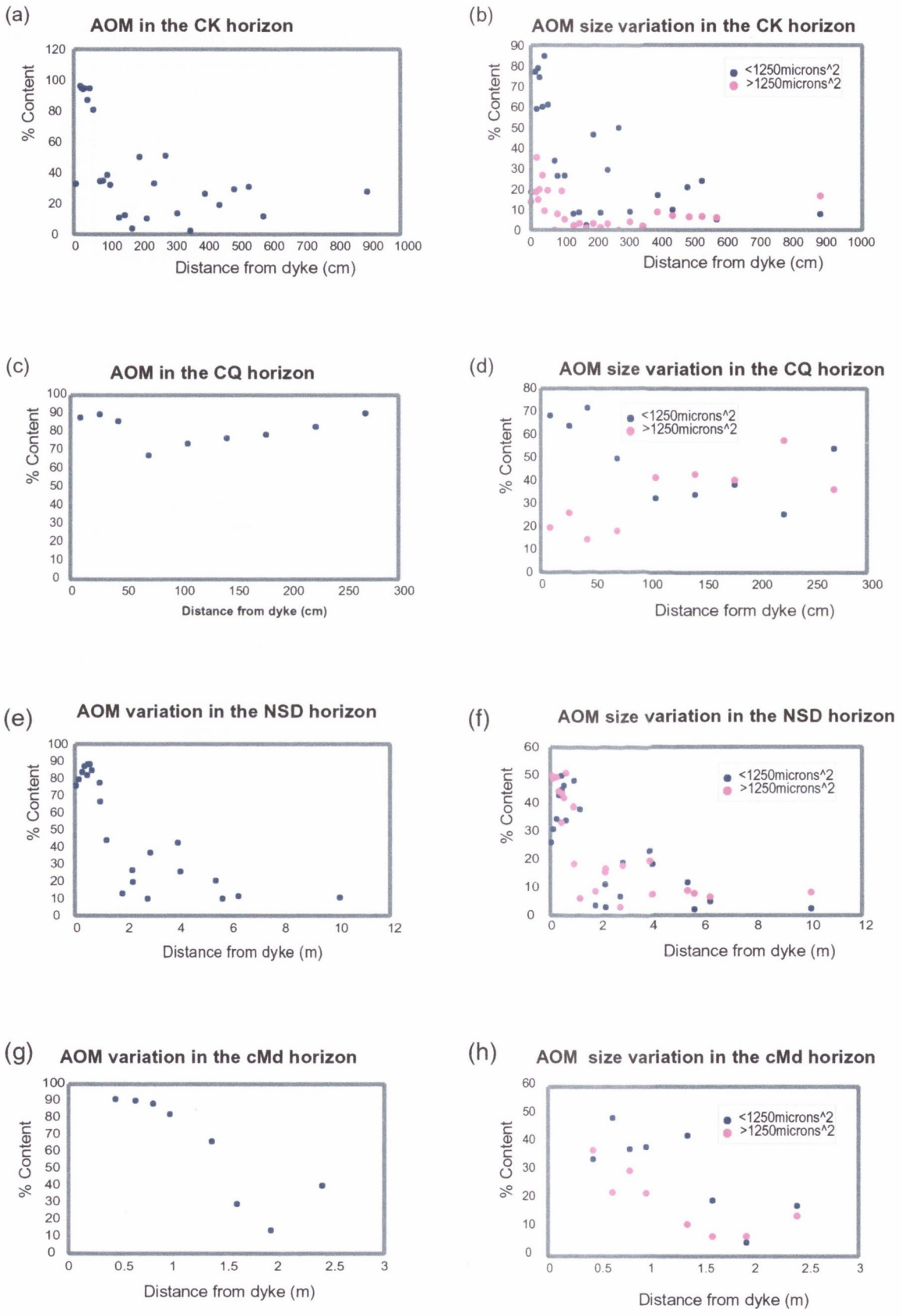

Figure 8.13 AOM content and size variation in the Carrickleck Dyke and North Star Dyke aureoles

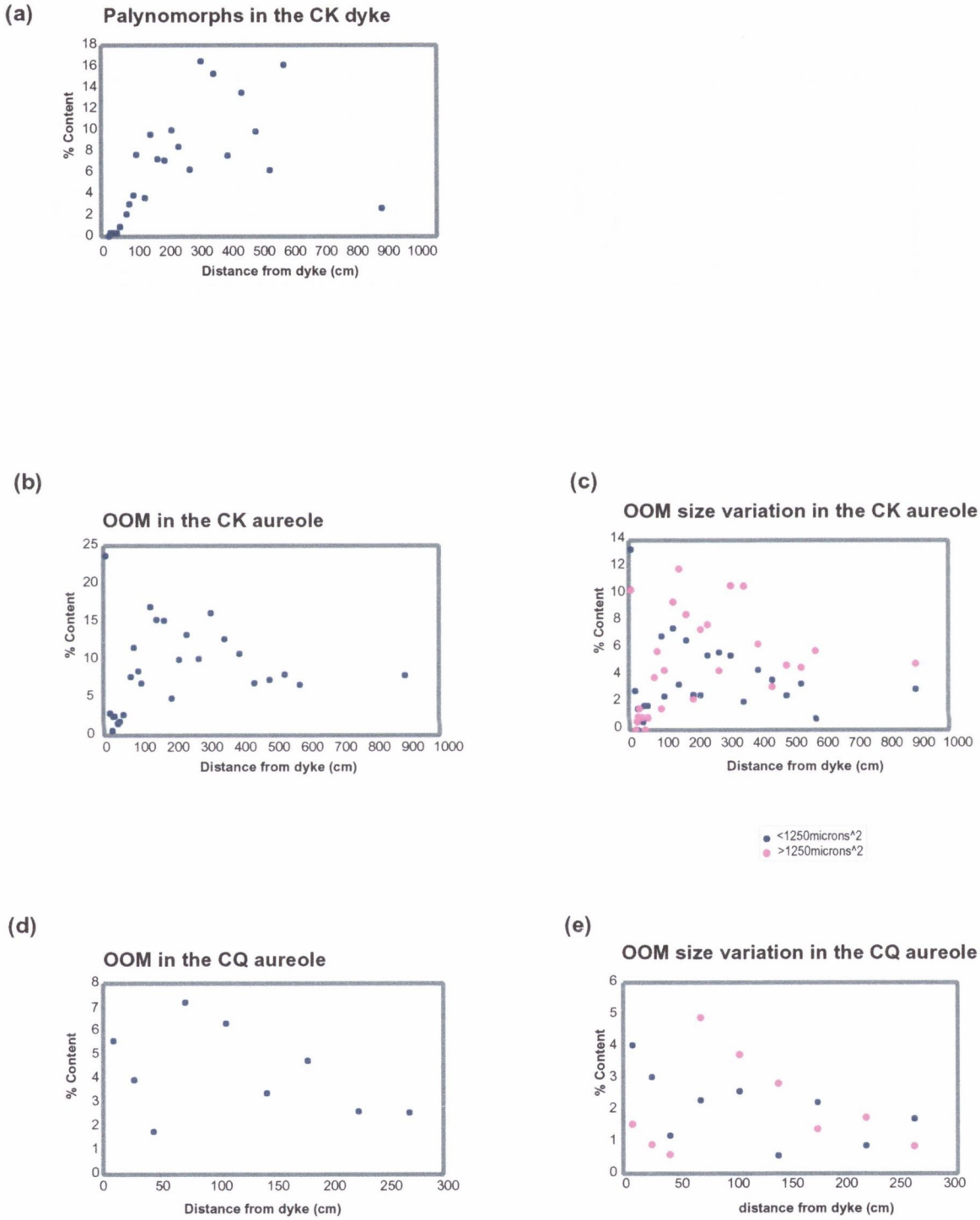

Figure 8.14(i) Palynomorph and OOM content and size variation in the Carrickleck Dyke aureole

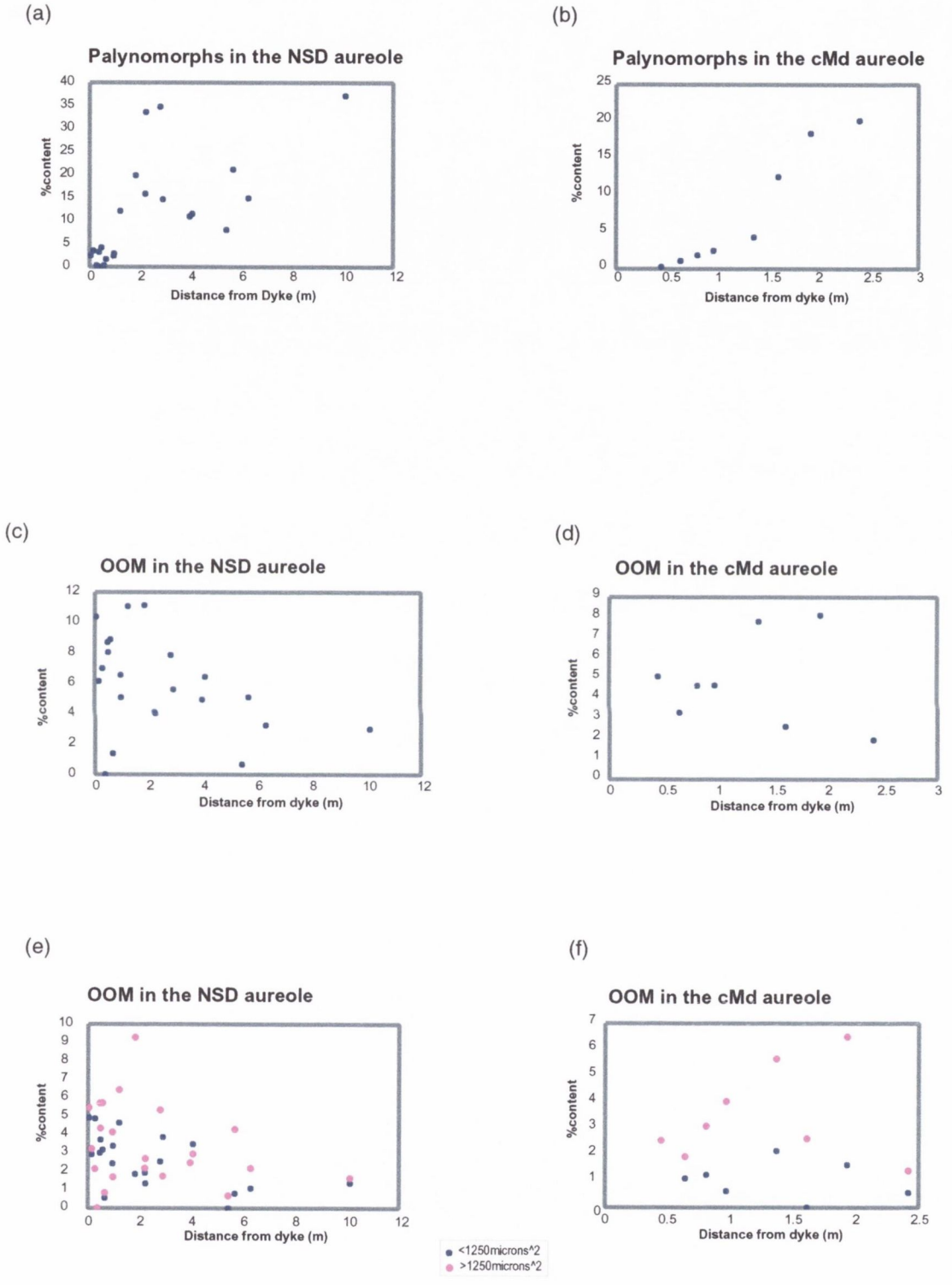

Figure 8.14(ii) palynomorph and OOM content and size variation in the North Star Dyke aureole

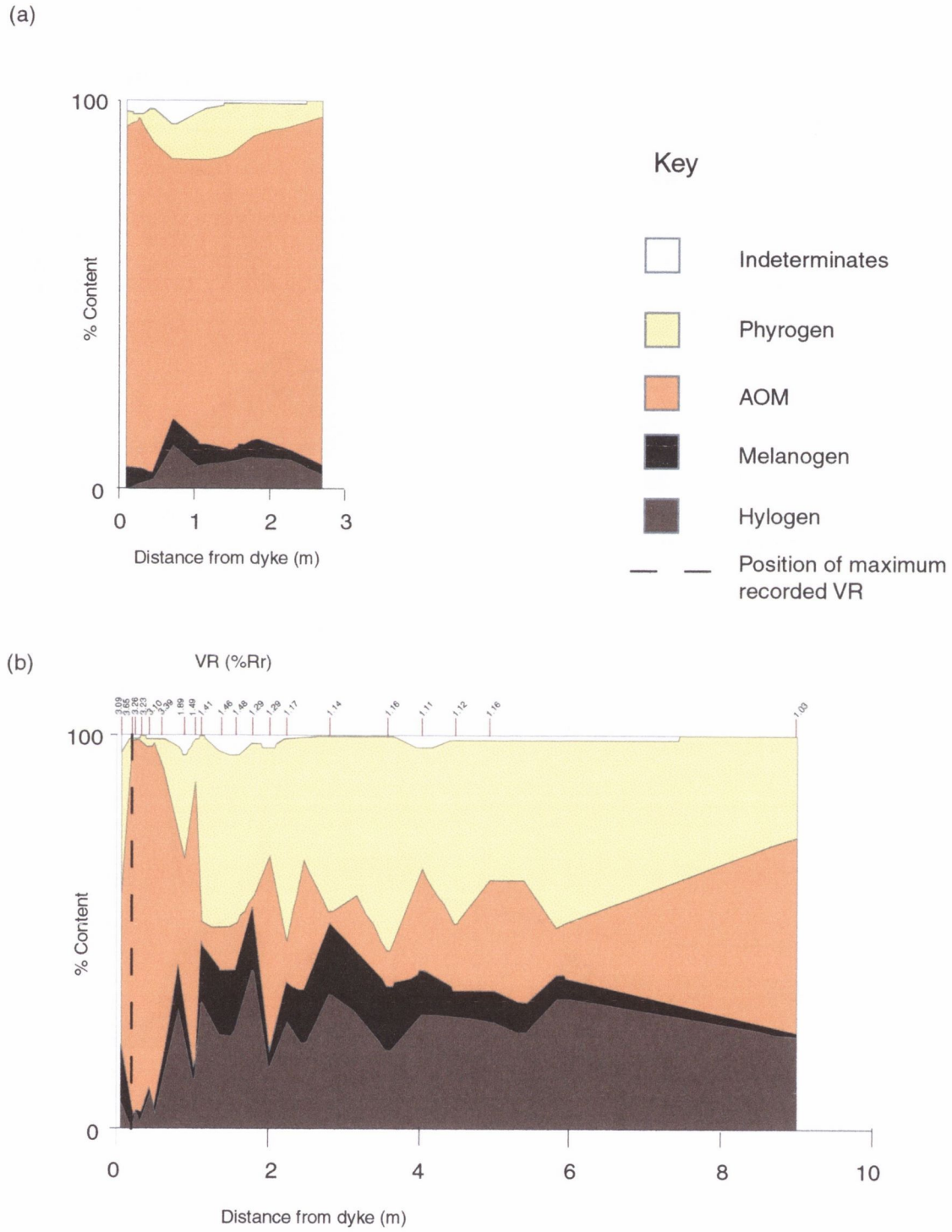

Figure 8.15 (i) Palynofacies variation in the Carrickleck Dyke aureole (a) CQ horizon (b) the CK horizon

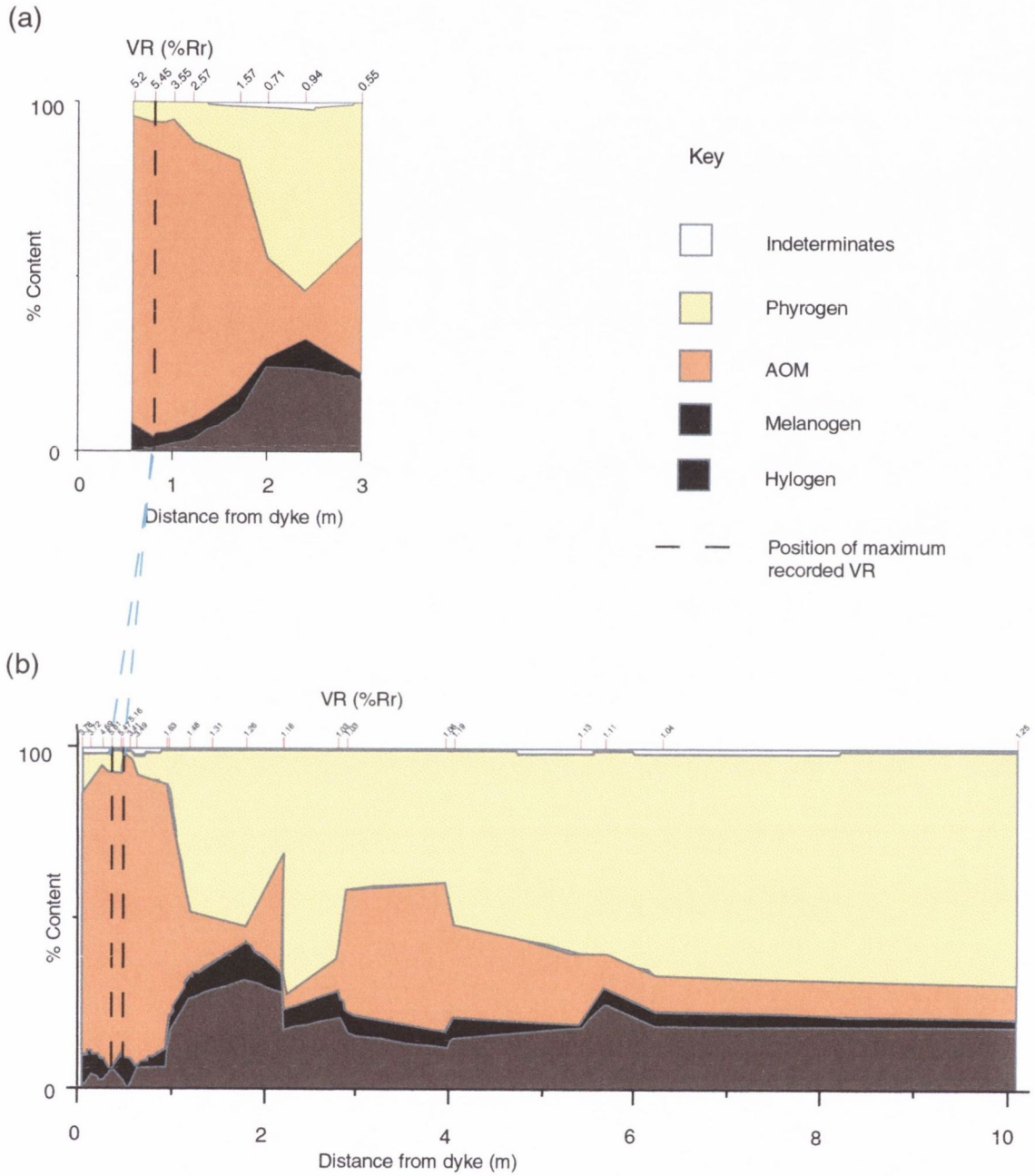

Figure 8.15 (ii) Palynofacies variation in the North Star Dyke aureole (a) cMd horizon (b) NSD horizon

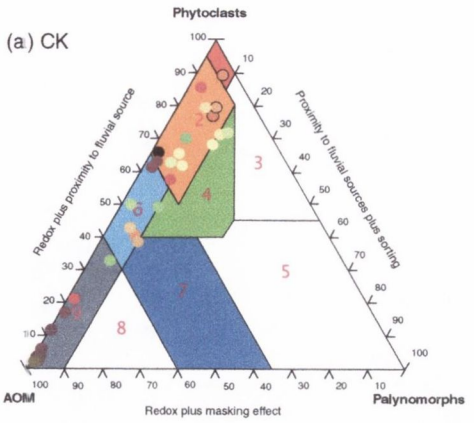

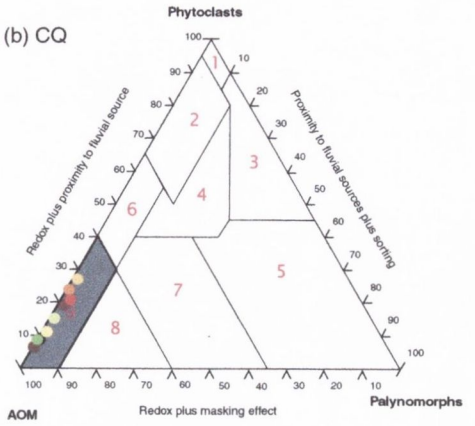

Sample	Perp Dist. from dyke (cm)	Palyn-omorphs	Phyto-clasts	AOM	VR (%Rr)
	6.74	1.098901	65.38462	33.51648	3.09
	20.22	0	3.536977	96.46302	3.65
	24.72	0	4.938272	95.06173	3.26
	29.21	0.310559	4.968944	94.7205	3.23
	33.74	0.311526	4.672897	95.01558	3.1
	42.69	0	11.8541	88.1459	3.39
	49.43	0.308642	4.320988	95.37037	
	60.22	0.900901	17.41742	81.68168	1.89
	80.89	2.071006	63.60947	34.31953	1.49
	89.88	2.824859	60.73446	36.44068	1.41
	103.36	1.497006	21.55689	76.94611	1.46
	112.35	9.142857	57.14286	33.71429	1.48
	139.31	3.746398	85.01441	11.23919	1.29
	157.29	9.973753	77.42782	12.59843	1.29
	179.76	7.395498	88.74598	3.858521	1.17
	202.23	7.333333	41	51.66667	1.14
	224.7	10.23392	79.23977	10.52632	1.16
	247.17	12.80788	36.94581	50.24631	1.1
	283.12	6.849315	41.91781	51.23288	1.12
	319.07	8.064516	78.3871	13.54839	1.16
	359.52	15.83113	71.50396	12.66491	1.11
	404.46	7.94702	64.56954	27.48344	1.12
	449.4	13.89646	68.11989	17.98365	1.14
	494.34	9.657321	62.3053	28.03738	1.03
	539.28	6.695464	62.41901	30.88553	1.1
	584.22	16.15599	72.14485	11.69916	1.07
	898.79	1.944444	50.83333	47.22222	1.07
	1617.83	5.18732	33.42939	61.38329	1.07
	6291.56	8.908046	50	41.09195	1.1
	7190.35	7.650273	69.67213	22.6776	1.08

Sample	Perp Dist. from dyke (cm)	Palyn-omorphs	Phyto-clasts	AOM
	20.22	0	9.872611	90.12739
	24.72	0	7.232704	92.7673
	29.21	0	12.30284	87.69716
	33.74	0	27.91411	72.08589
	42.69	0.299401	24.2515	75.4491
	49.43	2.39521	20.95808	76.64671
	60.22	1.436782	19.25287	79.31034
	80.89	0.57971	15.65217	83.76812
	89.88	0	9.537572	90.46243

1. Highlyproximal shelf or basin
2. Marginal dysoxic-anoxic basin
4. Shelf to basin transition
6. Proximal suboxic-anoxic shelf
7. Distal dysoxic-anoxic shelf
9. Distal suboxic-anoxic basin.

Figure 8.16 (i) Samples through the Carrickleck Dyke aureole plotted on the ternary plot of Tyson (1995). (a) the CK horizon; (b) the CQ horizon

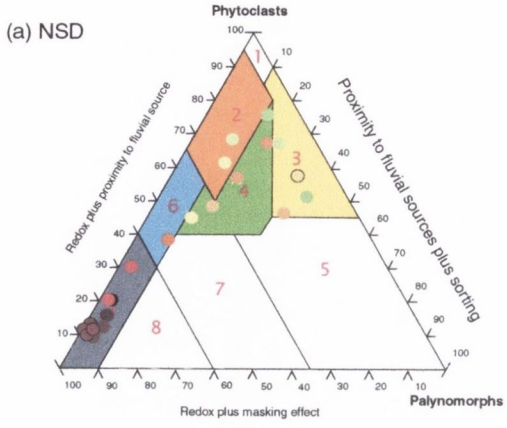

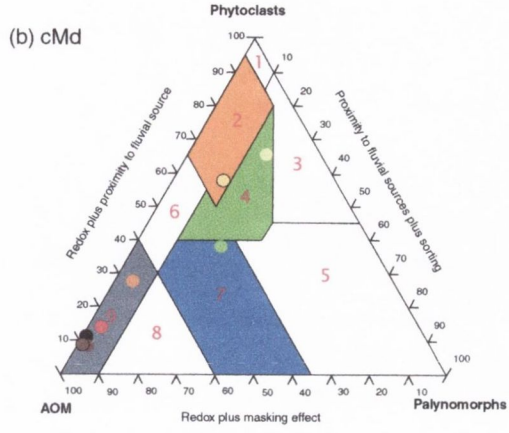

Sample	Perp Dist. from dyke (cm)	Palyn-omorphs	Phyto-clasts	AOM	VR (%Rr)
	0.04	2.406417	21.12299	76.47059	3.78
	0.15	3.519062	15.83578	80.64516	3.72
	0.28	0.31348	13.16614	86.52038	4.69
	0.37	3.225806	9.677419	87.09677	5.61
	0.47	4.216867	12.6506	83.13253	5.47
	0.49	0	11.49068	88.50932	5.16
	0.57	0.318471	11.1465	88.53503	3.41
	0.65	1.754386	11.9883	86.25731	3.49
	0.95	2.43309	19.70803	77.85888	2.82
	0.97	2.919708	30.41363	66.66667	1.63
	1.21	10.0295	37.75811	52.21239	1.48
	1.82	20.05348	67.37968	12.56684	1.26
	2.2	16.42157	56.86275	26.71569	1.05
	2.22	34.48276	46.15385	19.3634	1.03
	2.89	14.75728	48.54369	36.69903	1.06
	2.79	33.66093	56.75676	9.58231	1.03
	3.95	11.11111	45.27778	43.61111	1.06
	4.05	12.36264	61.26374	26.37363	1.19
	5.4	10.16166	68.82217	21.01617	1.13
	5.66	22.86501	66.94215	10.19284	1.11
	6.27	14.4357	74.54068	11.02362	1.04
	10.11	37.67313	51.80055	10.52632	1.25

Sample	Perp Dist. from dyke (cm)	Palyn-omorphs	Phyto-clasts	AOM	VR (%Rr)
	6.74	0.276243	11.32597	88.39779	5.2
	20.22	1.108033	8.864266	90.0277	5.45
	24.72	1.857585	9.287926	88.85449	3.55
	29.21	2.484472	14.90683	82.6087	2.57
	33.74	4.213483	28.37079	67.41573	1.57
	42.69	12.5	58.13953	29.36047	0.71
	49.43	20.22472	65.73034	14.04494	0.94
	60.22	21.53392	38.93805	39.52802	0.55

2. Marginal dysoxic-anoxic basin
3. Heterolithic oxic shelf (proximal shelf)
4. Shelf to basin transition
6. Proximal suboxic-anoxic shelf
7. Distal dysoxic-anoxic shelf
9. Distal suboxic-anoxic basin.

Figure 8.16 (ii) samples through the North Star Dyke aureole plotted on the Ternary plot of Tyson (1995). (a) the NSD horizon (b) the cMd horizon

8.8 SUMMARY

1. The mudrock horizons collected from the area around the North Star Dyke have similar palynofacies constituents. However, each horizon shows its own individual characteristics. NSD palynofacies is characteristically in a better state of preservation and contains a greater proportion of palynomorphs. cMd palynofacies contains membranous material, which has a characteristically strong fluorescence in the background samples. Neither the NSD nor BC horizons contain this fine group. The palynofacies material is also quite degraded.
2. The mudrock horizons collected from the area around the Carrickleck Dyke have distinctively different palynofacies content. The CQ horizon is dominated by the AOM fraction, with very small amounts of other OM. The CK horizon palynofacies is poorly preserved, and is also dominated by the AOM fraction. However, it does contain greater proportions and variety of palynomorphs and woody material.
3. There is not a predictable particle size distribution through the aureole (i.e. particles do not necessarily become obviously larger or smaller with proximity to the dyke).
4. Maximum proportions of AOM in aureole samples are usually recorded at the same position as the maximum, recorded VR.
5. Much of the organic material is broken down/amorphous and destroyed in the area adjacent to the dykes.
6. All organic material is blackened in the area adjacent to the dykes.
7. The samples collected from the area directly adjacent to the dykes all plot in area 9 of Tysons ternary diagram, a 'distal suboxic-anoxic basin'.

8.9 DISCUSSION

The similarity of each of the lithological horizons from Ballycastle, can be put aside when the organic residues for each of the individual horizons are examined. This gives some credence to the use of palynofacies assemblages as an indicator for different palynological facies. For example the survival of the very fine, membranous material observed in the cMd horizon, combined with the very poor preservation of palynomorphs, might imply that degradation was due to microbial rather than mechanical action. In contrast the NSD horizon contains a full range of palynological material, however the very fine OM seen in the cMd horizon is absent and much of the OM is ragged and rounded, implying greater mechanical degradation.

At Carrickleck, samples can again be differentiated by their palynofacies content. This again shows that the palynofacies assemblage has a place in the study of a sedimentary lithology.

All organic material in the areas adjacent to the dykes is black and damaged. This must be assumed to be a destructive effect of the heat of the intruding dykes.

AOM, in the 'oil industry' can be considered to be an indicator of the economic potential of a source rock. Each of the horizons examined in this study exhibit a tendency for the palynofacies assemblage to become AOM dominated with proximity to the dyke, even in the cases where AOM is not the dominant organic material in the 'background' samples. When a mudrock or shale is discovered, assessed and deemed to be in a 'mature' state, the presence of blackened AOM might easily be misinterpreted as indicating that the mudrock or shale has 'produced' and they might thus go in search of a reservoir and trap situation, or attempt to model the migration of the ghost fuel, when what they might simply be looking at is a rock that has been exposed to a short lived heating event and whose organic material has simply degraded broken and the smaller particles have amalgamated into an amorphous mass during sample preparation. The evidence from this study would imply that one must be very careful when interpreting the organic residues of potential source rock.

Tyson's ternary plot was designed for use with lithologies that are not 'overmature'. It was not designed to deal with material heated in this manner. However it is not uncommon in exploration to core rock and analyse blind (i.e. without necessarily knowing too much about the geology at depth). Use of this plot ought to be done with caution. Samples closest to the dykes for each horizon plots in area 9 of Tyson's ternary plot. Clearly this is not a correct representative facies, the apparent content being a function of the destructive influence of the dyke.

8.10 CONCLUSIONS

Palynofacies is altered by the heat of intrusion. Particularly in the region closest to the dyke.

Palynofacies affected by the elevated temperatures of a short lived intrusive heating event is reduced to an assemblage dominated by black AOM.

OM bearing rock collected from directly adjacent to a dyke could easily be misidentified as an 'overmature' (possible) source rock.

Palynofacies should probably only be used as a tool to identify a sedimentary facies, when the material has been matured to VR reflectance values ≤1.5%R_r, i.e. Tysons ternary plot should not be used when VR values are ≥1.5%R_r.

Applying the results of this study to the ternary plot of Tyson serves as a warning when analysing palynofacies that caution must always be applied, particularly when the full geological setting is not known.

9 THERMAL MODELLING

9.1 INTRODUCTION

In addition to the laboratory investigations using vitrinite reflectance, clay crystallinity, and thermal alteration indices, the models proposed by Delaney (1987, 1988) were used in an attempt to model the conductive cooling history of a mafic dyke. This was undertaken in order to establish the theoretical thermal evolution of the dyke aureole.

Temperature is a measure of the average kinetic energy of individual molecules, measured in degrees Kelvin or Celsius. **Thermal energy** refers to the total energy of all the molecules in an object. **Heat** refers to a transfer of energy from one object to another because of a difference in temperature. The direction of heat flow between two objects depends on their temperatures, not on how much thermal energy each has. Heat can be transferred from one place to another in three different ways - **conduction**, **convection** and **radiation**.

Heat **conduction** occurs in many materials, as the result of molecular collisions, (phonon conduction). Heat conduction takes place only if there is a temperature difference across an object that is it requires the presence of matter, most commonly a solid (Giancoli 1991, Beardsmore and Cull 2001). Heat **convection** is the process whereby heat is transferred by mass movement of molecules from one place to another. Whereas conduction involves molecules and/or electrons moving only over small distances and colliding, convection involves the movement of molecules over large distances. Convection occurs most commonly in fluids. **Radiation** essentially consists of electromagnetic waves, emitted from a body, which can transfer heat through near empty space unlike convection and conduction which both require the presence of matter for heat transfer.

9.1.1 THERMAL CONDUCTIVITY AND DIFFUSIVITY -TEMPERATURE DEPENDENT THERMAL PROPERTIES

Thermal conductivity (K), ($Wm^{-1}°C^{-1}$), is a measure of how easily heat is transmitted through a material.

Thermal diffusivity (k), (m^2s^{-1}), is the rate at which heat dissipates through a material and can be expressed as a function of conductivity

(1) $k=K/(\rho C)$ where k=thermal diffusivity (m^2s^{-1})
K= thermal conductivity ($Wm^{-1}°C$)
ρ= density (kgm^{-3})
C= specific heat (J/kg°C)

The coefficients of conductivity and diffusivity are calculated by 'least square fitting' a line to curves presented by experimental data (figure 9.1). The ranges for the conductivity and diffusivity of basalt and mudrock overlap substantially (table 9.1). This overlap in values seems to imply that it is reasonable to assume that the numbers produced in the paper by Delaney can be used for this model.
(Delaney 1988)
Data for K and k are described by the equations:

(2) $K=a_1+b_1/(273.15+\theta)$ Where a_1 & b_1 are the coefficients of K
(3) $K= a_2+b_2/(273.15+\theta)$ a_2 & b_2 are the coefficients of k
θ is temperature in °C

Thermal conductivity and diffusivity are physical properties of rocks, which can be used to describe heat flow. Both of these properties vary with lithology, (see table 9.1). Thermal conductivity and diffusivity are also temperature dependent properties. It is generally accepted that most minerals have thermal conductivities and diffusivities that decrease with increasing temperatures; they are roughly inversely proportional to temperature (Beardsmore and Cull 2001, Furlong 1991, Delaney 1988, 1987, Hanley *et al.* 1978). It is also generally accepted that K and k of most rocks show an inverse relationship to temperature (Carslaw and Jaeger 1959, Hanley *et al.* 1978, Delaney 1987, 1988, Furlong 1991, Midttømme and Roaldset 1999 and references therein, Beardsmore and Cull 2001). There are however reports of rocks that show increasing K and k with temperature (Midttømme and Roaldset 1999 and references therein). The thermal conductivity of rocks has been much studied and there are many cited values in the literature (Lovering 1935, Touloukian and Ho 1981, Furlong 1991, Beardsmore and Cull 2001). The property of thermal diffusivity has not received as much attention. Thermal property data for rocks at high temperatures (>500°C) are sparse. However thermal conductivity and diffusivity

appear to vary only slightly for temperatures between 300 and 700°C (Hanley *et al.* 1978, Furlong 1991).

LITERATURE SOURCES	units	Diffusivity	Rock type	Conductivity	units	LITERATURE SOURCES
Schon 1996, Delaney 1988	m^2/s	4.33- 7.75e-7	Basalt	0.54 -2.25	W/mdegC	*Barker 1996, *Beardsmore 1996, Schon 1996, Hanley *et al* 1978
Conor et al. 1997	m^2/s	7.23E-07	Basalt dry	1.7	W/mdegC	Conor *et al.* 1997
Conor et al. 1997	m^2/s	9.78E-07	Basalt wet	2.3	W/mdegC	Conor *et al.* 1997
			Granite	3.05	W/mdegk	Furlong *et al.* 1991
			Mudstone	1.6 -3.02	W/mdegK	*Beardsmore 1996, *Reiter and Tovar 1982,*Barker 1996, Bodell and Chapman 1982
Schon 1996	m^2/s	5.94E-7 - 15.3E-7	Argillites	0.25-3.01	W/mdegK	Schon 1996
Turcotte and Schubert 2002 and Schon 1996	m^2/s	4.24E-7 - 1.05E-6	Shale	1.6 - 2.9	W/mdegK	*Beardsmore 1996, Furlong *et al.* 1991, *Barker 1996, Turcotte and Schubert 2002
			Clay	0.38 - 3.02	W/mdegK	Schon 1996
			Claystone	1.8 - 2.9	W/mdegK	*Barker 1996, *Beardsmore 1996
Schon 1996	m^2/s	0.7-7.02E-7	Coal	0.18 - 0.4	W/mdegK	*Majorowicz and Jessop 1981, *Beach, Jones and Majorowicz (1987), Furlong *et al.* 1991
Schon 1996	m^2/s	2.54-20.4	Sandstone	0.38 - 6.50	W/mdegK	Schon 1996, Furlong et al. 1991
Hanley *et al.* 1978	m^2/s	7.45 E-6 - 1.24 E-5	Limestone	2.00 - 3.40	W/mdegK	Turcotte and Schubert 2002, Furlong *et al.* 1991

*Values found in Beardsmore and Cull 2001

Table 9.1 Some of the reported thermal conductivity and diffusivity values for a variety of lithologies.

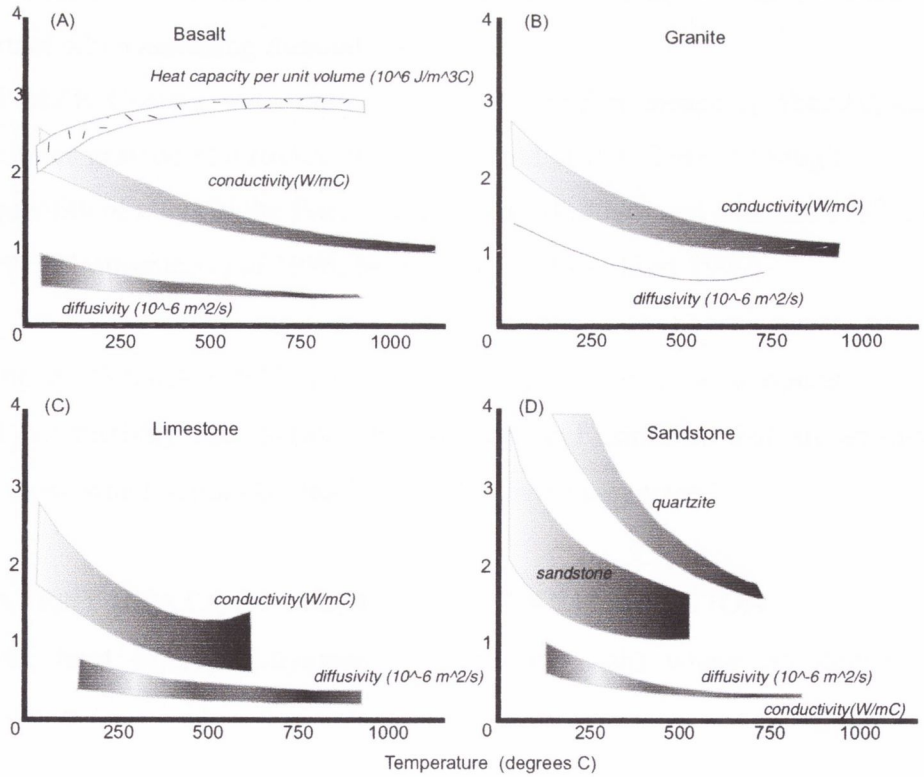

Figure 9.1 Variation of thermal diffusivity and conductivity with temperature for different lithologies (after Delaney 1987, 1988, data from Touloukian et al. 1981)

9.1.1.1 FACTORS INFLUENCING CONDUCTIVITY (K) AND DIFFUSIVITY (k)

FLUID CONTENT OF ROCK

The thermal conductivity and diffusivity of water is directly proportional to temperature. This means that for porous, saturated rock the estimation of the thermal properties becomes more difficult. "A rock with 10% porosity (ϕ) at modest temperatures and pressures may exhibit an increase in K of up to 40% if water saturated. At 20 MPa and 550°C, as characteristic pressure and temperature near a dyke contact at 2km depth, the conductivity of water is small so that the increase in conductivity due to water saturation is only 7%. The influence of water on K is therefore greatly temperature dependant" (Delaney 1988).

POROSITY, even when not hosting fluids, has been observed to be inversely proportional to the effective thermal conductivity of a rock (Delaney 1988, Midttømme and Roaldset 1999).

The **ANISOTROPIC NATURE** of sedimentary rocks also affects their thermal conductivity. Values measured parallel to the layering can be as much as twice that of those measured perpendicular to bedding (Midttømme *et al.* 1996, Schön 1996, Midttømme and Roaldset 1999,).

MINERALOGY Minerals have different thermal properties so that the rock composition is important when assessing thermal properties.

GRAIN SIZE Coarser sediments tend to have higher measured thermal conductivities than the finer grained claystones, mudstones and shales. This is thought to be due to the higher quantity of clays in the finer grained rocks (Gilliam and Morgan 1987, Demongodin *et al.* 1991, Midttømme *et al.*1996, Midttømme and Roaldset 1999).

According to Delaney (1987, 1988) "models that treat these temperature dependencies (thermal conductivity and thermal diffusivity) yield estimates that are as much as 75°C beneath those which would be predicted if they were neglected."

9.1.2 LATENT HEAT OF MAGMATIC CRYSTALLISATION

Magmatic heat of crystallisation (megaJm^{-3}) = (ρh) where ρ= density, h=heat of crystallisation.

9.1.2.1 FACTORS INFLUENCING THE LATENT HEAT OF MAGMATIC CRYSTALLISATION

Latent heat is released during the entire solidification history of the intrusion, rather than in the early stages as might be expected with crystallisation (Furlong 1991). The heat released by a cooling magma from its initial temperature to its solidus temperature depends on its chemistry and cooling rate. "For a quickly quenched, glassy magma, the heat released is $(\rho C)_m(\Theta_{mi} - \Theta_s)$; if cooled slowly to form a holocrystalline rock then a heat of crystallisation $(\rho h)_m$ is released also" (Delaney 1987), where ρ_m is the density of the magma, C_m is the heat capacity of the magma, Θ_{mi} is the initial temperature of the magma and Θ_s is the solidus temperature of the magma.

This means that the cooling time of the magma is important. Magmas intruded into cool host rocks high in the crust become too viscous to flow if subjected to even a 10% temperature drop (Delaney and Pollard 1982). This implies that thicker dykes are most likely to remain fluid for longer. Delaney gives the example of a thin dyke (2m) intruded at 1150°C into country rock at 50°C, with $k = 7.5 \times 10^{-6} m^2 s^{-1}$, which, would cool to 600°C in approximately 15 days, $\tau=1$ (where τ is dimensionless time); the dyke would lose most of its heat after 150 days $\tau=10$. The characteristic cooling time has the proportionality constant $t \propto T^2$, so that a dyke ten times thicker than another takes 100 times longer to cool (Delaney and Pollard 1982). In other words, "magmas that cool sufficiently slowly to release heat of crystallisation display effective diffusivities that can be expected to have a strong influence on temperatures and cooling durations" (Delaney 1987). Delaney (1987, 1988) has estimated that the heat of crystallisation can raise the initial temperature at the dyke contact by as much as 100°C.

9.2 PROGRAMS FOR THE CONDUCTIVE COOLING OF DYKES WITH TEMPERATURE-DEPENDENT THERMAL PROPERTIES AND HEAT OF CRYSTALLISATION (AFTER P.T. DELANEY 1988)

9.2.1 INTRODUCTION

Delaney (1988) has compiled four programs, written in Fortran77, which take into account the heat of crystallisation and the thermal dependence of thermal conductivity and thermal diffusivity. These models constitute 4 programs with 26 subroutines and functions. They are based on the Fouriers equation for heat flux and the heat conduction equation for temperature dependent thermal properties of Carslaw and Jaeger (1959). This assumes an

idealised dyke as a tabular body of thickness T, which conducts heat in directions perpendicular to the contact in areas that are not near the dyke tip. The reader is referred to the paper of Delaney 1987 for a more extensive discussion and explanation for the theory and algorithms used; for a more 'program specific' perspective of the work, Delaney 1988 is recommended. The latter paper also contains a complete copy of the code, for each of the programs.

There are two programs dedicated to the general solution of a cooling dyke. These are referred to as 'whole time' solutions, and apply throughout the entire cooling history of a dyke. The whole-time solutions work on the premise that the thermal property contrasts affect cooling rates early in the cooling history, and subsequently have less influence on the cooling rate. The other two programs are designed to allow more accurate estimates of the initial dyke-contact temperatures, i.e. at times less than that required for cooling to commence at the dyke centre. These are referred to as 'early time' solutions. Heat is contained primarily in the dyke early in the cooling history and in the host rocks in the later stages.

Analytical solutions, such as those proposed by Lovering (1935), and Carslaw and Jaeger (1959) are useful to quickly estimate cooling time, but numerical solutions are more important for those seeking accuracy to within 100°C (Delaney 1988). Analytical solutions require that thermal conductivity and diffusivity remain constant and thus can only account approximately for the effect of the heat of crystallisation associated with cooling.

The difference between the numerical and analytical solutions is greatest at the contact between host rock and dyke wall. They also result in differing cooling rates and total times.

9.2.2 FOUR PROGRAMS; FIVE SOLUTIONS

Early time solutions estimate the time taken after intrusion for the dyke to begin to cool at the centre. The **maximum temperature** experienced at the contact (distance (X)=0) at the time of intrusion (t=0), θ_{ci} (θ=temperature, c=contact, i=initial), is also calculated. Analytical early time solutions (*Earlya*), calculates higher θ_{ci} than the equivalent numerical solutions, *Earlyn* (*c.* $0.85\theta_{ci}(n):1\theta_{ci}(a)$).

Earlya also calculates a **quicker cooling rate** in the early stages of the cooling process than *Earlyn*.

Whole time solutions model the cooling of the dyke up to a specified time (controlled by the operator in Taud.dat file which must be written before the programs are run). Whole

time analytical solutions (*Wholea*) calculate a cooling time necessary for the dyke to cool to the ambient temperature of the host rock at time of intrusion, much greater than that of whole time numerical solutions (*Wholen*). *Wholen* can be solved using *Earlya* (*wnea*) or *Earlyn* (*wnen*) as starting conditions. *Wnea* solutions estimate times greater than wnen, for the complete cooling of the dyke. Calculated times for *wnea* and *wnen* are much closer than those of *Wholen* and *Wholea.*

9.2.3 THE WORKING MODEL

Early analytical programs model the early cooling history of the dyke, where 'early' implies from intrusion until the centre of the dyke begins to cool. Conductivity and diffusivity are assumed to be constant. Heat of crystallisation is an optional variable and can raise the contact temperature by *c.* 100°C. The advantage of the early time solutions, both numerical and analytical, is the possible increased accuracy of the calculations for distances less than T/4 from the dyke (where T= dyke thickness).

Early numerical programs solve for the early cooling history of the dyke, where 'early' implies from intrusion until the centre of the dyke begins to cool. Conductivity and diffusivity are assumed to vary with temperature. This forces a drop in initial contact temperature (relative to the contact temperature calculated by the early analytical solution) by approximately 100°C. Heat of crystallisation is an optional variable and can raise the initial contact temperature by *c.* 100 °C.

Whole time analytical solution assumes constant values for conductivity and diffusivity and calculates the initial temperature at the contact

$$\theta_{ci} = (K_m/K_h)/(K_m/K_h) + \text{root}(k_m/k_h)$$

$_m$ = magma

$_h$ = host rock

Whole time numerical solutions assume conductivity and diffusivity vary with temperature. The results of either the early analytical or early numerical solutions are used to provide initial conditions and are integrated using the 'Crank Nicholson method' a complicated mathematical method (Delaney 1987). When using early numerical solution for the whole time solution starting conditions, the model maintains higher temperatures at greater distances from the dyke for longer times, than are maintained when using the analytical early solution where high temperatures attained by the dyke are maintained for

shorter times i.e. higher starting T°C heat dissipates more quickly (see table 9.3).Varying the dyke width doesn't affect the maximum temperature attained (θ_{ci}), but it does affect the amount of time that the higher temperatures are sustained and it increases the amount of time necessary for the dyke to cool.

9.2.3.1 THE EFFECT OF VARYING PARAMETERS

PARAMETER	VALUE	UNIT
Dyke thickness	2.0	metres (m)
Ambient T Host rock	50	degrees
Temp. Intrusion of the Dyke	1150	Celsius (C)
Conductivity of Magma (Km)	2.25	W/m C
Conductivity of Mudrck (K)	2	W/m C
Coefficient of conductivity Magma a1 b1	0.6893 522	
Coefficient of conductivity Mudrock a1 b1	0.250 944	
Diffusivity of Magma	7.23E-07	m^2/s
Diffusivity of Mudrock	7.0E-07	m^2/s
Coefficient of diffusivity Magma a1 b1	3.06E-07 1.25E-04	
Coefficient of diffusivity Mudrock a1 b1	1.80E-07 2.50E-04	
Latent heat	9.00E+08	MJ/m^3
Solidus temperature	950	C
GUESS initial dyke contact temperature	700	C
GUESS lambda s	-0.4	
relative error	1.00E-04	
Number of dyke thicknesses from contact, and number of points per dyke thickness, where temperatures are to be calculated	3 30 (analytical) 19 30 (numerical)	
Times when temperatures are to be calculated are in file TAU.DAT (nondimensional) or DTAU.DAT (dimensional) (n/d)	d	
Read input from EARLYA.DAT (analytic early time) or EARLYN.DAT (nemuerical early time) (a/n)	a=analytical n=numerical	
number of time steps between tiimes TAU?	10	

Table 9.2 'Basic' sample input data for analytical and/or numerical model solutions

The addition of the heat of crystallisation is said to be of importance when the dyke is on the scale of hundreds of metres to kilometres (thickness). However including this parameter can raise the contact temperature of the dyke up to 100°C.

Varying the initial temperatures of the host rock and the intruding magma can have marked effects on θ_{ci}. These variables directly influence the initial temperatures and the cooling time is also therefore affected.

Heightened values of K and k result in a higher θ_{ci} and decreased cooling time. Lowering the values for K and k of the dyke result in a lower θ_{ci} and a longer cooling time, lowering the values for the host rock result in a higher θ_{ci} and an even longer cooling time than either the basic data set or the decreased values for the dyke.

Lowering the solidus temperature for the dyke results in higher θ_{ci} and longer cooling time.

θ_{ci} is most responsive to the ambient temperature of the host rock, magma temperature at time of intrusion, heat of crystallisation and to a lesser extent to K and k

Cooling time and **Rate** are most responsive to dyke thickness and ambient temperature of host rocks, K, k and dyke thickness.

		wnen solutions		early time solutions	
Parameter	new value	ci (C)	c after 154days	ea	en
basic solution		525	224	0.309	0.772
Dyke width	4m	525	389	1.543	3.086
	8m	525	513	7.716	15.432
Heat of crystallisation	900E+6M J/m^3	618	282	1.543	1.543
	900E+4M J/m^3	526	225	0.309	0.772
Magma T	900C	417	182	0.309	0.772
	1500C	679	283	0.309	0.772
Host Rock ambient temp	12	496	185.2	0.309	0.772
	150	596	322	0.309	0.772
thermal properties					
K & k both dyke and host rocks	K=5, k=1.5	543	177.5	7.407	7.407
K & k of dyke	K=1.5 k=4.9E-7	468.7	225	0.772	0.772
K &k of host rock	K=1.5 k=4.9E-7	586	265	0.309	0.772
Solidus temperature	400C	578	285	0.772	0.772

Table 9.3 The effect of varying test parameters. wnen = whole time numerical solutions; θ_{ci}=initial contact temperature; θ_c = contact temperature; basic solution is the solution for the parameters cited in Table 9.2

9.3 ASSUMPTIONS OF THE MODELS FOR THE NORTH STAR AND CARRICKLECK DYKES

- Each dyke is intruded instantaneously and is treated as a single intrusive event.
- Host rocks are dry and fully lithified at the time of intrusion, with negligible porosity and permeability.
- Dykes considered in this work are treated as being too small, and therefore having solidified too soon for buoyant hydrothermal circulation to have established. Thus all heats of reaction, other than the crystallization of the magma, and all heat transfer arising from fluid motion are assumed to be negligible.
- Thermal conduction, parallel to bedding, is the main form of heat transfer through the host rock.
- The dyke is idealised as a tabular body of thickness T. At all positions not near the dyke tip, heat is conducted only in directions normal to the contact

9.4 INPUT DATA

9.4.1 INDIVIDUAL DATA INPUT AND EXPLANATION

9.4.1.1 AMBIENT TEMPERATURE OF HOST ROCK

CARRICKLECK

CK samples are Namurian in age. The maximum pre-intrusion temperature, experienced by CK and CQ horizons from the Carrickleck Quarry, was achieved through burial in the latest Carboniferous – earliest Permian times (Fernandez 2000).

For the Kingscourt outlier the Upper Carboniferous sequence has a maximum present day thickness of 2,300' or 701.04m (Jackson 1965, pg 131). The Permo-Triassic sequence of the Kingscourt outlier has a maximum, present day, thickness of 550m (Naylor 1992). The upper Permian has a reported VR of 0.39%R_r assuming this to be due to a maximum burial, and invoking a regional thermal gradient of 22°Ckm^{-1}, then the maximum cover necessary to achieve this reflectance value is ~1.7km. Thus a total Tertiary cover of 2400m. Invoking a geothermal gradient of 22°Ckm^{-1} (Allen *et al.* 2002) gives an ambient temperature of [12 (surface temp)+ (2.4km x 22°Ckm^{-1})] 65°C has been assumed during dyke emplacement.

BALLYCASTLE

The maximum burial of the area around Ballycastle is thought to have occurred in the earliest Tertiary (Evans 1998). This would imply that the recorded VR from the background samples at Ballycastle are, ideally, recording the maximum ambient temperature of the host rock during dyke emplacement. However, there are conflicting VR readings from the dispersed vitrinite in the mudrock horizons and the coals (~1.0%R_r or 148°C and 0.55%R_r or 86°C respectively). Four input temperature temperatures were used:

1. maximum ambient temperature based on the vitrinite measured from the mudstone horizons
2. maximum ambient temperature based on the vitrinite measured from the mudstone horizon with coal lenses
3. calculated ambient temperature based on an estimate of overburden in the Tertiary and a regional geothermal gradient of 22°Ckm^{-1} (Allen *et al.* 2002)
4. as 3 but with an exaggerated gradient of 80°Ckm^{-1} that would be justified by Tertiary volcanics.

For the last two points an estimated maximum cover of 1122 m is assumed, (1000m Permian –Tertiary cover in the Tertiary (Naylor 1992) and 122m of Upper Carboniferous cover (Wilson and Robbie 1966)). Applying the assumed regional gradient of 22°Ckm^{-1}, and surface temperature of 12°C, would imply an ambient temperature of 36.68°C. Invoking an exaggerated local geothermal gradient of 80°C would imply an ambient temperature of 101.8°C. With an estimated minimum cover of 550m (Wilson and Robbie 1966) and a maximum geothermal gradient of 80°C/km^{-1} and a minimum thermal gradient of 22°C/km^{-1} the assumed temperatures become 56°C and 25 °C respectively.

9.4.1.2 TEMPERATURE OF INTRUDING MAGMA

CARRICKLECK

Unlike the North Star Dyke, the Carrickleck Dyke is rotten and there was very little detail that could be gathered from looking at the material. An average temperature for hot, fluid, basaltic magma was taken from the literature, 1150°C (Hughes 1982, Delaney 1987, 1988, Goodhue 1994, McCormack 1998).

BALLYCASTLE

Minerals are dominantly thin plagioclase laths and olivine in the chilled margin. Pyroxene was not present in the margin samples. The plagioclase laths observed in the chilled margin have 'fuzzy' ends, which implies, an undercooling temperature of no less than 200°C (Lofgren 1980) *i.e.* the temperature difference between host rock and the intruding magma chilled at the margin was no less than 200°C.

Whole rock XRF data were used in an attempt to estimate a maximum temperature for the magma at the time of intrusion of the North Star Dyke. The albite-anorthite-diopside system of (Bowen 1915) approximates magma from which gabbro and basalt (without orthopyroxene and olivine) crystallise (Hibbard 1993). Normalised data from the North Star Dyke plots beyond the 1450°C isotherm on the ternary plot (see figure 9.2). The ternary phase diagram of Bowen (1915)(figure 9.2), describes the albite-anorthite-diopside solid solution series constructed for a pure system. However, these dykes, as for most natural systems, are not the idealised pure/closed systems described by this phase diagram. For example the North Star Dyke contains augite instead of pure diopside and some dissolved H_2O are also contained (see App II for XRF normalised data). The presence of these 'impurities' lowers the system temperatures. The average temperature quoted in the literature is 1150°C (Thompson *et al.* 1972, Hughes 1982, Delaney 1987,1988).

9.4.1.3 SOLIDUS TEMPERATURE

An estimated solidus temperature of 950°C is taken for BC and CK from the literature (Hughes 1982, Delaney 1987, 1988).

9.4.1.4 DYKE WIDTH

CARRICKLECK

The Carrickleck dyke is a single intrusion, approximately 1.5m wide.

BALLYCASTLE

The North Star Dyke is a composite dyke, *c.* 4m in width, intruded in three steps *c.* 3.1m, 0.63m and 0.3m (oldest to youngest, outer to inner).

The margins of each separate intrusion are visible, however the contact margins of the secondary and tertiary intrusions are not strongly developed. It is therefore assumed that

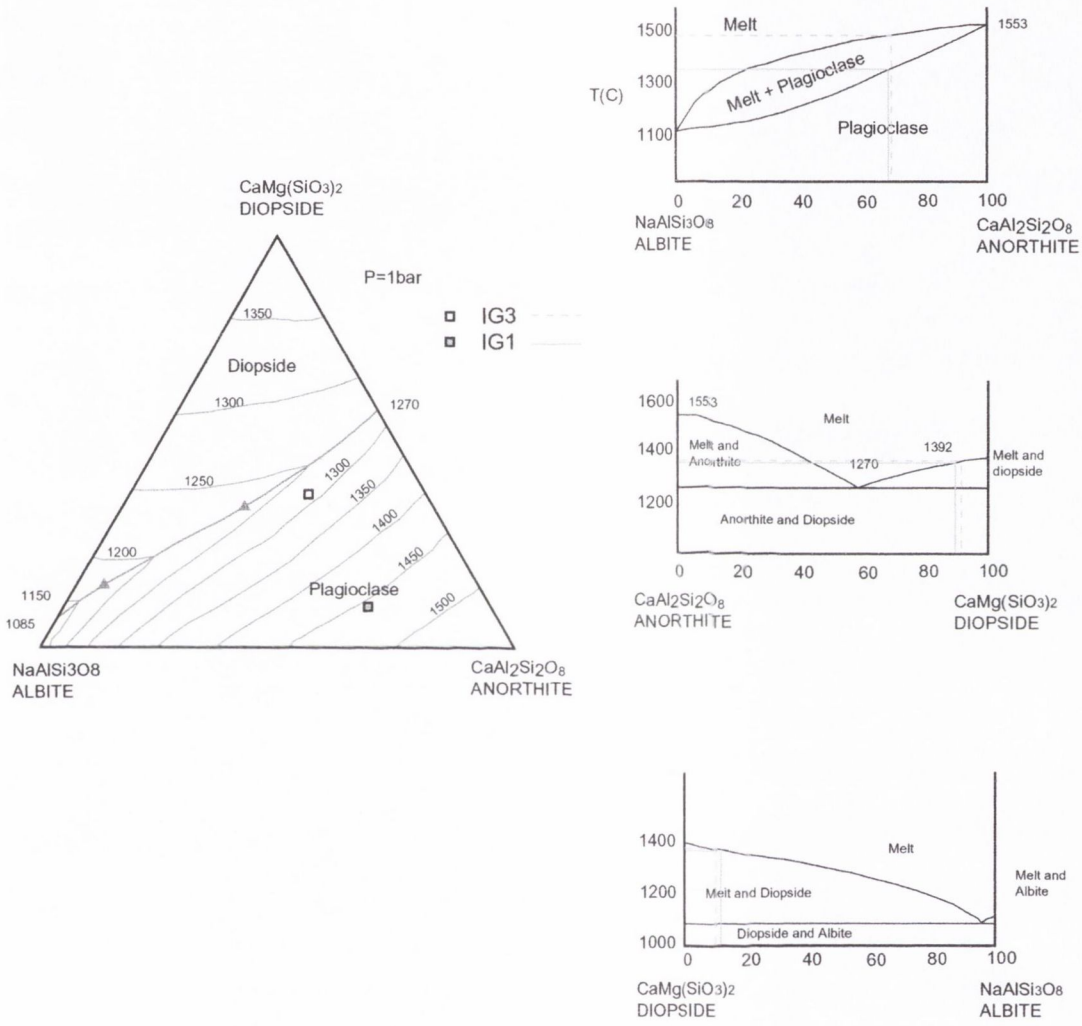

Figure 9.2 (a) Ternary phase diagram for the Albite-Anorthite-Diopside system at 1bar (Bowen 1915). A ternary system contains three binary systems: (b) Albite-Anorthite phase diagram, (c) Anorthite-Diopside phase diagram, and (d) Diopside-Albite phase diagram.

each successive intrusion came hot on the heels of the last. However the first intrusion must have been below its solidus temperature (<950°C pers comm. Dr. R. Merriman 2002) to allow the hot solid to fracture and admit new magma. The injection of fresh magma must have halted or reversed the cooling at the centre of the dyke, with an overall result that the dyke margin would have remained above ambient country rock temperature for longer than in the case of a single intrusive event. Thus, the effective heat flow time is assumed to have increased, perhaps on the order of days. It is assumed to be unlikely that the subsequent intrusions of magma would have had significant cooling time to allow them to release a heat of crystallisation.

However, the supposed increased time for effective heat flow should justify considering the dyke as a single 4m body.

9.4.1.5 THERMAL PROPERTIES OF ROCKS

Mudrock conductivity 2.0 $Wm^{-1}C^{-1}$

Basalt conductivity 2.25 $Wm^{-1}C^{-1}$ (see table 9.2, Delaney 1987, 1988)

Mudrock Diffusivity $7.0x10^{-7}$ m^2s^{-1} (average value, see table 9.2)

Basalt Diffusivity $7.5x10^{-7}$ m^2s^{-1} (average value, see table 9.2, Delaney 1988)

Conductivity coefficients			
Mudrock	0.250 (a)	944 (b)	(Delaney 1988)
Basalt	0.689 (a)	522 (b)	(Delaney 1988)
Diffusivity coefficients			
Mudrock	$1.80x10^{-7}$ (a)	$2.50x10^{-4}$ (b)	(Delaney 1988)
Basalt	$3.06x10^{-7}$ (a)	$1.25x10^{-4}$ (b)	(Delaney 1988)

9.5 RESULTS

9.5.1 MODELLING THE CARRICKLECK DYKE

The numerical method was used to model the Carrickleck situation (see figures 9.3 and 9.4). The model (*en*) gives a maximum contact temperature of 535°C. The contact temperature was calculated to remain above 500°C for up to 8 days. The model calculates that it would take approximately 0.42 years for the contact temperature to drop to less than 200°C and *c.* 42 years for the contact and dyke centre to reach the original ambient temperature of the intruded host rock. In the region directly adjacent to the dyke, VR estimated temperatures from the CK horizon are much lower than maximum temperatures (T_{max}) calculated by the model. Beyond 3m from the dyke contact the VR estimated temperatures were greater than T_{max} calculated by the model. This was to be expected however as it has been assumed that the CK horizon had achieved maximum burial in the latest Carboniferous.

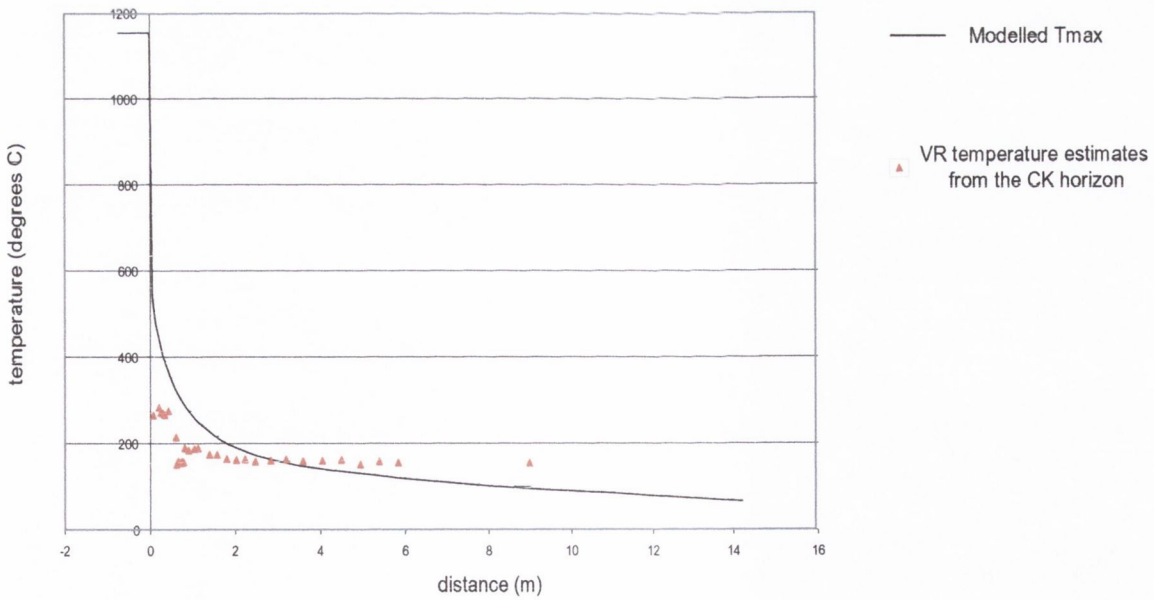

Figure 9.3 Modelled T_{max} and VR estimated temperature from the CK horizon in the Carrickleck dyke aureole. VR estimated temperatures beyond the aureole are expected to exceed those of the model as it has been assumed that maximum burial occurred in the Late Carboniferous.

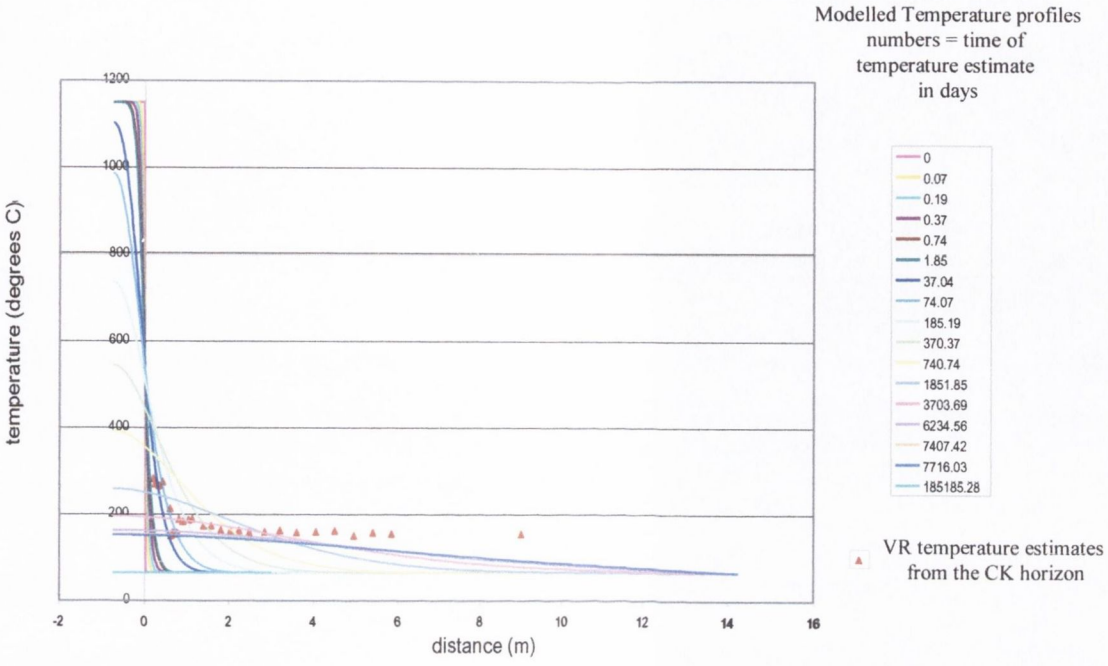

Figure 9.4 Modelled Temperature (T) profiles at selected time intervals the Carrickleck dyke aureole with VR estimated temperatures from the CK horizon.

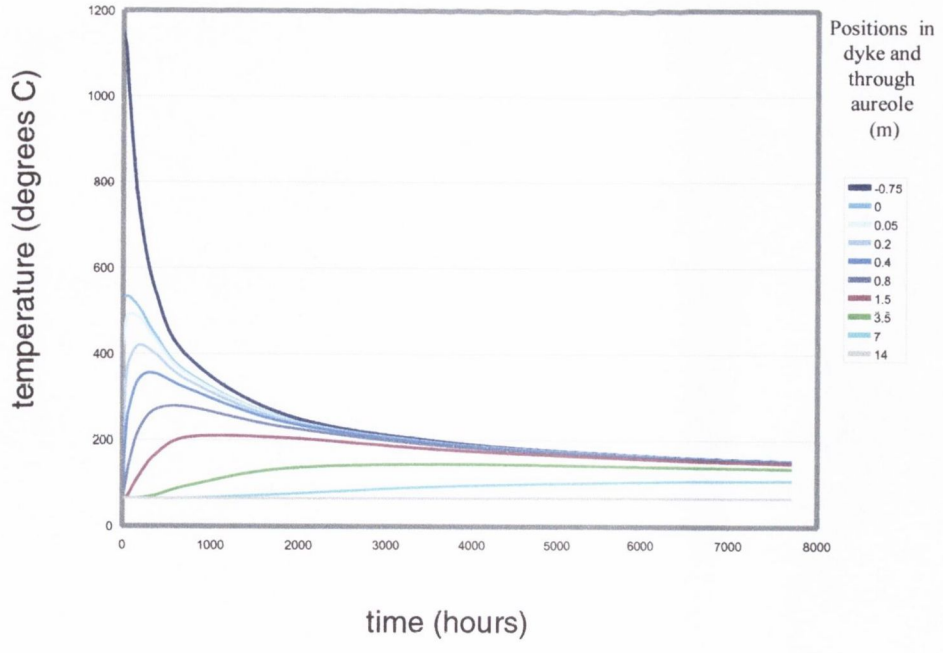

Figure 9.5 The thermal evolution through time of the dyke centre (-0.75m), the contact (0m) and some points in the Carrickleck Dyke aureole

9.5.2 MODELLING THE NORTH STAR DYKE

Due to the uncertain ambient temperature of the host rock (θ_{hi}) at the time of intrusion in the Ballycastle area five possible temperatures were considered. Each model calculates temperatures in the area immediately adjacent to the dyke margin. These temperatures are significantly elevated relative to the VR estimated temperatures from the BC, cMd and NSD horizons. Models using θ_{hi} greater than or equal to 86°C appear to best fit the VR estimated data (see figure 9.6). Based on the model of Delaney (1988), the maximum temperature range enjoyed at the North Star Dyke contact at the instant of intrusion was 505 – 686°C depending on the assumed ambient temperature of the host rock. Taking the intermediate temperature of 86°C, the model predicts a maximum contact temperature of 550°C (using numerical solutions-*en, wnen*), which would be sustained for less than a day. The contact temperature should be sustained at >500°C for ≤ 77days, and would be sustained at ≥200°C for ≤4yrs. It takes *c.* 200 years for the dyke centre to cool to the same temperature as the ambient temperature of the host rock.

Host Rock Ambient Temperature (°C)	Maximum Contact Temperature (°C)	>500 °C	>200 °C	Dyke Centre Temp = Host Rock Ambient Temperature
56	504	<30days	<4years	*c.* 200 years
37	514	>30/<77days	<4 years	*c.* 200 years
56	529	<50 days	<4 years	*c.* 200 years
86	543	<77days	<4 years	*c.* 200 years
102	543	<77days	<21 years	*c.* 200 years
148	594	<154days	<21years	*c.* 200 years

Table 9.4 Some of the basic data fom the modelled thermal evolution (wnen solution) of the North Star Dyke contact under different starting ambient host rock temperature conditions. Describing the amount of time that the contact be sustained aabove 500°C and 200°C, and how long it should take for the dyke centre to cool to the same temperature as the ambient host rock

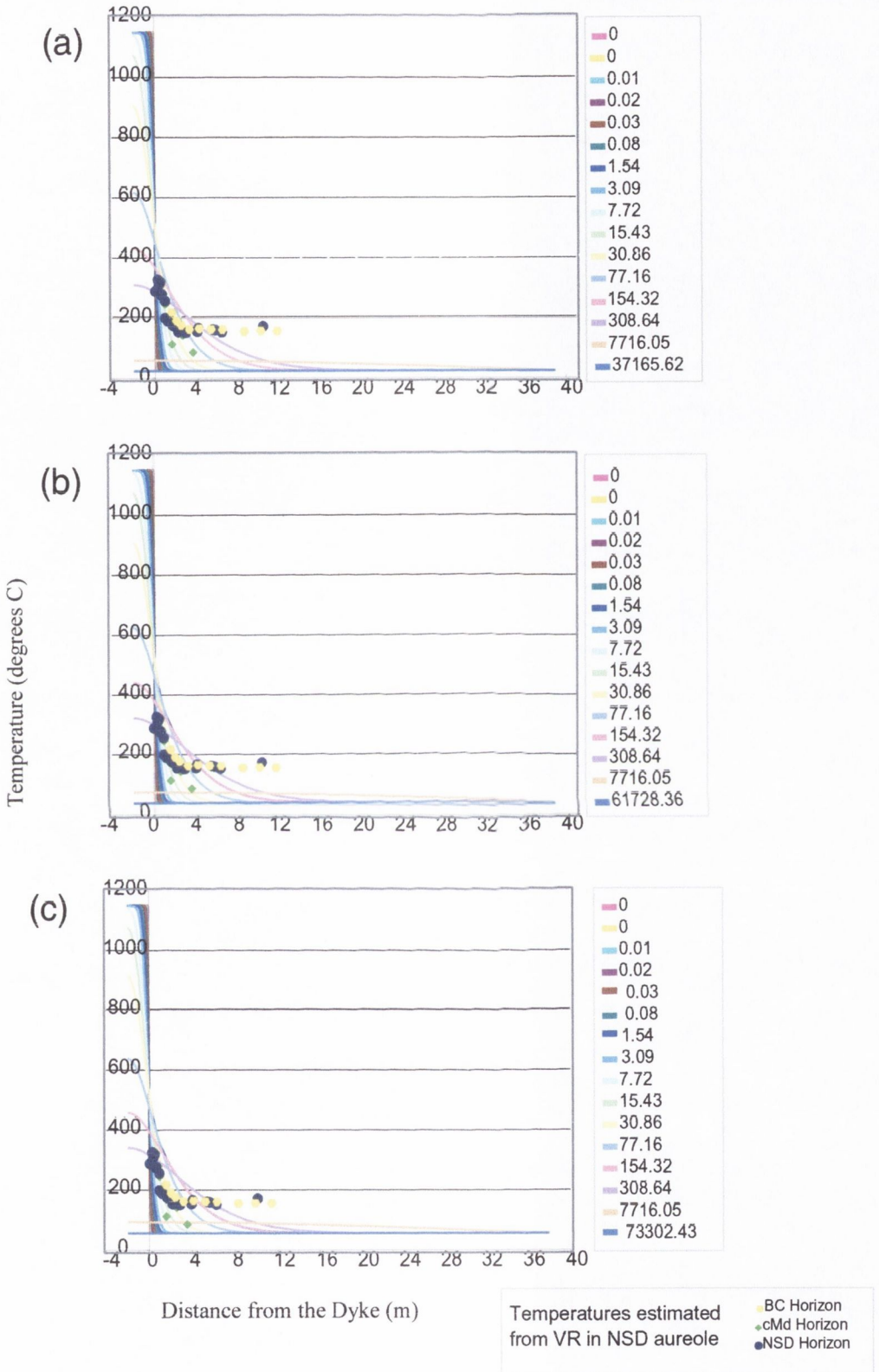

Figure 9.6(i) Modelled Temperature (T) profiles for the North Star Dyke aureole with VR estimated temperatures from the BC, cMd and NSD horizons. Assumed ambient temperature of host rocks (a) 24 ℃, (b) 37 ℃, and (c) 56 ℃. Profiles representing temperatures through the aureole at points in time (where the time is represented in days)

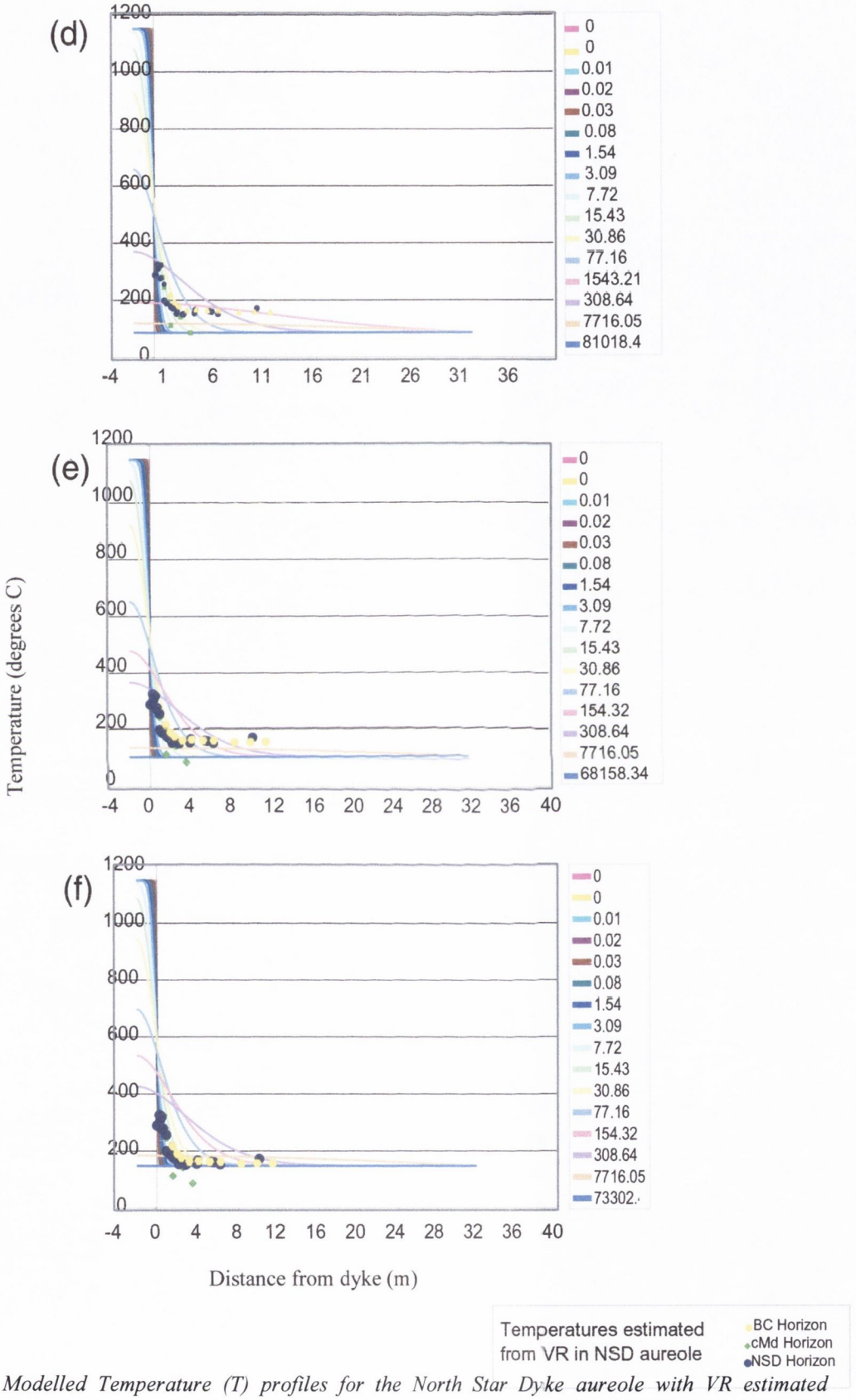

Figure 9.6(ii) Modelled Temperature (T) profiles for the North Star Dyke aureole with VR estimated temperatures from the BC, cMd and NSD horizons. Assumed ambient temperature of host rocks (d) 86, (e) 102 ℃, and (f) 148 ℃. Profiles representing temperatures through the aureole at points in time (where the time is represented in days)

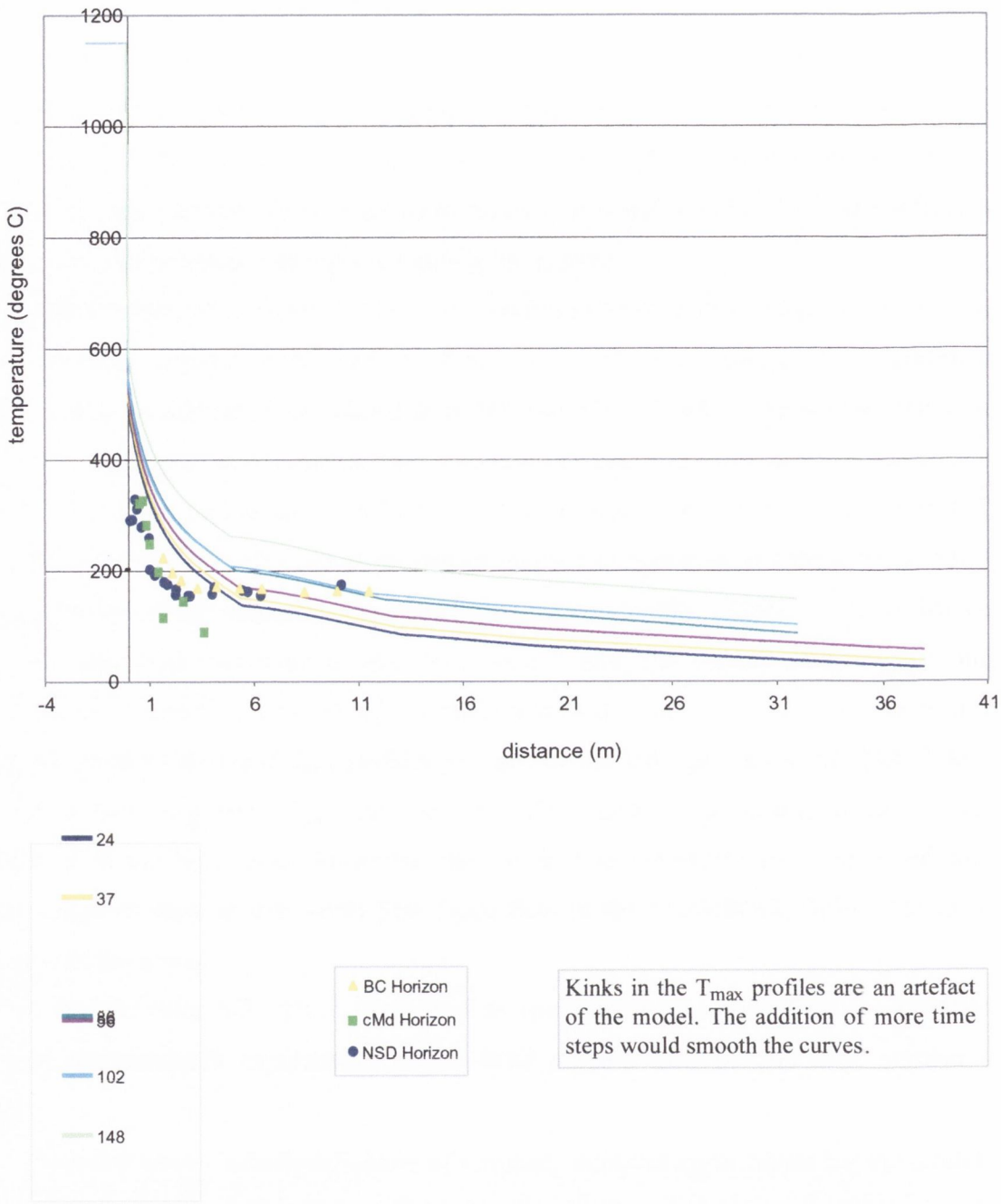

Figure 9.7 Modelled T_{max} profiles in the North Star Dyke aureole based on the various estimated ambient temperatures of host rock at time of intrusion. VR estimated temperatures from the NSD, BC, cMd horizons.

9.6 DISCUSSION

The model calculates a possible thermal evolution of the dyke aureole. The modelled profiles show similarities to the VR estimated profiles, which to some extent justifies their use for comparative purposes. The temperature disparity at <1m from the dyke contact between the modelled temperatures and VR estimates might imply that the reaction of vitrinite to elevated temperatures is not instantaneous. It might also however be a reflection on the model's imperfection as regards treating the system.

Based on the model of Delaney (1988), the maximum temperature range enjoyed at the North Star Dyke contact at the instant of intrusion was 505 – 686°C. The maximum, recorded contact temperature calculated from VR was 374 – 326°C, *c.* two-thirds the value of the model estimated maximum contact temperature. The maximum contact temperature was 288 – 326°C, *c.* half of the model estimated maximum contact temperature. Similarly for the Carrickleck Dyke the initial maximum contact temperature is estimated at 536°C (Delaney 1988) but the maximum recorded VR translates to 283 – 320°C, *c.* three fifths of the model estimated maximum contact temperature, and, the contact reflectance values translate to 265 – 295°C, *c.* one half of the calculated model maximum contact temperature.

The model predicts different T_{max} profiles for each of the settings. The North Star Dyke is predicted to have a greater T_{max} than the Carrickleck Dyke. This is due to the ambient temperature of the host rocks. However, the elevated temperatures are maintained for a greater length of time in the North Star Dyke than in the Carrickleck Dyke, due to the difference in thickness.

The fact that recorded VR values (converted to temperature) do not reflect the modelled maximum temperatures experienced in the dyke aureole may be due to a number of reasons:

- Operator error – misidentification of vitrinite, incorrect input values for the model.
- Insufficient heating duration at the contact for the vitrinite to equilibrate to the reflectance values equivalent to temperatures experienced and or estimated by the model.
- Inherent inaccuracies in Delaney's (1988) model.
- Temperature conversion equations are inaccurate or inadequate to model vitrinite values from this setting.
- Possibility of fluid in the aureole retarding reflectance values.

- Elevated initial temperatures may have forced volatiles out immediately which, were drawn to and concentrated at the contact along with any other fluids that might be present in the rock, forcing over pressure and suppression in this area.
- Heating duration and fluctuation may have hampered vitrinite reactions.

All of these reasons combined and other possibilities may be culpable for the inconsistencies between the modelled (Delaney 1988) and observed T_{max} (after VR conversion).

Barker *et al.* (1998) have compared T_{max} profiles from a number of dykes with a range of widths from various settings and compared them to four models of cooling in a host rock after dyke intrusion. The four models were computed to represent simple conduction, complex conduction, incipient convection and convection cell heat transfer (see figure 9.8). Barker *et al.* (1998) observed that within a dyke aureole the dominant style of heat flow can differ depending on the position within the aureole. They also concluded that where vitrinite reflectance decreases at the high temperatures reached near a dyke contact, this "change in vitrinite evolution may be due to the presence of water vapour and perhaps supercritical fluids changing the reaction path of the vitrinite".

The vitrinite profiles seen in this work exhibit steep slope increase in slope within *c.* 1m of the dykes and decrease in reflectance adjacent to the dykes (<0.25m), which may be a reflection of the varied dominant heat flow in the aureoles.

It is possible that the vitrinite reflectance could not conform to the model proposed by Delaney (1989) due to the presence of water vapour, and perhaps through that inference that the heat transfer particularly in the area directly adjacent to the dyke was not dominantly conductive but closer to what Barker *et al.* (1998) have referred to as complex conduction or incipient convection.

It is possible that the vitrinite reflectance could not conform to the model proposed by Delaney (1989) due to the presence of water vapour, and perhaps through that inference that the heat transfer particularly in the area directly adjacent to the dyke was not dominantly conductive but closer to what Barker *et al.* (1998) have referred to as complex conduction or incipient convection.

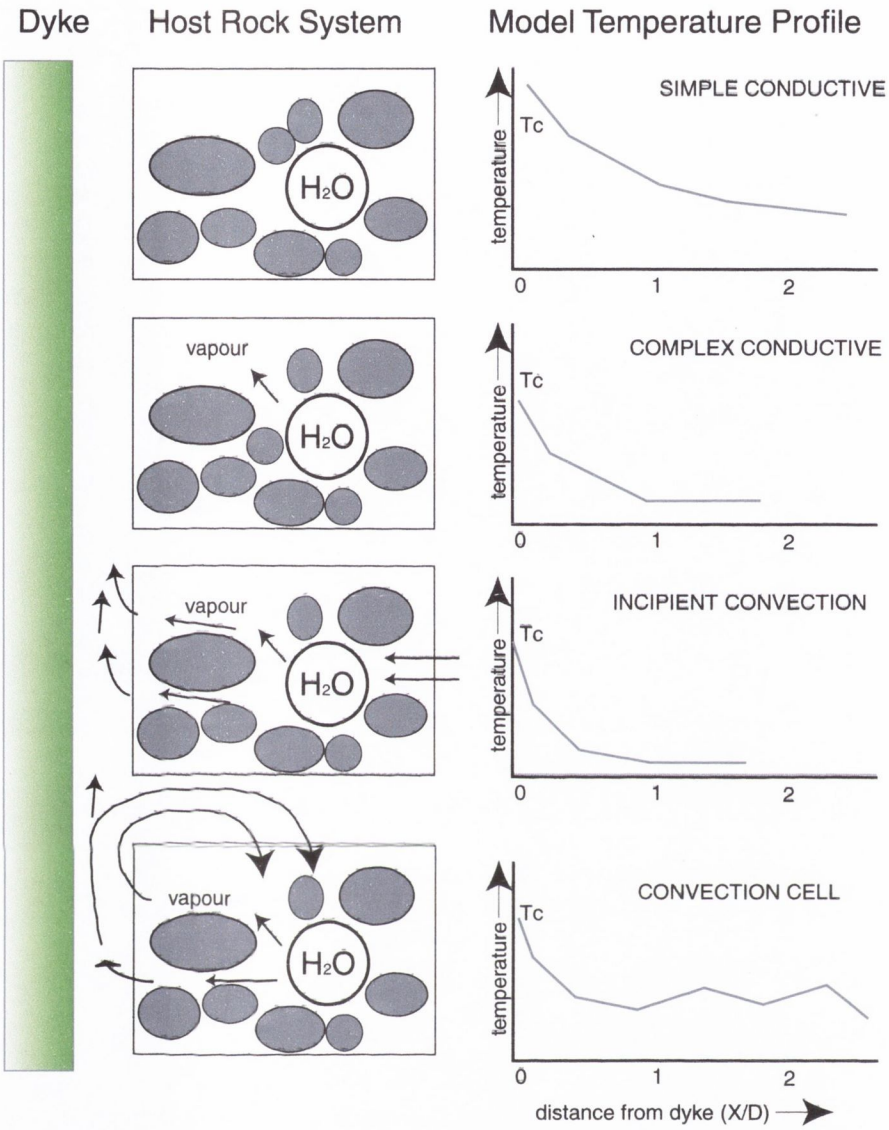

Figure 9.8 Four models of Barker (1998) describing four styles of heat transfer after the intrusion of a dyke. SIMPLE CONDUCTIVE – after intrusion pore water does not vaporise and is assumed to have negligible effect as a heat sink. COMPLEX CONDUCTIVE – after intrusion, pore water is assumed to absorb heat and vaporise. INCIPIENT CONVECTION – rapid cooling of the dyke after intrusion causes a rise of heated fluids near the dyke without the development of a recharge system. CONVECTION CELL – after intrusion a convection cell featuring the buoyant rise of heated fluids next to the dyke and recharge to the cooled fluids away from the dyke.

9.7 CONCLUSIONS

The Carrickleck Dyke must have cooled faster than the North Star Dyke.

The Carrickleck Dyke could not have sustained elevated aureole temperatures for as long as the North Star Dyke.

Modelled profiles show similarities to the VR estimated profiles.

The model of Delaney (1988), although it uses complicated algorithims and programming, cannot model the full complexities of the heat flow related to dyke intrusion, it can give estimates and ideals.

There is disparity at <1m from the dyke contact between the modelled temperatures and VR estimates. If the modelled temperatures are to be believed, then vitrinite reflectance values grossly underestimate the contact temperatures, and temperatures within 1m of the dyke. This can imply that the reaction of vitrinite to elevated temperatures is not instantaneous, or that it is being retarded in this area. It may also to some degree be due to inaccuracies in the model.

Barker *et al.* (1988) suggest that within an aureole at any one time there may be various styles of heat flow dominant in a particular region – complex or incipient conduction. Evidence from the VR relative to the models of Delaney and the idealised models of Barker et al. (1988) (figure 9.8) would suggest that this is what is occurring in the region *c.*<1m from dyke, both at Ballycastle and Carrickleck.

10 CONCLUSIONS

Vitrinite reflectance is sensitive to, and reacts quickly to increased temperatures. However, vitrinite takes longer to equilibrate at higher temperatures.

The reverse trend of VR values observed in the areas directly adjacent to the dykes may be due to a number of causes. It is thought however that they are due primarily to VR retardation, caused by overpressure created by vaporised fluids (probably connate waters) at the time of intrusion.

Vitrinite from directly adjacent to a dyke, does not register the true temperature to which it was exposed. Although longer periods of exposure to elevated temperatures results in higher reflectance values, in neither dyke aureole are there reflectance values which might be assumed to represent *c.* 1150°C (approximate temperature of intruding magma).

Temperature conversion equations reviewed and used in this work are either invalid in a dyke intrusion situation or are inadequate to relate the reflectance values of vitrinite in a dyke aureole, particularly vitrinite from less than 0.5m distance from the dyke.

Discrepancies in VR values between the NSD and cMd horizons is thought to be due to differences in the vitrinite in each horizon, *i.e.* the detrital vitrinite may be reworked, experienced varied transport conditions or it simply be different vitrinite sub types. Further work would need to be considered to confirm this.

Coal beyond the influence of the dyke yields background VR of 0.5%R_r, but vitrinite recovered from clastic sediments yield VR of 1.1-1.2%R_r. This might be interpreted in a number of ways:

4. Vitrinite recovered from the clastic lithologies might have been reworked.
5. Operator error with respect to correct identification of vitrinite
6. The obviously different depositional environments may have led to the concentrations of different starting vitrinites and thus varying maturation paths, leading to contrasting VR values

Mineralisation of the cMd coal lenses was probably a result of diagenesis.

There were fluids available to transport elements parallel to bedding, and the transport and precipitation of these elements were influenced to some extent by the dykes. It would appear that most of the changes observed occur within

The heat of dyke intrusion had a destructive effect on some of the clay minerals in the aureole mudrock horizons. Kaolinite is particularly sensitive to this, suffering a massive intensity drop in both aureoles at VR values of *c.* 1.5-1.6%R_r, equivalent to a

maximum temperature of *c.*210°C (after Barker and Goldstein 1990). This temperature is well less than half the temperature necessary to destroy the kaolinite structure using heat in the laboratory.

The illite peak decreases in intensity and 'sharpens' with proximity to the dykes.

Illite crystallite BMS are very small for each horizon, but they do present size fluctuations coincident with varying mineral intensities, and maximum sizes are observed in samples closest to the dyke.

Correlation between the VR and BMS profiles is indicative of the crystallite size being related, although not strongly, to the thermal influence of the dyke

The wave like patterns described by the intensity profiles is reminiscent of the modelled heat transfer in a dyke aureole with a convective component (Barker 1988, see chapter 9).

The influence of the post intrusion calcite fluid did not have a far reaching effect on the observed mineralogy of the aureole mudrocks.

The NSD horizon should be placed in the NC zone of the Carboniferous, straddling the Viséan-Namurian boundary.

Sporomorphs are destroyed in a dyke aureole, the destructive influence being greater with proximity to the dyke.

Only the more robust spore genera such as *Lycospora* and *Densospora* survive into the dyke contact.

Rock samples gathered in proximity to an intrusion are difficult to date using palynostratigraphy.

The thermal alteration index is showing consistency in each horizon with VR in the background samples.

AOM colour in the CQ horizon alters through a similar colour series as the spores of the CK horizon.

AOM colour alteration might also be used as a TAI, however, the material colour changes need to be calibrated.

Spore and AOM colour changes occur quite rapidly in response to the heat of intrusion.

TAI, although not as accurate or specific an indicator for lithological palaeotemperature, is more dependant on temperature than vitrinite, in this case at least.

Spore fluorescence reacts quickly, in geological time, to elevated temperatures.

Fluorescence quenching in the Carrickleck Dyke and the North Star Dyke aureole sample horizons indicates that the North Star Dyke has a more extensive aureole.

Fluorescence appears to react faster than VR to temperature, and maybe, like TAI, is also more temperature dependant than VR. More work would need to be undertaken to confirm this result. If fluorescence reacts more quickly than VR, then perhaps in the exploration operations, if the rock assessed contains material with a similar VR/spore fluorescence discrepancy it might be assumed that the core is adjacent to an intrusion and that the 'maturity' that is being assumed for this horizon is misleading.

Palynofacies analysis is a credible method for identifying lithological horizons, but can not stand alone as a tool for facies analysis and identification.

Organic material is blackened and broken down/destroyed by the elevated temperatures induced by dyke emplacement.

Palynofacies affected by the elevated temperatures of a short lived intrusive heating event is reduced to an assemblage dominated by black AOM.

Organic matter that is expose to these elevated temperatures becomes amorphous and can be mis-identified as 'mature/over-mature' AOM. This is a fact worthy of note when analysing organic residues, from samples taken for purposes of economic exploration.

Palynofacies should probably only be used as a tool to identify a sedimentary facies, when the material has been matured to VR reflectance values $\leq 1.5\%R_r$, i.e. Tysons ternary plot should not be used when VR values are $\geq 1.5\%R_r$.

The Carrickleck Dyke must have cooled faster than the North Star Dyke.

The Carrickleck Dyke could not have sustained elevated aureole temperatures for as long as the North Star Dyke.

Modelled profiles show similarities to the VR estimated profiles.

The model of Delaney (1988), although it uses complicated algorithms and programming, cannot model the full complexities of the heat flow related to dyke intrusion, it can give estimates and ideals.

There is disparity at <1m from the dyke contact between the modelled temperatures and VR estimates. If the modelled temperatures are to be believed, then vitrinite reflectance values grossly underestimate the contact temperatures, and temperatures within 1m of the dyke. This can imply that the reaction of vitrinite to elevated temperatures is not instantaneous, or that it is being retarded in this area. It may also to some degree be due to inaccuracies in the model.

Barker *et al.* (1988) suggest that within an aureole at any one time there may be various styles of heat flow dominant in a particular region – complex or incipient conduction. Evidence from the VR relative to the models of Delaney and the idealised models of Barker et al. (1988) (figure 9.8) would suggest that this is what is occurring in the region *c.*<1m from dyke, both at Ballycastle and Carrickleck.

BIBLIOGRAPHY

Abbott, M.L., 1963, *Lycopod fructifications from the Upper Freeport (No. 7) Coal in South Eastern Ohio*: Palaeontographica, **B112**, p. 93-118.

Ahn, J.H., and Peacor, D., R., 1986, *Transmission electron microscope data for rectorite: Implications for the origin and structure of 'fundamental particles'*: Clays and Clay Minerals, **34**, p. 180- 86.

Allen, P., A., and Allen, J., R., 1990, *Basin Analysis: principles and applications*, Blackwell Scientific Publications, 451 p.

Allen, P., A., Bennett, S., Cunningham, M., Carter, A., Gallagher, K., Lazzaretti, E., Galewsky, J., Densmore, A., L., Phillips, A., W.E., Naylor, D., and Solla-Hach, C., 2002, *The Post-Variscan Thermal and Denudational History of Ireland, in* Dore, A., ed., Exhumation of Atlantic Margins: London, Geological Society of London Special Publication.

Alpern, B., 1958, *Description de quelques microspores du Permo Carbonifère Français*: Revue Micropalaéontologique, **1**, p. 75-86.

Alpern, B., 1970, *Classification petrographique des constituants orgainques fossiles des roches sedimentaires*: Reçue de l'Institute Français du petrole, **25**, p. 339-383.

Alpern, B., Durand, B., Espitalie, J., and Tissot, B., 1972, *Localisation, characterisation et classification petrographique, des Substances organiques sedimentaires fossiles*, Advanced Organic Geochemistry: Oxford, Pergamon Press, p. 1-28.

Altaner, S., P., and Bethke, C., M., 1988, *Interlayer order in illite/smectite*: American Mineralogist, **73**, p. 766 - 774.

Altaner, S.P., Weiss, C.A.J., and Kirkpatrick, R.J., 1988, *Evidence from ^{29}Si NMR for the structure of mixed-layer illite/smectite clay minerals*: Nature, **331**, p. 699 - 702.

Anderton, R., Bridges, P.H., Leeder, M.R., and Sellwood, B.W., 1993, *A Dynamic Stratigraphy of the British Isles*: London, Chapman and Hall.

Andrews, H.N., and Pannell, E., 1942, *Contributions to our knowledge of American Carboniferous floras II. Lepidocarpon*: Ann. Mo. Bot. Gdn., **29**, p. 19-35.

Andrews, H.N., and Mamay, S.H., 1951, *A new American species of Bowmanites*: Botanical Gazzette, **113**, p. 158-165.

Andrews, J., E., 1987, *Jurassic clay mineral assemblages their post-depositional alteration: upper Great Estuarine Group, Scotland*: Geological Magazine, **124**, p. 261 - 271.

Artüz, S., 1957, *Die Sporae dispersae der Türkischen Steinkohle vom Zonguldak-Gebiet*: Istanbul Üniv. Fen Fak. Mecm., **B22**, p. 239-263.

Bailey, S.W., ed., 1984, *Micas*: Reviews in Mineralogy, **13**: Washington D.C., Mineralogical Society of America.

Bailey, S.W., 1988, *X-ray diffraction identification of the polytypes of mica, serpentine and chlorite*: Clays and Clay Minerals, **36**, p. 193-213.

Barker, C., E., 1983, *Influence of time on metamorphism of sedimentary organic matter in liquid-dominated geothermal systems, western North America*: Geology, **11**, p. 384 - 388.

Barker, C., E., 1988, *Geothermics of petroleum systems: Implications of the stabilisation of kerogen thermal maturation after a geologically brief heting duration at peak temperature*: United States Geological Survey Bulletin, **11870 Petroleum systems of the United States**, p. 26-29.

Barker, C., E., and Pawlewicz, M., J., 1993, *An empirical determination of the minimum number of measurements needed to estimate the mean random vitrinite reflectanc of disseminated organic matter:* Organic Geochemistry, **20**, p. 643 - 651.

Barker, C.E., and Halley, R.B., 1986, *Fluid inclusion, stable isotope, and vitrinite reflectance evidence for the thermal history of the Bone Spring Limestone, southern Guadalupe Mountains, Texas*, *in* Gautier, D.L., ed., Roles of Organic Matter in Sediment Diagenesis: Society of Economic Palaeontologists and Mineralogists Special Publication, **38**, Society of Economic Palaeontologists, p. 190-203.

Barker, C.E., and Pawlewicz, M.J., 1986, *The correlation of vitrinite reflectance with maximum temperature in humic organic matter*, *in* Bunterbath, G., and Stegena, L., eds., Paleogeothermics- evaluation of geothermal conditions in the geologic past: Lecture notes in Earth sciences, **5**: Berlin Heidelberg, Springer-Verlag (New York), p. 79-94.

Barker, C.E., and Goldstein, R.H., 1990, *Fluid-inclusion techniques for determining maximum temperature in calcite and its comparison to vitrinite*: Geology, **18**, p. 1003-1006.

Batten, D.J., 1973, *Use of palynologic assemblage types in Wealdon correlation*: Paleontology, **16**, p. 1-40.

Batten, D.J., 1980, *Use of transmitted light microscopy of sedimentary organic matter for evaluation of hydrocarbon source potential*: Proceedings of the IV International Palynological Conference, p. 589-594.

Batten, D.J., 1981, *Palynofacies, organic maturation and source potential for petroleum, in* J.Brooks, ed., Organic maturation studies and fossil fuel exploration, **1**, Academic Press, p. 201-.

Batten, D.J., 1982a, *Palynofacies, palaeoenvironments and petroleum*: Journal of Micropalaeontology, **1**, p. 107-114.

Batten, D.J., 1982b, *Palynofacies and salinity in the Purbeck and Weladen of Southern England, in* Banner, F.T., and Lord, A.R., eds., Aspects of Micropalaeontology, **1**: London, Allen and Unwin, p. 278-308.

Batten, D.J., 1996, *Chapter 26A, Palynofacies and palaeoenvironmental interpretation, in* Jansonius, J., and McGregor, D.C., eds., Palynology : Principles and applications, new directions, other applications and floral history: Palynology: Principles and Applications, **3**: Salt Lake City, Utah, AASP foundation, p. 1011 - 1064.

Batten, D.J., 1999, *Palynofacies analysis, in* Jones, T.P., and Rowe, N.P., eds., Fossil Plants and Spores; modern techniques, **1**: London, Geological Society, p. 194 -198.

Baxter, R.W., 1950, *Peltastrobus reedae: a new sphenopsid cone from the Pennsylvanian of Indiana*: Botanical Gazzette, **112**, p. 174-182.

Bayliss, G., 1974, *Geochemical Parameers reflecting geothermal diagenesis; relationships between organic matter types (kerogen) and petroleum.*: 8th Annual meeting of the American Association of Stratigraphic Palynologists, p. 2.

Bayliss, G.S., 1975, *Chemical changes attendant with thermal alteration of organic materials following deposition*: American Association of Stratigraphic Palynologists, **8th annual meeting, Houston**.

Beardsmore, G.R., and Cull, J.P., 2001, *Crustal Heat Flow: A guide to measurement and modelling*: Cambridge, Cambridge University Press, 324 p.

Berner, R.A., 1971, *Principles of Chemical Sedimentation*: NewYork, McGraw Hill, 240 p.

Berry, W., 1937, *Spores from the Pennington Coal, Rhea county, Tennessee*: American Midl. Nat., **18**, p. 155-160.

Bethke, C.M., 1986, *Inverse hydrologic analysis of the distribution and origin of Gulf Coast-type geopressured zones*: Journal of Geophysical Research, **91**, p. 6535 - 6545.

Bharadwaj, D.C., 1957a, *The Palynological investigations of the Saar coals*: Palaeontographica, **B101**, p. 73-101.

Bharadwaj, D.C., 1957b, *The spore flora of the Velener Schichten (Lower Westphalian D) in the Ruhr Coal measures*: Palaeontographica, **B102**, p. 110-138.

Bharadwaj, D.C., 1958, *On Porostrobus zeilleri Nathorst and its spores with remarks on the systematic position of P. bennholdi Bode and the phyllogeny of densosporites Berry*: Palaeobotanist, **7**, p. 67-75.

Bharadwaj, D.C., and Venkatachala, B.S., 1961, *Spore assemblage out of a Lower Carboniferous shale from Spitsbergen*: Palaeobotanist, **10**, p. 18-47.

Bishop, A.N., and Abbott, G.D., 1995, *Vitrinite reflectance and molecular geochemistry of Jurassic sediments: the influence of heating by Tertiary dykes (northwest Scotland)*: Organic Geochemistry, **22**, p. 165-177.

Bonijoly, M., Oberlin, M., and Oberlin, A., 1982, *A possible mechanism for natural graphite formation*: International Journal of Coal Geology, **1**, p. 283 - 312.

Bowen, N.L., 1915, *Crystallisation-differentiation in silicate liquids*: American Journal of Science, **39**, p. 175-191.

Bradford, M.R., 1977, *The distribution and paleoecology of the dinoflagellate cysts in the Persian Gulf and adjacent regions*: Ph.D. unpublished thesis, University of Saskatchewan, Saskatchewan, 555 p.

Brindley, G.W., and Brown, G., eds., 1980, *Crystal Structures of Clay Minerals and their X-Ray Identification*: Mineralogical Society, Monograph No. 5, **5**: London, Mineralogical Society, 495 p.

Brooks, J., 1981a, *Organic maturation of sedimentary organic matter and petroleum exploration: a review*, *in* Brooks, J., ed., Organic maturation and fossil fuel Exploration: London, Academic Press, p. 1-37.

Brooks, J., 1981b, *Organic Maturation Studies and Fossil Fuel Exploration*: London, Academic Press, 441 p.

Bruce, C.H., 1984, *Smectite dehydration, its relation to structural development and hydrocarbon accumulation in northern Gulf of Mexico Basin*: American Association of Petroleum Geologists Bulletin, **68**, p. 673 - 683.

Buiskool Toxopeus, J.M.A., 1983, *Selection criteria for the use of vitrinite reflectance as a maturity tool, in* Brooks, J., ed., Petroleum Geochemistry and exploration of Europe, **2**: Oxford, Blackwell Scientific publications, p. 295 - 307.

Bujak, J.P., Barss, M.S., and Williams, G.L., 1977a, *Offshore East Canadas organic type and colour and hydrocarbon potential*: The Oil and Gas Journal, **75**, p. 198-201.

Bujak, J.P., Barss, M.S., and Williams, G.L., 1977b, *Organic type and colour and hydrocarbon potential*: The Oil and Gas Journal, **75**, p. 96-100.

Burgess, J.D., 1974, *Microscopic examination of Kerogen (dispersed organic matter) in petroleum exploration*: Geological Society of America, Special paper, **153**, p. 19-30.

Burnham, A.K., and Sweeney, J.J., 1989, *A chemical kinetic model of vitrinite maturation and reflectance*: Geochimica et Cosmochimica acta, **53**, p. 2649-2657.

Burst, J.F., 1969, *Diagenesis of Gulf Coast clay sediments and its possible relation to petroleum migration*: American Association of Petroleum Geologists Bulletin, **53**, p. 73 - 93.

Bustin, R.M., 1983, *Heating during thrust faulting in the Rocky Mountains; friction or fiction?*: Tectonophysics, **95**, p. 309-328.

Bustin, R.M., 1988, *Sedimentology and characteristics of dispersed orgainc matter in Tertiary Niger Delta: origin of source rocks in a deltaic environment.*: American Association of Petroleum Geologists Bulletin, **72**, p. 277-298.

Bustin, R.M., Nouzaud, J.-N., and Ross, J.V., 1995a, *Natural graphitization of anthracite: experimental considerations*: Carbon, **33**, p. 679 - 691.

Bustin, R.M., Ross, J.V., and Nouzaud, J.-N., 1995b, *Mechanisms of graphite formation from kerogen: experimental evidence*: International Journal of Coal Geology, **28**.

Butterworth, M.A., and Williams, R.W., 1958, *The small spore floras of coals in the Limestone Coal group of the Lower Carboniferous of Scotland*: Transactions of the Royal Society of Edinburgh, **63**, p. 353-392.

Butterworth, M.A., Jansonious, J., Smith, A.H.V., and F.L., S., 1964, *Densosporites (berry) Potonie and Kremp and related genera*: C. r. congr. Strat. Geol. carbonif. Paris (1963), **1**, p. 1049-1057.

Carr, A.D., 2000, *Suppression and retardation of vitrinite reflectance, part 1. Formation and significance for hydrocarbon generation*: Journal of Petroleum Geology, **23**, p. 313 - 343.

Carslaw, H.A., and Jaeger, J.C., 1959, *Conduction of Heat in Solids*, Oxford University Press.

Carson, B., 1995, *Palynostratigraphy, palynofacies and hydrocarbon source potential of the Lower Carbonifeorus in two Boreholes from the Baltic Island of Rügen, Germany*: Ph.D. thesis, Trinity College Dublin, Dublin, 185 p.

Chaloner, W.G., 1953a, *On the megaspores of four species of Lepidostrobus*: Ann. Bot., **17**, p. 263 - 293.

Chaloner, W.G., 1953b, *A new species of Lepidostrobus containing unusual spores*: Geological Magazine, **90**, p. 97-110.

Chaloner, W.G., 1958, *A Carboniferous Selaginellites with Densosporites microspores*: Palaeontology, **1**.

Claret, J., Jardine, S., and Robert, P., 1981, *La Diversite des roches meres petrolieres: aspects geologiques et implications economiques a partir de quatre exemples*: Bulletin des Centres Recherche Exploration-Production Elf Aquitaine, **5**, p. 383-417.

Clarke, R.F.A., and Verdier, J.P., 1967, *An investigation of microplankton assemblages from the chalk of the Isle of Wight.*: Verhandelingen der Koninklijke Nederlandsche Akademie van Wetenschappen, Afdeeling Naturkunde, Series 1, **24**, p. 1-96.

Clayton, G., Coquel, R., Doubinger, J., Gueinn, K.J., Loboziak, S., Owens, B., and Streel, M., 1977, *Carboniferous Miospores of Western Europe: illustration and zonation. Report of commission internationale deMicroflore du paleozoique working group on Carboniferous stratigraphical palynology*: Mededelingen Rijks Geolische Dienst, **29**, p. 1-71.

Clayton, G., Haughey, N., Sevastopulo, G., Dimitrius , and Burnett, R., 1989, *Thermal maturation levels in the Devonian and Carboniferous rocks of Ireland.*

Clayton, G., Manger, W., L., and Owens, B., 1998, *Mississippian (Lower Carboniferous) miospores from the Cuyahoga and Logan Formation of northeastern Ohio, USA*: Journal of Micropalaeontology, **17**, p. 183-191.

Collins, A., 1990, *The 1-10 Spore Colour Index (SCI): a universally applicable colour maturation scale based on graded, picked, palynomorphs.*: Mededelingen Rijks Geologische Deinst, **45**, p. 39-47.

Combaz, A., 1964, *Les Palynofacies*: Revue de Micropaleontologie, **7**, p. 205-218.

Connan, J., 1974, *Time-temperature relation in oil genesis*: American Association of Petroleum Geologists Bulletin, **58**, p. 2516 - 2521.

Cook, A.C., Murchison, D.G., and Scott, E., 1972, *A British meta-anthracitic coal of Devonian age*: Geological Journal, **8**, p. 83-94.

Correia, M., 1971, *Diagenesis of sporopollenin and other comparable organic substances: Application to hydrocarbon research, in* Brooks, J., Grant, P.R., Muir, M., van Gijzel, P., and Shaw, G., eds., Sporopollenin; proceedings of a Symposium held at the Geology Dept., Imperial College London, 23-25 Sept., 1970: London, Academic Press.

Cox, K.G., Bell, J.D., and Pankhurst, R.J., 1979, *The Interpretation of igneous rocks*, **1**, Allan and Unwin.

Cramer, F.H., Diez, M., and C.R., D., 1972, *Early Paleozoic palynomorph provinces and paleoclimate and their spatial arrangement: acritarchs*: Paleontographica, **B138**, p. 107-188.

Creaney, S., 1989, *Reaction of organic material to progresive geological heating, in* Naeser, N.D., and McCulloh, T.H., eds., Thermal History of Sedimentary Basins: Methods and Case histories: New York, Springer Verlag, p. 37-52.

Dalla Torre, M., Ferreiro Mählmann, R., and Ernst, W.G., 1997, *Experimental study on the pressure dependence of vitrinite maturation*: Geochimica Cosmochimica Acta, **61**, p. 2921-2928.

Davies, E.H., 1985, *The miospore and dinoflagellate cyst Oppel zonation of the Lias, Portugal*: Palynology, **9**, p. 105-132.

Davies, J.R., McNestry, A., and Waters, R.A., 1991, *Paleoenvironments and palynofacies of a pulsed transgression: the late Devonian and early*

Dinantian (Lower Carboniferous) rocks of southeast Wales: Geological Magazine, **128**, p. 355-380.

de Vernal, A., Bilodeau, G., Hillaire-Marcel, C., and Kassou, N., 1992, *Quantitative assessment of carbonate dissolution in marine sediments from foraminifer linings versus shell ratios: Davis Strait, northwest North Atlantic.*: Geology, **20**, p. 527-530.

Decommer, H., 1982, *Étude palynoplanctologique et cadre sedimentologique du Jurassique et du Cretace du nord de la France*: Annales de la societe Geologique du Nord, **101**, p. 161-176.

Deer, W.A., Howie, R.A., and Zussman, J., 1982, *Framework Silicates*: Rock Forming Minerals, **4**: London, Longmans, Green and Co., 435 p.

Delaney, P., T., and Pollard, D., D., 1982, *Solidification of Basaltic Magma during flow in a dike*: American Journal of Science, **282**, p. 856-885.

Delaney, P., T., 1987, *Heat transfer theory applied to mafic dyke intrusions, in "Mafic Dyke swarms" ed.s H.C. Halls and W.F. Fahzig*: Geological Association of Canada, Special Paper, **34**, p. 31-46.

Delaney, P., T., 1988, *Fortran 77 programs for Conductive cooling of dikes with temperature - dependant thermal properties and heat of crystallization*: Computers and Geosciences, **14**, p. 181 - 212.

Demongodin, L., Pinoteau, B., Vasseur, G., and Gable, R., 1991, *Thermal conductivity and well logs: a case study in the Paris Basin*: Geophysical Journal International, **105**, p. 675-691.

Dettmann, M.E., 1963, *Upper Mesozoic microfloras from Southeastern Australia*: Proceedings of the Royal Society of Victoria, **77**, p. 1-148.

Drits, V.A., Eberl, D.D., and Srodo, J., 1998, *XRD measurement of mean thickness, thickness distribution and strain for illite-smectite crystallites by the Bertaut-Warren-Averbach technique*: Clays and Clay Minerals, **46**, p. 38-50.

Durand, B., ed., 1980a, *Kerogen: Insoluble organic matter from sedimentary rocks*, **1**: Paris, Editions Technip.

Durand, B., 1980b, *Sedimentary organic matter and kerogen. Definition and quantitative importance of kerogen*, *in* Durand, B., ed., Kerogen: Insoluble organic matter from sedimentary rocks, **1**: Paris, Editions Technip, p. 13-34.

Dybová, S., and Jachowicz, A., 1957a, *Microspores of the Upper Silesian coal measures*: Prace. Inst. Geol., **23**, p. 1-328.

Dybová, S., and Jachowicz, A., 1957b, *Microspore zones of the Carboniferous of the Ostrava-karvina region*: Sborn. Ustr. Ust. geol., **24**, p. 167-205.

Eberl, D.D., and Blum, A., 1993, *Illite crystallite thickness by X-ray diffraction, in* Reynolds , R.C.J., and Walker, J.R., eds., CMS Workshop Lectures, **5a**, p. 124 - 149.

Eberl, D.D., Drits, V.A., Srodon, J., and Nüesch, R., 1996, *MUDASTER: A program for calculating crystallite size distributions and strain from the shapes of X-ray diffraction peaks*:: U.S. Geological Survey, p. 55.

Eberl, D.D., Nüesch, R., Sucha, V., and Tsipursky, S., 1998, *Measurement of fundamental illite particle thicknesses by X-ray diffraction using PVP-10 intercalation*: Clays and Clay Minerals, **46**, p. 89-87.

Emeleus, C., and Preston, J., 1969, *Field Excursion Guide to the Volcanic rocks of Ireland*: Belfast, Doorman and Sons.

Erren, H., and Bredewout, J.W., 1991, *Model calculations on intrusive cooling and related coalification of the Peel-Erkelenz coalfield (The Netherlands and Germany)*: Geologie en Mijnbouw, **70**, p. 253 - 252.

Esposito, K.J., and Whitney, G., 1995, *Thermal Effects of Thin Igneous Intrusions on Diagenetic Reactions in a Tertiary Basin of Southwestern Washington.*: U.S. Geological Survey Bulletin 2085-C.

Evitt, W.R., 1963a, *A discussion and proposals concerning fossil dinoflagellates, hystrichospheres and acritarchs, I and II*: Proceedings of the National Academy of Sciences, Washington, **49**, p. 158-164.

Evitt, W.R., 1963b, *Occurrence of freshwater alga Pediastrum in Cretaceous marine sediments*: American Journal of Science, **261**, p. 890-893.

Felix, C.F., 1954, *Some American arborescent lycopod fructifications*: Ann. Mo. Bot. Gdn., **41**, p. 351-394.

Fernandez, P., M. C., 2000, *Investigation of the Stratigraphy, maturation and source-rock potential of Carboniferous Black Shales in the Dublin Basin*: Ph.D. thesis, Trinity College, Dublin, 218 (plus appendices) p.

Freed, R.L., and Peacor, D., R., 1992, *Diagenesis and the formation of authigenic illite rich I/S crystals in Gulf Coast shales: TEM study of clay seperates*: Journal of Sedimentary Petrology, **63**, p. 220 - 234.

Frey, M., 1987a, *Very low grade metamorphism of clastic sedimentary rocks, in* Frey, M., ed., Low Temperature Metamorphism: Glasgow, Blackie and son, p. 9-58.

Frey, M., ed., 1987b, *Low Temperature Metamorphism*: Glasgow and London; New York, Blackie and son, Great Britain; Chapman and Hall, USA, 351 p.

Frey, M., and Robinson, D., eds., 1999, *Low Grade Metamorphism*: Cambridge, Blackwell Science, 313 p.

Furlong, K.P., Hansen, R.B., and Bowers, J.R., 1991, *Modeling Thermal Regimes, in* Kerrick, D.M., ed., Contact Metamorphism, reviews in mineralogy, Mineralogical Society of America, **26**: Washington D.C., Kerrick, D.M., p. 437 - 505.

Giancoli, D.C., 1984, *General Physics*: London, Prentice/Hall international, 962 p.

Gibbs, R.J., 1965, *Error due to segragation in quantitative clay mineral x-ray diffraction mounting techniques.*: American Mineralogist, **50**, p. 741-751.

Gilliam, T.M., and Morgan, I.L., 1987, *Shale: Measurement of thermal properties*: ORNL/TM-10499: Oak Ridge National Laboratory.

Goodhue, R., J.D., 1996, *A Palynofacies, geochemical and maturation investigation of the Namurian rocks of County Clare*: Ph.D. thesis, Trinity College, Dublin, 168 p.

Goodhue, R., J.D. , and Clayton, G., 1998, *Organic maturation levels, thermal history and hydrocarbon source potential of the Namurian rocks of the Clare Basin, Ireland*: Marine and Petroleum Geology, **16**, p. 667 - 675.

Gray, J., and Boucout, A.J., 1975, *Color changes in pollen and spores: A review*: Geological Society of America Bulletin, **86**, p. 1019-1033.

Grayson, J.F., 1981, *Microspectrofluorescence and kerogen liquefaction, in* Brooks, J., ed., Organic Maturation Studies and Fossil Fuel Exploration: London, ISBN 0 - 12 - 135760 - 0, Publ Academic Press, p. 343 - 349.

Grebe, H., 1971, *A recommended terminology and descriptive method for spores*: C.I.M.P. - Microfossiles Organiques du Paleozoique, Les Spores, **4**, p. 1-34.

Gregory, W., A., Chinn, E., W., Sassein, R., and Hart, G., F., 1991, *Fluorescent microscopy of particulate organic matter: Sparta Formation and Wilcox Group, South Central Louisiana*: Organic Geochemistry, **17**, p. 1-9.

Gretener, P.E., and Curtis, C.D., 1982, *Role of temperature and time on organic metamorphism*: American Association of Petroleum Geologists Bulletin, **66**, p. 1124 - 1149.

Grieve, D.A., 1991, *Biaxial vitrinite reflectance in coals of the Elk Valley, southeastern British Colombia, Canada*: International Journal of Coal Geology, **19**, p. 185 - 200.

Grim, R.E., Bray, R.H., and Bradley, R.F., 1937, *The mica in argillaceous sediments*: American Mineralogist, **22**, p. 813 - 829.

Guennel, G.K., 1958, *Miospore analysis of the Pottsville Coals of Indiana*: Bulletin of the Geological Survey of Indiana, **13**, p. 101.

Guggenheim, S., Bain, D., C., Bergaya, F., Brigatti, M., F., Drits, V., A., Eberl, D., D., Formoso, M., L.L., Galan, E., Merriman, R., J., Peacor, D., R., Stanjek, H., and Watanabe, T., 2002, *Report of the Association Internationale Pour L'Etude des Argiles (AIPEA) Nomenclature Committee for 2001: Order, disorder and crystallinity in phyllosilicates and the use of the "crystallinity index"*: Clays and Clay Minerals, **50**, p. 406 - 409.

Habib, D., 1979, *Sedimentology of palynomorphs and palynodebris ion Cretaceous carbonaceous facies south of Vigo seamount., in* Sibuet, J.C., and Ryan, W.B.F., eds., Deep Drilling results in the Atlantic Ocean: Continentla margins and Paleoenvironments, American Geophysical Union, Maurice Ewing series, **47**: Washington D.C., US Government printing Office, p. 451-467.

Habib, D., and Miller, J.A., 1989, *Dinoflagellate species and organic facies evidence of marine transgression and regressio in the Atlantic coastal plain*: Paleogeography, Paleoclimatology and palaeoecology, **74**, p. 23-47.

Hacquebard, P.A., 1957, *Plant spores in coal from the Horton group (Mississippian) of Nova Scotia*: Micropaleontology, **3**, p. 301-324.

Hacquebard, P.A., and Barss, M.S., 1957, *A Carboniferous spore assemblage, in coal from the South Nahanni River area, Northwest Territories*: Bulletin of the Geological Survey of Canada, **40**, p. 1-63.

Hanley, E.J., Dewitt, D.P., and Roy, R.F., 1978, *The thermal diffusivity of eight well-characterized rocks for the temperature range 300-1000K*: Engineering Geology, **12**, p. 31-47.

Hart, G., F., 1986, *Origin and classification of organic matter in clastic systems*: Palynology, **10**, p. 1-23.

Hartung, W., 1933, *Die Sporenverhältnisse der Calamariaceen*: Arb. Inst. Paläobot., **3**, p. 95-149.

Hayes, J.B., 1970, *Polytypism of chlorite in sedimentary rocks*: Clays and Clay Minerals, **18**, p. 285-306.

Hendricks, S.B., and Teller, E., 1942, *X-ray interference in partially ordered layer lattices*: Journal of Chemical Physics, **10**, p. 147 - 167.

Hibbard, M.J., 1993, *Petrography to Petrogenesis*, Prentice Hall.

Higgs, K., 1975, *Upper Devonian and Lower Carboniferous miospore assemblages from Hook Head, County Wexford, Ireland*: Micropaleontology, **3**, p. 301 - 324.

Higgs, K., and Russell, K.J., 1981, *Upper Devonian microfloras from Southeast Iveragh, County Kerry, Ireland*: Geoloical Survey of Ireland Bulletin, **3**, p. 17-50.

Higgs, K., Clayton, G., and Keegan, J., 1988, *Stratigraphic and systematic palynology of the Tournasian rocks of Ireland.*: Geological survey of Ireland Special Paper, **7**, p. 1-82.

Hillier, S., and Marshall, J., 1988, *A rapid technique to make polished thin sections of sedimentary organic matter concentrates*: Journal of Sedimentary Petrology, **58**, p. 754 - 755.

Hoffmeister, W.S., Staplin, F.L., and Malloy, R.E., 1955, *Mississippian plant spores from the Hardinsburg formation of Illinois and Kentucky*: Journal of Palaeontology, **29**, p. 372-399.

Hood, A., Gutjahr, C.C.M., and Heacock, R.L., 1975, *Organic metamorphism and the generation of Petroleum*: The American Association of Petroleum Geologists Bulletin, **59**, p. 986 - 996.

Horst, U., 1943, *Mikrostratigraphischer Beitrag zum Vergleich des Namur von West Oberschlesien und Mahrisch-Ostrau. Die Mega- und Mikrosporen der hauptsachlichen Floze beider Riviere.*, Techn. Hochsch. Berlin, Berlin.

Horst, U., 1955, *Die sporae dispersae des Namurs von Westoberschliesen und Mahrisch-Ostrau*: Paleontographica, **B98**, p. 137-236.

Hoskins, J.H., and Abbott, M.L., 1956, *Selaginellites crassicinctus, a new species from the Desmoinesian Series of Kansas*: American Journal of Botany, **43**, p. 36-46.

Houseknecht, D., W., and Weesner, C., M.B., 1997, *Rotational reflectance of dispersed vitrinite from the Arkoma Basin*: Organic Geochemistry, **26**, p. 191 - 206.

Hower, J., and Mowatt, T.C., 1966, *The mineralogy of illite and mixed-layer illite/montmorillonite*: American Mineralogist, **51**, p. 825-854.

Hower, J., Eslinger, E.V., Hower, M.E., and Perry, E.A., 1976, *Mechanism of burial metamorphism of argillaceous sediments*: Geological Society of America Bulletin, **87**, p. 725 - 737.

Huang, W.-L., 1996, *Experimental study of vitrinite maturation: effects of temperature, time, pressure, water and hydrogen index*: Organic Geochemistry, **24**, p. 233-241.

Hughes, C.J., 1982, *Chapter 6 Physical properties and chemistry of magmas, in* Hughes, C.J., ed., Igneous petrology: Developments in Petrology, **7**: Amsterdam, Elsevier Scientific Publishing Company, p. 551.

Hughes, N.F., and Playford, G., 1961, *Palynological reconnaissance of the Lower Carboniferous of Spitsbergen*: Micropaleontology, **7**, p. 27-44.

Hyde, H.A., and Williams, D.W., 1944, *Right word*: Pollen Anal. Circ., **8**, p. 6.

Ibrahim, A.C., 1932, *Beschreibung von sporenformen aus Flöz Ägir; in Potonié, Sporenformen aus den Flözen Ägir un Bismarck des Ruhr gebietes*: Neues Jb. Miner. Geol. Palaont. BeilBd., **67**, p. 447-449.

Ibrahim, A.C., 1933, *Sporenformen des Ägirhorizontes des Ruhrreviers.*: Neues Jahrbuch Miner. Geol. Palaont. BeilBd., **67**, p. 447-449.

ICCP, 1998, *The new vitrinite classification (ICCP System 1994)*: Fuel, **77**, p. 349 - 358.

Ischenko, A.M., 1958, *Spore-pollen analysis of the Lower Carboniferous sediments of the Dneiper-Donets Basin*: Akad. Nauk. Ukr. S.S.S.R. Trudy Inst. geol. Nauk. Ser. Strat. Palaeont., **11**, p. 1-185.

Jackson, J.S., 1955, *The Carboniferous succession of the Kingscourt outlier with notes on the Permo-Triass*: Ph.D. thesis, Trinity College, Dublin.

Jackson, J.S., 1965, *The Upper Carboniferous (Namurian & Westphalian) of Kingscourt, Ireland*: Scientific Proceedings of the Royal Dublin Society, Series A, **2, No. 8**: Dublin, The Royal Dublin Society, Balls Bridge, 152 p.

Jacob, H., 1964, *Neue Erkenntnisse auf dem Gebiet der Lumineszenzmikroskopie fossiler Brennstoffe*: Fortschritte Geol. Rheinland und Westfalen., **12**, p. 569 - 588.

Jansonious, J., 1962, *Palynology of Permian and Triassic sediments, Peace River area, Western Canada*: Palaeontographica, **B110**, p. 35-98.

Johnsson, M., J., Howell, D., G., and Bird, K., J., 1993, *Thermal maturity patterns in Alaska: implications for tectonic evolution and hydrocarbon potential*: The American Association of Petroleum Geologists Bulletin, **77**, p. 1874 - 1903.

Johnston, T.P., and Rundle, C.C., 1993, *K-Ar results from dolerite in Co. Fermanagh Northern Ireland: Evidence for Late Cretaceous Igneous activity.*: Irish Journal of Earth Sciences, **12**, p. 65-74.

Jones, R.W., and Edison, T.A., 1978, *Microscopic observations of kerogen related to geochemical parameters with emphasis on thermal maturation, in* Oltz, D.F., ed., Low Temperature metamorphism of kerogens and clay minerals. The Pacific Section. SEPM.: The pacific Section: SEPM: Los Angeles, Society of Economic Palaeontologists and Mineralogists, p. 1-12.

Karweil, J., 1955, *The metamorphisis of coals from the stand point of physical chemistry*: Z. Dt. Geol., **107**, p. 132-139.

Kisch, H.J., 1969, *Coal-rank and burial-metamorphic mineral facies*: Advances in organic Geochemistry: Oxford, Pergamon Press, Oxford, 407 - 424 p.

Kisch, H.J., 1983, *Mineralogy an petrology of burial diagenesis (burial metamorphism) and incipient metamorphism in clastic rocks, in* Larsen, G., and G.V., C., eds., Diagenesis in Sedimemts and Sedimentary Rocks 2: Amsterdam, Elsevier, p. 289-493 and 513-541.

Kisch, H.J., 1987, *Correlation between indicators of very low grade metamorphism, in* Frey, M., ed., Low Temperature Metamorphism: Glasgow-London, Blackie, p. 227-300.

Klaus, W., 1960, *Sporen der karnischen Stufe der ostalpinen Trias*: Jb. geol. Reichsanst. Wien, **5**, p. 107-183.

Knox, E.M., 1948, *The microspores in coals of the Limestone Coal Group in Scotland.*: Transactions of the Institution of Mineral Engineers of London, **107**, p. 155-163.

Knox, E.M., 1950, *The spores Lycopodium, Phylloglossum, Selaginella and Isoëtes and their value in the study of microfossils of Palaeozoic age*: Transactions of the Botanical Society of Edinburgh, **5**, p. 211-357.

Koch, J., and Schellschmidt, R., 2001, *02/00750: Vitrinite reflectance as a function of temperature - relation between coalification and temperature of espcially coal formation*: Fuel and Energy Abstracts.

Komarek, J., and Morga, R., 2002, *Relationship between the maximum and the random reflectance of vitrinite for coal from the Upper Silesian Coal Basin (Poland)*: Fuel, **81**, p. 969 - 971.

Kosanke, R.M., 1950, *Pennsylvanian spores of Illinois and their use in correlation*: Bulletin of the Illinois Geological Survey, **74**, p. 1-128.

Lam, K., and Porter, R., 1977, *The distribution of palynomorphs in the Jurassic of the Brora outlier, Northeastern Scotland*: Journal of the Geological Society of London, **134**, p. 45-55.

Landais, P., Rochdi, A., Largeau, C., and Derenne, S., 1983, *Chemical characterisation of torbanites by transmission micro-FTIR spectroscopy: origin and extent of compositional heterogeneiities*: Geochimica et Cosmochimica Acta, **57**, p. 2529-2539.

Levine, J., Ross, and Davis, A., 1984, *Optical anisotropy of coals as an indicator of tectonic deformation, Broad Top Coal Field, Pennsylvania*: Geological Society of America Special Bulletin, **95**, p. 100 - 108.

Lofgren, G., 1980, *Experimental studies on the dynamic crystallization of silicate melts*, *in* Hargaves, ed., Physics of magmatic processes, Princeton University Press, p. 478-551.

Long, G., and Neglia, S., 1968, *Composition du l'eau interstitielle des argilles des minéraux argileaux*: Revue de l'Institut Français du Pétrole, **23**, p. 53-69.

Loose, F., 1932, *Beschreibung von Sporenformen aus Flöz Bismarck*, *in* Potonié, R., ed., Sporenformen aus den Flözen Ägir und Bismarck des Ruhrgebeites, **69**, p. 449-452.

Loose, F., 1934, *Sporenformen aus dem Flöz Bismarck des Ruhrgebeites*: Arb. Inst. Palaobot. Berlin, **4**, p. 127-164.

Lopatin, N.W., 1971, *Temperature and geological time as factors in coalification*: Akademia Nauk SSSR Izvestiya Ser. Geologischeskaya, **3**, p. 95-106.

Lorente, M.A., 1990, *Textural characteristics of organic matter in several subenvironments of the Orinoco Upper Delta*: Geologie en Mijnbouw, **69**, p. 263-278.

Love, L.G., 1960, *Assemblags of small spores from the lower Oil-Shale Group of Scotland*: Proceedings of the Royal Society of Edinburgh, **67**, p. 99-126.

Love, L.G., and Neves, R., 1963, *Palynological evidence on the age of the Carboniferous of Inninmore*: Geological Society of Glasgow Transactions, **25**, p. 61-71.

Lovering, T.S., 1935, *Theory of Heat conduction applied to geological problems*: Geological Society of America Bulletin, **46**, p. 69-94.

Luber, A.A., and Waltz, I.E., 1938, *Classification and stratigraphical value of spores of some Carboniferous coal deposits in the U.S.S.R.*: Trav. Inst. geol. U.R.S.S., **105**, p. 1-45.

Luber, A.A., and Waltz, I.E., 1941, *Atlas of Microspores and pollen grains of the Palaeozoic of the U.S.S.R.*: Trans. All-Un. Sci. Res. Inst. geol (VSEGEI), **139**, p. 1-107.

Lynch, L., and Reynolds , R.C.J., 1985, *The stoichiometry of the smectite-illite reaction: program with abstracts*: 21st annual Meeting of the Clay Minerals Society, p. 84.

MacEwan, D.M.M., 1956, *Fourier transform methods for studying scattering from lamellar systems: I A direct method for analysing interstratified mixtures*: Kolloidschrift, **34**, p. 69-73.

MacEwan, D.M.M., 1958, *Fourier transform methods for X-ray scattering from lamellar systems:II. The calculation of X-ray diffraction effects for various types of interstratification*: Kolloidschrift, **156**, p. 61-67.

MacEwan, D.M.M., and Wilson, M.J., 1980, *Interlayer and intercalation complexes of clay minerals*, *in* Brindley, G.W., and Brown, G., eds., Crystal Structures of Clay Minerals and Their X-Ray Identification: Mineralogical Society Monograph, **5**: London, The Mineralogical Society, with financial assistance from, The Royal Society, p. 495.

MacIntyre, R.M., McMenamin, T., and Preston, J., 1975, *K-Ar results from western Ireland and their bearing on the timing and siting of Thulean magmatism*: Scottish Journal of Geology, **11**, p. 227-249.

Mackenzie, A.S., and Quigley, T.M., 1988, *Principles of geochemical prospect appraisal*: American Association of Petroleum Geologists Bulletin, **72**, p. 399-415.

Mamay, S.H., 1950, *Some American Carboniferous fern fructifications*: Ann. Mo. Bot. Gdn., **37**.

Mamay, S.H., 1954, *Two new plant genera of Pennsylvanian age from Kansas coal balls*: Professional papers of the U.S. Geological Survey, **254-D**, p. 81-95.

Manum, S.B., and Throndsen, T., 1978, *Dispersed organic matter (kerogen) in the Spitsbergen Tertiary*: Norsk Polarinstitut Arbok, p. 179-187.

Marshall, A.E., and Williams, J.E., 1970, *Palynology of the Yoredale "Series" in the Roman Wall district of Western Northumberland, Northern England*: Congres Avance Études Stratigraphic Geologie Carbonifères, Compte Rendu, **6**, p. 1147-1148.

Marshall, J.E.A., 1990, *Determination of thermal maturity*, *in* Briggs, D.E.G., and Crowther, P.R., eds., Palaeobiology, a synthesis, p. 511 - 515.

Marshall, J.E.A., and Yule, B., 1999, *Chapter 31 Spore Colour Measurement*, *in* Jones, T.P., and Rowe, N.J., eds., Fossil plants and spores: modern techniques: London, Geol. Soc. Lond.

Masran, T.C., and Pocock, A.J., 1981, *The classification of plant-derived particulate organic matter in sedimentary rocks*, *in* Brooks, J., ed., Organic Maturation and Fossil Fuel Exploration, **1**: London, Academic Press, p. 145-176.

McCormack, N., J., 1998, *The thermal history of the South Portugese Zone*: PhD thesis, Trinity College, Dublin.

McHardy, W.J., Wilson, M.J., and Tait, J.M., 1982, *Electron microscope and X-ray diffraction studies of filamentous illitic clay from sandstones of the Magnus field*: Clay Minerals, **17**, p. 23 - 29.

McIntyre, D.J., 1972, *Effect of experimental metamorphism on pollen in a lignite*: Geoscience and Man, **4**, p. 111-117.

McPhilemy, B., 1989, *Palynology and palynofacies of some Lower Carboniferous sections in Northwest Ireland*: PhD thesis, Trinity College, Dublin, Dublin.

McTavish, R.A., 1978, *Pressure retardation of vitrinite diagenesis, offshore Northwest Europe*: Nature, **271**, p. 648-650.

Menning, M., Zdzislaw, B., Kullman, J., Stuppel, D., and Weyer, D., 2000, *On the number of Carboniferous series and stages*: Newsletter on Carboniferous Stratigraphy, IUGS subcommission for Carboniferous stratigraphy, **18**, p. 9.

Merriman, R., J., and Kemp, S., J., 1996, *Clay minerals and sedimentary basin maturity*: Mineralogical Society Bulletin, **111**, p. 7-8.

Merriman, R., J., 2002a, *The Magma-to-mud cycle*: Geology Today, **18**, p. 67 - 71.

Merriman, R., J., 2002b, *Contrasting clay mineral assemblages in British Lower Palaeozoic slate belts: the influence of geotectonic setting*: Clay Minerals, **37**, p. 207 - 219.

Merriman, R.J., and Frey, M., 1999, *Patterns of very low grade metapelites in metapelitic rocks*, *in* Frey, M., and Robinson, D., eds., Low-Grade Metamorphism: Oxford, Blackwell Science, p. 61-107.

Metcalfe, I., 1997, *Revision of the Carboniferous part of the IUGS stratigraphic chart*: Carboniferous Newsletter, **15**, p. 15.

Midttømme, K., Roaldset, E., and Brantjes, J.G., 1996, *Conductivity of alluvial sediments from the Ness formation, Oseberg Area, North Sea*: EAEG 58th conference, ectended abstracts, **2**, p. 552.

Midttømme, K., and Roaldset, E., 1999, *Thermal conductivity of sedimentary rocks: uncertainties in measurement and modelling*, *in* Aplin, A.C., Fleet, A.J., and Macquaker, J.H.S., eds., Muds and Mudstones: Physical and Fluid Flow Properties: The Geologcal Society Special Publication, **158**: London, The Geological Society, p. 45-60.

Moore, D., M., and Reynolds , R.C.J., 1997, *X-Ray Diffraction and the Identification and Analysis of Clay Minerals*: Oxford-NewYork, Oxford University Press, 378 p.

Morton, J.P., 1985, *Rb-Sr evidence for punctuated illite/smectite diagenesis in the Oligocene Frio Formation, Texas Gulf Coast*: Bulletin of the Geological Society of America, **96**, p. 114-122.

Murchison, D.G., Cook, A.K., and Raymond, A.C., 1985, *Optical properties of organic matter in relation to thermal gradients and structural deformation*: Philosophical Transactions of the Royal Society of London, **A.315**, p. 157-186.

Mussett, A.E., Dagley, P., and Skelhorn, R.R., 1988, *Time and duration of activity in the British Tertiary Igneous Province*, *in* Morton, A.C., and Parson, L.M., eds., Early Tertiary Volcanism and the opening of the NE Atlantic: Geological Society of London, special publication, **39**: London, Oxford Bell, p. 337-348.

Nadeau, P.H., Tait, J.M., McHardy, W.J., and Wilson, M.J., 1984a, *Interstratified XRD characteristics of physical mixtures of elementary clay particles*: Clay Minerals, **19**, p. 67-76.

Nadeau, P.H., Wilson, M.J., McHardy, W.J., and Tait, J.M., 1984b, *Interstratified clays as fundamental particles*: Science, **225**, p. 923 - 925.

Nadeau, P.H., Wilson, M.J., McHardy, W.J., and Tait, J.M., 1985, *Interstratified clays as fundamental particles: a reply*: Clays and Clay Minerals, **33**, p. 560.

Naumova, S.N., 1953, *Spore pollen complexes of the Upper Devonian of the Russian platform and their stratigraphical value*: Trav. Inst. Sci. geol. Akad. Nauk S.S.S.R., **143**, p. 1-154.

Naylor, D., 1992, *The post-Variscan history of Ireland*, *in* Parnell, J., ed., Basins on the Atlantic Seaboard: Petroleum Geology, Sedimentology and Basin evolution; Geological Society Special Publication, **62**: London, Geological Society, p. 255-275.

Neves, R., 1961, *Namurian plant spores from the southern Pennines, England*: Palaeontology, **4**, p. 247-279.

Neves, R., 1964, *Knoxisporites (Potonié and Kremp) Neves 1961*: C. r. congr. Strat. Géol. carbonif. Paris (1963), **1**, p. 1063-1069.

Neves, R., and Owens, B., 1966, *Some Namurian Camerate miospores from the English Pennines*: Pollen Spores, **8**, p. 337-360.

Newman, A.C.D., ed., 1987, *Chemistry of Clays and Clay Minerals*: Mineralogical Society Monograph No 6, **6**: London, Longman Scientific and Technical, 480 p.

Ohr, M., Halliday, A., N., and Peacor, D., R., 1991, *Sr and Nd isotopic evidence for punctuated clay diagenesis, Texas Gulf Coast*: Earth and Planetary Science Letters, **105**, p. 110-126.

Ottenjann, K., Teichmüller, M., and Wolf, M., 1974, *Spektrale Fluoreszenz - Messungen an Sporoniten mit Auflicht - Anregung, eine Mikroskopische*

methode zur Bestimmung des Inkohlungsgrades gering inkohlter kohlen: Fortschritte Geol. Rheinland und Westfalen, **24**, p. 1 - 36.

Ottenjann, K., Teichmüller, M., and Wolf, M., 1975, *Spectral fluorescence measurements of sporinites in reflected light and their application for coalification studies*: Colloque International Paris 1973 Petrographie de la matiere organique des sediments; Relations avec la palaeotemperature et le potentiel petrolier, p. 49 - 65.

Ottenjann, K., 1988, *Fluorescence alteration and its value for studies of maturation and bituminization*: Organic Geochemistry, **12**, p. 309 - 321.

Peacor, D., R., 1998, *Implications of TEM data for the concept of fundamental particles*: The Canadian Mineralogist, **36**, p. 1397 - 1408.

Pearce, J.A., and Cann, J.R., 1973, *Tectonic setting of basic volcanic rocks determined using trace element analyses*: Earth and Planetary Science Letters, **19**, p. 290 - 300.

Pearson, D.L., 1982, *Approaching a pollen/spore standard*: Palynology, **6**, p. 289.

Pearson, D.L., 1984, *Pollen/Spore colour standard. Phillips petroleum company exploration projects section, in* Traverse, A., ed., Palaeopalynology, **1**: Boston, Hyman and Unwin, p. 416/417.

Perry, E.A., and Hower, J., 1972, *Late stage dehydration in deeply buried pelitic sediments*: Bulletin of the American Association of Petroleum Geologists, **56**, p. 2013-2021.

Peters, K.E., Ishiwatari, R., and Kaplan, I.R., 1977, *Color of Kerogen as Index of Organic Maturity*: The American Association of Petroleum Geologists Bulletin, **61**, p. 504-510.

Pickard, N.A.H., Jones, G.L., Rees, J.G., Somerville, I.D., and Strogen, P., 1992, *Lower Carboniferous Stratigraphy (Dinantian) stratigrahy and structure of the Walterstown-Kentstown area, Co. Meath*: Geological Journal, **27**, p. 35-58.

Playford, G., 1962, *Lower Carboniferous microfloras of Spitsbergen*: Palaeontology, **4 & 5**, p. 550-618.

Pollastro, R.M., and Barker, C.E., 1986, *Application of clay mineral, vitrinite reflectance and fluid inclusion studies to the thermal and burial history of the Pinedale Anticline, Green River Basin, Wyoming*: The Society of Economic Paleontologists and Mineralogists, p. 73-83.

Potonié, H., 1893, *Die Flora des Rotliegenden von Thüringen*: Kgl. Preuss. Geol., **L. -A. 9**, p. 1-298.

Potonié, R., and Kremp, G., 1954, *Die Gattungen der palaozoischen Sporae dispersae und ihre Stratigraphie*: Geol. Jb., **69**, p. 111-194.

Potonié, R., and Kremp, G., 1955, *Die sporae dispersae des Ruhrkarbons, ihre Morphographie und Stratigraphie mit Ausblicken auf Arten anderer Gebeite und Zeitabschnitte: Teil I*: Palaontographica, **B98**, p. 1-136.

Potonié, R., 1956, *Synopsis der Gattungen der Sporae dispersae.Teil I. Sporites.*: Beih. Geol. Jb., **23**, p. 1-103.

Potonié, R., 1962, *Synopsis der Sporae in situ.*: Beih. Geol. Jb., **52**, p. 1-204.

Powell, A.J., Dodge, J.D., and Lewis, J., 1990, *Late Neogene to Pleistocene palynological facies of Peruvian continental margin upwelling, leg 112, in* Summer Hayes, C.P., Prell, W.L., and Emeis, K.C., eds., Proceedings of the Ocean Drillling Project, Scientific Results, **64**: London, Geological Society of London Special Publication, p. 215-226.

Powers, M.C., 1967, *Fluid-release mechanisms in compacting marine mudrocks and their importance in oil exploration*: American Association of Petroleum Geologists Bulletin, **51**, p. 1240 - 1254.

Preston, J., 1981, *Tertiary Igneous Activity, in* Holland, C., H., ed., Geology of Ireland, **1**: Dublin, p. 213-222.

Price, L.C., 1983, *Geologic time as a parameter in organic metamorphism and vitrinite reflectance as an absolute palaeogeothermometer*: Journal of Petroleum Geology, **6**, p. 5-38.

Price, L.C., and Wenger, M., 1992, *The influence of pressure on petroleum generation and maturation suggested by aqueous pyrolysis*: Organic Geochemistry, **19**, p. 141-159.

Radforth, N.W., 1938, *An analysis and comparison of the structural features of Dactylotheca plumosa Artis sp. and Senftenbergia ophiodermatica Göpert sp.*: Transactions of the Royal Society of Edinburgh, **59**, p. 385 - 396.

Radforth, N.W., 1939, *Further contributions to our knowledge of the fossil Schizaeaceae: genus Senftenbergia*: Transactions of the Royal Society of Edinburgh, **59**.

Rankin, A., H., 1989, *Fluid inclusions*: Geology Today, p. 21-24.

Reed, F.D., 1938, *Notes on some plant remains from teh Carboniferous of Illinois*: Botanical Gazzette, **100**, p. 324-335.

Remy, R., 1960, *Bowmanites nindeli n. sp.*: Mber. Deutsch Akadamie Wissenschaft Berlin, **1**, p. 257-260.

Remy, W., and Remy, R., 1957, *Durch Mazeration fertilier Farne des Paläozoikums gewonnene Sporen*: Palaönt. Z., **31**, p. 55-65.

Richey, J.E., 1961, *Scotland: The Tertiary Volcanic Districts*: British Regional Geology: Edinburgh, Her Majestys Stationary Office, 120 p.

Robert, P., 1981, *Classification of organic matter by means of fluorescence; application to hydrocarbon source rocks*: International Journal of Coal Geology, **1**, p. 101 - 137.

Robison, C.R., van Gijzel, P., and Darnell, L.M., 2000, *The transmittance color index of amorphous orgainc matter: a thermal maturity indicator for petroleum source rocks.*: International Journal of Coal Geology, **43**, p. 83 - 103.

Ross, J.V., and Bustin, R.M., 1997, *Vitrinite anisotropy resulting from simple shear experiments at high temperature and high confining pressure*: Coal Geology, **33**, p. 153 - 168.

Schemel, M.P., 1950, *Carboniferous plant spores from Daggatt county, Utah*: Journal of Palaeontology, **24**, p. 232-244.

Schopf, J.M., Wilson, L.R., and R., B., 1944, *An annotated synopsis of palaeozoic fossil spores and the definition of generic groups*: Rep. Invest. Ill. Geol. Surv., **91**, p. 1-72.

Sevastopulo, G., Dimitrius, 1981, *Lower Carboniferous, in* Holland, C., H., ed., A Geology of Ireland: Edinburgh, Scottish Academic Press.

Sevastopulo, G.D., and Wyse-Jackson, P., 2001, *Carboniferous (Dinantian), in* Holland, C., H., ed., A Geology of Ireland: Edinburgh, Scottish Academic Press.

Shaw, H.F., 1980, *Clay minerals in sediments and sedimentary rocks, in* Hobson, G.D., ed., Developments in Petroleum Geology - 2: Barking Essex, Applied Science Publishers.

Sigal, J., 1965, *Palynofacies: un neologisme illogique et superflu*: Revue de Micropaleontology, **8**, p. 59-60.

Smart, G., and Clayton, T., 1985, *The progressive illitization of interstratified illite-smectite from Carboniferous sediments of northern England and its relationship to organic maturity indicators*: Clay Minerals, **20**, p. 455-466.

Smith, A.H.V., and Butterworth, M.A., 1967, *Miospores in the coal seams of the Carboniferous of Great Britain*: *Special Papers in Palaeontology*, **1**: London, University Press, Oxford, 1-324 p.

Smith, J., 1996, *A palynofacies analysis of the Dinantian (Asbian) Glenade Sandstone Formation of the Leitrim Group, northwest Ireland*: Geological Society Special Publication, **no. 107**, p. 437-448.

Somers, G., 1952, *A preliminary study of the fossil spore content of the Lower Jubilee Seam of the Sydney Coalfield, Nova Scotia*: Nova Scotia Research Foundation, p. 1-30.

Somers, Y., 1972, *Revision du genre Lycospora Schopf, Wilson et Bentall, Microfossiles organiques du paleozoique*: Commission Internationale de Microflore du Paleozoique, Centre National de la Recherche Scientifique., **5 Spores**.

Srodon, J., and Eberl, D., D., 1984, *Illite*, *in* Bailey, S.W., ed., Micas: Reviews in mineralogy, **13**: Washington D.C., Mineralogical Society of America, p. 495- 544.

Srodon, J., Elass, F., McHardy, W.J., and Morgan, D.J., 1992, *Chemistry of illite-smectite infrared from TEM measurements of fundamental particles*: Clay Minerals, **27**, p. 137-158.

Stach, E., Mackowsky, M.T., Teichmuller, M., Taylor, G.H., Chandra, D., and Teichmuller, R., 1982, *Stachs Textbook of Coal Petrology*: Berlin and Stuttgart, Gebruder Borntraeger, 535 p.

Stach, E., Mackowsky, M.T., Teichmuller, M., Taylor, G.H., Chandra, D., and Teichmuller, R., 1986, *Stachs Textbook of Coal Petrology*: Berlin and Stuttgart, Gebruder Borntraeger, 535 p.

Stancliffe, R.P.W., 1989, *Microforaminiferal linings: their classification, biostratigraphy and paleoecology, with special reference to specimens from British Oxfordian sediments*: Micropaleontology, **35**, p. 337-352.

Staplin, F.L., and Jansonious, J., 1964, *Elucidation of some Paleozoic densospores*: Palaeontographica, **114**, p. 95-117.

Staplin, F.L., 1969, *Sedimentary organic matter, organic metamorphism and oil and gas occurrence*: Bulletin of Canadian Petroleum Geology, **17**.

Stopes, M.C., 1935, *On the petrology of banded bituminous coals*: Fuel, **14**, p. 4-13.

Streel, M., 1964, *Une association de spores du Givetien inférieur de la Vesdre, à Goè (Belgique)*: Annales de la societe Géologique du Belgium, **87**, p. 1-30.

Strogen, P., Somerville, I., D., Pickard, N., A.H., and Jones, G., Ll., 1995, *Lower Carboniferous (Dinantian) Stratigraphy and structure in the Kingscourt Outlier, Ireland*: Geological Journal, **30**, p. 1-23.

Sullivan, H., James, 1962, *Distribution of miospores through coals and shales of the Coal Measures sequence exposed in Wernddu claypit, Caerphilly (South Wales)*: Geoloical Society of London Quarterly Journal, **118**, p. 353-373.

Sullivan, H., James, 1964, *Miospores from the Drybrook Sandstone and associated measures in the Forest of Dean Basin, Gluocestershire*: Palaeontology, **7**, p. 353-373.

Sullivan, H., James, 1965, *Palynological Evidence concerning the regional differentiation of upper Mississippian floras.*: Pollen et spores, **7**, p. 539 - 563.

Sullivan, H., James, and Marshall, A.E., 1966, *Visèan spores from Scotland*: Micropaleontology, **12**, p. 265-285.

Sweeney, J., and Burnham, A., K., 1990, *Evaluation of a simple model of vitrinite reflectance based on chemical kinetics*: American Association of Petroleum Geologists Bulletin, **74**, p. 1559 - 1570.

Sweeney, J.J., and Burnham, A.K., 1989, *A Chemical kinetic model of vitrinite maturation and reflectance*: Geochimica Cosmochimica Acta, **53**, p. 2649-2657.

Talibudeen, O., and Goulding, K., W.T., 1983, *Apparent charge heterogeneity in kaolins in relation to their 2:1 phyllosilicate content*: Clays and Clay Minerals, **31**, p. 137 - 142.

Tappan, H., 1980, *The Paleobiology of Plant Protists*: San Francisco, Freeman, 1028 p.

Taylor, G.H., Teichmüller, M., Davis, A., Diessel, C.F.K., Littke, R., and Robert, P., 1998, *Organic Petrology*, **1**: Berlin, Gebrüder Borntraeger, 704 p.

Taylor, G.T., 1982, *Methanogenic Bacteria*: Progress in Industrial Microbiology, **16**, p. 231-330.

Taylor, H.P., and Forrester, R.W., 1971, *Low O^{18} igneous rocks from the intrusive complexes of Skye, Mull and Ardnamurchan, Western Scotland*: Journal of Petrology, **12**, p. 465-497.

Teichmüller, M., and Teichmüller, R., 1967, *Diagenesis of coals (Coalification)*, *in* Larsen, G., and Chilingar, G., eds., Diagenesis in Sediments, p. 391 - 415.

Teichmüller, M., 1982, *Origin of Petrographic constituents of coal*, *in* Stach, E., Mackowsky, M.T., Teichmüller, M., Chandra, D., Teichmüller, R., Murchison, D.G., and Zierke, F., eds., Stach's Textbook of Coal Petrology: Berlin, Gebrüder Borntraeger, p. 219-294.

Teichmüller, M., 1987, *Organic material and very low grade metamorphism*, *in* Frey, M., ed., Low Temperature Metamorphism: Glasgow and London; New York, Blackie; Chapman and Hall, p. 114-161.

Thomas, and Spicer, 1987, *The evolution and Palaeobiology of land plants.*: Ecology, Phytogeography and Physiology series, **2**: London and Sydney, Portland Oregon, Croom and Helm, London and Sydney. Discorides Press.

Thompson, R.N., Esson, J., and Dunham, A.C., 1972, *Major element chemical ariation in the Eocene lavas of the Isle of Skye, Scotland.*: Journal of Petrology, **13**, p. 219-253.

Till, R., 1974, *Statistical Methods for the Earth Scientist - An introduction*: London, Macmillan, 154 p.

Ting, F.T.C., 1981, *Uniaxial and biaxial virtrinite reflectance models and their Relationship to Paleotectonics*, *in* Brooks, J., ed., Organic Maturation Studies and Fossil Fuel Exploration: London, Academic Press, p. 379 - 392.

Ting, T.C., 1977, *Quantitative flourescence microscopy and fluorescence characteristics of thermally altered liptinites*: Palynology, **1**, p. 27-32.

Tobin, R., C., and Claxton, B., L., 2000, *Multidisciplinary thermal maturity studies using vitrinite reflectance and fluid inclusion microthermometry: a new calibration of old techniques*: The American Association of Petroleum Geologists Bulletin, **84**, p. 1647 - 1665.

Touloukian, Y.S., Judd, W.R., and Roy, R.F., 1981, *Physical Properties of Rocks and Minerals*: McGraw Hill/ CINDAS Data Series on Material Properties Volume II - 2, **II**: New York, McGraw Hill Book Company, 548 p.

Traverse, A., 1988a, *Palaeopalynology*, **1**: Boston, Unwin Hyman, 600 p.

Traverse, A., ed., 1988b, *Sedimentation of Organic Particles*: Cambridge, Cambridge University Press, 544 p.

Traverse, A., 1996, *Chp.2 Nomenclature and taxonomy: systematicsPalynology*, *in* Jansonius, J.a.M., D.C. (e.d.s), ed., Palynology: Principles and applications, **vol. 1 pp 227 - 260, ISBN 9-931871-03-4**, American Association of Stratigraphic Palynologists Foundation, p. 227 - 260, ISBN 9-931871-03-4.

Tschudy, R., H., and Scott, R., A., *Aspects of Palynology*: New York, Wiley Interscience.

Tyson, R.V., 1993, *Palynofacies analysis*, *in* Jenkins, D.J., ed., Applied Micropalaeontology: Dordrecht, Kluwer, p. 153-191.

Tyson, R.V., 1995, *SEDIMENTARY ORGANIC MATTER : organic facies and palynofacies*, **1**: London, Chapall & Hall, 615 p.

Van Gijzel, P., 1981, *Applications of the Geomicrophotometry of Kerogen, Solid Hydrocarbons and Crude Oils to Petroleum Exploration*, *in* Brooks, J., ed., Organic Maturation Studies and Fossil Fuel Exploration, **1**: London, Academic Press, p. 351 - 377.

Van Gijzel, P., 1982, *Characterisation and identification of kerogen and bitumen and determination of thermal maturation by means of qualitative microscopical techniques*, *in* F.L., S., Dow, W.G., Milner, C.W.D., O'Connor, D.I., Pocock, S.A.J., van Gijzel, P., Welte, D.H., and Yukler, M.A., eds., How to assess Maturation and paleotemperatures: Society of Economic Paleontologists and Mineralogists, Short course No.7 Tulsa, p. 289.

Velde, B., and Nicot, E., 1985, *Diagenetic clay mineral composition as a function of pressure, temperature and chemical activity*: Journal of sedimentary petrology, **55**, p. 541-547.

Velde, H., Fermont, W.J.J., David, P., Pagnier, H.J., and Visscher, H., 1996, *Environmental influence on maturity parameters in Carboniferous coals of the Netherlands*: Coal Geology, **30**, p. 37 - 64.

Visscher, H., 1971, *The Permian and Triassic of the Kingscourt Outlier, Ireland; A palynological investigation related to regional stratigraphical problems in the Permian and Triassic of Western Europe*: Geological Survey of Ireland, Special Paper, **No. 1**, p. 1-114.

Walton, J., 1957, *On Protopitys (Göppert): with a description of a fertile specimen 'Protopitys scotia' sp. nov. from the calciferous Sandstone series of Dumbartonshire*: Transactions of the Royal Society of Edinburgh, **63**, p. 333-339.

Waples, D.W., 1980, *Time and Temperature in Petroleum formation: application of Lopatin's method to petroleum exploration*: AAPG American Association of Petroleum Geologists, **64**, p. 916-926.

Warr, L.N., and Nieto, F., 1998, *Crystallite thickness and defect density of phyllosilicates in low temperature metamorphic pelites: a TEM and XRD study of clay mineral crystallinity-index standards*: The Canadian Mineralogist, **36**, p. 1453 - 1474.

Whittaker, M.F., and Butterworth, M.A., 1978, *Palynology of Carboniferous strata from the Ballycastle area, Co. Antrim, Northern Ireland*: Palynology, **2**, p. 147-158.

Wilson, H.E., and Robbie, J.A., 1966, *Geology of the country around Ballycastle*: Memoirs of the Geological Survey, Ministry of Commerce.

Wilson, H.E., 1972, *Regional Geology of Northern Ireland*: British Regional Geology: Belfast, Her Majestys Stationery Office, 115 p.

Wilson, H.E., and Manning, P.I., 1978, *Geology of the Causeway coast: memoir for one inch geological sheet 7*, **1**: Belfast, Her Majesty's Stationery Office, 72 p.

Wilson, L.R., and Coe, E.A., 1940, *Descriptions of some unassigned plant microfossils from the Des Moines series of Iowa*: Proceedings of Iowa Academic Science, **51**, p. 329-332.

Wilson, L.R., 1958, *Photographic illustrations of fossil spore types from Iowa*: Okla. Geol. Notes, **18**, p. 99 - 100.

Wood, D., A., 1988, *Relationships between thermal maturity indices calculated using Arrhenius equation and Lopatin method: Implications for petroleum exploration*: The American Association of Petroleum Geologists Bulletin, **72**, p. 115-134.

Yule, B.L., Roberts, S., and Marshall, J.E.A., 2000, *The thermal evolution of sporopollenin*: Organic Geochemistry, **31**, p. 859-870.

Ziegler, P., Alfred, 1990, *Geological Atlas of Western and Central Europe*

APPENDIX I

TABLES

Table 1 Sample Catalogue

Table 2 XRF Data

Table 3 Mean Random Reflectance and Temperature Conversion for dispersed vitrinite

Table 4 Mean Random Reflectance values for coal samples

Table 5 Clays and Clay mineral, peak reflection number[], position (°2θ), Angstrom values (Å), and intensity (I), for identification on XRD, oriented, air-dried, ethylene glycol and DMSO solvated.

Table 6 Minerals identified in respective samples

Table 7 Mineral peak intensity values and mudmaster best mean size values

Table 8 Palynology Count – absolute numbers

Table 9 Palynology Count – percent content

Table 10 Palynology Count – presence of spore genera (%)

Table 11 Palynofacies – divisions and absolute counts

Table 12 Palynofacies – divisions and percent content

Table 13 Palynofacies – divisions after Tyson (1995) and Bujak *et al.* (1977), absolute numbers and percent content

TABLE 1 Sample catalogue

					Analyses undertaken on samples					
Project Sample #	TCD catalogue #	Dist. from dyke (m)	Litholgy	description	Palynology	Thermal alteration	Palyno-facies	VR	XRD	XRF
NSD1	49954	0.04	mudrock	aureole horizon	x	x	x	x	x	x
NSD2	49955	0.15	mudrock	aureole horizon	x	x	x	x	x	
NSD3	49956	0.28	mudrock	aureole horizon	x	x	x	x	x	x
NSD4	49957	0.37	mudrock	aureole horizon	x	x	x	x	x	
NSD5	49958	0.47	mudrock	aureole horizon	x	x	x	x	x	x
NSD6	49959	0.49	mudrock	aureole horizon	x	x	x	x	x	
NSD7	49960	0.57	mudrock	aureole horizon	x	x	x	x	x	
NSD8	49961	0.65	mudrock	aureole horizon	x	x	x	x	x	
NSD9	49962	0.95	mudrock	aureole horizon	x	x	x	x	x	
NSD10	49963	0.97	mudrock	aureole horizon	x	x	x	x	x	
NSD11	49964	1.21	mudrock	aureole horizon	x	x	x	x	x	
NSD13	49966	1.65	mudrock	aureole horizon	x	x	x	x	x	
NSD14	49967	1.82	mudrock	aureole horizon	x	x	x	x	x	
NSD15	49968	2.2	mudrock	aureole horizon	x	x	x	x	x	x
NSD16	49969	2.22	mudrock	aureole horizon	x	x	x	x	x	
NSD17	49970	2.89	mudrock	aureole horizon	x	x	x	x	x	
NSD18	49971	2.79	mudrock	aureole horizon	x	x	x	x	x	
NSD19	49972	3.95	mudrock	aureole horizon	x	x	x	x	x	
NSD20	49973	4.05	mudrock	aureole horizon	x	x	x	x	x	
NSD21	49974	5.4	mudrock	aureole horizon	x	x	x	x	x	
NSD22	49975	5.66	mudrock	aureole horizon	x	x	x	x	x	
NSD23	49976	6.27	mudrock	aureole horizon	x	x	x	x	x	
NSD24	49977	10.11	mudrock	aureole horizon	x	x	x	x	x	x
BC1	37765	11.42	mudrock	aureole horizon		x		x	x	
BC2	37766	9.9	mudrock	aureole horizon		x		x	x	
BC3	37767	8.32	mudrock	aureole horizon		x		x	x	
BC4	37768	6.29	mudrock	aureole horizon		x		x	x	
BC5	37769	5.24	mudrock	aureole horizon		x		x	x	
BC6	37770	4.11	mudrock	aureole horizon		x		x	x	
BC7	37771	3.2	mudrock	aureole horizon		x		x	x	
BC8	37772	2.43	mudrock	aureole horizon		x		x	x	
BC9	37773	2.01	mudrock	aureole horizon		x		x	x	
BC10	37774	1.58	mudrock	aureole horizon		x		x	x	
cMd1	56067	0.46	mudrock	aureole horizon with coal lenses		x	x	x	x	
cMd2	56068	0.63	mudrock	aureole horizon with coal lenses		x	x	x	x	
cMd3	56069	0.8	mudrock	aureole horizon with coal lenses		x	x	x	x	
cMd4	56070	0.96	mudrock	aureole horizon with coal lenses		x	x	x	x	
cMd5	56071	1.36	mudrock	aureole horizon with coal lenses		x	x	x	x	
cMd6	56072	1.6	mudrock	aureole horizon with coal lenses		x	x	x	x	
cMd7	56073	2.56	mudrock	aureole horizon with coal lenses		x	x	x	x	
cMd8	56074	3.55	mudrock	aureole horizon with coal lenses		x	x	x	x	
Cuo1	56075	9.65	coal	lenses in the cMd aureole horizon				x		
Cuo2	56076	4.55	coal	lenses in the cMd aureole horizon				x		
Cuo3	56077		coal	lenses in the cMd aureole horizon				x		
Cuo4	56078	2.85	coal	lenses in the cMd aureole horizon				x		
Co1	56079	9.65	coal	lenses in the cMd aureole horizon				x		
Co2	56080	4.55	coal	lenses in the cMd aureole horizon				x		
Co4	56081	2.85	coal	lenses in the cMd aureole horizon				x		
		(m above s.l.)								
CL9	56099	106.5	coal	horizons from the Gobb section				x		
CL10	56100	70	coal	horizons from the Gobb section				x		
CL11	56101	69.2	coal	horizons from the Gobb section				x		
CL12	56102	56	coal	horizons from the Gobb section				x		
CL13	56103	55	coal	horizons from the Gobb section				x		
CL14	56104	52.5	coal	horizons from the Gobb section				x		
CL15	56105	48	coal	horizons from the Gobb section				x		
CL16	56106	45.5	coal	horizons from the Gobb section				x		
		Dist. from dyke (m)								
CK1	56107	0.07	mudrock	aureole horizon		x	x	x	x	x
CK2	56108	0.2	mudrock	aureole horizon		x	x	x	x	x
CK3	56109	0.25	mudrock	aureole horizon		x	x	x	x	
CK4	56110	0.29	mudrock	aureole horizon		x	x	x	x	
CK5	56111	0.34	mudrock	aureole horizon		x	x	x	x	
CK6	56112	0.47	mudrock	aureole horizon		x	x	x	x	x
CK7	56113	0.5	mudrock	aureole horizon		x	x		x	
CK8	56114	0.6	mudrock	aureole horizon		x	x	x	x	
CK9	56115	0.81	mudrock	aureole horizon		x	x	x	x	
CK10	56116	0.9	mudrock	aureole horizon		x	x	x	x	
CK11	56117	1.03	mudrock	aureole horizon		x	x	x	x	
CK12	56118	1.12	mudrock	aureole horizon		x	x	x	x	
CK13	56119	1.39	mudrock	aureole horizon		x	x	x	x	
CK14	56120	1.57	mudrock	aureole horizon		x	x	x	x	
CK15	56121	1.8	mudrock	aureole horizon		x	x	x	x	
CK16	56122	2.02	mudrock	aureole horizon		x	x	x	x	

TABLE 1 Sample catalogue *continued*

CK17	56123	2.25	mudrock	aureole horizon		x	x	x	x	
CK18	56124	2.48	mudrock	aureole horizon		x	x	x	x	x
CK19	56125	2.83	mudrock	aureole horizon		x	x	x	x	
CK20	56126	3.19	mudrock	aureole horizon		x	x	x	x	
CK21	56127	3.59	mudrock	aureole horizon		x	x	x	x	
CK22	56128	4.05	mudrock	aureole horizon		x	x	x	x	
CK23	56129	4.49	mudrock	aureole horizon		x	x	x	x	
CK24	56130	4.94	mudrock	aureole horizon		x	x	x	x	
CK25	56131	5.39	mudrock	aureole horizon		x	x	x	x	
CK26	56132	5.84	mudrock	aureole horizon		x	x	x	x	
CK27	56133	8.99	mudrock	aureole horizon		x	x	x	x	
CK28	56134	26.28	mudrock	aureole horizon		x	x	x	x	
CK29	56135	62.92	mudrock	aureole horizon		x	x	x	x	
CK30	56136	72.9	mudrock	aureole horizon		x	x	x	x	x
CQ 0.1	56137	0.1	mudrock	aureole horizon		x	x		x	
CQ0.3	56138	0.3	mudrock	aureole horizon		x	x		x	
CQ0.5	56139	0.5	mudrock	aureole horizon		x	x		x	
CQ0.8	56140	0.8	mudrock	aureole horizon		x	x		x	
CQ1.2	56141	1.2	mudrock	aureole horizon		x	x		x	
CQ1.6	56142	1.6	mudrock	aureole horizon		x	x		x	
CQ2.0	56143	2	mudrock	aureole horizon		x	x		x	
CQ2.5	56144	2.5	mudrock	aureole horizon		x	x		x	
CQ3.0	56145	3	mudrock	aureole horizon		x	x		x	
(NSD)IG1	56146		basalt	dyke margin sample					x	x
(NSD)IG2	56147		basalt	dyke main intrusion					x	x
(NSD)IG3	56148		basalt	dyke 3rd intrusion					x	x
CKa	56149		basalt	dyke margin sample						x
CKb	56150		basalt	dyke body sample						

TABLE 2 XRF data *OMAC and GEOMAR refer to the two different laboratories that analysed the samples*

OMAC

	Ckiga		CK 1	CK2	CK 6	CK 18	CK 30
%SiO2	42.51		53.69	55.93	55.66	52.26	49.86
%Al2O3	10.84		18.2	18.49	19.16	18.19	20.73
Fe2O3	11.2		6.53	5.53	5.39	7.67	8.2
%MgO3	14.85		1.57	1.62	1.53	1.41	1.44
%CaO	9.58		3.42	2.29	1.97	3.31	0.93
%Na2O	1.43		0.26	0.13	0.17	0.15	0.04
%K2O	0.14		3.91	3.46	3.65	2.94	2.97
%TiO2	0.99		0.98	1.01	1.04	0.96	1.06
%P2O5	0.13		0.14	0.14	0.14	0.13	0.11
%MnO	0.19		0.08	0.12	0.09	0.11	0.08
%Cr2O3	0.101		0.019	0.02	0.023	0.019	0.024
%LOI	7.4		10.9	11	11	12.7	14.3

	NSDig 1	NSDig 2	NSD1	NSD 3	NSD 5	NSD 15	NSD 24
%SiO2	45.58	46.4	49.87	50.57	53.04	48.75	28.53
%Al2O3	15.66	15.35	17.68	18.79	19.27	18.63	12.57
Fe2O3	11.41	10.67	9.9	7.12	5.98	6.57	7.36
%MgO3	7.96	9.94	3.84	3.76	3.66	2.83	6.08
%CaO	9.77	10.29	0.51	0.44	0.84	3.35	16.32
%Na2O	2.29	2.29	0.55	0.58	0.47	0.16	0.06
%K2O	0.21	0.2	2.8	3.67	3.73	2.88	2.47
%TiO2	1	0.95	1.45	1.46	1.52	1.5	0.91
%P2O5	0.11	0.1	0.13	0.12	0.15	0.12	0.14
%MnO	0.14	0.19	0.23	0.08	0.04	0.07	0.21
%Cr2O3	0.109	0.118	0.028	0.028	0.026	0.025	0.015
%LOI	5.6	3.4	12.8	12	10.9	14.8	25.1

GEOMAR

Channel	unit	NSDIG1	NSDIG2
SiO2	%	44.99	45.88
TiO2	%	0.94	0.87
Al2O3	%	16.65	15.98
Fe2O3	%	12.47	10.9
MnO	%	0.12	0.19
MgO	%	8.27	9.79
CaO	%	8.76	10.54
Na2O	%	1.95	1.92
K2O	%	0.33	0.21
P2O5	%	0.12	0.1
Co	ppm	74	67
Cr	ppm	873	783
Ni	ppm	423	347
V	ppm	249	240
Zn	ppm	81	76
Ce	ppm	<10	20
La	ppm	<14<	<14
Nb	ppm	4	4
Ga	ppm	16	13
Pb	ppm	7	9
Pr	ppm	<4	<4<
Rb	ppm	6	6
Ba	ppm	765	373
Sr	ppm	148	139
Th	ppm	<4	<4<
Y	ppm	26	23
Zr	ppm	69	64
SUM	%	94.94	96.63
H20	%	4.45	2.85
CO2	%	0.37	0.47

TABLE 3 *Mean Random Reflectance and Temperature Conversion for dispersed vitrinite*

Sample No	Dist. from dyke (m)	VR (%Rr)	SD	T (C) Barker and Pawlewicz 1980	T (C) Barker 1988	T (C) Barker and Goldstein 1990
NSD1	0.04	3.84	0.49	324	288	322
NSD2	0.15	3.87	0.47	326	289	323
NSD3	0.28	5.55	0.46	374	326	366
NSD4	0.37	4.69	0.4	352	309	346
NSD5	0.47	5.09	0.5	362	317	356
NSD6	0.49	5.16	0.5	364	319	357
NSD7	0.57	3.41	0.23	311	276	308
NSD8	0.65	3.49	0.35	314	278	311
NSD9	0.95	2.82	0.32	287	256	285
NSD10	0.97	1.63	0.18	216	199	220
NSD11	1.21	1.48	0.2	204	189	209
NSD13	1.65	1.31	0.18	188	176	194
NSD14	1.82	1.26	0.25	183	172	190
NSD15	2.2	1.05	0.14	160	153	168
NSD16	2.22	1.16	0.19	173	163	180
NSD17	2.89	1.03	0.18	158	151	166
NSD18	2.79	1.03	0.16	158	151	166
NSD19	3.95	1.06	0.14	160	154	169
NSD20	4.05	1.19	0.22	176	166	183
NSD21	5.4	1.13	0.16	170	161	177
NSD22	5.66	1.11	0.29	167	159	174
NSD23	6.27	1.04	0.18	159	152	167
NSD24	10.11	1.25	0.26	182	171	189
cMd1	0.46	5.2	0.5	365	319	358
cMd2	0.63	5.45	0.49	371	324	364
cMd3	0.8	3.55	0.4	316	280	313
cMd4	0.96	2.57	0.19	275	246	274
cMd5	1.36	1.57	0.16	212	195	216
cMd6	1.6	0.71	0.06	110	112	121
cMd7	2.56	0.94	0.19	146	142	155
cMd8	3.55	0.55	0.07	77	86	91
BC1	11.42	1.1	0.17	166	158	173
BC2	9.9	1.11	0.15	167	159	174
BC3	8.32	1.09	0.17	165	157	172
BC4	6.29	1.16	0.18	173	163	180
BC5	5.24	1.17	0.19	174	164	181
BC6	4.11	1.2	0.18	177	167	176
BC7	3.2	1.17	0.21	174	164	181
BC8	2.43	1.34	0.22	191	178	197
BC9	2.01	1.53	0.23	208	192	213
BC10	1.58	1.98	0.23	241	219	243

TABLE 3 continued

Mean Random Reflectance and Temperature Conversion for dispersed vitrinite

Sample No	Dist. from dyke (m)	VR (%Rr)	SD	T (C) Barker and Pawlewicz 1980	T (C) Barker 1988	T (C) Barker and Goldstein 1990
CK1	0.07	3.09	0.36	298	265	296
CK2	0.2	3.65	0.26	320	283	316
CK3	0.25	3.26	0.38	305	271	303
CK4	0.29	3.23	0.26	304	270	302
CK5	0.34	3.1	0.42	299	266	297
CK6	0.47	3.39	0.44	310	275	307
CK8	0.6	1.89	0.37	235	214	258
CK9	0.81	1.49	0.21	205	189	209
CK10	0.9	1.41	0.2	198	184	203
CK11	1.03	1.46	0.24	202	187	207
CK12	1.12	1.48	0.33	204	189	209
CK13	1.39	1.29	0.28	186	174	192
CK14	1.57	1.29	0.29	186	174	192
CK15	1.8	1.17	0.28	174	164	181
CK16	2.02	1.14	0.26	171	162	178
CK17	2.25	1.16	0.24	173	163	180
CK18	2.48	1.1	0.14	166	158	173
CK19	2.83	1.12	0.26	168	160	176
CK20	3.19	1.16	0.36	173	163	180
CK21	3.59	1.11	0.2	167	159	174
CK22	4.05	1.12	0.27	168	160	176
CK23	4.49	1.14	0.24	171	162	178
CK24	4.94	1.03	0.25	158	151	166
CK25	5.39	1.1	0.17	166	158	173
CK26	5.84	1.07	0.18	163	155	170
CK27	8.99	1.07	0.25	163	155	170
CK28	26.28	1.07	0.32	163	155	170
CK29	62.92	1.1	0.24	166	158	173
CK30	72.9	1.08	0.16	164	156	171

TABLE 4 *Vitrinite Reflectance data for coal samples*

Mean Random reflectance resullts for randomly

Sample No	(m above s.l.)	VR (%Rr)	SD
Cl9	106.5	1.14	0.31
Cl10	70	0.53	0.07
Cl11	69.2	0.56	0.07
Cl12	56	0.51	0.06
Cl13	55	0.48	0.06
Cl14	52.5	0.5	0.06
Cl15	48	0.55	0.07
Cl16	45.5	0.78	0.16

Mean Random reflectance results for randomly oriented coal samples from the cMd horizon in

Sample No	Dist. from dyke (m)	VR (%Rr)	SD
Cuo1	9.65	0.53	72
Cuo2	4.55	0.44	49
Cuo4	2.85	0.54	75

Rmax and Rmin results for oriented coal lenses collected from the cMd horizon in the North Star Dyke aureole

		(parallel to bedding)		(perpendicular to bedding)	
Sample No	Dist. from dyke (m)	Rmax	Rmin	Rmax	Rmin
Co1	9.65			0.48	0.45
Co2	4.55	0.45	0.4	0.46	0.4
Co4	2.85	0.48	0.4	0.58	0.5

CLAY MINERALS

air-dried

	[001]			[002]			[003]			[004]			[005]						
		d ( )	I		d ( )	I		d ( )	I		d ( )	I		d ( )	I				
smectite	5.88	15	100	7.1	12.6	variable	17.74	5	variable	23.07	3.75	variable	29.5	3.03	variable				
chlorite (Fe rich)	6.2	14.24	c. 25	12.5	7.08	80-100	18.75	4.73	18	25	3.56	c. 50	31.6	2.83	<18				
illite	8.9	9.94	100	17.8	4.98	37.5	26.7	3.34	75	35.9	2.5	25							
pyrophillite (triclinic)	9.6	9.2	100							19.2	4.6	30				[111]	28.8	3.07	90
kaolinite	12.4	17.16	100	24.8	3.57	100	37.78	2.38	60										

ethylene glycol solvated

smectite	5.2	16.9	10	10.3	8.46		15.7	5.64		20.98	4.23		26.3	3.38					

DMSO solvated

kaolinite	7.82	11.3	100	25.84	3.73	100													

NON-CLAY MINERALS

	hkl	d ( )	*I*	*hkl*	d ( )	*I*	*hkl*	d ( )	*I*	*hkl*	d ( )	*I*	*hkl*	d ( )	*I*
quartz	[010]	20.9	4.26	35	[100]	26.6-9	3.34	100							
Ca Plagioclase (anorthite)	[204]	27.8	3.21	100	[204]	28	3.18	100	[202]	22	4.04	52	[220]	28.4	3.13	41
Na plagioclase (lo albite)	[002]	27.95	3.19	100												
K-feldspar (lo microcline	[220]	27.42	3.25	100	[202]	27.08	3.29	48								
calcite	[104]	29.36	3.04	100												
dolomite	[104]	30.92	2.89	100												
ankerite	[104]	30.82	2.9	100												
halite		31.7	3.82	100												
gypsum	[020]	11.58	7.56	100	[121]	20.84	4.27	50	[031]	23.36	3.79	20	[141]	29.18	3.06	55
apatite	[211]	31.8	2.78-.81	100												
pyrite	[200]	33.02	2.71	85												

TABLE 5 *XRD powder data for the minerals identified in the Carrickleck and Ballycastle samples (after Moore and Reynolds 1997 and Brindley and Brown 1984)*

Sample No.	smectite	chlorite	illite	pyrophillite	kaolinite	quartz	Ca plagioclase	Na plagioclase	K feldspar	calcite	Mg, Fe Carbonates	gypsum	apatite	pyrite	Comment
BC1		3	2*		3	1			1	1	1				uneven chlorite reflections regularly identified implying less iron rich phase
BC2		3	2*		3	1				2	1			1	
BC3		3	2*		3	1			1	2	1		1		
BC4		3	2*		3	1			1	2	1			1	
BC5		3	2*		3	1			1	2	1				
BC6		3	2*		3	1				1	1				
BC7		3	2*		3	1				1	2				
BC8		3	2*		3	1			1		1			1	
BC9		3	2*		3	1			1		2				
BC10		3	2*		3	1			1	2	1			1	
cMd1	3	1	2	1	2		2						2	1	uneven chlorite reflections regularly identified implying less iron rich phase
cMd2	3	2	2		2	1	2								
cMd3	3	2	2		2	1	2						1	1	
cMd4	3	2	2		2	1	2			1					
cMd5		3	3*		3	2			2					1	
cMd6		3	2*		3	1			1		1				
cMd7		3	2*		3	1									
cMd8		3	2*		3	1					1				
NSD1	3	2	2		2		2						1	1	uneven chlorite reflections regularly identified implying less iron rich phase
NSD2	3	2	2		2	1	2						1		
NSD3	3	2	2		2		1								
NSD4	3	2	3		2	1	2								
NSD5	3	2	3		2	1	1								
NSD6	3	2	3	1	2	1			1		1		1		
NSD7	3	2	2		2	1	1						1		
NSD8	2	2	2		2	1					1				
NSD9	2	2	2	2	3	1			1	1			1		
NSD10	1	2	3	1	3	1			1		1			1	
NSD11		3*	3	1	3	1		1	1				1		
NSD13		3*	2		3	1									
NSD14		3*	2		3	1									
NSD15		3*	2		3	1					1			1	
NSD16		3*	2		3	1			1				1	1	
NSD17		3*	2		3	1			1						
NSD18		3*	2		3	1					1		1	1	
NSD19		3*	2		3	1			1						
NSD20		3*	2		3	1			1	0	1				
NSD21		3*	2		3	1			0	0	1				
NSD22		3*	2		3	1			1	1	1				
NSD23		3*	2		3	1									
NSD24		2*	2		3	1			1	2	2			1	

Sample No.	smectite	chlorite	illite	pyrophillite	kaolinite	quartz	Ca plagioclase	Na plagioclase	K feldspar	calcite	Mg, Fe Carbonates	gypsum	apatite	pyrite	Comment
CK1		3	2	?	3	3				?					Areas where f'spar of one type or another is very messy hump
CK2		3	2	?	3	1									
CK3		2	3*	?	2	3									
CK4		2	3*		2	3	?								
CK5		2	3*	?	2	3									
CK6		2	3*		2	2									
CK7				?	1	3						3			
CK8			3*	2	2	3				1					
CK9		2	3*	2	2	2				1		1			
CK10		2	3*		3	2									
CK11		2	3*	?	3	2				1					
CK12		2	3*	?	3	2									
CK13		2	3*		3	2									
CK14		2	2*		3	2					1				
CK15		2	2*		3	2									
CK16		2	3*		3	2									
CK17		2	2*		3	2									
CK18		2	3*		3	2									
CK19		2	3*		3	2								1	
CK20		2	2*		3	2									
CK21		2	3*		3	2									
CK22		2	3*		3	2									
CK23		2	3*		3	2				1					
CK24		2	3*		3	2									
CK25		2	3*		3	2			?						
CK26		2	3*		3	2			?						
CK27		2	3*		3	2			?						
CK28		2	3*		3	2			?		1			1	
CK29		2	3*		3	2			?		1			1	
CK30		3	3*		3	2								1	
CQ0.1		3	2		2	3									Areas where f'spar of one type or another is very messy hump
CQ0.3		3	2		3	3			1						
CQ0.5		3	3*		2	3									
CQ0.8			1*			1						3			
CQ1.2		3	3*		2	3				1	1				
CQ1.6		3	3*		2	3									
CQ2.0		3	3*		2	2					?				
CQ2.5		3	3*		2	3				1					
CQ3.0		3	2*		2	3				2	1				

1=trace component
2=minor component
3=major component
*=expandable component

TABLE 6 *minerals identified in the Carrickleck and Ballycastle samples*

TABLE 7 *Clay mineral peak intensity values and Mudmaster illite crystallite Best Mean Size values for Ballycastle*

Sample No.	Distance from dyke (m)	VR (%Rr)	illite crystallite MUDMASTER calculated Best Mean size (nm)	illite 001 intensity (air dried)	illite 001 intensity (ethylene glycol solvated)	kaolinite 001 / chlorite 002 intensity (air dried)	calcite 104 intensity (air dried)	Mg, Fe carbonate104 intensity (air dried)
BC1	11.42	1.1	3.1	107		564	72	79
BC2	9.9	1.11	3.1	69		493	118	40
BC3	8.32	1.09	3.1	124		620	85	58
BC4	6.29	1.16	3.2	100		871	125	13
BC5	5.24	1.17	3.1	180		894	155	34
BC6	4.11	1.2	3.2	201		1051	75	52
BC7	3.2	1.17	3.2	170		844	0	172
BC8	2.43	1.34	3.1	286		1157	24	30
BC9	2.01	1.53	3.1	64		180	0	95
BC10	1.58	1.98	3.1	58		148	248	47
cMd1	0.46	5.2	3.3	165		122		
cMd2	0.63	5.45	3.3	145		113		
cMd3	0.8	3.55	3.3	135		130		
cMd4	0.96	2.57	3.3	204		255		
cMd5	1.36	1.57	3.3	140		338		
cMd6	1.6	0.71	2.7	74		670		
cMd7	2.56	0.94	3.6	108		849		
cMd8	3.55	0.55	3.3	149		865		
NSD1	0.04	3.84	3.1	235	175	179		
NSD2	0.15	3.87	3.3	198	113	95		
NSD3	0.28	5.55	3.6	170	98	54		
NSD4	0.37	4.69	3.4	157	71	46		
NSD5	0.47	5.09	3.4	238	111	100		
NSD6	0.49	5.16	3.3	108	115	112		
NSD7	0.57	3.41	3.2	340	109	187		
NSD8	0.65	3.49	3.2	136	91	141		
NSD9	0.95	2.82	3.1	120	95	121		
NSD10	0.97	1.63	3.1	124	81	165		
NSD11	1.21	1.48	3.2	253	104	606		
NSD13	1.65	1.31	3.3	98	103	648		
NSD14	1.82	1.26	3.4	284	96	1086		
NSD15	2.2	1.05	3.3	130	119	991		
NSD16	2.22	1.16	3.2	148	111	1191		
NSD17	2.79	1.03	3.1	127	80	1147		
NSD18	2.89	1.03	3.1	165	88	1053		
NSD19	3.95	1.06	2.9	170	131	1287		
NSD20	4.05	1.19	3	80	34	790		
NSD21	5.4	1.13	3.6	155	120	969		
NSD22	5.66	1.11	3.1	78	34	636		
NSD23	6.27	1.04	3.3	107	95	1077		
NSD24	10.11	1.25	3.3	145	72	838		

TABLE 7 *Clay mineral peak intensity values and Mudmaster illite crystallite Best Mean Size values for Carrickleck*

Sample No.	Distance from dyke (m)	VR (%Rr)	illite crystallite MUDMASTER calculated Best Mean size (nm)	illite 001 intensity (air dried)	illite 001 intensity (ethylene glycol solvated)	kaolinite 001 / chlorite 002 intensity (air dried)
CK1	0.0674	3.09	3.3	142		212
CK2	0.2022	3.65	3.6	125		323
CK3	0.2472	3.26	3.7	291		137
CK4	0.2921	3.23	4	222		135
CK5	0.3374	3.1	4	269		140
CK6	0.4269	3.39	3.8	519		240
CK8	0.6022	1.89	3.5	90		109
CK9	0.8089	1.49	3.2	126		124
CK10	0.8988	1.41	3.3	335		316
CK11	1.0336	1.46	3.5	294		351
CK12	1.1235	1.48	3.5	522		481
CK13	1.3931	1.29	3.6	326		485
CK14	1.5729	1.29	3.5	284		494
CK15	1.7976	1.17	3.2	320		458
CK16	2.0223	1.14	3.4	392		487
CK17	2.247	1.16	3.1	187		293
CK18	2.4717	1.1	3.5	366		460
CK19	2.8312	1.12	3.5	432		499
CK20	3.1907	1.16	3.6	228		533
CK21	3.5912	1.11	3.3	335		530
CK22	4.0446	1.12	3.5	435		526
CK23	4.494	1.14	3.3	236		385
CK24	4.9434	1.03	3.3	405		585
CK25	5.3928	1.1	3.7	508		503
CK26	5.8422	1.07	3.8	331		461
CK27	8.9879	1.07	3.4			
CK28	16.1783	1.07	4	404		596
CK29	62.9156	1.1	3.5	263		466
CK30	71.9035	1.08	3.1	353		459
CQ 0.1	0.0899		3.1	58		99
CQ0.3	0.27		3.2	66		115
CQ0.5	0.44		3.2	122		70
CQ0.8	0.72		3.4	48		0
CQ1.2	1.08		3.8	179		151
CQ1.6	1.44		3.7	226		140
CQ2.0	1.8		3.5	216		147
CQ2.5	2.25		3.2	121		94
CQ3.0	2.7		3.4	108		72

APPENDIX I

TABLE 8 *PALYNOLOGY COUNT absolute numbers*

	N24	N23	N22	N20	N19	N18	N17	N16	N15	N14	N11	N10	N9	N8	N7	N6	N5	N4	N3	N2	N1
Acanthotriletes spp.	4	1																			
Calamospora spp.	5	1	1	6	5	3	4	6			3										
Cingulizonates spp. (+n24.16)	4	27	15	10	13	15	9	15	14	6	5		2				3				6
Cingulizonates bialatus	19	8	14	1	3	11	2	4	4												
Convolutispora spp.	2		1	3	2		3	6	1	1											
Crassispora maculosa	1	6	2	1	2	2	1	2	2	1											
Densosporites spp.	10	1	6	17	8		2		10	33	10	6	6	6	6	6	3	5	6	1	5
Densosporites triangularis	1			1				1		2											
Diatomozonptriletes sp.				1																	
Discernisporites sp.																					
Grandispora spinosa				1				1													
Knoxisporites spp.																					
Laevigatosporites minimus							1														
Laevigatosporites spp.			1	3			1		3	4											
Laevigatosporites minimus		2	1	1	5	2															
Laevigatosporites vulgaris	5	4			3	1		2													
Leiotriletes spp.		2	1	1		3		3	1												
Leiotriletes priddyi				1																	
Leiotriletes tumidus							1								1						
Lycospora noctuina	8	9	2	9	10	1	4	9	12	13	2		5	7	1						
Lycospora pusilla	67	67	124	69	80	167	163	138	117	74	44		54	60	40						
Lycospora sp.	30	45	11	73	55	13	12	19	16	20	51	91	117	113	80	82	139	131	70	112	32
Murospora spp.																					
Punctatisporites sp.	2	2	1	1	2	1		1		4											
Punctatisporites minutus	4	1	3		3	2			1												
Punctatisporites punctatus	2	4	4	2		1	1														
Punctatosporites c.f. granifer						1															
Pustulatisporites pustulatus						1															
Raistrickia nigra																	1				
Reticulatisporites spp.		1	1	1		1		1		1											
Reticulatisporites polygonalis	1		2					1													
Rotaspora spp.																					
Rotaspora knoxi																					
Schulzospora spp.	1	2						5	1	1											1
Schulzospora campyloptera	5	1					1														
Schulzospora elongata	2	1																			
Secarisporites remotus						1				1											
Stenozonotriletes coronatus			1		1	1		2	2												
Tripartites vetustus	1				1				2												
Triquitrites marginatus									1												
Verrucosisporites nodosus									1												
Indeterminates	126	115	109	98	107	73	95	84	112	139	185	203	116	114	172	212	154	164	224	187	256
Total	300	300	300	300	300	300	300	300	300	300	300	300	300	300	300	300	300	300	300	300	300

TABLE 9 PALYNOLOGY COUNT *percent content*

	N24	N23	N22	N20	N19	N18	N17	N16	N15	N14	N11	N10	N9	N8	N7	N6	N5	N4	N3	N2	N1
Acanthotriletes spp.	1	0	0	0	0	0	0	0	0	0	0	0	0	0	0	0	0	0	0	0	0
Calamospora spp.	2	0	0	2	2	1	1	2	0	0	1	0	0	0	0	0	0	0	0	0	0
Cingulizonates spp. (+n24.16)	1	9	5	3	4	5	3	5	5	2	2	0	1	0	0	0	1	0	0	0	2
Cingulizonates bialatus	6	3	5	0	1	4	1	1	1	0	0	0	0	0	0	0	0	0	0	0	0
Convolutispora spp.	1	0	0	1	1	0	1	2	0	0	0	0	0	0	0	0	0	0	0	0	0
Crassispora maculosa	0	2	1	0	1	1	0	1	1	0	0	0	0	0	0	0	0	0	0	0	0
Densosporites spp.	3	0	2	6	3	0	1	0	3	11	3	2	2	2	2	2	1	2	2	1	2
Densosporites triangularis	0	0	0	0	0	0	0	0	0	1	0	0	0	0	0	0	0	0	0	0	0
Diatomozonptriletes sp.	0	0	0	0	0	0	0	0	0	0	0	0	0	0	0	0	0	0	0	0	0
Discernisporites sp.	0	0	0	0	0	0	0	0	0	0	0	0	0	0	0	0	0	0	0	0	0
Grandispora spinosa	0	0	0	0	0	0	0	0	0	0	0	0	0	0	0	0	0	0	0	0	0
Knoxisporites spp.	0	0	0	0	0	0	0	0	0	0	0	0	0	0	0	0	0	0	0	0	0
Laevigatosporites minimus	0	0	0	0	0	0	0	0	0	0	0	0	0	0	0	0	0	0	0	0	0
Laevigatosporites spp.	0	0	0	1	0	0	0	0	1	1	0	0	0	0	0	0	0	0	0	0	0
Laevigatosporites minimus	0	1	0	0	2	1	0	0	0	0	0	0	0	0	0	0	0	0	0	0	0
Laevigatosporites vulgaris	2	1	0	0	1	0	0	1	0	0	0	0	0	0	0	0	0	0	0	0	0
Leiotriletes spp.	0	1	0	0	0	1	0	1	0	0	0	0	0	0	0	0	0	0	0	0	0
Leiotriletes priddyi	0	0	0	0	0	0	0	0	0	0	0	0	0	0	0	0	0	0	0	0	0
Leiotriletes tumidus	0	0	0	0	0	0	0	0	0	0	0	0	0	0	0	0	0	0	0	0	0
Lycospora noctuina	3	3	1	3	3	0	1	3	4	4	2	0	3	4	0	0	0	0	0	0	0
Lycospora pusilla	22	22	41	23	27	56	54	46	39	24	15	0	18	19	13	0	0	0	0	0	0
Lycospora sp.	10	15	4	24	18	4	4	6	5	7	16	30	38	37	27	27	46	44	23	37	11
Murospora spp.	0	0	0	0	0	0	0	0	0	0	0	0	0	0	0	0	0	0	0	0	0
Punctatisporites sp.	1	0	0	0	1	0	0	0	0	1	0	0	0	0	0	0	0	0	0	0	0
Punctatisporites minutus	1	0	1	0	1	1	0	0	0	0	0	0	0	0	0	0	0	0	0	0	0
Punctatisporites punctatus	1	1	1	1	0	0	0	0	0	0	0	0	0	0	0	0	0	0	0	0	0
Punctatosporites c.f. granifer	0	0	0	0	0	0	0	0	0	0	0	0	0	0	0	0	0	0	0	0	0
Pustulatisporites pustulatus	0	0	0	0	0	0	0	0	0	0	0	0	0	0	0	0	0	0	0	0	0
Raistrickia nigra	0	0	0	0	0	0	0	0	0	0	0	0	0	0	0	0	1	0	0	0	0
Reticulatisporites spp.	0	0	0	0	0	0	0	0	0	0	0	0	0	0	0	0	0	0	0	0	0
Reticulatisporites polygonalis	0	0	1	0	0	0	0	0	0	0	0	0	0	0	0	0	0	0	0	0	0
Rotaspora spp.	0	0	0	0	0	0	0	0	0	0	0	0	0	0	0	0	0	0	0	0	0
Rotaspora knoxi	0	0	0	0	0	0	0	0	0	0	0	0	0	0	0	0	0	0	0	0	0
Schulzospora spp.	0	0	0	0	0	0	0	0	0	0	0	0	0	0	0	0	0	0	0	0	0
Schulzospora campyloptera	2	0	0	0	0	0	0	0	2	0	0	0	0	0	0	0	0	0	0	0	0
Schulzospora elongata	1	0	0	0	0	0	0	0	0	0	0	0	0	0	0	0	0	0	0	0	0
Secarisporites remotus	0	0	0	0	0	0	0	0	0	0	0	0	0	0	0	0	0	0	0	0	0
Stenozonotriletes coronatus	0	0	0	0	0	0	0	1	1	0	0	0	0	0	0	0	0	0	0	0	0
Tripartites vetustus	0	0	0	0	0	0	0	0	1	0	0	0	0	0	0	0	0	0	0	0	0
Triquitrites marginatus	0	0	0	0	0	0	0	0	0	0	0	0	0	0	0	0	0	0	0	0	0
Verrucosisporites nodosus	0	0	0	0	0	0	0	0	0	0	0	0	0	0	0	0	0	0	0	0	0
Indeterminates	42	38	36	32	35	24	32	28	37	47	62	68	39	38	57	71	51	55	75	62	85
Total	100	100	100	100	100	100	100	100	100	100	100	100	100	100	100	100	100	100	100	100	100

TABLE 10 PALYNOLOGY COUNT *presence of spore genera (%)*

	N24	N23	N22	N20	N19	N18	N17	N16	N15	N14	N11	N10	N9	N8	N7	N6	N5	N4	N3	N2	N1	
Acanthotriletes spp.	1	0	0	0	0	0	0	0	0	0	0	0	0	0	0	0	0	0	0	0	0	0
Calamospora spp.	2	0	2	2	2	1	1	2	0	0	1	0	0	0	0	0	0	0	0	0	0	0
Cingulizonates spp.	8	12	10	4	5	8	4	6	6	2	2	0	1	0	0	0	1	0	0	0	2	
Convolutispora spp.	1	0	0	1	1	0	1	2	0	0	0	0	0	0	0	0	0	0	0	0	0	
Crassispora maculosa	0	2	1	0	1	1	0	1	1	0	0	0	0	0	0	0	0	0	0	0	0	
Densosporites spp.	4	0	2	6	3	0	1	0	3	12	3	2	2	2	2	2	1	2	2	1	2	
Diatomozonptriletes sp.	0	0		0	0	0	0	0	0	0	0	0	0	0	0	0	0	0	0	0	0	
Discernisporites sp.	0	0		0	0	0	0	0	0	0	0	0	0	0	0	0	0	0	0	0	0	
Grandispora spinosa	0	0		0	0	0	0	0	0	0	0	0	0	0	0	0	0	0	0	0	0	
Laevigatosporites spp.	2	2	1	1	3	1	1	1	1	1	0	0	0	0	0	0	0	0	0	0	0	
Leiotriletes spp.	0	1	0	1	0	1	0	1	0	0	0	0	0	0	0	0	0	0	0	0	0	
Lycospora sp.	35	40	45	50	48	60	60	56	49	35	32	30	59	60	40	27	46	44	23	37	11	
Murospora spp.	0	0	0	0	0	0	0	0	0	0	0	0	0	0	0	0	0	0	0	0	0	
Punctatisporites sp.	3	2	3	1	2	1	0	0	0	1	0	0	0	0	0	0	0	0	0	0	0	
Punctatosporites c.f. granifer	0	0	0	0	0	0	0	0	0	0	0	0	0	0	0	0	0	0	0	0	0	
Pustulatisporites pustulatus	0	0	0	0	0	0	0	0	0	0	0	0	0	0	0	0	0	0	0	0	0	
Raistrickia nigra	0	0	0	0	0	0	0	0	0	0	0	0	0	0	0	0	1	0	0	0	0	
Reticulatisporites spp.	0	0	1	0	0	0	0	1	0	0	0	0	0	0	0	0	0	0	0	0	0	
Rotaspora spp.	0	0	0		0	0	0	0	0	0	0	0	0	0	0	0	0	0	0	0	0	
Schulzospora spp.	3	1	0		0	0	0	2	0	0	0	0	0	0	0	0	0	0	0	0	0	
Secarisporites remotus	0	0			0	0	0	0	0	0	0	0	0	0	0	0	0	0	0	0	0	
Stenozonotriletes coronatus	0	0	0		0	0	0	1	1	0	0	0	0	0	0	0	0	0	0	0	0	
Tripartites vetustus	0	0	0		0	0	0	0	1	0	0	0	0	0	0	0	0	0	0	0	0	
Triquitrites marginatus	0	0	0		0	0	0	0	0	0	0	0	0	0	0	0	0	0	0	0	0	
Verrucosisporites nodosus	0	0	0		0	0	0	0	0	0	0	0	0	0	0	0	0	0	0	0	0	
Indeterminates	42	38	35	32	35	24	32	28	37	47	62	68	39	38	57	71	51	55	75	62	85	
Total	100	100	100	100	100	100	100	100	100	100	100	100	100	100	100	100	100	100	100	100	100	

TABLE 11 PALYNOFACIES *count divisions and absolute numbers (<1250^2 µm)*

		<1250^2														
Sample No.	Perp Dist(m	T. wood		OOM		Plant tissue				Palynomorphs			AOM			
		Sy	Sn	ang	rndd	ribbed	fibrous	membranou	no df st	spores W	sps B	mgsp pcs	AOM	CPM	Indeterminat	
CK 1	0.07	6	6	51	3	9	0	5	48	3	1	0	74	0	11	
CK 2	0.20	0	0	12	0	0	0	1	0	0	0	0	309	0	0	
CK 3	0.25	2	10	0	0	0	0	0	1	0	0	0	236	0	0	
CK 4	0.29	0	4	6	0	0	0	0	0	1	0	0	316	0	1	
CK 5	0.34	0	0	4	0	0	0	0	4	0	1	0	298	0	0	
CK 6	0.43	1	11	2	0	0	0	0	2	1	0	0	240	0	0	
CK 7	0.49	1	1	7	0	0	0	0	4	1	0	0	339	0	2	
CK 8	0.60	4	18	7	0	1	0	2	12	1	1	0	245	0	2	
CK 9	0.81	56	17	15	0	4	0	0	46	8	0	0	135	0	4	
CK 10	0.90	36	12	23	0	6	1	0	45	6	7	0	106	0	12	
CK 11	1.03	58	12	28	0	6	0	0	83	3	9	0	77	0	9	
CK 12	1.12	49	0	10	0	22	0	7	49	14	12	0	106	0	2	
CK 13	1.39	32	9	30	0	11	1	3	94	14	0	0	32	0	4	
CK 14	1.57	31	8	13	0	6	1	1	48	11	16	0	35	0	9	
CK 15	1.80	48	4	26	0	8	1	0	57	10	11	0	10	0	8	
CK 16	2.02	26	0	10	0	6	1	0	28	9	5	0	186	0	10	
CK 17	2.25	36	10	10	0	6	0	5	64	23	7	0	34	0	0	
CK 18	2.47	25	4	22	0	8	3	0	25	14	6	0	118	0	1	
CK 19	2.83	37	0	2	21	0	8	0	26	7	12	0	199	0	1	
CK 20	3.19	59	1	22	0	18	18	5	0	52	8	0	36	0	1	
CK 21	3.60	62	0	8	0	26	0	3	38	31	17	0	4	0	10	
CK 22	4.04	54	3	18	0	19	0	3	25	18	3	0	68	0	9	
CK 23	4.49	42	1	14	1	6	4	2	41	30	13	0	40	0	3	
CK 24	4.94	36	0	10	0	5	1	1	30	18	6	0	84	3	0	
CK 25	5.39	27	17	14	0	6	0	5	37	11	3	0	96	0	2	
CK 26	5.84	38	0	3	0	23	0	2	24	32	8	0	21	0	6	
CK 27	8.99	60	0	12	0	15	3	0	50	5	3	0	32	2	0	
CK 28	16.18	41	0	3	0	10	0	0	13	6	9	0	196	1	1	
CK 29	62.92	54	0	7	0	19	1	0	33	19	8	0	132	0	0	
CK 30	71.90	45	0	24	0	25	0	0	45	10	9	0	72	0	0	
CQ 0.1	0.09	0	0	16	0	1	1	0	11	0	0	0	273	0	7	
CQ0.3	0.30	4	1	12	0	0	0	0	5	0	0	0	255	0	7	
CQ0.5	0.44	0	7	5	0	0	0	1	27	0	0	0	287	0	8	
CQ0.8	0.72	6	8	9	0	0	0	1	20	0	0	0	198	0	12	
CQ1.2	1.08	3	0	10	0	1	0	3	28	0	1	0	130	0	6	
CQ1.6	1.44	2	3	2	0	0	1	2	20	1	6	0	136	0	2	
CQ2.0	1.80	8	9	9	1	2	0	0	12	0	4	0	154	0	2	
CQ2.5	2.25	8	0	4	0	0	0	0	8	0	1	0	102	0	0	
CQ3.0	2.70	5	6	7	0	0	0	0	14	0	0	0	216	0	0	
NSD 1	0.04	0	1	20	0	7	0	1	16	0	10	0	103	1	2	
NSD 2	0.15	0	11	12	0	2	0	0	11	7	5	0	120	2	4	
NSD 3	0.28	1	6	18	1	2	2	2	7	1	0	0	134	4	1	
NSD 4	0.37	4	13	0	0	0	0	2	11	11	2	0	157	15	0	
NSD 5	0.47	5	0	12	0	1	0	0	2	14	0	0	193	6	1	
NSD 6	0.49	0	4	15	0	0	0	0	7	0	0	0	167	12	1	
NSD 7	0.57	0	0	13	0	0	1	0	6	1	0	0	174	11	0	
NSD 8	0.65	2	11	2	0	1	0	3	9	7	0	0	136	0	2	
NSD 9	0.95	3	5	10	0	5	0	0	15	10	0	0	154	0	0	
NSD 10	0.97	17	27	13	1	5	0	1	27	11	1	0	192	0	0	
NSD 11	1.21	19	0	19	0	14	3	0	23	30	4	0	146	6	10	
NSD 14	1.82	24	6	7	0	15	1	0	33	38	28	0	13	2	4	
NSD 15	2.20	44	18	8	0	9	1	1	70	0	54	0	44	0	0	
NSD 16	2.22	29	0	5	0	11	0	0	12	86	25	0	12	0	1	
NSD 17	2.89	31	9	15	0	12	0	4	69	5	46	0	76	0	2	
NSD 18	2.79	31	18	10	0	2	0	2	54	0	121	0	27	0	0	
NSD 19	3.95	21	8	10	0	11	3	3	59	12	23	0	88	4	0	
NSD 20	4.05	34	0	14	0	25	3	4	36	21	19	0	70	3	3	
NSD 21	5.40	22	0	0	0	35	2	4	92	11	13	0	47	0	3	
NSD 22	5.66	40	1	3	0	23	1	1	33	49	16	0	9	0	2	
NSD 23	6.27	58	0	4	0	33	1	2	32	29	14	0	18	1	4	
NSD 24	10.11	37	0	5	0	19	1	2	24	93	26	0	10	0	3	
cMd 1	0.57	0	0	10	0	2	0	2	7	1	0	0	129	9		
cMd 2	0.80	3	0	4	0	1	0	2	6	4	0	0	190	7	1	
cMd 3	1.00	1	0	5	0	4	0	1	1	6	0	0	151	1	0	
cMd 4	1.20	9	0	2	0	7	0	0	9	10	0	0	149	6	0	
cMd 5	1.70	20	0	9	0	9	0	4	10	15	1	0	160	11	6	
cMd 6	2.00	67	0	0	0	35	0	6	41	31	16	0	74	5	6	
cMd 7	2.40	29	0	6	0	24	1	5	35	41	25	0	18	1	3	
cMd 8	3.00	40	0	2	0	7	0	1	27	60	12	0	66	6	1	

KEY

Sy = structure visible
Sn = structure not visible

Ang. = angular
Rndd = rounded

No df st = no definitive structure

Spores W = spores whole
Spores B = spores broken
Mgsp pcs = megaspore pieces
AOM = Amorphous Organic Matter
CPM = Coagulated Particulate Matter

<1250^2µm, >1250^2µm

TABLE 11 PALYNOFACIES *count divisions and absolute numbers (>1250^2 µm)*

Sample No.	Perp Dist(m	T. wood		OOM		Plant tissue				Palynomorphs			AOM		Indeterminate
ite		Sy	Sn	ang	rndd	ribbed	fibrous	membranou	no df st	spores W	sps B	mgsp pcs	AOM	CPM	
CK 1	0.07	16	2	41	0	7	0	1	58	0	0	0	56	0	4
CK 2	0.20	0	0	0	0	0	0	0	1	0	0	0	76	0	1
CK 3	0.25	0	2	2	0	0	0	0	1	0	0	0	143	0	1
CK 4	0.29	0	1	4	0	0	0	0	5	0	0	0	60	0	1
CK 5	0.34	5	0	6	0	0	0	0	0	0	0	0	81	0	1
CK 6	0.43	6	16	4	0	1	0	0	5	0	0	0	108	0	2
CK 7	0.49	4	0	0	0	0	0	0	0	0	0	0	39	0	1
CK 8	0.60	8	7	2	1	2	2	0	1	0	1	0	78	0	2
CK 9	0.81	45	6	15	0	9	0	0	28	0	0	0	2	0	8
CK 10	0.90	23	12	23	0	12	1	2	33	0	0	0	33	0	7
CK 11	1.03	15	0	6	0	0	0	0	9	0	3	0	77	0	3
CK 12	1.12	36	0	18	0	24	2	0	21	2	2	0	22	0	1
CK 13	1.39	42	9	31	7	17	3	0	38	0	0	0	11	0	10
CK 14	1.57	53	6	43	4	14	5	3	55	3	8	0	14	0	10
CK 15	1.80	97	11	32	3	14	3	0	39	1	6	0	5	0	6
CK 16	2.02	28	1	9	0	19	3	0	21	3	12	0	14	0	6
CK 17	2.25	48	10	28	1	18	3	24	50	5	6	0	7	0	5
CK 18	2.47	54	0	31	0	18	0	0	39	3	10	0	14	0	5
CK 19	2.83	27	0	17	0	15	2	2	9	2	4	2	4	0	1
CK 20	3.19	55	0	43	0	19	8	0	27	0	6	0	18	0	3
CK 21	3.60	70	0	41	1	33	3	1	30	5	8	0	5	0	1
CK 22	4.04	58	0	25	0	14	6	0	20	5	5	0	37	0	10
CK 23	4.49	59	6	11	2	12	12	1	50	0	12	0	30	5	3
CK 24	4.94	72	0	19	0	23	1	3	37	9	6	0	29	1	5
CK 25	5.39	50	11	18	0	11	3	16	31	7	3	0	27	0	4
CK 26	5.84	94	0	23	0	40	2	7	24	16	9	0	26	0	1
CK 27	8.99	60	0	20	0	20	5	2	32	2	2	0	74	6	0
CK 28	16.18	34	0	10	0	8	1	0	8	0	6	0	49	0	4
CK 29	62.92	53	0	5	0	11	6	0	10	6	2	0	33	0	0
CK 30	71.90	75	0	25	2	16	1	0	19	3	9	0	15	3	1
CQ 0.1	0.09	0	0	6	0	0	0	0	2	0	0	0	78	0	2
CQ0.3	0.30	0	0	4	0	1	0	0	2	0	0	0	103	0	5
CQ0.5	0.44	1	0	2	0	0	0	0	2	0	0	0	57	0	1
CQ0.8	0.72	21	9	20	0	2	1	0	8	0	0	0	71	0	14
CQ1.2	1.08	14	3	15	0	6	0	0	8	0	0	0	166	0	6
CQ1.6	1.44	19	0	11	0	1	2	3	11	0	2	0	171	0	1
CQ2.0	1.80	15	0	6	3	1	0	1	9	0	1	0	161	0	1
CQ2.5	2.25	22	0	7	0	6	1	0	7	0	1	0	230	0	2
CQ3.0	2.70	2	0	3	0	1	0	0	0	0	0	0	145	0	1
NSD 1	0.04	0	0	21	1	2	0	0	16	0	0	0	166	33	0
NSD 2	0.15	0	7	12	1	5	0	1	2	2	0	0	184	12	1
NSD 3	0.28	1	1	9	0	0	0	0	2	0	0	0	188	9	9
NSD 4	0.37	0	6	0	0	1	0	0	2	0	0	0	177	0	0
NSD 5	0.47	0	0	22	1	2	1	0	4	1	1	0	120	12	0
NSD 6	0.49	1	0	16	1	0	0	0	0	0	0	0	105	68	1
NSD 7	0.57	1	0	19	4	0	0	0	0	0	0	0	95	72	1
NSD 8	0.65	2	8	3	0	1	0	0	3	0	0	0	203	0	6
NSD 9	0.95	6	12	17	0	4	0	0	6	0	0	0	155	0	0
NSD 10	0.97	12	4	6	1	5	1	0	4	0	0	0	73	0	0
NSD 11	1.21	21	0	26	0	29	0	0	11	10	4	0	9	16	1
NSD 14	1.82	46	5	37	0	14	7	3	63	3	11	0	32	3	4
NSD 15	2.20	13	10	9	0	22	0	2	21	1	9	0	62	0	3
NSD 16	2.22	32	3	11	0	33	10	3	33	10	14	0	53	14	3
NSD 17	2.89	18	2	6	1	6	1	0	19	0	7	0	71	0	0
NSD 18	2.79	18	18	21	0	7	1	3	35	1	17	0	12	0	0
NSD 19	3.95	14	7	9	1	5	3	2	30	0	9	0	77	1	0
NSD 20	4.05	23	0	12	0	48	10	8	27	3	2	3	28	2	1
NSD 21	5.40	50	0	3	0	16	0	3	46	0	8	7	35	0	3
NSD 22	5.66	59	1	17	0	34	5	9	41	8	12	4	26	5	1
NSD 23	6.27	20	0	9	0	73	12	4	41	3	13	0	21	5	2
NSD 24	10.11	34	0	7	0	27	3	7	38	11	19	0	32	1	1
cMd 1	0.57	0	0	10	0	2	0	0	0	0	0	0	150	77	0
cMd 2	0.80	0	0	8	1	0	0	1	8	0	0	0	89	74	1
cMd 3	1.00	4	0	12	1	2	0	0	6	1	0	0	121	81	0
cMd 4	1.20	1	0	16	0	2	1	2	9	0	0	0	88	87	1
cMd 5	1.70	25	0	23	0	9	0	2	8	0	1	0	43	43	2
cMd 6	2.00	29	0	10	0	16	1	0	19	0	2	0	26	13	2
cMd 7	2.40	64	0	26	0	35	6	3	24	1	6	4	23	13	5
cMd 8	3.00	39	0	6	0	10	1	3	16	2	6	4	57	34	0

KEY

Sy = structure visible
Sn = structure not visible

Ang. = angular
Rndd = rounded

No df st = no definitive structure

Spores W = spores whole
Spores B = spores broken
Mgsp pcs = megaspore pieces
AOM = Amorphous Organic Matter
CPM = Coagulated Particulate Matter

<1250^2µm, *>1250^2µm*

TABLE 12 PALYNOFACIES *count divisions and absolute numbers (>1250^2 µm)*

KEY

Sy = structure visible
Sn = structure not visible

Ang. = angular
Rndd = rounded

No df st = no definitive structure

Spores W = spores whole
Spores B = spores broken
Mgsp pcs = megaspore pieces
AOM = Amorphous Organic Matter
CPM = Coagulated Particulate Matter

<1250^2µm, *>1250^2µm*

Palynofacies divisions % content

Sample No.	Perp Distcr T. wood Sy	Sn	Total wood	OOM ang	OOM rndd	Total OOM	Plant tissue ribbed	Plant tissue fibrous	membranou no df st	Total plant ti Palynomorphs spores W	Palynomorphs sps B	mgsp pcs	Total palyno AOM	Total palyno AOM	CPM	Total AOM	Indeterminate
CK 1	0.07	5	2	7	23	1	24	4	0	1	26	31	1	0	0	1	33	0	33	4
CK 2	0.20	0	0	0	3	0	3	0	0	0	0	0	0	0	0	0	96	0	96	0
CK 3	0.25	1	3	4	1	0	1	0	0	1	1	0	0	0	0	0	95	0	95	0
CK 4	0.29	0	1	1	2	0	2	0	0	0	1	0	0	0	0	0	94	0	94	1
CK 5	0.34	1	0	1	2	0	2	0	0	0	1	0	0	0	0	0	95	0	95	0
CK 6	0.43	2	7	9	2	0	2	0	0	0	2	0	0	0	0	0	87	0	87	1
CK 7	0.46	1	0	1	2	0	2	0	0	1	1	0	0	0	0	0	95	0	95	1
CK 8	0.90	3	6	9	2	0	2	1	1	0	3	6	0	0	1	1	81	0	81	1
CK 9	0.91	25	6	31	8	0	8	3	0	0	19	22	2	0	0	2	34	0	34	3
CK 10	0.96	16	6	22	12	0	12	4	1	1	20	26	1	2	0	3	35	0	35	5
CK 11	1.03	7	3	10	8	0	8	2	0	0	23	25	1	3	0	4	38	0	38	3
CK 12	1.12	21	0	21	7	0	7	12	1	2	18	33	4	4	0	8	32	0	32	1
CK 13	1.38	18	4	22	15	2	17	7	1	1	33	42	4	0	0	4	11	0	11	4
CK 14	1.57	23	4	27	14	1	15	5	2	1	26	34	4	6	0	10	12	0	12	5
CK 15	1.80	36	4	40	15	1	16	5	1	0	24	30	3	4	0	7	4	0	4	3
CK 16	2.02	13	0	13	5	0	5	6	1	0	12	19	3	4	0	7	50	0	50	4
CK 17	2.25	21	5	26	10	0	10	6	1	7	28	42	7	3	0	10	10	0	10	1
CK 18	2.47	17	1	18	13	0	13	6	1	0	16	23	4	4	0	8	33	0	33	2
CK 19	2.83	19	0	19	5	5	10	4	2	1	9	16	2	4	1	6	51	0	51	1
CK 20	3.19	29	0	29	16	0	16	9	6	1	7	23	13	4	0	17	14	0	14	1
CK 21	3.80	41	0	41	12	0	12	15	1	1	17	34	9	6	0	15	2	0	2	3
CK 22	4.04	23	1	24	11	0	11	8	2	1	11	22	6	2	0	8	26	0	26	5
CK 23	4.46	30	2	32	6	1	7	4	4	1	23	32	7	6	0	13	17	2	19	2
CK 24	4.94	27	0	27	7	0	7	7	1	1	17	26	7	3	0	10	28	1	29	1
CK 25	5.39	31	7	38	8	0	8	4	1	5	17	27	5	2	0	7	31	0	31	1
CK 26	5.84	33	0	33	7	0	7	16	1	2	12	31	12	4	0	16	12	0	12	2
CK 27	6.99	22	0	22	8	0	8	9	2	0	20	31	2	1	0	3	26	1	27	0
CK 28	16.18	26	0	26	3	0	3	4	0	0	5	9	1	4	0	5	61	0	61	1
CK 29	62.82	27	0	27	3	0	3	8	2	0	11	21	6	3	0	9	41	0	41	0
CK 30	71.90	32	0	32	12	1	13	10	0	0	16	26	3	4	0	7	22	1	23	0
CQ 0.1	0.09	0	0	0	6	0	6	0	0	0	3	3	0	0	0	0	88	0	88	2
CQ0.3	0.30	1	0	1	4	0	4	0	0	0	2	2	0	0	0	0	90	0	90	3
CQ0.5	0.44	0	2	2	2	0	2	0	0	0	7	7	0	0	0	0	86	0	86	2
CQ0.8	0.72	7	2	9	7	0	7	1	0	0	7	8	0	0	0	0	67	0	67	6
CQ1.2	1.08	4	1	5	6	0	6	2	0	1	9	12	0	0	0	0	74	0	74	3
CQ1.6	1.44	5	1	6	3	0	3	0	1	1	8	10	0	0	0	0	77	0	77	1
CQ2.0	1.80	6	2	8	4	1	5	1	0	0	5	6	0	2	0	2	77	0	79	1
CQ2.5	2.25	7	0	7	3	0	3	1	0	0	4	5	0	1	0	1	83	0	83	1
CQ3.0	2.70	2	1	3	3	0	3	0	0	0	3	3	0	1	0	1	90	0	90	0
NSD 1	0.04	0	0	0	10	0	10	2	0	0	8	10	0	2	0	2	67	8	75	1
NSD 2	0.15	0	4	4	6	0	6	2	0	0	3	5	2	1	0	3	76	3	79	1
NSD 3	0.28	1	2	3	7	0	7	1	1	1	2	5	0	0	0	0	81	3	84	2
NSD 4	0.37	1	5	6	0	0	0	0	0	0	3	3	3	0	0	3	83	4	87	0
NSD 5	0.47	1	0	1	8	0	8	1	0	0	2	3	4	0	0	4	78	3	81	0
NSD 6	0.49	0	1	1	8	0	8	0	0	0	2	2	0	0	0	0	68	20	88	1
NSD 7	0.57	0	0	0	8	1	9	0	0	0	2	2	0	0	0	0	67	21	88	0
NSD 8	0.66	1	5	6	1	0	1	1	0	1	3	5	2	0	0	2	85	0	85	2
NSD 9	0.95	2	4	6	7	0	7	2	0	0	5	7	2	0	0	2	77	0	77	0
NSD 10	0.97	7	8	15	5	0	5	2	0	0	8	10	3	0	0	3	66	0	66	0
NSD 11	1.21	7	0	7	11	0	11	11	1	0	9	21	10	2	0	12	39	5	44	3
NSD 14	1.62	18	3	21	11	0	11	7	2	1	24	34	10	10	0	20	11	2	13	2
NSD 15	2.20	16	7	23	4	0	4	8	0	1	13	23	9	0	0	16	27	0	27	1
NSD 16	2.22	14	1	15	4	0	4	11	2	1	18	32	0	16	0	16	16	3	19	1
NSD 17	2.69	12	3	15	5	0	5	4	0	1	11	25	24	10	0	34	16	3	19	1
NSD 18	2.79	9	9	18	8	0	8	2	0	1	22	27	1	13	0	14	37	0	37	0
NSD 19	3.95	9	4	13	5	0	5	4	2	1	22	29	3	8	0	11	41	1	42	0
NSD 20	4.05	15	0	15	6	0	6	18	3	3	16	40	6	5	1	11	24	1	25	1
NSD 21	5.40	22	0	22	1	0	1	13	0	2	34	49	3	5	2	8	20	0	20	0
NSD 22	5.66	25	1	26	5	0	5	14	2	2	18	36	14	7	1	21	9	1	10	1
NSD 23	6.27	19	0	19	3	0	3	26	3	2	18	49	8	7	0	15	10	2	12	2
NSD 24	10.11	18	0	18	3	0	3	11	1	2	16	30	26	11	0	37	10	0	10	1
cMd 1	0.57	0	0	0	5	0	5	1	0	1	2	4	0	0	0	0	70	21	91	0
cMd 2	0.80	1	0	1	3	0	3	0	0	1	3	4	1	0	0	1	70	21	91	1
cMd 3	1.00	1	0	1	4	0	4	2	0	0	2	4	2	0	0	2	68	21	89	0
cMd 4	1.20	2	0	2	5	0	5	2	0	1	4	7	2	0	0	2	59	23	82	0
cMd 5	1.70	13	0	13	8	0	8	4	0	2	4	10	4	1	0	5	51	15	66	2
cMd 6	2.00	22	0	22	3	0	3	13	0	1	15	29	8	5	0	13	25	4	29	2
cMd 7	2.40	23	0	23	8	0	8	15	2	2	15	34	11	8	0	19	10	4	14	2
cMd 8	3.00	19	0	19	2	0	2	4	0	1	11	16	16	4	0	20	31	9	40	0

TABLE 13 PALYNOFACIES *divisions after Tyson (1995), absolute counts and % cnotent*

		TYSON					
		ABSOLUTE COUNT			%		
Sample No.	Perp Dist(m)	Palynomorph	Phytoclast	AOM	Palynomorph	Phytoclast	AOM
cMd 1	0.57	1	41	320	0	11	88
cMd 2	0.80	4	32	325	1	9	90
cMd 3	1.00	6	30	287	2	9	89
cMd 4	1.20	8	48	266	2	15	83
cMd 5	1.70	15	101	240	4	28	67
cMd 6	2.00	43	200	101	13	58	29
cMd 7	2.40	72	234	50	20	66	14
cMd 8	3.00	73	132	134	22	39	40
NSD 1	0.04	9	79	286	2	21	76
NSD 2	0.15	12	54	275	4	16	81
NSD 3	0.28	1	42	276	0	13	87
NSD 4	0.37	14	42	378	3	10	87
NSD 5	0.47	14	42	276	4	13	83
NSD 6	0.49	0	37	285	0	11	89
NSD 7	0.57	1	35	278	0	11	89
NSD 8	0.65	6	41	295	2	12	86
NSD 9	0.95	10	81	320	2	20	78
NSD 10	0.97	12	125	274	3	30	67
NSD 11	1.21	34	128	177	10	38	52
NSD 14	1.82	75	252	47	20	67	13
NSD 15	2.20	67	232	109	16	57	27
NSD 16	2.22	130	174	73	34	46	19
NSD 17	2.89	76	250	189	15	49	37
NSD 18	2.79	137	231	39	34	57	10
NSD 19	3.95	40	163	157	11	45	44
NSD 20	4.05	45	223	96	12	61	26
NSD 21	5.40	44	298	91	10	69	21
NSD 22	5.66	83	243	37	23	67	10
NSD 23	6.27	55	284	42	14	75	11
NSD 24	10.11	136	187	38	38	52	11
CK 1	0.07	4	238	122	1	65	34
CK 2	0.20	0	11	300	0	4	96
CK 3	0.25	0	16	308	0	5	95
CK 4	0.29	1	16	305	0	5	95
CK 5	0.34	1	15	305	0	5	95
CK 6	0.43	0	39	290	0	12	88
CK 7	0.49	1	14	309	0	4	95
CK 8	0.60	3	58	272	1	17	82
CK 9	0.81	7	215	116	2	64	34
CK 10	0.90	10	215	129	3	61	36
CK 11	1.03	5	72	257	1	22	77
CK 12	1.12	32	200	118	9	57	34
CK 13	1.39	13	295	39	4	85	11
CK 14	1.57	38	295	48	10	77	13
CK 15	1.60	23	276	12	7	89	4
CK 16	2.02	22	123	155	7	41	52
CK 17	2.25	35	271	36	10	79	11
CK 18	2.47	26	75	102	13	37	50
CK 19	2.83	25	153	187	7	42	51
CK 20	3.19	25	243	42	8	78	14
CK 21	3.60	60	271	48	16	72	13
CK 22	4.04	24	195	83	8	65	27
CK 23	4.49	51	250	66	14	68	18
CK 24	4.94	31	200	90	10	62	28
CK 25	5.39	31	289	143	7	62	31
CK 26	5.84	58	259	42	16	72	12
CK 27	8.99	7	183	170	2	51	47
CK 28	16.18	18	116	213	5	33	61
CK 29	62.92	31	174	143	9	50	41
CK 30	71.90	28	255	83	8	70	23
CQ 0.1	0.09	0	31	283	0	10	90
CQ0.3	0.30	0	23	295	0	7	93
CQ0.5	0.44	0	39	278	0	12	88
CQ0.8	0.72	0	91	235	0	28	72
CQ1.2	1.08	1	81	252	0	24	75
CQ1.6	1.44	8	70	256	2	21	77
CQ2.0	1.80	5	67	276	1	19	79
CQ2.5	2.25	2	54	289	1	15	84
CQ3.0	2.70	0	33	313	0	10	90

APPENDIX II

VITRINITE REFLECTANCE HISTOGRAMS

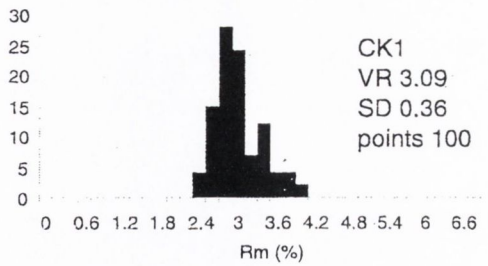

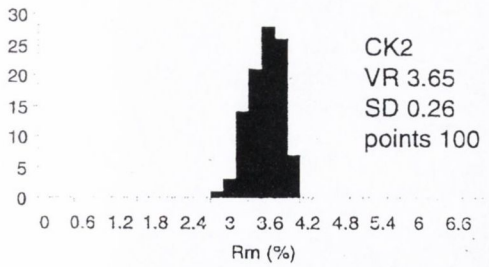

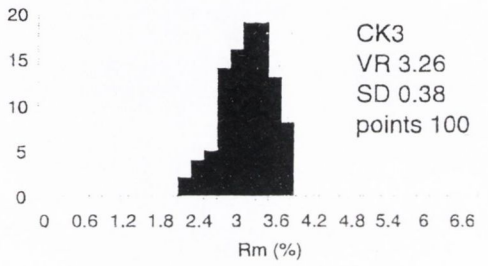

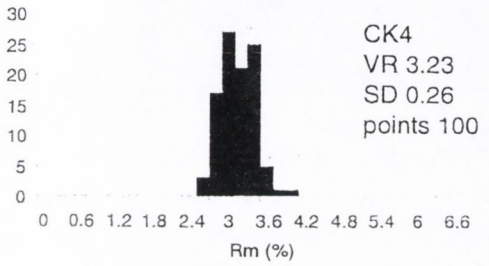

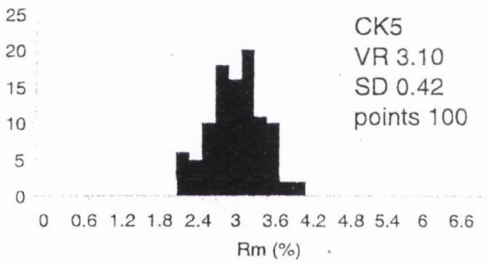

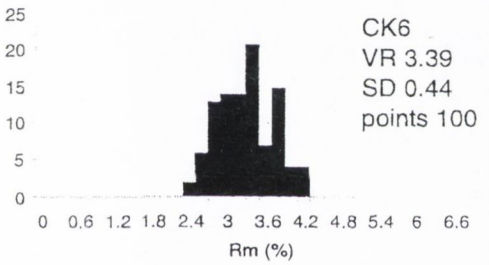

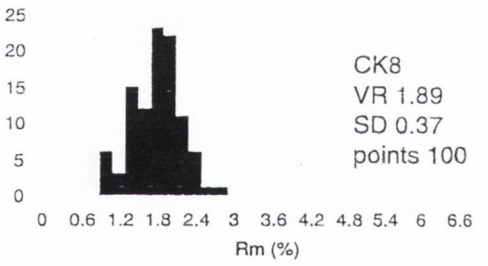

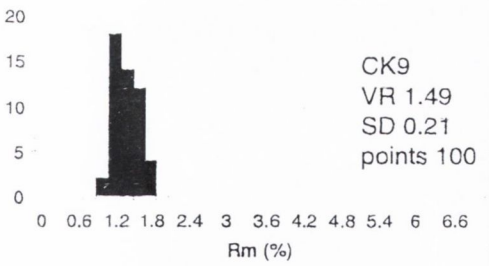

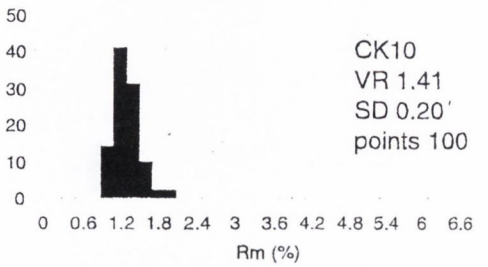

Histograms for Vitrinite results for samples CK1-10 in the CK traverse; Carrickleck Dyke aureole.

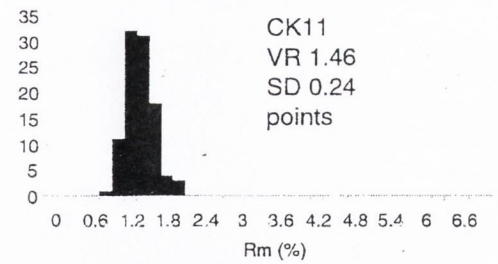

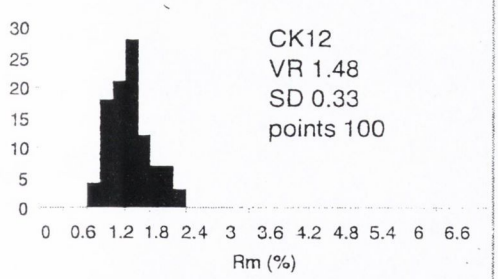

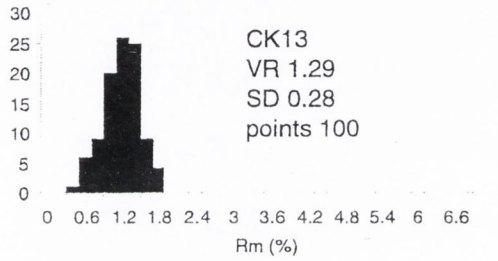

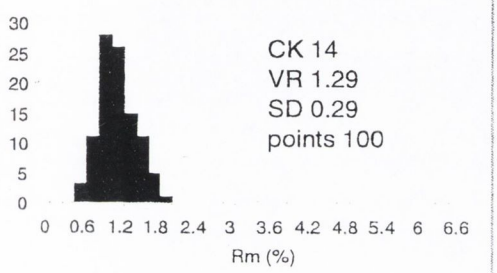

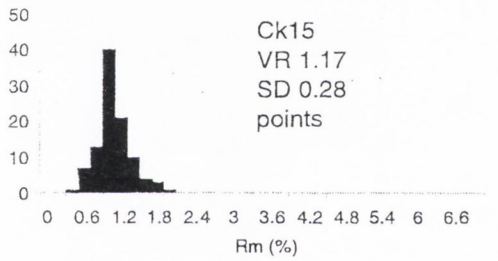

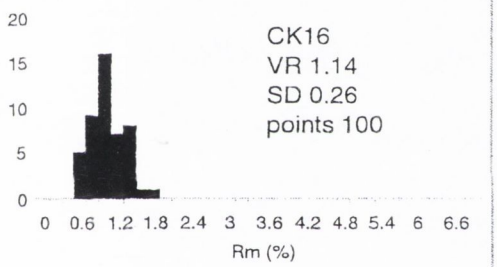

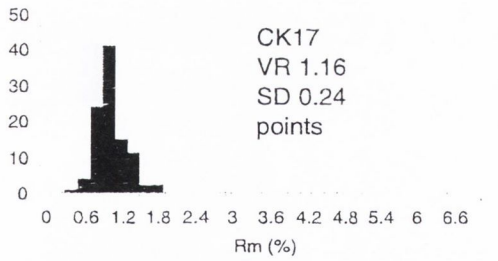

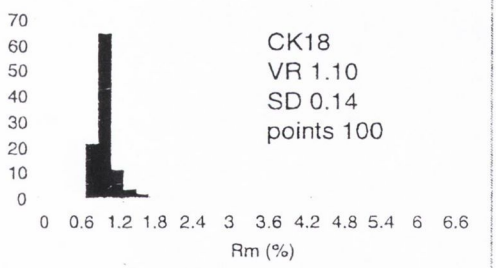

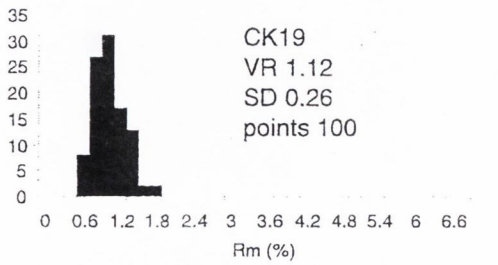

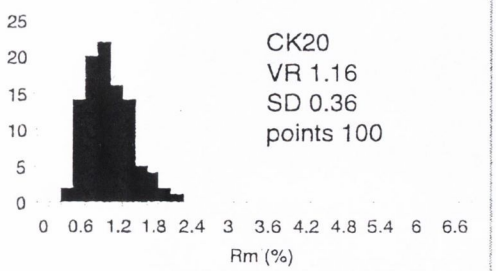

Histograms for Vitrinite results for samples CK11-20 in the CK traverse; Carrickleck Dyke aureole.

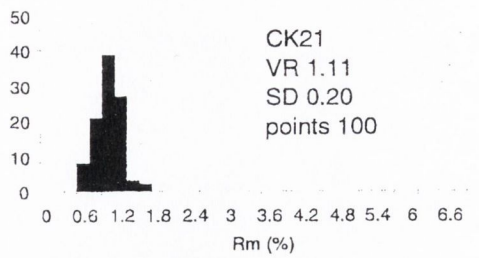

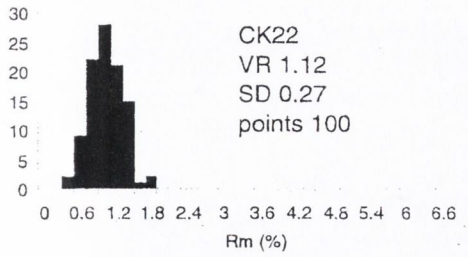

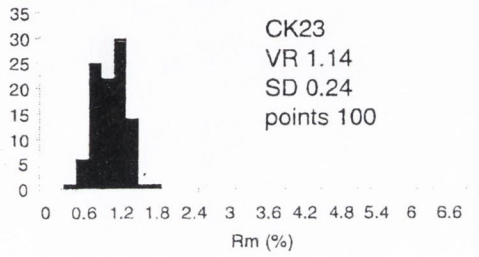

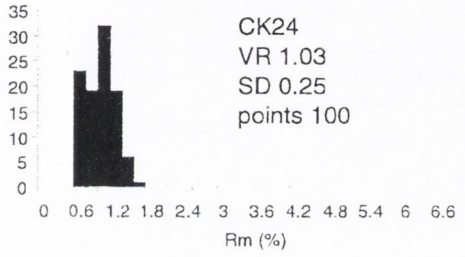

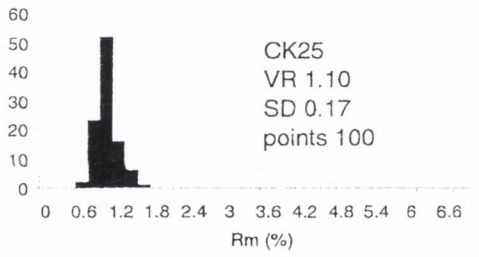

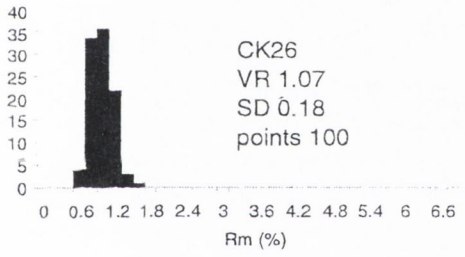

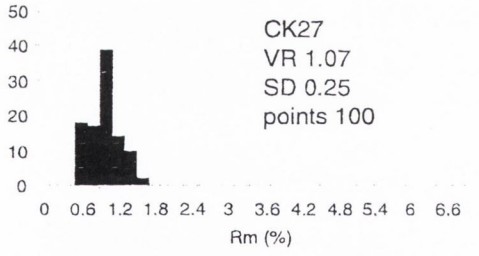

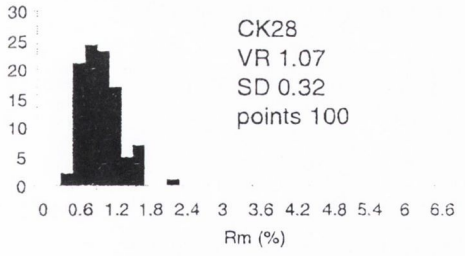

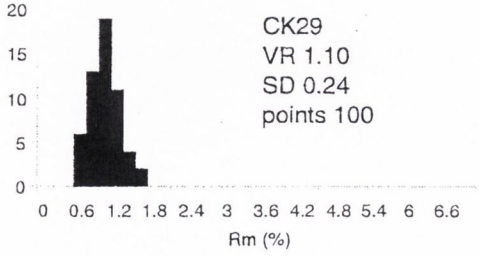

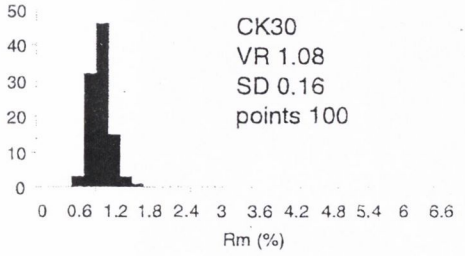

Histograms for Vitrinite results for samples CK21-30 in the CK traverse; Carrickleck Dyke aureole.

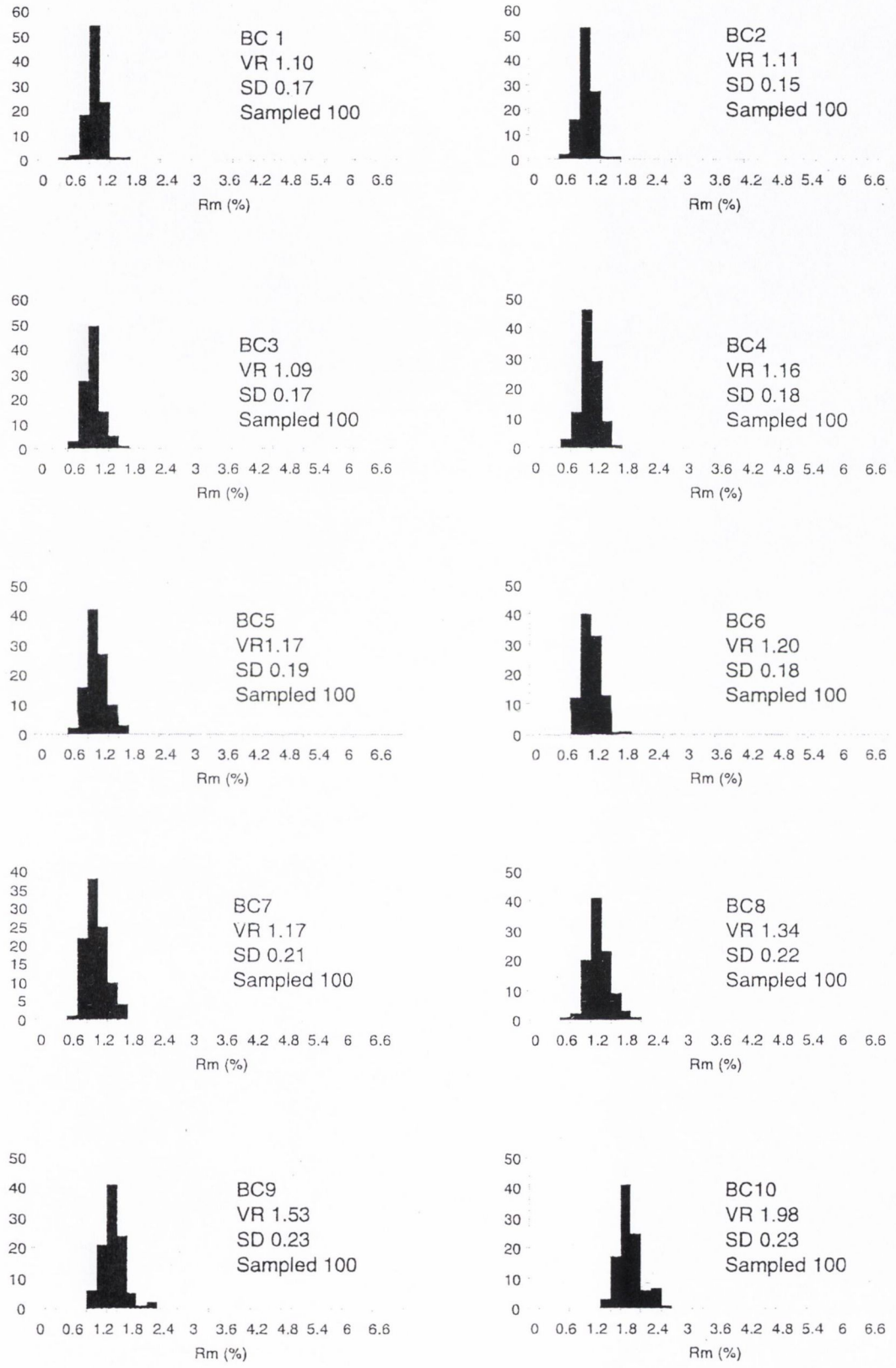

Histograms for Vitrinite results for samples BC 1-10 from the North Star Dyke aureole.

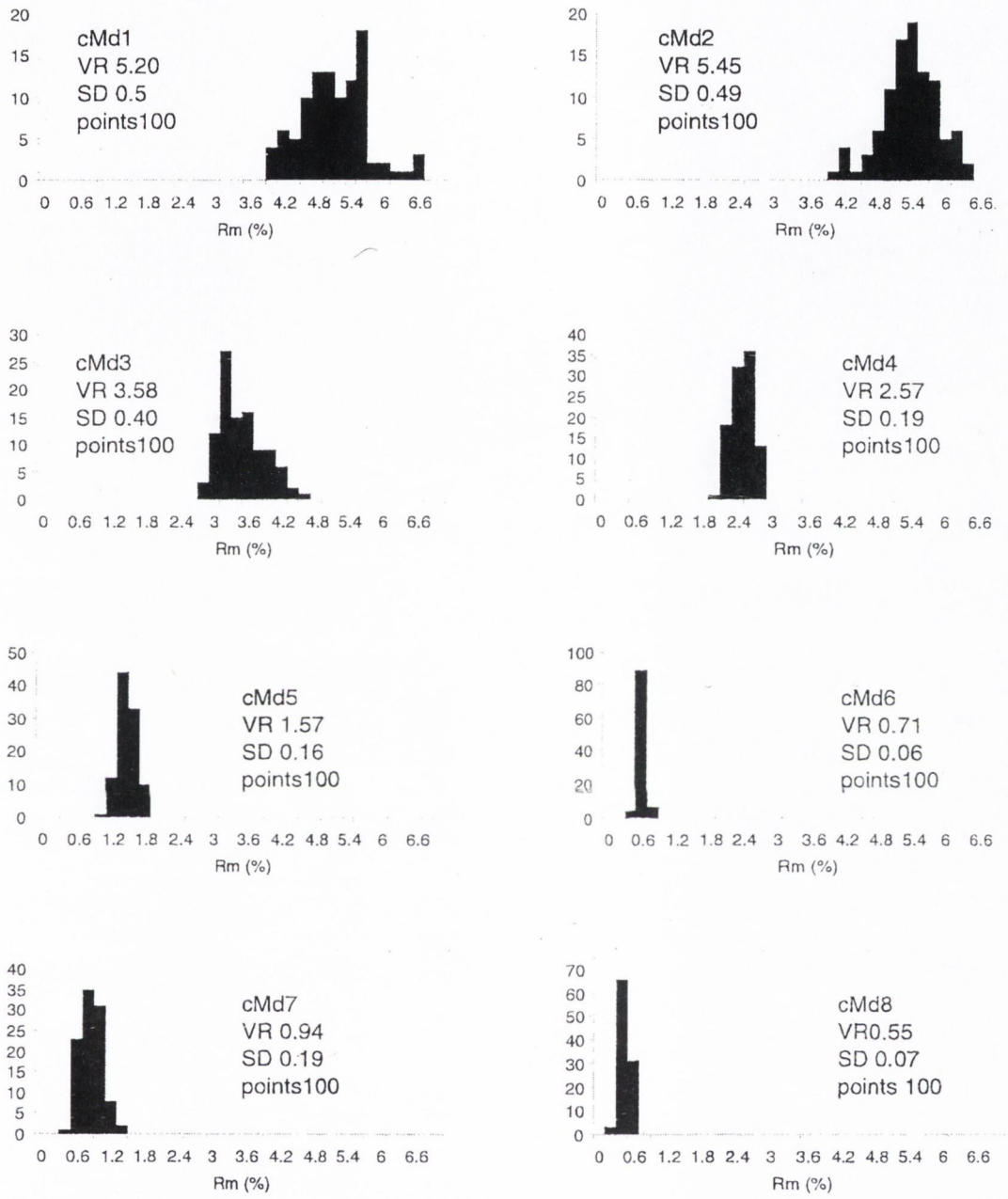

Histograms for Vitrinite results for samples cMd 1-8 from the North Star Dyke aureole

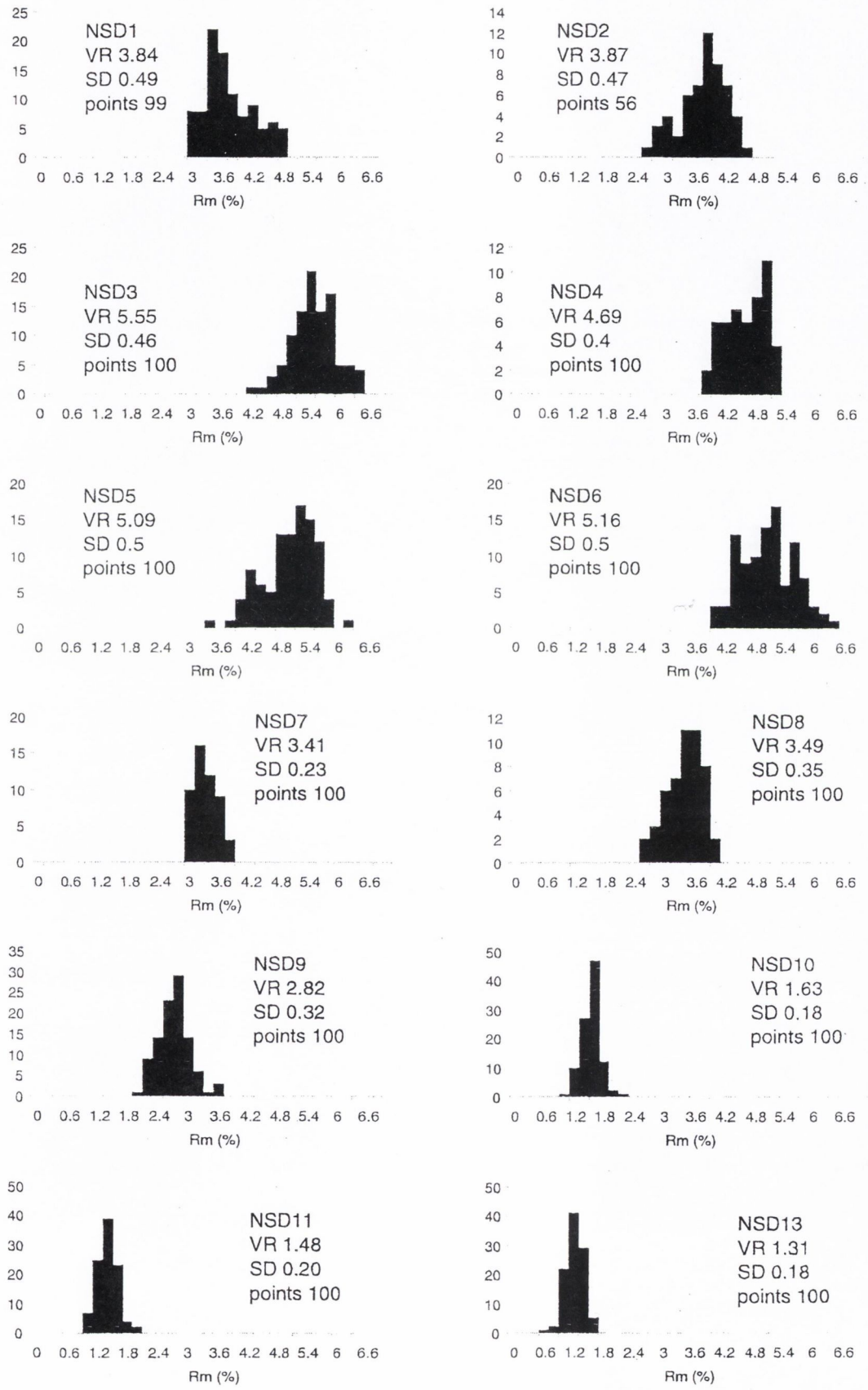

Histograms for Vitrinite results for samples NSD 1-13 from the North Star Dyke aureole

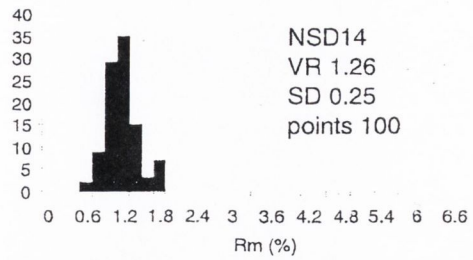

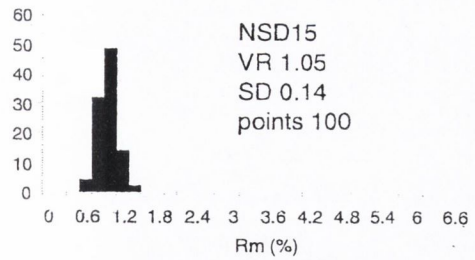

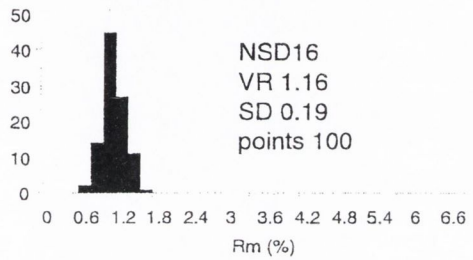

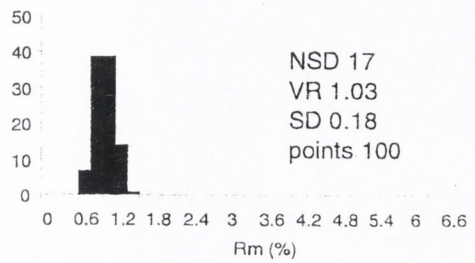

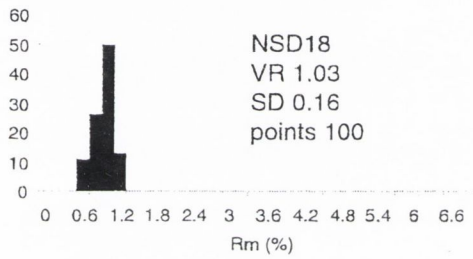

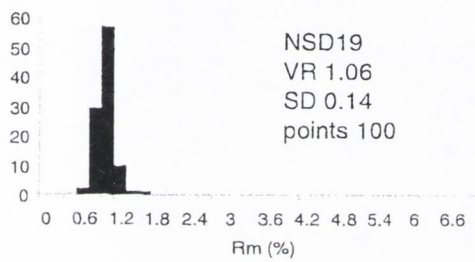

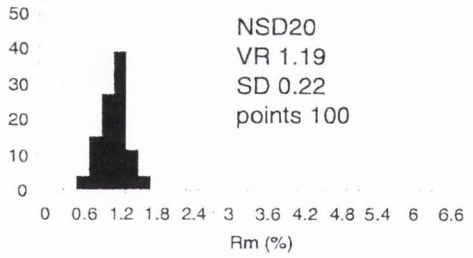

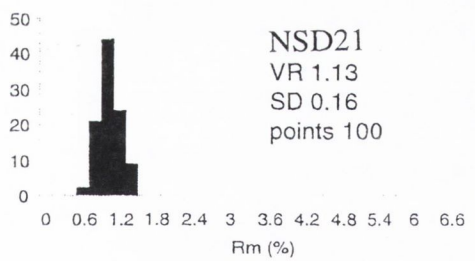

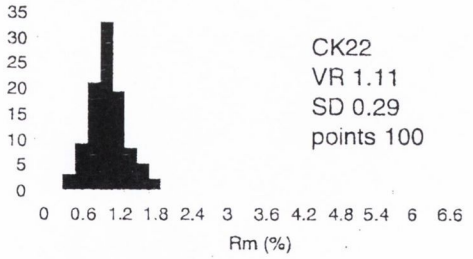

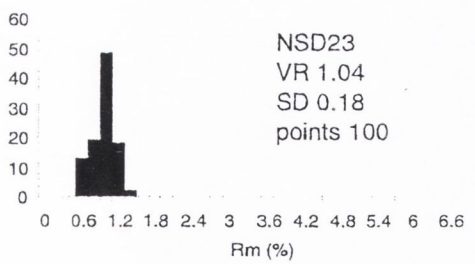

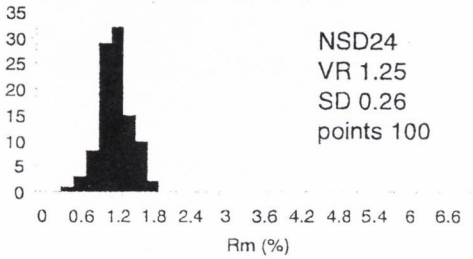

Histograms for Vitrinite results for samples NSD 14-24 from the North Star Dyke aureole

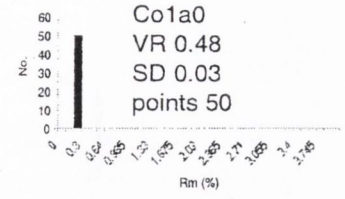

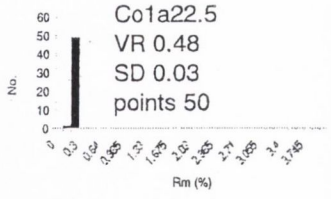

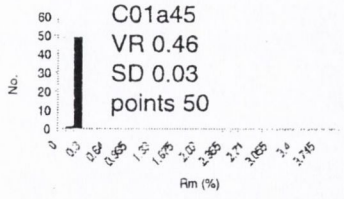

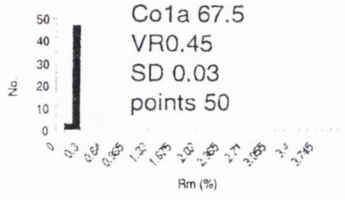

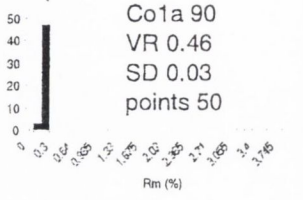

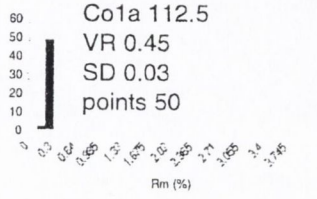

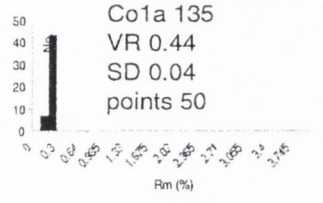

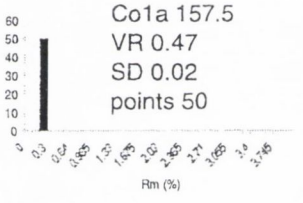

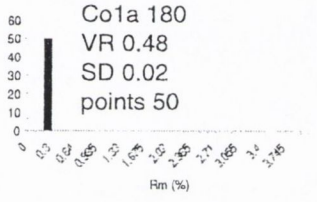

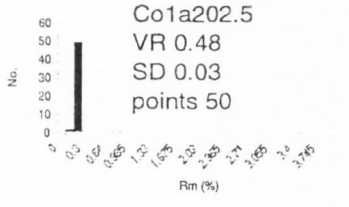

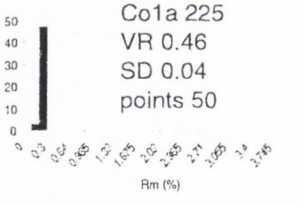

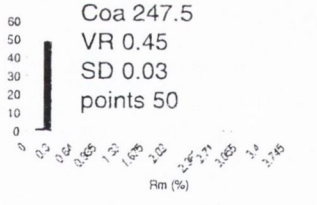

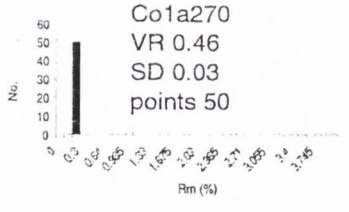

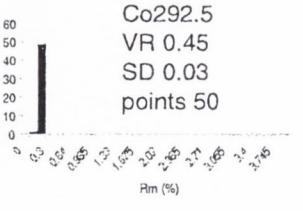

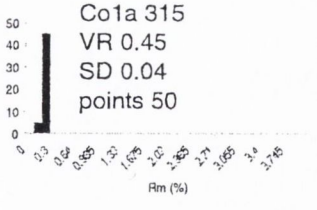

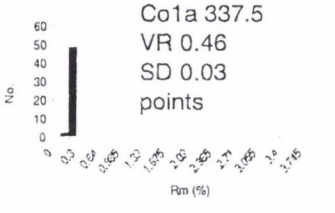

Histograms for Co1a , oriented coal lens collected from the cMd horizon. Measurements taken on the lense face perpendicular to bedding.

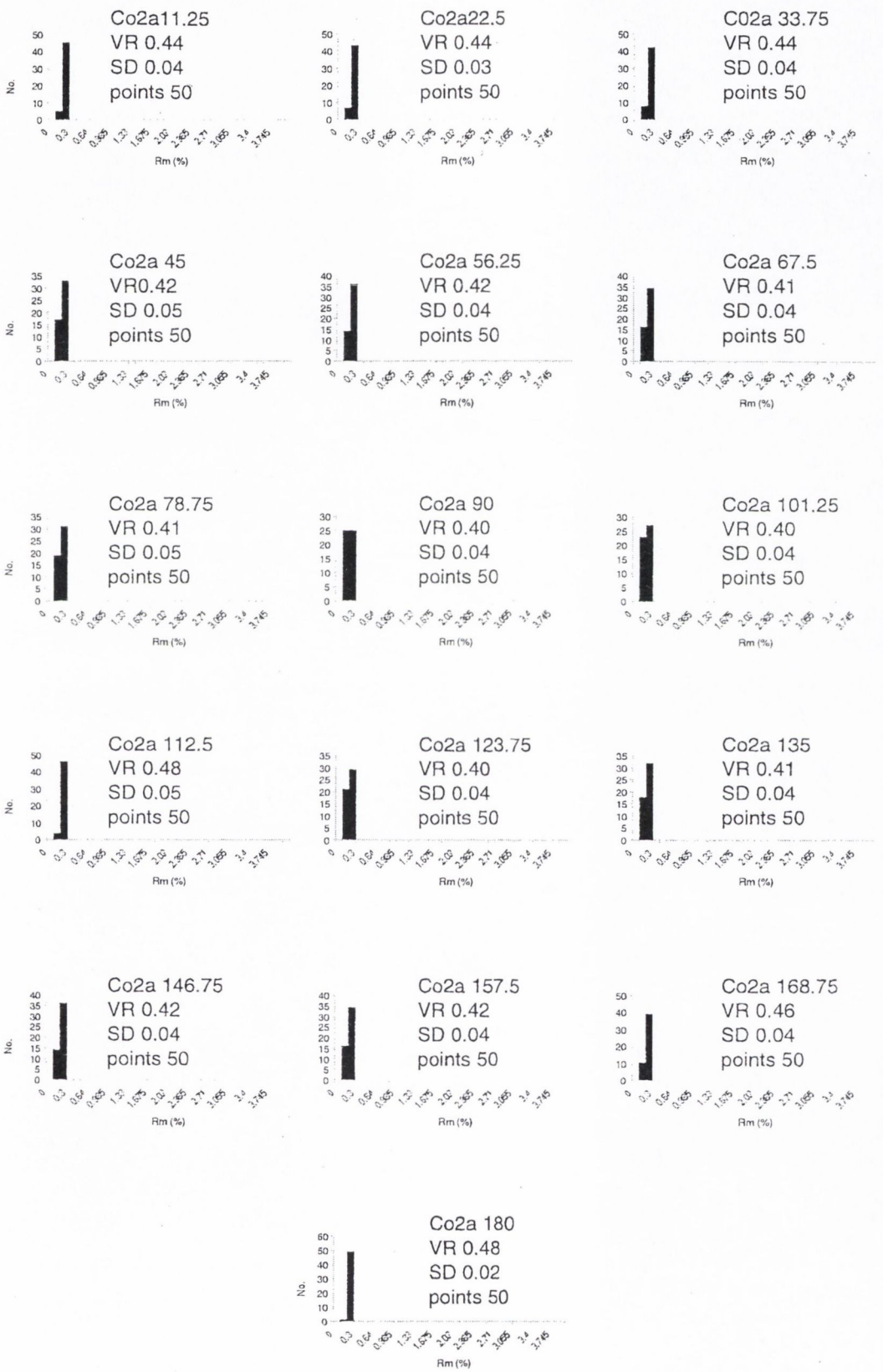

Histograms for Co2a , oriented coal lens collected from the cMd horizon. Measurements taken on the lense face cut perpendicular to bedding and strike.

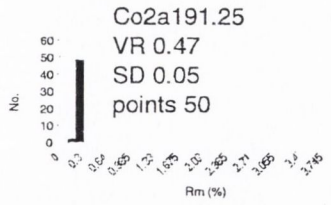

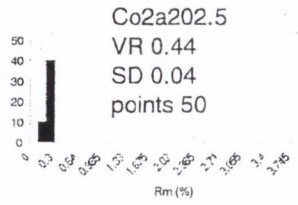

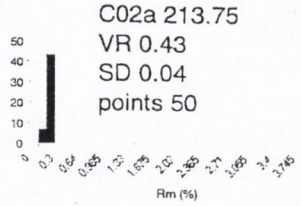

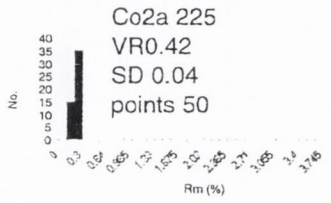

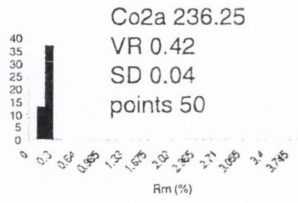

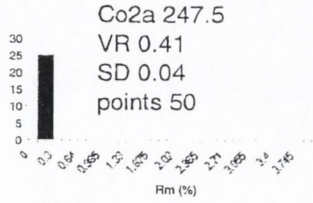

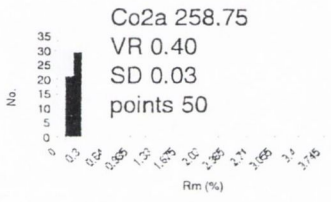

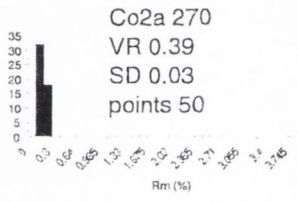

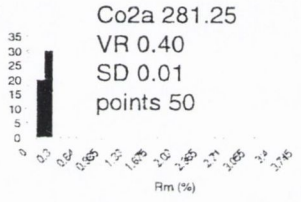

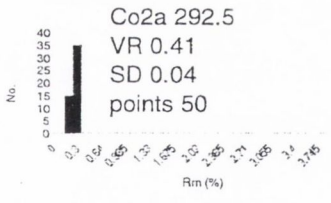

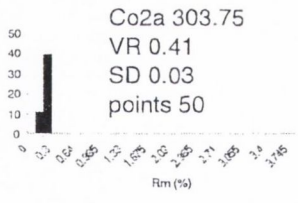

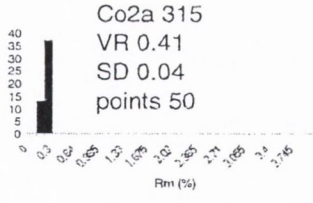

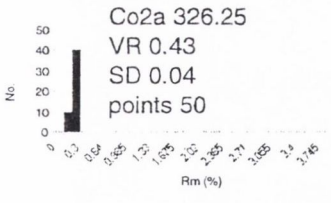

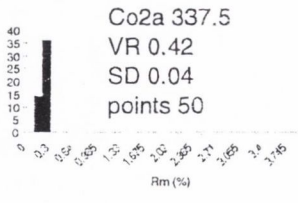

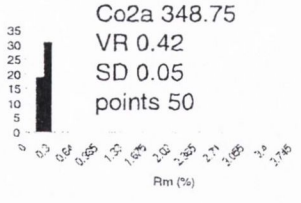

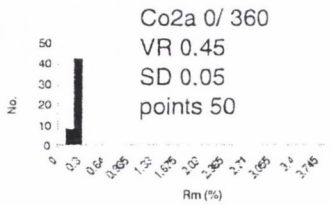

Histograms for Co2a , oriented coal lens· collected from the cMd horizon. Measurements taken on the lense face cut perpendicular to bedding and strike.

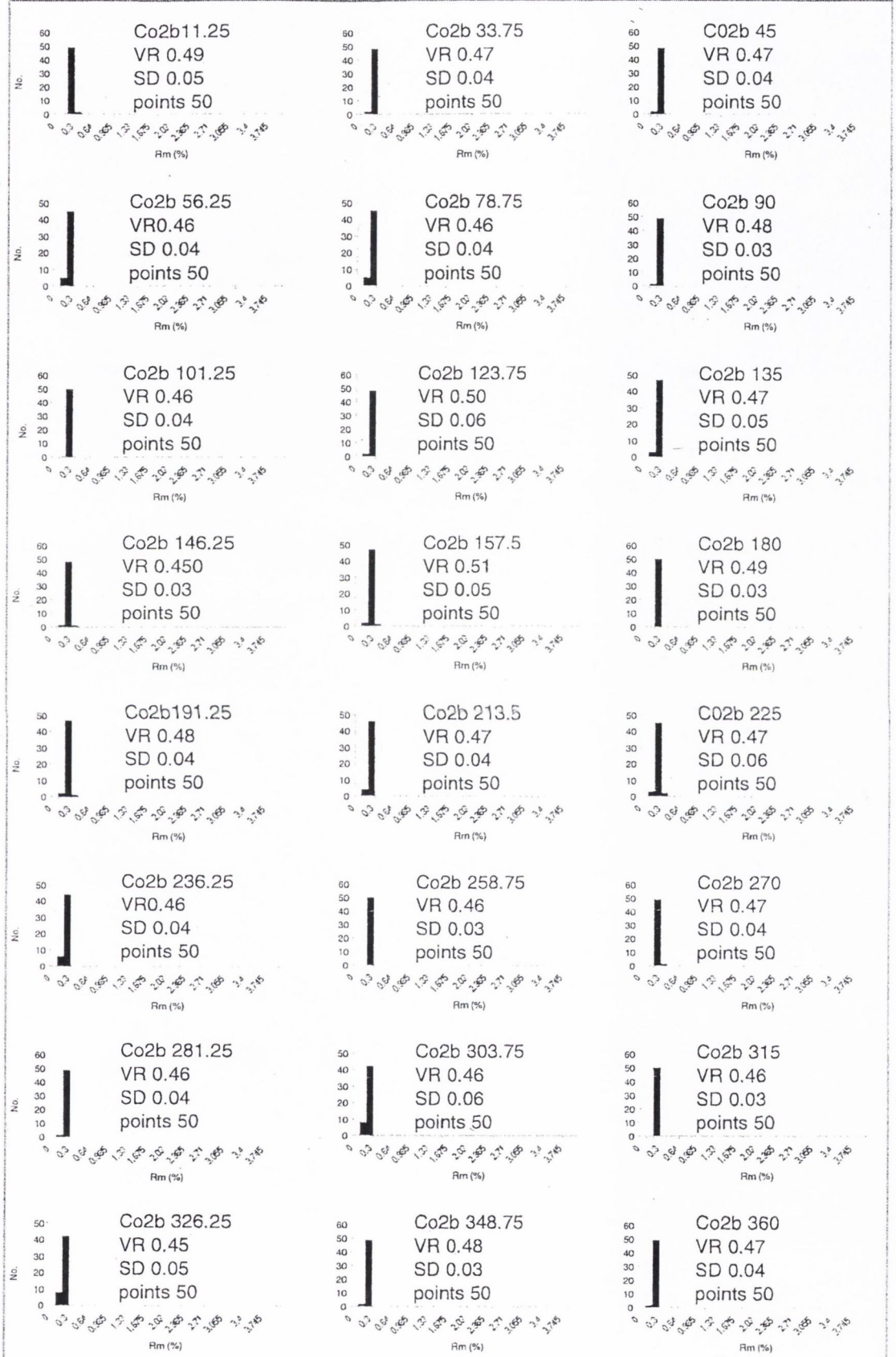

Histograms for Co2b , oriented coal lens collected from the cMd horizon. Measurements taken on the lense face cut parallel to bedding and strike.

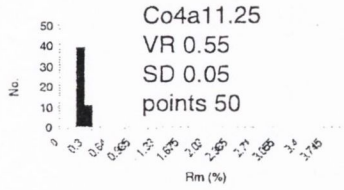

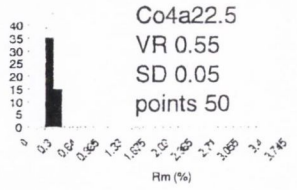

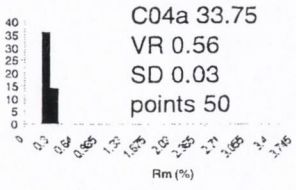

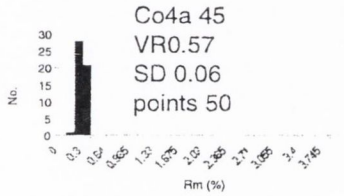

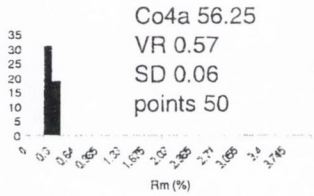

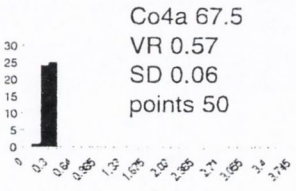

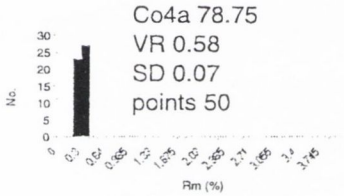

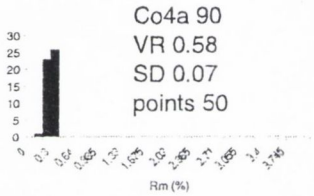

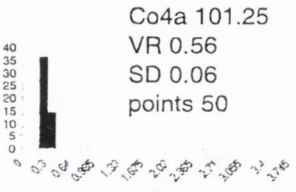

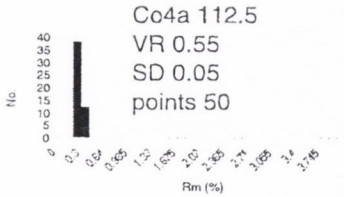

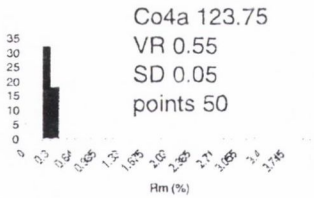

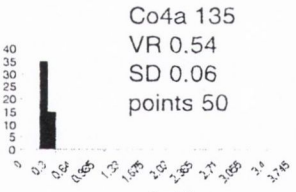

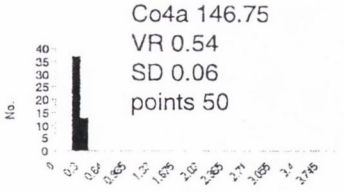

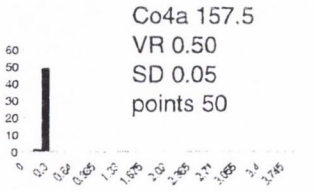

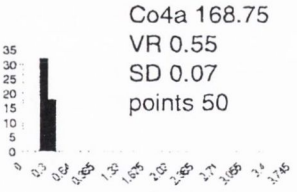

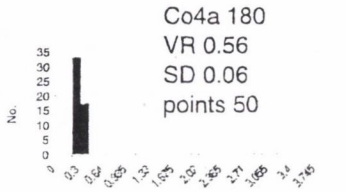

Histograms for Co4a , oriented coal lens collected from the cMd horizon. Measurements taken on the lense face cut perpendicular to bedding and strike.

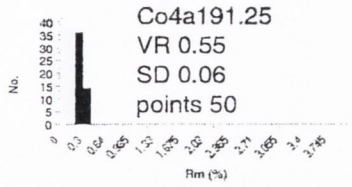

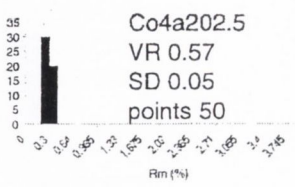

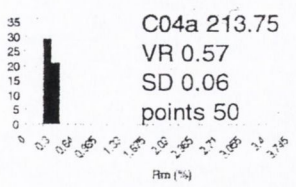

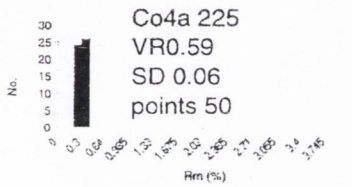

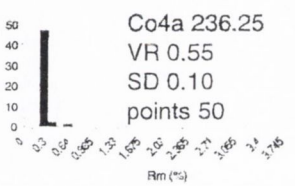

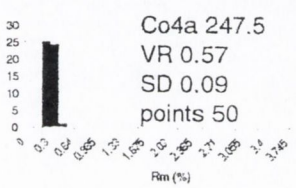

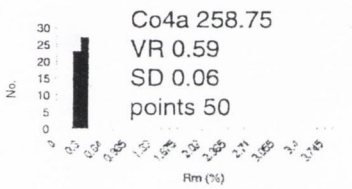

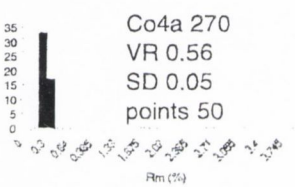

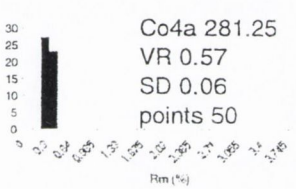

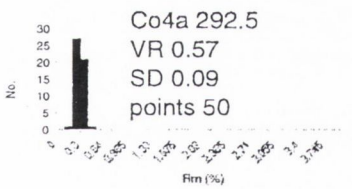

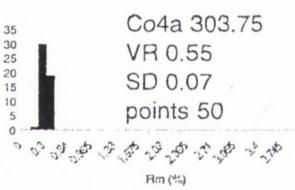

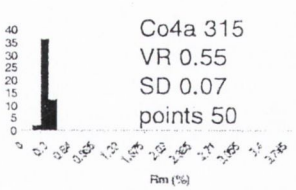

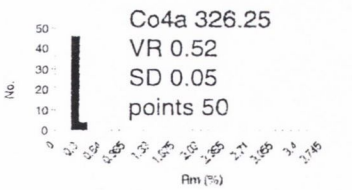

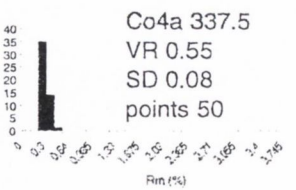

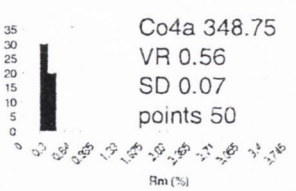

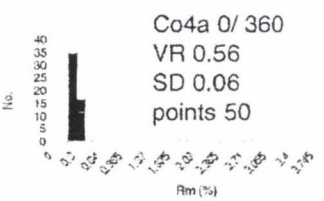

Histograms for Co4a , oriented coal lens collected from the cMd horizon. Measurements taken on the lense face cut perpendicular to bedding and strike for Rmax and Rmin measurements.

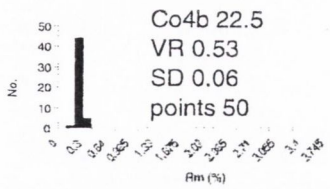

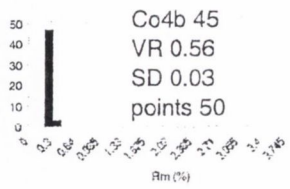

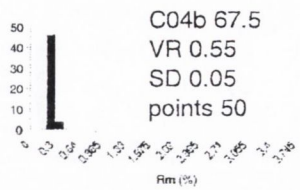

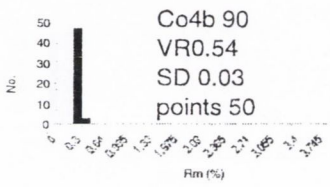

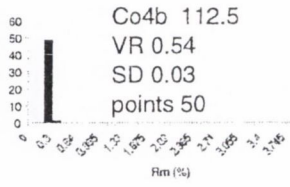

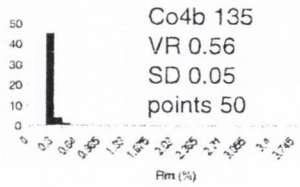

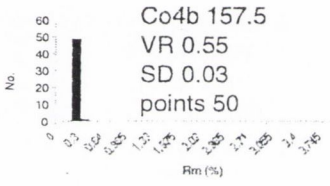

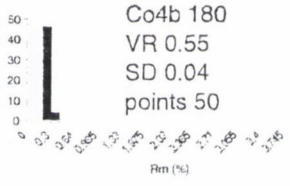

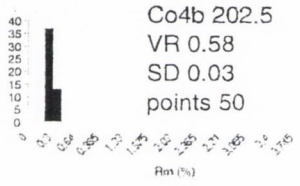

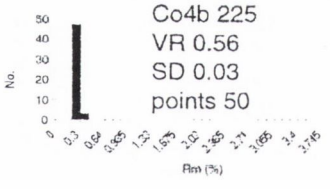

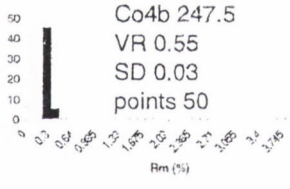

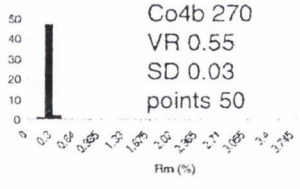

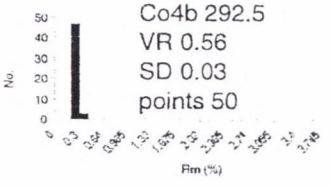

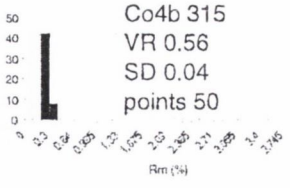

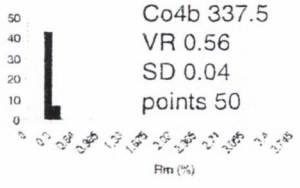

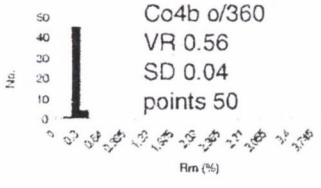

Histograms for Co4b , oriented coal lens collected from the cMd horizon. Measurements taken on the lense face cut perpendicular to bedding and parallel to strike, for Rmax and Rmin.

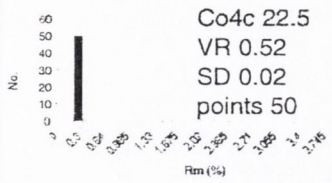

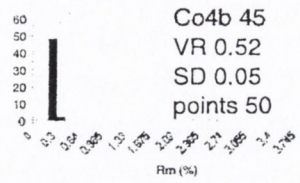

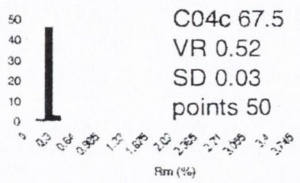

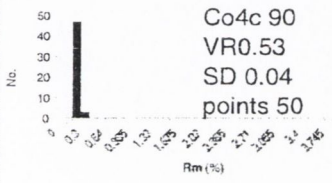

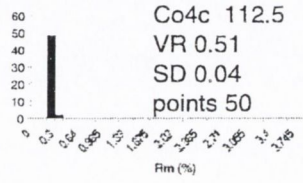

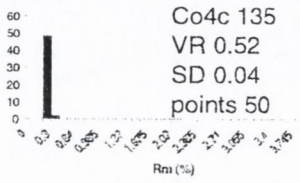

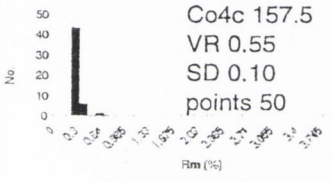

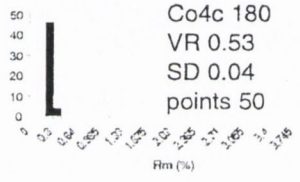

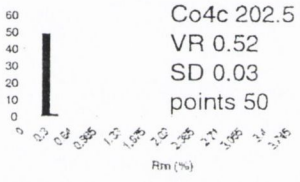

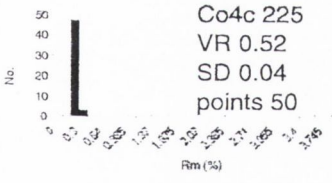

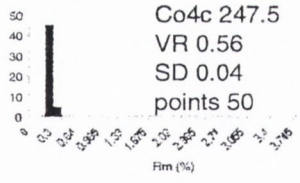

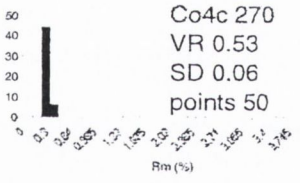

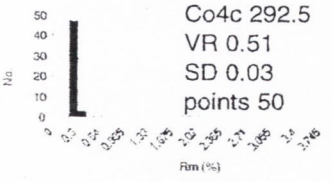

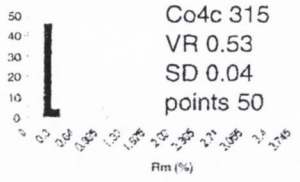

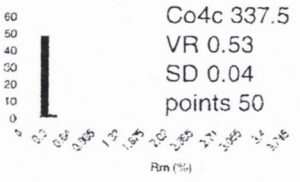

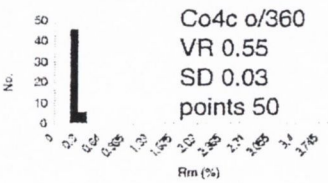

Histograms for Co4c, oriented coal lens collected from the cMd horizon. Measurements taken on the lense face cut parallel to bedding and strike, for the prupose of Rmax and Rmin measurements.

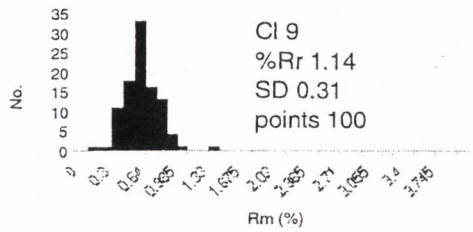

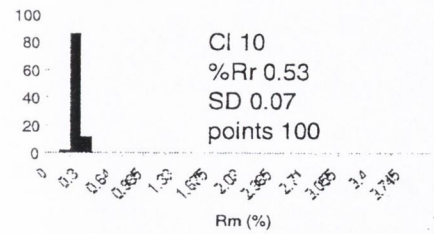

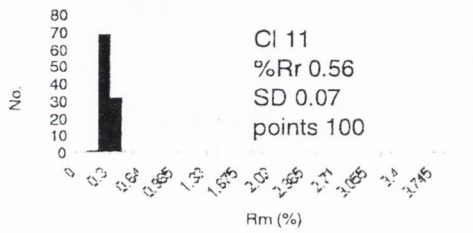

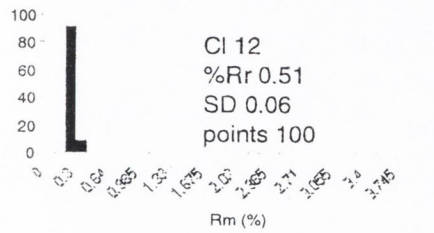

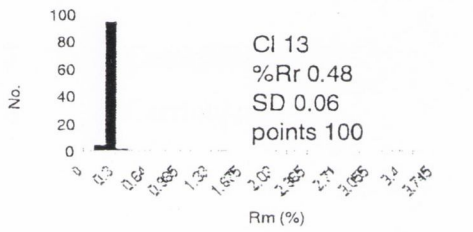

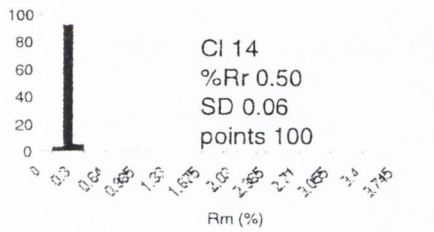

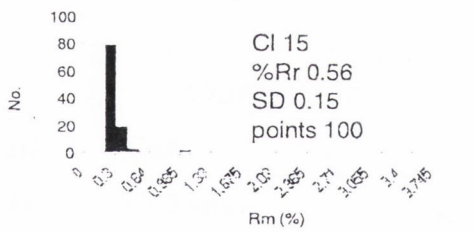

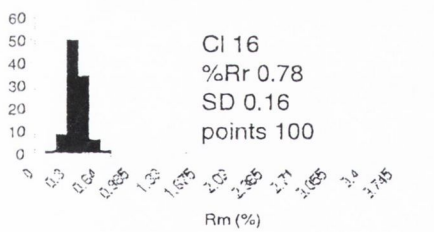

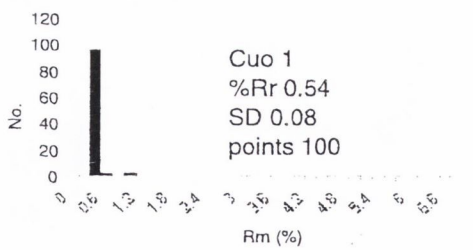

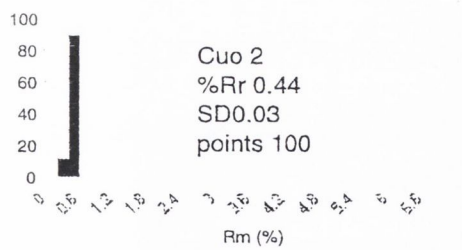

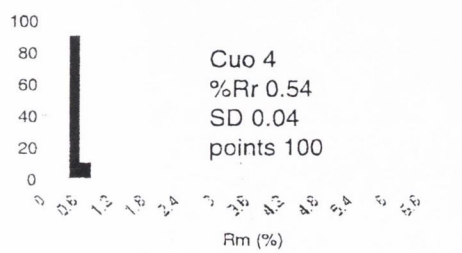

Histograms of mean random vitrinite reflectance for Coal samples collected from the Gobbsection (Cl 9-16) Ballycastle and unoriented coal samples collected from the cMd horizon (Cuo 1, 2, 4), in the North Star Dyke Aureole.

APPENDIX III

PLATES

PETROGRAPHIC PLATES

Plate 1 North Star Dyke, sample IG1, PPL and XPL

Plate 2 North Star Dyke, sample IG2, PPL and XPL

Plate 3 North Star Dyke, sample IG3, PPL and XPL

Plate 4 Carrickleck Dyke, sample IGA, XPL, Calcite vein

Plate 5 Carrickleck Dyke, sample IGA, PPL and XPL

Plate 6 Carrickleck Dyke, Sample IGB, XPL, Olivine grain

CATHODE LUMINESCENCE

Plate 7 Carrickleck Dyke, sample IGA, calcite veining, TL and CL

Plate 8 Carrickleck Dyke, sample IGA, calcite veining, TL and CL

FLUID INCLUSION

Plate 9 Carrickleck Dyke, sample IGA, fluid inclusion in calcite, TL

COAL LENSES FROM THE cMd HORIZON

Plate 10 Co1

Plate 11 Co2 and Co4

Plate 12 Co4

MIOSPORE PHOTOMICROGRAPHS

Plate 13

Plate 14

Plate 15

THERMAL ALTERATION INDEX VARIATION

Plate 16 CK TAI spore and AOM alteration

Plate 17 CQ TAI AOM alteration

Plate 18 cMd TAI spore and AOM alteration

Plate 19 NSD TAI spore and AOM alteration

PALYNOFACIES VARIATION

Plate 20 CK1 - 10

Plate 21 CK11 - 20

Plate 22 CK21 - 30

Plate 23 CQ0.1 - 3

Plate 24 cMd1 - 8

Plate 25 NSD1 - 12

Plate 26 NSD13 – 24

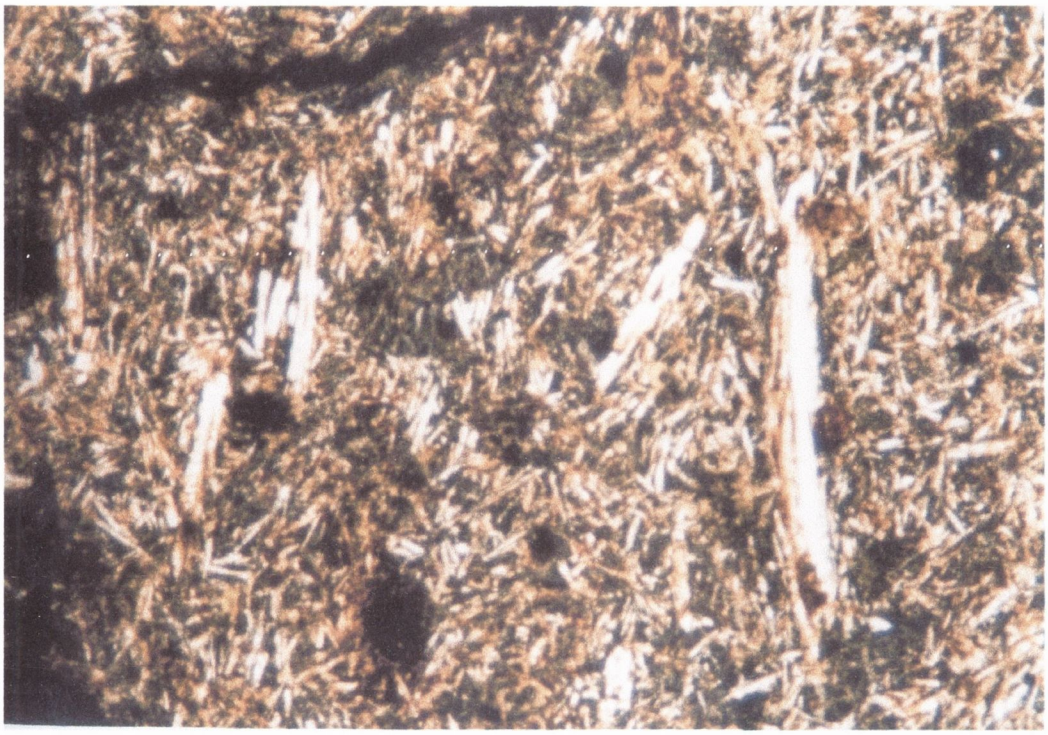

PLATE 1 North Star Dyke, sample IG1, plan 1.2 objective, plates in PPL (above) and XPL (below). Microcrystalline groundmass of feldspar and opaque minerals. Larger plagioclase laths aligned c. parallel to dyke margin. High degree of alteration, some of the alteration material has a green tinge in PPL, chlorite? Thin vein of opaque material in upper left handside of plates.

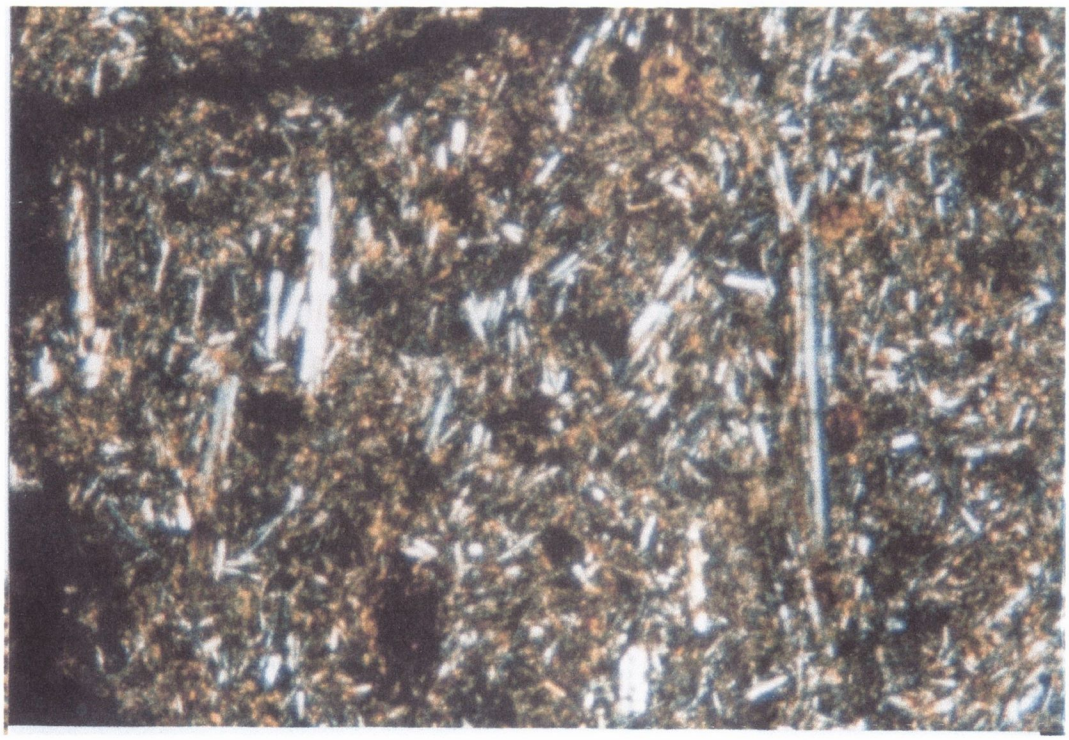

1mm

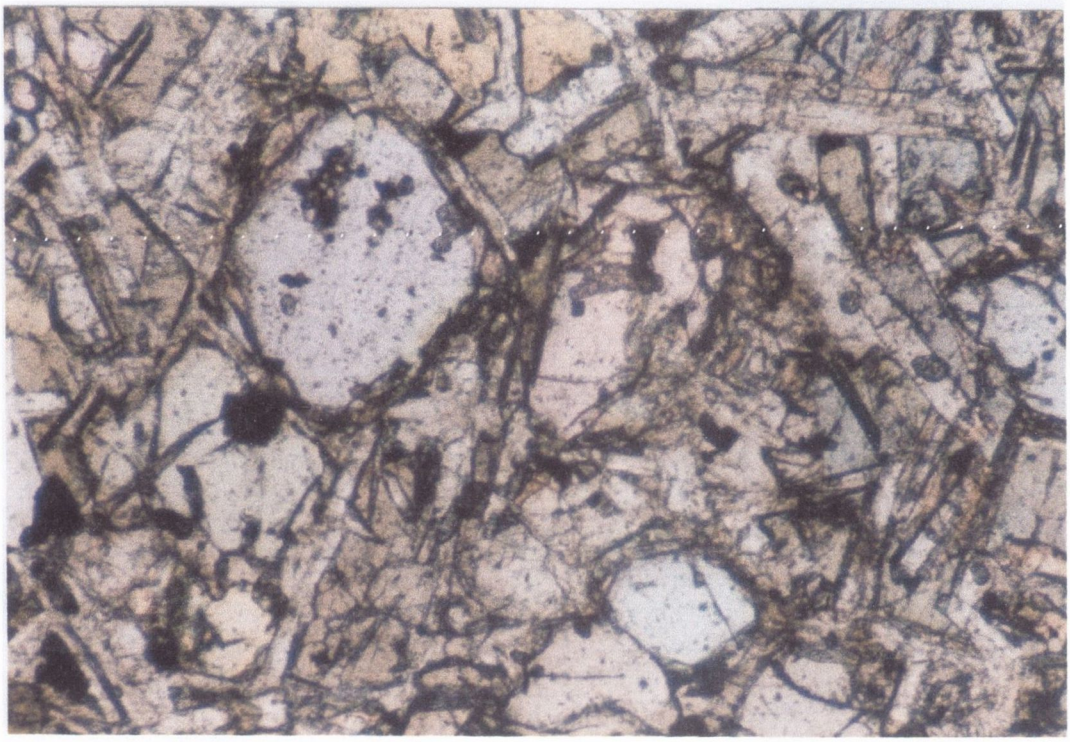

PLATE 2 North Star Dyke, sample IG2, plan 5 objective. Sub-ophitic texture with plagioclase chadocrysts and pyroxene (augite) oikocrysts. Anhedral intergranular olivine. Note some inclusion in the olivines and embayment of the olivine crystal, in the middle right hand side , filled with abutting plagioclase crystal.

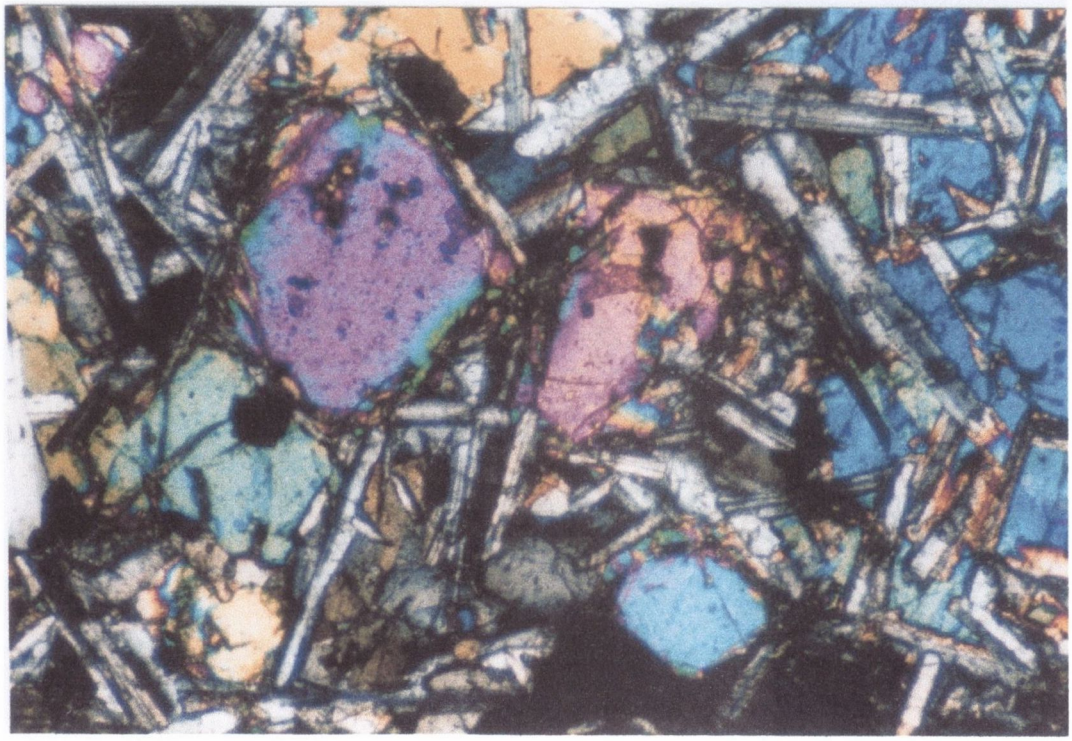

0.5 mm

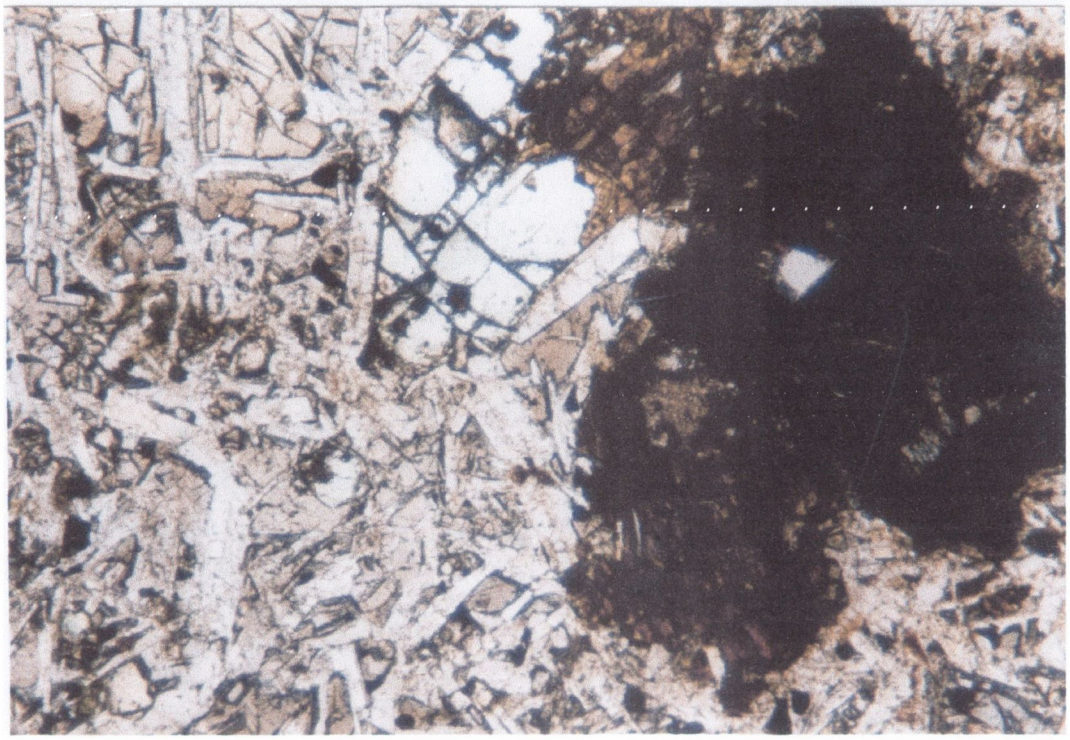

PLATE 3 North Star Dyke, sample IG3, plan 1.2 objective. Left ahnd side: seriate texture feldspars in a feldspar/augite/olivine and opaque mineral groundmass. Top left shows sub-ophitic texture-large pyroxene and partly enclosed feldspars. Right hand side: large brown mass of alteration material, top middle shows a large partially altered, euhedral olivine.

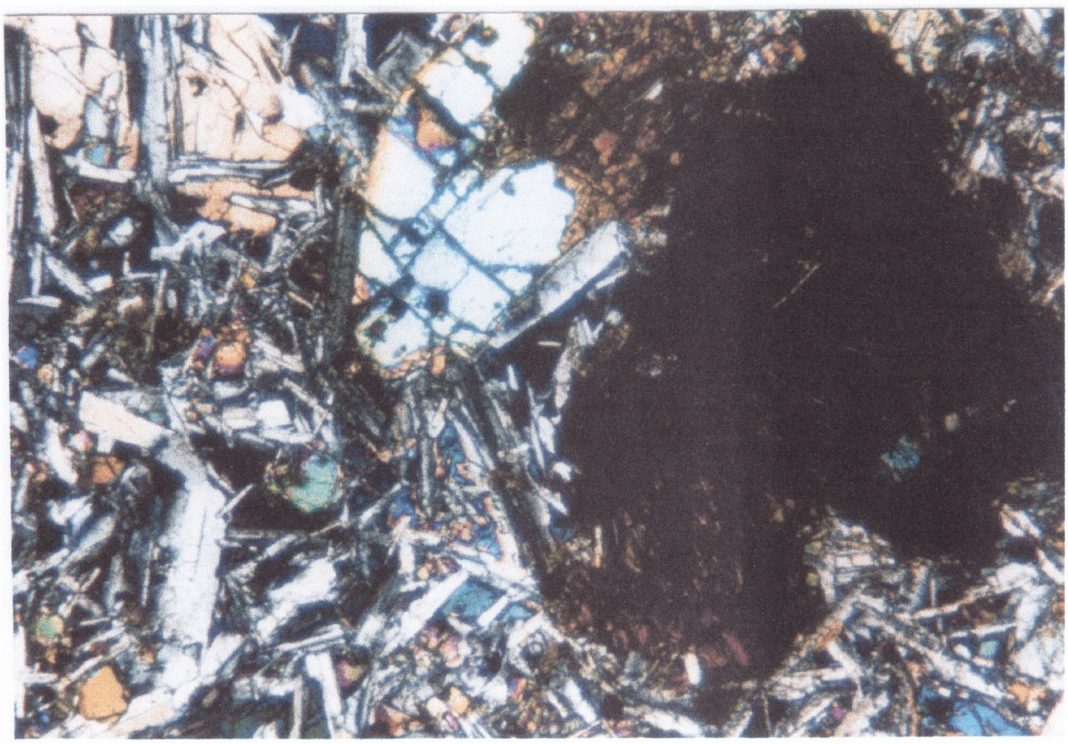

1mm

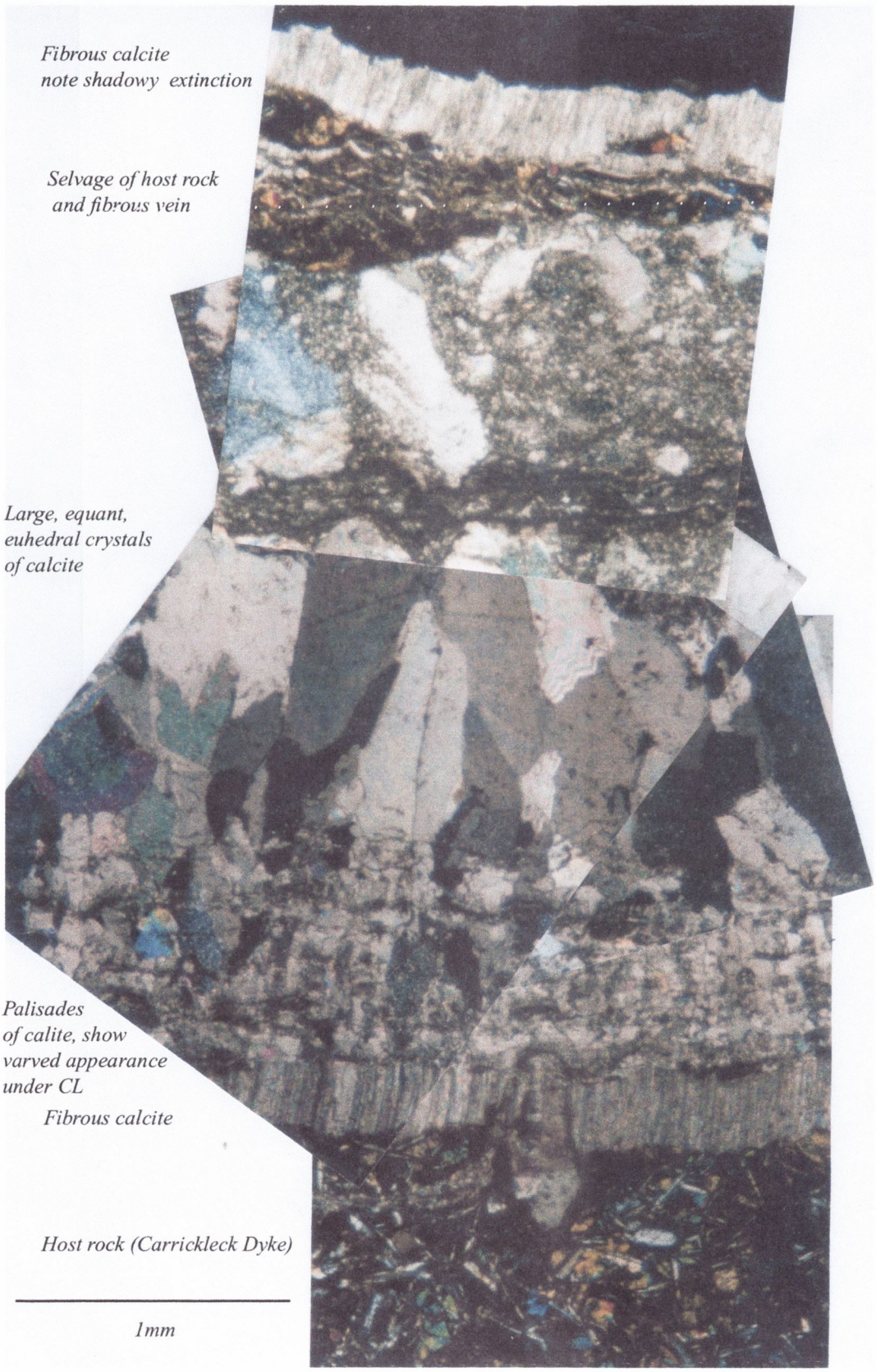

PLATE 4 Carrickleck Dyke, sample IGA, plan 1.2 objective. 4mm wide calcite filled vein.

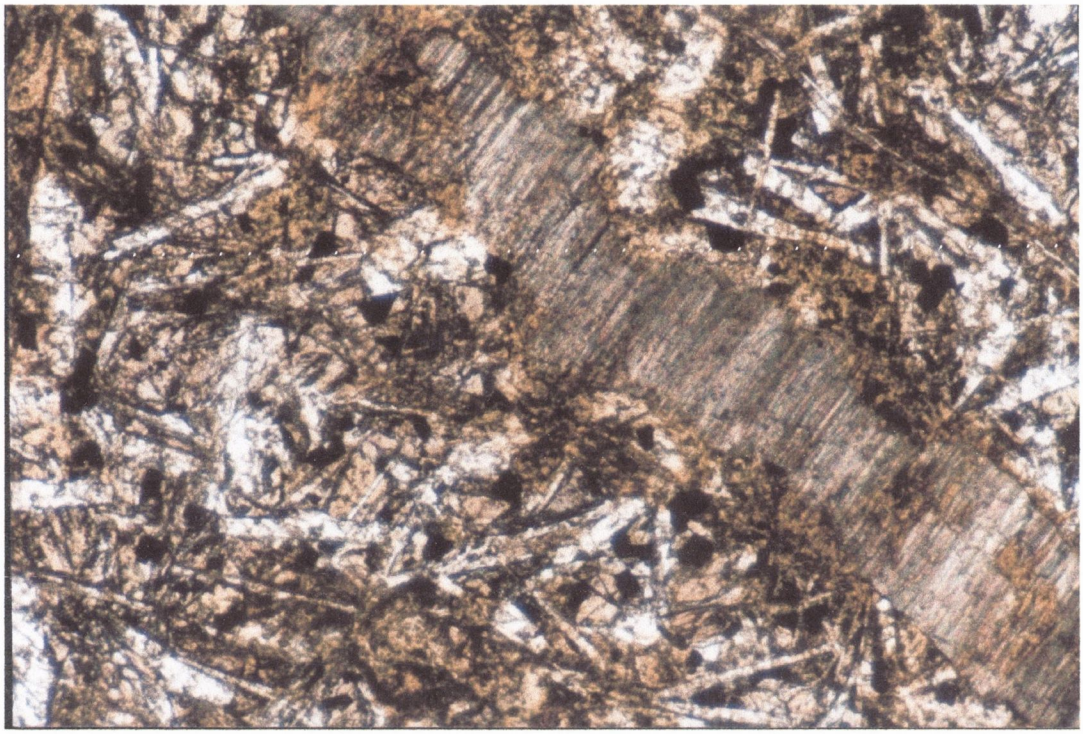

PLATE 5 Carrickleck Dyke, sample IGA, plan 5 objective. Fibrous calcite filled vein, preferentially altered at the margins, cross-cutting sub-ophitic feldspar and pyroxene groundmass. Entire area shows alteration to a brown and green tinted material. Up to 10% opaque minerals present.

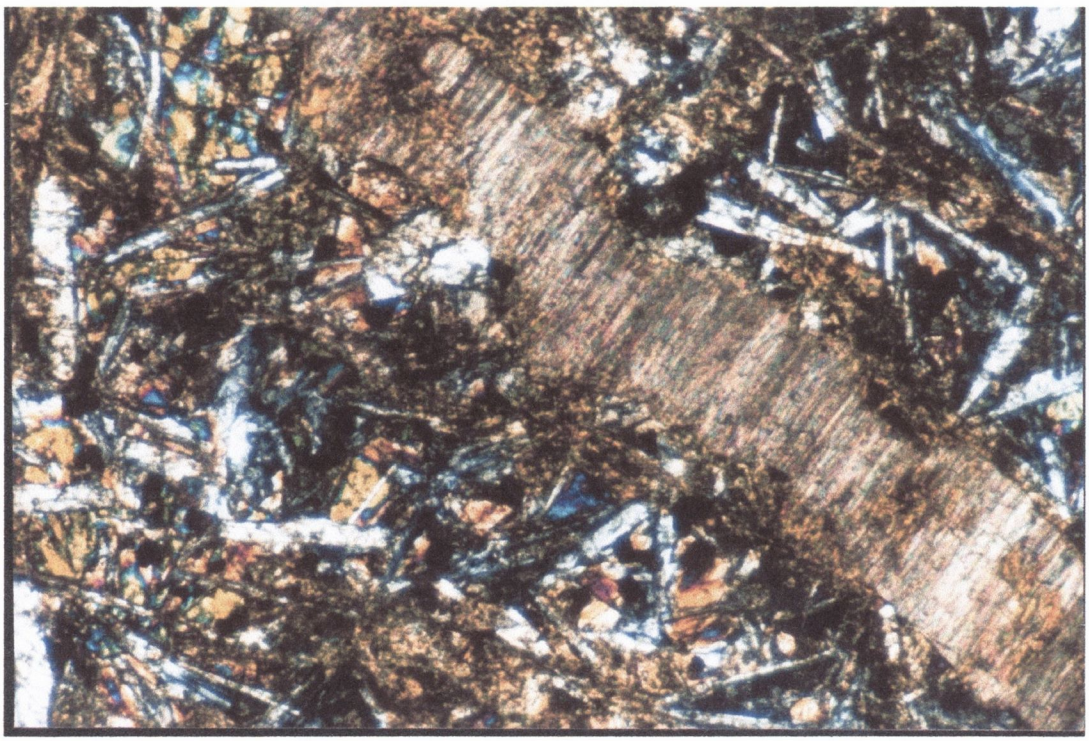

0.5mm

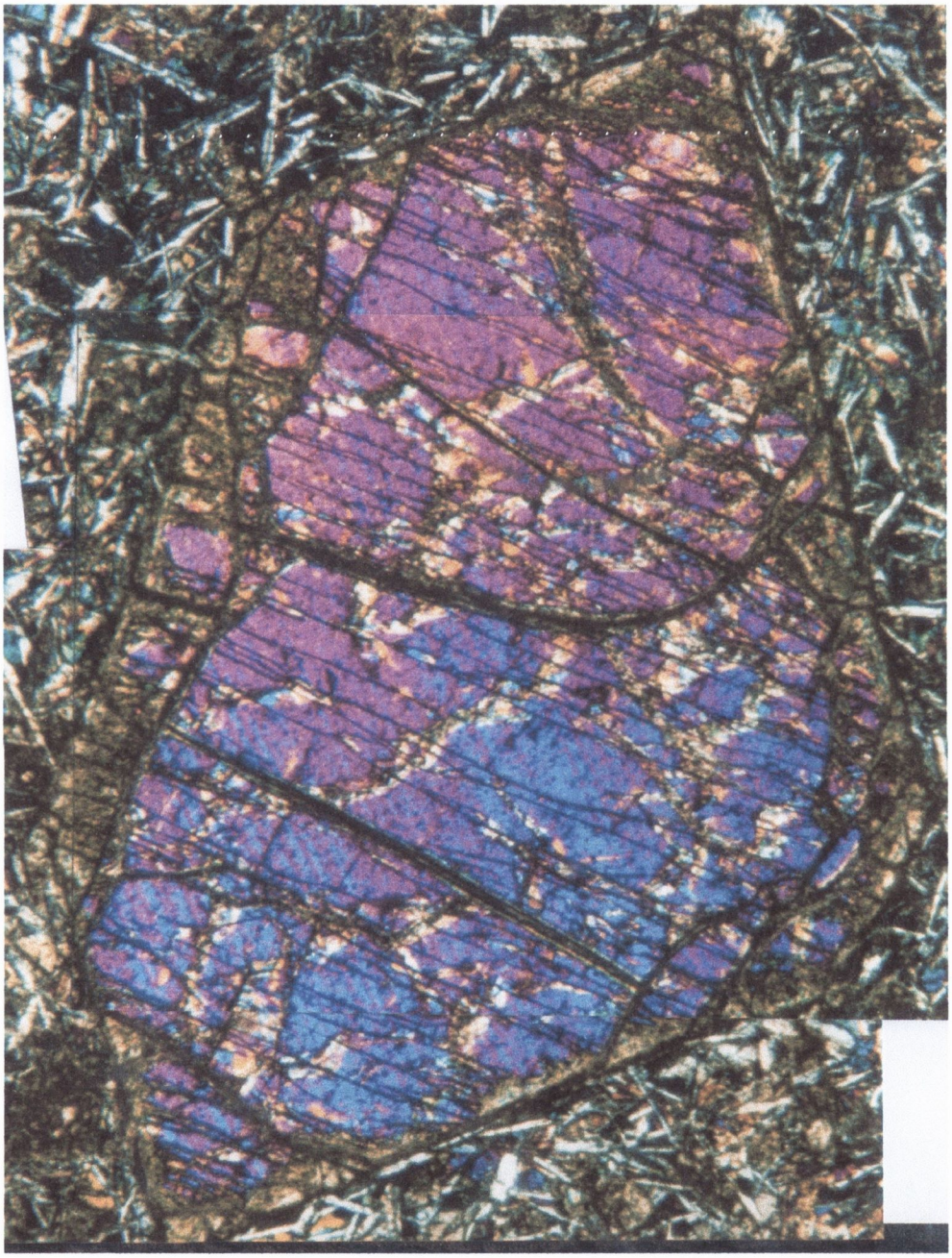

1mm

PLATE 6 Carrickleck Dyke, sample IGb, plan 1.2 objective. Large (3.84mm) euhedral, olivine phenocryst. Preferential alteration around the edges and along fractures.

(a)

(b)

1mm

PLATE 7 Calcite veining in the Carrickleck dyke. (a) Transmited light (TL), (b) Cathode Luminescence (CL). Fibrous ferroan calcite veins (blue in CL) bound a composite calcite vein. Note the replacement of the ferroan calcite with the second phase cacite.

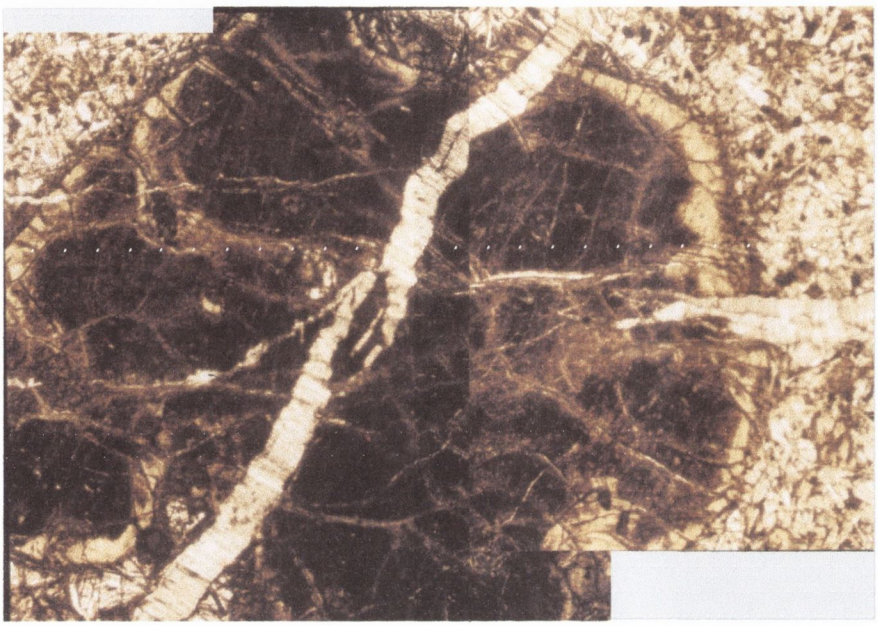

Plate 8 A highly altered olivine crystal in a groundmass of feldspar (blue in CL). The olivine is fractured and cross cut by a fibrous ferroan calcite vein. A second calcite vein also cross cuts the olivine and the ferroan calcite vein, and preferrentially develops a network of fine calcite veins.

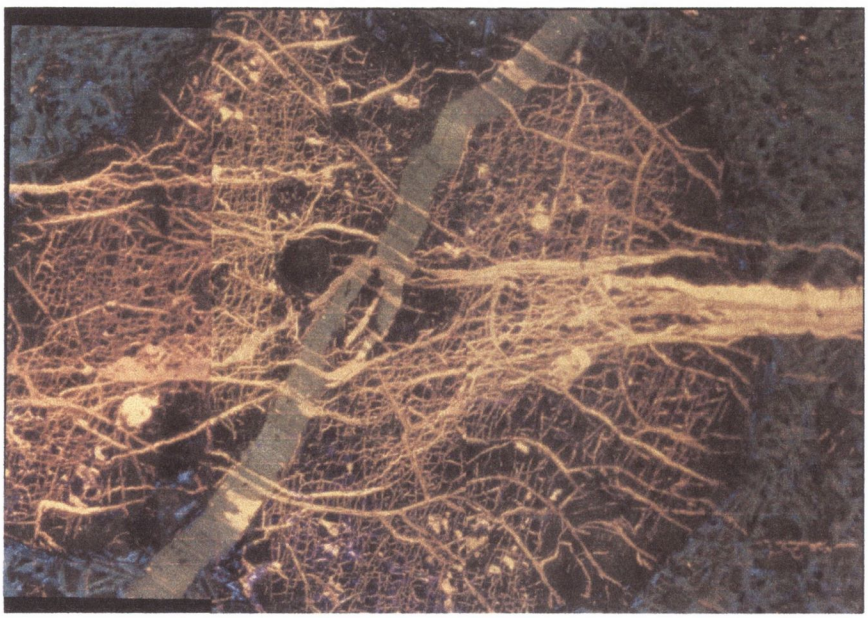

1 mm

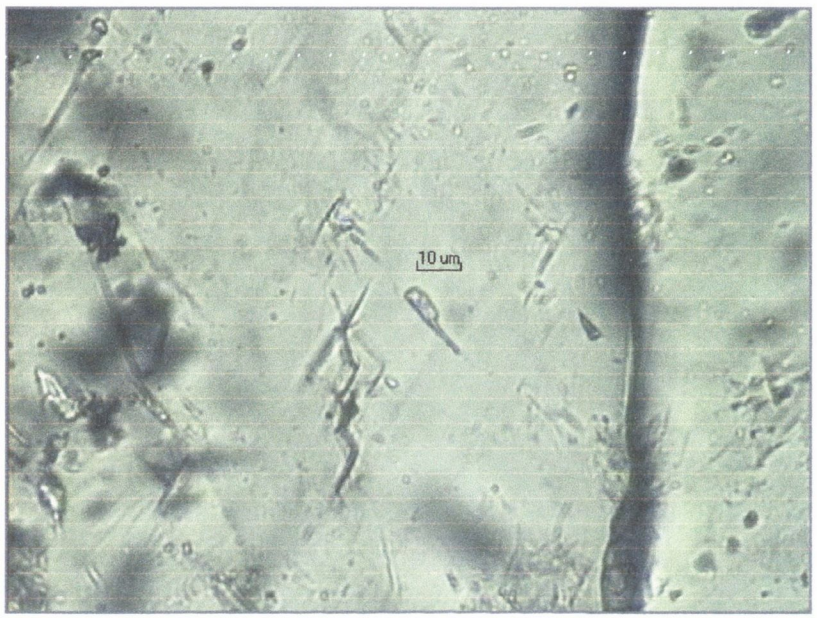

PLATE 9 Negative crystal shape characteristic of fluid inclusions observed in the euhedral calcite crystals found in veins in the Carickleck dyke. In order to distingish whether these are holes, artefacts of escaped fluids or are filled with a solid mass, the material would need to be observed using SEM.

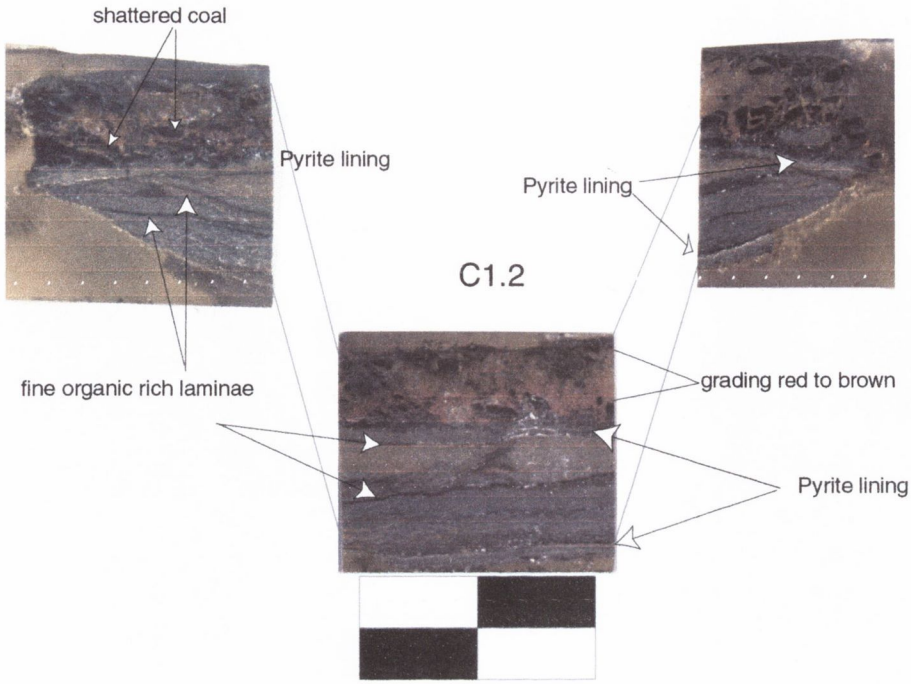

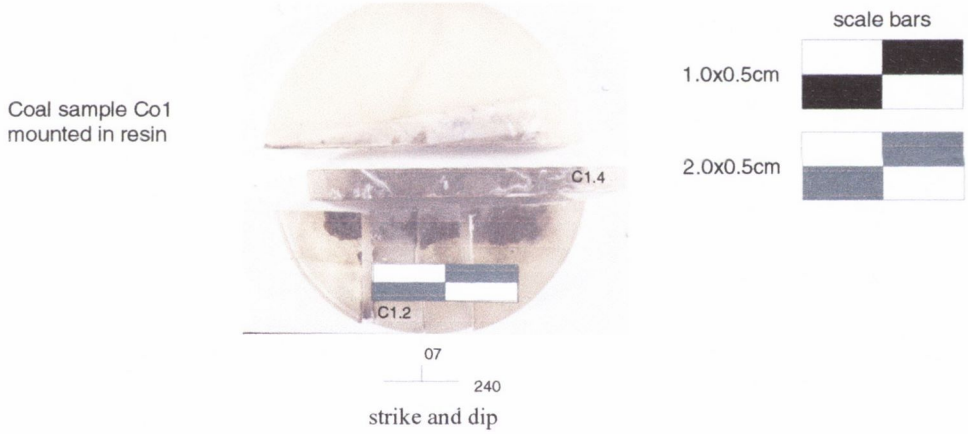

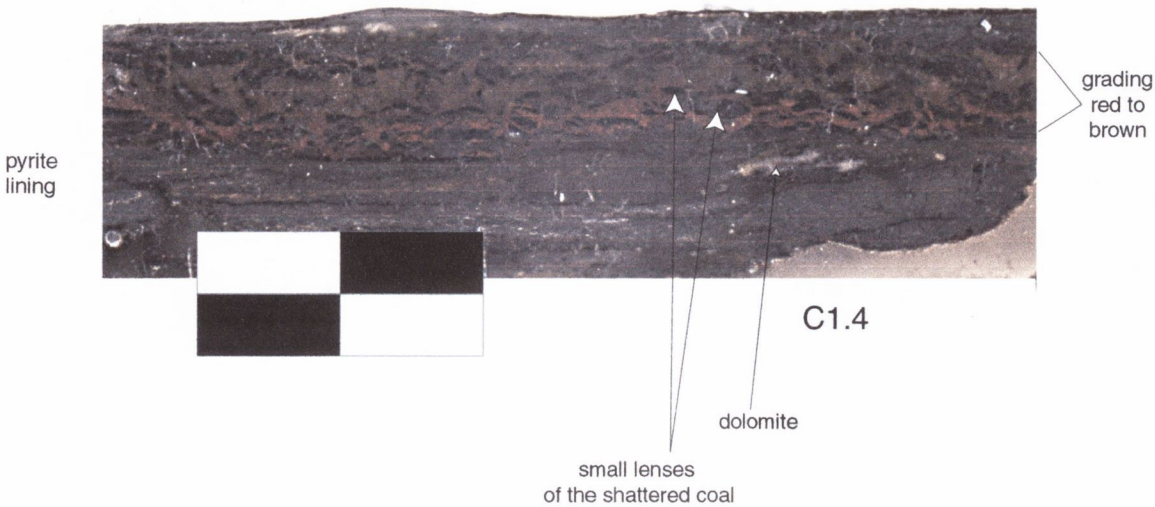

PLATE 10 Co1, mounted in resin and cut at right angles to bedding, showing the effects of fluids on the lens

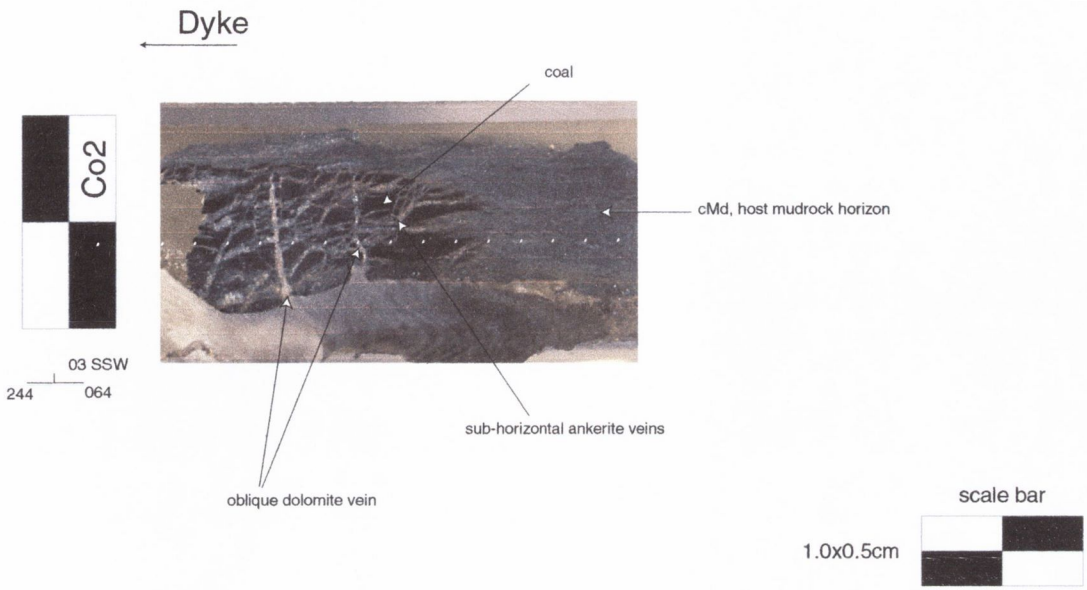

PLATE 11 (a) Section of Co2 Coal lense cut perpendicular to bedding. This sample exhibits a similar fracture and fill system as that seen in Co4.

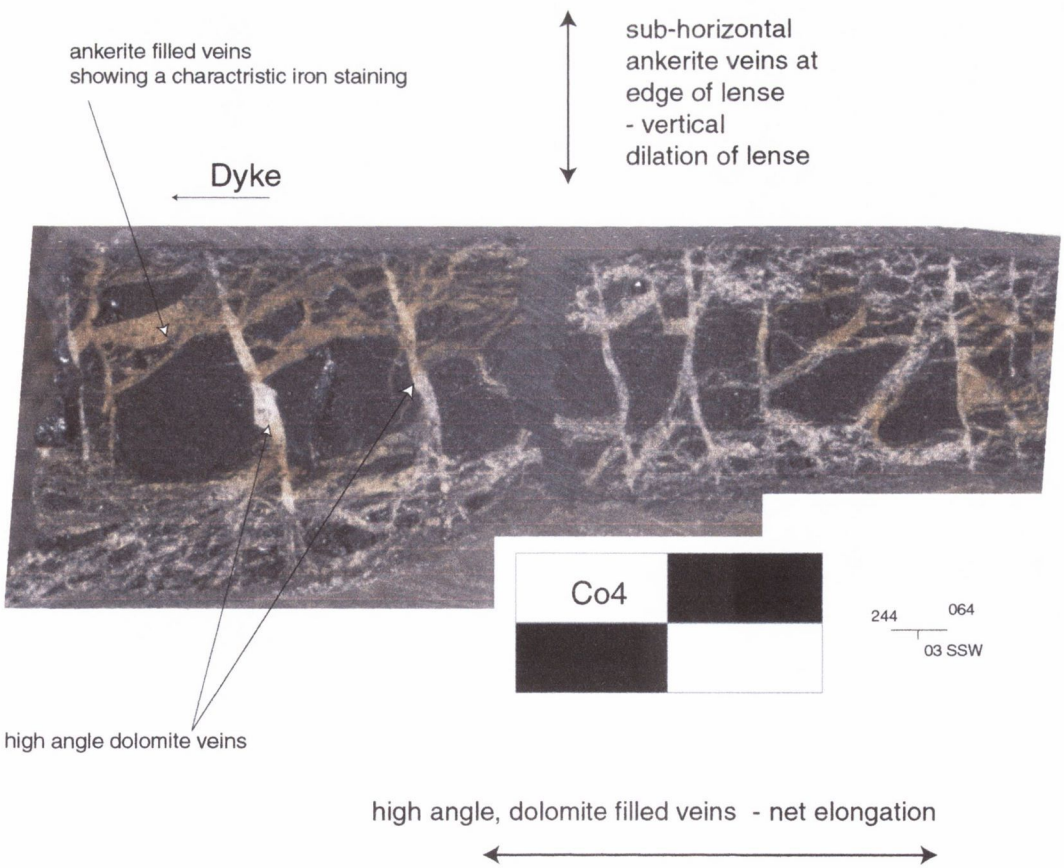

PLATE 11 (b) A section from Co4 Coal lense showing the fracture system and fill, assumed to be asociated with burial.

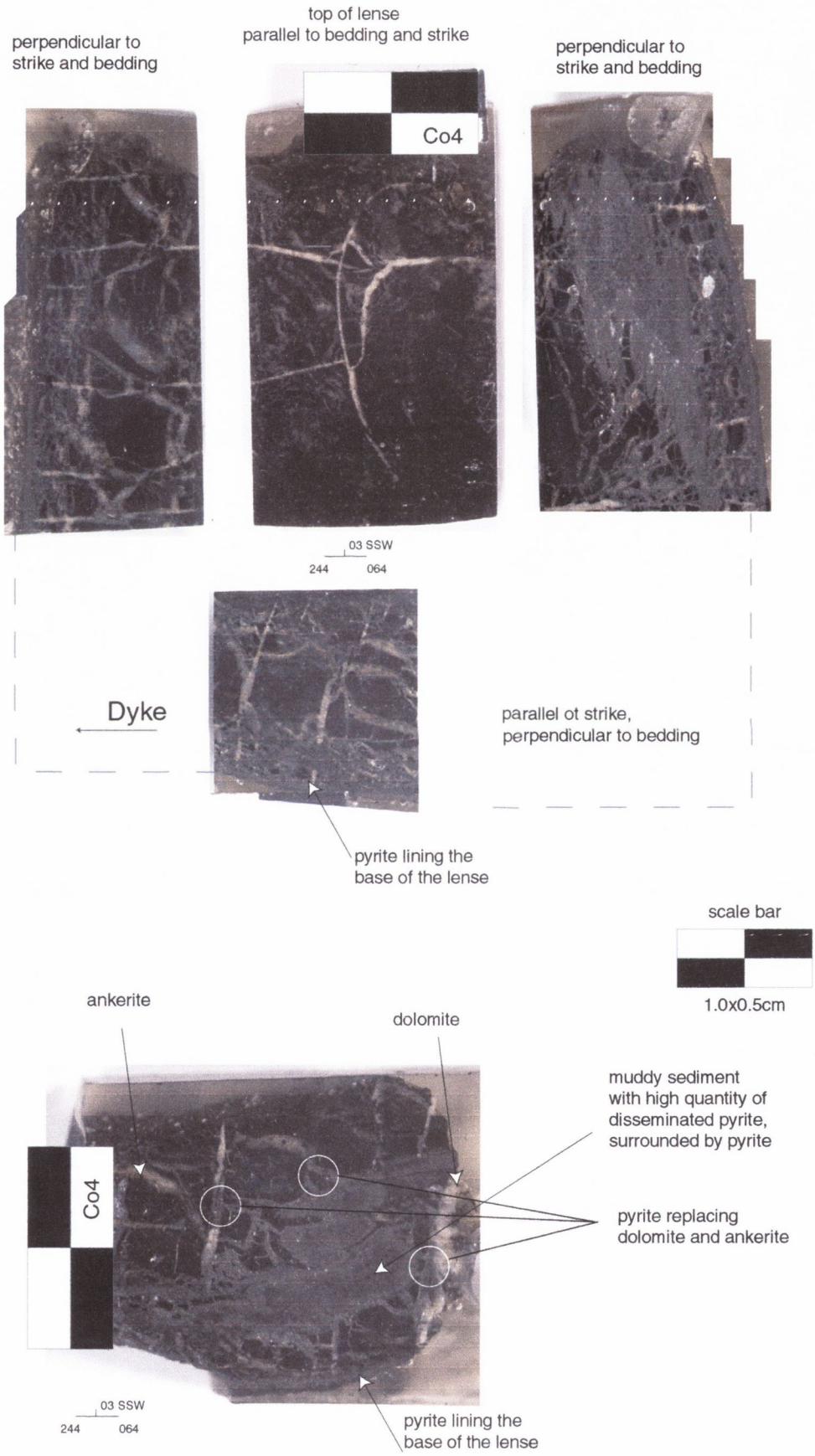

PLATE 12 Sections from the Co4 coal lense showing the complex relations between the ankerite, dolomite and pyrite phases in the coal lense

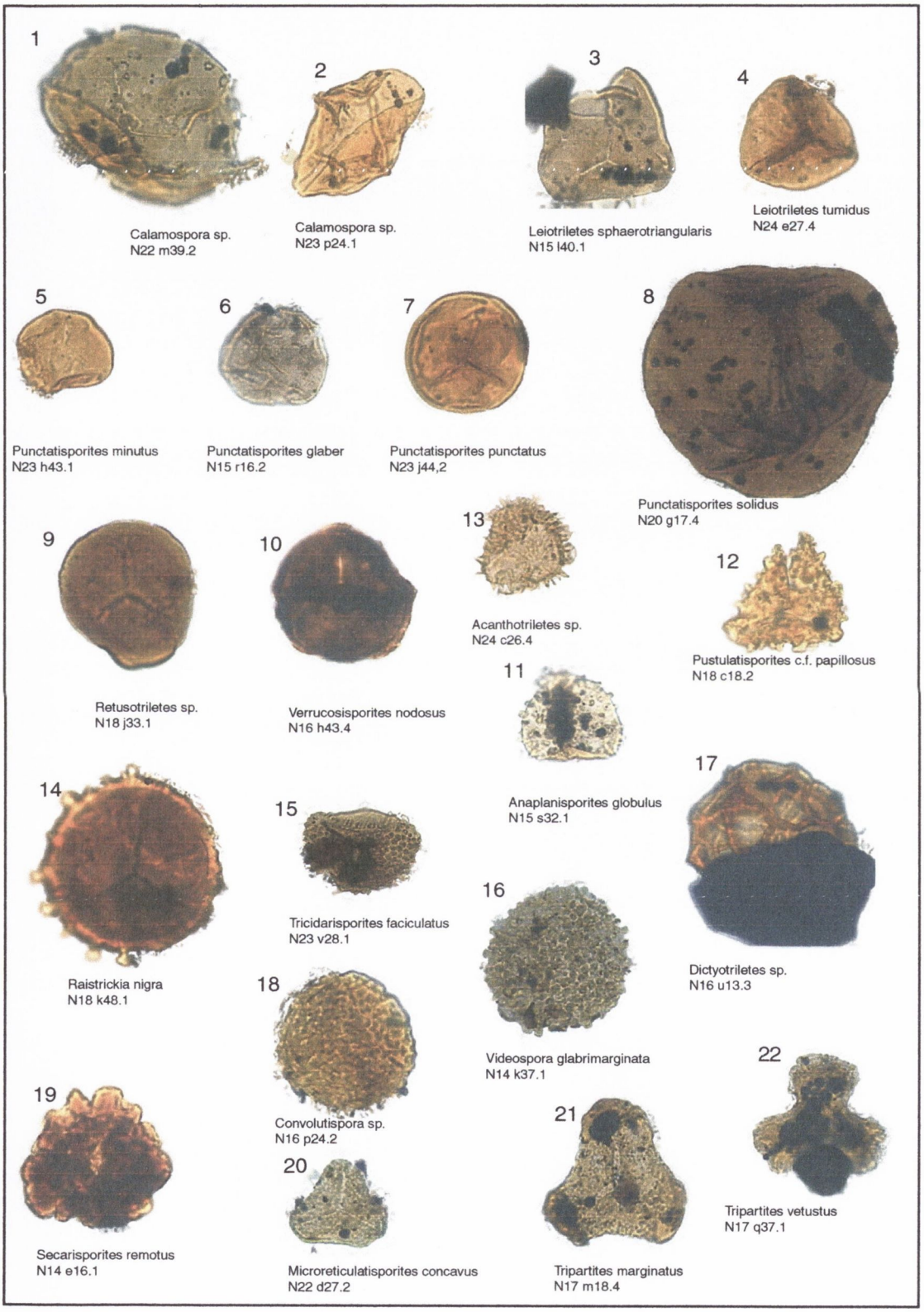
1
Calamospora sp.
N22 m39.2
2
Calamospora sp.
N23 p24.1
3
Leiotriletes sphaerotriangularis
N15 l40.1
4
Leiotriletes tumidus
N24 e27.4
5
Punctatisporites minutus
N23 h43.1
6
Punctatisporites glaber
N15 r16.2
7
Punctatisporites punctatus
N23 j44,2
8
Punctatisporites solidus
N20 g17.4
9
Retusotriletes sp.
N18 j33.1
10
Verrucosisporites nodosus
N16 h43.4
13
Acanthotriletes sp.
N24 c26.4
12
Pustulatisporites c.f. papillosus
N18 c18.2
11
Anaplanisporites globulus
N15 s32.1
14
Raistrickia nigra
N18 k48.1
15
Tricidarisporites faciculatus
N23 v28.1
16
Videospora glabrimarginata
N14 k37.1
17
Dictyotriletes sp.
N16 u13.3
18
Convolutispora sp.
N16 p24.2
19
Secarisporites remotus
N14 e16.1
20
Microreticulatisporites concavus
N22 d27.2
21
Tripartites marginatus
N17 m18.4
22
Tripartites vetustus
N17 q37.1
50 microns

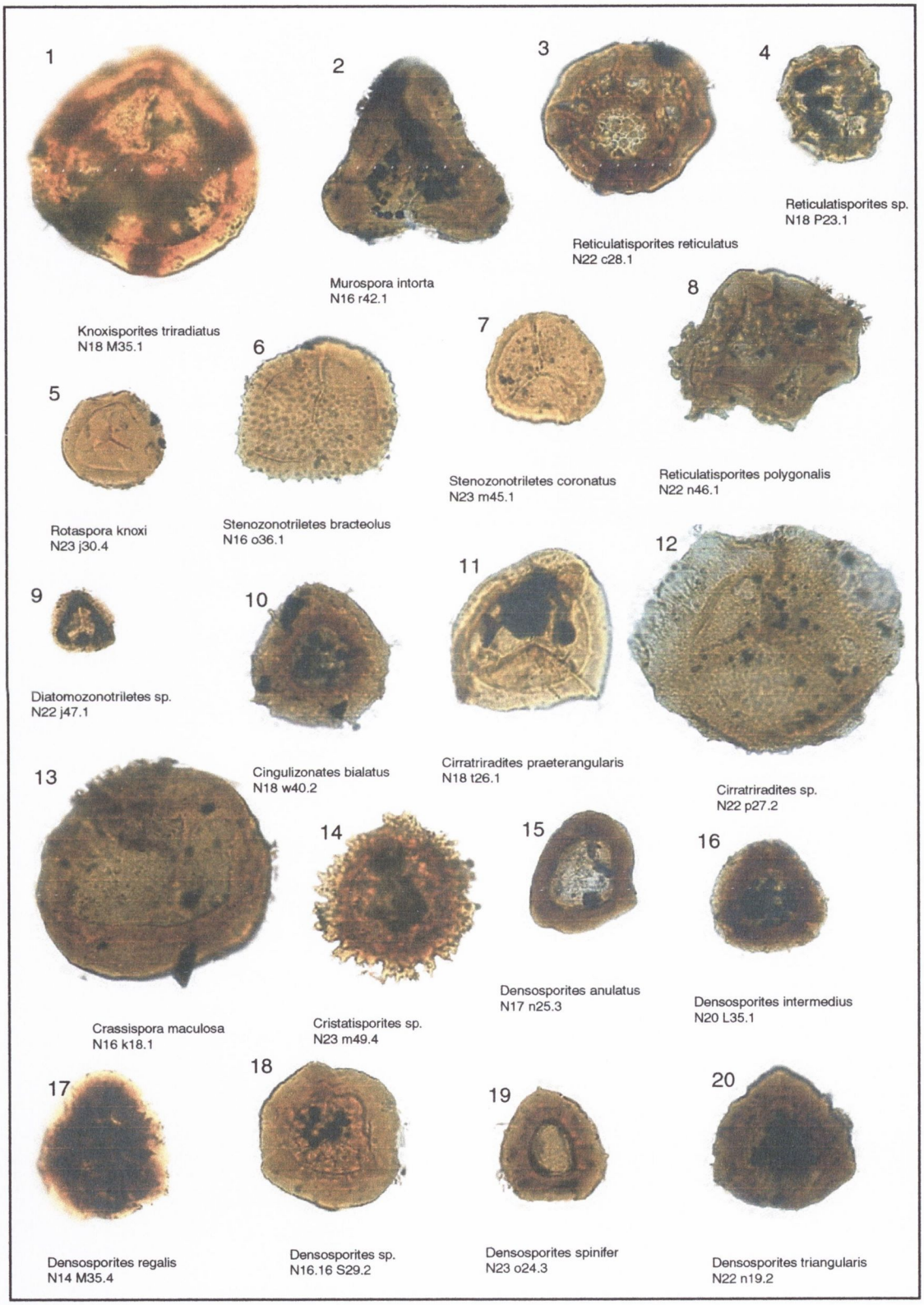
1
Knoxisporites triradiatus
N18 M35.1
2
Murospora intorta
N16 r42.1
3
Reticulatisporites reticulatus
N22 c28.1
4
Reticulatisporites sp.
N18 P23.1
5
Rotaspora knoxi
N23 j30.4
6
Stenozonotriletes bracteolus
N16 o36.1
7
Stenozonotriletes coronatus
N23 m45.1
8
Reticulatisporites polygonalis
N22 n46.1
9
Diatomozonotriletes sp.
N22 j47.1
10
Cingulizonates bialatus
N18 w40.2
11
Cirratriradites praeterangularis
N18 t26.1
12
Cirratriradites sp.
N22 p27.2
13
Crassispora maculosa
N16 k18.1
14
Cristatisporites sp.
N23 m49.4
15
Densosporites anulatus
N17 n25.3
16
Densosporites intermedius
N20 L35.1
17
Densosporites regalis
N14 M35.4
18
Densosporites sp.
N16.16 S29.2
19
Densosporites spinifer
N23 o24.3
20
Densosporites triangularis
N22 n19.2
50 microns

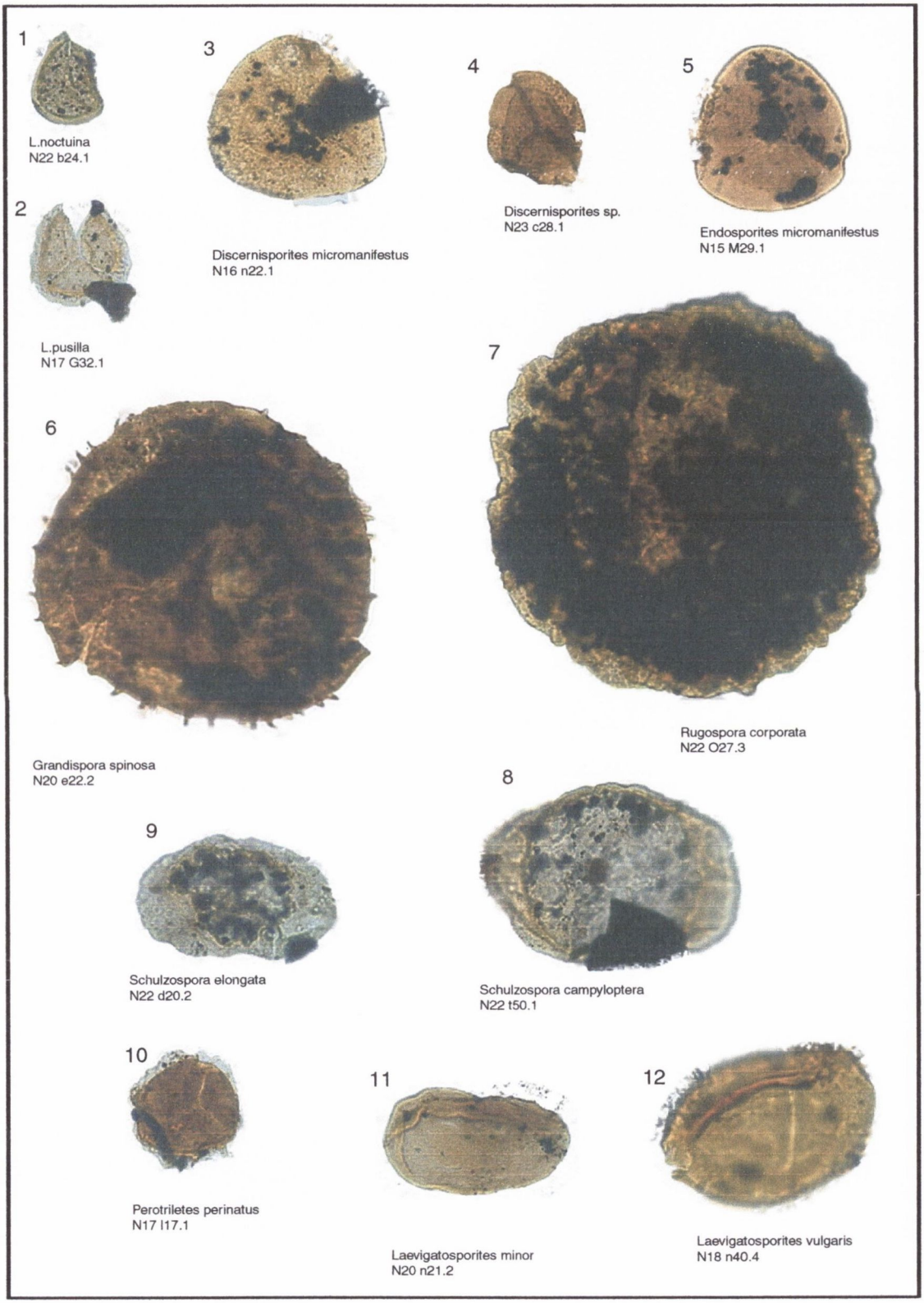
1
L.noctuina
N22 b24.1
2
L.pusilla
N17 G32.1
3
Discernisporites micromanifestus
N16 n22.1
4
Discernisporites sp.
N23 c28.1
5
Endosporites micromanifestus
N15 M29.1
6
Grandispora spinosa
N20 e22.2
7
Rugospora corporata
N22 O27.3
8
Schulzospora campyloptera
N22 t50.1
9
Schulzospora elongata
N22 d20.2
10
Perotriletes perinatus
N17 l17.1
11
Laevigatosporites minor
N20 n21.2
12
Laevigatosporites vulgaris
N18 n40.4

50 microns

1	2	3	4	6	7	8	9	10	11	12	13	14	15
Non-fluorescing material													
Perpendicular distance from dyke (cm):													
6.74	20.22	24.72	29.21	33.74	49.43	60.22	80.89	89.88	103.36	112.35	139.31	157.29	179.76
VR (Rr%):													
3.09	3.65	3.26	3.23	3.10	-	1.89	1.49	1.41	1.46	1.48	1.29	1.29	1.17

16	17	18	19	20	21	22	23	24	25	26	27	28	29	30
Fluorescing material														
202.23	224.70	247.17	283.12	319.07	359.52	404.46	449.4	494.34	539.28	584.22	898.79	1617.83	6291.56	7190.35
1.14	1.16	1.10	1.12	1.16	1.11	1.12	1.14	1.03	1.1	1.07	1.07	1.07	1.10	1.08

Explanation for PLATE 16 CK TAI spore and AOM thermal alteration (all images at x500mag).

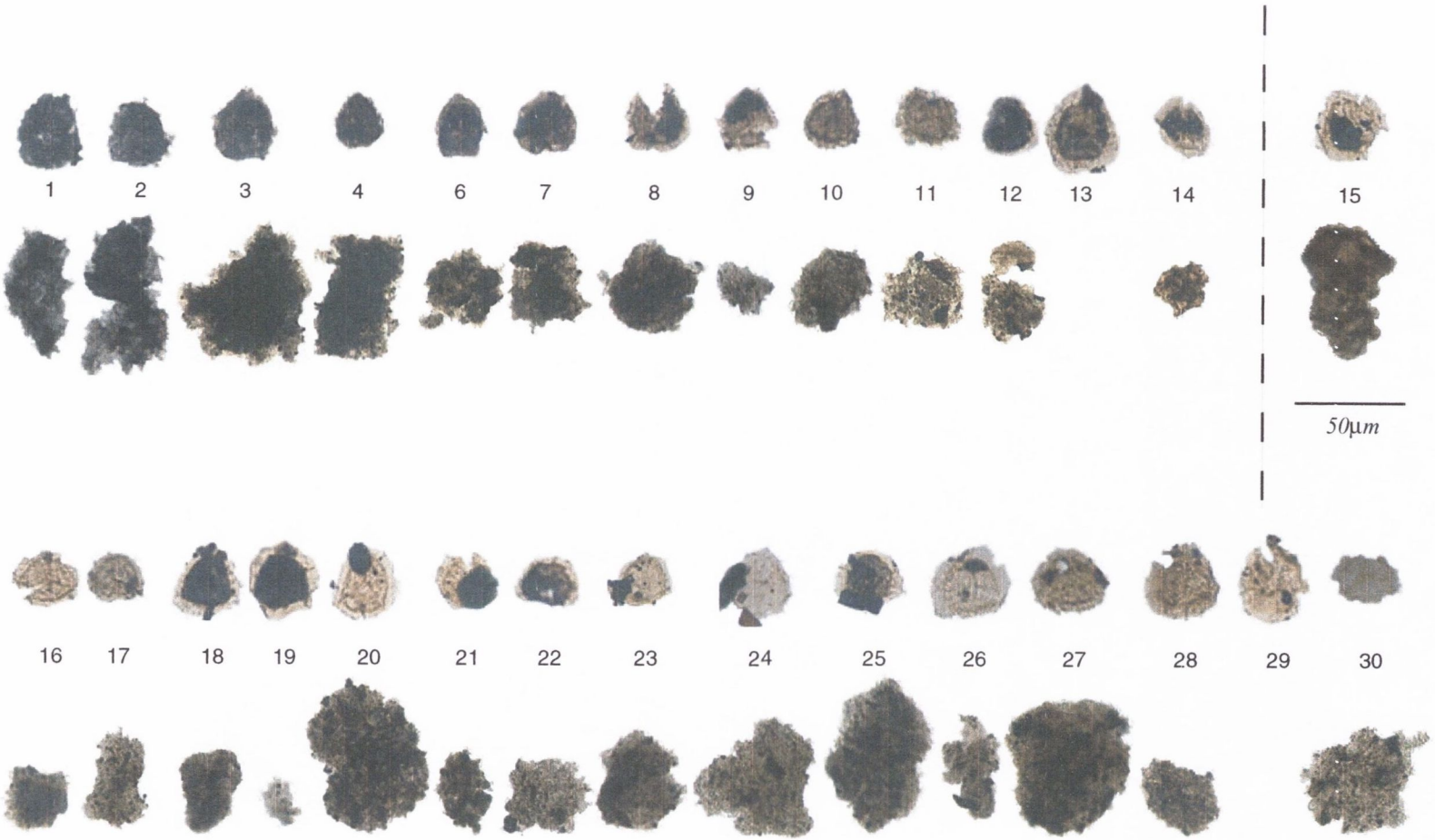

PLATE 16 CK TAI spore and AOM thermal alteration (all images at x500mag).

Sample No.

0.1	0.5	0.8	1.2	1.6	2.o	2.5	3.0

Perpendicular distance from the dyke (m)

0.09	0.44	0.72	1.08	1.44	1.80	2.25	2.7

non-fluorescing material

fluorescing material

50μm

PLATE 17 CQ AOM thermal alteration

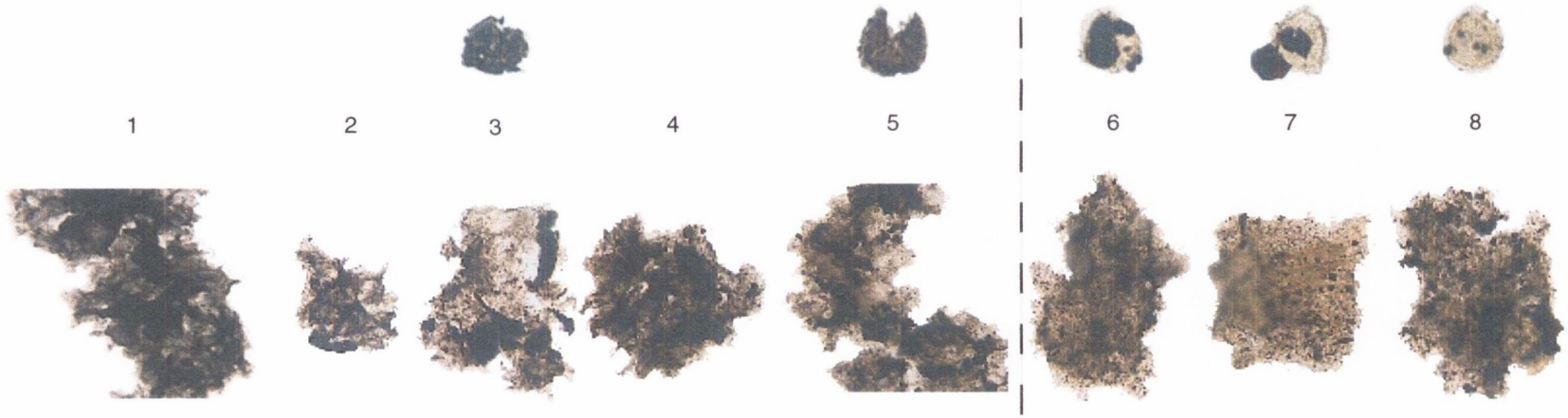

1	2	3	4	5	6	7	8
Perpendicular distance from dyke (m):							
0.46	0.63	0.80	0.96	1.36	1.60	2.56	3.55
VR (%Rr)							
5.2	5.45	3.55	2.57	1.57	0.71	0.94	0.55

Non-fluorescing material

Fluorescing material

50μm

Plate 18 cMd TAI for spore and AOM

Non-fluorescing material

1	2	3	4	5	6	7	8	9	10	11
Perpendicular distance from dyke (m):										
0.04	0.15	0.28	0.37	0.47	0.49	0.57	0.65	0.95	0.97	1.21
VR (Rr%):										
3.78	3.72	4.69	5.61	5.47	5.16	3.41	3.49	2.82	1.63	1.48

Fluorescing material

14	15	16	17	18	19	20	21	22	23	24
1.82	2.20	2.22	2.79	2.89	3.95	4.05	5.40	5.66	6.27	10.11
1.26	1.05	1.16	1.03	1.03	1.06	1.19	1.13	1.11	1.17	1.28

Explanation for PLATE 6.6 NSD spores and AOM thermal alteration

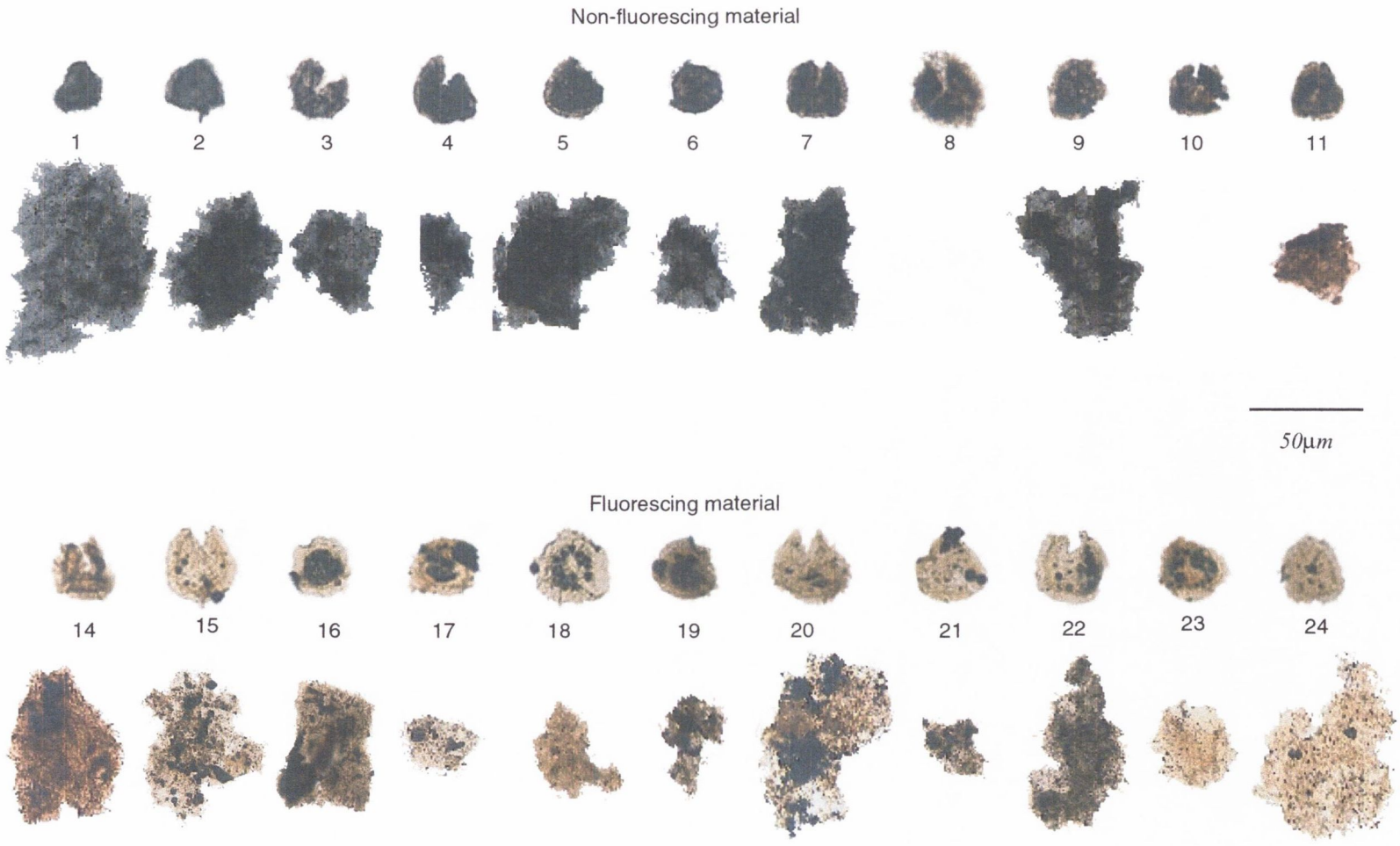

PLATE 19 NSD spores and AOM thermal alteration

Sample no.	CK 1	CK 2	CK 3	CK 4	CK 5	CK 6	CK 7	CK 8	CK 9	CK 10
Distance from dyke (m)	0.07	0.2	0.25	0.3	0.34	0.43	0.5	0.6	0.81	0.9
VR (%Rr)	3.09	3.65	3.26	3.23	3.10	3.39		1.89	1.49	1.41
Translucent wood										
Opaque Organic Matter										
Non-woody plant matter										
palynomorph										
AOM										
Zooclast										

50 microns

PLATE 20 CK compilation palynofacies, illustrating particles found in each sample through the CK horizon of the Carrickleck Dyke aureole

Sample no.	CK 11	CK 12	CK 13	CK 14	CK 15	CK 16	CK 17	CK 18	CK 19	CK 20
Distance from dyke (m)	1.0	1.1	1.4	1.6	1.8	2.0	2.2	2.5	2.8	3.2
VR (%Rr)	1.46	1.48	1.29	1.29	1.17	1.14	1.16	1.1	1.12	1.16
Translucent wood										
Opaque Organic Matter										
Non-woody plant matter										
palynomorph	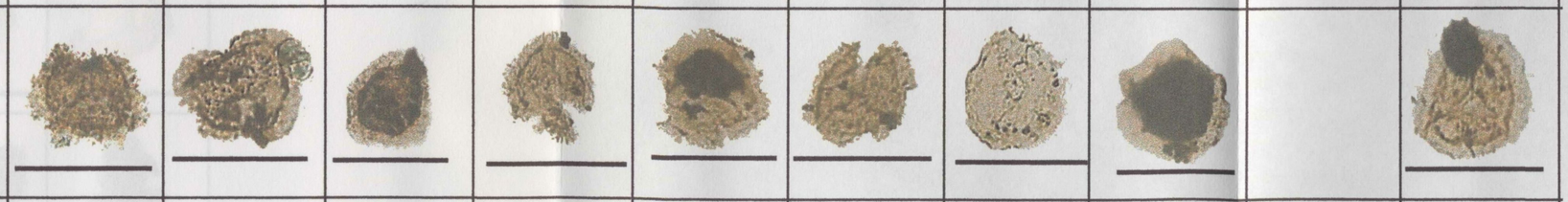									
AOM	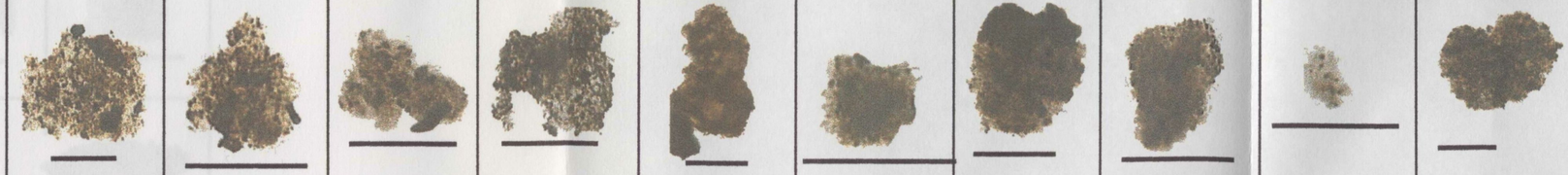									
Zooclast	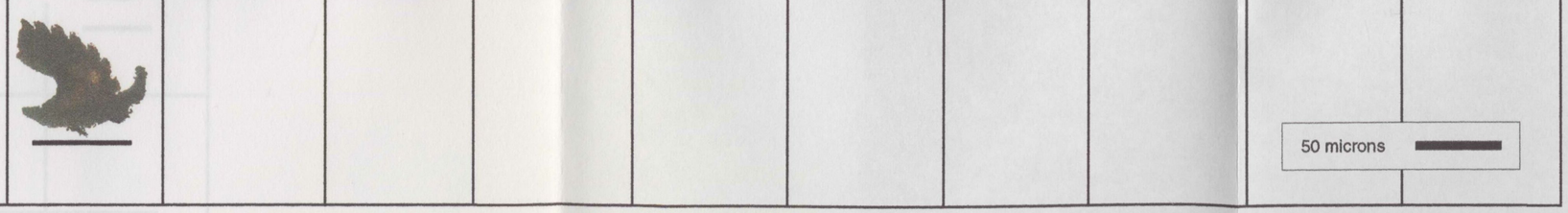									

PLATE 21 CK compilation palynofacies, illustrating particles found in each sample through the CK horizon of the Carrickleck Dyke aureole

Sample no.	CK 21	CK 22	CK 23	CK24	CK 25	CK 26	CK27	CK 28	CK 29	CK 30
Distance from dyke (m)	3.6	4.1	4.5	5.0	5.4	5.8	9.0	16.2	63.1	71.9
VR (%Rr)	1.11	1.12	1.14	1.03	1.03	1.07	1.07	1.07	1.10	1.08
Translucent wood	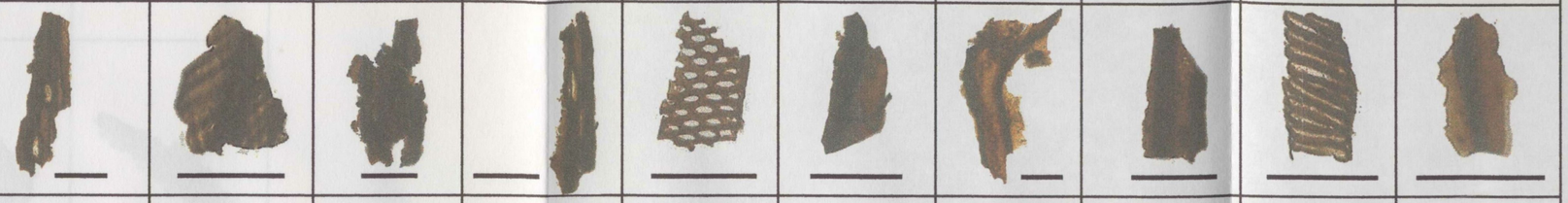									
Opaque Organic Matter	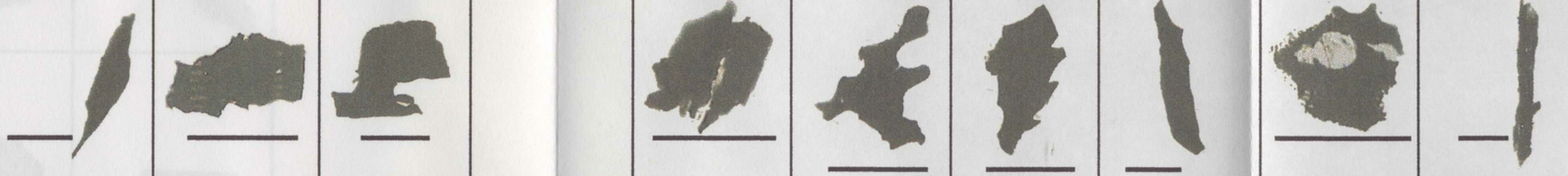									
Non-woody plant matter										
Palynomorph	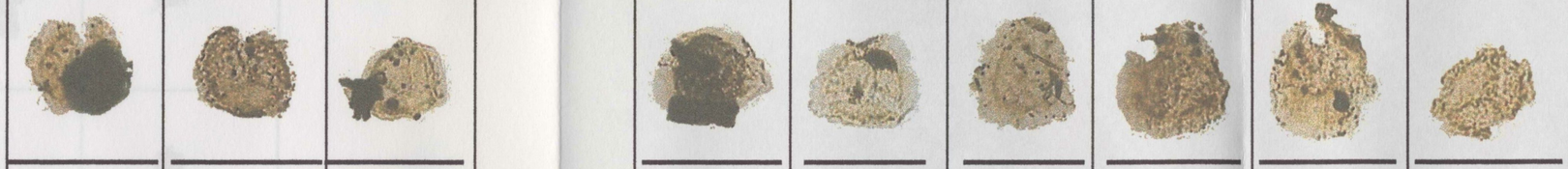									
AOM	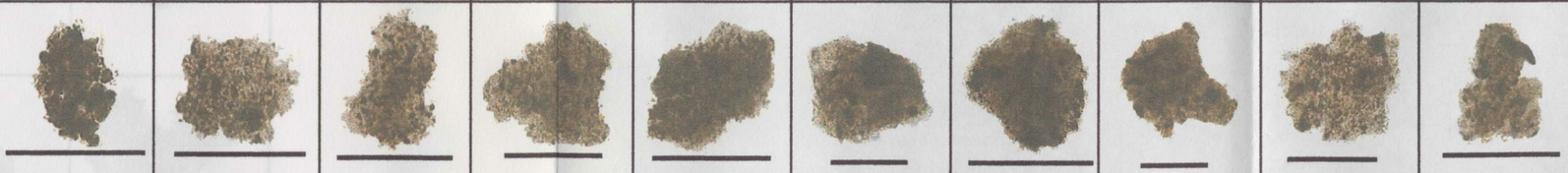									
Zooclast	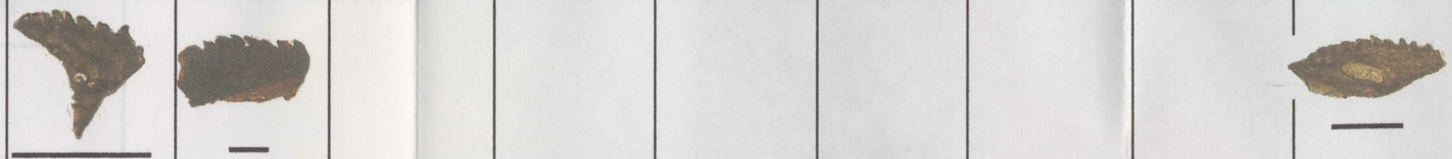									
Indeterminate	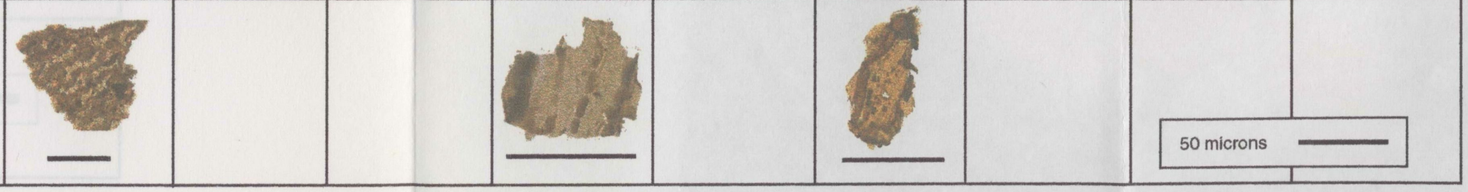									

50 microns

PLATE 22 CK compilation palynofacies, illustrating particles found in each sample through the CK horizon of the Carrickleck Dyke aureole

Sample no.	CQ 0.1	CQ 0.3	CQ 0.5	CQ 0.8	CQ 1.2	CQ 1.6	CQ 2.0	CQ 2.5	CQ 3.0
Distance from dyke (m)	1.82	2.20	2.22	2.89	2.79	3.95	4.05	5.40	5.66
Translucent wood									
Opaque Organic Matter									
Non-woody plant matter									
Palynomorph									
AOM									
Zooclast									
Indeterminate									

50 microns

PLATE 23 CQ compilation palynofacies, illustrating particles found in each sample through the CQ horizon of the Carrickleck Dyke aureole

Sample no.	cMd 1	cMd 2	cMd 3	cMd 4	cMd 5	cMd 6	cMd 7	cMd 8
Distance from dyke (m)	0.46	0.63	0.80	0.96	1.36	1.60	2.56	3.55
VR (%Rr)	5.20	5.45	3.55	2.57	1.57	0.71	0.94	0.55
Translucent wood								
Opaque Organic Matter								
Non-woody plant matter								
Palynomorph								
AOM								

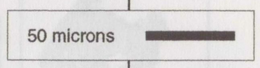

PLATE 24 cMd compilation palynofacies, illustrating particles found in each sample through the cMd horizon of the North Star Dyke aureole

Sample no.	NSD 1	NSD 2	NSD 3	NSD 4	NSD 5	NSD 6	NSD 7	NSD 8	NSD 9	NSD 10	NSD 11
Distance from dyke (m)	0.04	0.15	0.28	0.37	0.47	0.49	0.57	0.65	0.95	0.97	1.21
VR (%Rr)	3.78	3.72	4.69	5.61	5.47	5.16	3.41	3.49	2.82	1.63	1.48
Translucent wood											
Opaque Organic Matter											
Non-woody plant matter											
palynomorph											
AOM											
Zooclast											
Indeterminate											

50 microns

PLATE 25 NSD compilation palynofacies, illustrating particles found in each sample through the NSD horizon of the North Star Dyke aureole

Sample no.	NSD 14	15	16	17	18	19	20	21	22	23	24
Distance from dyke (m)	1.82	2.20	2.22	2.89	2.79	3.95	4.05	5.40	5.66	6.27	10.11
VR (%Rr)	1.26	1.05	1.16	1.03	1.03	1.06	1.19	1.13	1.11	1.04	1.25
Translucent wood											
Opaque Organic Matter	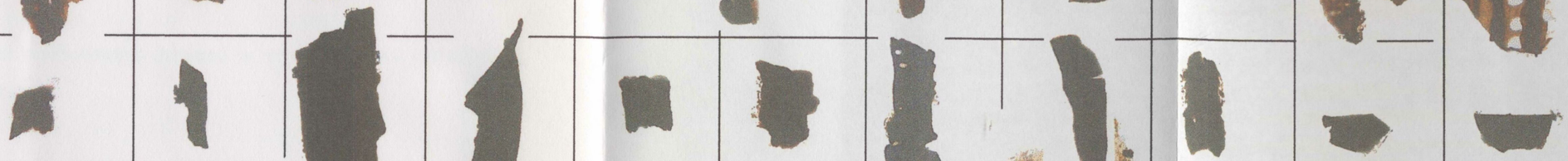										
Non-woody plant matter	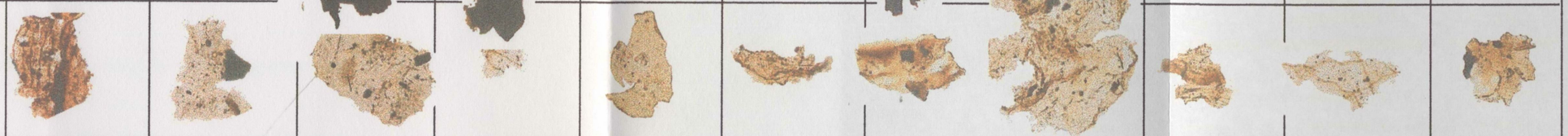										
palynomorph	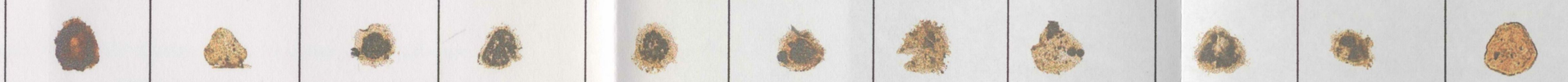										
AOM	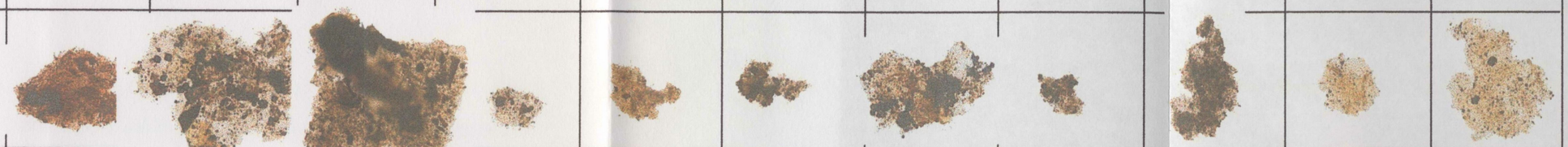										
Zooclast											
Indeterminate											

50 microns

PLATE 26 NSD compilation palynofacies, illustrating particles found in each sample through the NSD horizon of the North Star Dyke aureole

APPENDIX IV

PALYNOFACIES DICTIONARY

APPENDIX VII : Dictionary of Palynofacies Terminology

Acritarch – Group Palynomorph, subgroup phytoplankton. After the Greek *akritos* meaning 'doubtful'; *arche* meaning 'origin', introduced by Evitt (1963). Extremely varied form.

Angiosperm - seed bearing plant on which the ovules are borne in an ovary which develops into a fruit after fertilisation; any flowering plant.

Anoxic Environment - aquatic environments depleted in oxygen; where virtually all aerobic biological activity has ceased.

Clast - from the Greek *klastos* meaning 'broken in pieces'.

Cuticle - a botanical term referring to the waxy layer coating the epidermis

or

- used in coal literature for any thin, translucent, tissue like material

Diagenesis – a process through which the system tends to come to equilibrium under conditions of shallow burial where the sediment usually becomes consolidated (Brooks 1981)

Dispersed Organic Matter – (DOM) used by Burgess (1974) to describe the organic matter in sediments (i.e. what Tyson 1995 is calling kerogen) but this phrase is also used by coal petrologists to distinguish between the organic matter in coals and that in other lithologies.

Exine - the part of the pollen wall outside the exine (Reitsma, 1970)

Facies - describes a spatially segregated and broadly coeval body of sediment deposited within a specific depositional environment or by a specific depositional mechanism (Tyson, 1995).

Fading effect - exposure of pollen and spores to UV radiation under the microscope leads to decompositon or alteration of their walls. The exposure caused a fading effect of the fluorescence intensities.

Gelified material – woody phytoclasts showing botanical structure and intra-clast porosity (Tyson 1995)

(non-) gelified material – woody phytoclasts, which are homogenous and massive.

Geothermal gradient – heat flow is the transfer of thermal energy from the interior of the earth to the earth surface, where it is dissipated. It is normally expressed in the rate of increase of temperature with depth i.e. geothermal gradient, as related to the thermal conductivity of the rocks in which it is measured (Brooks 1981).

Gymnosperm - seed bearing plant on which the ovules are borne naked on open scales (e.g. cones)

Higher/Vascular plants - pteridophytes, gymnosperms, angiosperms

Humic - a word normally used to refer to products of peat formation which consist not only of tissue and cellular structures of land plants but also of carbonised (fusinised) OM s.a. charcoal and other oxidised remains (Batten 1981).

Hylogen – (*hylo-*, the Greek root means 'matter') the woody tissue of land plants

Intine - cell wall proper (cell membrane)

Isospores – produced by the more lowly vascular plants (e.g. clubmosses, horsetails, and most ferns). Multiple, identical spores (e.g. from a tetrad), that give rise to a free living gametophyte generation in homospory (Brasier 19).

Kerogen - (*Keros,* Greek meaning 'wax-' or 'oil-forming' and the root *-gen* meaning 'that which produces.')

The word was first proposed by A. CrumBrown (in Steuart 1912) when describing OM present in the Lothian oil shales as "the carbonaceous matter in shale that gives rise to crude oil in distillation"

The word has been used in various senses throughout the literature. Brooks (1981) and Durand (1980) believe that the term Kerogen should not have any genetic inference for either the origin of the constituents in the sediment or even from the viewpoint of postulated hydrocarbon generation products.

1. the OM in shales, which, when heated yields oil.(A. Crum Brown in Steuart, 1912) thus in an optically restricted sense kerogen can be used to describe only the unstructured, essentially amorphous OM (Batten 1981)
2. Tissot et *al.* (1974) classify Kerogen as the OM recovered from sedimentary rocks which fit into one of 3 categories according to their H/C v^s O/c content (after Van Krevelans diagram 1961)

   Type 1 - most commonly Lacustrine in origin, rich in algae and microbial lipids

   Type 2 - Marine, algae, zooplankton and other marine organisms accumulated in a marine environment.

   Type 3 - Detritus derived from land plants.
3. The total insoluble organic matter in a sediment (Burgess, 1974 and Bayliss, 1975) or in the optical sense Burgess (1974) defines kerogen as a finely disseminated organic material freed from a sedimentary rock after acid treatment.
4. Hunt (1979) broadened the above optical definition to disseminated organic matter of sedimentary rocks insoluble in non oxidising acids bases and organic solvents. Not preparations take the material through all of these steps!!
5. the fraction of OM which is insoluble in the usual organic solvents (Durand 1980) very broad and all encompassing

6. the disseminated OM of rocks that is insoluble in non-oxidising mineral acids, bases and organic solvents (Brooks 1981)
7. kerogen is a term that is often incorrectly used to encompass all OM in a rock. Brooks (1981) feels that the organic fraction extractable with solvents should be separate from kerogen. His preferred definition being "the disseminated organic matter of rocks that is insoluble in non-oxidising mineral acids and bases and organic solvents" furthermore the term kerogen should have no genetic significance concerning the origin of the constituents in the sedimentary organic matter or even from the viewpoint of hydrocarbon generation products.
8. Tissot and Welte 1984- define kerogen as the organic constituents of sedimentary rocks that are insoluble in both aqueous alkaline and common organic solvents (this is equivalent to the humin of soil scientists).
9. Tyson (1995) classifies fossil organic matter in ancient sediments as kerogen, and sees palynological organic matter as kerogen viewed in transmitted.
10. Kerogen is a chemical term, introduced by organic geochemists, for organic matter which is not soluble in organic solvents (Frey, 1987).

Labile organic fraction – the organic fraction that is consumed before burial.

Lower plants - algae, bryophyta

Maceral – a word initially introduced by Stopes (1935) originally meaning "a distinctive and comprehensive word tallying with the word mineral…they (macerals) are the descriptive equivalent of the inorganic units composing most rock masses and universally called minerals", likening macerals in coals to minerals in rocks.

Maceration - softening or separation as a result of soaking.

Maturation- maturation of organic matter is a chemical response to increasing thermal stress experienced by the sediment, producing many and varied changes in the original organic constituents of the sediment. It is regarded as taking place subsequent to diagenesis

(where low temperature chemical reactions are important) produces changes in the insoluble kerogen and in the soluble bitumen (Williams and Douglas, 1981)

Metabolizable material - sugar and amino acids

Microspore – 20 -50μm in diameter, these are small male spores.

Megaspore – 200 - 400μm in diameter, these are large female spores.

Miospore- an umbrella term for isospores, microspores and (small)megaspores

Organic maturation - the process leading to hydrocarbon generation as a result of time and temperature induced geochemical structural and compositional changes in the OM (Brooks 1981).

Palynofacies Powell *et al.* (1990) defines palynofacies as a distinct assemblage of HCL and HF insoluble particulate organic matter (palynoclasts) whose composition reflects a particular sedimentary environment. However it is treated here as an indication of a set of characteristics that with others characterises the rock rather than a method for definitive identification.

Palynofacies analysis - is defined as the identification of characteristics of rock facies through the palynological study of their contained organic matter (after Batten 1999, Tyson 1995, Powell 1990, and Combaz 1964). Thus analysis requires that all types of HCl and HF resistant organic matter recovered from rock or sediment samples by palynological extraction methods be examined. It is a useful if blunt tool.

Palynology- derived by Hyde and Williams (1944) from the Greek verb *palunein* (meaning to sprinkle, to dust), a term coined to encompass the study of spores and pollen.

Palynomorph - (term coined by R.A. Scott and introduced by Tschudy 1961) all discrete HCl and HF resistant organic walled (unicellular, multi-cellular or colonial) microfossils that may be present in palynological preparations.

Palynomorphs can be fungal spores and small fructifications, polychaete jaws, the extinct chitinazoans, animal and vegetable tissue fragments algal cysts, isospores, microspores, megaspores and pollen (Jansonius and McGregor 1996). That is any microscopic specimen resistant to HCl, HF, H_2NO_3, $NHOH_3$

Phyco- - in composition, seaweed (Greek *Phykos*, meaning seaweed). Used with respect to algae.

Phytoclast - a controversial term introduced by Bostick (1971, p84) to describe those dispersed clay to fine sized particles of altered plant matter that are apparently derived from land plants. "Grains of clastic organic matter similar to coal…called phytoclasts as many of them have relict plant structures…consist of plant spores and pollen, leaf cuticles and fragments that have bordered pits, ribs, fibres, or cellular structure. Bostick however also included floccules of probably mostly algal debris or poorly preserved liptinite plus low reflectance vitrinite.

Tyson on the other hand chooses to define the term by restricting it to what are literally clasts by excluding the Palynomorph and amorphous materials (also suggested by Alpern (1980) and Hart (1986).

Phytoclasts fragments of plant derived material. Plant fossils with characteristic features associated with terrestrial adaptation (stomata, cuticle, xylem, wind dispersed spores) do not appear until late Silurian time (Chaloner *et al.* 1991). There are some cases of isolated spores and tissue fragments in earlier Silurian sediments and late Ordovician material but the nature of the plants that produced them is not clear (Chaloner *et al.* 1991).

Phytocoenoses – fossil plant assemblages

Pollen – is a multicellular spore, whose function is dispersal to reach the female cone directly and to proceed with fertilisation

Protista – (*Gr Protistos* very first, *protos* first) a large group of unicellular organisms on the borderline between the plant and animal kingdoms. Tappan 1980 lists the Blue and green algae, bacteria, rhodophyta, acritarchs, dinoflagellates, silicoflagellates, diatoms, calcareous nannoplankton as plant protists.

Pteridophyte – the term "pteridophyte" has no natural-classification significance (Traverse 1988) but is useful in the palynological sense to embrace the whole complex of free-sporing (seedless) vascular plants

Pterophyta – ferns

Refractory organic fraction – that fraction of organic matter that survives diagenesis to become a potential source of hydrocarbons.

Sapropel (Potonié 1908, 1910) - "a gel derived from organic debris which has putrefied in an anaerobic medium". The current usage of Sapropel implies amorphous OM has had algal origin. However AOM does not always originate from algal material and the initial definition does not imply that algal involvement was actually necessary.

Sapropelic OM - consists of decomposition and polymerisation products of both algal and vascular plants; this alteration has usually taken place when the supply of oxygen is limited. In addition it includes cuticles, spores dinoflagellate cysts and other biological clastic entities which have well defined morphologies (Batten 1981)

Spore – the term spore refers to any single celled or few celled body, produced as a means of propagating a new individual.

Sporopollenin - the name for the highly resistant chemical substance/substances in the exine of the pollen wall and the exosporium of a large number of spore walls (Jonker 1971)

Van Krevelan Diagram (1961)- classifies OM into 3 principal categories:

Sapropelic, Mixed Sapropelic/humic and ligneous according to their relative proportions of H/c v^s O/C.

Vascular / Higher plants – any plant which has an internal system for conduction and transport of fluids and or nutrients around its body. Pteridophytes, gymnosperms, angiosperms.

APPENDIX V

XRD TRACES AND DATA

Figure 1 CK horizon compilation traces

Figure 2 CQ horizon compilation traces

Figure 3 BC horizon compilation traces

Figure 4 cMd horizon compilation traces

Figure 5 NSD horizon compilation traces

Figure 6 XRD air dried trace for the North Star Dyke (IG1)

CD with raw XRD trace data in Excel 2000 format

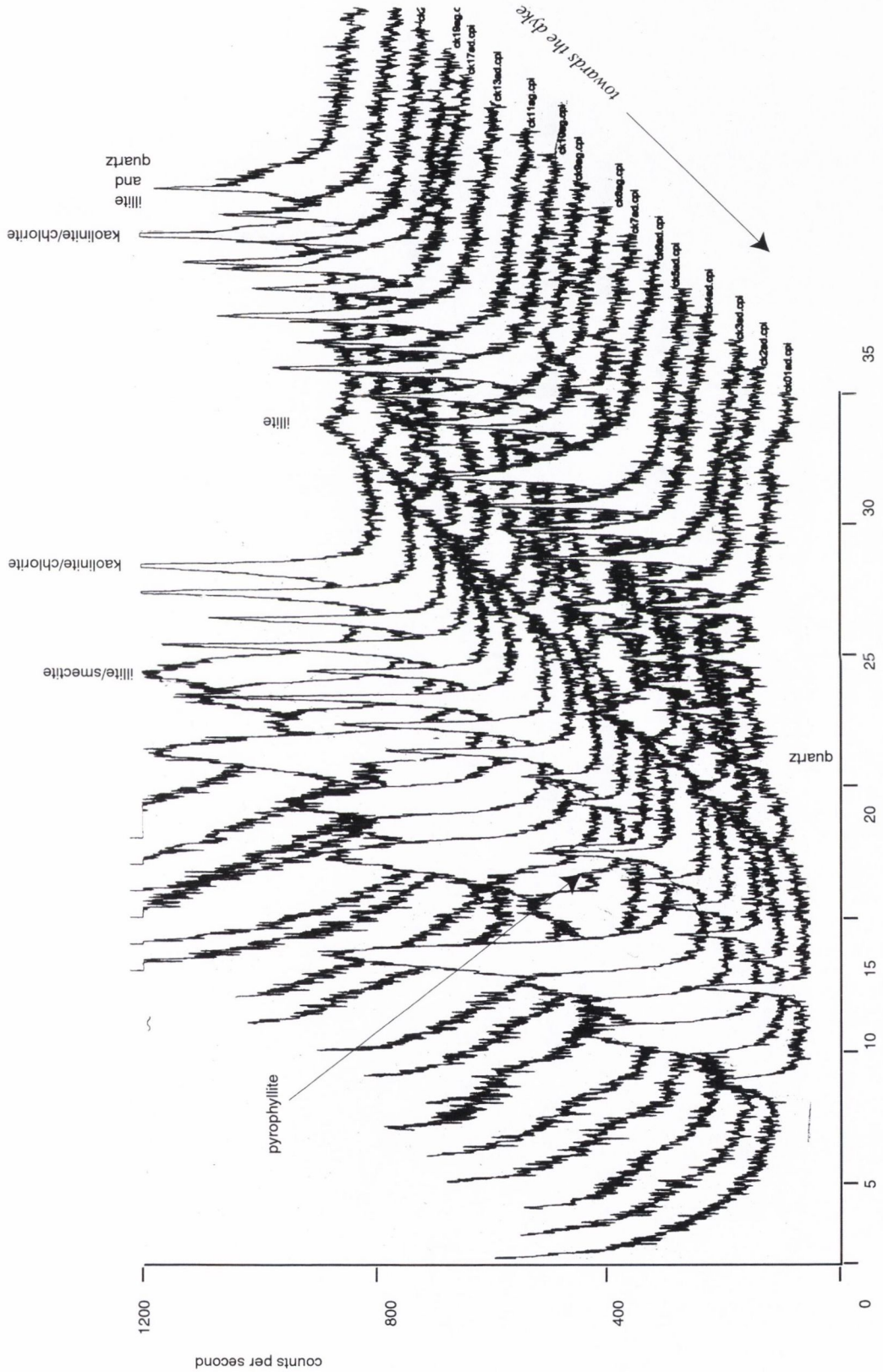

Figure 1 CK horizon air-dried traces

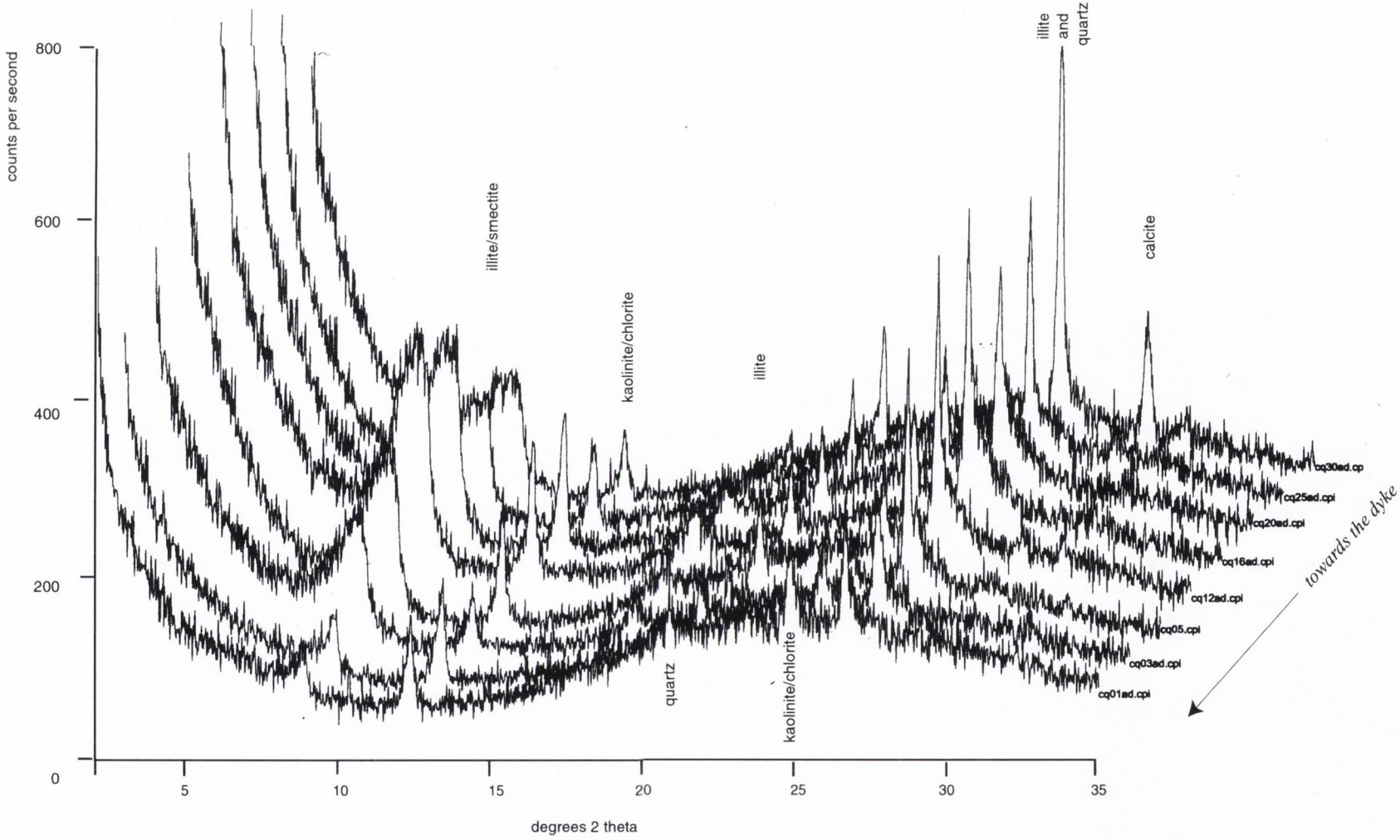

Figure 2 CQ horizon air-dried traces

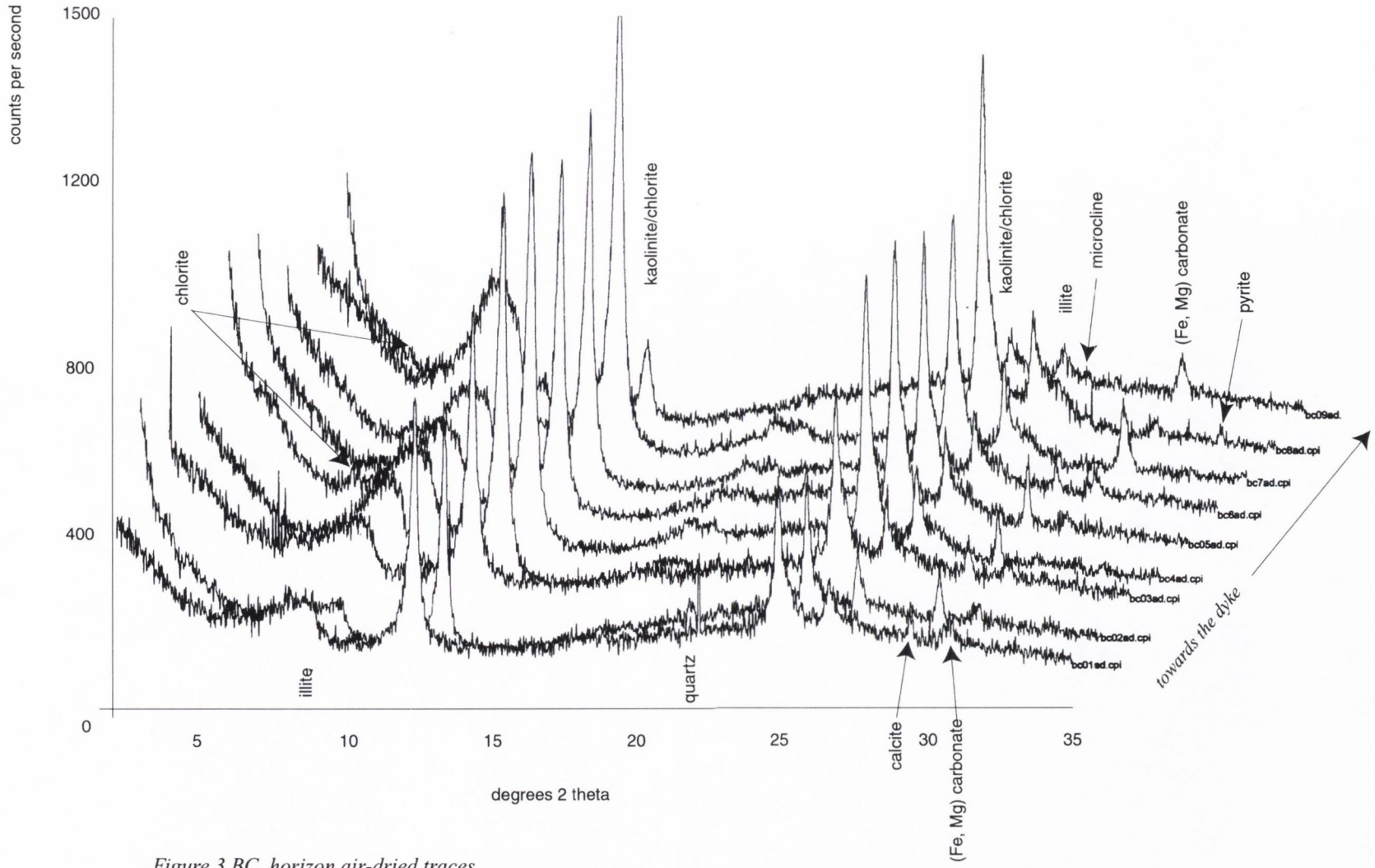

Figure 3 BC horizon air-dried traces

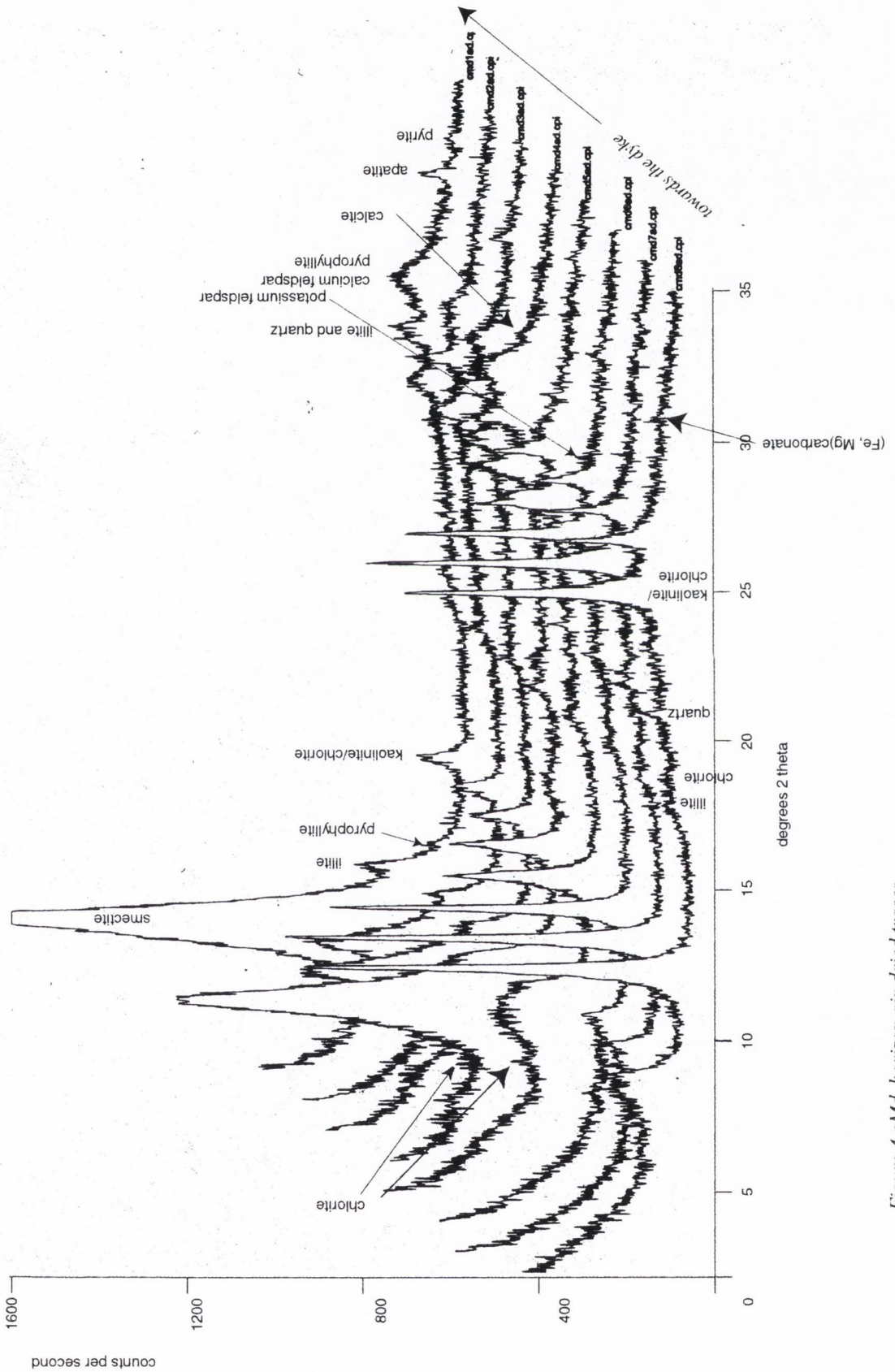

Figure 4 cMd horizon air-dried traces

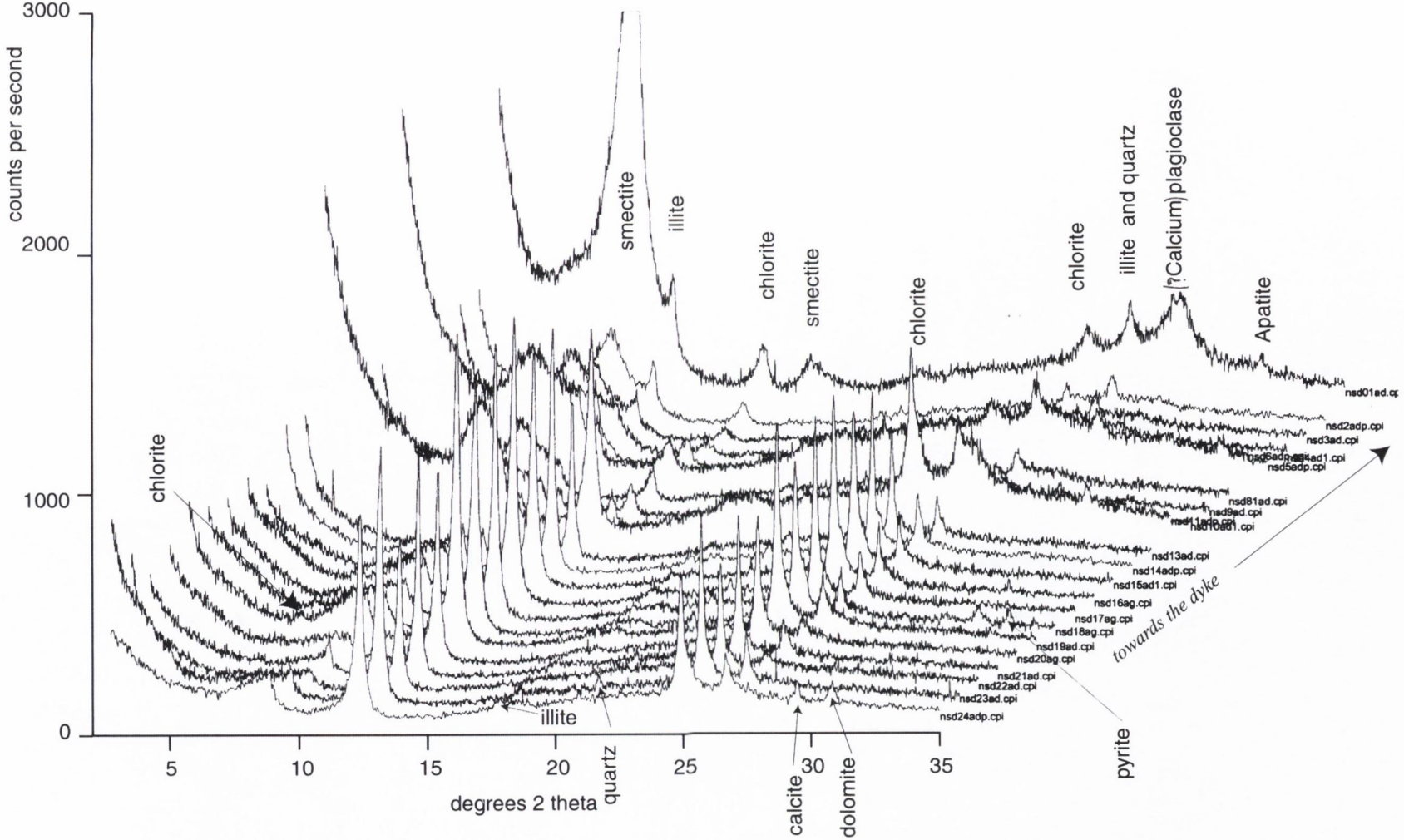

Figure 5 NSD horizon air-dried traces

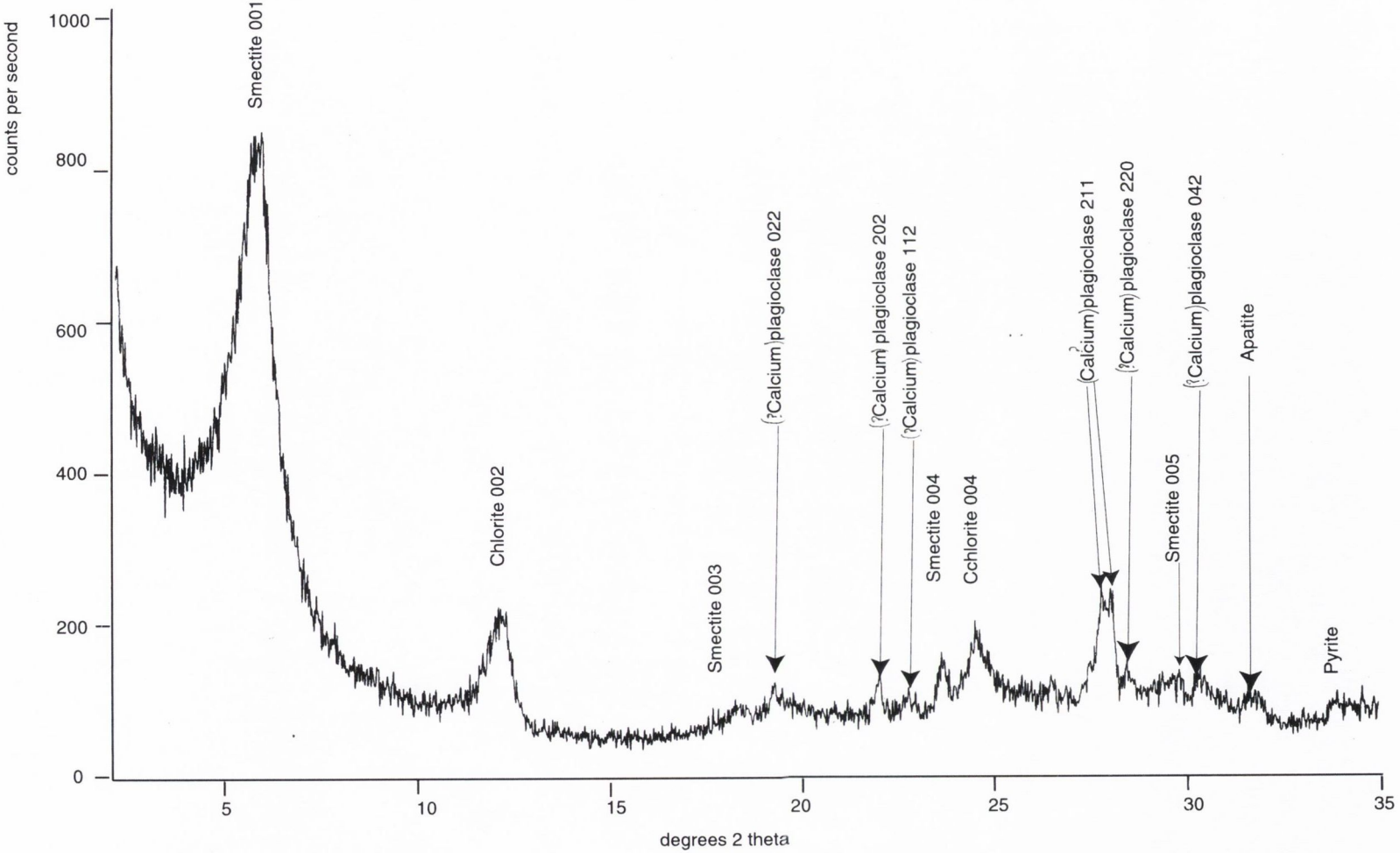

Figure 6 XRD air dried trace for the North Star Dyke